

METHODS IN MOLECULAR MEDICINE™

Renal Cancer

Methods and Protocols

Edited by

Jack H. Mydlo, MD



Humana Press

Renal Cell Carcinoma

Clinical Features and Management

Paul Russo

1. Introduction

In 1999 it was estimated that renal cell carcinoma (RCC) would account for 29,990 new cancer cases diagnosed in the United States (61% in men and 39% in women), and lead to 11,600 deaths. RCC accounts for 2–3% of all malignancies in adults and causes 2.3% of all cancer deaths in the United States annually (**1**). Approx 4% of all RCC cases are bilateral at some point in the life of the patient. Data from over 10,000 cases of renal cancer entered in the Connecticut Tumor Registry suggests an increase in the incidence of renal cancer from 1935–1989; in women the incidence increased from 0.7 to 4.2 in 100,000, and in men from 1.6 to 9.6 in 100,000 (**2**). Factors implicated in the development of RCC include cigarette smoking, exposure to petroleum products, obesity, diuretic use, cadmium exposure, and ionizing radiation (**3–9**).

In the last 20 yr, the surgical management of RCC has evolved. Radical nephrectomy is no longer considered the only approach to RCC and modifications in the radical nephrectomy—relating specifically to adrenalectomy and regional lymph-node dissection—are now widely accepted. In the last 10 yr, reports from major centers have shown the effective application of partial nephrectomy, or nephron-sparing surgery, in the treatment of small, incidentally discovered renal tumors. In the last 5 yr, advances in endosurgical instrumentation have allowed dedicated investigators to explore laparoscopic and laparoscopically assisted nephrectomy as alternatives to open surgical techniques. Finally, the limits of operative treatment for advanced cases of RCC are being explored, including the role of surgery in locally recurrent RCC, in renal tumors involving the inferior vena cava, and in the treatment of patients with metastatic disease.

2. Clinical Presentation

2.1. Incidental Presentation and Differential Diagnosis

The widespread use of abdominal computed tomography, ultrasonography, and MRI in the evaluation of nonspecific abdominal complaints has lead to the increased detection of the incidental renal mass or incidentaloma, from 10–15% to over 50% during the last 20 yr (*10–12*). Some urologists use office transabdominal ultrasound as part of the routine history and physical exam of every new patient visit, thus further increasing, the possibility of an incidental tumor discovery (*13*). Another source of incidentally detected renal tumors is with patients undergoing imaging in the follow-up care of other malignancies. Twenty-seven percent of patients with RCC will have a diagnosis of at least one other malignancy in their lifetime—the most common being breast cancer, prostate cancer, colorectal cancer, bladder cancer, and non-Hodgkin's lymphoma (*14*).

Incidentally discovered renal tumors are confined within the renal capsule (P2 or less) in 75% of cases, and are associated with a 5-yr survival rate of at least 75% following operative treatment (*15–17*). When compared to symptomatic RCC, incidentally discovered RCC tumors are significantly smaller in size (mean 5 cm), have a lower P stage, and are associated with a high likelihood of survival. Analysis of histological grade and DNA ploidy pattern reveals no differences between incidental RCC and symptomatic RCC (*18*). The resulting stage migration in RCC has resulted in a decrease in the incidence of metastatic disease to less than 20% and improved 5-yr survival (*19*). The incidental discovery of smaller renal carcinomas has also encouraged the more liberal application of partial nephrectomy (nephron-sparing surgery) (*20*). Today, over one-half of surgically resected cases of RCC are detected without clinical symptoms, and the likelihood of complete resection with partial or radical nephrectomy is great.

The differential diagnosis of a renal mass includes benign cyst (simple, complex, hemorrhagic), pseudotumors (column of Bertin), angiomyolipoma, vascular malformation, lymphoma, sarcoma, adult Wilm's tumor, or metastatic tumor. When a clinician is faced with a solid renal mass, approx 90% of such masses will be RCCs or the benign-behaving variant of RCC (oncocytoma) (*21*). In general, preoperative percutaneous needle biopsy or aspiration of the clinically localized solid renal mass is not recommended because of the high rate of RCC or oncocytoma in such masses, the low rate of metastatic tumors (<5%) presenting as a solid renal mass, concerns regarding the high rate of false-negative results, and the possibility of causing bleeding or tumor-tract seeding (*22*). With these concerns in mind, percutaneous needle biopsy is reserved for patients with obvious metastatic disease for which tissue confirmation of RCC will allow systemic treatment or access to a clinical trial (*23*).

2.2. Bilateral Renal Tumors

Bilateral RCC occurs in approx 4% of all RCC cases, and may be hereditary or sporadic in origin. Hereditary forms of RCC, such as von Hippel-Lindau (VHL) disease, hereditary papillary renal cell carcinoma (HPRC), and familial renal oncocytoma, differ in general from sporadic, unilateral forms of RCC because they tend to be multifocal and bilateral, and occur at a younger age (third to fifth decade). In von Hippel-Lindau disease, other potentially life-threatening neoplasms—such as CNS hemangioblastoma and pheochromocytoma, as well as cystic changes in the kidney, pancreas, and epididymis—are commonly associated with the bilateral renal tumors. The VHL tumor-suppressor gene has been cloned and localized to the short arm of chromosome 3 (24–29). Hereditary papillary RCC has been described as a distinct form of inherited renal cancer that does not display a loss of heterozygosity at chromosome 3/VHL (30,31). In addition, the nearly benign variant of RCC—oncocytoma—can present as bilateral tumors with a familial distribution (32), has been found to exhibit an array of chromosomal abnormalities, including the loss of the Y chromosome and abnormalities in chromosome 1 and 22, and can have a hereditary pattern of inheritance (33).

RCC can also present as a bilateral tumor without evidence of hereditary or familial involvement. Histologic patterns in these patients are predominantly clear-cell (59%), followed by papillary (17%) and oncocytoma (10%). In this cohort of patients, 66% presented synchronously (34). Bilateral RCC provides a surgical challenge that balances complete resection with attempts to maintain adequate renal function off dialysis.

2.3. Symptomatic Presentation

RCC is associated with a wide array of systemic symptoms—including microscopic and gross hematuria, anemia, polycythemia, hypercalcemia, weight loss, malaise, acute varicocele, and fever—and has been referred to by some as the internist's disease (35). Physical examination is performed with special attention to supraclavicular and cervical lymph nodes, the presence of a palpable abdominal mass, the presence of a bruit, lower-extremity edema, varicocele, SC nodules, and penile or vaginal metastases. Laboratory evaluation should include a CBC, serum calcium, liver function studies, and a serum creatinine. A reversible abnormality in liver function, called Stauffer's syndrome, can also be observed. Today, less than 5% of patients present with the classic Virchow's triad of hematuria, flank pain, and flank mass. Of all RCC cases, the rate of those presenting with metastatic or locally advanced disease is approx 30% (36).

2.4. Extent of Disease Evaluation

The extent of disease evaluation should include a chest x-ray and abdominal CT scan to focus on the regional nodes and lung, the most common sites of early metastatic disease (37,38). An abdominal CT scan can correctly predict the T-stage in 80% of cases (38). If a nodule on the chest X-ray is observed, then a chest CT is indicated to rule out multiple pulmonary metastases. Chest CT has a greater yield of finding metastatic nodules in a patient with a large primary tumor (39). A bone scan is not routinely performed unless the patient has an elevated alkaline phosphatase or complains of bone pain (37). If the CT scan raises the possibility of renal vein or inferior vena-caval extension, then Doppler ultrasound or MRI is performed to define the uppermost level of the thrombus (40). CT of the brain is not routinely performed unless the patient complains of a headache, manifests a neurologic deficit, or experiences a seizure. As an aid to the operating surgeon, angiography, is utilized in selected cases if partial nephrectomy is planned and the tumor is centrally located.

3. Staging

Prior to surgery a tumor stage is assigned. Two staging systems—the Robson system (41) and UICC TMN classification (42)—are utilized in RCC. Descriptive limitations in the Robson system include regional node involvement and renal vein or inferior vena-cava involvement. The TMN staging system more explicitly describes the extent of the local and regional disease and is thus preferred at our institution. The current AJCC staging system was recently modified in 1998 to include all tumors as T1 that are 7 cm or less (Table 1). This represents a change from the 1993 system that described T1 tumors as those less than 2.5 cm. Prospective validation of the 1998 AJCC system is anticipated. Neither staging system currently differentiates the metastatic potentials of the variants of RCC where tumor size may be less important than histopathology, ranging from the potentially aggressive conventional clear-cell carcinoma, to the intermediate papillary and chromophobe carcinoma, to the only rarely metastatic oncocytic tumors (43–45). When prognostic factors are viewed together, size has the greatest prognostic impact on conventional clear-cell RCC. In time, staging systems will probably also incorporate histologic subtypes into the prognosis of renal tumors.

The most important prognostic determinants of 5-yr survival are the local extent of the tumor (organ-confined disease-TMN P1, Robson stage I, 70–80%; or extending into perinephric fat TMN P3a or Robson stage II, 60–70%), the presence of regional nodal metastases (single, multiple, contralateral, fixed, or juxtaregional-Robson IIIb or TMN N1, N2, 5–20%), and the presence of metastatic disease at presentation (Robson IVb or TMN M1, 0–5%). Other adverse prognostic indicators usually associated with locally advanced or metastatic

Table 1
TNM Clinical Classification

T-primary tumor			
Tx	Primary tumor cannot be assessed		
T0	No evidence of primary tumor		
T1	≤7.0 cm; limited to kidney		
T2	>7.0 cm; limited to the kidney		
T3	Tumor extends into major veins or invades adrenal gland or perinephric tissues but not beyond the Gerota fascia		
T3a	Tumor invades adrenal gland or perinephric tissues but not beyond the Gerota fascia		
T3b	Tumor grossly extends into renal vein(s) or vena cava below the diaphragm		
T3c	Tumor grossly extends into vena cava above the diaphragm		
T4	Tumor invades beyond the Gerota fascia		
N-regional lymph nodes			
NX	Regional lymph nodes cannot be assessed		
N0	No regional lymph node metastasis		
N1	Metastasis in a single regional lymph node		
N2	Metastasis in more than one regional lymph node		
M-distant metastasis			
Mx	Distant metastasis cannot be assessed		
M0	No distant metastasis		
M1	Distant metastasis		
Stage grouping			
Stage I	T1	N0	M0
Stage II	T2	N0	M0
Stage III	T1	N1	M0
	T2	N1	M0
	T3	N0, N1	M0
Stage IV	T4	N0, N1	M0
	Any T	N2	M0
	Any T	Any N	M1

tumors include high pathologic grade, sarcomatoid histology, large tumor size (>10 cm), weight loss, hypercalcemia, and an elevated sedimentation rate (46).

3. Surgical Treatment of RCC

Despite recent exciting breakthroughs in our understanding of the molecular biology of RCC and its histologic variants, surgical resection still remains the

only effective treatment for clinically localized renal tumors. The historical approach to renal tumors focused on simple nephrectomy, which was supplanted by perifascial or radical nephrectomy that was presumed—but never proven—to be a more effective operation. As migration to an earlier stage during detection of renal tumors has occurred—resulting from the above described advances in abdominal imaging—partial nephrectomy in general, and nephron-sparing surgery in particular, have emerged as effective alternatives to radical nephrectomy in appropriately selected cases. Careful case selection has enabled the surgical resection of renal tumors with vena-caval tumor extension, limited metastatic disease, and isolated local recurrence. Although laparoscopy must be considered investigational, advances in instrumentation may substantially enhance the appeal of this minimally invasive approach, which limits perioperative morbidity and hospital stay.

4.1. Radical Nephrectomy

Using a thoracoabdominal incision, Mortensen (1948) reported the first radical nephrectomy—an operation that removed all of the contents of Gerota's fascia in an attempt to address the 13% of patients with renal tumors that invaded the perinephric fat (47). The radical nephrectomy was popularized in the 1960s by Robson, who described this operation as the perifascial resection of the tumor-bearing kidney, along with perirenal fat, regional lymph nodes, and the ipsilateral adrenal gland (48). In 1969, Robson reported the results of radical nephrectomy and described a 65% survival rate for tumors confined within Gerota's fascia (Robson stage 1 and 2), but the finding of regional nodal metastases led to less than a 30% 5-yr survival rate (49).

Depending on the surgeon's preference—relating mainly to patient's body habitus, the tumor size, and tumor location—the radical nephrectomy can be performed through an eleventh-rib flank incision, a transperitoneal midline or subcostal incision, or a transthoracic incision. In retroperitoneal nephrectomy, the peritoneum and pleura are dissected off the perirenal soft tissues and Gerota's fascia, exposing the kidney. In transabdominal approaches to the kidney, the colon, small intestine, liver, pancreas and spleen (for left-sided tumors) are mobilized, exposing the great vessels and the kidney within Gerota's fascia. During the radical nephrectomy, the surgeon gains early control of the renal hilum and ligates and divides the renal artery and the renal vein. Approx 20% of people have multiple renal arteries, leading the surgeon to carefully identify, ligate, and divide any aberrant renal, lumbar, or tumor vessels that may supply the kidney. The classic radical nephrectomy is completed with an ipsilateral adrenalectomy and regional lymph-node dissection, typically skeletonizing the ipsilateral great vessel (vena cava or aorta). A more complete retroperitoneal lymph-node dissection is performed if metastatic lymph nodes are discovered at the time of radical nephrectomy.

Despite the wide acceptance of radical nephrectomy by urologic surgeons over the last 25 yr (**49–51**), no data have convincingly confirmed the need for the component parts of the operation (i.e., the need for adrenalectomy (**52**), or the need for and extent of lymph-node dissection) (**53,54**). Randomized comparisons with and without the component parts comparing radical nephrectomy to simple nephrectomy have not yet been described. At the same time, the evolution of nephron-sparing operations during the era of the incidental renal tumor detection has now been fully established as a legitimate alternative to radical nephrectomy (**20,55–60**).

4.2. Lymph Node Dissection

Lymphatic drainage from the kidneys is a complex process, and differs depending on the side. The right kidney drains into precaval, retrocaval, and interaortocaval nodes (not paracaval), whereas the left kidney drains to the para-aortic, preaortic, and retroaortic nodes. In renal cancer, regional lymph nodes can be enlarged because of a benign inflammatory response or from metastatic involvement (**61**). In a series of 163 patients with operable RCC, preoperative CT scanning was falsely negative in five patients, two with grossly enlarged hilar nodes (>2.5 cm), and three with micrometastatic disease in nodes <1 cm. Of 43 patients with preoperative CT scans demonstrating enlarged regional nodes (1–2.2 cm, median 1.4 cm), 18 patients (42%) had metastatic RCC, and in 25 patients (58%) the enlarged nodes were inflammatory. The cause of the reactive regional nodes may be related to an immune response secondary to necrosis within the primary tumor. Given the current limitations of CT scanning, no patient should be denied a potentially curative resection based on regional lymph-node enlargement alone.

Although the original description of the radical nephrectomy described a concomitant and complete retroperitoneal lymph-node dissection with skeletonization of both the inferior vena cava and aorta, most urological surgeons rarely perform an operation of this extent today. A node dissection clearing the ipsilateral great vessel and the renal hilum is generally done. Clinical data compiled over the last 25 yr leaves little doubt that the finding of even a single positive lymph node represents an ominous prognostic sign, with most series reporting less than 20% 5-yr survivors. It is unknown whether complete lymph-node dissection at the time of radical nephrectomy provides a therapeutic advantage to the patient.

The accepted rationale for lymph-node dissection in RCC is: to improve staging accuracy, to resect micrometastatic disease, and to determine if enlarged regional nodes are inflammatory or metastatic (**61**). Improvement in staging accuracy would better identify patients at high risk for systemic disease and would provide a rational basis for entry of such patients into poor risk-

adjuvant trials. Lymph-node metastasis, in the absence of other metastatic disease, occurs in approx 10–15% of cases. (53,54,62–64). Guiliani and colleagues correlated tumor stage with degree of lymph-node metastases and found that tumors confined to Gerota's fascia had a 13% rate of positive nodes, whereas for tumors beyond Gerota's fascia the rate was 37% (62). This issue is further complicated today by our enhanced understanding of the different histologic subtypes and the impact of histology on prognosis. Currently there is no available data on the risk of nodal metastases as correlated to histologic subtype.

Proponents of extended lymph-node dissection argue that the resection of microscopically involved nodes (palpably normal) can add a therapeutic benefit as well as reduce the possibility of local tumor recurrence in more potentially aggressive primary tumors. Golimbu and colleagues described 52 patients who underwent radical nephrectomy and regional lymph-node dissection, and compared the outcome to 141 patients with palpably normal nodes undergoing radical nephrectomy alone. Lymph-node dissection added no apparent survival benefit for patients with stage I tumors, but a 10–15% survival benefit in stage II tumors suggested some therapeutic benefit (65). This study and others like it are subject to selection biases that can only be clarified in a prospective and randomized trial. Because of differences in operative lymphadenectomy templates, it is difficult to compare lymph-node data from one institution to the next. The ultimate impact of lymphadenectomy can only be assessed by a prospective and randomized trial where the surgical templates for operation are uniformly agreed upon and carefully adhered to, and the data is controlled for tumor stage and histologic subtype.

At the present time, the therapeutic impact of regional lymphadenectomy in RCC remains controversial, yet it is reasonable to perform complete retroperitoneal lymphadenectomy for large tumors (>T1) when metastatic lymph nodes are documented at the time of radical nephrectomy. A regional node dissection (ipsilateral great vessel and hilar nodes) should at the very least be done in other cases. Node dissection is unnecessary in the case of small renal tumors treated by partial nephrectomy or laparoscopic techniques, since the expected yield approaches zero. This approach will provide prognostic information valuable for patient counseling as well as entry into appropriate adjuvant clinical trials (66).

4.3. Adrenalectomy

Adrenalectomy has traditionally been included as a component of the radical nephrectomy (47–49), yet the therapeutic impact has not been fully defined. With stage migration to an earlier-stage renal tumor, clarification of the therapeutic value of adrenalectomy is now required, particularly because the approach to small renal tumors by partial nephrectomy and laparoscopy is underway. The mechanisms by which metastatic disease can gain access to the

adrenals could be as follows: direct extension through perinephric soft tissues; hematogenous spread through ipsilateral adrenal veins, or the systemic circulation; and lymphatic spread. Sagalowsky and colleagues reported an incidence of adrenal metastases of 4.3% in 695 nephrectomies (52). Adrenal metastases were more likely to occur in patients with tumors that occupied the entire kidney or the upper pole, and were most common in tumors with advanced T-stage. Thirty percent of patients also had evidence of metastatic disease to regional nodes or distant sites. Despite resection of the affected adrenal gland, in 21 of the 30 cases of metastatic disease in the adrenals, 17 patients (81%) died of their disease—most within 26 mo of resection. There is little doubt that metastatic disease in the adrenals is an ominous prognostic sign similar to that of nodal metastases. This experience closely parallels that of surgical oncologists resecting isolated adrenal metastases from other primary cancer sites, such as lung and breast, where 5-yr survival rates of 24% can be achieved with resection—particularly if the patients had a disease-free interval greater than 6 mo (67). In addition, improvements in preoperative imaging with CT and MRI have allowed highly accurate assessment of the status of the adrenals prior to operation. Gill and colleagues correctly cleared the adrenals in 119 patients who had their adrenals preoperatively confirmed as uninvolved at the time of radical nephrectomy. Conversely, when the adrenal gland appeared abnormal on preoperative imaging, 24% of patients were found to have metastatic involvement (68).

Although its potential therapeutic advantage is probably very small, ipsilateral adrenalectomy is still performed for large renal tumors—particularly those involving the upper pole of the kidney, or for those patients with preoperative imaging suggesting an adrenal abnormality. For small renal tumors treated by partial nephrectomy or laparoscopic nephrectomy, adrenalectomy is unnecessary.

4.4. Laparoscopic Renal Cancer Surgery

Reports from several centers have described a preliminary experience with laparoscopic radical and partial nephrectomy for the resection of small renal tumors. As described, the techniques offer the patient a shorter postoperative recovery and hospital stay, but lead to long operations even in the hands of the few expert laparoscopic surgeons in the United States committed to the development of this approach. Thanks to the efforts of these committed investigators, laparoscopic techniques have evolved, allowing for 5-port transperitoneal resection of kidneys for both benign and malignant disease as well as for donor nephrectomy (69–72).

As with many laparoscopic procedures, the benefits of reduced hospital stay, reduced analgesic requirements in the postoperative period, and a more rapid return to normal activities and work for the patient were offset by the increases

in operating time (double that for patients undergoing open nephrectomies). In addition, delivering the surgical specimen by organ entrapment techniques and tissue morcellation led to concerns about possible seeding of the peritoneal cavity or port sites with tumor cells, as well as inaccuracies in pathological assessment. In an attempt to address some of these concerns, investigators have recently utilized a 6.5-cm suprapubic incision to deliver the specimen intact (72). In the initial combined American laparoscopic nephrectomy experience of 185 cases, complications occurred in 12% of patients with benign diseases of the kidney and in 34% of patients with renal cancer. Intraoperative complications related to vascular injury, splenic injury, and pneumothorax led to open surgical intervention in 8 of 185 cases (73).

Tumors most amenable to laparoscopic resection (P1) are now being aggressively approached by partial nephrectomy in the strategy known as “nephron-sparing” surgery. To date, this method provides local control and cure rates similar to radical nephrectomy, with a low expected rate (1–3%) of local recurrence (or new tumor formation) in the operated kidney (55–60). Laparoscopic surgeons have been applying added instrumentation such as intraoperative ultrasound, the laparoscopic tourniquet, and the argon-beam coagulator to initiate a preliminary experience with laparoscopic partial nephrectomy for both benign and malignant lesions (74,75). In these laparoscopic partial nephrectomies, the operating team, through separate ports, uses the tourniquet to hold and compress the designated site of renal incision and the argon beam to coagulate the cut renal surface. Long-term reports detailing late complications and tumor control rates are anticipated.

Reports have appeared in the literature describing a procedure for laparoscopically assisted nephrectomy—a procedure which makes use of an abdominal incision to hand-assist in the mobilization and removal of the specimen. This approach seemed to substantially shorten the operating time while still allowing for the rapid recovery found in the totally laparoscopic procedure (76,77). Laparoscopically assisted abdominal surgery has certainly gained a place in the operative approach to certain gynecologic and colorectal tumors, and may play a future role in the management of renal tumors.

Santiago and colleagues recently reported the use of laparoscopically assisted renal cyst aspiration in patients with complex renal cysts. After the cyst fluid was sent for immediate cytology, 5 of 31 patients (14%) were found to have cystic RCC and they elected to have a radical or partial nephrectomy performed (78). Despite the innovative clinical research techniques involving laparoscopic renal surgery described here, to date most major centers have not committed resources to these techniques. Even in the hands of clinical investigators whose major interest is laparoscopy, the procedures are long and often complicated, and subject to a very steep learning curve. Many institutions

such as ours, where operating-room time is in great demand, await the long-term results of this initial experience as well as the technical improvements which may make laparoscopic renal surgery more popular.

4.5. Partial Nephrectomy

Partial nephrectomy is utilized for the resection of suspicious renal masses in situations in which standard radical nephrectomy would render the patient functionally anephric, necessitating dialysis. Partial nephrectomy is performed in the setting of bilateral renal tumors (either synchronous or asynchronous) (13) or for resection of a mass in a solitary kidney. In addition, when the kidney contralateral to the tumor-containing kidney is functionally impaired from hypertension, diabetes mellitus, congenital abnormality, calculus disease, or nephropathy, partial nephrectomy is required. A functioning renal remnant of at least 20% is needed to maintain a patient off dialysis (79,80).

The widespread use of abdominal computed tomography and ultrasonography during the diagnostic imaging of nonspecific abdominal complaints has led to the increased detection of incidental renal masses (81–84). Currently, approx 90% of such renal masses are RCCs or renal oncocytomas, and the remaining masses are benign complex cysts or unusual tumors such as sarcoma or metastases (21). Reclassification of oncocytoma in the family of renal cortical neoplasms (such as clear-cell or conventional, papillary, or chromophobe) is justified because these tumors retain a small (<3%) but well-documented metastatic potential (43). Despite this obvious stage migration to a smaller renal mass, incidentally discovered RCCs display no significant differences in histologic type, nuclear grade, DNA ploidy, or survival in stage 1 cases when compared to symptomatic tumors—suggesting that, if left undetected and untreated, these tumors will enlarge and acquire a metastatic potential (85). In addition, current radiologic techniques of CT, US, or MRI do not distinguish the small renal cortical neoplasms on the basis of histologic subtype.

If partial nephrectomy could lead to substantial loss of renal substance, placing the patient at risk for temporary dialysis, a preoperative consultation with renal medicine is obtained. At the time of surgery a temporary central venous dialysis catheter is placed to facilitate postoperative management if significant renal insufficiency should occur. The usual approach taken to expose the kidney is through an eleventh-rib, extraperitoneal flank incision. Following complete mobilization of the kidney within Gerota's fascia, the adrenal gland is carefully dissected free of the kidney. Vessel loops are applied to the proximal ureter and the isolated main renal artery. Prior to placement of a bulldog vascular clamp across the renal artery, a mannitol drip is initiated (12.5 g/200 cc) to further limit renal tubular damage.

The use of hypothermia with ice slush allows the partial nephrectomy to be performed in a nearly bloodless field. Following renal-artery cross clamping, ice slush is quickly applied to the kidney for 10–15 min, allowing the kidney to cool to approx 20°C. In all cases, partial nephrectomy with at least a 1-cm rim of surrounding normal renal parenchyma is performed to remove the renal mass, and a frozen section of the base of the specimen is sent to document a clear surgical margin. Tumor enucleation is not performed, because of the high likelihood of tumor infiltration of the pseudocapsule in the enucleation plane. The renal tumor may be resected by wedge resection, major polar resection, major transverse resection—and in very unusual circumstances—extracorporeal partial nephrectomy with autotransplantation. In the case of bilateral renal tumors, the operations are staged 4–6 wk apart.

Following resection of the mass, a running 4-0 absorbable suture is used to repair any rents in the collecting system and large venous channels, and to suture ligate any obvious arteries. Following release of the bulldog clamp, the kidney is carefully checked for bleeding and firm pressure is held on the kidney over the resection margins for several min to assure adequate hemostasis. The argon-beam coagulator (ABC) is used to thoroughly coagulate the renal cortex. Perinephric fat and/or surgicel are used to fill the resection cavity. Several liver sutures (0-chromic) are placed through pledgets of surgicel or perinephric fat to prevent tearing of the renal capsule as the resection margins are brought together, providing final venous hemostasis. Ureteral stents are not routinely used. A penrose drain is placed in the perinephric space through a separate skin incision and left in place for 2–4 d or until there are no signs of significant serous or urinary drainage.

A study from the Cleveland Clinic of 216 patients with sporadic RCC undergoing partial nephrectomy supports the effectiveness of partial nephrectomy. In their report, 47 patients had bilateral synchronous tumors, 95 patients had RCC in a solitary kidney, 57 patients had associated azotemia, medical, or urologic disease necessitating renal preservation, and 17 patients had renal tumors with a normal opposite kidney (nephron-sparing). Eighty-three percent of patients had T1-2 or T3a tumors. The 5-yr cancer-specific survival rate in this series was 87% (T1,2 94%, T3a 79%). Survival in unilateral RCC was 95%, synchronous RCC 85%, or asynchronous bilateral RCC 73%. Local recurrence developed in 9 of 216 patients (4%). The local recurrence rate was higher in large, symptomatic tumors (6.7%) as opposed to small, incidentally discovered tumors (1.1%) (66). The partial nephrectomy, with its' low perioperative morbidity and low recurrence rates, represents a significant improvement in the surgical management of RCC.

Partial nephrectomy techniques are currently being applied electively to such renal masses, in the case of a normal contralateral kidney, in the approach termed *nephron-sparing surgery* (59,60,86–88). Preliminary results from

several centers describe local recurrence rates of $<2\%$ (**81,89–91**), and excellent disease-free survival at 5 yr, despite the reported presence of tumor multicentricity ranging from 6–25% (**92–95**). In addition, careful intraoperative palpation with biopsy and resection of suspicious renal nodules and cysts—coupled with the application of intraoperative ultrasonography—allows the operating surgeon a final opportunity to identify any small satellite tumors (**96,97**). Rarely, the kidney may be covered with many tumor nodules in addition to the main index tumor, undetected by preoperative imaging studies—a definite contraindication to partial nephrectomy (**98**).

The complications of partial nephrectomy relate to hemorrhage, ureteral obstruction, renal insufficiency, and urinary fistula formation. In general, delayed postoperative bleeding is manifested with gross hematuria, bloody drainage from the drain site, or retroperitoneal bleeding with flank mass. Conservative measures such as bedrest, serial hemoglobin determinations, and frequent vital signs are usually sufficient to allow natural clotting mechanisms to control the bleeding. On rare occasions, arteriography with selective embolization or open surgical exploration with ligation of the bleeding vessel is indicated.

Persistent flank drainage (>10 d) indicates a urinary fistula—a diagnosis that can be confirmed by sending the fluid for BUN/creatinine. In the absence of distal ureteral obstruction, most urinary fistulas will close spontaneously as minor rents in the collecting system epithelialize and heal. Inadequate flank drainage can lead to a perinephric collection that may require percutaneous or open drainage. Rarely, a small clot can cause ureteral obstruction and contribute to increased pressure on the freshly repaired collecting system, allowing urinary extravasation. Once the ureteral clot is lysed by urokinase (produced by the kidney), the obstruction is alleviated. Occasionally a double J ureteral stent is placed to bypass the temporary obstruction. The development of postoperative renal insufficiency is dependent on the extent of tumor resection and the amount of viable total renal parenchyma remaining after the partial resection. The Cleveland Clinic reported an acute renal insufficiency rate of 26% in partial nephrectomies performed in a solitary kidney (**99**).

A late complication first reported with partial nephrectomy relates to the possibility of glomerular damage as a result of hyperfiltration, leading to proteinuria and possible progressive renal insufficiency (**100,101**). Follow-up of patients who have had partial nephrectomy in a solitary kidney should include a 24-h urinary protein determination. If significant proteinuria is detected (>150 mg/d), then dietary modification or treatment with a converting enzyme inhibitor may be required.

4.6. Resection of Vena-Cava Tumor Extension

The propensity for RCC to extend into the renal vein and vena cava poses challenging surgical issues. Approximately 23% of RCCs will display renal-vein extension, and in 7% there will be direct extension of the thrombus into the vena cava (**102**). Although the imaging studies of CT and abdominal ultrasound can detect vena-caval tumor thrombus, MRI most effectively determines the uppermost extent of the thrombus and has made vena cavography obsolete (**103**). Vena-caval tumor thrombus may extend from infrahepatic cava (type 1 and 2) to the level of the hepatic veins (type 3), to the supradiaphragmatic or intraatrial vena cava (type 4). There are also case reports of thrombus extension into the right ventricle. Approx 90% of vena-caval tumor thrombi are below the level of the diaphragm. Most patients with RCC and vena-caval tumor thrombus are entirely symptomless but patients can present with pulmonary emboli, clinical evidence of peripheral venous hypertension (leg edema, collateral venous distention, right-sided varicocele, or caput medusae), and positional hypotension. Most primary renal tumors with vena-caval extension are large (mean 10 cm). An aggressive metastatic evaluation (brain CT and bone scan) should be done prior to surgery, since the finding of metastatic disease is an absolute contraindication to resection (**104**).

The degree of extension into the vena cava dictates the surgical techniques required to remove the tumor and thrombus, often with the assistance of a cardiovascular surgical team. Following exploratory laparotomy and exclusion of nodal or visceral metastases, distended collateral tumor vessels are carefully ligated and divided. Care must be taken not to overly manipulate the tumor to avoid dislodging the thrombus and causing an intraoperative pulmonary embolism. A Moritz or DeWeese clip is placed on the inferior vena cava above the thrombus, early in the operation, to protect against intraoperative embolism. The placement of the clip can be done through an incision in the central tendon of the diaphragm at the level of the suprahepatic vena cava. If possible, the renal artery should be ligated and divided early to decrease perfusion to the kidney and tumor. Isolation of the vena cava is achieved by ligating all lumbar and gonadal vessels to the cava. Vessel loops are placed on the contralateral renal vein and proximal and distal vena cava, effectively isolating the cava containing the tumor thrombus. For tumor thrombus with infrahepatic caval involvement, the thrombus can often be milked back toward the kidney and isolated with a Satinsky clamp. Incision into the cava at the ostium of the renal vein allows delivery of the thrombus, which may be facilitated by a Fogarty or Foley catheter placed above the thrombus, inflated, and then pulled toward the ostium of the renal vein. If the thrombus is free-floating, the vena cavotomy is closed. If there is evidence of direct caval-wall invasion, the affected section of cava is resected and sent as a separate specimen. The vena cava is closed primarily or occasionally, and a vascular patch graft (Gore-Tex or Dacron) is required to provide an adequate lumen.

As the tumor thrombus extends cephalad toward the right atrium, other surgical techniques are utilized in order to decrease blood flow and achieve adequate exposure. These include a thoracoabdominal incision with complete liver mobilization and a 20-min compression of the porta hepatis (Pringle maneuver), venovenous bypass (*105*), and cardiopulmonary bypass with or without hypothermic circulatory arrest (*106*).

Despite the many advances in cardiovascular surgery allowing a surgical approach to RCC that has spread to the inferior vena cava and right atrium, resection is still associated with a perioperative mortality approaching 10%—depending on the local extent of the primary tumor and the level of vena-caval extension (*107,108*). The prognosis in tumors involving the vena cava depends upon the P stage of the tumor, the absence of nodal disease, and whether the thrombus is free-floating within the caval lumen or directly invades the caval wall (*109,110*). Hatcher described the important difference between IVC invasion and free-floating extension into the IVC for prognosis (*108*). In a series of 44 patients, those with free-floating extension of tumor into the IVC had a 69% 5-yr survival (median 9.9 yr). Those with direct IVC invasion had a 25% 5-yr survival (median 1.2 yr) which could be affected to 57% if the involved segment of IVC wall could be resected completely.

Inferior vena-cava extension—in the absence of regional nodal or distant metastatic disease and following complete surgical resection—is associated with adjusted 5- and 10-yr survival rates in the range of 50% (*107,108*). The prognosis did not seem to depend on the level of IVC involvement up to and including the right atrium. In patients with IVC involvement and other adverse prognostic indicators (extrafascial spread, lymph-node or distant metastases), 5-yr survival was 18% (median < 0.9 yr) (*108*). The importance of the presence or absence of metastatic disease at the time of diagnosis of RCC invading the venous system is provided by Libertino and colleagues in an update of a 24-yr experience with 100 patients with RCC extending into the renal vein, vena cava, or right atrium. Of the 72% of patients with no metastatic disease at the time of diagnosis and complete resection, median survival was 21.1 yr (5 yr, 64%, 10 yr, 57%). Patients resected and found to have metastatic disease had a median survival of 2.5 yr and a 5-yr survival of 20% with no survivors beyond 8 yr (*111*).

4.7. Resection of Local Tumor Recurrence

Local recurrence without evidence of metastatic disease is a distinctly rare event in RCC, and is usually a precursor for the development of metastatic disease. Most local recurrences are symptomatic upon presentation, yet surveillance CT scans can now detect local recurrence in up to 30% of patients undergoing radical nephrectomy and 5% of patients selected for partial nephrectomy prior to the onset of symptoms. Local recurrence within the renal fossa may occur through the following possible mechanisms: incomplete

resection of large primary tumor, incomplete or nondissection of regional lymph nodes or adrenal-bearing microscopic disease at the time of nephrectomy, in-transit metastatic disease in perinephric soft tissues not resected at the time of radical nephrectomy, or metastatic deposit in the perinephric soft tissues. Local recurrences are more common in patients with large, locally advanced primary tumors and metastatic regional nodes. Historically, local recurrences in the renal bed without metastatic disease were reported in approx 5% of patients undergoing radical nephrectomy (112–114). Because of the high likelihood that metastatic disease will occur following the detection of a local recurrence, it is reasonable to repeat an extensive metastatic evaluation in 3–6 mo before embarking upon a plan to resect.

Resection of local recurrence is justifiable following a completely negative extent of disease evaluation, and assuming the overall condition of the patient is good. Esrig and colleagues reported the results of operative management of 11 patients with isolated local recurrence during a 17-yr period at USC Medical Center. In this series, the average time to local recurrence was 31 mo, and all but two patients had abdominal symptoms identifying the recurrence. There were two perioperative deaths—one from disease progression and one from surgical complications related to concomitant small-bowel resection. Five patients in this small series survived longer than 35 mo with no evidence of recurrent disease (114).

In this series—as well as in our own experience—there is little question that surgery for local recurrence is a formidable procedure which often requires en bloc resection of adjacent muscle, bowel, spleen, pancreas, or liver, and patients should be aware that this approach falls into the realm of heroic surgery. Although there are some long-term survivors of such a surgical approach, it is unknown whether this represents a true therapeutic effect or if survival is still within the often protracted natural history of the disease. Radiation therapy for palliation of symptoms from a local recurrence or observation alone also remain reasonable options for treatment in selected patients, but this approach is not associated with complete remission.

4.8. Role of Surgical Resection of the Primary Tumor in Patients with Metastatic Disease

Despite extensive clinical investigation with systemic chemotherapy, hormonal therapy, and biologic response modifiers, alone or in combination, only 5–10% of patients with metastatic renal cell carcinoma will survive 5 yr. In addition, some patients with metastatic renal cancer may have prolonged periods of disease stabilization and occasional spontaneous regressions in some or all disease sites, clouding the impact of therapeutic interventions (7–9). Although there are case reports suggesting a therapeutic impact of nephrec-

tomy in the face of metastatic disease, enthusiasm must be tempered in the context of an unpredictable and often protracted natural history. In the face of metastatic renal cancer, surgery has been used to induce spontaneous remission, to debulk primary tumor prior to entry into clinical trials, and to resect limited metastatic disease.

Resection of the primary tumor is not indicated as a means of inducing spontaneous regression of metastatic disease. This rare but real phenomenon (<1%) has not been definitively linked to the operation itself, and has been observed in the absence of surgical intervention (115).

There is controversy regarding the role of nephrectomy prior to systemic therapy with biologic response modifiers. The theoretical advantages are reduction of a large, potentially immunosuppressive tumor burden, and prevention of complications related to the primary tumor during systemic therapy. On rare occasions, a highly symptomatic tumor is removed when conservative measures at palliation are unsuccessful. Surgical mortality has been reported for 2–11% for patients with large primary renal tumors and metastatic disease. The possibility that the patient may not recover sufficiently well after preparatory radical nephrectomy to receive systemic immunotherapy must be considered. In one large series of 195 patients with metastatic RCC, 121 patients (62%) were eligible for high-dose interleukin-2 following cytoreductive nephrectomy, leading to a response rate of 18%. In that series, 40% of the patients who underwent nephrectomy ultimately did not receive immunotherapy—a result of complications of nephrectomy or clinical deterioration from disease progression (116).

The approach followed at our center is to consider nephrectomy following immunotherapy in patients who have received a major response in metastatic sites. This approach spares unnecessary surgical morbidity and mortality in patients who are not destined to respond, allows for pathological assessments of the primary tumor after systemic therapy, and raises the possibility that surgery can consolidate to a complete surgical response those patients experiencing a major response to the systemic agent. (7–9,117,118).

4.9. Surgical Resection of Metastatic Disease

In 1939, Barney and Churchill reported the first case of a patient who underwent both nephrectomy and excision of a single pulmonary metastases, only to die 23 yr later of coronary-artery disease (119). During the last 60 yr, the surgical resection of limited metastatic disease (*metastectomy*) has been performed in some centers in the absence of effective systemic therapies. The selection criteria for this aggressive surgical management have not been well-defined. Several variables have been evaluated for their prognostic significance in an attempt to select patients destined to benefit from such operations. These vari-

ables include the site and number of metastatic deposits, completeness of resection, the performance status of the patient, and the disease-free interval from treatment of the primary tumor to the diagnosis of metastatic disease. In those patients who have solitary metastases and have undergone complete resection, 5-yr survival rates between 35–60% have been reported. Despite successful resection of metastatic disease and associated patient survival, there is no evidence from any clinical studies that the surgical intervention itself, as opposed to the well-documented and unpredictable natural history of RCC, lead to the observed outcome (*120–130*).

In a recent report from Memorial Sloan-Kettering Cancer Center, prognostic factors for survival were investigated in 278 patients who underwent surgical metastectomy. Favorable features for survival were a disease-free interval of greater than 12 mo vs less than 12 mo (55% vs 9% 5-yr overall survival), solitary vs multiple sites of metastases (54% vs 29% 5-yr overall survival), and age younger than 60 yr (49% vs 35% 5-yr survival). The survival period was longer when the solitary site of resection was the lung (54%, 5-yr survival) compared to the brain (18%, 5-yr survival). Twenty-nine percent of patients with completely resected multiple sites of metastases within a given site survived 5 yr, suggesting that complete resection of all metastatic deposits was more important than the number of metastatic deposits within a given site (*131*).

There is little doubt that careful patient selection, coupled with complete surgical resection of metastatic disease in a background of the long and often unpredictable natural history of RCC—can yield the results described here. The integration of metastectomy with systemic immunotherapies is an approach to metastatic RCC that warrants investigation. Pogrebniak and colleagues reported a study of 23 patients who underwent resection of pulmonary metastases from RCC—of which 15 had previously been treated with IL-2-based immunotherapy. Patients with resectable lesions had a longer survival (mean 49 mo, median not yet reached) than those patients with unresectable lesions (median 16 mo). In this study, survival was not dependent on the number of nodules removed (*132*). Patients with metastatic RCC should be offered surgery if it is likely that a curative metastectomy can be performed. Favorable subgroups include those with a solitary site of metastases and a DFT of greater than 1 yr.

5. Rational Follow-up Strategies After Surgical Treatment of RCC

No uniform guidelines have been established for the follow-up of patients who have undergone surgical treatment of RCC. Despite emerging evidence that some patients can benefit from aggressive surgical treatment of limited metastatic disease, various practices exist among urologic surgeons regarding

the management of recurrent disease and the timing of referrals of patients to medical and radiation oncologists. The intensity of follow-up and the tests ordered during follow-up also vary from center to center (*133–138*). In the absence of effective systemic therapy for metastatic disease, overly compulsive follow-up may diagnose asymptomatic metastatic disease earlier, but may not necessarily provide a therapeutic advantage. Excessive costs and patient anxiety may also occur unnecessarily during this follow-up.

Follow-up strategies were proposed from a nephrectomy series by Sandock and colleagues after a detailed analysis of the pattern of metastatic disease progression, sites of metastatic failure, and the efficacy of tests required to diagnose recurrence (*134*). These investigators reviewed 137 patients with node-negative, nonmetastatic RCC who underwent radical nephrectomy between 1979 and 1993 at the Case Western Reserve-affiliated hospitals. Recurrence correlated closely with the clinical stage of the tumor at the time of diagnosis. Using the older AJCC classification ($T1 < 2.5$ cm), no patients with T1 disease relapsed, and 15% of patients with T2 and 53% of patients with T3 tumors relapsed. Of the 19 patients in whom pulmonary metastases developed, 14 (74%) had cough, dyspnea, pleuritic chest pain, or hemoptysis. In all patients with pulmonary metastases, metastatic disease was diagnosed by an ordinary chest X-ray. Of the 13 patients in this series who developed intraabdominal metastatic disease, 12 (92%) complained of abdominal symptoms or had abnormal liver function studies that led to the diagnosis. All 10 patients who developed bone metastases complained of new bone pain that directed the diagnosis by plain film and bone scan. Only one patient had an isolated brain metastasis, which was associated with CNS symptoms and was confirmed by brain CT. Two patients developed cutaneous metastases that were detected during the physical examination. In this series, 85% of patients who experienced a recurrence of their disease did so during the first 3 yr after nephrectomy, with the remaining relapses occurring between 3.4 and 11.4 yr.

Levy and colleagues from the M. D. Anderson Cancer Center tracked the pattern of recurrence in 286 patients with P1-3N0 or Nx RCC, who had surgery between 1985 and 1995. Perhaps reflecting the stage migration that has occurred in RCC over the last 10 yr, 59 of 92 (62%) patients diagnosed with metastatic disease were asymptomatic, including 32 detected by routine chest X-ray and 12 detected by routine blood work. Isolated asymptomatic intraabdominal metastases were diagnosed by surveillance CT scan in only six patients (9%) (*139*). As in the Sandock study, as the P stage increased the likelihood of recurrence increased from 7% for P1 and 27% for P2, and 39% for P3, leading the authors to conclude that a stage-specific surveillance protocol would tailor the follow-up evaluation intensity with the relative risk of recurrence.

Based on these limited retrospective data, it is our practice to recommend six monthly visits for P1 (AJCC 1998, tumors <7cm) patients to include history and physical examination and annual chest X-ray for a total of 3 yr, and then yearly thereafter. For P2 and P3 tumors, the chest X-ray interval is increased to every 6 mo for 3 yr, and then yearly thereafter. The routine use of excessive abdominal CT scanning is discouraged, because the costs are high and the detection of asymptomatic local disease recurrence is very low. Specialized scans such as bone scans, CT of the brain, and abdominal CT are not routinely performed unless directed by specific patient signs or symptoms.

RCC is notorious for unusual, late, symptomatic, and metastatic recurrences in organs such as the pancreas, thyroid, skin, duodenum, and adrenal glands. These recurrences are often mistaken for new primary tumors, and aggressive surgical resection is undertaken (*131,140–142*). Experiences with late, isolated recurrences in RCC again highlight often long and unpredictable natural history of RCC.

The increasing use of partial nephrectomy requires specialized follow-up of the operated kidney and—when nephron-sparing is used—the normal contralateral kidney. Satellite or secondary smaller RCCs may be clinically undetected at the time of partial nephrectomy, and may in time develop into a second primary tumor or a local recurrence. The incidence of satellite tumors seems to increase with the size of the index tumor. In a clinical pathological study addressing this issue in nephrectomy specimens, the rate of satellite tumors was approx 10% in 257 kidney tumors less than 5 cm in diameter (*142*). Whether each satellite tumor—many of which were microscopic in nature—had the capacity to develop into a clinically significant tumor could not be addressed by the study. The search for evidence of satellite tumors depends to a large extent on the compulsiveness of the pathological prosector (*143*). Careful intraoperative inspection of the kidney with the use of intraoperative ultrasound allows the surgeon a final chance to detect satellite tumors, and the opportunity to resect them or proceed to radical nephrectomy.

A special category of patients predisposed to RCC is those with end-stage renal disease—a condition that effects more than 200,000 Americans. Acquired renal cystic disease, a condition defined as multiple cysts involving greater than 25% of the kidney—is a likely precursor lesion to RCC, and occurs in 80–95% of patients undergoing hemodialysis and 30–45% of patients undergoing peritoneal dialysis. Acquired cystic disease has also been reported in kidney-transplant recipients. This condition affects 45% of patients within the first 3 yr of dialysis, with a 5–30% likelihood that these patients will develop RCC. Approx 15% of patients will present with metastatic RCC. Patients who develop acquired cystic disease in transplant allografts may have an accelerated disease course because of immunosuppressive medications. For all patients undergoing dialysis, or transplant recipients, aggressive evaluation of microscopic or gross hematuria and

annual upper-tract imaging (ultrasound or CT) are recommended. With improved medical management of end-stage renal disease, this category of patients with RCC will be an increasingly challenging management problem (*144–149*).

For patients with VHL disease, the RCC component of the disease occurs in 50% of patients, and is often bilateral and multifocal. In patients with a known diagnosis of VHL, biannual upper-tract imaging (CT, USG) is recommended, and aggressive imaging of family members is also performed. When bilateral RCC is encountered, the treatment options of bilateral partial nephrectomies—often requiring reoperations—vs bilateral nephrectomies with dialysis confront the operating surgeon (*150,151*). Novick and Strem reviewed nine patients with VHL disease treated with partial nephrectomy. One patient died of metastatic disease at 43 mo, one patient was alive without evidence of disease at 74 mo, and the remaining seven patients required repeated operations. Only three patients were not on dialysis. Despite improvements in the techniques of partial nephrectomy, for patients with VHL, bilateral nephrectomies with dialysis may be a safer alternative (*152*).

6. Systemic Approaches to the Treatment of Metastatic RCC

Patients with metastatic RCC have a poor prognosis, with 5-yr survival proportion of less than 10% for patients presenting with Stage 4 disease (*7,153*). RCC is resistant to chemotherapy and hormonal therapy, and no agent or combination of agents currently achieves a response in more than 10% of patients (*154*). Two agents with minimal antitumor activity—vinblastine and floxuridine (FUDR)—are seemingly active in RCC, but response rates in a recent trial were just 6% (*9*). Multidrug resistance associated with the MDR-1 gene and its protein product P-glycoprotein are believed to be responsible for the resistance of RCC to chemotherapeutic drugs (*155*). Attempts to enhance the response proportion with agents known to reverse multidrug resistance—such as cyclosporin, nifedipine, and tamoxifen, unfortunately—were unsuccessful (*156*). Despite exciting and promising basic research, treatment of metastatic RCC patients with cytokines such as IL-2 and interferon alpha have led to responses in only 10–20% of patients treated (*9*). Complicating matters is the observation that pretreatment clinical factors such as hemoglobin, serum LDH, corrected calcium, nephrectomy, and Karnofsky performance status were independent risk factors predicting survival. Patients could be stratified by these risk factors, and patients with favorable or intermediate risk factors were more likely to benefit from investigative therapies. Attempts to couple biological response modifiers with chemotherapy (i.e., interferon alpha plus vinblastine) are associated with enhanced systemic toxicity, but not improved survival (*9,157*). Metastatic RCC is associated with a prolonged and variable clinical course, and in certain patients, spontaneous regression of metastatic deposits

has been documented (158). It is usually the practice of medical oncologists at our center to carefully observe an asymptomatic patient until clinical disease progression is documented. Metastatic RCC is a disease where the application of novel treatment strategies based on the improved understanding of the tumor biology may increase the therapeutic potential.

7. Conclusions

The widespread availability of abdominal ultrasound, MRI, and CT scanning has increased the diagnosis of incidental renal tumors, which now comprise the vast majority of the new cases diagnosed each year. With the detection of renal tumors at an earlier stage, partial nephrectomy and nephron-sparing surgery have evolved as effective alternatives to radical nephrectomy. The poor prognostic findings of involved regional lymph nodes or ipsilateral adrenal metastases have led to more selective operations on those sites in the face of incidental tumor detection. Technological advances have allowed for the development by dedicated surgical investigators of techniques of laparoscopic and laparoscopically assisted nephrectomy. Although not widely employed, further improvements in technology may widen the appeal of these approaches to selected renal tumors.

Advances in cardiovascular surgical techniques have made possible the resection of RCC with tumor thrombi involving the inferior vena cava—although this approach is still associated with significant perioperative mortality, depending on the degree of caval involvement. In highly selected cases, resection of limited metastatic disease is recommended, particularly if the disease-free interval is greater than 12 mo and there is only a single site of metastatic disease. Whether metastectomy is therapeutic or fits within the realm of the often long and unpredictable natural history of RCC is unknown. Strategies for follow-up are based primarily on the *P* stage of the operated tumor.

Small, incidental tumors have an excellent prognosis and require little in the way of post-operative imaging. As the *P* stage increases, the likelihood of developing metastatic disease increases, necessitating biannual chest X-ray in addition to history and physical exam. Symptom-directed bone scans and CT scans are effective in identifying most recurrences in patients with large, poorly-differentiated tumors. Patients requiring specialized follow-up programs include those treated by partial nephrectomy and those with end-stage renal disease, acquired cystic disease of the kidney, and VHL disease.

The well-documented resistance of RCC to systemic treatments by chemotherapy, hormonal therapy, and biologic response modifiers—alone or in combination—provides a great incentive for researchers to make advances in tumor biology, the understanding of etiologic factors, tumor prevention, and developmental therapeutics. Although patients have undergone experimental

therapies and experienced significant tumor reductions leading to partial and occasionally complete responses, most patients are resistant to these treatments. New and effective systemic treatments for RCC must be developed—hopefully through an enhanced understanding of the basic tumor biology of RCC.

References

1. Landis, S. H., Murray, T., Bolden, S., and Wingo, P. A. (1999) Cancer statistics. *Cancer J. Clin.* **49**, 8–31.
2. Katz, D. L., Zheng, T., Holford, T. R., and Flannery, J. (1994) Time trends in the incidence of renal carcinoma: analysis of Connecticut Tumor Registry data: 1935–1989. *Int. J. Cancer* **57**–63.
3. Kreiger, N., Marrett, L. D., Dodds, L., et al. (1993) Risk factors for renal cell carcinoma: results of a population-based case-control study. *Cancer Causes Control* **4**, 101–110.
4. Finkle, W. D., McLaughlin, J. K., Rasgon, S. A., et al. (1993) Increased risk of renal cell cancer among women using diuretics in the United States. *Cancer Causes Control* **4**, 555–558.
5. McCredie, M. and Stewart, J. H. (1992) Risk factors for kidney cancer in New South Wales—I. Cigarette smoking. *Eur. J. Cancer* **28**, 2050–2054.
6. Mellemgaard, A., Engholm, G., McLaughlin, J. K., and Olsen, J. H. (1994) Risk factors for renal cell carcinoma in Denmark. Role of weight, physical activity, and reproductive factors. *Int. J. Cancer* **56**, 66–71.
7. Motzer, R. J., Bander, N. H., and Nanus, D. M. (1996) Renal cell carcinoma. *N. Engl. J. Med.* **335**, 865–875.
8. Linehan, W. M., Shipley, W. U., and Parkinson, D. R. (1997) Cancer of the kidney and ureter, in *Cancer Principles and Practice of Oncology* (DeVita V. T., Hellman S., and Rosenberg, S. A., eds.), Lippincott-Raven, Philadelphia, PA, pp.1271–1300.
9. Motzer, R. J., Russo, P., Nanus, D. M., and Berg, W. J. (1997) Renal cell carcinoma. *Curr. Probl. Cancer* **21**, 189–232.
10. Smith, S. J., Bosniak, M. A., Megibow, A. J., et al. (1989) Renal cell carcinoma. Earlier discovery and increased detection. *Radiology* **170**, 699–703.
11. Levine, E., Huntrakoon, M., and Wetzel, C. H. (1989) Small renal neoplasms. Clinical, pathologic, and imaging features. *Am. J. Roentgenol.* **153**, 69–73.
12. Konnack, J. W. and Grossman, H. B. (1990) Renal cell carcinoma as an incidental finding. *J. Urol.* **134**, 1094–1096.
13. Porena, M., Vespasiani, G., Rosi, P., et al. (1992) Incidentally detected renal cell carcinoma: role of ultrasonography. *J. Clin. Ultrasound* **20**, 395–400.
14. Rabbani, F., Grimaldi, G., and Russo, P. (1998) Multiple primary malignancies in renal cell carcinoma. *J. Urol.* **160**, 1255–1259.
15. Tsukamoto, T., Kumamoto, Y., Yamazaki, K., et al. (1991) Clinical analysis of incidentally found renal carcinomas. *Eur. Urol.* **19**, 109–113.
16. Aslaksen, A. and Gothlin, J. H. (1991) Imaging of solid renal masses. *Curr. Opin. Radiat.* **3**, 654662.

17. Aso, Y. and Homma, Y. (1992) A survey on incidental renal cell carcinoma in Japan. *J. Urol.* **147**, 340–343.
18. Sasaki, Y., Homma, Y., Hosaka, Y., et al. (1994) Clinical and flow cytometric analysis of renal cell carcinomas with reference to incidental or non-incidental detection. *Jpn. J. Clin. Oncol.* **24**, 32–36.
19. Kessler, O., Mukamel, E., Hadar, H., et al. (1994) The impact of the improved diagnosis of renal cell carcinoma on the course of the disease. *J. Surg. Oncol.* **57**, 201–204.
20. Novick, A. C. (1993) Renal-sparing surgery for renal cell carcinoma. *Urol. Clin. N. Am.* **20**, 277–282.
21. Silver, D. A., Morash, C., Brenner, P., Campbell, S., and Russo, P. (1997) Pathological findings at the time of nephrectomy for renal mass. *Ann. Surg. Oncol.* **4**, 570–574.
22. Campbell, S. C., Novick, A. C., Herts, B., Fischler, D. F., Meyer, J., Levin, H. S., and Chen, R. N. (1997) Prospective evaluation of fine needle aspiration of small, solid, renal masses: accuracy and morbidity. *Urology* **50**, 25–29.
23. Nicfero, J. and Coughlin, B. F. (1993) Diagnosis of renal cell carcinoma: value of fine needle aspiration cytology in patients with metastases or contraindications to nephrectomy. *Am. J. Roentgenol.* **161**, 1303–1305.
24. Linehan, W. M., Lerman, M. I., and Zbar, B. (1995) Identification of the von Hippel-Lindau (VHL) gene. Its role in renal cancer. *JAMA* **273**, 564–570.
25. Gnarr, J. R., Glenn, G. M., Latif, F., Anglard, P., Lerman, M. I., Zbar, B., and Linehan, W. M. (1993) Molecular genetic studies of sporadic and familial renal cell carcinoma. *Urol. Clin. N. Am.* **20**, 207–216.
26. Lubensky, I. A., Gnarr, J. R., Bertheau, P., Walther, M. M., Linehan, W. M., and Zhuang, Z. (1996) Allelic deletions of the VHL gene detected in multiple microscopic clear cell renal lesions in von Hippel-Lindau disease patients. *Am. J. Pathol.* **149**, 2089–2094.
27. Gnarr J. R., Tory K., Weng Y., Schmidt L., Wei M. H., Li H., Latif, F., et al. (1994) Mutations of the VHL tumour suppressor gene in renal carcinoma. *Nat. Genet.* **7**, 85–90.
28. Anglard, P., Tory, K., Brauch, H., Weiss, G. H., Latif, F., Merino, M., Lerman, M., et al. (1991) Molecular analysis of genetic changes in the origin and development of renal cell carcinoma. *Cancer Res.* **51**, 1071–1077.
29. Franklin, J. R., Figlin, R., and Beldegrun, A. (1996) Renal cell carcinoma: basic biology and clinical behavior. *Semin. Urol. Oncol.* **14**, 208–215.
30. Zbar, B., Tory, K., Merino, M., Schmidt, L., Glenn, G., Choyke, P., Walther, M. M., et al. (1994) Hereditary papillary renal cell carcinoma. *J. Urol.* **151**, 561–566.
31. Zbar, B., Glenn, G., Lubensky, I. A., Choyke, P., Walther, M. M., Magnusson, G., Bergerheim, U. S. R., et al. (1995) Hereditary papillary renal cell carcinoma: clinical studies in 10 families. *J. Urol.* **153**, 907–912.
32. Weirich, G., Glenn, G., Junker, K., Merino, M., Storkel, S., Lubensky, I., Choyke, P., Pack, S., Amin, M., Walther, M. M., Linehan, W. M., and Zbar, B. (1998) Familial renal oncocytoma: clinicopathological study of 5 families. *J. Urol.* **160**, 335–340.

33. van den Berg, E., Dijkhuizen, T., Storkel, S., Brutel de la Riviere, G., Dam, A., Mensink, A., Oosterhuis, J. W., et al. (1995) Chromosomal changes in renal oncocytomas. *Cancer Genet. Cytogenet.* **79**, 164–168.
34. Grimaldi, G., Reuter, V. E., and Russo, P. (1998) Bilateral non-familial renal cell carcinoma. *Ann. Surg. Oncol.* **5**, 548–552.
35. Skinner, D. G., Colvin, R. B., Vermillion, C. D., et al. (1971) Diagnosis and management of renal cell carcinoma: A clinical and pathological study of 309 cases. *Cancer* **28**, 1165–1177.
36. Mevorach, R. A., Segal, A. J., Tersegno, M. E., et al. (1992) Incidental diagnosis and review of natural history. *Urology* **39**, 519–522.
37. Newhouse, J. H. (1993) The radiologic evaluation of the patient with renal cancer. *Urol. Clin. N. Am.* **20**, 231–246.
38. Tammela, T. L., Leinonen, A. S., and Kontturi, M. J. (1991) Comparison of excretory urography, angiography, ultrasound and computed tomography for T category staging of renal cell carcinoma. *Scand. J. Urol. Nephrol.* **25**, 283–286.
39. Lim, D. J. and Carter, M. F. (1993) Computerized tomography in the preoperative staging for pulmonary metastases in patients with renal cell carcinoma. *J. Urol.* **150**, 1112.
40. Myneni, L., Kricak, H., and Carroll, P. R. (1991) Magnetic resonance imaging of renal carcinoma with extension into the vena cava: staging accuracy and recent advances. *Br. J. Urol.* **68**, 571–578.
41. Robson, C. J., Churchill, B. M., and Andersen, W. (1969) The results of radical nephrectomy for renal cell carcinoma. *J. Urol.* **101**, 297–301.
42. Fleming, I. D., Cooper, J. S., Hanson, D., et al. (1998) *AJCC Cancer Staging Manual*. 5th ed. Lippincott-Raven, Philadelphia, PA, pp. 215–218.
43. Perez-Ordenez, B., Hamed, G., Campbell, S., Erlandson, R. A., Russo, P., Gaudin, P. B., and Reuter, V. E. (1997) Renal oncocytoma: a clinicopathologic study of 70 cases. *Am. J. Surg. Pathol.* **21**, 871–883.
44. Bryant, D. A., Sheinfeld, A. G., Russo, P., Gaudin, P. B., and Reuter V. E. (1998) Conventional renal cell carcinoma: A clinicopathologic study of 183 cases from 1991 to 1994. *Mod. Pathol.* **11**, 77A.
45. Reuter, V. E., Sheinfeld, A. G., Hamed, G., Campbell, S., Gaudin, P., and Russo, P. (2000) Papillary renal cell carcinoma: A clinicopathologic study of 83 tumors. *Am. J. Surg. Pathol.* in press.
46. Thrasher, J. B. and Paulson, D. E. (1993) Prognostic factors in renal cancer. *Urol. Clin. North. Am.* **20**, 247–262.
47. Mortensen, H. (1948) Transthoracic nephrectomy. *J. Urol.* **60**, 855–858.
48. Robson, C. J. (1963) Radical nephrectomy for renal cell carcinoma. *J. Urol.* **89**, 37–41.
49. Robson, C. J., Churchill, B. M., and Andersen, W. (1969) The results of radical nephrectomy for renal cell carcinoma. *J. Urol.* **101**, 297–301.
50. Patel, N. P. and Lavengood, R. W. (1978) Renal cell carcinoma: natural history and results of treatment. *J. Urol.* **119**, 722–726.
51. Sene, A. P., Hunt, L., McMahon, R. F., et al. (1992) Renal carcinoma in patients undergoing nephrectomy: analysis of survival and prognostic factors. *Br. J. Urol.* **70**, 125–134.

52. Sagalowsky, A. I., Kadesky, K. T., Ewalt, D. M., and Kennedy, T. J. (1994) Factors influencing adrenal metastases in renal cell carcinoma. *J. Urol.* **151**, 1181–1184.
53. Herrlinger, J. A., Schrott, K. M., Schott, G., et al: What are the benefits of extended dissection of the regional lymph nodes in the therapy of renal cell carcinoma? *J. Urol.* **146**, 1224–1227.
54. Ditonno, P., Traficante, A., Battaglia, M., et al. (1992) Role of lymphadenectomy in renal cell carcinoma. *Prog. Clin. Biol. Res.* **378**, 169–174.
55. Licht, M. R. and Novick, A. C. (1993) Nephron-sparing surgery for renal cell carcinoma. *J. Urol.* **145**, 1–7.
56. Steinbach, F., Stockle, M., Muller, S. C., et al. (1992) Conservative surgery of renal cell tumors in 140 patients: 21 years of experience. *J. Urol.* **148**, 24–29.
57. Thrasher, J. B., Robertson, J. E., and Paulson, D. F. (1994) Expanding indications for conservative renal surgery in renal cell carcinoma. *Urology* **43**, 160–168.
58. Butler, B. P., Novick, A. C., Miller, D. P., et al. (1995) Management of small unilateral renal cell carcinomas: radical versus nephron-sparing surgery. *Urology* **45**, 34–40.
59. Herr, H. W. (1994) Partial nephrectomy for renal cell carcinoma with a normal opposite kidney. *Cancer* **73**, 160–162.
60. Herr, H. W. (1999) Partial nephrectomy for unilateral renal carcinoma and a normal contralateral kidney: 10 year follow-up. *J. Urol.* **161**, 33–35.
61. Studer, U. E., Scherz, S., Scheidegger, J., Kraft, R., Sonntag, R., Ackermann, D., and Zingg, E. J. (1990) Enlargement of regional lymph nodes in renal cell carcinoma is often not due to metastases. *J. Urol.* **144**, 243–245.
62. Guilian, L., Giberti, C. Martorana, G., and Rovida, S. (1990) Radical extensive surgery for renal cell carcinoma: Long-term results and prognostic factors. *J. Urol.* **143**, 468–473.
63. Herrlinger, A., Schrott, K. M., Schott, G., and Siegel, A. (1984) Results of 382 transabdominal radical nephrectomies for renal cell carcinoma with partial and complete en- bloc lymph node dissection. *World J. Urol.* **2**, 113–120.
64. Phillips, P. E. and Messing, E. M. (1993) Role of lymphadenectomy in the treatment of renal cell carcinoma. *Urology* **41**, 9–15.
65. Golimbu, M., Joshi, P., Sperber, A., et al. (1986) Renal cell carcinoma. Survival and prognostic factors. *Urology* **27**, 291–301.
66. Wood, D. P. (1990) Role of lymphadenectomy in renal cell carcinoma. *Urol. Clin. N. Am.* **18**, 421–426.
67. Kim, S. H., Brennan, M. F., Russo, P., Burt, M. E., and Coit, D. G. (1998) The role of surgery in the treatment of clinically isolated adrenal metastases. *Cancer* **82**, 389–394.
68. Gill, I. S., McClennan, B. L., Kerbl, K., et al. (1994) Adrenal involvement from renal cell carcinoma: Predictive value of computerized tomography. *J. Urol.* **152**, 1082–1085.
69. Gill, I. S., Kerbl, K., and Clayman, R. V. (1993) Laparoscopic surgery in urology: Current applications. *Am. J. Roentgenol.* **160**, 1167–1170.
70. Kerbl, K., Clayman, R. V., McDougall, E. M., and Kavoussi, L. R. (1994) Laparoscopic nephrectomy: the Washington University experience. *Br. J. Urol.* **73**, 231–236.

71. McDougall, E. M., Clayman, R. V., and Elashry, O. (1995) Laparoscopic nephroureterectomy for upper tract transitional cell carcinoma: the Washington University Experience. *J. Urol.* **154**, 975–980.
72. Kavoussi, L. R., Kerbl, K., Capelouto, C. C., McDougall, E. M., and Clayman, R. V. (1993) Laparoscopic nephrectomy for renal neoplasms. *Urology* **42**, 603–608.
73. Gill, I. S., Kavoussi, L. R., Clayman, R. V., et al. (1995) Complications of laparoscopic nephrectomy in 185 patients: A multi-institutional review. *J. Urol.* **154**, 479–483.
74. Winfield, H. N., Donovan, J. F., Lund, G. O., Kreder, K. J., Stanley, K. E., Brown, B. P., Loening, S. A., and Clayman, R. V. (1995) Laparoscopic partial nephrectomy: Initial experience and comparison to the open surgical approach. *J. Urol.* **153**, 1409–1414.
75. Kerbl, K. and Clayman, R. V. (1994) Advances in laparoscopic renal and ureteral surgery. *Eur. Urol.* **25**, 1–6.
76. Hayakawa, K., Nishiyama, T., Ohashi, M., Ishikawa, H., and Hata, M. (1997) A trial of laparoscopic assisted radical nephrectomy. *Jpn. J. Urol.* **88**, 801–806.
77. Nishiyama, T. and Terunuma, M. (1995) Laparoscopy-assisted radical nephrectomy in combination with minilaparotomy: report of initial 7 cases. *Int. J. Urol.* **2**, 124–127.
78. Santiago, L., Yamaguchi, R., Kaswick, J., and Bellman, G. C. (1998) Laparoscopic management of indeterminate renal cysts. *Urology* **52**, 379–383.
79. Novick, A. C., Stroom, S., Montie, J. E., Pontes, J. E., Siegel, S., Montague, D., and Goormastic, M. (1989) Conservative surgery for renal cell carcinoma: A single center experience with 100 patients. *J. Urol.* **141**, 835–839.
80. Provet, J., Tessler, A., Brown, J., Golimbu, M., Bosniak, M., and Morales, P. (1991) Partial nephrectomy for renal cell carcinoma: indications, results and implications. *J. Urol.* **145**, 472–476.
81. Licht, M. R., Novick, A. C., and Goormastic, M. (1994) Nephron sparing surgery in incidental versus suspected renal cell carcinoma. *J. Urol.* **152**, 39–42.
82. Smith, S. J., Bosniak, M. A., Megibow, A. J., et al. (1989) Renal cell carcinoma. Earlier discovery and increased detection. *Radiology* **170**, 699–703.
83. Levine, E., Huntrakoon, M., and Wetzel, C. H. (1989) Small renal neoplasms. Clinical, pathologic, and imaging features. *Am. J. Roentgenol.* **153**, 69–73.
84. Rodriguez, R., Fishman, E. K., and Marshall, F. F. (1995) Differential diagnosis and evaluation of the incidentally discovered renal mass. *Semin. Urol. Oncol.* **13**, 246–253.
85. Sasaki, Y., Homma, Y., Hosaka, Y., et al. (1994) Clinical and flow cytometric analysis of renal cell carcinomas with reference to incidental or non-incidental detection. *Jpn. J. Clin. Oncol.* **24**, 32–36.
86. Licht, M. R. and Novick, A. C. (1993) Nephron sparing surgery for renal cell carcinoma. *J. Urol.* **149**, 1–7.
87. Lerner, S. E., Hawkins, C. A., Blute, M. L., Grabner, A., Wollan, P. C., Eickholt, J. T., and Zincke, H. (1996) Disease outcome in patients with low stage renal cell carcinoma treated with nephron sparing or radical surgery. *J. Urol.* **155**, 1868–1873.

88. Morgan, W. R. and Zincke, H. (1990) Progression and survival after renal-conserving surgery for renal cell carcinoma: experience in 104 patients and extended follow-up. *J. Urol.* **144**, 852–857.
89. Steinbeck, F., Stackle, M., Muller, S. C., et al. (1992) Conservative surgery of renal tumors in 140 patients: 21 years of experience. *J. Urol.* **148**, 24–29.
90. Thrasher, J. B., Robertson, J. E., and Paulson, D. F. (1994) Expanding indications for conservative renal surgery in renal cell carcinoma. *Urology* **43**, 160–168.
91. Marberger, M., Pugh, R. C. B., Auvert, J., et al. (1981) Conservative surgery of renal cell carcinoma: the EIRSS experience. *Br. J. Urol.* **53**, 528–532.
92. Whang, M., O'Toole, K., Bixon, R., Brunetti, J., Ikeguchi, E., Olsson, C. A., Sawczuk, I. S., and Benson, M. C. (1995) The incidence of multi focal renal cell carcinoma in patients who are candidates for partial nephrectomy. *J. Urol.* **154**, 968–971.
93. Nissenkorn, I. and Bernheim, J. (1995) Multicentricity in renal cell carcinoma. *J. Urol.* **153**, 620–622.
94. Cheng, W. S., Farrow, G. M., and Zincke, H. (1991) The incidence of multicentricity in renal cell carcinoma. *J. Urol.* **146**, 1221–1223.
95. Kletscher, B. A., Qian, J., Bostwick, D. G., Andrews, P. E., and Zincke, H. (1995) Prospective analysis of multifocality in renal cell carcinoma: influence of histological pattern, grade, number, size, volume and DNA ploidy. *J. Urol.* **153**, 904–906.
96. Gilbert, B. R., Russo, P., Zirinsky, K., Fair, W. R., and Vaughan, E. D. (1988) Intraoperative sonography. Application in renal cell carcinoma. *J. Urol.* **139**, 582–584.
97. Assimos, D. G., Boyce, H., Woodruff, R. D., Harrison, L. H., McCullough, D. L., and Kroovand, R. L. (1991) Intraoperative renal ultrasonography: a useful adjunct to partial nephrectomy. *J. Urol.* **146**, 1218–1220.
98. Gohji, K., Hara, I., Gotoh, A., Eto, H., Miyake, H., Sugiyama, T., Okada, H., Arakaawa, S., and Kamidon, S. (1998) Multifocal renal cell carcinoma in Japanese patients with tumors with maximal diameters of 50 mm or less. *J. Urol.* **159**, 1144–1147.
99. Campbell, S. C., Novick, A. C., Streem, S. B., Klein, E., and Licht, M. (1994) Complications of nephron sparing surgery for renal tumors. *J. Urol.* **151**, 1177–1180.
100. Novick, A. C. and Schreiber, M. I. (1995) The effect of angiotensin converting enzyme inhibition on nephropathy in patients with a remnant kidney. *Urol.* **46**, 785–789.
101. Novick, A. C., Gephardt, G., Guiz, B., et al. (1991) Long term follow up after partial removal of solitary kidney. *N. Engl. J. Med.* **325**, 1058–1062.
102. Kallman, D. A., King, B. F., Hattery, R. R., et al. (1992) Renal vein and inferior vena cava tumor thrombus in renal cell carcinoma: CT, US, MRI and venacavography. *J. Comp. Assist. Tomogr.* **16**, 240–247.
103. Goldfarb, D. A., Novick, A. C., Lorig, R., Bretan, P. N., Montie, J. E., Pontes, J. E., Streem, S. B., and Siegel, S. W. (1990) Magnetic resonance imaging for assessment of vena cava thrombi: A comparative study with venacavography and computerized tomography scanning. *J. Urol.* **144**, 1100–1104.

104. Blute, M. L., Zincke, H., and Utz, D. C. (1994) Surgical management of renal cell carcinoma with intracaval involvement. *AUA Update Series* **13**, 21–27.
105. Burt, M. (1991) Inferior vena caval involvement by renal cell carcinoma: use of venovenous bypass as adjunct during resection. *Urol. Clin. N. Am.* **18**, 437–444.
106. Klein, E. A., Kaye, M. C., and Novick, A. C. (1991) Management of renal cell carcinoma with vena caval thrombi via cardiopulmonary bypass and deep hypothermic circulatory arrest. *Urol. Clin. N. Am.* **18**, 445–447.
107. Libertino, J. A., Zinman, L., and Watkins, E. . (1987) Long-term results of resection of renal cell carcinoma with extension into the inferior vena cava. *J. Urol.* **137**, 21–24.
108. Hatcher, B. A., Anderson, E. E., Paulson, D. F., et al. (1991) Surgical management and prognosis of renal cell carcinoma invading the vena cava. *J. Urol.* **145**, 20–23.
109. Langenburg, S. E., Blackbourne, L. H., Sperling, J. W., et al. (1994) Management of renal tumors involving the inferior vena cava. *J. Vasc. Surg.* **20**, 385–388.
110. Montie, J. E., el Ammar, R., Pontes, J. E., et al. (1991) Renal cell carcinoma with inferior vena cava tumor thrombi. *Surg. Gyn. Obst.* **173**, 107–115.
111. Swierewski, D. J., Swierewski, M. J., and Libertino, J. A. (1994) Radical nephrectomy in patients with renal cell carcinoma with venous, venal caval, and atrial extension. *Am. J. Surg.* **168**, 205–209.
112. Persenty, R. A., Richard, F., Pradel, J., et al. (1984) Local recurrence after nephrectomy for primary renal cancer. CT recognition. *J. Urol.* **13**, 246–249.
113. Campbell, S. C. and Novick, A. C. (1994) Management of local recurrence following radical nephrectomy or partial nephrectomy. *Urol. Clin. N. Am.* **21**, 593–599.
114. Esrig, D., Ahlering, T. E., Liskovsky, G., et al. (1992) Experience with fossa recurrence of renal cell carcinoma. *J. Urol.* **147**, 1491–1494.
115. McCaffrey J. A., Motzer R. J: What is the role of nephrectomy in patients with metastatic renal cell carcinoma. *Semin. Oncol.* **23 (Suppl.)**, 19,20.
116. Walther, M. M., Yang, J. C., Pass, H. I., Linehan, W. M., and Rosenberg, S. A. (1997) Cytoablative surgery before high dose interleukin-2 based therapy in patients with metastatic renal cell carcinoma. *J. Urol.* **158**, 1675–1678.
117. Rackley, R., Novick, A., Klein, E., Bukowski, R., McLain, D., and Goldfarb, D. (1994) The impact of adjuvant nephrectomy on multimodality treatment of metastatic renal cell carcinoma. *J. Urol.* **152**, 1399–1403.
118. Sella, A., Swanson, D. A., Ro, J. Y., Putnam, J. B., Amato, R. J., Markowitz, A. B., and Logothetis, C. J. (1993) Surgery following response to interferon-alpha-based therapy for residual renal cell carcinoma. *J. Urol.* **149**, 19–21.
119. Barney, J. D. and Churchill, E. J. (1939) Adenocarcinoma of the kidney with metastasis to the lung: cured by nephrectomy and lobectomy. *J. Urol.* **42**, 269–276.
120. deKernion, J. B., Ramming, K. P., and Smith, R. B. (1978) The natural history of metastatic renal cell carcinoma: a computer analysis. *J. Urol.* **120**, 148–152.
121. Giuliani, L., Giberti, C., Martorana, G., et al. (1990) Radical extensive surgery for renal cell carcinoma: long-term results and prognostic factors. *J. Urol.* **143**, 468–473.

122. Golimbu, M., Joshi, P., Sperber, A., et al. (1986) Renal cell carcinoma: survival and prognostic factors. *Urology* **27**, 291–301.
123. Maldazys, J. D. and deKernion, J. B. (1986) Prognostic factors in metastatic renal carcinoma. *J. Urol.* **136**, 376–379.
124. McNichols, D. W., Segura, J. W., and DeWeerd, J. H. (1981) Renal cell carcinoma: long-term survival and late recurrence. *J. Urol.* **126**, 17–23.
125. Neves, R. J., Zincke, H., and Taylor, W. F. (1988) Metastatic renal cell cancer and radical nephrectomy: identification of prognostic factors and patient survival. *J. Urol.* **139**, 173–1176.
126. Golimbu, M., Al-Askari, S., Tessler, A., et al. (1986) Aggressive treatment of metastatic renal cancer. *J. Urol.* **136**, 805–807.
127. Kierney, P. C., van Heerden, J. A., Segura, J. W., et al. (1994) Surgeon's role in the management of solitary renal cell carcinoma metastases occurring subsequent to initial curative nephrectomy: an institutional review. *Ann. Surg. Oncol.* **1**, 345–352.
128. Kjaer, M. (1987) The treatment and prognosis of patients with renal adenocarcinoma with solitary metastasis. 10 year survival results. *Int. J. Radiat. Oncol. Biol. Phys.* **13**, 619–621.
129. Klugo, R. C., Detmers, M., Stiles, R. E., et al. (1977) Aggressive versus conservative management of stage IV renal cell carcinoma. *J. Urol.* **118**, 244–246.
130. O'Dea, M. J., Zincke, H., Utz, D. C., et al. (1978) The treatment of renal cell carcinoma with solitary metastasis. *J. Urol.* **120**, 540–542.
131. Kavolius, J. P., Mastorakos, D. P., Pavolvich, C., Russo, P., Burt, M. E., and Brady, M. S. (1998) Resection of metastatic renal cell carcinoma. *J. Clin. Oncol.* **16**, 2261–2266.
132. Pogrebniak, H. W., Haas, G., Linehan, W. M., et al. (1992) Renal cell carcinoma: resection of solitary and multiple metastases. *Ann. Thorac. Surg.* **54**, 33–38.
133. Montie, J. E. (1994) Follow-up after partial or total nephrectomy for renal cell carcinoma. *Urol. Clin. N. Am.* **21**, 589–592.
134. Sandock, D. S., Seftel, A. D., Resnick, M. I. (1995) A new protocol for the follow-up of renal cell carcinoma based on pathological stage. *J. Urol.* **154**, 28–31.
135. Bottiger, L. E. (1969) Prognosis in renal carcinoma. *Cancer* **26**, 780–787.
136. Heney, N. M. and Nocks, B. N. (1982) The influence of perinephric fat involvement on survival in patients with renal cell carcinoma extending into the inferior vena cava. *J. Urol.* **128**, 18–20.
137. Lieber, M. M., Tomera, F. M., Taylor, W. F., et al. (1981) Renal adenocarcinoma in young adults: survival and variables affecting prognosis. *J. Urol.* **125**, 164–168.
138. Selli, C., Hinshaw, W. M., Woodard, B. H., et al. (1983) Stratification of risk factors in renal cell carcinoma. *Cancer* **52**, 899–903.
139. Levy, D. A., Slaton, J. W., Swanson, D. A., and Dinney, C. P. (1998) Stage specific guidelines for surveillance after radical nephrectomy for local renal cell carcinoma. *J. Urol.* **159**, 1163–1167.
140. McNichols, D. W., Segura, J. W., DeWeerd, J. H. (1981) Renal cell carcinoma: long-term survival and late recurrence. *J. Urol.* **126**, 17–23.

141. Takatera, H., Maeda, O., Oka, T., et al. (1986) Solitary late recurrence of renal cell carcinoma. *J. Urol.* **136**, 799, 800.
142. Jacqmin, D., Saussine, C., Roca, D., et al. (1992) Multiple tumors in the same kidney: incidence and therapeutic implications. *Eur. Urol.* **21**, 32–34.
143. Lee, S. E. and Kim, H. H. (1994) Validity of kidney-preserving surgery for localized renal cell carcinoma. *Eur. Urol.* **25**, 204–208.
144. Dunnill, M. S., Millard, P. R., and Oliver, D. (1977) Acquired cystic disease of the kidneys: a hazard of long-term intermittent maintenance hemodialysis. *J. Clin. Pathol.* **30**, 868–877.
145. Katz, A., Sambolos, K., and Oreopoulos, D. G. (1987) Adult cystic disease of the kidney in association with chronic ambulatory peritoneal dialysis. *Am. J. Kidney Dis.* **9**, 426–429.
146. Gehrig, J. J., Gottheiner, J. I., and Swenson, R. S. (1985) Acquired cystic disease of the end stage kidney. *Am. J. Med.* **79**, 609–620.
147. Matson, M. A. and Cohen, E. P. (1990) Acquired cystic kidney disease: occurrence, prevalence, renal cancers. *Medicine* **69**, 217–226.
148. Sasagawa, I., Nakada, T., Kubota, Y., et al. (1994) Renal cell carcinoma in dialysis patients. *Urologia Internationalis* **53**, 79–81.
149. Williams, J. C., Merguerian, P. A., Schned, A. R., Morrison, P. M. (1995) Acquired renal cystic disease and renal cell carcinoma in an allograft kidney. *J. Urol.* **153**, 395, 396.
150. Maher, E. R., Yates, J. W., Harries, R., et al. (1990) Clinical features and natural history of von Hippel-Lindau disease. *Q. J. Med.* **77**, 1151–1163.
151. Maher, E. R., Bentley, E., Payne, S. J., et al. (1992) Presymptomatic diagnosis of von Hippel-Lindau disease with flanking DNA markers. *J. Med. Genet.* **29**, 902–905.
152. Novick, A. C. and Streem, S. B. (1992) long-term follow up after nephron-sparing surgery for renal cell carcinoma in von Hippel-Lindau disease. *J. Urol.* **147**, 1488–1490.
153. Vogelzang, N. J., Stadler, W. M. (1998) Kidney cancer. *Lancet* **352**, 1691–1696.
154. Figlin, R. A. (1999) Renal cell carcinoma: management of advanced disease. *J. Urol.* **151**, 381–387.
155. Rodenburg, C. J., Nooter, K., and Herweijer, H. (1991) Phase 2 study of vinblastine and cyclosporin-A to circumvent multidrug resistance in renal cell cancer. *Ann. Oncol.* **2**, 305–306.
156. Motzer, R. J., Lyn, P., Fischer, P., et al. (1995) Phase I/II trial of dexverapamil plus vinblastine for patients with advanced renal cell carcinoma. *J. Clin. Oncol.* **13**, 1958–1965.
157. Minasian, L. M., Motzer, R. J., Gluck, L., et al. (1993) Interferon alfa-2a in advanced renal cell carcinoma: treatment results and survival in 159 patients with long-term follow-up. *J. Clin. Oncol.* **11**, 1368–1375.
158. Vogelzang, N. J., Priest, E. R., and Borden, L. (1992) Spontaneous regression of histologically proved pulmonary metastases from renal cell carcinoma: a case with 5-year follow up. *J. Urol.* **148**, 1247–1248.

Pathology of Kidney Tumors

David J. Grignon

1. Introduction

1.1. Classification

The classification of epithelial tumors of the kidney has undergone considerable change in the last two decades. Systems based on cytoplasmic characteristics and cytogenetic analysis have expanded our understanding of this group of tumors. These new, nontraditional systems have led to the development of a more clinically significant pathological classification (*1,2*). Although many questions remain unanswered and debate continues concerning the validity of these proposals, research studies on epithelial neoplasms of the kidney must take these advances into consideration. Scientific studies of any type should incorporate information regarding the type of tumor(s) included in the study group. This chapter briefly reviews the accepted subtypes of renal epithelial neoplasms, with a focus on the morphological features that distinguish them.

1.2. The “Mainz” System

In 1986, Thoenes et al. (*3*) proposed a system based primarily on the cytoplasmic characteristics of tumor cells. This allowed for a greater subdivision of renal epithelial tumors, into what the authors believed would be clinically significant categories. This approach has been adopted in whole or in part by most urologic pathologists, and, combined with cytogenetic information forms the basis for the recent consensus classification (*4,5*). The basic categories consist of clear-cell, chromophobe-cell, chromophil-cell, mixed tumors, collecting-duct carcinoma, and oncocytoma.

1.3. Cytogenetic Classification

Based on his work as well as that of other investigators, Kovacs proposed a classification of renal epithelial tumors, taking into consideration consistent patterns of cytogenetic abnormalities (6). There is remarkable correlation of the cytogenetic abnormalities with the histologic subtypes described by Thoenes et al. (3).

1.3.1. Nonpapillary Carcinoma (3p–)

This group includes clear-cell renal-cell carcinoma (RCC), and granular (eosinophil subtype of clear cell of Thoenes et al. [3]). renal cell carcinomas not included in other groups. Clear-cell RCC with a pure or partial papillary architecture is also classified here. Up to 98% of cases in this group have the 3p- abnormality (von Hippel Lindau gene mutation) (7). Other frequent abnormalities include 5q+ (70%) and 14q- (41%). The 3p- abnormality is viewed as the primary cytogenetic event in the development of RCC, and does not correlate with clinical aggressiveness; more “malignant” tumors have an accumulation of multiple additional cytogenetic changes.

1.3.2. Papillary Renal Tumors (+7, +17)

Papillary tumors, as defined cytogenetically, are limited to papillary or tubulopapillary neoplasms with columnar or cuboidal eosinophilic or basophilic cells (chromophil tumors of Thoenes, et al.) (3). The small, tubulopapillary cortical lesions that many accept as “adenoma” have trisomy 7 and 17 in up to 100% of cases, but have no other cytogenetic abnormalities. Papillary carcinomas also have the +7 (75%) and +17 (80%) changes, as well as a variety of other abnormalities, including +3q, +8, +12, +16, and +20. Kovacs has argued that cytogenetic analysis can differentiate benign from malignant tumors in this subset (6).

1.3.3. Chromophobe RCC (–1, –2, –6, –10, –13, –17, and –21)

Chromophobe-cell RCC have been evaluated cytogenetically with a consistent but unusual pattern of abnormality with multiple monosomies. Over 80% of cases studied have shown loss of all seven chromosomes indicated here (8).

1.3.4. Oncocytoma

These tumors have shown a lack of consistent cytogenetic abnormalities. The most common are translocations involving the breakpoint region 11q13 and –Y and –1 (2).

1.4. Consensus Classification

Consensus meetings held in Heidelberg, Germany, and Rochester resulted in a working classification being developed and recommended for use (4,5). This classification is a natural extension of the work of Thoenes et al. (3,6) and

Kovacs, and takes into consideration the clinical relevance of these various entities. The classification is presented in **Table 1**. The entities making up this classification scheme are detailed individually in **Subheading 2**.

2. Renal Cortical Adenoma

2.1. Clinical Features

The frequency of small epithelial lesions in the cortex of kidneys has been found to be between 7% and 23% in autopsy series (9). Eble and Warfel reported on a series of 400 consecutive autopsies in which the kidneys were carefully sectioned and examined; (10) and epithelial cortical lesions were found in 83 instances (21%) with increasing frequency with advanced age (10% in 21–40-yr-olds vs 40% in 70–90-yr-olds). Papillary adenomas have been reported in up to one-third of patients in association with acquired cystic disease (11). These appear earlier than carcinomas in this patient group, and are believed to represent the precursor lesion.

2.2. Pathologic Features

Cortical adenomata are grossly identifiable from as small as 1 mm, are well-circumscribed, yellow to gray in color, and are located in the cortex. The majority are tubular, papillary, or tubulo-papillary in architecture, most often corresponding to the basophil cell type as described by Thoenes et al. (3). The cells have round to oval nuclei with stippled to clumped chromatin and inconspicuous nucleoli. Cytoplasm is scant and amphophilic to basophilic. Although well-defined criteria for the distinction of adenoma from carcinoma have yet to be defined, the consensus conference agreed on a working definition until additional information is available. In this system, adenoma is defined as a lesion less than 5 mm in diameter, having a tubulopapillary architecture and a low nuclear grade (4,12).

3. Metanephric Adenoma/Adenofibroma

3.1. Clinical Features

This rare lesion has only recently been described in detail (13–15). It occurs at any age, but is most common in middle age, with a 2:1 female preponderance. Approximately 50% are incidental findings, with others presenting with polycythemia, abdominal/flank pain, mass, or hematuria. Incidental cases may coexist with RCC. The cases reported to date have not recurred or metastasized.

3.2. Pathologic Features

There is a wide range of sizes, with the largest reported case measuring 15 cm. Metanephric adenoma is well-circumscribed, solid or lobulated, and grayish-white. Small cysts and calcifications may be present. It is composed of uniform, round tubules embedded in a loose stroma. Individual cells have small,

Table 1
Classification of Renal Epithelial Tumors

Benign
Papillary adenoma
Oncocytoma
Metanephric adenoma/adenofibroma
Malignant
Conventional (clear-cell) carcinoma
Papillary carcinoma
Chromophobe carcinoma
Collecting-duct carcinoma
Unclassified RCC

regular nuclei, with absent or inconspicuous nucleoli and scant cytoplasm. Less often, papillary or microcystic architectures are seen. Hemorrhage, necrosis, and calcifications including psammoma bodies—are common. The cells do not contain glycogen, and immunohistochemical studies suggest a distal nephron or collecting-duct origin (14). Recent cytogenetic data suggests a relationship with papillary tumors based on the presence of trisomy 7 and 17 (16).

4. Oncocytoma

4.1. Clinical Features

In 1976, Klein and Valensi identified a subset of renal tumors composed of oncocytes exhibiting a benign clinical behavior (17)—an observation subsequently confirmed by several groups (18–20). Oncocytoma comprises approx 4% of kidney tumors in adults, with most detected over age 50; there is a male-to-female ratio of approximately 2–3:1. The majority are discovered as incidental findings, although oncocytoma may present with hematuria or a palpable mass. Origin from the intercalated cell of the collecting duct has been postulated (21).

4.2. Pathologic Features

Oncocytoma is a circumscribed mass with a homogeneous tan or mahogany-brown color. In some cases, bilateral and multifocal lesions are found. In rare cases there are innumerable lesions present—a situation that has been termed "oncocytomatosis" (22). Areas of hemorrhage may be seen, but necrosis is absent. A stellate central scar is characteristic; however, in smaller lesions the scar may not be well-developed and will only be demonstrable on histologic examination. Oncocytoma may coexist with RCC.

The tumor is composed entirely of cells with abundant and intensely eosinophilic cytoplasm, exhibiting coarse granularity. Focal cytoplasmic vacuolization may be present (23). The cells are typically cuboidal, but may be columnar and are arranged in well-defined nests which are peripherally closely packed but separated by a loose stroma toward the central region (**Fig. 1**). This corresponds to the central scar that may be evident grossly. Cystic change may be seen, and hemorrhage—when present—is frequently associated with these areas. Less often, a tubular or microcystic architecture is found. Nuclei are regular and round to oval in shape, with granular chromatin and central nucleoli. The presence of cells with bizarre pleomorphic nuclei is well-recognized, and believed to be degenerative in nature. Mitoses are absent, and applying strict criteria, the finding of even a single mitotic figure excludes oncocytoma as a diagnosis. In a review of 80 cases, Amin et al. (20) identified a total of two mitotic figures in the entire series, demonstrating the rarity of this finding. The importance of this criterion is highlighted by a report from Memorial Sloan-Kettering Cancer Center. In this series, 16% of tumors reported as oncocytoma had 1–2 mitotic figures per 10 high-powered fields, and there were two cases (3%) which had apparently developed metastases (24).

4.3. Special Studies

Oncocytoma reacts positively for low mol-wt cytokeratin, and does not express vimentin (25). There is positive reactivity for epithelial-membrane antigen (21). Hale's colloidal iron stain is negative. Lectins show a pattern consistent with collecting-duct origin (21). Ultrastructurally, the cells are filled with mitochondria.

5. Conventional (Clear Cell) Carcinoma

5.1. Clinical Features

Clear-cell RCC accounts for approx 70% of all adult epithelial kidney tumors in surgically resected series; thus, it is reflected in much of the literature on RCC (3). The tumor is believed to originate in the proximal tubule. The characteristic cytogenetic abnormalities, found in over 90% of clear-cell RCC cases, involve the short arm of chromosome 3 (3p) (2,6). In many cases, there is loss of the entire short arm; yet other aberrations such as deletions and translocations are described. Studies in patients with von Hippel-Lindau disease have led to the recognition of the von Hippel-Lindau gene (26). The vast majority of cases occur in adults over 40 yr of age, although no age group is spared—even children. There is a male preponderance, with approx a 2:1 ratio. RCC occurs with greater frequency in a few well-described inherited conditions, including von Hippel-Lindau disease (27) and tuberous sclerosis (28).

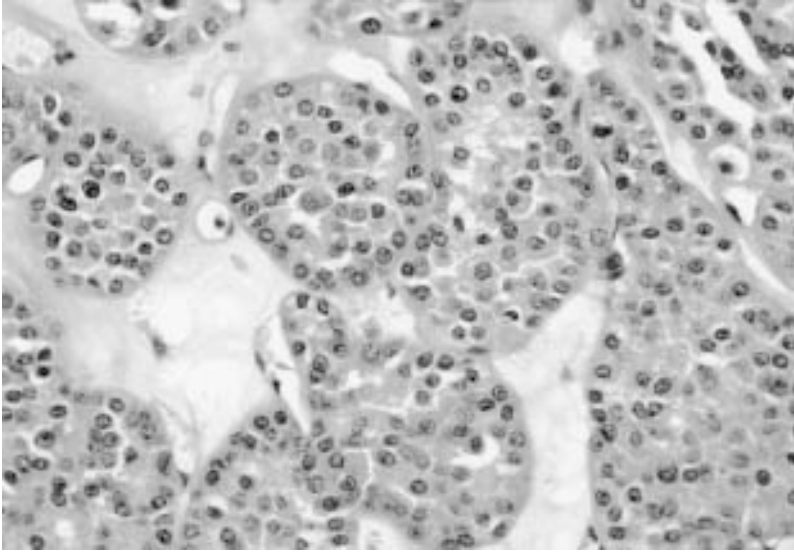


Fig. 1. Renal oncocytoma. The tumor is composed of uniform cells with granular eosinophilic cytoplasm arranged in nests embedded in a loose fibrous stroma.

5.2. Pathologic Features

The most characteristic gross feature of conventional (clear-cell) RCC is a bright yellow color caused by abundant lipid in the tumor. The neoplasm can range in size from millimeters to massive, weighing several kilograms. There is an apparent trend for tumors to be smaller in size, as increasing numbers are discovered earlier. Most present a variegated appearance, with hemorrhage and necrosis; brown areas may reflect old hemorrhage and soft, fleshy grayish-white areas frequently indicate a sarcomatoid component. Fibrosis can impart a firm grayish-white color, usually in the center of the lesion. Most are well-circumscribed, with a thin capsule or pseudocapsule separating the tumor from adjacent tissues. Cystic change occurs in as many as 15% of cases. Bilateral tumors are found in approx 1% of patients, and are more frequent in patients with von Hippel-Lindau disease and tuberous sclerosis.

Clear-cell tumors have transparent, structureless (empty) cytoplasm with well-defined cell borders. The cytoplasm contains variable amounts of glycogen and lipid; mucin stains are negative. In some cells, there is fine eosinophilic material around the nucleus (clear-cell eosinophilia), a feature often associated with high nuclear grades. The nuclei in clear-cell RCC tend to be round to oval and fairly regular, although considerable heterogeneity may exist in a single tumor. The nuclear characteristics have proven to be a significant predictor of behavior. Many studies have now demonstrated the independent

significance of nuclear grading as a prognostic indicator (29,30). Architecturally, clear-cell RCC may display several patterns; compact-alveolar, tubular, and microcystic are the most common. In the former, the small nests are separated by a well-developed sinusoidal vascular network (**Fig. 2**). Cystic change is common and rarely may produce a predominantly cystic lesion.

5.3. Special Studies

Clear-cell RCC characteristically coexpresses cytokeratin (low mol-wt) and vimentin, a feature of diagnostic importance (31). High mol-wt cytokeratins are not expressed. Carcinoembryonic antigen (CEA) is not expressed. Cells contain abundant glycogen and are mucin-negative. The Hale's colloidal iron stain is negative, although the iron pigment which is often present will stain.

6. Papillary Carcinoma

6.1. Clinical Features

Papillary (chromophil) RCC comprises 10–15% of RCC in surgical series (3,32–34). As emphasized by Delahunt and Eble (33), the term “papillary” in this context is a “name” rather than a “descriptor.” Age ranges from childhood to elderly, with most occurring in middle age; there is a male preponderance (2–4:1). It has been generally considered that chromophil RCC has a better prognosis than the clear-cell type, yet there is limited data available comparing the two types on a stage-for-stage basis. The overall 5-yr survival for papillary carcinoma is >80%, compared to 40–50% for clear-cell carcinoma. Using historical controls, Amin et al. found improved survival to be independent of stage (34).

Cytogenetically, papillary RCC is characterized by trisomy 7 and 17 with loss of the Y chromosome. Trisomies of other chromosomes—including 8, 12, 16, and 20—are also reported, although less frequently (35,36). Studies of hereditary papillary RCC have indicated the presence of a papillary RCC gene, recently reported to be the proto-oncogene *c-met*, located at 7q31.1-34 (37,38). The origin of papillary RCC is uncertain. Tumors express antigens related to both proximal and distal tubules. Some reports have suggested that the eosinophilic subtype originates in the proximal tubules, and the basophilic type in the distal tubules (39).

6.2. Pathologic Features

Papillary RCC is well-circumscribed, and often is surrounded by a thick capsule. The tumor is tan to brown to red-brown in color. It often reflects hemorrhage with a friable cut surface, giving an impression of extensive necrosis; the amount of necrosis is often less than suspected from the gross appearance. Cystic degeneration may be prominent, and areas of calcification may be grossly evident.

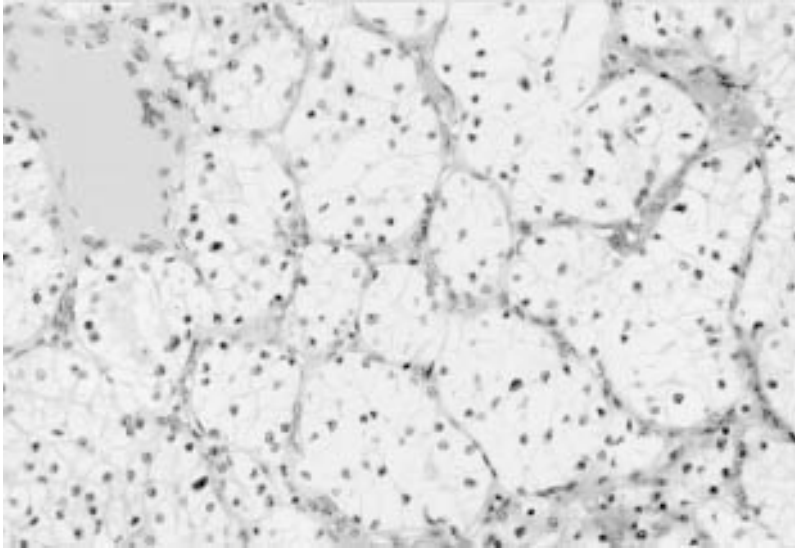


Fig. 2. Conventional (clear-cell) renal carcinoma. In this typical example the tumor cells have clear cytoplasm and are arranged in small nests that are separated from each other by a prominent sinusoidal vascular network.

The majority of tumors have a papillary or tubulo-papillary architecture. These may be tightly packed, resulting in a highly cellular tumor. The papillary structures often contain large numbers of foamy macrophages in the stalks (**Fig. 3**). The papillary stalks may be sclerotic or edematous, with broad papillae. Hemorrhage is often present, with abundant hemosiderin that is frequently within the tumor-cell cytoplasm. Psammoma bodies may be present, but are an inconsistent feature. Sarcomatoid morphology occurs, but is distinctly rare. These tumors tend to have dense granular cytoplasm, and are subclassified as basophil or eosinophil types. Less frequently, both coexist, resulting in so-called duophil neoplasms. In the basophil type, nuclei are typically small and hyperchromatic, with dense chromatin and occasional nuclear grooves, and mitoses are rare. Eosinophil tumors have cuboidal to columnar cells with more abundant and intensely eosinophilic cytoplasm. Eosinophil tumors are of higher nuclear grade (**33,34**), and in one report were more often locally advanced (**33**).

6.3. Special Studies

Papillary tumors express low mol-wt cytokeratins including cytokeratin 7: in one series, 83% of basophil and 20% of eosinophil tumors were CK7-positive (**40**). The reported coexpression of vimentin has ranged from 0–80%

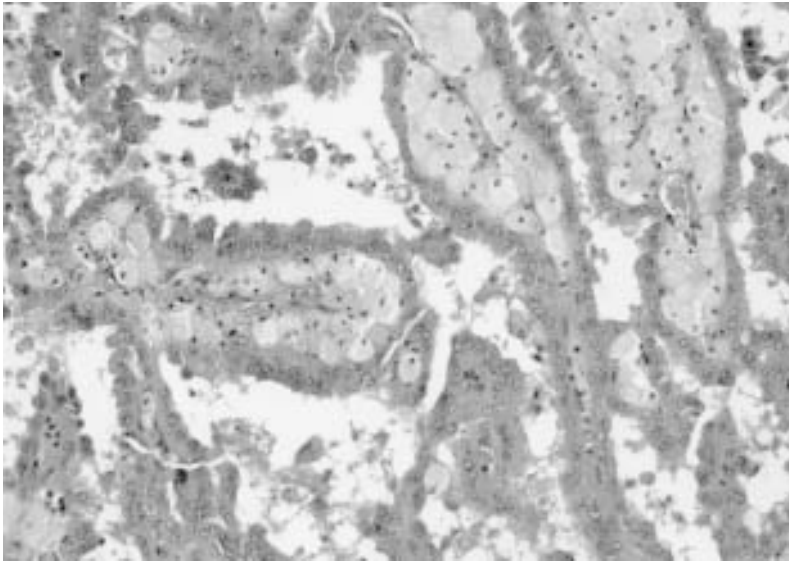


Fig. 3. Papillary carcinoma. This example of the eosinophilic type of papillary carcinoma is composed of tall columnar tumor cells with abundant eosinophilic cytoplasm covering the papillary stalks. Note the presence of abundant foamy macrophages within the papillary cores.

(33,40). *Ulex europaeus*, a marker of collecting-duct epithelium, is negative (33). Weak reactivity to CEA has been reported in a few cases (32). The cells contain scant glycogen, and do not stain with Hale's colloidal iron (except for the hemosiderin). Ultrastructurally, the cytoplasm is complex, with abundant organelles (3).

7. Chromophobe Carcinoma

7.1. Clinical Features

Chromophobe-cell carcinoma was first defined as a distinctive pathologic entity by Thoenes and colleagues in 1985 (41), comprising approx 5% of adult renal epithelial tumors. It occurs predominantly in middle-aged patients, and does not exhibit a sex preference. Emerging data indicates that it has a better prognosis than conventional RCC (42,43). Chromophobe carcinoma is believed to arise from intercalated cells in the renal collecting ducts (44). Cytogenetically, the tumor is distinctive, with the presence of multiple monosomies involving chromosomes 1, 2, 10, 13, 6, 21, and 17 (in descending order of frequency) (45,46).

7.2. Pathologic Features

Chromophobe carcinoma has a homogeneous tan to brown color, similar to that seen in renal oncocytoma. A central scar is not a feature, and areas of hemorrhage and necrosis may be present. Cystic degeneration is rare, and usually only small cysts are seen.

Microscopically, chromophobe tumors have two forms: a classical type and an eosinophilic variant. The typical appearance (*classical variant*) is of cells with voluminous pale eosinophilic cytoplasm, often with perinuclear clearing and more intense staining adjacent to the cell membrane (**Fig. 4**). Careful examination shows the cytoplasm to have a more reticular than granular appearance. Nuclei tend to be centrally located, but may be eccentric and have coarse chromatin with variable nucleoli. The nuclear membrane may be wrinkled, producing a raisin-like appearance. Mitoses are usually present, but may be scant. In a small percentage of cases, the cytoplasm shows a more intense eosinophilia mimicking renal oncocytoma (*eosinophilic variant*). These cells also often have perinuclear clearing, and in most instances, classical areas can be found (at least focally). Sarcomatoid variants are rare, but have been described (47).

7.3. Special Studies

Through immunohistochemistry, tumors express low mol-wt cytokeratin but not vimentin (25,48). Epithelial-membrane antigen is expressed (42). Hale's colloidal iron is uniformly positive, with a reticular pattern of cytoplasmic staining (25,49). The ultrastructural features are highly distinctive, with the cytoplasm containing abundant vesicular structures (50). Occasionally these contain internal smaller vesicles. It has been suggested that these vesicles derive from the mitochondrial membrane. The cells also contain variable numbers of mitochondria, and in the eosinophilic variant these may be quite numerous.

8. Collecting-Duct Carcinoma

8.1. Clinical Features

The first description of collecting-duct carcinoma is attributed to Mancilla-Jimenez et al. who described three cases of papillary RCC in which atypical hyperplastic changes were noted in the collecting-duct epithelium (51). Since then, several reports have appeared further detailing the clinical and pathologic features of this tumor (52,53), and the topic has recently been reviewed by Srigley and Eble (54). Although few cases have been reported to date, some clinical comments may be made. These tumors occur in a younger age group than typical RCC and have a very aggressive course. In a study from the M.D. Anderson Cancer Center, the median survival of 10 patients was only 22 mo (55). Davis and colleagues recently reported an association between sickle-cell disease and a tumor they termed *renal medullary carcinoma*; these

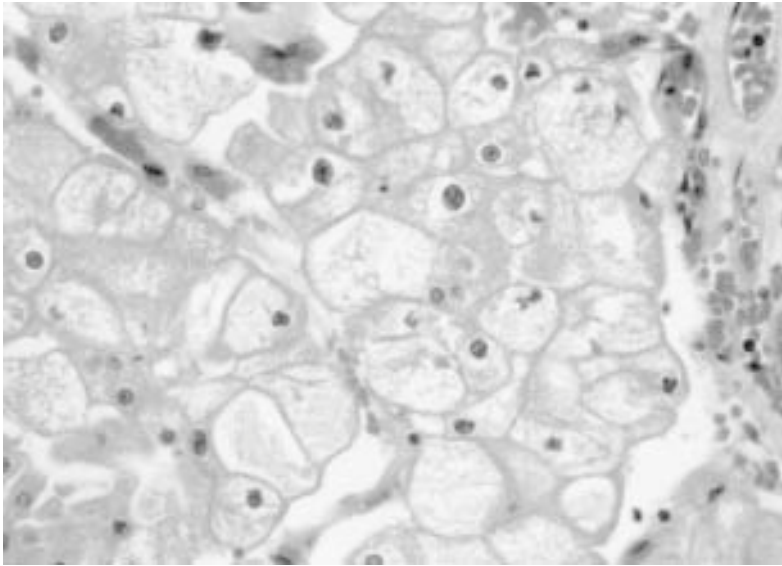


Fig. 4. Chromophobe carcinoma. In the classical type illustrated in this photomicrograph, the tumor cells have voluminous cytoplasm with a reticular appearance and apparent thick-cell membranes resulting from the concentration of organelles at the periphery of the cytoplasm.

also were postulated to originate in the collecting ducts (56). The presentation is similar to other malignant kidney tumors. The cases of this variant reported to date have been very aggressive, with most dying within 1 yr of diagnosis. Finally, low-grade tumors of putative collecting-duct origin have also been reported; and these patients have a good prognosis, with 1 in 10 dying of tumor (57).

Cytogenetic analysis of collecting-duct carcinoma has yielded variable results (2). Among the most frequent findings have been monosomy of chromosome 18 (58), and loss of heterozygosity on chromosome 1q (59).

8.2. Pathologic Features

Collecting-duct carcinoma is located in the renal medulla, although in larger tumors this may not be apparent. It has an infiltrative growth pattern with a white or gray color, and variegation is common, with frequent areas of necrosis. The classical histology is a mixed papillary and infiltrative tubular architecture. The infiltrative component is associated with stromal desmoplasia (Fig. 5). In most cases, foci of dysplasia or “carcinoma *in situ*” may be found in the collecting ducts. Typically, the tumors are of high nuclear grade, corresponding to Fuhrman grades 3 or 4. Sarcomatoid differentiation has been reported in collecting-duct carcinoma (60).

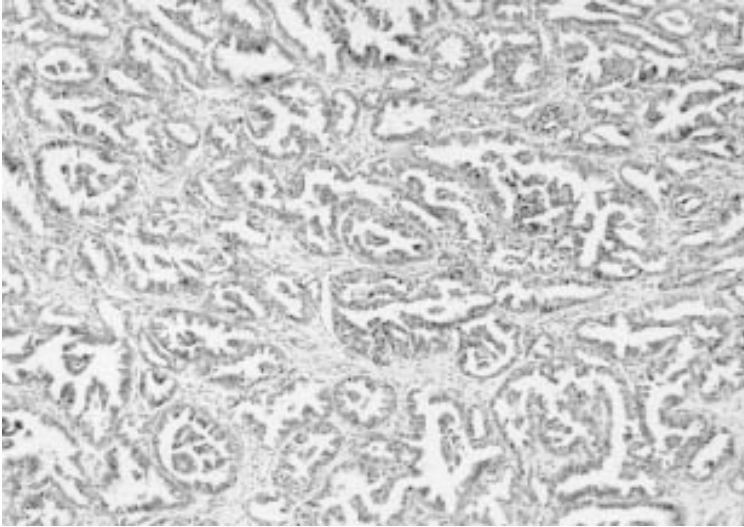


Fig. 5. Collecting-duct carcinoma. The tumor in this case shows a complex papillary ductal architecture with a desmoplastic stroma in the background.

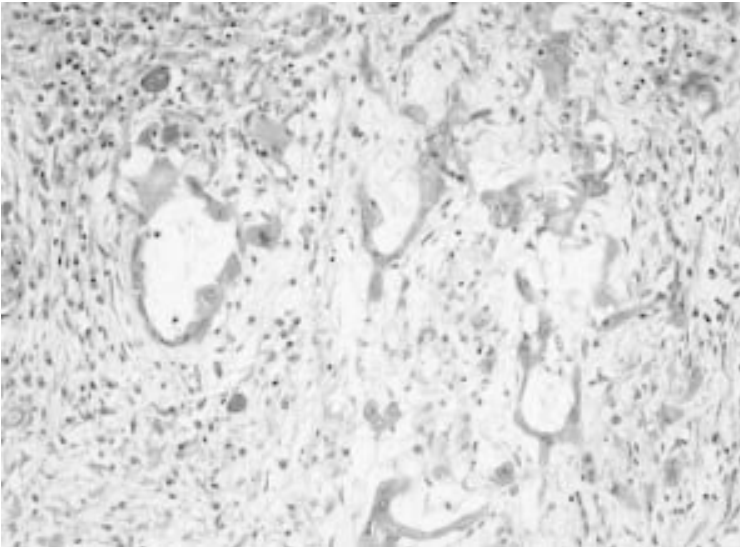


Fig. 6. Medullary carcinoma. In this case the tumor shows the “yolk sac-like” architecture that is most characteristic of this variant of collecting-duct carcinoma.

With medullary carcinoma, the most characteristic feature is a reticular or yolk sac-like appearance combined with adenoid cystic-like areas (**Fig. 6**). In

other areas, tumor cells occur in sheets. An infiltrate of polymorphonuclear leukocytes is usually present. Individual cells have pleomorphic nuclei, with frequent mitoses. In most cases, a prominent desmoplastic stromal response is noted. Sickled erythrocytes may be identified.

Low-grade tumors of presumed collecting-duct origin have been characterized by a predominantly tubulocystic pattern of growth. Mucin positivity was a feature of all cases described, including cytoplasmic staining.

8.3. Special Studies

Collecting-duct carcinoma usually contains relatively small amounts of glycogen, and occasionally focal cytoplasmic mucin is present (61). Immunohistochemical studies support a collecting-duct origin with positivity for high mol-wt cytokeratin (cytokeratin 19), peanut-lectin agglutinin, and *U. europus* agglutinin (53).

References

1. Fleming, S. (1993) The impact of genetics on the classification of renal carcinoma. *Histopathology* **22**, 89–92.
2. Zambrano, N. R., Lubensky, I. A., Merino, M. J., Linehan, W. M., and Walther, M. M. (1999) Histopathology and molecular genetics of renal tumors: toward unification of a classification system. *J. Urol.* **162**, 1246–1258.
3. Thoenes, W., Störkel, S., and Rumpelt, H. J. (1986) Histopathology and classification of renal cell tumors (adenomas, oncocytomas, and carcinomas). *Path. Res. Pract.* **181**, 125–143.
4. Störkel, S., Eble, J. N., Adlakha, K., Amin, M., Blute, M. L., and Bostwick, D. G. (1997) Classification of renal cell carcinoma: workgroup 1. *Cancer* **80**, 987–989.
5. Kovacs, G., Akhtar, M., Beckwith, B. J., Bugert, P., Cooper, P., Cooper, C. S., Delahunt, B., Eble, J. N., Fleming, S., Ljungberg, B., Medeiros, L. J., Moch, H., Reuter, V. E., Ritz, E., Roos, G., Schmidt, D., Srigley, J. R., Störkel, S., van den Berg, E., and Zbar, B. (1997) The Heidelberg classification of renal cell tumors (editorial). *J. Pathol.* **183**, 131–133.
6. Kovacs, G. (1993) Molecular differential pathology of renal cell tumors. *Histopathology* **2**, 1–8.
7. Gnarr, J. R., Tory, K., Weng, Y., Schmidt, L., Wei, M. H., Li, H., Latif, F., Liu, S., Chen, F., and Duh, F. M. (1994) Mutations of the VHL tumour suppressor gene in renal carcinoma. *Nat. Genet.* **7**, 85–90.
8. Schwerdtle, R. F., Störkel, S., Neuhaus, C., Brauch, H., Weidt, E., Brenner, W., Hohenfellner, R., Huber, C., and Decker, H. J. (1996) Allelic losses at chromosomes 1p, 2p, 6p, 10p, 13q, 17p and 21q significantly correlate with the chromophobe subtype of renal cell carcinoma. *Cancer. Res.* **56**, 2927–2930.
9. Grignon, D. J. and Eble, J. N. (1998) Papillary and metanephric adenomas of the kidney. *Semin. Diagn. Pathol.* **15**, 41–53.
10. Eble, J. and Warfel, K. (1991) Early human renal cortical epithelial neoplasia. *Mod. Pathol.* **4**, 45A.

11. Hughson, M. D., Buchwald, D., and Fox, M. (1986) Renal neoplasia and acquired cystic kidney disease in patients receiving long-term dialysis. *Arch. Pathol. Lab. Med.* **110**, 592–601.
12. Delahunt, B. and Eble, J. N. (1997) Papillary adenoma of the kidney: an evolving concept. *J. Urological Pathol.* **7**, 99–112.
13. Jones, E. C., Pins, M., Dickersin, R. D., and Young, R. H. (1995) Metanephric adenoma of the kidney: a clinicopathological, immunohistochemical, flow cytometric, cytogenetic and electron microscopic study of seven cases. *Am. J. Surg. Pathol.* **19**, 615–626.
14. Davis, C. J. Jr., Barton, J. H., Sesterhenn, I. A., and Mostofi, F. K. (1995) Metanephric adenoma: clinicopathological study of fifty patients. *Am. J. Surg. Pathol.* **19**, 1101–1114.
15. Gatalica, Z., Grujic, S., Kovatich, A., and Petersen, R. O. (1996) Metanephric adenoma: histology, immunophenotype, cytogenetics, ultrastructure. *Mod. Pathol.* **9**, 329–333.
16. Brown, J. A., Anderl, K. L., Borell, T. J., Qian, J., Bostwick, D. G., and Jenkins, R. B. (1997) Simultaneous chromosome 7 and 17 gain and sex chromosome loss provide evidence that renal metanephric adenoma is related to papillary renal cell carcinoma. *J. Urol.* **158**, 370–374.
17. Klein, M. J. and Valensi, Q. J. (1976) Proximal tubular adenomas of the kidney with so-called oncocytic features: a clinicopathologic study of 13 cases of a rarely reported neoplasm. *Cancer* **38**, 906–914.
18. Merino, M. J. and LiVolsi, V. A. (1982) Oncocytomas of the kidney. *Cancer* **50**, 1852–1856.
19. Barnes, C. A. and Beckman, E. N. (1983) Renal oncocytoma and its congeners. *Am. J. Clin. Pathol.* **79**, 312–318.
20. Amin, M. B., Crotty, T. B., Tickoo, S. K., and Farrow, G. M. (1997) Renal oncocytoma: a reappraisal of morphologic features with clinicopathologic findings in 80 cases. *Am. J. Surg. Pathol.* **21**, 1–12.
21. Lyzak, J. S., Farhood, A., and Verani, R. (1994) Intracytoplasmic lumens in renal oncocytoma and possible origin from intercalated cells of the collecting duct. *J. Urol. Pathol.* **2**, 135–151.
22. Warfel, K. A. and Eble, J. N. (1982) Renal oncocytomatosis. *J. Urol.* **127**, 1179–1180.
23. Slagel, D. and Bonsib, S. M. (1995) Renal oncocytoma with unusual features: case report and review of morphologic variants of oncocytoma. *J. Urol. Pathol.* **3**, 223–233.
24. Perez-Ordenez, B., Hamed, G., Campbell, S., Erlandson, R. A., Russo, P., Gaudin, P. B., and Reuter, V. E. (1997) Renal oncocytoma: a clinicopathologic study of 70 cases. *Am. J. Surg. Pathol.* **21**, 871–883.
25. DeLong, W. H., Sakr, W. A., and Grignon, D. J. (1996) Chromophobe renal cell carcinoma: a comparative histochemical and immunohistochemical study. *J. Urol. Pathol.* **4**, 1–8.

26. Ogawa, O., Kakehi, Y., Ogawa, K., Koshiba, M., Sugiyama, T., and Yoshida, O. (1991) Allelic loss at chromosome 3p characterizes clear cell phenotype of renal cell carcinoma. *Cancer. Res.* **51**, 949–953.
27. Solomon, D. and Schwartz, A. (1988) Renal pathology in von Hippel-Lindau disease. *Hum. Pathol.* **19**, 1072–1079.
28. Washecka, R. and Hanna, M. (1991) Malignant renal tumors in tuberous sclerosis. *Urology* **37**, 340–343.
29. Fuhrman, S. A., Lasky, L. C., and Limas, C. (1982) Prognostic significance of morphologic parameters in renal cell carcinoma. *Am. J. Surg. Pathol.* **6**, 655–663.
30. Grignon, D. J., Ayala, A. G., El-Naggar, A. K., Wishnow, K. I., Ro, J. Y., Swanson, D. A., McLemore, D., Giacco, G. G., and Guinee, V. F. (1989) Renal cell carcinoma: a clinicopathologic and DNA flow cytometric analysis of 103 cases. *Cancer* **64**, 2133–2140.
31. El-Naggar, A. K., Ro, J. Y., and Ensigen, L. G. (1993) Papillary renal cell carcinoma: clinical implication of DNA content analysis. *Hum. Pathol.* **24**, 316–321.
32. Renshaw, A. A. and Corless, C. L. (1995) Papillary renal cell carcinoma: histology and immunohistochemistry. *Am. J. Surg. Pathol.* **19**, 842–849.
33. Delahunt, B. and Eble, J. N. (1997) Papillary renal cell carcinoma: a clinicopathologic and immunohistochemical study of 105 tumors. *Mod. Pathol.* **10**, 537–544.
34. Amin, M. B., Corless, C. L., Renshaw, A. A., Tickoo, S. K., Kubus, J., and Schultz, D. S. (1997) Papillary (chromophil) renal cell carcinoma: histomorphologic characteristics and evaluation of conventional pathologic prognostic parameters in 62 cases. *Am. J. Surg. Pathol.* **21**, 621–635.
35. Kovacs, G. (1989) Papillary renal cell carcinoma: a morphologic and cytogenetic study of 11 cases. *Am. J. Pathol.* **134**, 27–34.
36. Van Den Berg, E., van der Hout, A. H., Oosterhuis, J. W., et al. (1993) Cytogenetic analysis of epithelial renal-cell tumours: rRelationship with a new histopathological classification. *Int. J. Cancer* **55**, 223–227.
37. Zbar, B., Glenn, G., Lubensky, I., Choyke, P., Walther, M. M., Magnusson, G., Bergerheim, U. S., Pettersson, S., Amin, M., and Hurley, K. (1995) Hereditary papillary renal cell carcinoma: clinical studies in 10 families. *J. Urol.* **153**, 907–912.
38. Schmidt, L., Duh, F. M., Chen, F., Kishida, T., Glenn, G., Choyke, P., Scherer, S. W., Zhuang, Z., Lubensky, I., Dean, M., Allikmets, R., Chidabaram, A., Bergerheim, U. R., Feltis, J. T., Casadevall, C., Zamarron, A., Bernues, M., Richard, S., Lips, C. J., Walther, M. M., Tsui, L. C., Geil, L., Orcutt, M. L., Stackhouse, T., and Zbar, B. (1997) Germline and somatic mutations in the tyrosine kinase domain of the MET proto-oncogene in papillary renal carcinomas. *Nat. Genet.* **16**, 68–73.
39. Hughson, M. D., Johnson, L. D., Silva, F. G., and Kovacs G. (1993) Nonpapillary and papillary renal cell carcinoma: a cytogenetic and phenotypic study. *Mod. Pathol.* **6**, 449–456.
40. Gatalica, Z., Kovatich, A., and Miettinen, M. (1995) Consistent expression of cytokeratin 7 in papillary renal-cell carcinoma: An immunohistochemical study in formalin-fixed, paraffin-embedded tissues. *J. Urol. Pathol.* **3**, 205–211.

41. Thoenes, W., Störkel, S., and Rumpelt, H.-J. (1985) Human chromophobe cell renal carcinoma. *Virchows Arch. (Cell Pathol.)* **48**, 207–217.
42. Akhtar, M., Kardar, H., Linjawi, T., McLintock, J., and Ali, M. A. (1995) Chromophobe cell carcinoma of the kidney: a clinicopathologic study of 21 cases. *Am. J. Surg. Pathol.* **19**, 1245–1256.
43. Thoenes, W., Störkel, S., Rumpelt, H.-J., Moll, R., Baum, H. P., and Werner, S. (1988) Chromophobe cell renal carcinoma and its variants—a report on 32 cases. *J. Pathol.* **155**, 277–287.
44. Störkel, S., Steart, P. V., Drenckhahn, D., and Thoenes, W. (1989) The human chromophobe cell renal carcinoma: its probable relation to intercalated cells of the collecting duct. *Virchows Arch. (Cell Pathol.)* **56**, 237–245.
45. Kovacs, A. and Kovacs, G. (1992) Low chromosome number in chromophobe renal cell carcinomas. *Genes Chromosomes Cancer* **4**, 267–268.
46. Speicher, M. R., Schoell, B., du Manoir, S., Schrock, E., Ried, T., Cremer, T., Störkel, S., Kovacs, A., and Kovacs, G. (1994) Specific loss of chromosomes 1,2,6,10,13,17, and 21 in chromophobe renal cell carcinomas revealed by comparative genomic hybridization. *Am. J. Pathol.* **145**, 356–364.
47. Aizawa, S., Chigusa, M., Ohno, Y., and Suzuki, M. (1997) Chromophobe cell renal carcinoma with sarcomatoid component: a report of two cases. *J. Urol. Pathol.* **6**, 51–59.
48. Pitz, S., Moll, R., Störkel, S., and Thoenes, W. (1987) Expression of intermediate filament proteins in subtypes of renal cell carcinomas and in renal oncocytomas. *Lab. Invest.* **56**, 642–653.
49. Tickoo, S. K., Amin, M. B., and Zarbo, R. J. (1998) Colloidal iron staining in renal epithelial neoplasms, including chromophobe renal cell carcinoma: emphasis on technique and patterns of staining. *Am. J. Surg. Pathol.* **22**, 419–424.
50. GerHarz, C.-D., Moll, R., Störkel, S., Ramp, U., Thoenes, W., and Gabbert, H. E. (1993) Ultrastructural appearance and cytoskeletal architecture of the clear, chromophilic, and chromophobe types of human renal cell carcinoma in vitro. *Am. J. Pathol.* **142**, 851–859.
51. Mancilla-Jimenez, R., Stanley, R. J., and Blath, R. A. (1976) Papillary renal cell carcinoma. *Cancer* **38**, 2469–2480.
52. Fleming, S. and Lewi, H. J. E. (1986) Collecting duct carcinoma of the kidney. *Histopathology* **10**, 1131–1141.
53. Rumpelt, H. J., Störkel, S., Moll, R., Scharfe, T., and Thoenes, W. (1991) Bellini duct carcinoma: further evidence for this rare variant of renal cell carcinoma. *Histopathology* **18**, 115–122.
54. Srigley, J. R. and Eble, J. N. (1998) Collecting duct carcinoma of kidney. *Semin. Diagn. Pathol.* **15**, 54–67.
55. Dimopoulos, M. A., Logothetis, C. J., Markowitz, A., Sella, A., Amato, R., and Ro, J. Collecting duct carcinoma of the kidney. *Br. J. Urol.* **71**, 388–391.
56. Davis, C. J., Jr., Mostofi, F. K., and Sesterhenn, I. A. (1995) Renal medullary carcinoma: the seventh sickle cell nephropathy. *Am. J. Surg. Pathol.* **19**, 1–11.

57. MacLennan, G. T., Farrow, G. M., and Bostwick, D. G. (1997) Low-grade collecting duct carcinoma of the kidney: report of 13 cases of low-grade mucinous tubulocystic renal carcinoma of of possible collecting duct origin. *Urology* **50**, 679–684.
58. Gregori-Romero, M. A., Morell-Quadreny, L., and Llombart-Bosch, A. (1996) Cytogenetic analysis of three Bellini duct carcinomas. *Genes Chromosomes Cancer* **15**, 170–172.
59. Steiner, G., Cairns, P., Polascik, T. J., Marshall, F. F., Epstein, J. I., Sidransky, D., and Schoenberg, M. (1996) High-density mapping of chromosomal arm 1q in renal collecting duct carcinoma: region of minimal deletion at 1q32.1-32.2. *Cancer Res.* **56**, 5044–5046.
60. Baer, S. C., Ro, J. Y., Ordonez, N. G., Maiese, R. L., Loose, J. H., Grignon, D. J., and Ayala, A. G. (1993) Sarcomatoid collecting duct carcinoma: a clinicopathologic and immunohistochemical study of five cases. *Hum. Pathol.* **24**, 1017–1022.
61. Kennedy, S. M., Merino, M. J., Linehan, W. M., Roberts, J. R., Robertson, C. N., and Neumann, R. D. (1990) Collecting duct carcinoma of the kidney. *Hum. Pathol.* **21**, 449–456.

Telomerase Assay in Renal Cancer

William W. Zhang and Laurence H. Klotz

1. Introduction

Telomeres are repeating sequences located at each end of eukaryotic chromosomes. These sequences function to protect chromosome positioning and replication (**1–3**). In vertebrates, telomere DNA consists of tandem repeats of TTAGGG, 10–15 kb pairs long (**4**). In most normal cells, DNA replication during mitosis results in the loss of telomere sequences 50–100 bp at the 5' ends of DNA termini (**1,5**). This sequence loss is mandated by the end-replication-splicing problem (**Fig. 1**). Thus, telomeres progressively shorten with age in somatic cells in culture and in vivo. In contrast, cancer cells and malignant cell lines retain telomere length despite repeated mitosis (**6**). This is believed to be an essential component of immortalization for most cells.

In most immortalized cells and normal cells that replicate interminably (i.e., testis germ cells), the loss of telomere length is prevented by telomerase. Telomerase was first demonstrated in Tetra-hymena and then in other ciliates and established cell lines (**7,8**). It is a ribonucleoprotein enzyme and contains three components: the telomerase RNA component, telomerase-associated protein 1, and telomerase reverse transcriptase (**9**). Using a segment of its RNA component as a template (**10**), the enzyme synthesizes telomeric repeats onto chromosomal ends under assistance from the protein component and reverse transcriptase. By reactivating this enzyme, malignant cells maintain their telomere length. Harley et al. introduced a cellular senescence-immortalization theory in 1990 (**11,12**), and Wright and Shay further proposed that cells must pass two checkpoints before immortalization (**13**) (**Fig. 2**). The first stage represents normal cellular senescence (mortality stage 1). At the second stage, the telomeres become critically shortened and a stage of proliferative crisis is

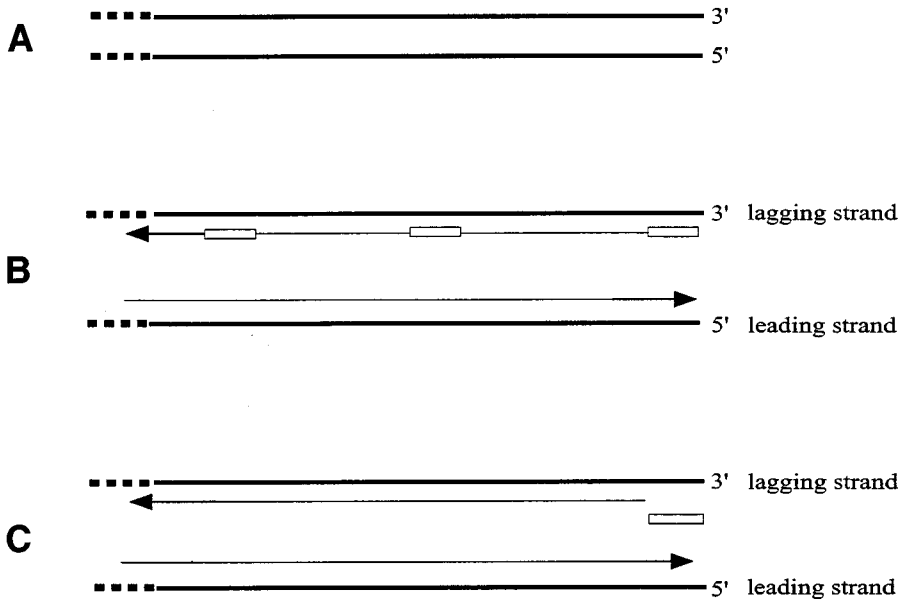


Fig. 1. End-replication problem. As the replication fork proceeds from left to right, the leading strand proceeds to replicate one strand of original DNA (*see B*). The direction of the lagging strand is opposite to the direction of the replication fork and relies on the ligation of Okazaki fragments, which are primed with short stretches. Most RNA primer is never replaced with DNA (*see C*). Consequently, each round of replication produced a daughter chromosome. These are deficient in the sequences corresponding to the original 3' ends.

reached with severe genomic instability (mortality stage 2). During this stage, in rare cells, activation of telomerase leads to synthesis of TTAGGG repeats and a balanced compensation of the end-replication problem. This may be an essential and rate-limiting step in the immortalization process of a tumor cell.

Telomerase activity is present in cell lines of renal, bladder, and prostate cancers, and a high proportion of primary malignancies of the genitourinary tract including kidney, ureter, bladder, prostate and testis cancers (**3,10,14–28**). Telomerase activity has been detected in 198 of total 289 (69%) of RCC (26 of 35 in Rohde et al. (**14**); 40/56 in Mehle et al. (**16**); 11 of 12 in Gelmini et al. (**18**); 36 of 47 in Kinoshita et al. (**19**); 28 of 50 in Yoshida et al. (**20**); 29 of 45 in Mehle et al. (**28**); 28 of 44 in Muller et al. (**23**); 2 of 3 (67%) renal pelvis carcinomas (1 of 2 in Rohde et al. (**14**); 1 of 1 in Kyo et al. (**17**) and 12 of 12 (100%) Wilms tumor (6 of 6 in Kim et al. (**3**); 6 of 6 in Yashima et al. (**15**)). In most of these cases (73 of 83, 88%) the adjacent normal renal tissue in the cancer-bearing

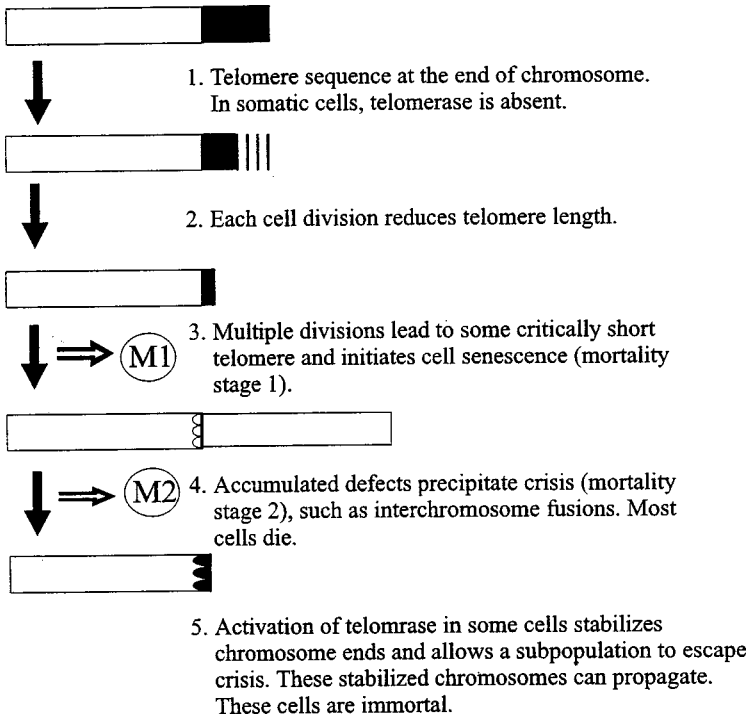


Fig. 2. Telomerase role in cellular senescence and immortalization.

kidneys were telomerase-negative (4 of 6 in Kim et al. (3); 29 of 35 in Rohde et al. (14); 10 of 12 in Kyo et al. (17); 30 of 30 in Kinoshita et al. (19). In benign renal tumors, none of six angiomyolipomas or four oncocytomas contained telomerase activity (14,23). No normal tissue in a total of 141 samples from either non-cancer-bearing kidneys or histologically normal renal tissues had telomerase activity (0 of 9 in Rohde et al. (14); 0 of 3 in Yashima et al. (15); 0 of 56 in Mehle et al. (16); 0 of 21 in Yoshida et al. (20); 0 of 52 in Muller et al. (23).

All 18 renal malignant cell lines studied by Kim et al. and Kinoshita et al. had telomerase activity (3,19).

Telomerase was also found in 12% of adjacent normal tissue from cancer-bearing kidneys. This may be a result of occult cancer cells deep in the histologically characterized surface of the cancer area, or may be attributed to early molecular alterations of cancer that are histologically inapparent (10).

The high incidence of telomerase activity detected in renal malignancies is consistent with the findings from other sites such as lung, colorectal, gastric, breast, prostate, and liver cancers (3,5,10,22,24-26). Detection of telomerase activity in a high proportion of renal tumors suggests that this enzyme may

play a role in renal carcinogenesis or cancer progression (14). The fact that about one-third of renal cancers are telomerase-negative implies that information from these studies may have prognostic value (10,27) and could thus improve the classification of renal tumors (19).

Studies of the correlation between telomerase activity and various prognostic clinical and pathologic parameters (tumor size, clinical stage, DNA ploidy, histological grade, and clinical outcome) have reported variable results (14,16,19,20,23). The studies have been confounded by small numbers and short follow-up. Whether telomerase activity differentiates between clear-cell and non-clear-cell types in renal cell carcinoma (RCC) is also unknown (14,19). Two studies of a total of 91 RCCs (47 cases in Kinoshita et al. (19); 44 cases in Muller et al. (23)) found that telomerase activity was less frequent in chromophobe renal-cell malignancies compared to clear-cell carcinomas (19). This suggests that chromophobe tumors, which do not have a 3p deletion/mutation (although they show many other chromosomal losses) may not consist of immortalized cells. This has been proven in clinical observations of the benign nature of this tumor.

Recent investigations have suggested that the loss of genes on the short arm of chromosome 3 plays an important role in downregulation of telomerase activity in RCC (28–30). Loss of heterozygosity of 3p (particularly at 3p21.2-p14.2 and 3p24.3-p24.1) has been shown to correlate closely with the presence of telomerase activity. Previous studies have demonstrated that microcell transfer of chromosome 3 can suppress cell growth, induce senescence, and downregulate telomerase expression (31,32). Microcell transfer of the 3p21.1-14.1 region has been shown to suppress telomerase activity in cell lines lacking 3p. Thus, this region appears to harbor a gene directly involved in the regulatory pathway of telomerase. A possible scenario regarding RCC, telomerase activation, and 3p deletion is the deletion of a gene on 3p, inactivation of the telomerase gene at a late stage by deletion or mutation of the second 3p allele resulting in further telomere reduction and proliferative crisis, and activation of telomerase and abrogation of the proliferative crisis. Conversely, inactivation of 3p may directly induce telomerase activity. Further analysis of the 3p region which regulates telomerase activation is warranted.

Telomerase activity is measured using a PCR-based assay, the Telomeric Repeat Amplification Protocol (TRAP) (3,5). Telomerase activity measured by the TRAP assay depends on the number of cancer cells and the quality of sample and the techniques applied in the assay. Contamination of the extracts by either ribonucleases or PCR product contaminants may produce false-negative or false-positive results. The assay is dependent upon stringent handling and storage of samples.

Analysis of telomerase activity was first presented *in vitro* by Greider et al. and Morin (7,8,33). The highly sensitive and efficient PCR-based TRAP assay was described by Kim et al. in 1994 (3). The TRAP assay permits large-scale analysis of telomerase activity in human cells and tissues.

2. Materials

2.1. Equipment

1. Skin-biopsy punch, 2.0–3.0 mm in diameter.
2. Kontes tube with motorized pestles (Fisher Scientific).
3. Refrigerated microcentrifuge.
4. Pipetman, aerosol-resistant tips (RNase-free) and tubes.
5. 0.5-mL polymerase chain reaction (PCR) tubes.
6. Thermocycler.
7. Vertical gel electrophoresis apparatus and power supply.
8. Gel dryer.
9. PhosphorImager.

2.2. Solutions and Reagents

2.2.1. Tissue Sample Preparation

Washing buffer: 10 mM HEPES-KOH (pH 7.5), 1.5 mM MgCl₂, 10 mM KCl, 1 M dithiothreitol (DTT), store at 4°C.

2.2.2. Extraction of Telomerase Protein

1. Lysis buffer: 10 mM Tris-HCl (pH 7.5), 1 mM MgCl₂, 1 mM EGTA, 1 mM phenylmethylsulfonyl fluoride, 5 mM β -mercaptoethanol, 0.5% 3-[(3-cholamidopropyl)diethylamino]-1-propanesulfonate (CHAPS, Pierce), 10% glycerol, aliquoted and store at 4°C.
2. Protein Assay Reagent (Bio-Rad Cat. No. 500-0002).

2.2.3. TRAP Assay Setup

1. Preparation of CX primer (0.05 μ g/ μ L).
 - a. CX primer sequence: 5'-CCCTTACCCTTACCCTTACCCTAA-3', custom-made and anion-exchange HPLC-purified.
 - b. CX primer is diluted to 0.05 μ g/ μ L, and 2 μ L of the primer is sealed onto the bottom of a PCR reaction tube with 10 μ L of molten wax in advance before the experiment, and then allowed to solidify at room temperature. Tubes are stored at 4°C until use.
2. Preparation of TRAP reaction buffer:
 - a. 50 μ L 50X dNTPs (deoxynucleoside triphosphates) mix (1.25 mM): dATP 0.625 μ L, dGTP 0.625 μ L, dTTP 0.625 μ L, dCTP 0.625 μ L, distilled water 47.5 μ L, aliquoted and store at 4°C.
 - b. Taq DNA polymerase (Boehringer Mannheim).

- c. 10X PCR Buffer II (without MgCl_2 , Boehringer Mannheim)
- d. T4g 32 Protein (Boehringer Mannheim).
- e. TS primer sequence: 5'-AATCCGTCGAGCAGAGTT-3', custom-made and anion-exchange HPLC purified.
- f. $[\alpha\text{-}^{32}\text{P}] \text{dCTP}$ (Amersham).
- g. TRAP reaction mixture contains 20 mM Tris-HCl (pH 8.3), 1.5 mM MgCl_2 , 63 mM KCl, 0.005% Tween-20, 1 mM EGTA, 50 mM each of deoxynucleoside triphosphate, 0.1 μg TS primer, 1 μg T4g32 protein, 2 U Taq DNA polymerase, 0.4 μL $[\alpha\text{-}^{32}\text{P}] \text{dCTP}$ (10 $\mu\text{Ci/mL}$, 3000 Ci/mmol), and 2 μL cell extract.

2.2.4. Telomerase Extension

PCR reaction mix (master mix) (50 μL /assay): 48 μL TRAP reaction buffer, 2 μL cell extract.

2.2.5. Electrophoresis

1. 1 L 5X TBE buffer stock: 54 g Tris base, 27.5 g boric acid, 3.72 g EDTA (pH8.0), add distilled water to 1000 mL, store at room temperature.
2. 40% polyacrylamide stock: 96.7 g acrylamide, 3.3 g acrylamide *bis* (mono/*bis* = 19:1), add distilled water to 250 mL, store at 4°C.
3. 30 mL 12% nondenaturing polyacrylamide gel: 10 mL 40% polyacrylamide stock, 6 mL 5X TBE buffer, 14 mL dH_2O , 0.075 mL 10% ammonium persulfate, 0.025 mL TEMED.
4. Polyacrylamide gel electrophoresis (PAGE) loading buffer stock: 0.25 g Bromophenol blue, 0.25 g xylene cyanol, 50 mL glycerol, add distilled water to 100 mL.

3. Methods (3,10,33)

3.1. Main Protocol of TRAP Assay

1. Tissue-sample preparation: save at -80°C until use.
2. Extraction of telomerase protein.
3. Protein conc. measurement (Bradford assay). Save at -80°C until use.
4. Telomerase extension.
5. PCR amplification.
6. Electrophoresis (11–15% polyacrylamide gel).
7. Autoradiography or phosphorimaging.
8. Data analysis.

3.2. Tissue Sample Preparation

1. Specimens from patients are obtained.
2. Tissue samples are stored at -80°C in the tissue bank until use. The procedure for preparation should be finished as quickly as possible within 1 h.
3. Tissue samples are slightly thawed quickly, and a core of the tissue is punched by skin-biopsy punch from histologically predefined areas of the sample.

4. The tissue core is quickly washed once with ice-cold washing buffer and centrifuged in full speed at 4°C. Carefully remove all the buffer, and then store at -80°C or proceed directly to the next step.

3.3. Extraction of Telomerase Protein

1. When preparing extraction, resuspend tissue core immediately in ice-cold lysis buffer in a Kontes tube.
2. The added amount of lysis buffer is adjusted 2 $\mu\text{L}/\text{mg}$ tissue sample or 200 μL / 10^5 – 10^6 cells.
3. Homogenize tissue sample with Kontes matching pestles rotated at 450 rpm, incubate for 20–25 min on ice, and centrifuge at 16,000g for 20 min at 4°C. Supernatants are aliquoted, collected, and stored at -80°C.
4. Protein conc. of the extract is measured by the Bradford assay (Bio-Rad method).
5. Telomerase in frozen extracts is stable for at least 1 yr at -80°C, and can be multiply thawed and frozen.

3.4. TRAP Assay Setup

1. Thaw reagents and store on ice.
2. The PCR tubes containing CX primer (0.05 $\mu\text{g}/\mu\text{L}$) are used as PCR reaction tubes and marked with codes including samples needed to measure and control.
3. Multiple controls are essential, including negative and positive controls. The negative controls use (in lieu of extract): lysis buffer only, and heat- or RNase-treated extract. These allow the exclusion of a false-positive result from contamination of the soln. The positive control requires an extract with known telomerase activity. This permits an elimination of contamination by RNase as the cause of a negative result.
4. Prepare TRAP reaction buffer 48 $\mu\text{L}/\text{assay}$: add the following reagents to the PCR tube with 2 μL CX primer (0.05 $\mu\text{g}/\mu\text{L}$): distilled water 23.5 μL , 10X PCR buffer II 10 μL , MgCl_2 (25 mM) 5 μL , EGTA (20 mM) 2.5 μL , dNTPs (1.25 mM) 2 μL , TS primer (0.05 $\mu\text{g}/\mu\text{L}$) 2 μL , T4 gene 32 protein (5 $\mu\text{g}/\mu\text{L}$) 0.2 μL , Taq DNA polymerase 0.4 μL , [α - ^{32}P]dCTP 0.4 μL .

3.5. Telomerase Extension

1. For telomerase extension, 2 μL cell extract (6 μg , 3 $\mu\text{g}/\mu\text{L}$) is added to the in **Subheading 3.4., step 4** PCR reaction buffer (48 $\mu\text{L}/\text{assay}$), total 50 μL , mixed well and incubated on ice for 20–30 min to allow extension of TS primer by telomerase.
2. For quantitative analysis, 5 attograms of a 150-bp internal telomerase assay standard (ITAS) is added to the reaction mix in **step 1**.
3. For serial dilution analysis (*see Subheading 3.10. Data analysis*), the 2- μL cell extract is diluted by lysis buffer at 10-fold, 100-fold, and 1000-fold, and then added to the reaction mix.
4. The TRAP assay is based on a polymerase chain reaction (PCR), in which enzymatic telomerase extracted from tissue sample adds a number of telomeric repeats (TTAGGG) onto the 3' end of an oligonucleotide primer (TS). The extended products then serve as templates and are amplified by the PCR using the upstream

primer TS and the downstream primer CX. This generates a ladder of PCR products at increments of six bases. The oligonucleotides begin at a length of 50 bp. In this protocol, the TS primer serves both as a substrate oligonucleotide for telomeric extension and as an upstream primer for PCR amplification. Using this exquisitely sensitive protocol, telomerase activity can be detected from as few as 1–10 telomerase-expressing cells (27,36).

5. Since telomerase is a ribonucleoprotein, ribonucleases (RNase)-free conditions must be maintained in all materials and equipment.
6. There are several telomerase detection kits available from commercial companies (33,34). TRAP-eze Telomerase™ Detection Kit (Oncor Inc.) has been commercialized since 1996. Telomerase PCR Elisa (Boehringer Mannheim or Perkin-Elmer) is a method which uses nonradioactive techniques. These commercial kits decrease sampling time and increase standardization.

3.6. PCR Amplification

1. 7–10 μ L mineral oil is added to each sample, and the entire sample is transferred to a thermocycler for PCR amplification.
2. PCR protocol: 94°C, 2 min; 94°C, 30 s, 50°C, 20 s, 72°C, 30 s, for 30–35 cycles; then 72°C, 5–7 min.

3.7. Electrophoresis

1. After PCR amplification is finished, add 5 μ L of PAGE loading buffer into each PCR reaction tube.
2. Load and run 25 μ L of this on 12% nondenaturing polyacrylamide gel (vertical, 17 \times 13.5 cm) in 0.5X TBE buffer until the Bromophenol blue just runs off the gel. Run time is 2–3 h using 250 V, 20 mA.

3.8. Dry Gel

1. Transfer and dry the gel in a gel dryer at 80°C, 1–1.5 h.

3.9. Visualization

1. The gel is exposed to a Kodak XB-1 film with an intensifying screen for autoradiography at –80°C overnight, or to a PhosphorImager screen using ImageQuant software at room temperature.
2. The level of telomerase activity is determined by the density of ladder signals, the number of ladders, and the ratio of the ladder to the control density (16).

3.10. Data Analysis

For a valid TRAP assay, all of the conditions in **steps 1–4** should be met:

1. The control lanes must show the appropriate outcome, or analysis of the experimental extracts cannot proceed.
2. A telomerase positive extract produces a ladder of products at six base increments starting at 50 nucleotides. Faint bands less than 50 bp in size at the low end of the gel are considered as primer dimers or other byproducts rather than a telomerase

product ladder. A commercial 50 bp DNA marker provides a molecular ladder to analyze telomerase PCR products. If the extract is telomerase negative, no band will be visible.

- 3. Visual analysis depends on the method employed in the TRAP assay: radiola-beled detection or nonradioactive detection. Radiolabeled detection requires autoradiography or PhosphorImage.

Radioisotope detection was first recommended by Kim et al. (3). Nonradioactive methods for visualization have recently been described (14,17,35). The nonradio-active technique is generally less quantitative than the radioisotopic detection.

- 4. Quantitative analysis:
 - a. To quantitate telomerase activity, an internal telomerase assay standard is used (10,14,33), and the analysis is quantitated by PhosphorImage. The molecular size of the internal standard recommended by Wright et al. is 150 bp derived from a fragment of rat myogenin (14,36). In its commercial kit, Oncor Inc. introduced another oligonucleotide sequence—a 36-bp internal standard. Either of the internal standards can be amplified by PCR. The corresponding product can be separated from the telomerase products by electrophoresis without interference with the visualization of the telomerase ladder. By comparing the signal strength of the telomerase ladder with that of the inter-nal standard, a quantitative value for the level of telomerase activity is obtained. The oligonucleotide standards also identify false-negative tumor samples resulting from Taq polymerase inhibitors.

Telomerase activity is quantitated by PhosphorImage analysis by evaluating each lane of the gels separately. The lanes are separated into two peak areas for evalua-tion: one peak for the internal amplification standard and one for the telomerase products. A ratio of telomerase products to internal standard is determined and subsequently plotted graphically using a logarithmic scale (33).

- b. Relative telomerase activity (semiquantitative analysis). Telomerase activity can also be estimated by serial dilutions. Lysate extracts containing 6 µg protein with previously verified positive activity are diluted by lysis buffer at 10X, 100X, and 1000X dilutions. The diluted extracts are then added to reac-tion buffer for TRAP assay. Comparing signals by autoradiography or PhosphorImage, relative telomerase activity can be classified into:

Dilution		10X	100X	1000X
Telomerase activity	Low degree	+	–	–
	Medium degree	+	+	–
	High degree	+	+	+

3.11. Explanations for a Telomerase Assay Result

3.11.1. For a False-Negative Result

In addition to a telomerase negative extract, there are several mechanisms for a false-negative assay:

- 1. RNA degrades quickly. Rapid freezing of tissue specimens in dry ice or liquid nitrogen is crucial to maintaining the enzymatic activity of the cells.

2. During tissue preparation with homogenization, the specimen must be kept on ice and centrifuged in full speed at 4°C.
3. Contamination with RNase in the TRAP assay will also produce a negative assay.

3.11.2. For a False-Positive Result

1. A positive telomerase assay in normal tissue may reflect contamination by occult cancer cells hidden deep in the specimen. In theory, 1–10 telomerase-positive cancer cells may result in a positive assay (27,36). In general, pathological characterization evaluates only the surface of the block. On a sample punched from a characterized block, the presence of cancer cells deep in the surface cannot be excluded. In one study of telomerase in prostate cancer and benign prostatic hyperplasia, Zhang et al. found that 4 of 11 samples taken from adjacent areas of cancer-bearing glands were telomerase-positive (10). In studies investigating telomerase activity in RCCs, 12% of 83 samples from the adjacent normal renal tissue of the cancer-bearing kidneys had telomerase activity, compared with no telomerase activity in 89 samples from either non-cancer-bearing kidneys or historically normal renal tissues. The telomerase activity may be caused by contamination by occult cancer cells hidden deep in the specimen. It is also possible that early in carcinogenesis, telomerase activation occurs prior to visible histologic alterations.
2. A false-positive assay may also occur as a result of contamination by telomerase present on inadequately cleaned equipment.

4. Notes

1. Because telomerase is a ribonucleoprotein and the standard TRAP assay is a highly sensitive PCR-based assay, it is extremely important to reduce the risk of contamination by RNase and PCR product contamination. The following rules should be applied and maintained:
 - a. Always use a clean lab coat and wear gloves. A surgical mask is also recommended for use during extractions and while setting up the reactions.
 - b. Use DEPC-treated distilled water for all solutions.
 - c. Use fresh aliquots of each component of the assay, including 50X dNTPs, TRAP buffer, Taq, primers, and DEPC-treated water.
 - d. Use RNase-free tips, tubes, and solutions.
 - e. To minimize carryover contamination, a specifically designed TRAP station is highly recommended.
2. To validate results, the same experiment should be repeated once.

References

1. Harley, C. and Villepontear, B. (1995) Telomeres and telomerase in aging and cancer. *Curr. Opin. Genet. Dev.* **5**, 249–255.
2. Blackburn, E. H. (1990) Telomeres: structure and synthesis. *J. Biol. Chem.* **265**, 5919–5921.
3. Kim, N. W., Piatyszek, M. A., Prowse, K. R., Harley, C. B., West, M. D., Ho, P. L. C., Coviello, G. M., Wright, W. E., Weinrich, S. L., and Shay, J. W. (1994)

Specific association of human telomerase activity with immortal cells and cancer. *Science* **22**, 2011–2015.

4. de Lange, T., Shiue, L., Myers, R. M., Cox, D. R., Naylor, S. L., Killery, A. M., and Varmus, H. E. (1990) Structure and variability of human chromosome ends. *Mol. Cell Biol.* **10**, 518–527.
5. Bacchetti, S. and Counter, C. M. (1995) Telomeres and telomerase in human cancer. *Int. J. Oncol.* **7**, 423–432.
6. Counter, C. M., Avilion, A. A., Lefevre, C. E., Stewart, N. G., Greider, C. W., Harley, C. B., and Bacchetti, S. (1992) Telomere shortening associated with chromosome instability is arrested in immortal cells which express telomerase activity. *EMBO J.* **11**, 1921–1929.
7. Greider, C. W. and Blackburn, E. H. (1985) Identification of a specific telomere terminal transferase activity in tetrahymena extracts. *Cell* **4**, 405–413.
8. Morin, G. B. (1989) The human telomere terminal transferase enzyme is a ribonucleoprotein that synthesized TTAGGG repeats. *Cell* **59**, 521–529.
9. Horikawa, I., Oshimura, M., and Barrett, J. C. (1998) Repression of the telomerase catalytic subunit by a gene on human chromosome 3 that induced cellular senescence. *Mol. Carcinog.* **22**, 65–72.
10. Zhang, W., Kapusta, L. R., Slingerland, J. M., and Klotz, L. H. (1998) Telomerase activity in prostate cancer, prostatic intraepithelial neoplasia, and benign prostatic epithelium. *Cancer Res.* **58**, 619–621.
11. Harley, C. B., Futcher, A. B., and Greider, C. W. (1990) Telomeres shorten during aging of human fibroblasts. *Nature* **345**, 458–460.
12. Rhyu, M. S. (1995) Telomeres, telomerase, and immortality. *J. Natl. Cancer Inst.* **87**, 884–894.
13. Wright, W. E. and Shay, J. W. (1992) The two-stage mechanism controlling cellular senescence and immortalization. *Exp. Gerontol.* **27**, 383–389.
14. Rohde, V., Sattler, H. P., Oehlenschlaeger, B., Forster, S., Zwergel, T., Seitz, G., and Wullich, B. (1998) Genetic changes and telomerase activity in human renal cell carcinoma. *Clin. Cancer Res.* **4**, 197–202.
15. Selli, C., Hinshaw, W. M., Woodard, B. H., and Paulson, D. F. (1983) Stratification of risk factors in renal cell carcinoma. *Cancer* **52**, 899–903.
16. Mehle, C., Piatyszek, M. A., Ljungberg, B., Shay, J. W., and Roos, G. (1996) Telomerase activity in human renal cell carcinoma. *Oncogene* **13**, 161–166.
17. Kyo, S., Kunimi, K., Uchibayashi, T., Namiki, M., and Inoue, M. (1997) Telomerase activity in human urothelial tumors. *Am. J. Clin. Pathol.* **107**, 555–560.
18. Gelmini, S., Caldini, A., Becherini, L., Capaccioli, S., Pazzagli, M., and Orlando, C. (1998) Rapid, quantitative nonisotopic assay for telomerase activity in human tumors. *Clin. Chem.* **44**, 2133–2138.
19. Kinoshita, H., Ogawa, O., Mitsumi, K., Kakehi, Y., Terachi, T., and Yoshida, O. (1998) Low frequency of positive telomerase activity in a chromophobe subtype of renal cell carcinoma. *J. Urol.* **159**, 245–251.
20. Yoshida, K., Sakamoto, S., Sumi, S., Higashi, Y., and Kitahara, S. (1998) Telomerase activity in renal cell carcinoma. *Cancer* **83**, 760–766.

21. Yoshida, K., Sugino, T., Tahara, H., Woodman, A., Bolodeoku, J., Nargund, V., Fellows, G., Goodison, S., Tahara, E., and Tarin, D. (1996) Telomerase activity in bladder carcinoma and its implication for noninvasive diagnosis by detection of exfoliated cancer cells in urine. *Cancer* **89**, 362–269.
22. Mao, L., El-Naggar, K., Fan, Y., Lee, J. S., Lippman, S. M., Kayser, S., Lotan, and Hong, W. K. (1996) Telomerase activity in head and neck squamous cell carcinoma and adjacent tissues. *Cancer Res.* **56**, 5600–5604.
23. Muller, M., Heicappell, R., Krause, H., Sachsinger, J., Porsche, C., and Miller, K. (1999) Telomerase activity in malignant and benign renal tumors. *Eur. Urol.* **35**, 249–255.
24. Counter, C. M., Hirte, H. W., Bacchetti, S., and Harley, C. B. (1994) Telomerase activity in human ovarian carcinoma. *Proc. Natl. Acad. Sci. USA* **91**, 2900–2904.
25. Chadeneau, C., Hay, K., Hirte, H. W., Gallinger, S., and Bacchetti, S. (1997) Telomerase activity associated with acquisition of malignancy in human colorectal cancer. *Cancer Res.* **58**, 1863–1867.
26. Hiyama, K., Hiyama, E., Ishioka, S., Yamakido, M., Inai, K., Gazdar, A. F., Piatyszek, M. A., and Shay, J. W. (1995) Telomerase activity in small-cell and non-small-cell lung cancers. *J. Natl. Cancer Inst.* **87**, 895–902.
27. Kim, N. W. (1997) Clinical implications of telomerase in cancer. *Eur. J. Cancer* **33**, 781–786.
28. Mehle, C., Lindblom, A., Ljungberg, B., Stenling, R., and Roos, G. (1998) Loss of heterozygosity at chromosome 3p correlates with telomerase activity in renal cell carcinoma. *Int. J. Oncol.* **13**, 289–295.
29. Horikawa, I., Oshimura, M., and Barrett, J. C. (1998) Repression of the telomerase catalytic subunit by a gene human chromosome 3 that induces cellular senescence. *Mol. Carcinog.* **22**, 65–72.
30. Ohmura, H., Tahara, H., Suzuki, M., Ide, T., Shimizu, M., Yoshida, M. A., Tahara, E., Shay, J. W., Barrett, J. C., and Oshimura, M. (1995) Restoration of the cellular senescence program and repression of telomerase by human chromosome 3. *Jpn. J. Cancer Res.* **86**, 899–904.
31. Rimessi, P., Gualandi, F., Morelli, C., Trabanelli, C., Wu, Q., Possati, L., Montesi, M., Barrett, J. C., and Barbanti-Brodano, G. (1994) Transfer of human chromosome 3 to an ovarian carcinoma cell line identifies 3 regions on 3p involved in ovarian cancer. *Oncogene* **9**, 3467–3473.
32. Uzawa, N., Yoshida, M. A., Oshimura, M., and Ikeuchi, T. (1995) Suppression of tumorigenicity in three difference cell lines of human oral squamous cell carcinoma by introduction of chromosome 3p via microcell mediated chromosome transfer. *Oncogene* **11**, 1997–2004.
33. Holt, S. E., Norton, J. C., Wright, W. E., and Shay, J. W. (1996) Comparison of the telomeric repeat amplification protocol (TRAP) to the new TRAP-eze telomerase detection kit. *Methods Cell Sci.* **18**, 237–248.
34. Muller, M., Krause, H., Heicappell, R., Tischendorf, J., Shay, J. W., and Miller, K. (1998) Comparison of human telomerase RNA and telomerase activity in urine for diagnosis of bladder cancer. *Clin. Cancer Res.* **4**, 1949–1954.

35. Heine, B., Hummel, M., Muller, M., Heicappell, R., Miller, K., and Stein, H. (1998) Non-radioactive measurement of telomerase activity in human bladder cancer, bladder washings, and in urine. *J. Pathol.* **184**, 71–76,
36. Wright, W. E., Shay, J. W., and Piatyszek, M. A. (1995) Modifications of a telomeric repeat amplification protocol (TRAP) result in increase reliability, linearity and sensitivity. *Nucleic Acids Res.* **23**, 3794–3795.

Suggested Reading

- Kim, N. W., Piatyszek, M. A., Prowse, K. R., Harley, C. B., West, M. D., Ho, P. L. C., Coviello, G. M., Wright, W. E., Weinrich, S. L., and Shay, J. W. (1994) Specific association of human telomerase activity with immortal cells and cancer. *Science* **22**, 2011–2015.
- Holt, S. E., Norton, J. C., Wright, W. E., and Shay, J. W. (1996) Comparison of the telomeric repeat amplification protocol (TRAP) to the new TRAP-eze telomerase detection kit. *Methods Cell Sci.* **18**, 237–248.

Comparative Genomic Hybridization

Joseph C. Presti, Jr.

1. Introduction

Comparative genomic hybridization (CGH) allows a genome-wide survey of the relative copy number of tumor DNA in a single hybridization. The tumor-cell DNA (Test DNA) is hybridized together with a sex-matched normal DNA (Reference DNA) onto normal metaphase spreads. Test DNA and Reference DNA are labeled with fluorochrome-conjugated reagents of different color, thereby allowing the detection of genetic imbalance in the abnormal cells.

Critical factors in the entire process that determine the quality of the hybridization are the metaphase slides and the Test DNA. The notes added after each section in this chapter provide valuable hints for achieving a high-quality hybridization. High-quality CGH shows good DAPI chromosomal banding, evenly hybridized green and red colors along the length of the chromosomes, and minimal background staining.

CGH is a straightforward method for the first screening of genetic changes in a specimen. Its resolution is limited to the 10 Mb range. Other techniques can be applied for further characterizing the determined genetic changes, like FISH or repeating the CGH hybridization of the same DNA probe onto a bacterial artificial chromosome contiguous (BAC-contig) of the region of interest instead of the metaphase spread.

Here we describe the application of CGH to DNA extracted from paraffin-embedded blocks through microdissection of tumor areas identified by a pathologist.

2. Materials

2.1. Chromosome Preparation from Cultured Peripheral Blood Cells

1. Phytohemagglutinin: 100X (Gibco-BRL).
2. Hank's balanced salt solution (HBSS)
3. Methotrexate: dissolve 0.5 mg methotrexate (Sigma) in 100 mL HBSS. Sterilize by filtration through a 0.22- μ m filter.
4. Thymidine: dissolve 25 mg thymidine (Sigma) in 100 mL HBSS. Sterilize by filtration through a 0.22 μ m filter.
5. colcemid: 10 μ g/mL (Gibco-BRL).
6. KCl hypotonic solution: 75 mM KCl.
7. Methanol/acetic-acid: HPLC-grade absolute methanol/glacial acetic-acid (3:1).

2.2. DNA Microdissection from Paraffin Blocks

1. Xylene.
2. Methyl green.
3. PCR DNA extraction buffer: 10 mM Tris-HCl (pH 8.0), 1.5 mM $MgCl_2$, 50 mM KCl, 1 mg/mL gelatin, 0.5% Tween-20, 0.4 mg/mL proteinase K (Sigma).
4. Proteinase K (PK): Store as 20 mg/mL aliquots at $-20^{\circ}C$; can be refrozen a few times.

2.3. Degenerate Oligonucleotide Primer-Polymerase Chain Reaction

1. DOP primer: 5'-CCG-ACT-CGA-GNN-NNN-NAT-GTG-G-3'. Use at 1.4 mM.
2. Topoisomerase-1: Promega (10 U/ μ L).
3. Sequenase-Vers 2 (USB/Amersham): Use at 1:8 with Sequenase dilution buffer.
4. *Taq* polymerase (Boehringer): 5 U/ μ L (use 2 U/sample).
5. dNTPs (Boehringer): use stock of 100 mM each.
6. 10X *Taq* buffer (Boehringer): 100 mM Tris-HCl, 2 mM $MgCl_2$, 500 mM KCl, 1 mg/mL gelatin.
7. 1X PCR buffer: 10 mM Tris-HCl (pH 8.0); 1.5 mM $MgCl_2$, 50 mM KCl, 0.2 mM dNTPs, 2 μ M DOP primer.
8. Preamplification mix: 1X PCR buffer containing 0.2 μ L/sample $MgCl_2$ (50 mM) and 0.1 μ L/sample topoisomerase.

2.4. Nick-Translation (NT)

1. BSA: 10 mg/mL (Gibco-BRL).
2. 10X A4: 200 μ M each dATP, dCTP, and dGTP (Gibco-BRL); 500 μ M Tris-HCl, pH 7.2, 200 μ M $MgCl_2$; 100 mM mercaptoethanol; 100 μ g/mL BSA (Gibco-BRL). Store at $-20^{\circ}C$.
3. FITC-dUTP: 25 nm (Dupont/NEN).
4. Dig-11-dUTP: 25 nm (Boehringer Mannheim).
5. Biotin-dATP: 25 nm (Gibco-BRL).
6. DNA Pol-1: 10 U/ μ L (from Gibco-BRL (BIONICK kit)).
7. 10X enzyme mix (from Gibco-BRL (BIONICK kit)).
8. DNA Pol-1/DNase I: (from the "slow enzyme" mix from Gibco-BRL (BIONICK kit)).

2.5. Hybridization

1. High-quality human metaphase preparations from a male donor (*see Subheading 2.1.*).
2. *Cot*I-DNA: 1 mg/mL (Gibco). It is recommended to measure the conc.
3. MM1CGH: 50% formamide in 2X SSC pH 7.0 with 10% (w/v) dextran sulfate (Sigma).
4. Denaturation Solution (DN): 70% formamide in 2X SSC, pH 7.0.
5. 20X SSC: 3 M NaCl, 0.3 M NaCitrate, pH 7.0.

2.6. Washing

1. Triton X-100.
2. Hybridization wash solution: 50% formamide in 2X SSC, pH 7.0.
3. PN: Mix solution A and solution B until pH 8.0 is reached (ratio approx 1:5). Solution A: 0.1 M Na₂HPO₄ 0.1% Nonidet P-40. Solution B: 0.1 M NaH₂PO₄ 0.1% Nonidet P-40.
4. Preblock solution: 4X SSC/1% BSA.
5. Rhodamine-conjugated anti-digoxigenin: 1 µg/mL (Boehringer Mannheim).
6. FITC avidin: 5 µg/mL (Vector Laboratories).
7. 4, 5-Diamino-2-phenyl-indole (DAPI): 100 µg/mL in dH₂O, kept in aliquots at -20°C protected from the light.
8. DAPI in antifade: 0.1-0.2 µg/mL DAPI in phenylenediamine antifade mounting medium.

2.7. Imaging

1. Fluorescence microscope equipped with digital imaging system.
2. SCIL-image software package.

3. Methods

3.1. Chromosome Preparation from Cultured Peripheral Blood Cells

T-lymphocytes in whole blood are stimulated with phytohemagglutinin. The proliferating cells are synchronized, exposing them to methotrexate for 17 h followed by a thymidine release. Metaphase cells are obtained by treating cell cultures with Colcemid—which arrests cells in the mitosis phase, leading to an accumulation of cells in metaphase. The cells are treated with a hypotonic KCl solution, fixed with methanol/acetic acid, spread onto ethanol-washed slides, and air dried. Examine the slides for good chromosome spreading and morphology by phase-contrast microscopy; the cell density should not be too high, many well-spread metaphases, little cytoplasm around the metaphases and little debris. The slides are optimized for CGH through an aging process, keeping them in a dry container at -20°C for several weeks. The dropping can be optimized by changing the settings of a thermotron.

3.2. DNA Microdissection from Paraffin Blocks

Methyl green is a water soluble stain used for staining of microdissected slides instead of hematoxylin and eosin (H&E), which has been found to interfere with DOP-PCR amplification. It is usually only necessary to stain and microdissect one slide, but two slides are used when the target is less than 1 mm in diameter.

3.2.1. Deparaffinization

1. Xylene 2X, 3 min each.
2. 100% ethanol, 2 min.
3. 95% ethanol, 2 min.
4. 70% ethanol, 2 min.
5. 50% ethanol, 2 min.
6. dH₂O, 2 min.

3.2.2. Methyl Green Staining

1. 0.1–1% Methyl green (approx 15–60 se).
2. The section should not be too dark. The methyl green concentration can be varied if sections are generally too dark or too light. It is advisable to start with a lower concentration.
3. dH₂O 1–5 min (depending on how blue/green the tissue is).
4. Air-dry upright.
5. The slide is now ready for photographing and microdissection. It is advisable to use soon, but the slide can be stored for a few wk if necessary.

For each tumor, two adjacent 5- μ sections are cut from the paraffin block. One section is stained with hematoxylin and eosin, and the second section is stained with methyl green (0.1%). All sections are photographed. Using the adjacent H&E section for orientation, the tumor area for CGH analysis is analyzed. The selected areas are recovered by carefully scraping away surrounding tissue with a disposable #11 scalpel blade. A new #15 blade with a droplet of PCR DNA extraction buffer is used to transfer desired regions into sterile 0.5-mL tubes containing 15 μ L of PCR DNA extraction buffer (additional 5 μ L PCR DNA extraction buffer for each mm² of microdissected tissue.). Mineral oil (20 μ L) is placed over the sample and incubated at 55°C overnight in a shaking water bath. Fresh proteinase K (0.3 μ L of 20 mg/mL stock) is added daily through the oil for an additional 2 d. Proteinase K is inactivated at 95°C for 15 min. DNA is separated from the oil and transferred into new tubes. All steps are handled carefully to avoid crossover contamination for subsequent PCR reactions.

3.3. Degenerate Oligonucleotide Primer (DOP)-PCR CGH

Microdissected DNA is amplified according to Guan et al. (1). In cases using less than 1 mg DNA, the DNA is amplified based on the DOP-PCR protocol of Willenbacher et al. (2). Samples are amplified in duplicate, in separate PCR reactions.

Briefly, a 1–2 μL aliquot of microdissected DNA is added to 5 μL of 1X PCR buffer containing 0.2 μL 50 mM MgCl_2 and 0.1 μL TOPOisomerase I (Promega), covered with oil. The samples are incubated at 37°C for 30 min, then at 96°C for 10 min. The TOPO pretreatment is followed by 5 cycles of sequenase treatment (1 min denaturing at 94°C; 2–5 min annealing at 30°C, 3-min extension at 37°C). The sequenase (USB) (0.3 μL of a 1:8 dilution) is added through the oil during the annealing step for each cycle. All samples must have at least 2 min of annealing, but no more than 5 min. Preamplification is followed by 1 cycle at 95°C for 10 min, and 45 μL of 1X PCR buffer with 2 U *Taq* DNA Polymerase (Boehringer) is added during the last 5 min through the oil, followed by additional oil overlay. This is followed by 35 cycles at 94°C for 1 min, 56°C for 1 min, and 72°C for 3 min, with a final extension at 72°C for 5 min.

PCR-amplified DNA (3 μL) is run on 1% agarose ethidium bromide-stained gel to determine the resulting PCR product size. Each PCR experiment includes samples of normal female genomic DNA (isolated from peripheral blood), MPE600 (breast-cancer-cell line with known CGH aberrations, *see* Fig. 1), and a blank to check for PCR contamination. Fifty nanograms of reference or MPE600 cell-line DNA yield approx 2–3 μg of amplified DNA, ranging in size from 200 bp–6 kb. Microdissected DNA yields up to 1 μg of PCR product, with sizes averaging approx 600 bp in size (ranging from 100 bp–2 kb).

3.4. Nick Translation of DNA for CGH

The principle of nick translation (NT) is the nicking the DNA with DNAses and incorporating modified nucleotides through the simultaneous 5'-3' exonucleolytic activity and 3'-5' elongation activity of DNA polymerase I. These modified nucleotides allow the detection of the probe, which can be:

1. Direct: The nucleotides are labeled with a fluorochrome, like FITC-dUTP, and visualized directly under the fluorescence microscope after the hybridization.
2. Indirect: The NT incorporates modified nucleotides, such as Dig-11-dUTP and biotin-dATP, which are detected indirectly through an additional reaction.

The size of the nick-translated probes is probably the most important aspect for CGH success. Depending on the size of the initial DNA the reaction is varied from the standard protocol (*see* Table 1), changing the enzyme (fast or low activity), its amount and the incubation time. Refer to **Subheading 4** for details.

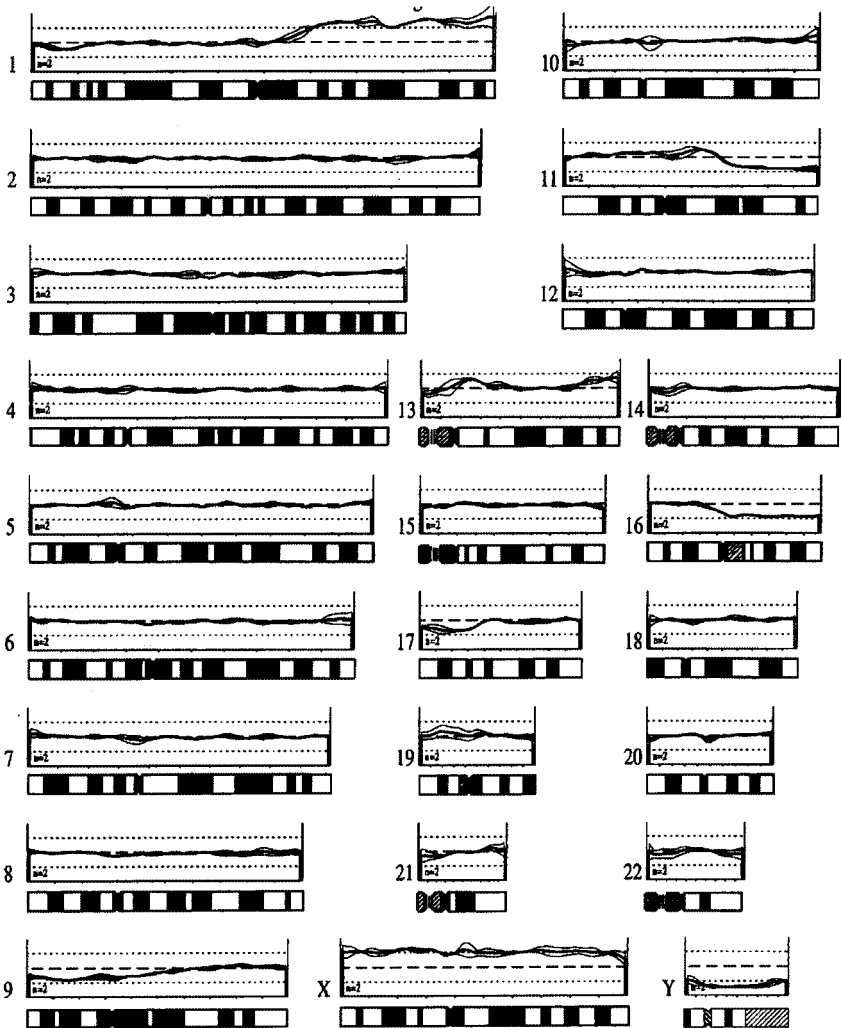


Fig. 1. CGH profile showing the changes of the control cell line MPE600: gains of 1q,11q13,13q12, 13q32-qter and losses of 9p, 11q14-qter, 16q and 17p. Test and Reference DNA are not sex matched, therefore the X-chromosome appears gained and the Y-chromosome appears to be lost.

1. Prepare reaction mixtures per 50 μ L adding enzymes last.
2. Incubate reaction mixtures for 60 min at 15°C.
3. Stop reaction by heating at 70°C for 15 min.
4. Run 3–5 μ L of probe on 1% agarose gel to check size. Product should run as a smear ranging from 0.3–2.3 kb.
5. Store probes at –20°C.

Table 1
Standard Protocol for Nick Translation

Label	Biotin-dATP	Digox-dUTP	FITC-dUTP	Texas Red dUTP
10X biotin dNTP	5 μ L	0 μ L	0 μ L	0 μ L
10X A4 dNTP	0 μ L	5 μ L	5 μ L	5 μ L
Modified dUTP	0 μ L	1 μ L	1 μ L	1 μ L
DNA Pol-1	1 μ L	1 μ L	1 μ L	1 μ L
DNA Pol/ DNase (additional)	(2.5–5 μ L)	(2.5–5 μ L)	(2.5–5 μ L)	(2.5–5 μ L)
DNA (1 μ g) from 50 μ L DOP-PCR	25 μ L fresh or 45 μ L microdissected	25 μ L fresh or 45 μ L microdissected	25 μ L fresh or 45 μ L microdissected	25 μ L fresh or 45 μ L microdissected
ddH ₂ O				
Total reaction volume	50 μ L	50 μ L	50 μ L	50 μ L

3.5. Hybridization

DNA from tumor and a sex-matched normal control are labeled by NT with fluorochrome-conjugated reagents of different color, e.g., Did-11-dUTP/anti-dig rhodamine (tumor) and fluorescein -14-dUTP (normal). They are mixed with unlabeled Cot-1 DNA to block binding to repetitive sequences, and are then denatured and hybridized to a normal male lymphocyte metaphase spread for 2–3 d at 37°C. To check the hybridization quality for each set of samples, a NT PCR normal control and MPE600 (breast-cancer-cell line with known CGH aberrations, *see Fig. 1*) are hybridized against the same reference PCR probe used against the test samples. To confirm results, it is recommended to perform replicate hybridizations using other label combinations. The labels for test and normal DNAs are reversed when using fresh DNA. This explains the term “inverse” CGH for the replicate CGH reaction. For microdissected DNA the label Did-11-dUTP/antidig rhodamin works best. Therefore, we recommend to change in the “inverse” CGH only the reference DNA label using biotin-dUTP/FITC-avidin instead of fluorescein-14-dUTP. Artifacts appear as losses of chromosomes 1p, 19, and 22 and gains of chromosomes 4, 9p, and 13q (*see Fig. 2*). If appreciable artifact occurs, then alternative labels are used—such as indirect CGH (*see Subheading 3.3.*).

3.5.1. Reprecipitate DNAs

1. Add the following DNAs to a 1.5-mL centrifuge tube, mixing with pipet as shown in **Table 2**.
2. Add 1/10th vol of 3M Na acetate, mixing with pipet.

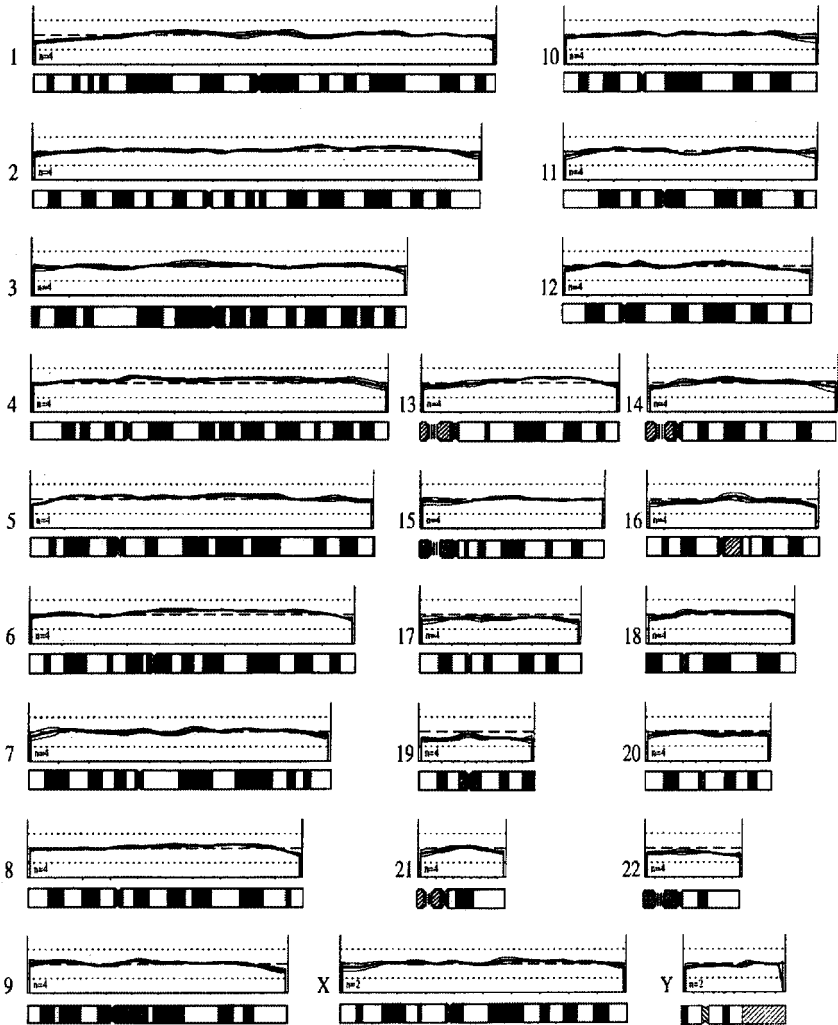


Fig. 2. CGH profile of a normal control showing typical artifacts, losses of 1p33-pter, 19 and 22 and gains of 4 and 13q21-q33.

3. Add 2.5X (original) vol 100% EtOH to precipitate DNA, and vortex gently.
4. Spin 30 min at 14,000 rpm, 4°C.
5. Decant supernatant; blot dry, being careful to avoid DNA pellet.
6. Add 10 μ L of MM1CGH/H₂O mix (70% MM1CGH/30% H₂O).
7. Carefully dissolve with pipet, and gently vortex.
8. Quickly spin (1 s) to bring vol to bottom of tube.

Table 2
Hybridization Mixture

Direct CGH	“Inverse” CGH
20 µg Cot-I DNA (approx 20 µL)	20 µg Cot-I DNA (approx 20 µL)
approx 200 µg digoxigenin-labeled DNA (approx 20–40 µL of DOP-PCR)	approx 200 ng digoxigenin-labeled DNA (approx 20–40 µL of DOP-PCR)
approx 200 ng FITC-labeled DNA (approx 20–40 µL of DOP-PCR)	approx 200 DNA biotin-labeled DNA (approx 20–40 µL of DOP-PCR)

3.5.2. Denature Slides

1. Select slides with spots in a good location, with plenty of metaphases, and little or no cytoplasm around the metaphases or nuclei.
2. Mark each spot on the back of the slide with a diamond pen.
3. Prewarm slide on 37°C hot plate for 1 min.
4. Denature prewarmed slides in 70% formamide/2X SSC for 2.5–10 min at 73°C inside a Coplin jar (time will vary depending on slide batch).
5. Denature no more than three slides at a time.
6. Dehydrate slides through 70, 85, and 100 ethanol, 2 min each.
7. Wipe the backs of each slide and air-dry upright on kimwipes.

3.5.3. Hybridization

1. Place slides on 37°C warmer 1–2 min before adding probes.
2. Denature probe mix at 70–75°C for 5 min.
3. Apply denatured probe immediately onto warmed slide on the hot plate.
4. Coverslip (18 mm) and seal with rubber cement.
5. Let rubber cement dry 5 min on warmer.
6. Incubate for 2–3 d at 37°C in a humid chamber.

3.6. Washing and Staining

Slides are washed to remove unbound probe, and DNA is counterstained with DAPI (blue) to produce a banding pattern used for chromosome identification. The relative binding of tumor (red; Dig-11-dUTP) and normal (green; FITCdUTP) DNAs along each metaphase chromosome reflects the relative abundance of DNA sequences in the tumor. Thus, DNA sequences that were overrepresented in the tumor show relatively increased red fluorescence, and those regions that were underrepresented in the tumor appear with relatively decreased red fluorescence. The labeled normal DNA serves as a control for regional variations in the ability to hybridize to the target chromosomes. This DNA can be taken from a different source than the tumor DNA. “Inverse” labeling CGH is performed on all samples (tumor DNA NT with Dig-11-dUTP and normal DNA with Biotin dATP) for confirmation of all alterations.

The fluorochromes are light-sensitive, thus, it is recommended to keep the exposure to light of the slides at a minimum. After removing the coverslip and going through the washing steps allow the slides to dry evenly. Apply DAPI on completely dried slides. The slides can be kept for 1–2 wk in the refrigerator before acquiring the images.

1. Remove rubber cement. Slide coverslips off gently.
2. Wash three times for 12 min each at 45°C in 50% formamide/2XSSC.
3. Wash once for 10 min at 45°C in 2X SSC.
4. Wash once for 10 min at RT in 2X SSC.
5. Remove slide, quickly blot back (to remove excess liquid).
6. Add 85 μ L of 4X SSC/1% BSA preblock solution (kept in aliquots in freezer).
7. Gently cover with a 24/50 mm coverslip.
8. Incubate for 5 min, then gently remove coverslip.
9. Add 85 μ L of a mix of anti-digoxigenin-rhodamine/FITC avidin (at 1:200/1:400 in preblock solution).
10. Gently cover with a 24/50 mm coverslip.
11. Incubate for 45–60 min (protecting from light). Gently remove coverslip.
12. Wash 10 min each at RT in 4X SSC, then 4X SSC/0.1%Triton, then 4X SSC.
13. Rinse slides two times in ddH₂O for 5–10 min each, air-dry upright.
14. Apply 8.0 μ L of 0.2 μ g/mL DAPI in antifade (22-mm coverslip).
15. Let sit at RT for at least 2 h. Do not collect images the same day as Day 2 staining.

3.7. Imaging

A quantitative image-processing system is used for the acquisition and processing of sequential three-color images using filters for green (fluorescein), red (Texas red), and blue (DAPI) fluorescence. Software programs based on the SCILImage software package are used to display and overlay multicolor images in pseudocolors, and to contrast-stretch the images to enhance green and red color differences and the blue DAPI banding. Green-to-red ratios of each chromosome are then plotted as a function of distance from the *p* terminus to *q* terminus (left to right). A semiautomatic karyotyping based on the fluorescence banding pattern in the DAPI image identifies the specific chromosomes. Generally, four ratio profiles are averaged for each chromosome (two separate metaphases) to reduce noise. The metaphases should show little chromosomal condensation, few overlapping or touching chromosomes with relatively straight conformation, minimal background staining, and a smooth, nongranular hybridization pattern. Centromeric and heterochromatic regions are excluded from interpretation. Green-to-red ratios greater than 1.20 are considered as gains of genetic material, whereas ratios less than 0.8 are considered as losses of genetic material (3). Imbalances are scored by CGH only if they are present in both hybridizations (CGH and inverse CGH).

Table 3
Recommended Digest Mixtures

Sample	DNA	Enzyme	Enzyme vol.	Time	Probe size
PCR amplified Fresh DNA (50 μ L)	25 μ L	10X or slow	3–5 μ L	60 min	100–2000 bp
PCR amplified microdissected DNA(50 μ L)	40 μ L	10X or slow	3–5 μ L	60 min	100–600 bp

4. Notes

1. Since the metaphase spread is the most critical factor in CGH, we recommend using a controlled chamber for achieving consistent metaphase quality during slide dropping.
2. The cell-culture synchronization yields a greater number of mitotic cells, and will result in metaphases with similar chromosome lengths.
3. Metaphase slides are commercially available from Vysis.
4. For keeping the times in the sequenase step, do not amplify more than 13 tubes at a time.
5. Remember to include sufficient normal DNA reactions for the planned CGH, a positive PCR/CGH control, and a PCR blank negative control.
6. For PCR of fresh DNA (from unfixed material), 50 ng input DNA is used per 50 μ L PCR reaction.
7. For PCR of paraffin DNA (from formalin-fixed/paraffin-embedded tissue), it is best to add only 1 μ L of DNA per 50 μ L PCR reaction. The reaction may be inhibited (less product) if more than 2 μ L of the DNA extraction solution is added.
8. Adjust probe size to a smear between 0.1–1.5 kb by repeating the NT. PCR products are usually smaller, ranging from 0.1–0.6 kb.
9. The 10X enzyme is the “fast enzyme.” If the 10X enzyme is cutting the DNA too small, then try varying the amount and/or time of incubation. The standard conc. for fresh DNA is 3–5 μ L of the 10X enzyme mix for 60 min. Incorporation decreases appreciably below 2 μ L or less than 40 min. If the mix is still cutting too small with these minimum amounts, then try the “slow” enzyme. The “slow” enzyme is less active than the 10X enzyme mix from the BioNick kit. If you need to use this, then try 60 min using 5 μ L first, and adjust conditions as needed. This enzyme is better for smaller DNA and/or degraded DNA.
10. The recommended volume of enzyme and time of incubation are shown in **Table 3**.
11. The conc. of the *Cot*I-DNA should be measured before using.
12. The amount of probe DNA used can vary, and should be adjusted depending on the intensity of the product. Best results are obtained using the following vol of the approx 1 μ g/50 μ L NT product:
PCR product from fresh DNA: 20 μ L. Depending on the label use 20 μ L of FITC or biotin-labeled probe, or 15 μ L of Texas red-labeled probe, or 10 μ L of dioxigenin-labeled probe for each CGH reaction.

PCR product from microdissected DNA: 45 μ L. If the digoxigenin-labeled probe size is good (>600 bp), only 30–40 μ L of the probe still yields a good CGH result.

13. It is important to adhere closely to the denaturation times. Thus, prepare the slides in batches of no more than three at a time.
14. The quality of the slides used is the second major variable in CGH. Each new batch should be tested under different conditions, such as adjusting denaturation time and temperature.

References

1. Guan, X. Y., Trent, J. M., and Meltzer, P. S. (1993) Generation of band-specific painting probes from a single microdissected chromosome. *Hum. Mol. Genet.* **2**, 1117–1121.
2. Willenbacher, R. F., Zelman, S. J., Ferrell, L. D., Moore, D. H., Waldman, F. M. (1997) Chromosomal alterations in ulcerative colitis-related neoplastic progression. *Gastroenterology* **113**, 791–801.
3. Piper, J., Rutovitz, D., Sudar, D., Kallioniemi, A., Kallioniemi, O., Waldman, F. W., Gray, J. W., and Pinkel, D. (1995) Computer image analysis of comparative genomic hybridization. *Cytometry* **19**, 10–26.

Analyzing the *FHIT* Gene by RT-PCR, Western Blotting, and Immunohistochemistry

Raffaele Baffa, Coleen M. Calviello, Teresa Druck,
and Leonard G. Gomella

1. Introduction

FHIT (fragile histidine triad) is a tumor-suppressor gene located at chromosome band 3p14.2. The genomic locus, which is greater than 1 Mb, contains 10 small exons that make up the 1.1-kb *FHIT* cDNA. The coding region starts in exon 5 and stops in exon 9, producing a 16.8-kDa cytoplasmic protein. The *FHIT* locus contains the hereditary renal cell carcinoma (RCC) t(3;8) translocation, and also encompasses the *FRA3B* common fragile region (for review, *1*). Numerous studies have proven that the *FHIT* gene is inactivated by deletions in both primary tumors and cell lines derived from head and neck, stomach, lung, and kidney cancers (*2–6*). Since *FHIT* is inactivated in so many cancers, it is essential to learn its normal function and analyze how the loss of its function contributes to the progression and development of cancer. For example, an early event in the lungs of a smoker is breakage at the *FHIT* locus, causing a reduced or absent *FHIT* protein expression in the preneoplastic lesions. Compensation for the functional loss of *FHIT* via a recombinant, nonfragile *FHIT* gene may prove therapeutically useful (*7,8*). Our studies have also shown that the *FHIT* gene is altered or absent in the majority of transitional-cell carcinoma (TCC) cases of the bladder examined (*9*). Through the utilization of molecular techniques such as those described here, *FHIT* alterations may be detected in an early stage of cancer, and thus prove to be a useful diagnostic tool to prevent cancer progression.

FHIT inactivation is easily observed by immunological and molecular methods such as reverse transcription-polymerase chain reaction (RT-PCR); Southern, Northern, and Western blotting; and immunohistochemistry.

RT-PCR allows the detection of amplification products from cancer-cell mRNA with *FHIT* exon deletions. Cancer-derived cell lines and/or tumors, which may have *FHIT* deletions, frequently express aberrant RT-PCR products, and do not generate the normal size *FHIT* product. *FHIT* protein alterations are frequently detectable in Western analysis when the protein band is absent or barely discernable in those cell lines isolated from carcinomas. Immunohistochemical studies of *FHIT* expression in human cancers show that *FHIT* is strongly detected in normal epithelial cells. Those sections which show a reduction in the expression of *FHIT* generally exhibit altered cell morphology. A direct correlation between DNA and RNA alterations and low expression or absence of *FHIT* protein has been demonstrated (1,10). All of the techniques—RT-PCR, Southern, Northern, and Western blotting, and immunohistochemistry—are extensively utilized in the exploration of *FHIT* abnormalities. This chapter examines the most commonly utilized procedures: RT-PCR, Western blotting, and immunohistochemistry.

2. Solutions

2.1. Reverse Transcription (RT) Protocol

1. Aerosol pipet tips.
2. Gloves.
3. RNase-free 1.5-mL Eppendorf tubes.
4. 5 μ g total RNA.
5. DEPC (diethyl pyrocarbonate) water.
6. Reverse transcriptase (e.g., Superscript, Gibco, Gaithersburg, MD).
7. Oligo mix: 10 μ L .5 μ g/ μ L oligo-dT (12-18-mer), 10 μ L random primers 50 ng/ μ L.
8. 10X PCR buffer: 100 mM Tris-HCl, 500 mM KCl, 150 mM MgCl₂.
9. dNTP mix: add equal vol of 10 mM stocks of dATP, dGTP, dCTP, dTTP.
10. Miscellaneous mix: 4 μ L 10X PCR buffer, 2 μ L 0.1 M DTT, 1 μ L dNTP mix.
11. Ice.
12. Water bath (70°C, 42°C).
13. Thermal cycler.

2.2. PCR Protocol

1. cDNA (e.g., RT product).
2. 10X PCR buffer: 100 mM Tris-HCl, 500 mM KCl, 150 mM MgCl₂.
3. dNTP mix: add equal vol of 10 mM stocks of dATP, dGTP, dCTP, dTTP.
4. *Taq* polymerase (5 U/ μ L).
5. Forward and reverse primers (20 ng/ μ L) (**Table 1**).
6. Sterile distilled water.
7. Ice.
8. Thin-walled PCR tubes (200 or 500 μ L).
9. Thermal cycler.
10. Mineral oil (if thermal cycler does not have a heated lid).

Table 1
Primer Sequences

Sequence (5'-3')	Primer name	Orientation	Position (nucleotides)
CATCCTGGAAGCTTTGAAGCTCA	5U2	Forward	-222 to -200
TCCGTAGTGCTATCTACAT	5U1	Forward	-162 to -144
TCAACTGTGAGGACATGTCG	3D7	Forward	-14 to -5
AACATTTCCATGGGACCTCTTC	3D5	Forward	212-232
CTATGAGGAGCTCCAGAAAC	3D3	Forward	339-358
TCACTGGTTGAAGAATACAGG	3D2	Reverse	579-592
CATGCTGATTCAAGTTCCTCTTGG	3D1	Reverse	523-545
TCTGATTCAAGTTCCTCTTGG	3D4	Reverse	376-395
ATGTTTTTCCACCACTGTCC	3D6	Reverse	197-216
TGAGATGTTGGCCAAATCTG	3D8	Reverse	8-27

Primers 5U1, 5U2, 3D1, and 3D2 are the primers described by Ohta (12).

2.3. Analysis of PCR Products by Gel Electrophoresis

1. 10X Tris-borate electrophoresis buffer (TBE): 108 g Tris base, 55 g boric acid, and 40 mL of 0.5 M EDTA pH 8 (11). Adjust volume to 1 L with distilled water. Store at room temperature.
2. 6X loading buffer: 0.25% bromophenol blue, 0.25% xylene cyanol, 30% glycerol.
3. Agarose.
4. Ethidium bromide (1% solution).
5. Horizontal gel electrophoresis system.
6. Power supply.
7. UV light box.
8. Camera.

2.4. Preparation of Protein for Gel Electrophoresis

1. Cell lysis buffer: 150 mM NaCl, 1% NP 40, 2 mM EDTA, 1 mM DTT, 50 mM, Tris-HCl, pH 8.0.
2. Protease inhibitors: 10 mg/mL each of chymostatin, leupeptin, aprotinin, and pepstatin.
3. 0.1 M PMSF.
4. Ice.
5. 100 mm Petri dish of subconfluent cells (or 4×10^6 cells).
6. Cell scraper.
7. Hot plate or boiling water.

2.5. Gel Electrophoresis

1. Protein electrophoresis vertical gel apparatus.
2. Syringe.

3. Power supply.
4. Wide-range molecular weight marker (e.g., Sigma Chemicals, St. Louis, MO).
5. 5X loading buffer: 5% SDS, 10% glycerol, 5% bromophenol blue, 0.5% xylene cyanol, and 5% β -mercaptoethanol.
6. 4–20% Tris glycine precast gels (e.g., Bio-Rad, Hercules, CA).
7. 1X running buffer: 25 mM Tris, pH 8.3, 192 mM glycine and 0.1% (w/v) SDS.

2.6. Electrotransfer

1. Distilled water.
2. Whatman 3MM paper.
3. Indelible marker.
4. Gloves.
5. Forceps.
6. Power supply.
7. Nitrocellulose membrane.
8. Serological pipet (glass or plastic).
9. Electroblot transfer system.
10. Transfer buffer (makes 1 L): 14 g glycine, 3 g Tris base, 1 g SDS, 200 mL methanol, adjust volume to 1 L with distilled water.

2.7. Blocking/Antibody Probing

1. Rocker or shaker.
2. 10X Tris-buffered Saline (TBS): 24.2 g Tris base, 80 g NaCl, 38 mL 1 M HCl, bring to pH 8.0, add distilled water to 1 L. Store at room temperature.
3. TBS-Tween: 2.5 mL Tween-20, 50 mL 10X TBS stock, adjust volume to 500 mL with distilled water. Refrigerate at 4°C.
4. Nonfat dry milk powder (available from grocery stores).
5. Ponceau S (optional), 0.1% Ponceau S, 5% trichloroacetic acid (TCA).
6. A sealable plastic bag or small container that will hold the membrane.
7. Clear plastic wrap.
8. *FHIT* rabbit polyclonal antibody (Zymed, San Francisco, CA).
9. Horseradish peroxidase-labeled anti-rabbit antibody.

2.8. Detection of Protein Bands

1. X-ray cassette and film.
2. Detection system (e.g., ECL by Amersham, Arlington Heights, IL).
3. Clear plastic wrap.
4. Plastic container slightly larger than membrane.
5. Paper towels.
6. Forceps.
7. Laboratory tape.

2.9. Deparaffinization

1. Xylene (histological grade).
2. 100% ethanol.

3. 70% ethanol.
4. Phosphate-buffered saline (PBS).
5. Distilled water.
6. Paper towels.

2.10. Staining

1. PAP pen (Dako, Carpinteria, CA).
2. 0.01 M Citrate buffer pH 6.0.
3. Microwave.
4. 3% hydrogen peroxide diluted in methanol.
5. Distilled water.
6. *FHIT* rabbit polyclonal antibody (Zymed, San Francisco, CA).
7. Harry's modified hematoxylin.
8. Biotinylated anti-rabbit secondary antibody.
9. Slide holders/Coplin jars.
10. 2,4-diamino benzidine (DAB).
11. Phosphate-buffered saline (PBS).
12. Coverslips.
13. Mounting medium (e.g., Permount, Fisher, Pittsburgh, PA).
14. An indelible marker that will write on the slide.
15. Staining kit (e.g., LSAB kit, Dako).
16. Goat serum.

3. Methods

3.1. RT-PCR

Remember to keep all reagents on ice. Ensure that all reagents are available before beginning the protocol. It is advisable to complete calculations for a two “master mixes”—oligo mix and miscellaneous mix—before experimentation. (see **Notes 1** and **2**).

3.1.1. RT-PCR Reactions

1. Bring 5 µg of total RNA to a 12-µL volume with DEPC water.
2. Add 2 µL of oligo mix to each sample.
3. Place at 70°C for 10 min.
4. Quench on ice.
5. Briefly centrifuge.
6. Add 7 µL miscellaneous mix to each sample. Mix well by pipetting.
7. Place at 42°C for 2 min.
8. Add 1 µL reverse transcriptase.
9. Place in thermal cycler using the following conditions: 42°C for 50 min, followed by 70°C for 15 min, and an indefinite extension at 4°C.
10. The product may be stored at -20°C for subsequent use.

3.1.2. PCR Reactions

1. Prepare a PCR “master mix” by adding 1 μ L of forward primer, 1 μ L of reverse primer, 2.5 μ L of 10X PCR buffer, 0.5 μ L of dNTP mix, 0.25 μ L *Taq*, and enough water to bring the vol to 24 μ L for one reaction (*see Note 2*).
2. Distribute “master mix” to each tube.
3. Add 1 μ L cDNA (obtained after the steps in **Subheading 3.1.1.** is completed) to an appropriately labeled thin-walled PCR tube.
4. Flick tube to mix.
5. Add a layer of mineral oil if required by thermal cycler.
Always include a positive and negative control for the PCR reaction (*see Note 1*).

3.1.3. PCR Parameters

These conditions are optimal for the primers described in **Table 1**.

1. Initial denaturation: 94°C for 3 min.
2. 30 cycles of 94°C for 30 s, 62°C for 30 s, 72°C for 1 min.
3. Final extension at 72°C for 5 min.
4. The reaction can be stored at 4°C before loading the gel.

3.1.4. Analysis of PCR Products by Gel Electrophoresis

1. Make a 1% agarose gel by dissolving 1 g agarose for every 100 mL 1X TBE buffer.
2. Add 2 μ L ethidium bromide solution.
3. Pour into gel-casting tray with comb and allow the gel to solidify.
4. To each sample, add 1/5 vol of loading buffer.
5. Load samples into the gel wells.
6. Electrophorese samples into gel.
7. Visualize bands on a UV light box.
8. Take a photograph. (A 1% agarose gel showing amplification products of cell lines with normal and aberrant *FHIT* transcripts is shown in **Fig. 1**.)

3.1.5. Nested PCR (if necessary)

Because levels of *FHIT* expression are low, another round of amplification with primers nested between the first set of primers is sometimes necessary. Set up a new “master mix” using a pair of nested primers. Distribute this “master mix” to a new set of PCR tubes before adding 1 μ L of the first round product. Thermal-cycler conditions are the same as in the first amplification (*see Table 2* for troubleshooting).

3.2. Western Blotting

1. It is helpful to precut the membrane to the size of the gel, and to cut the Whatman 3MM paper slightly larger than the gel.
2. After the membrane and Whatman 3MM paper are cut, begin to presoak membrane and Whatman 3MM paper for approx 30 min in transfer buffer prior to transfer. No rocking is needed.



Fig. 1. Analysis of the expression of the *FHIT* gene by nested RT-PCR in three prostate adenocarcinomas and autologous benign epithelium (A,B,C). Normal *FHIT* transcript is expressed in normal prostatic glands (N). Abnormal *FHIT* transcripts are detected in prostatic tumors (T).

Table 2
Troubleshooting (RT-PCR)

Problem	Probable cause	Recommendation
No/little PCR product	Insufficient template RNA amount	a. Increase amount of RNA template in cDNA reaction.
	Template RNA-degraded	a. Prepare fresh RNA b. Check RNA prep by electrophoresis prior to RT-PCR.
RT-PCR product smears	Reaction not optimal	a. Check all reagents.
	Amplification product	a. Check all reagents. b. Check cycling conditions. c. Check the Mg ²⁺ concentration. d. Decrease template concentration.
Nonspecific products	Annealing temperature	a. Increase annealing temperature. b. Decrease the amount of template.
	DNA contamination	a. Use a new control by performing only the PCR (omit RT). No product will be generated if sample is free of DNA.

3. It is useful to include a positive control lysate that expresses *FHIT*. This ensures that the antibody works.

3.2.1. Preparation of Protein Lysates

It is useful to include a *FHIT*-expressing cell as a positive control.

1. Add 500 μL of cell lysis buffer to cells.
2. Place on ice while using cell scraper to remove cells from surface.
3. Pipet protein lysate into 1.5-mL tube.
4. Centrifuge for 10 min, 12,000g, 4°C.
5. Remove supernatant and store at -80°C until ready to use. Store in aliquots because repeated freeze-thaw may degrade the protein.

3.2.2. Gel Electrophoresis of Proteins

1. In a 1.5-mL tube add 75 μg total protein, 4 μL 5X loading buffer, and water for a total vol of 20 μL .
2. Boil protein samples before loading for 5 min.
3. Centrifuge 5 min, 12,000g, at room temperature.
4. Allow samples to cool to room temperature.
5. While the samples cool, rinse the lanes with the syringe, using the running buffer in the tank.
6. Load samples in the gel.
7. Run gel between 150 and 200 V until the bromophenol blue reaches the end of the gel. The gel voltage may be adjusted according to time constraints.

3.2.3. Transfer of Proteins to Nitrocellulose Membrane

1. Open cassette with black side down to the lab bench.
2. Place the sponge down.
3. Add Whatman 3MM paper.
4. Add gel.
5. Place the membrane on the gel and smooth out air bubbles using a pipet. (Always handle the membrane with forceps!)
6. Add another piece of Whatman 3MM.
7. Place second sponge over gel and close cassette.
8. Lock the cassette.
9. Place cassette into the apparatus. The black should face the back part of the apparatus.
10. Add the cooling core. (**Remember to refreeze core prior to subsequent use.**)
11. Run transfer 1 h at 100 V.

3.2.4. Viewing Protein Bands (Optional)

The Ponceau S stain is reversible, and may be used to view the protein transferred to the membrane.

1. Ponceau S stain membrane (Ponceau is reusable).
2. Rinse membrane with TBS (Note the relative amounts of protein in each lane).
3. Continue by blocking the membrane with 5% nonfat dry milk in Tween-TBS (see Subheading 3.2.5.).

3.2.5. Blocking and Application of Antibodies

1. Place membrane in 5% milk solution to block overnight at 4°C or 3 h at room temperature. *FHIT* antibody is diluted in 5% milk solution 1:1500 and placed on the membrane, which should be placed in a small container or sealed bag, and allowed to shake for 1 h at room temperature or overnight at 4°C. Occasionally, we add β -actin antibody at a 1:2500 dilution to the blot. This controls for protein concentration in each lane. (A Western blot showing the expression of β -actin is shown in **Fig. 2**.)
3. Wash membrane 10 min twice with TBS/Tween.
4. Apply to the membrane the secondary antibody: horseradish peroxidase conjugated anti-rabbit diluted (check with antibody source for suggested dilution) in 5% milk solution.
5. Incubate for 1 h, shaking, at room temperature, or overnight at 4°C.
If β -actin is also used, be sure to add antimouse antibody to the secondary antibody solution.
6. Wash in TBS-Tween for 15 min, then wash for 10 min twice.

3.2.6. Analysis of Protein Expression by Chemiluminescence

Follow the manufacturer's protocol for the chemiluminescent kit. We prefer the ECL kit by Amersham.

1. After the membrane has been treated with the reagents in the chemiluminescent kit, place the moist membrane in clear plastic wrap and tape it to the cassette for exposure to radiograph film.
2. Take multiple exposures as needed until optimal darkness of bands is achieved.
3. *FHIT* generates a band at 16.8 kDa. (A Western blot analysis of cell lines with an absence or reduction of the *FHIT* protein is shown in **Fig. 2**.) See **Table 3** for troubleshooting.

3.2.7. Stripping and Reprobing Membranes

If the membrane is needed for future antibody probing, it is necessary to strip the membrane according to the protocols listed in the chemiluminescent kit. It is important that the membrane remains moist. We accomplish this by placing the membrane in a freezer bag with 5 mL of TBS-Tween. The bag is sealed and allowed to remain at 4°C until stripping and/or reprobing is necessary.

3.3. Immunohistochemistry

3.3.1. Deparaffinizing

This procedure is only necessary when the specimens have been embedded in paraffin. Deparaffinization of the slides must be done before the slides are stained. It is helpful to have the Coplin jars in the correct order, filled with the appropriate chemical, and labeled properly so that slide staining may proceed in an orderly fashion.

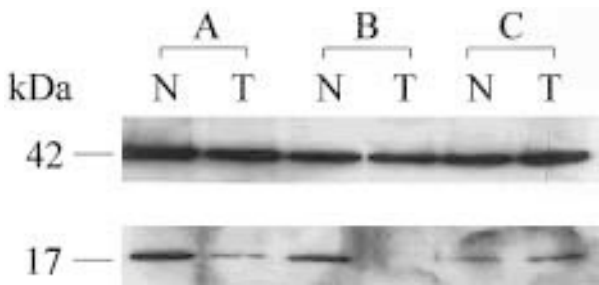


Fig. 2. Western blot analysis of *FHIT* protein. Lower panel shows *FHIT* expression in three prostatic adenocarcinomas and autologous benign glands (A,B,C). Normal *FHIT* protein is expressed in benign prostatic epithelium (N). *FHIT* protein is undetectable or shows lower expression in prostatic tumors (T). The upper panel shows β -actin expression for the same membrane.

Table 3
Troubleshooting (Western blotting)

Problem	Probable cause	Recommendation
No signal	No transfer of proteins	a. Ponceau S stain membrane. b. Stain gels with dye to check transfer efficiency. c. Check that the membrane and anode are correctly oriented. d. Check for air bubbles/gel membrane distortion.
	Protein degradation Detection system	a. Make fresh lysates. a. Low affinity of primary or secondary antibody. b. Chemiluminescent reagents inactive.
Weak signal	Insufficient amount of protein	a. Load more protein. b. Expose film longer. c. Poor transfer.
High background	High concentration of antibody	a. Decrease antibody concentration
	Inadequate blocking	a. Ensure blocking solution is prepared correctly. b. Increase blocking time.
	Inadequate washes	a. Increase wash time. b. Increase the number of wash changes.

Table 4
Checklist for Deparaffinizing Slides

	Chemical	Time (min)
✓	Xylene	5
✓	Xylene	5
✓	100% Ethanol	3
✓	100% Ethanol	3
✓	70% Ethanol	3
✓	70% Ethanol	3
✓	Distilled water	5
✓	Distilled water	2
✓	Distilled water	2
✓	PBS	5

1. Allow slides to soak in xylene for 5 min.
2. Tap on a paper towel.
3. Allow slides to soak in a fresh bath of xylene for 5min.
4. Transfer to 100% ethanol for 3 min.
5. Transfer to a fresh bath of 100% ethanol for 3 min.
6. Tap on a paper towel.
7. Allow to stand in 70% ethanol 3 min.
8. Transfer to a fresh bath of 70% ethanol for 3 min.
9. Allow slides to soak in distilled water for 5 min.
10. Transfer to a fresh bath of distilled water and allow slides to soak for 2 min.
11. Soak in PBS for 5 min (*see Table 4*).

3.3.2. Slide Staining

If cells are used in the staining process, the cells should be fixed on the slides before staining. We recommend following the protocol developed by the manufacturers of the various staining kits. The *FHIT* antibody should be used at a dilution of 1:1000 (*see Fig. 3*).

4. Notes

1. RT-PCR pointers: When working with RNA, careful precautions should be taken so that the RNA does not degrade. RNA extraction should be preformed in a separate area from that used to process PCR products. The use of gloves, lab coats, and aerosol pipet tips also decreases the risk of contamination/degradation of the RNA. Spilling the tiniest amount of a PCR reaction may result in a release of PCR products into the laboratory workspace, which may carry over into subsequent PCR reactions and thus cause false results (**13**).
A negative control for RT (no RNA template) should be included and used as a negative control for the PCR reaction.

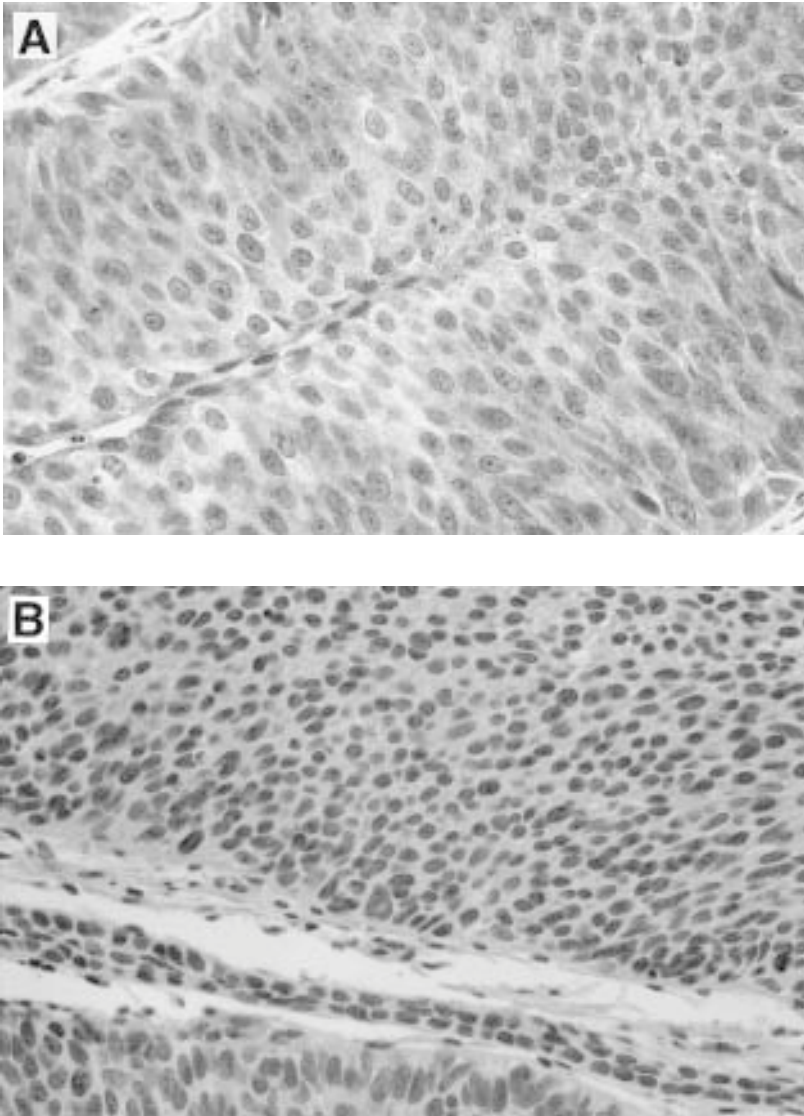


Fig. 3. *FHIT* immunostaining in transitional-cell carcinoma (TCC) of the urinary bladder. Papillary TCCs showing uniform *FHIT* expression (A) (X250) and complete absence of *FHIT* protein (B) (X200).

2. Master mixes: Make enough master mix for one reaction more than the number of samples to be amplified. This ensures an adequate master mix for every sample despite of pipet calibration errors.

References

1. Druck, T., Berk, L., and Huebner, K. (1998) FHITness and cancer. *Oncol. Res.* **10**, 341–345.
2. Mao, L., Fan, Y., Lotan, R., and Hong, W. (1996) Frequent abnormalities of *FHIT*, a candidate tumor suppressor gene, in head in neck cancer. *Cancer Res.* **56**, 5128–5131.
3. Virgilio, L., Shuster, M., Gollin, S., Veronese, M. L., Ohta, M., Huebner, K., and Croce, C. M. (1996) *FHIT* gene alterations in head and neck squamous cell carcinomas. *Proc. Natl. Acad. Sci. USA* **93**, 9770–9775.
4. Baffa, R., Veronese, M. L., Santoro, R., Mandes, B., Palazzo, J., Rugge, M., Santoro, E., Croce, C. M., and Huebner, K. (1998) Loss of *FHIT* expression in gastric carcinoma. *Cancer Res.* **57**, 4708–4714.
5. Fong, K., Biesterveld, T., Virmani, A., Wistuba, I., Sekido, Y., Alder, S. A., Ahmadian, M., Ong, S. T., Rassool, F. V., and Zimmerman, P. V. (1997) *FHIT* and FRA3B 3p14.2 allele loss are common in lung cancer and pre-neoplastic bronchial lesions and are associated with cancer related *FHIT* cDNA splicing aberrations. *Cancer Res.* **57**, 2256–2267.
6. Velickovic, M., Delahunt, B., and Grebe, S. (1999) Loss of heterozygosity at 3p14.2 in clear cell renal carcinoma is an early event and is highly localized to the *FHIT* gene locus. *Cancer Res.* **59**, 1323–1326.
7. Sozzi, G., Tornielli, S., Tagliabue, E., Sard, L., Pezzella, F., Pastorino, U., Minoletti, F., Pilotti, S., Ratecliffe, C., Veronese, M. L., Goldstraw, P., Huebner, K., Croce, C. M., and Pierotti, M. A. (1997) Absence of Fhit protein in primary lung tumors and cell lines with *FHIT* gene abnormalities. *Cancer Res.* **57**, 5207–5212.
8. Ji, L., Fang, B., Yen, N., Fong, K., Minna, J. D., and Roth, J. A. (1999) Induction of apoptosis and inhibition of tumorigenicity and tumor growth by adenovirus vector-mediated fragile histidine triad (*FHIT*) gene overexpression *Cancer Res.* **59**, 3333–3339.
9. Baffa, R., Gomella, L. G., Vecchione, A., Bassi, P., Mimori, K., Sedor, J., Calviello, C. M., Gardiman, M., Minimo, C., Strup, S. E., McCue, P. A., Kovatich, A. J., Pagano, F., Huebner, K., and Croce, C. M. (2000) Loss of FHIT expression in transitional cell carcinoma of the urinary bladder. *Am. J. Pathol.* **156**, 419–424.
10. Huebner, K., Sozzi, G., Brenner, C., Pierotti, M., and Croce, C. M. (1999) Fhit loss in lung cancer. *Adv. Oncol.* **15**, 3–9.
11. Sambrook, J., Fritsch, E. F., and Maniatis, T. (1989) *Molecular Cloning: A Laboratory Manual*, 2nd ed., Cold Spring Harbor Laboratory Press, Cold Spring Harbor, NY.
12. Ohta, M., Inoue, H., Cotticelli, M., Kastury, K., Baffa, R., Palazzo, J., Siprashvili, Z., Mori, M., McCue, P., Druck, T., Croce, C., and Huebner, K. (1996) The *FHIT* gene, spanning the chromosome 3p14.2 fragile site and renal carcinoma-associated t(3;8) breakpoint, is abnormal in digestive tract cancers. *Cell* **84**, 587–597.
13. Kwok, S. and Higuchi, R. (1989) Avoiding false positives with PCR. *Nature* **339**, 237–238.

Detection of Apoptosis in Renal Cell Carcinoma

Kenneth J. Pienta and Jeffrey F. Williams

1. Introduction

Apoptosis is a selective process of programmed cell death that plays an important role in both physiologic and malignant states. In neoplastic disease, the rate at which a tumor grows depends on cell deletion as well as cell proliferation. It has been shown in several types of tumors that more aggressive tumors usually have a higher proliferative activity as well as an increased rate of apoptosis. The same characteristics seem true of renal neoplasms, as the frequency of apoptosis has been positively correlated with tumor grade, stage, and size in renal cell carcinoma (RCC) (1). Apoptosis is closely related to proliferative activity, tumor differentiation, and depth of invasion in transitional-cell carcinoma of the renal pelvis and ureter (2). The mechanisms of cell-cycle control, proliferation, and apoptosis are key issues in the biology and prognosis of RCCs. The expression of bcl-2 and p53 has been implicated in the control of apoptosis in tumorigenesis, and as a possible pathway to which cancer treatments could be directed. A reciprocal correlation was found between apoptosis and p53 positivity in RCC suggesting that the presence of mutant p53 is a negative regulator of apoptosis (3).

Classically, apoptosis is characterized by specific morphological changes such as shrinkage of cytoplasm, condensation, and fragmentation of the cell nucleus, and membrane blebbing. These changes may be noted in routine histology in hematoxylin and eosin (H&E)-stained sections, but assessment with conventional light microscopy may underestimate apoptosis. Only cells at the end stages of the process show characteristic cell shrinkage and chromatin fragmentation. Another complicating factor is the low frequency in which apoptotic cells usually are observed—a result of the short duration of the morphological changes.

The difficulty of morphologic identification of apoptosis has led to the development of other methods to study apoptosis. The biochemical hallmark of apoptosis is the fragmentation of genomic DNA—an irreversible event that demonstrates the cell's commitment to death. DNA fragmentation has been shown to result from activation of an endogenous nuclear endonuclease that selectively cleaves DNA into oligosomal-length fragments. When these fragments are analyzed on agarose-gel electrophoresis, they form a distinctive ladder pattern consisting of multiples of approx= 180 bp subunits (4). The detection of the DNA ladder pattern in agarose gels is considered a hallmark of apoptosis, and is a widely performed method.

DNA ladder analysis has its limitations. It cannot identify cells that are undergoing apoptosis *in situ*. Noncarcinoma—cells including neutrophils and lymphocytes—may also undergo apoptotic cell death. It also been shown that large DNA fragmentation occurs prior to the subsequent degradation of DNA into oligosomal lengths, and in some cells the final degradation may not even take place. Though not definitive, the detection of DNA ladder pattern by gel electrophoresis provides an additional criterion to define cell death as apoptotic. Kits are commercially available that may simplify the process (Apoptotic DNA Ladder Kit, Roche Molecular Biochemicals).

The detection of the DNA ladder pattern may detect apoptosis in cell populations, but has limited value in the identification of cells undergoing apoptosis in the majority of clinical materials. Another technique allows for study of apoptosis *in situ*. As described previously, DNA fragmentation is a characteristic event that often occurs in the early stages of apoptosis. DNA strand breaks can be detected by enzymatic labeling of the free 3'-OH ends with modified nucleotides (X-dUTP, X = biotin, DIG, or fluorescein). A suitable labeling enzyme is terminal deoxynucleotidyl transferase (TdT), which is able to label blunt ends of double-stranded DNA breaks. This method was reported by Gavreli et al. (5) and is termed 3'-OH nick-end labeling, or TdT-mediated deoxyuridine triphosphate (dUTP) biotin nick-end labeling (TUNEL). With this relatively simple, rapid procedure, excellent results may be obtained with formalin-fixed, paraffin-embedded tissue. Adherent cell cultures, cytopins, and cell smears have all been successfully used.

To allow exogenous enzymes to enter the cell, the plasma membrane must be permeabilized prior to the enzymatic reaction. To avoid loss of DNA from the cells, the cells must be fixed with formaldehyde or glutaraldehyde before permeabilization. This fixation cross-links low-molecular-weight DNA to other cellular constituents, and prevents its extraction during the permeabilization step.

The labeled free ends of DNA may be detected in a second incubation step with (strept) avidin or an anti-DIG antibody. The immunocomplex is easily visible if the (strept) avidin or an anti-DIG antibody is conjugated with a reporter molecule (e.g., fluorescein, AP, or POD).

In contrast to the indirect method, fluorescein-dUTP may be used to directly label DNA strand breaks, which allows for the detection of the incorporated nucleotides with a fluorescence microscope or a flow cytometer. Direct labeling with fluorescein-dUTP offers several advantages. Direct labeling produces less nonspecific background with sensitivity equal to indirect labeling, and thus it is as powerful as the indirect method of detecting apoptosis. Furthermore, the fluorescence may be converted into a colorimetric signal if an antifluorescein antibody conjugated with a reporter enzyme is added to the sample.

Various commercially available kits may make the overall process easier (*In Situ* Cell Death Detection Kit, Roche Molecular Biochemicals, Apop Tag in situ apoptosis detection kit, Oncor Inc). The following protocol, adopted from Gavreli et al. (1993) with permission, describes an indirect TUNEL labeling assay using end-labeling of DNA with peroxidase-conjugated streptavidin. It is a useful technique for studying cell smears, adherent cells, cytopsmns, and frozen or fixed tissue sections.

1.1. Tissue and Cell Culture Preparation

Tissue blocks are immediately fixed in 8% paraformaldehyde in PBS. Tissue blocks are cut at 3 μ m and placed on glass slides. Paraffin sections should be deparaffinized in xylene for 5 min and hydrated through graded concentrations of ethanol.

Cell suspensions should be centrifuged, resuspended with 4% paraformaldehyde, and plated on silane-coated glass slides. The cell-culture smears may be immediately air-dried and stained using the May-Grunwald-Giemsa method or alcohol-fixed and stained the Papanicolaou's method. Smears may be fixed in various fixatives (4% paraformaldehyde, 8% paraformaldehyde, methanol, or Carnoy fixative) for 120 min. After fixation, smears may be stored at -20°C in 50% glycerol or air-dried and stored at 4°C until use. Smears may also be air-dried without fixative and stored at 4°C until use for up to 3 mo.

2. Materials

1. Proteinase K (20 $\mu\text{g}/\text{mL}$, Sigma Chemical Co.).
2. TdT labeling buffer: 30 mM Trizma-base, pH 7.2, 140 mM/L sodium cacodylate, 1 mM cobalt chloride.
3. Deoxynucleotidyl transferase (TdT) (United States Biochemical, Cleveland, OH).
4. Biotinylated uridine triphosphate (UTP) (Boehringer Mannheim or Yamanouchi).
5. Peroxidase-conjugated streptavidin (Vector Laboratories, Burlingame, CA).
6. Diaminobenzidine hydrogen peroxide solution (50 mL of PBS containing 50 mg of diaminobenzidine and 30 μL of hydrogen peroxide).
7. Terminating buffer: 300 mM sodium citrate and 30 mM sodium chloride.
8. DNase I (Sigma Chemical Co., St. Louis, MO, or Stratagene Co., La Jolla, CA).

3. Methods

3.1. TUNEL Assay Steps

1. Wash deparaffinized sections or smears with distilled water.
2. Treat with proteinase K for 20 min at room temperature.
3. Wash with distilled water for 2 min.
4. Block endogenous peroxidase activity by incubating tissue sections with 0.3% hydrogen peroxide for 30 min. Incubate smears with 0.3% hydrogen peroxide for 10 min.
5. Wash with distilled water.
6. Immerse slides in TdT labeling buffer for 10 min.
7. Incubate the slides with diluted terminal deoxynucleotidyl transferase (TdT and biotinylated uridine triphosphate for 90 min at 37°C. (2 μ L TdT and 5 μ L of biotinylated dUTP in 100 μ L of TdT buffer).
8. Rinse slides in terminating buffer for 15 min at room temperature.
9. Wash sections with distilled water for 5 min.
10. Blocking may be performed using 2% BSA in phosphate-buffered saline (PBS) for 10 min. Rinse in distilled water and immerse in PBS for 5 min.
11. Incubate sections with peroxidase-conjugated streptavidin for 30 min at room temperature.
12. Wash twice with PBS for 5 min.
13. Develop slides by immersing in diaminobenzidine hydrogen peroxide solution for 5–8 min.
14. The slides may be counterstained with 0.5% methyl green solution.
15. Mount slides in an aqueous mounting medium (Gel/Mount, Crystal/Mount, Biomeda Corp.)
16. Positive control: treat smears or sections with 1 μ Lg/mL of DNase I in TdT buffer for 10 min.
17. Negative control: incubate slides in TdT buffer without TdT.
18. Determine the apoptotic index. Select the most positively stained areas of apoptotic cells. Count at least 100 tumor cells per slide. The apoptotic index is measured as the number of TdT-mediated dUTP-biotin nick and positive cells per 100 carcinoma cells.

Negative controls should not have nuclear staining. Positive control sections should have staining of all nuclei—a dark-brown staining reaction. The differentiation between necrotic and apoptotic cells may present some difficulty, as necrotic tumor cells also contain fragmented DNA. Apoptosis usually involves individual cells with nuclei or nuclear fragments that are strongly stained. Often there is an absence of cytoplasm, but if present, it is usually not stained. Necrosis often involves large areas with hundreds of confluent cells. These cells not only display nuclear staining, but also diffuse cytoplasmic staining.

4. Notes (adapted from ref. 7)

1. Nonspecific TUNEL Labeling: DNA-strand breaks induced by UV irradiation during tissue embedding may lead to nonspecific labeling. Use a different embedding material that does not require UV irradiation. Acid tissue fixatives (e.g., mathacarn, Carnoy's fixative) cause DNA-strand breaks, and better results may be obtained using buffered 4% paraformaldehyde as a fixative.
2. Endogenous nuclease activity may occur soon after tissue preparations. Fix tissues immediately after organ harvest, or perfuse fixative through an intact animal if necessary. Another cause of nonspecific TUNEL labeling is a too-high TdT concentration during TUNEL labeling. Reduce concentration of TdT by diluting it 1:2 or 1:3 with TUNEL dilution buffer (Roche Molecular Biochemical) containing 30 mM Tris (pH 7.2), 140 mM sodium cacodylate, and 1 mM CoCl_2 .
3. Endogenous alkaline phosphatase activity during converter reaction may also result in nonspecific TUNEL labeling. Block endogenous alkaline phosphatase activity by adding 1 mM levamisole to the AP substrate solution.
4. Endogenous peroxidase activity during converter reaction: Before permeabilizing cells, block endogenous POD activity by immersing the slides in a solution of 0.3% H_2O_2 in methanol.
5. Nonspecific binding of antifuorescein antibody conjugate during converter reaction. Block nonspecific sites with normal antisheep serum. Block nonspecific sites with PBS containing 3% BSA for 20 min.
6. High background may result from formalin fixation, which causes yellow staining of cells containing melanin precursors. Use methanol fixation (this may lead to a reduction in TUNEL-labeling sensitivity)
7. TUNEL labeling mix too concentrated can lead to high background. Reduce concentration of labeling mix by diluting it 1:2 with TUNEL dilution buffer.
8. Endogenous alkaline phosphatase activity during converter reaction. Block by adding 1 mM levamisole to the AP substrate solution.
9. Endogenous peroxidase activity during converter reaction. Before permeabilizing cells, block endogenous POD activity by immersing the slides in a solution of 0.3% H_2O_2 in methanol.
10. Nonspecific binding of antifuorescein antibody conjugate during converter reaction. Block nonspecific sites with PBS containing 3% BSA or normal antisheep serum (20 min).
11. Ethanol and methanol fixation. Use buffered 4% paraformaldehyde as fixative.
12. Extensive crosslinking during prolonged fixation reactions may lead to low TUNEL labeling. This may be alleviated by reducing the fixation time or using buffered 2% paraformaldehyde as fixative.
13. Insufficient permeabilization of cells, so TUNEL reagents cannot reach nuclei. Pretreat with proteinase K (concentration and time must be optimized empirically). Pretreat with 0.01 M sodium citrate for 30 min at 70°C. Increase TUNEL incubation time.

14. Restricted access of TUNEL reagents to nuclei, caused by paraffin-embedding. After dewaxing tissue sections, treat with proteinase K. Immerse dewaxed tissue sections in 200 mL 0.01 M citrate buffer (pH 6.0) and treat with microwave irradiation (370 W, 5 min). Note: conditions must be experimentally optimized for each tissue.)
15. Inadequate DNase treatment (DNase concentration too low). For cyrosections, apply 1 μ g/mL DNase. For paraffin-embedded tissue sections, apply 0.5 mg/mL DNase. For other samples, apply 1 U/mL DNase in a solution of 10 mM Tris-HCL (pH 7.4), 10 mM NaCl, 5 mM $MnCl_2$, 0.1 mM $CaCl_2$, 25 mM KCl; incubate for 30 mins at 37°C. Use an alternative DNase buffer, 10 mM Tris-HCl (pH 7.5), 1 mM $MgCl_2$, 1 mg/mL BSA.

References

1. Todd, D., Guang, Y., Brown, R. W. , Cao, J., D'Agati, V., Thompson, T. S., and Truong, L. D. (1996) Apoptosis in renal cell carcinoma: detection by in situ end-labeling of fragmented DNA and correlation with other prognostic factors. *Hum. Pathol.* **27**, 1012–1017.
2. Musada, M., Takano, Y., Iki, M., Asakura, T., Hasiba, T., Noguchi, S., and Hosaka, M. (1997) Apoptosis in transitional cell carcinoma of the renal pelvis and ureter: association with proliferative activity, bcl-2 expression, and prognosis. *J. Urol.* **158**, 750–753.
3. Tannapfel, A., Hahn, H. A., Katalinic, A., Fietkau, R. J., Kuhn, R., Wittekind, C. W. (1997) Incidence of apoptosis, cell proliferation and p53 expression in renal cell carcinomas. *Anticancer Res.* **17**, 1155–1162.
4. Walker, P. R., Kokileva, L., Leblanc, J., Sikorska, M. (1993) Detection of the initial stages of DNA fragmentation in apoptosis. *Biotechniques* **15**, 1032–1040.
5. Gavrieli, Y., Sherman, Y., Ben-Sasson, S. A. (1992) Identification of programmed cell death in situ via specific labeling of nuclear DNA fragmentation. *J. Cell Biol.* **119**, 493–501.
6. Sasano, H., Yamaki, H., and Nagura, H. (1998) Detection of apoptotic cells in cytology specimens: an application of TdT-mediate dUTP-biotin nick end labeling to cell smears. *Diagn. Cytopathol.* **18(6)**, 398–402.
7. Wylie, A. et al. (1998) Apoptosis and cell proliferation. Boehringer Mannheim Biochemicals. 2nd ed., pp. 24–28, 106–108.

Fluorescence *In Situ* Hybridization (FISH) to Metaphase and Interphase Chromosomes

Jill A. Macoska

1. Introduction

The unambiguous identification of human chromosomes became possible with the discovery and implementation of G-banding techniques (*1*). Almost immediately, investigators developed various methods to physically map specific DNA sequences to banded chromosomes. A commonly used early technique involved the hybridization *in situ* of radioactively labeled probes to heat-denatured human metaphase chromosomes (reviewed in *2*). These techniques were efficient, yet costly, time-consuming, and technically difficult. Isotopic hybridization *in situ* was rapidly superseded by nonisotopic techniques—especially those utilizing fluorescently labeled probes (*3–6*). This chapter describes basic methodology for the accomplishment of metaphase and interphase fluorescence *in situ* hybridization (FISH).

2. Materials

1. 20 X SSC : 3 M NaCl, 300 mM sodium citrate.
2. 10X Phosphate-buffered saline (PBS): 27 mM KCl, 14 mM KH₂PO₄, 1.37 M NaCl, 43 mM NaH₂PO₄·7H₂O, to 1 L with dd H₂O.
3. 4% Paraformaldehyde (200 mL)
 - a. Heat 130 mL ddH₂O to 60°C (on heated stir plate, using a thermometer in separate water-filled vessel on same plate in a chemical fume hood).
 - b. Add 8 g paraformaldehyde (weigh out in fume hood; avoid exposure to skin and lungs) and magnetic stir bar.
 - c. While stirring, add 2 N NaOH drop by drop until paraformaldehyde goes into solution (some white particulate matter will remain).
 - d. Remove from heat and add 70 mL of 3X PBS.
 - e. Check pH; adjust to pH 7.2 with 1 N HCl, if necessary.

From: *Methods in Molecular Medicine*, vol. 53: *Renal Cancer: Methods and Protocols*
Edited by: J. H. Mydlo © Humana Press Inc., Totowa, NJ

- f. Cool to room temperature, then filter-sterilize.
- g. Store at 4°C; use for up to 2 wk.
4. 1X Phosphate-buffered detergent (PBD) for 1 L: 12.34 g Na_2HPO_4 (diabasic) to 0.1 M, 0.82 g NaH_2P_4 (monobasic) to 0.1 M, 5.0 mL Nonidet P-40 to 0.5%, to 1 L with dd H_2O .
5. Biotin-detection solution for 1 mL (make fresh each time): 2 μg fluorescein-avidin or rhodamine-avidin (Vector Laboratories or Molecular Probes), 1 mg BSA (to 1%), 200 μL of 20X SSC (to 4X), to 1 mL with dd H_2O .
6. Biotinylated antiavidin solution for 1 mL: 2 μg biotinylated antiavidin antibodies (Vector Laboratories or Molecular Probes), 1 mg BSA (to 1%), 200 μL of 20X SSC (to 4X), to 1 mL with dd H_2O .
7. Biotin amplification solution for 1 mL: 4–5 μg fluorescein-avidin (Vector Laboratories or Molecular Probes), 1 mg BSA (to 1%), 200 μL of 20X SSC (to 4X), to 1 mL with dd H_2O .
8. Digoxigenin-selection solution for 1 mL (make fresh each time): 10 μg rhodamine- or fluorescein-conjugated Fab fragment of sheep antidigoxigenin (Boehringer Mannheim), 1 mg BSA (to 1%), 200 μL of 20 XSSC (to 4X), to 1 mL with dd H_2O .
9. Digoxigenin-amplification solution: 5–7 μg fluorescein-conjugated rabbit antisheep IgG (Sigma or Molecular Probes), 1 mg BSA (to 1%), 200 μL of 20X SSC (to 4X), to 1 mL with dd H_2O .

3. Methods

3.1. Preparation of Fluorescently Labeled Probes

3.1.1. Selection of Probe DNA

Fluorescently labeled DNA probes to either unique or repetitive sequences (e.g., centromere-specific probes or chromosome-paint probes) are commercially available (Vysis, Inc., Downer's Grove, IL). Other than a heat-denaturation step (*see Subheading 3.12., step 2*), no other manipulations are usually required to prepare these probes for hybridization, and their use is straightforward. However, the investigator may wish to develop unique sequence probes to map specific DNA sequences to human metaphase chromosomes, or to quantitate homologous genomic DNA sequences in metaphase or interphase cell nuclei. In these cases, probe DNA must be prepared and labeled for *in situ* hybridization.

A major requirement for proper selection of probe DNA is that it must be large enough to provide a fluorescent signal of sufficient intensity for visualization. Typically, probes must exceed 10 kb to ensure adequate posthybridization visualization. This necessarily implies that most probes will comprise recombinant DNAs containing genomic DNA sequences, although large cDNA clones may be suitable for FISH experiments. Cosmid (30–50 kb), P1 (50–100 kb), BAC, or PAC (100–200 kb) and YAC (0.5–2.0 Mb) DNAs are all large enough to provide a sufficient fluorescent signal for visualization after hybrid-

ization. Yet, the use of such large DNA sequences, often invokes two potential “problems” that must be addressed: (1) genomic DNA probes—especially those comprising larger (>50 kb) sequences—will likely contain repetitive sequences—e.g., Alu repeats or rapidly reannealing (Cot-1) sequences. Repetitive sequences must be “masked” or “blocked” to avoid nonspecific probe binding during the hybridization process; (2) large probes must be made smaller through restriction enzyme digestion to permit entry into cell nuclei when performing interphase FISH. Solutions to both of these problems are offered under **Subheading 3.2., steps 12 and 13.**

3.1.2. Selection of Fluorophores (Fluorescent Dyes)

Fluorescence depends upon three events: excitation, emission, and detection. Specific types of molecules called fluorophores (often, polyaromatic hydrocarbons or heterocyclic compounds) are excited (absorb energy in the form of photons) from a light source (mercury or xenon bulbs or lasers). The fluorophore exists in this excited state for a short period of time, then returns to the ground state. In order to return to the ground state, the fluorophore must dissipate energy, which is accomplished through the emission of photons. The energy of the emitted photons is less than that of the photons originally absorbed by the fluorophore, so that the emission spectra of a given fluorophore is different from its excitation spectra. Therefore, optical filters specific for the emission spectra of the fluorophores allow detection and visualization of emitted photons—the process typically referred to as “fluorescence” (7).

3.1.3. Emission Spectra

Fluorophores typically used in basic FISH experiments have emission spectra in either the “green” (fluorescein, Cy3) or “red” (rhodamine, Texas red, Cy5) ranges. These are conjugated to deoxyribonucleotides, and are available from many vendors (Amersham, Dupont NEN, Molecular Probes), for easy incorporation into probe DNA sequences. The use of appropriate optical filters (*see Subheading 3.20.2.*) allows the simultaneous visualization of two or more fluorescently labeled probe DNAs bound to metaphase or interphase chromosomes (**Fig. 1**).

3.1.4. Direct Fluorescence Labeling

Probe DNA is labeled through nick-translation (NT) with an appropriate nucleotide fluorophore (**Fig. 2**). Many molecular biology reagent vendors provide “kits” for the NT of DNA; the following is a generic NT protocol that can be modified for the incorporation of specific fluorescent dyes. (NOTE: these and all subsequent steps should be performed with minimal exposure to ambient light to avoid inadvertent excitation of the fluorophores.)



Fig. 1. Posthybridization appearance of fluorescent signal. The diagram shows the appearance of chromosomes hybridized simultaneously to two fluorescently labeled probes, one specific to the chromosome centromere (black dots), and one specific for sequences on the short arm of the chromosome (gray dots). Metaphase chromosomes (left) localize the probes as expected, to each sister chromatid of the homologous chromosome pair. Interphase chromosomes (right) localize the probes in an apparently more random manner because of the uncondensed state of the target DNA. In both cases, the hybridization pattern of each probe indicates that the homologous target DNA sequences are present in normal diploid dosage. Because the metaphase chromosomes represent duplicated DNA, four signals for each probe are observed; for the interphase chromosomes, two signals for each probe are present.

3.2. NT Protocol for Labeling DNA Sequences with Fluorophore-Conjugated Deoxynucleotides

1. 2.5 μL of a 1-mM “mix” of dNTPs (to a final concentration of 50 μM). (Omit the fluorophore-conjugated nucleotide analog from the dNTP mix—e.g., if fluorescein-dUTP is used, omit dTTP from the reaction mix.)
2. 5.0 μL of 10X buffer (500 mM Tris-HCl, pH 7.8; 100 mM 2-mercaptoethanol).
3. 50 mM MgCl_2 .
4. 5.0 μL of DNA probe sequence, 1 μg total.
5. 1.0 μL of DNA polymerase I (5–15 U).
6. 1.0 μL of 0.1 $\mu\text{g}/\mu\text{L}$ DNase I (can be made by diluting 1 mg/mL stock into 10,000 μL 20 mM Tris-HCl (pH 7.5) and 500 $\mu\text{g}/\text{mL}$ BSA).
7. 35.5 μL ddH₂O.
8. to 50 μL total vol.
9. Incubate the reaction for 15–60 min at 15°C.
10. Stop the reaction with the addition of 1.0 μL of 0.5 M EDTA (pH 8.0).
11. Eliminate unincorporated fluorophore (which can cause “background” fluorescence later) by passing the labeled probe DNA through a Sephadex G50-type spin column. These columns are commercially available from many vendors (e.g., Millipore, Worthington, Amersham Pharmacia Biotech).
12. If the labeled probe DNA will be used for interphase FISH, it should be digested with an appropriate restriction endonuclease to cut the DNA into fragments ≤ 20 kb. This can usually be accomplished using six-cutter enzymes such as *EcoRI*,

*Hind*III, or *Bam*HI. However, the optimal enzyme for these purposes should be assessed prior to probe labeling.

13. The labeled probe DNA should be ethanol-precipitated in the presence of Cot-1 DNA (10 µg) (Life Technologies, Inc.), Yeast tRNA (25 µg) and sonicated salmon testes DNA (25 µg) and 1/10 vol of 3 M sodium acetate, then resuspended in 10 µL high-quality formamide (Fluka Chemical).

3.3. Indirect Fluorescence Labeling

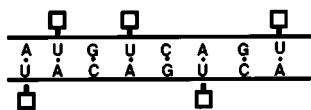
1. Indirect fluorescence labeling differs from direct labeling because the fluorophore is attached to an antibody rather than directly to a nucleotide (**Fig. 2**). Indirect fluorescence labeling utilizes the avidin/biotin system, where a biotin-containing nucleotide is incorporated into probe DNA using NT techniques (as described in **Subheading 3.2.** for direct labeling). After hybridization of probe DNA to “target” DNA (metaphase chromosomes or interphase nuclear DNA), fluorophore-labeled avidin is applied to the slide, which binds biotin. Because there are four biotin-binding sites per avidin molecule, “empty” biotin-binding sites can be utilized for binding biotinylated antiavidin antibody molecules. These, in turn, are available for binding additional fluorophore-labeled avidin molecules, thus “amplifying” the fluorescent signal. A less commonly used amplification system employs digoxigenin-labeled nucleotide incorporation into probe DNA. Multiple sheep antidigoxigenin antibodies (the source of the final fluorescent signal) bind the digoxigenin-labeled probe DNA and can, in turn, be bound by fluorophore-labeled rabbit antisheep antibodies, thus “amplifying” the fluorescent signal (7,8).
2. The primary advantage of both the biotin/avidin and digoxigenin systems is that they allow amplification of the fluorescent signal. The primary disadvantage of each of these indirect fluorescence-labeling techniques is that “noise” or “background” fluorescence increases with each additional sandwich “layer,” resulting in a trade-off between signal amplification and noise levels.
3. Probes for indirect fluorescence labeling are prepared as described in **Subheading 3.2.** except that a biotinylated or digoxigenin-labeled nucleotide is used.

3.4. Preparation of “Target” DNA

3.4.1. Preparation of Metaphase Chromosomes from Peripheral Blood

1. Using *FISH*, the chromosomal localization of unique DNA sequences can be determined for normal human metaphase chromosomes. To obtain such chromosomes, collect 5–10 cm³ human peripheral blood from a male donor (to ensure presence of the *Y* chromosome) into a heparinized tube (green cap) via venapuncture.
2. Inoculate 0.25–0.5 mL of whole blood into 5 mL RPMI media supplemented to 10% with fetal calf serum in T25 flask. Add 50 µL of sterile 100X PHA (Life Technologies) and incubate the flask for 2–4 d.
3. Synchronize the cells at the S phase of the cell cycle by adding 50 µL of 10 µM methotrexate. Incubate the cells overnight (at least 16 h), and then release the methotrexate block by the addition of 50 µL 1 mM thymidine.

A Direct Fluorescence Labeling



biotin
 avidin
 digoxigenin
 fluorophore
 antibody

B Indirect Fluorescence Labeling

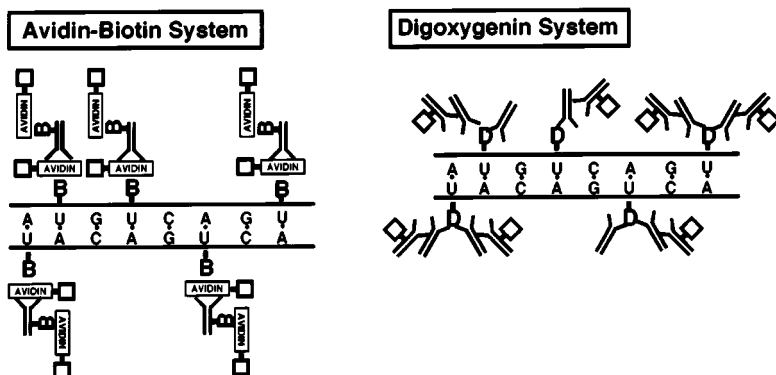


Fig. 2. Direct and indirect fluorescence labeling of probe DNAs. (A) Direct Fluorescence Labeling. As indicated in the diagram, the fluorophore is conjugated directly to deoxyribonucleotides (here, dUTP), which is incorporated into the probe DNA via NT (*see text*). (B) Indirect fluorescence labeling. In the avidin-biotin system (left), biotin is conjugated to the deoxyribonucleotides (here, dUTP) and is incorporated into the probe DNA via NT. Fluorescently labeled avidin then binds the biotin molecules, and can in turn be bound by biotin-conjugated antiavidin antibodies. The binding of additional fluorophore-conjugated avidin molecules to these biotin sites “amplifies” the fluorescent signal. In the digoxigenin system (right), digoxigenin-labeled deoxyribonucleotides (here, dUTP), are incorporated into the probe DNA via NT. Multiple sheep antidigoxigenin antibodies (the source of the final fluorescent signal) bind the digoxigenin-labeled probe DNA and can in turn be bound by fluorophore-labeled rabbit antisheep antibodies, thus “amplifying” the fluorescent signal.

4. Allow the cells to proceed through DNA synthesis for about 4 h, then add 25 μ L of 10 μ g/mL Colcemid.
5. Incubate the cells for 30 min, transfer to a 15-mL conical tube, and centrifuge at room temperature for 10 min at 180g to pellet the cells.
6. Aspirate off most of the supernatant, leaving approx 0.25 mL in tube.
7. Gently resuspend the cells in this small amount of liquid by tapping the tube and/or pipetting three to four times through a wide-bore plastic disposable pipet. Add 6 mL of 75 mM KCl (hypotonic solution) and gently mix by tapping the tube.

8. Incubate the released cell nuclei for 15 min at room temperature, then fix by adding 10–12 drops of ice-cold Carnoy's (3:1 methanol:acetic acid) and gently mixing.
9. Centrifuge at room temperature for 10 min at 180g to pellet the nuclei.
10. Aspirate all but 0.5 mL of the fixative and resuspend the nuclei by gently pipetting up and down using a wide-bore plastic disposable pipet.
11. Gradually add fixative a few drops at a time, followed by gentle mixing up to a final vol of 6.0 mL.
12. Incubate on ice for 2 h, then pellet the nuclei as described in **step 9**.
13. Resuspend the pellet in 4 mL fixative, pellet, then 2 mL fixative.
14. Store the nuclei at 4°C until use (**8**).

3.5. Preparation of Metaphase Spreads

1. Label the frosted edge of lint-free glass microscope slides with the sample identity in pencil.
2. Using a squirt bottle, thoroughly wash the slides and blot dry.
3. Spin down the fixed-cell nuclei and, using a 12-in Pasteur pipet, resuspend the nuclei in 0.5–1.0 mL fresh Carnoy's.
4. Holding the pipet full of nuclei in one hand and the slide in the other, tilt the slide at a 30–45° angle away from the pipet and position the pipet and slide as far apart as comfortably possible.
5. Apply 4–5 drops of nuclei/fixative to the slide, reverse the tilt of the slide, and sit the slide in an ice bucket (frosted edge on ice).
6. Cover the ice bucket and let the slides dry for 10–15 min.
7. Check the slides using phase-contrast microscopy to ensure that the slides contain an adequate number of well-spread metaphases.
8. If the number of metaphases is insufficient, centrifuge the nuclei and resuspend in a smaller vol of Carnoy's.
9. If the metaphase chromosomes are not well-spread, increase the distance between the slide and the pipet when “dropping” the nuclei.
10. Store prepared slides in light-tight slide boxes at room temperature.

3.6. G-Banding

1. The sequence of manipulations shown in **Table 1** should be followed for successful G-banding.
2. The key step in this process is the appropriate digestion of chromosomal proteins (chromatin) with trypsin; underdigestion yields poorly banded chromosomes, whereas overdigestion yields puffy, fragile chromosome preparations.
3. Make a fresh 0.02% trypsin solution each time by diluting 4 µL of 5% trypsin into 1 mL of HBSS (-Ca²⁺, -Mg²⁺).
4. For best results, use a fresh Giemsa stain for each procedure by adding 2 mL of Gurr's Giemsa to a solution containing 25 mL of 1 mM Na₂HPO₄ (dibasic) and 25 mL of 1 mM NaH₂PO₄ (monobasic) (**2,8**).
5. After the slides are banded, evaluate them under light microscopy. The slides can be temporarily coverslipped and viewed under oil immersion.

Table 1
G-Banding Protocol for Metaphase Chromosomes

Step	Solution	Incubation Time
1	0.02% trypsin	0.5–2.0 min
2	HBSS (-Ca ²⁺ , -Mg ²⁺)	Dip 4X
3	70% ethanol	Dip 4X
4	95% ethanol	Dip 4X
5	Air-dry	
6	Giemsa stain	2–3 min
7	ddH ₂ O	Rinse well
8	Air-dry	

6. Fields displaying well-spread metaphase chromosomes should be photographed and their *x,y* coordinates noted.
7. The photographs can be utilized to identify specific chromosomes from their G-banding patterns and, later, to pinpoint the physical location of hybridized DNA probe sequences.

3.7. Preparation of Touch Preps for Interphase FISH

1. If fresh tissues are available, cells may be obtained for analysis by gently pressing a charged microscope slide (e.g., ProbeOn Plus slides, Fisher Scientific) against a freshly cut surface.
2. Allow the slides to air-dry, and fix the adherent cells by immersing the slide into Carnoy's (3:1 methanol:acetic acid) three times for 5 min each, then air-dried (9).

3.8. Preparation of Disaggregated Nuclei for Interphase FISH

1. To avoid the "slice artifact" associated with hybridization to cut tissue sections, some investigators prefer to utilize whole nuclei isolated from archival (formalin-fixed, paraffin-embedded) tissue sections.
2. These procedures entail the preparation of thick (50- μ) tissue slices, which are dewaxed in xylenes three times for 10 min each, then rehydrated through successive 2-min incubations in 95%, 80%, and 70% ethanol.
3. After a 20-min incubation in 2X standard saline citrate (SSC) at 75°C, the slide is incubated in 0.5% pepsin (2.5 g pepsin dissolved into 100 mL of 0.9% NaCl) for 30–60 min at 37°C and the cells are disaggregated by drawing them repeatedly through a 21-gauge needle.
4. The cells are pelleted, washed in 1 mL of 1X PBS, pelleted again, resuspended in a minimal quantity of 1X phosphate-buffered saline (PBS), pipetted onto charged slides (ProbeOn Plus, Fisher Scientific).
5. The slides are air-dried overnight and fixed for 15 min in Carnoy's (9).

3.9. Preparation of Tissue Sections for Interphase FISH

1. Both archival (formalin-fixed, paraffin-embedded) and frozen tissue sections can be utilized for interphase FISH.
2. In either case, tissue should be sectioned onto charged slides (e.g., ProbeOn Plus, Fisher Scientific) to avoid tissue detachment during the hybridization and washing processes.
3. To avoid nuclear overlaps, the thickness of the tissue sections should not exceed 5–6 μ .

3.10. Preparation of Frozen Tissue Sections

Remove slides from freezer. Once thawed, prepare a series of Coplin jars containing the following solutions and follow these incubation steps (**10**):

1. Fix the slides in 4% paraformaldehyde for 15 min.
2. Wash three times in 2X SSC.
3. Incubate the slides in 20% sodium metabisulfite for 15 min at 43°C.
4. Wash three times in 2X SSC.
5. Incubate the slides for 2 min each in: 70%, 80%, 90%, and 100% ethanol.
6. Dip in acetone.
7. Air-dry the slides.
8. Digest the slides at 37°C in 0.1X protein-digesting enzyme (Oncor, Inc.) for 20–30 min (tissue-dependent).
9. Wash three times in 2X SSC.
10. Incubate the slides for 2 min each in: 70%, 80%, 90%, and 100% ethanol.
11. Dip in acetone.
12. Air-dry the slides.

3.11. Preparation of Archival Tissue Sections

1. “De-wax” paraffin-embedded archival tissue sections by incubating the slides at 50–55°C for 3–5 h.
2. Prepare a series of Coplin jars containing the following solutions and follow these incubation steps to prepare the slides for hybridization (**10–12**):
3. Incubate the slides in three changes of xylenes for 10 min each.
4. Dehydrate in two changes of 100% ethanol for 5 min each.
5. Equilibrate in 2X SSC at 75°C for 20 min.
6. Digest with 4 mg/mL pepsin (Sigma Chemical) dissolved in 0.9% NaCl (pH 1.5) for 20–25 min (tissue-dependent).
7. Dip in ddH₂O.
8. Place in 2X SSC for 5 min; use immediately. Blot off excess SSC from edges of slide prior to hybridization.

3.12. Hybridization to Metaphase Chromosomes

1. The probe should be labeled as described in **Subheading 3.2.** and resuspended in 10 μ L formamide.
2. Denature the probe solution at 75°C for 10 min, then allow the probe and repetitive sequences to anneal at 37°C for 3–5 h. This will serve to “block” repetitive sequences in the probe from binding to the target chromosome sequences.
3. In the meantime, digest the slides containing the metaphase spreads with 100 μ g/mL RNase in 2X SSC for 1 h at 37°C.
4. Rinse the slides four times in 2X SSC for 2 min each, dehydrate through 70% ethanol, 80% ethanol, and 95% ethanol for 2 min each, and air-dry.
5. Just prior to hybridization, prewarm the slides by incubating them for 15 min at 37°C on a hot plate or slide warmer, then denature them in a solution of 70% formamide/2X SSC at 70°C for 2 min.
6. Immediately plunge them into ice-cold 70% ethanol for 2 min, followed by cold 80%, 90%, then 100% ethanol, for 2 min each.
7. Allow the slides to air dry (**8,13,14**).
8. Briefly spin the probe solution in a microcentrifuge to collect the 10 μ L mixture at the bottom.
9. Carefully apply the probe to the slide, coverslip (gently tap out any trapped air bubbles), seal the perimeter of the coverslip with rubber cement, and incubate the slide in a humidified chamber sealed with parafilm for 12–24 h at 37°C. A simple humidified chamber may be constructed by adding a 5-mm layer of water to the bottom of a pipet tip box, setting the slide on the tip rack, and sealing the cover of the box to the bottom of the box with parafilm.

3.13. Hybridization to Disaggregated Nuclei

1. Just prior to hybridization, prewarm the slides in a solution of 2X SSC for 30 min at 37°C, then denature them in a solution of 70% formamide/2X SSC at 70°C for 2 min.
2. Immediately plunge them into ice-cold 70% ethanol for 2 min, followed by cold 80%, 90%, then 100% ethanol, for 2 min each.
3. Allow the slides to air-dry. Apply the probe and hybridize as described in **Subheading 3.12.**

3.14. Hybridization to Touch Preps

1. Treat as described in **Subheading 3.13.** for disaggregated nuclei, and hybridize as described in **Subheading 3.12.**

3.15. Hybridization to Tissue Sections

1. After resuspension in 10 μ L formamide, the probe should be combined with an equal vol of hybridization solution (to a final concentration of 25% dextran sulfate, 2.5 μ g/mL BSA, 2.5X SSC).
2. Incubate the probe mixture for 5 min at 75°C to completely denature the probe, then place immediately on ice.

- Carefully apply the probe mixture to the slide, coverslip (gently tap out any trapped air bubbles), and seal the perimeter of the coverslip with rubber cement.
- Incubate the slide for 10 min at 90°C, then 12–24 h at 37°C in a humidified chamber sealed with parafilm (as described in **Subheading 3.12.**) (10).

3.16. Washing

- Washing after hybridization to metaphase chromosomes: Prepare a series of wash solutions and incubate the slides as follows:

Wash 1	50% formamide/ 2X SSC	20 min	37°C
Wash 2	2X SSC	20 min	37°C
Wash 3	1X SSC	20 min	37°C
Wash 4	1X phosphate-buffered saline (PBS)	20 min	room temperature

- Remove the coverslip from the slide by swishing it in Wash 1, and wash the slides with shaking (preferably on a rotary shaker) successively in Washes 1–3. After Wash 4, the slides may be temporarily stored at 4°C prior to visualization (8,13,14).
- Washing after hybridization to interphase chromosomes: Use the following wash protocol after hybridization to disaggregated nuclei, touch preps, and frozen or archival tissue sections. Prepare a series of wash solutions and incubate the slides as follows:

Washes 1–3	50% formamide/ 2X SSC	2 min	45°C
Wash 4	2X SSC	2 min	45°C
Wash 5	2X SSC/0.1% NP40	2 min	45°C
Wash 6	2X SSC/0.1% NP40	2 min	room temperature
Wash 7	1X PBS	20 min	room temperature

Excessive background may be removed when necessary by additional washing at 70°C for 2–5 min (10).

3.17. Visualization of Metaphase Chromosomes Hybridized with Biotin- or Digoxigenin- Labeled Probes

Visualization of probes labeled with biotin- or digoxigenin-containing deoxynucleotides requires binding to a fluorophore-conjugated antibody. For biotin- or digoxigenin-labeled probes:

- Transfer the freshly washed slides to a coplin jar containing 4X SSC.
- Add 50 μ L of the appropriate detection solution.
- Cover with a 22-mm \times 30-mm-sized square of parafilm.
- Incubate in a humidified chamber for 60 min at 37°C.
- Remove parafilm.
- Wash sequentially at room temperature for 10 min each in:
 - 4X SSC
 - 4X SSC/0.1% Triton-X 100
 - 4X SSC
- Blot dry and counterstain or amplify (see **Subheading 3.18.**) (8).

3.18. Amplification of Signal from Biotin- or Digoxigenin-Labeled Probes

3.18.1. Amplification of Signal from Biotin-Labeled Probes

If slide is already coverslipped, remove coverslip and soak slide in 4X SSC/0.1% Triton X-100. Blot edge of slide to remove excess liquid. Follow this procedure:

1. Add 50 μ L biotin detection solution.
2. Cover with a 22-mm \times 30-mm-sized square of parafilm.
3. Incubate in a humidified chamber for 30 min at 37°C.
4. Remove parafilm.
5. Wash 15 min in 4X SSC/0.1 % Triton X-100 at room temperature with gentle shaking.
6. Blot edge of slide to remove excess liquid.
7. Add 50 μ L biotin amplification solution.
8. Cover with a 22-mm \times 30-mm-sized square of parafilm.
9. Incubate in a humidified chamber for 30 min at 37°C.
10. Remove parafilm.
11. Wash 15 min in 4X SSC/0.1 % Triton X-100 at room temperature with gentle shaking.
12. Wash 15 min in 4X SSC at room temperature with gentle shaking.
13. Proceed with counterstaining and visualization (8).

3.19. Amplification of Signal from Digoxigenin-Labeled Probes

This procedure is identical to that for biotin-labeled probes, except that digoxigenin-detection and amplification solutions should be utilized.

1. Visualization and amplification of interphase chromosomes hybridized with biotin- or digoxigenin-labeled probes: Detection (and amplification, if desired) of biotin- or digoxigenin-labeled probes hybridized to interphase chromosomes within disaggregated nuclei, touch preps, or tissue sections) should be carried out as described in **Subheading 3.17.** and **3.18.** for metaphase chromosomes.
2. Counterstaining: DNA counterstaining is typically utilized to offer “contrast” between metaphase chromosomes or cell nuclei and the probe fluorophore. A popular counterstain used in conjunction with “green” fluorophores is propidium iodide, whereas a more generic counterstain used in conjunction with “green” or “red” fluorophores is DAPI.
3. To counterstain with propidium iodide or DAPI:
 - a. Apply 50 μ L of propidium iodide or DAPI stain to the slide.
 - b. Coverslip.
 - c. Incubate for 10 min at room temperature (in a light-tight box).
 - d. Wash briefly in 1X SSC.
 - e. Blot edges of slide dry.
 - f. Add 10–20 μ L antifade (e.g., Vectashield, Vector).
 - g. Coverslip.

4. Examine briefly via microscopy. If slide is overstained, incubate in 1X PBD with shaking at room temperature for 30–60 min; blot edges of slide dry, apply antifade, and examine. Repeat if necessary.
5. If probes were biotin- or digoxigenin-labeled, the fluorescent signal may be amplified at this time, if desired.
6. If no further manipulations are anticipated, the coverslip should be sealed permanently to the slide with nail polish.
7. The slide should be stored at -20°C ; strong fluorescent signals will be visible for 2–3 mo.

3.20. Microscopy

1. All large microscope vendors (Zeiss, Olympus, Nikon) manufacture research microscopes.
2. Prior to using or purchasing this type of microscope, it is essential to confirm that the optics of the microscope are suitable for use with oil-immersion (63X and 100X) objectives, and for image reproduction, whether film- or electronic-based.

3.20.1. Illumination

1. Most fluorescence-based microscopy utilizes conventional light microscopes outfitted with mercury bulbs (50 or 100 W). Xenon lamps are sometimes utilized, and lasers are becoming more common as light sources, especially in conjunction with confocal microscopy. Nevertheless, mercury lamps remain the most accessible forms of illumination for fluorescence microscopy, and this chapter assumes that most readers will utilize mercury-based illumination.
2. *Note:* it is essential that only trained personnel should replace and calibrate the mercury bulbs themselves. Failure to perform this procedure correctly can result in faulty illumination and visualization, and can actually damage the lamp housing itself. Furthermore, the fluorescence microscope should be regularly serviced so that the lenses and objectives can be cleaned and the optics can be checked and recalibrated, if necessary.

3.20.2. Emission Filters

1. All the major microscope vendors (e.g., Zeiss, Olympus, Nikon) and others (Omega, Chroma) sell emission filters for fluorescence microscopes that match the emission spectra of specific fluorophores.
2. Single-pass filters are the most restrictive in that they allow detection of only a narrow wavelength of emitted light and are suitable for visualization of only one fluorophore or counterstain.
3. Double-pass and triple-pass filters allow detection of two or three fluorophore/counterstain combinations, respectively.
4. Thus, a dual FISH experiment simultaneously analyzing the copy number of Cy3- and Cy5-tagged DNA probes in a specimen counterstained with DAPI would require the use of a triple-pass filter capable of detecting light emitted by the specimen in all three emission wavelengths.

5. Because of spectral overlaps and quenching issues, it is often desirable to visualize specimens with multiple filters to optimally detect fluorescent signals.

3.20.3. Image Capture

1. The visualization of fluorescent signals emanating from DNA probes requires high-resolution microscopy. Therefore, the experimental specimens must be visualized under oil immersion, using either $\times 63$ or $\times 100$ objectives.
2. Once properly focused, the image itself can be captured using conventional photography or electronically as a digital image.
3. For conventional photography, a 35-mm camera should be attached to the microscope using a camera mount available from most vendors (e.g., Zeiss, Olympus, and Nikon).
4. High-speed (ASA 400) color slide or print film should be used, and exposure times should be determined empirically for the particular microscope/camera setup used.
5. Typically, exposure times of less than 60 s suffice for bright fluorescent images, whereas duller or photobleached images may require exposure times up to 120 s.
6. For electronically generated images using CCD cameras, the camera controls themselves and associated computer-imaging software packages allow great flexibility.
7. Optimal parameters for electronic image capture should be determined empirically for the particular microscope/camera/software package used.

3.21. Fluorescent Signal Quantitation

3.21.1. Metaphase Chromosomes

1. Whether utilized for physical mapping or dosage assessment, the fluorescent signal produced by the hybridization of DNA probes to metaphase chromosomes must be quantitated.
2. For physical mapping, a direct comparison between G-banded and hybridized chromosomes mapping to the same x,y coordinates on a slide provides the best means for mapping probe DNA sequences to chromosomal bands (**Fig. 3**).
3. The major criteria for assessing chromosomal localization for unique DNA sequences is the presence of probe signals at the same position on each of the two sister chromatids per chromosome, for a total of four signals per homologous chromosome pair.
4. Failure to observe a fluorescent signal at the same position on all four chromatids suggests incomplete hybridization, possibly caused by technical error or incomplete homology between probe and target sequences.
5. If the latter is true, the probe localization could be spurious and should not be interpreted as indicative of physical chromosomal localization.
6. Signal quantitation becomes more problematic when it is used to assess DNA sequence dosage. This is especially true when the target DNA is from aberrant cells; e.g., short-term cultures of malignant cells, or immortalized or transformed cultured cells.

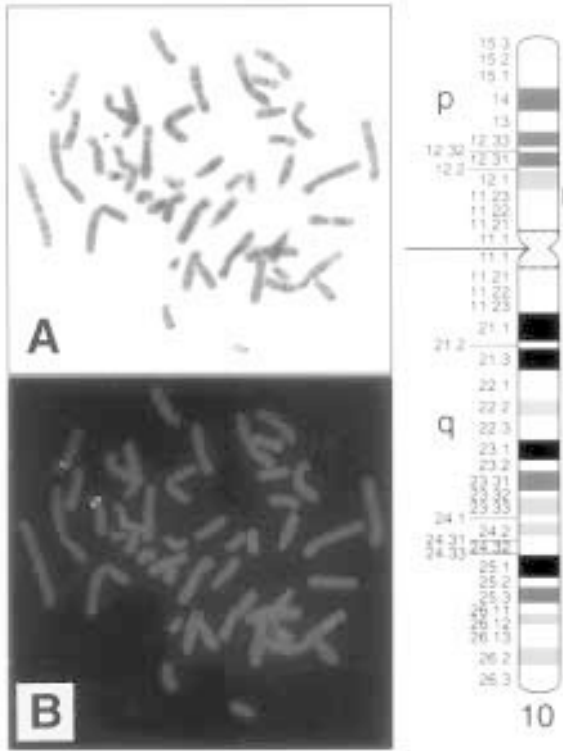


Fig. 3. Localization of probe sequences to metaphase chromosomes. Probe YAC 746-G-7 DNA was labeled with biotin-dUTP via NT, hybridized to metaphase chromosomes, and visualized as described in the text. **(A)** Trypsin-Giemsa—banded metaphase chromosomes prior to hybridization with YAC 746-G-7 DNA. **(B)** The same chromosomes following FISH with YAC 746-G-7. Both chromosomes 10 demonstrate hybridization on both chromatids at position 10p11.2 with the YAC probe. Right: Ideogram of chromosome 10 delineating the region of hybridization at 10p11.2 (vertical bar). Reprinted with permission from **ref. 14**.

7. Metaphase FISH can reliably distinguish copy number for unique probe DNA sequences provided the target genome is “stable” and does not vary from cell to cell, and the metaphase spreads examined are complete so that all chromosomes are represented.
8. As seen in **Fig. 4A**, a cosmid probe DNA specific for unique sequences mapping to 8q11 is represented as expected at the pericentromeric region of the *q* arm of an apparently normal homolog for chromosome 8 (small arrow). However, the same probe is represented twice on an aberrant iso(8q) chromosome (large arrow), and examination of several metaphase spreads verified this observation. Therefore, there are clearly three copies of this unique sequence present in the genome of HT-29 colon carcinoma cells.

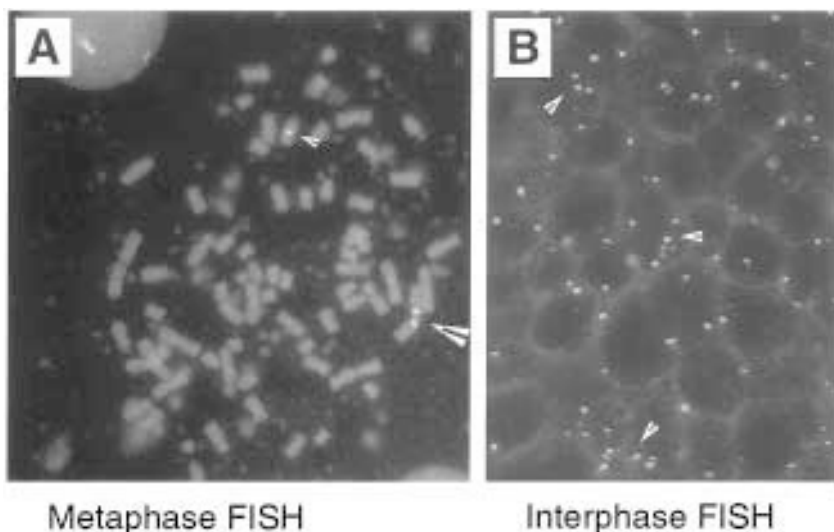


Fig. 4. FISH of abnormal metaphase and interphase chromosomes. **(A)** Metaphase FISH. A cosmid DNA probe, cCI8-209, specific for sequences mapping to the 8q13.1-q13.3 chromosomal region, was directly labeled with fluorescein-dUTP via NT, hybridized to metaphase chromosomes from the HT-29 colon carcinoma cell line, and visualized as described in the text (18). The probe sequences localized as expected at the pericentromeric region of the *q* arm of an apparently normal homologue for chromosome 8 (small arrow). However, the same probe is represented twice on an aberrant iso(8q) chromosome (large arrow), and examination of several metaphase spreads verified this observation. Therefore, there are clearly three copies of this unique sequence present in the genome of HT-29 colon carcinoma cells. **(B)** Interphase FISH. A probe specific for the centromere of chromosome 8 was hybridized *in situ* to a prostate-tumor tissue section using procedures described in the text. The probe DNA was specific for more than two signals in homologous “target” DNA in several nuclei (small arrows). Subsequent quantitation and statistical evaluation verified that all or part of chromosome 8 exists in “extra” copies in this tumor tissue.

3.21.2. Interphase Chromosomes

1. The fluorescent signal produced by the hybridization of DNA probes to interphase chromosomes may be quantitated to assess sequence dosage. This requires enumeration of the number of probe signals observed per nucleus.
2. It is essential to carefully delineate nuclear boundaries, and to avoid areas of potential nuclear overlaps caused by variations in tissue thickness.
3. The use of a simple chart, similar to that shown as follows, may be used to keep track of the number of signals observed per probe per nucleus:

Nucleus	Number of signals observed		
	Probe A	Probe B	Probe C
1	0	1	2
2	2	1	2
3	1	2	1
4	2	2	1
5	2	0	2

4. Data from various *x,y* coordinates on the slide should be recorded on such charts, and notes should be made regarding pertinent features of tissue architecture or histology (e.g., if all the data values are from a single tumor focus or gland).

3.22. Statistical Analysis

Chi square statistical tests can be performed over several metaphase spreads to ensure the veracity of chromosomal localization information for specific probes. Chi square tests can also be used to test for statistically significant differences between cell populations (e.g., normal and malignant) hybridized with the same probes to touch preps or disaggregated nuclei.

1. The use of sectioned tissues—either frozen or archival—however, introduces a factor termed “slice artifact” that must enter into any calculations of DNA sequence copy number.
2. Analysis of data from several studies demonstrated that 60–80% of probe signals in normal, sectioned tissue appear as two signals/nucleus as a consequence of tissue sectioning (10–12).
3. The actual percentage of nuclei that exhibit disomy for probe DNA sequences should be determined empirically from normal control tissues, and depends mainly on tissue thickness and hybridization efficiency.
4. For example, if a series of six normal tissues demonstrated two signals in 65, 70, 68, 75, and 78 of nuclei examined, then a mean of 71.2% of nuclei demonstrated two signals, with a standard deviation of $\pm 5.3\%$.
5. Therefore, a normal “range” for disomy would be defined as 65.9–76.5% of nuclei exhibiting two signals.
6. If the percent nuclei exhibiting disomy falls below 65.9%, one could reasonably conclude that some deletion or loss of sequences homologous to probe DNA sequences has occurred in the cell population examined.
7. However, the criteria used to define alterations of sequence dosage must be delimited rather stringently to avoid inaccurate assessments of DNA sequence gains or losses.
8. A prudent criteria for sequence loss would be defined as the average percent nuclei exhibiting disomy in normal tissues minus twice the standard deviation, or $X-2SD$.

9. In the example given earlier, the observation of two fluorescent signals for probe DNA in less than 60.6% of cell nuclei would indicate significant loss of homologous genomic sequences in the tissues examined.
10. Assigning criteria for alterations of sequence dosage using deviations from the mean, however, will be accurate only if deviations from the mean are minimal.
11. Standard deviation values that exceed 10% of the total number of nuclei examined in normal tissues indicate an excessively broad range for percent nuclei considered disomic, which suggests problems with hybridization efficiencies or with the accuracy of the histologic evaluation of the tissues examined.
12. Finally, evaluation of gains in sequence dosage requires the enumeration of three or more probe signals in cell nuclei. These values must be obtained for normal as well as other tissues, since uneven tissue thickness and tissue architecture may contribute to nuclear “overlaps” whose evaluation could lead to erroneous conclusions regarding sequence amplifications.
13. Calculations similar to those described here can be performed to determine the mean number of nuclei observed with three or more signals homologous to probe sequences in normal tissues, and to determine the standard deviation from the mean.
14. Nuclei with a number of probe signals $\geq X+2D$ can then be defined as exhibiting gain or amplification of genomic sequences homologous to the probe sequences.

3.23. The Future of FISH

The advent of other fluorescence-based techniques useful for the identification of numerical and structural alterations of genomic DNA sequences has greatly expanded the repertoire of techniques under the FISH umbrella. Comparative genomic hybridization, or CGH, allows the simultaneous detection of DNA sequence gains or losses at a chromosome band-scale of resolution (**15**). The use of various fluorophores in different combinations to label chromosome-specific probes has allowed the development of unique fluorescent “signatures” for each human autosome and sex chromosome. Such combinatorial labeling has made possible the evolution of spectral karyotyping—or SKY, which permits the ready identification of numerical and structural chromosome alterations too complex for identification using conventional G-banding techniques (**16,17**). It is clear that fluorescence-based techniques will continue to evolve, and will likely provide critical tools for achieving insight into disease progression and prognosis.

4. Notes

1. All probes representing essentially the same DNA sequence are not alike. It is not unusual to find that recombinant DNAs that overlap with the same genomic sequence are dissimilarly suited for use as FISH probes. One probe may contain more troublesome repetitive sequences, have a higher annealing temperature, or prove more resistant to restriction enzyme digestion. If one probe provides unsatisfactory results, another should be tried until one is found that can provide consistent, reliable hybridization results.

2. Good optical filters for capturing emission photons from excited fluorophores are essential for adequate visualization and quantitation of FISH data. Check that the emission spectra of all optical filters “matches” those of the fluorophores in use. For example, rhodamine and Texas red and often used interchangeably, as both produce a strong “red” fluorescent signal. However, the maximum emission for rhodamine is 520 nm, whereas that of Texas red is 615 nm. It is unlikely that the same optical filter will equally capture emitted photons from both of these fluorophores—especially since the best filters have rather narrow spectral ranges.
3. Passing the labeled probe DNA through a Sephadex G50-type spin column should eliminate unincorporated fluorophore (which can cause “background” fluorescence later). These columns are commercially available from many vendors (e.g., Millipore, Worthington, Amersham, Pharmacia Biotech). Although some investigators prefer to skip this step, we have found it essential for the elimination of posthybridization background fluorescence. This is important, as background fluorescence contributes significantly to “noise,” which greatly reduces the ability to detect true “signal” fluorescence.
4. When possible, direct fluorescent labeling should be utilized rather than indirect labeling. Direct labeling cuts down on background fluorescence and “noise,” and overall produces a much cleaner signal than indirect labeling. Bear in mind, however, that the use of small probes, e.g., large cDNAs or small cosmids (5–20 kb), may require indirect labeling to sufficiently amplify the signal for visualization and quantitation.
5. “Target” preparation is just as important as probe preparation for FISH experiments. Metaphase chromosomes should be G-band quality prior to hybridization. Tissue sections—whether frozen or archival—should have high-quality morphology to compensate for the expected degradation of morphology consequent to the manipulations required for used for interphase FISH.
6. When preparing metaphase chromosomes for FISH (or banding), all pipetting manipulations must be accomplished *very gently* to avoid disruption of nuclear membranes and dispersal of chromosomes prior to slide preparation. Otherwise, an insufficient number of metaphase spreads and/or incomplete metaphase spreads will result.
7. “Dropping” fixed nuclei onto slides to make metaphase spreads is an acquired skill. This procedure should be practiced holding the pipet at different distances from the slide to achieve the desired dispersal and “spread” of chromosomes on the slide. Check dried slides “dropped” from various distances under the microscope to determine which distance works best to achieve the desired result.
8. If the concentration of nuclei for use in making metaphase spreads is low, the nuclei should be spun down and resuspended in a smaller vol of fixative. Alternatively, 3–4 drops (rather than one or two) can be dropped onto a slide to increase the number of metaphase spreads; however, use of more than four drops will result in “sheeting” and flow of material off the slide (which defeats the purpose of using more drops).

9. Coverslips should be attached to slides temporarily during hybridization using rubber cement rather than other glues or clear nail polish. Rubber cement provides a watertight, flexible adhesive that can be easily removed after hybridization without disturbing the underlying tissue or metaphase spreads. To remove the rubber cement, secure the coverslip by pressing gently but firmly on it. This will prevent the coverslip from sliding (and possibly shearing or distorting the underlying tissue or chromosomes) while the rubber cement is being removed. Peel the rubber cement off with a small forceps (such as a jeweler's forceps) and discard.
10. Coverslips should never be forcibly removed from hybridized slides. Rather, gently swish the coverslipped slide in a beaker of room temperature 2X SSC until the coverslip slips off the slide, and then proceed with posthybridization washes.
11. If additional washing must be conducted to reduce excessive background after the slide has been coverslipped and examined under the microscope, the coverslip may be removed by holding the slide under running cold water until the coverslip slides off. Quickly put the slide into wash buffer and proceed with washing.
12. In order to avoid photo bleaching, the minimal amount of illumination possible should be utilized when visualizing slides for probe signal location and quantitation. Some microscopes can be outfitted with rheostat-like illumination controls (e.g., the Zeiss attract), while others utilize various filters to cut down on the amount of light transmitted through the slide. Weak signals sometimes preclude both quantitation and image capturing of the same slide coordinates, since either process may photobleach the probe signal.
13. Although double-pass or triple-pass emission filters are most useful for the image-capture of slides hybridized to multiple fluorescent probes, single-pass filters should always be used for probe quantitation. Spectral overlaps within multiple-pass filters can actually reduce the ability of these filters to detect the total fluorescent output from each probe. Therefore, probe signals often appear less "bright" or intense using multiple-pass filters compared to single-pass filters. As a result, quantitation using multiple-pass filters often under-estimates the number of probe signals extant compared to quantitation performed using single-pass filters.
14. The successful use of FISH to physically map the location of probe sequences to metaphase chromosomes is, in turn, critically dependent on the use of G-banded chromosomes and well-localized metaphase spreads. The x,y coordinates of each photographed metaphase spread must be recorded and logged along with an identifier that can be used to match the photo with the coordinates. This will allow a later side-by-side comparison of hybridized and G-banded chromosomes used to identify the band position of DNA sequences homologous to probe sequences.
15. Although probe signal enumeration is fairly straightforward for metaphase chromosomes, the opposite is true for interphase preparations—especially for those utilizing cut sections. The evaluation of cut sections requires enumeration of the number of probe signals observed per nucleus, which in turn requires the careful delineation of nuclear boundaries. This is where optimal counterstaining plays a key role in successful signal quantitation. If counterstained correctly, individual cell nuclei

should be clearly delineated, and a process of focusing up and down in the z direction should allow successful capture of all fluorescent signals. Areas where cell nuclei are not clearly delineated—often at the edges of the tissue section, or in areas where the section may have folded or torn—should not be analyzed.

16. When enumerating probe signal in tissue sections, notes should be made regarding pertinent features of tissue location, architecture or histology. For example, x,y coordinates should be recorded for each area analyzed, and particular histological features, such as the appearance of the tumor area analyzed, should be noted. This will enable the evaluation of potential “focal” manifestations of genetic alterations in renal tumors, or of “field cancerization” in adjacent normal renal epithelium.
17. As stated in the text, the use of sectioned tissues, either frozen or archival, introduces a factor termed “slice artifact” that must enter into any calculations of DNA sequence copy number. Simply stated, slice artifact is the apparent loss of probe signal caused by the loss of portions of cell nuclei that are literally sliced off during tissue sectioning. The magnitude of slice artifact will vary depending upon tissue type and section thickness. The calculation of slice artifact is equivalent to $100 - N$, where N is the percent of nuclei exhibiting two signals for the probe (or disomy) in normal tissues. To accurately calculate slice artifact, the percent of nuclei exhibiting disomy for probe sequences should be assessed for several normal tissue specimens. Ideally, the percent of nuclei exhibiting disomy should be determined for normal tissues from the same specimens harboring the renal tumors examined—e.g., if 25 renal tumors are analyzed, then 25 specimens of normal renal tissues from those same cases should also be analyzed. If normal tissues are not available for all cases, then as many cases as possible should be analyzed. This will ensure that the subsequent statistical analysis will be carried out with a population large enough to avoid spurious estimates of disomy and slice artifact.

To calculate slice artifact, first calculate the average percent disomy for normal tissues. If 20 normal tissue specimens are examined—and the average percent disomy is 80% with a standard deviation of 5%—then the slice artifact can be safely calculated as 20% ($100 - 80$). This means that the percentage of nuclei exhibiting sequence deletions in tumor tissues must exceed 20% for those deletions to be considered authentic. Furthermore, spurious estimates of disomy and slice artifact can be avoided if more stringent criteria for sequence losses are adopted. This entails defining slice artifact as $\geq (100 - N + 2[SD])$, where N again equals the percent of nuclei exhibiting disomy for the probe, and $2[SD]$ equals twice the standard deviation from the average percent nuclei exhibiting disomy, in normal tissues. Thus, the percent nuclei in tumor tissues demonstrating less than two signals per nucleus would have to be $\geq (100 - 80 + 2[5])$, or $\geq 30\%$, for true sequence loss to be assessed for that tumor.

It should be noted that standard deviation values that exceed 10% of the total number of nuclei examined in normal tissues indicate an excessively broad range for percent disomy, which suggests problems with hybridization efficiencies or with the accuracy of the histologic evaluation of the tissues examined.

References

1. Seabright, M. (1971) A rapid banding technique for human chromosomes. *Lancet* **2**, 971–972.
2. Henderson, A. S. (1982) Cytological hybridization to mammalian chromosomes. *Int. Rev. Cytol.* **76**, 1–46.
3. Bauman, J. G. and Duijn, P. (1981) Hybrido-cytochemical localization of specific DNA sequences by fluorescence microscopy. *Hist. J.* **13**, 723–733.
4. Landegent, J. E., Jansen in de Wal, N., van Ommen, G. J., Bass, F., de vijlder, J. J., van Duijn, P., and Van der Ploeg, M. (1985) Chromosome localization of a unique gene by non-autoradiographic in situ hybridization. *Nature* **317**, 175–177.
5. Hopman, A. H., Wiegant, J., Raap, A. K., Landegent, J. E., van der Ploeg, M., and van Duijn, P. (1986) Bi-color detection of two target DNAs by non-radioactive in situ hybridization. *Histochemistry* **85**, 1–4.
6. Cremer, T., Landegent, J., Bruckner, A., Scholl, H. P., Schardin, M., Hager, H. D., Devilee, P., Pearson, P., and van der Ploeg, M. (1986) Detection of chromosome aberrations in the human interphase nucleus by visualization of specific target DNAs with radioactive and non-radioactive in situ hybridization techniques: diagnosis of trisomy 18 with probe L1.84. *Hum. Genet.* **74**, 346–352.
7. Johnson, I. D. (1996) Introduction to fluorescent techniques in *Handbook of Fluorescent Probes and Research Chemicals*, 6th ed. (Spence, M. T. Z., ed.), Molecular Probes, Inc., Eugene, OR, pp. 1–4.
8. Knuutila, S. (1999) Cytogenetics, in *Current Protocols in Human Genetics*, Volume 1 (Dracopoli, N. C., Haines, J. L., Korf, B. R., Moir, D. T., Morton, C. C., Seidman, C. E., Seidman, J. G., and Smith, D. R., eds.), John Wiley and Sons, Inc., New York, pp. 4.0.1–4.7.32.
9. Afify, A., Bland, K. I., and Mark, H. F. L. (1996) Fluorescent *in situ* hybridization assessment of chromosome 8 copy number in breast cancer. *Breast Cancer Res. Treat.* **38**, 201–208.
10. Macoska, J. A., Trybus, T. M., Sakr, W. A., Wolf, M. C., Benson, P. D., Powell, I. J., and Pontes, J. E. (1994) Fluorescence in situ hybridization (FISH) analysis of 8p allelic loss and chromosome 8 instability in human prostate cancer. *Cancer Res.* **54**, 3824–3830.
11. Wolman, S. R., Macoska, J. A., Micale, M. A., and Sakr, W. A. (1992) An approach to definition of genetic alterations in prostate cancer. *Diagn. Mol. Pathol.* **1**, 192–199.
12. Macoska, J. A., Micale, M. A., Sakr, W. A., Benson, P. D., and Wolman, S. R. (1993) Extensive genetic alterations in prostate cancer revealed by dual PCR and FISH analysis. *Genes, Chromosomes, and Cancer* **8**, 88–97.
13. Lawrence, J. B., Villnave, C. A., and Singer, R. H. (1988) Sensitive, high-resolution chromatin and chromosome mapping in situ: presence and orientation of two closely integrated copies of EBV in a lymphoma line. *Cell* **52**, 51–61.
14. Takahashi, E., Hori, T., and Sutherland, G. R. (1990) Mapping of the human type II collagen gene (COL2A1) proximal to fra(12)(q13.1) by nonisotopic hybridization. *Cytogenet. Cell Genet.* **54**, 84–85.

- 14a. Trybus, T. M., Burgess, A. C., Wojno, K. J., Glover, T. W., and Macoska, J. A. (1996) Distinct Areas of Allelic Loss on Chromosomal Regions 10p and 10q in Human Prostate Cancer. *Cancer Res.* **56**, 2263–2267.
15. Kallioniemi, A., Kallioniemi, O.-P., Sudar, D., Rutovitz, D., Gray, J. W., Waldman, F., and Pinkel, D. (1992) Comparative genomic hybridization for molecular cytogenetic analysis of solid tumor. *Science* **258**, 818–821.
16. Ried, T., Baldinin, A., Rand, T. C., and Ward, D. C. (1992) Simultaneous visualization of seven different DNA probes by *in situ* hybridization using combinatorial fluorescence and digital imaging microscopy. *Proc. Natl. Acad. Sci. USA* **89**, 1388–1392.
17. Speicher, J. R., Ballard, S. G., and Ward, D. C. (1996) Karyotyping human chromosomes by combinatorial multi-fluor FISH. *Nat. Genet.* **12**, 368–375.
18. Fujiwara, Y., Emi, M., Ohata, H., Kato, Y., Nakajima, T., Mori, T., and Nakamura, Y. (1993) Evidence for the presence of two tumor suppressor genes on chromosome 8p for colorectal carcinoma. *Cancer Res.* **53**, 1172–1174.

Polymerase Chain Reaction Detection of DNA Sequence Deletions

Jill A. Macoska

1. Introduction

Allelic loss of human chromosome sequences contributes to tumorigenesis through the inactivation of putative tumor-suppressor genes. The Knudson hypothesis proposes that deletion or mutation must affect both alleles of the gene in order to disable tumor suppression (*1*). As might be expected, the effect of “two hits” on tumor-suppressor gene integrity—e.g., deletion of one allele and mutation of the remaining allele—would disable the gene from encoding gene product. The von Hippel-Lindau (VHL) gene is an example of a tumor-suppressor gene that fulfills the Knudson hypothesis—e.g., one mutant allele is inherited in the germline, and the other is mutated or deleted somatically in many clear-cell renal cell carcinomas (recently reviewed in *ref. 2*).

The polymerase chain reaction (PCR) provides a powerful tool to analyze DNA purified from clinical samples to physically locate and “map” frequently deleted DNA sequences at multiple genetic loci (*see Figs. 1 and 2*) (*3–5*). As described in detail here, PCR-based deletion-mapping experiments require very small quantities of tissue and typically utilize only 50–100 ng of DNA per reaction. The DNA is amplified using oligonucleotide primers (18–25 bp in length) specific for sequences flanking highly polymorphic short tandem repeats (STRs). The STRs can be comprised of dinucleotide (“CACAA”-type), trinucleotide, or tetranucleotide repeated sequences. The number of tandem repeats comprising STRs is frequently different (hence, polymorphic) for alleles of the same locus. Thus, loci containing STRs are highly heterozygous, and alleles of such loci can be distinguished upon gel electrophoresis of the PCR products because they will migrate differently in polyacrylamide or agarose

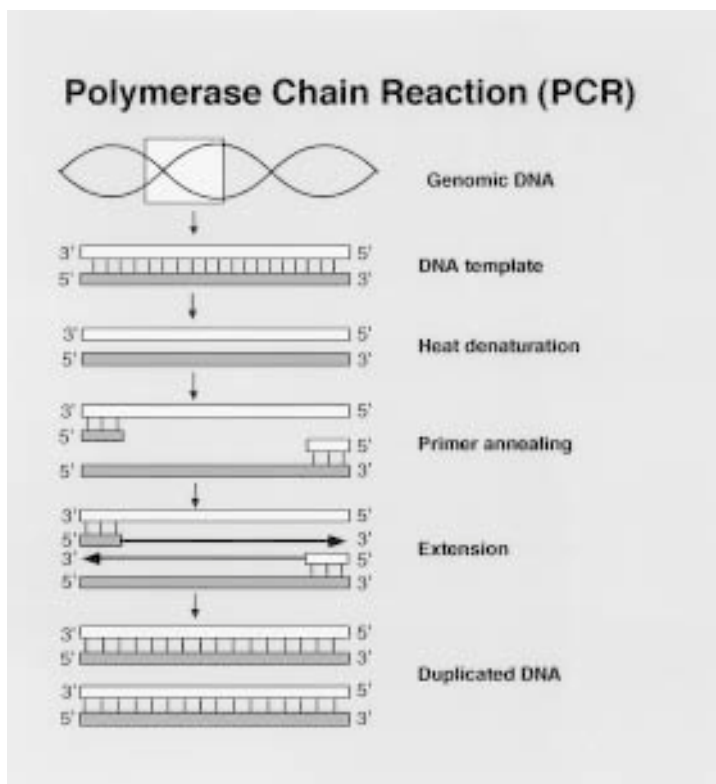


Fig. 1. Polymerase chain reaction. A schema for the polymerase chain reaction is shown. A portion of genomic DNA serves as the template for the amplification reactions. After heat denaturation, oligonucleotide primers anneal to the template, and Taq polymerase replicates and extends nascent DNA strands in the 5'→3' direction from the 3' ends of the primers. DNA that is duplicated or amplified in this manner can then serve as templates for further amplification reactions.

gels (*see Fig. 2*) (6). This differential migration distinguishes the two alleles 70–80% of the time for sequences containing dinucleotide repeats, and to a lesser degree for sequences containing tri- or tetranucleotide repeats. The highly polymorphic nature of STR sequences, combined with the polymerase chain reaction, provide a quick and reliable means to perform deletion mapping of specific chromosomal regions in human tumors.

2. Materials

1. Fresh tissue digestion buffer (10 mL)
 - a. 0.25 mL of 4 M NaCl
 - b. 0.1 mL of 1 M Tris-HCl, pH 8.

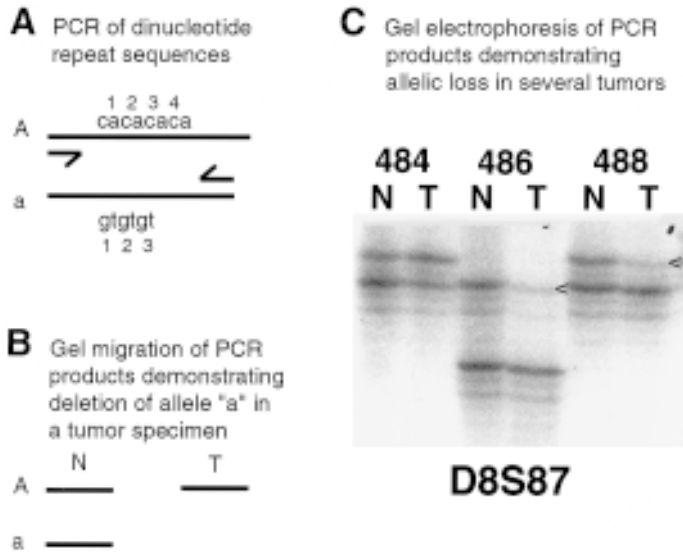


Fig. 2. PCR analysis of DNA from clinical specimens. (A) PCR of dinucleotide repeat sequences. A DNA sequence containing dinucleotide repeat sequences is shown. The "A" allele contains four CA repeats, whereas the "a" allele contains three repeats. Arrows show the positions of oligonucleotide primers. (B) Gel migration of PCR products demonstrating deletion of allele "a" in a tumor specimen. PCR amplification of the sequence shown in (A) for DNA derived from normal or tumor specimens results in a large product for allele A and a smaller product for allele a, consistent with the number of CA repeats present in each sequence. Both alleles are evident in DNA from the normal specimen, whereas the a allele is deleted in DNA from the tumor specimen and does not amplify in the PCR reaction. (C) Gel electrophoresis of PCR products demonstrating allelic loss in two tumors. DNA from normal and tumor specimens from cases 484, 486, and 488 was amplified with radiolabeled primers specific for a dinucleotide repeat sequence within the D8S87 locus and electrophoresed on a 6% denaturing acrylamide sequencing gel. Although two alleles at this locus are evident in DNA from all three normal specimens, the upper allele is deleted and did not amplify in DNA from tumors 486 and 488 (indicated by <).

- c. 0.5 mL of 0.5 M EDTA, pH 8.0
- d. 0.05 mL of 10% sodium dodecyl sulfate
- e. 0.1 mL of 10 mg/mL proteinase K (Sigma)
- Add 9 mL ddH₂O and filter-sterilize; make fresh for each use.
2. Tissue section digestion mixture (500 μ L)
 - a. 50 μ L GeneAmp[®] 10X PCR buffer II (Perkin Elmer)
 - b. 5.0 μ L Proteinase K (10 mg/mL)
 - Add 445 μ L ddH₂O; make fresh for each use.

3. TE for 100 mL:
 - a. 1.0 mL 1 M Tris-HCl, pH 7.5–8.0
 - b. 0.2 mL 0.5 M EDTA, pH 8.0Add 98.8 mL ddH₂O; filter-sterilize or autoclave and store at 4°C.
4. PBS (Phosphate-buffered saline) for 500 mL:
 - a. 4.0 g NaCl
 - b. 0.1 g KCl
 - c. 1.1 g Na₂HPO₄·7H₂O
 - d. 0.1 g KH₂PO₄Add ddH₂O to 1 L; filter-sterilize and store at 4°C.
5. STE for 10 mL:
 - a. 100 µL of 1 M Tris-HCl, pH 8.0
 - b. 250 µL of 4 M NaCl
 - c. 20 µL of 0.5 M EDTA, pH 8.0
 - d. Add 9.63 mL of ddH₂O, filter-sterilize, and store at 4°C. Warm to room temperature prior to use; vortex to redissolve precipitated salt.
6. 10X TBE buffer for 1 L:
 - a. Tris base: 108.0 g (89 mM, 1X)
 - b. Boric acid: 55.0 g (89 mM, 1X)
 - c. EDTA: 5.9 g (2 mM, 1X).Bring to 1 L with ddH₂O, autoclave, and store at room temperature. Dilute 1:9 to 1X prior to use.
7. Formamide loading dye for 10 mL:
 - a. 50 µL 2N NaOH (to 10 mM)
 - b. 8.95 mL formamide
 - c. 0.5 mL 0.05% bromophenol blue
 - d. 0.5 mL 0.05% xylene cyanol.

3. Methods

3.1. Purification of DNA

3.1.1. Purification of DNA from Fresh Tissue

1. Tissues should be quick-frozen in liquid nitrogen upon excision. Tissue chunks no larger than 1 cm³ should be pulverized using a prechilled mortar and pestle, suspended in 5–10 mL fresh tissue digestion buffer, tightly capped, and incubated for 8–16 h at 50°C with gentle agitation or rotation.
2. After digestion, the DNA/buffer mixture will be highly viscous. Add an equal vol of 25:24:1 phenol:chloroform:isoamyl alcohol, invert several times, and centrifuge at 2000g for 20 min at 4°C in swinging bucket rotor. The DNA solution will appear as an upper aqueous layer separated from the organic layer by a white interface.
3. Carefully pipet off the aqueous layer into a new tube using a large-bore plastic disposable pipet.
4. Extract the aqueous layer again with phenol:chloroform:isoamyl alcohol, then with 24:1 chloroform:isoamyl alcohol.

5. Estimate the vol of the aqueous layer and add 1/2 vol of 7.5 M ammonium acetate, mix, then add 2–3 vol of 100% ice-cold ethanol. The DNA should immediately come out of solution and appear as a stringy precipitate. Pellet the DNA by centrifuging at 2000g for 30 min at 4°C in swinging bucket rotor, let the pellet air-dry by placing the tube in a semi-inverted position (watch for “slippery” pellets!), and resuspend the DNA in 0.5–1.0 mL TE.
6. Read the optical density of 1–10 µL aliquots of the DNA in a spectrophotometer at 260λ and 280λ using ultraviolet illumination. The 260/280 ratio should be between 1.5 and 2.0; a smaller value indicates protein contamination, and a higher value suggests that the DNA is not completely in solution. Electrophorese a 1 µg aliquot of the DNA on a 1.0% agarose gel using a high molecular weight marker (e.g., λ DNA cut with *HindIII*). The DNA should migrate at a molecular weight above 20 kb (e.g., at or above the 23 kb λ/*HindIII* band). Evidence of “smearing” below 20 kb suggests DNA degradation; if so, the DNA should be reprepced, taking care not to shear the DNA at any step. DNA that appears to be less concentrated than indicated by the spectrophotometer readings may be contaminated with RNA; if so, digest the DNA with RNase (RNase-It, Stratagene) at 37°C for 1 h, extract once with 25:24:1 phenol:chloroform:isoamyl alcohol, and precipitate as described in **step 5**.

3.1.2. Purification of DNA from Sectioned Tissue

1. Tissue preparation and digestion: This protocol is used to prepare DNA from sectioned archival tissues (formalin-fixed, paraffin-embedded) or cryostat sections for PCR analysis.
2. For archival tissue: Melt excess wax off the slides by incubating them at 55–60°C for 2 h in an upright metal slide rack. Transfer the slides to a glass coplin jar and wash three times for 10 min each in xylene (approx 40 mL/wash). Wash the slides in three changes of 100% ethanol at 2 min per wash. Rehydrate the slides through 2-min incubations in 95% ethanol, 80% ethanol, and 70% ethanol. Incubate the slides in 0.1 N HCl for 20 min (this helps disrupt crosslinks). Rinse the slides in two changes of 1X PBS for 5 min each. Continue as described in **step 4**.
3. For cryostat sections: Take slides from the –80°C freezer and thaw. Continue with **step 4**.
4. DNA Purification: Scrape the desired tissue area off the slide using a fresh, one-sided razor blade for each specimen. Carefully push the tissue section into a 0.5-mL microcentrifuge tube with a 200-µL pipet tip. Depending upon the size of the tissue section, add 50–100 µL of Tissue Section Digestion Mixture and incubate 12–16 h at 37°C with shaking. Inactivate the proteinase K by heating the samples at 95°C for 20 min; cool quickly on ice, and store at –20°C until use. (NOTE: failure to adequately inactivate proteinase K will result in digestion of *Taq* polymerase enzyme in subsequent PCR reactions!).

3.1.3. Purification of DNA from Cultured Cells

1. Cultured-cell preparation and digestion: Trypsinize cells; when detached, add 2 vol of media and transfer to a 15-mL (or larger) snap-cap or screw-cap centri-

fuge tube. Centrifuge at 300g to gently pellet the cells. Decant and discard the supernatant. You may freeze cells at -80°C at this step, or proceed directly to DNA purification.

2. DNA purification: Resuspend the cells in 1–5 mL (1 mL for T25 flask; 5 mL for T150 flask) of Fresh Tissue Digestion Buffer and proceed as for DNA purification from fresh tissue (*see Subheading 3.1.1., step 2*).

3.2. Polymerase Chain Reaction

3.2.1. Preparation of Oligonucleotide Primers

1. Using computer software written for this purpose (several primer design software programs are available through the Internet website <<http://www.nises.affrc.go.jp/~hinomoto/PrimerDesign.html>>), choose suitable oligonucleotide primers for the sequence of interest.
2. Keep in mind that the “best” primer pairs will anneal to the template sequence at temperatures $\geq 55^{\circ}\text{C}$; will be at least 18 nt but less than 25 nt long; will not internally bond to form hairpin loops, and will not potentially “dimerize”—e.g., bind preferably to each other rather than to the template sequence.
3. Dimerization may occur if five or more basepair matches occur between the two primers.
4. Less than five basepair matches between the two primers is acceptable IF the 3' end sequences of either primer are not involved, as “tying up” the 3' end of either primer will greatly reduce the ability of the primer to bind template sequences and will reduce PCR reaction efficiency.
5. The oligonucleotide primers should be stored in sterile water at a concentration of 100 ng/ μL (this will produce a final concentration approximate to 1 μM in the PCR reaction; *see Subheading 3.2.2., step 3*).

3.2.2. The Polymerase Chain Reaction

The actual PCR reactions may be conducted using a variety of thermocyclers. The following protocol is intended for Peltier-type thermocyclers, and may require modification for use with gradient-type thermocyclers.

3.2.2.1. TUBES VS PLATES

The type of heat block provided with the thermocycler determines whether microcentrifuge tubes or microtiter plates can be used as reaction vessels. 96-well microtiter plates are preferred for high-throughput applications—e.g., extensive deletion mapping, allelotyping, genotyping, or microarray production. Polypropylene thin-walled tube plates are preferred for these purposes, and must be used with a sealing device such as lids, pop-tops or sticky film tops (e.g., Titer-Tops from Diversified Biotech). Thin-walled 0.2-mL or 0.5-mL polypropylene microcentrifuge tubes can be used to carry out smaller experiments, and are available from a number of manufacturers.

3.2.2.2. PRIMER RADIOLABELING

1. Optimal deletion mapping avoids the production of nonspecific or artifactual PCR products and, therefore requires the use of a 5' end-labeled oligonucleotide primer in the reaction mixture (7,8).
2. This primer is the same as one of the two (forward or reverse) oligonucleotide primers used in the PCR reaction itself. Primers are 5' end-labeled using T4 kinase as follows:
3. Using radioisotope handling precautions, make up the following reaction mixture in a 0.2-mL or 0.5-mL microcentrifuge tube (if labeling several primers, microtiter plates may be used):
 - a. 1.25 μ L 10X kinase buffer (supplied with T4 kinase).
 - b. 1.0 μ L T4 kinase (New England Biolabs).
 - c. 1.0 μ L 100 ng/ μ L oligonucleotide primer.
 - d. 3.0 μ L γ 32PdCTP (3000 Ci/mmol) (New England Nuclear).
 - e. 6.25 μ L ddH₂O.

Vortex the mixture, spin down briefly in a microcentrifuge, and incubate the reaction in the thermalcycler for 30 min at 37°C, then 15 min at 65°C. Add 80 μ L of STE, mix, and use immediately or store (behind a lucite shield!) for up to 1 wk at -20°C.

3.2.2.3. THE PCR REACTION

1. For each 20 μ L PCR reaction, use:
 - a. 5.0 μ L DNA (up to 100 ng).
 - b. 3.2 μ L of a 2 mM mixture of dGTP, dATP, dTTP and dCTP.
 - c. 2.0 μ L 1X PCR buffer (50 mM KCl, 10 mM Tris-HCl, pH 8.3, 2.5 mM MgCl₂).
 - d. 1.0 μ L of the "forward" oligonucleotide primer (approx 1 μ M final concentration).
 - e. 1.0 μ L of the "reverse" oligonucleotide primer (approx 1 μ M final concentration).
 - f. 0.5–1.0 μ L 5' end-labeled oligonucleotide primer.
 - g. 19.0 μ L of ddH₂O.
 - h. 1.0 μ L *Taq* Polymerase* (1 U; ADD LAST).
2. If several reactions will be run at once, a master mix should be made up by
 - a. aliquotting the DNA into the separate reactions vessels,
 - b. adding the various components in multiples of the number of desired reactions + 1 in a separate tube, then
 - c. aliquotting 15 μ L of the master mix to each reaction vessel for final vol of master mix + DNA = 20 μ L.
3. This process must be accomplished quickly, on ice, to prevent primer dimerization and nonspecific primer/template annealing (or use "hot start" or other similar methods to avoid this problem).
4. Just prior to cycling, the reactions should be mixed and spun down.
5. Mineral oil should be overlayed onto the reactions, if required, to prevent condensation under the lid of the reaction vessel. Swinging buckets that accommodate microtiter plates are available for most table-top and floor-model centrifuges.

Some thermalcyclers are equipped with “hot tops” or “hot bonnets” that eliminate the need for the addition of mineral oil to the reaction vessels prior to cycling.

3.2.2.4. CYCLING PARAMETERS

1. PCR reactions are typically heated to 95°C for 5 min (to completely denature the template), then cycled at 95°C for 30–60 s, 50–60°C (primer dependent) for 30–60 s, and 72°C for 30–60 s, for 30–40 cycles.
2. A final “extension” round at 72°C for 5–10 min may be added at the end, and the reactions cooled to 4°C to inhibit the *Taq* polymerase and stop the reactions.
3. Once cycling is completed, the reactions may be used immediately or stored at –20°C prior to electrophoresis.

3.2.2.5. MOLECULAR WEIGHT MARKERS

1. In order to properly identify PCR products on the gel, and to aid in estimating gel electrophoretic time, it is advisable to run molecular weight markers on each gel.
2. There are many commercially available low molecular weight DNA markers that can be conveniently end-labeled aliquotted, and stored for up to 1 mo at –20°C.
3. The left and right outer gel lanes should be loaded with radiolabeled molecular weight markers; these can even be used to construct migration plots (distance traveled in gel on linear x axis vs molecular weight of DNA fragment on semilogarithmic y axis) to determine the sizes relevant to PCR product bands, if necessary.

3.2.2.6. GEL ELECTROPHORESIS

1. Typical deletion-mapping PCR reactions are electrophoresed through 6% acrylamide/7 *M* urea sequencing gels in 1X TBE buffer.
2. The choice of comb used for these applications is entirely up to the investigator; however, shark-tooth combs typically provide the easiest mode for well formation on these types of gels.
3. Prior to electrophoresis, 5–10 μ L of formamide loading dye is added to each PCR reaction. After mixing, the reactions may be heated at 70°C for 5 min (optional). 10–20 μ L (depending upon well capacity) of each reaction is loaded onto the gel, which is then electrophoresed at 50 W.
4. The length of time the gel is electrophoresed depends upon the length of the PCR product(s) being resolved on the gel.
5. The migration of molecular weight markers relative to the xylene cyanol and bromophenol blue dye fronts can be used to gauge sufficient electrophoretic time to resolve specific PCR products.
6. At the completion of electrophoresis, the gel must be removed from the glass plates and dried.
7. To accomplish this, the gel sandwich must be placed horizontally on a benchtop and the top plate must be pried off using a one-sided razor blade or spatula for leverage.
8. A large piece of filter paper is then laid on top of the gel, gently pressed down, and the filter + gel is peeled off of the bottom plate.
9. The gel is then covered in plastic wrap and dried on a large bed gel dryer.

3.2.2.7. IMAGING

1. The dried gel may be imaged either through autoradiography or Phosphor Imaging.
2. For autoradiography, the gel must be exposed to large-format X-ray film in a light-tight film cassette for a sufficient length of time to produce an image.
3. Strong signals require only short exposures at room temperature; weak signals may require longer exposures using intensifying screens at -70°C .
4. In either case, multiple exposures may be required to sufficiently image all of the PCR products on the gel.
5. For Phosphor Imaging, using a Molecular Dynamics STORM or other similar system. The exposure times may be greatly reduced and do not require X-ray film for imaging. Instead, the images are stored directly as digital images, which may be evaluated using the provided software and imported into various graphics platforms for visualization, text labeling, etc.

3.2.2.8. SCORING ALLELIC LOSS: *LOSS OF HETEROZYGOSITY*

1. Allelic loss is typically scored when the ratio of allelic signal intensities at heterozygous loci in tumor tissue is $\leq 50\%$ of that for the same alleles in normal tissue from the same patient.
2. To eliminate bias and reduce error, it is useful to have two observers independently “score” allelic loss if it is assessed by visual inspection alone (7,8).
3. Alternatively, the signal intensities of the PCR product bands may be read as optical densities or as areas under a curve using software provided with the gel imaging system or from other sources (e.g., NIH Image) (see **Fig. 3** and **Table 1**).
4. Again, allelic loss is assessed if the ratio value for allelic bands in the tumor tissues is $\leq 50\%$ that of normal tissue from the same patient.
5. In **Fig. 3**, it is apparent that tumors from cases 1 and 3 demonstrate loss of heterozygosity (LOH), whereas the tumor from case 2 demonstrates equal retention of both alleles.
6. Densitometric analysis of the gel in **Fig. 3** demonstrates reductions in PCR amplicon signal intensity for one of two alleles from tumors 1, 3, and 4 compared to corresponding normal tissues.
7. The ratio of allelic signal intensities for tumors 1, 3, and 4 is 70%, 60%, and 34% that of the normal tissues, respectively.
8. Note that the allelic signal intensities for tumors from cases 1 and 3 actually exceed 50% that of the normal tissues, but would likely be assessed as demonstrating loss of heterozygosity (LOH) by visual inspection alone.

3.2.2.9. ALLELIC IMBALANCE

1. The polymerase chain reaction will sometimes preferentially amplify one PCR product over another in the same reaction. Thus, the ratio of signal intensities for two alleles of the same locus amplified from DNA derived from normal tissue may not equal 1.0 for all reactions.

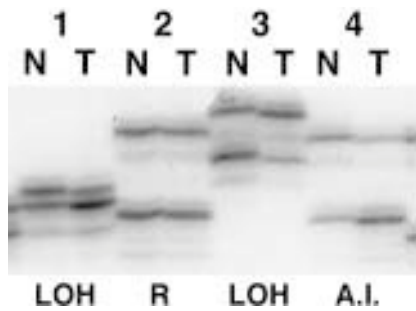


Fig. 3. PCR detection of DNA sequence deletions in tumor specimens. DNA from normal and tumor specimens from cases 1–4 was amplified with radiolabeled primers specific for a dinucleotide repeat sequence within the NEFL locus and electrophoresed on a 6% denaturing acrylamide sequencing gel. The signal intensities of the upper allele for tumor 1 and lower allele for tumor 3 are diminished compared to that of the corresponding normal tissues, consistent with loss of heterozygosity (LOH). In case 4, the signal intensities of the two alleles are “inverted” in the normal sample compared to the tumor sample, consistent with “allelic imbalance” (AI). Case 2 shows equivalent signal intensities for the two alleles in normal and tumor specimens, consistent with retention of diploid dosage for this locus (R).

Table 1
Gel Image Analysis for Allelic Quantitation

Case	Tissue	Allele 1 ^a	Allele 2 ^a	Ratio 1/2	Ratio T/N	Tumor Allelotype
1	Normal	3013	3057	0.99		
	Tumor	2676	3826	0.70	0.70	LOH
2	Normal	3616	3802	0.95		
	Tumor	3685	3662	0.99	1.04	Retained
3	Normal	3998	4435	1.11		
	Tumor	4245	2852	0.67	0.60	LOH
4	Normal	2742	1779	1.54		
	Tumor	1805	3422	0.53	0.34	Allelic Imbalance

^a These values denote the area under the curve for each allele. From Fig. 3.

2. This complicates comparisons with allelic ratios from the corresponding tumor samples, and makes assessment of allelic loss difficult.
3. Therefore, another criteria termed “allelic imbalance” is sometimes invoked to assess allelic loss (9).
4. An example of allelic imbalance is shown by case 4 in Fig. 3 and Table 1.

5. Note that the signal intensities of the two alleles are “inverted” in the normal sample compared to the tumor sample, so that the ratio of allele 1 to allele 2 is 1.54 in the normal sample and 0.53 in the tumor sample.
6. The tumor sample demonstrates only 34% of the allelic signal intensity apparent in the normal tissue, and thus clearly demonstrates allelic loss.
7. However, this assessment would have been difficult or even “missed” by visual inspection alone.

4. Notes

1. For best results, choose STR sequences with few alleles (<6) where the lengths of the most common alleles differ by >2 bp, and the lengths of the PCR products are <200 bp. Following these criteria will greatly reduce any potential confusion caused by the interpretation of data from loci with a large number of closely spaced alleles. Tri- and tetranucleotide repeats fulfill these criteria most consistently, but are not as commonly represented in the genome as dinucleotide repeats, and may not map to the region of interest. Finally, because the quality of starting material (state of tissue preservation, mode of tissue fixation) may vary throughout an experiment, the use of STR sequences that produce relatively “short” PCR products will ensure successful amplification in most cases.
2. Although PCR conditions are readily available for most STRs, one should always run temperature “trials” for each new STR. These trials consist of “test” PCR reactions using high molecular weight genomic DNA from a normal donor (e.g., purified from peripheral lymphocytes), where the DNA is amplified with the new STR at the suggested annealing temperature (T), and at temperatures equivalent to $T - 5^{\circ}\text{C}$ and $T + 5^{\circ}\text{C}$. This ensures utilization of the proper temperature for the chosen template, reagents, and conditions.
3. Fresh tissue must be harvested and snap-frozen quickly to ensure later purification of high quality (high molecular weight) DNA. Fixed tissue should be totally immersed in fixative for appropriate periods of time (depending upon tissue volume; overnight fixations are not optimal) to ensure uniform and complete tissue fixation with minimal DNA degradation. Degradation will be apparent if PCR amplification succeeds for smaller, but not larger (>200 bp) amplicons. DNA purified from archival tissue will be degraded down to segments no larger than 2000 bp; this is to be expected and can be dealt with effectively by choosing STRs (*see Note 2*) that produce smaller amplicons (<200 bp).
4. When choosing suitable oligonucleotide primers to the sequence of interest, keep in mind that the “best” primer pairs will anneal to the template sequence at temperatures $\geq 55^{\circ}\text{C}$; will be at least 18 nt but less than 25 nt long; will not internally bond to form hairpin loops, and will not potentially “dimerize”—e.g., bind preferably to each other rather than to the template sequence. Dimerization may occur if five or more basepair matches occur between the two primers. Less than five base-pair matches between the two primers are acceptable IF the 3' end sequences of either primer are not involved, as “tying up” the 3' end of either primer will greatly reduce the ability of the primer to bind template sequences

and will reduce PCR reaction efficiency. The oligonucleotide primers should be stored in sterile water at a concentration of 100 ng/ μ L (this will produce a final concentration approximate to 1 μ M in the PCR reaction).

5. Failure to adequately inactivate proteinase K will result in digestion of *Taq* polymerase enzyme in subsequent PCR reactions. Incubation at 95°C for at least 20 min is required to inactivate proteinase K; if subsequent PCR amplifications are unsuccessful, repeat the high-temperature incubation.
6. Although some investigators directly incorporate radioactivity into PCR products by substituting one of the dNTPs with a α^{32} PdNTP, we have found that “cleaner” reactions are obtained using a 5' end-labeled oligonucleotide primer in the reaction mixture. This primer is the same as one of the two (forward or reverse) oligonucleotide primers used in the PCR reaction itself. It is interesting to note that the forward and reverse primers do not always behave equally in subsequent PCR reactions; therefore, both should be end-labeled and used separately to determine which one provides “cleaner” and more consistent reactions.
7. Proper safety precautions must be used when handling radioactive materials. The use of multiple labeled primers within one experiment entails the potential exposure of the user to hundreds of milliCuries of radiation. Lucite shields, protective clothing (including double gloves), eye protection (for use with 32 P), disposable “sleeves” (used over lab coat sleeves) and continual monitoring with a Geiger counter are essential for the safe handling of radioactive isotopes.
8. Proper safety precautions must also be used when handling acrylamide. Acrylamide is a neurotoxin, and is especially dangerous in powdered form. Gloves should be worn, and disposable face masks can be worn, if desired, when acrylamide is weighed out and dissolved. Removal of gas bubbles from acrylamide may be accomplished by mixing the dissolved acrylamide on a stir plate in an one-armed flask under vacuum; this will reduce the appearance of bubbles in the gel and will help the gel polymerize faster. Catalyzed acrylamide can be placed in an ice bucket to retard polymerization in the flask when pouring the gel.
9. Care must be taken when prying the two plates of the gel “sandwich” apart so that the gel does not tear or slide off the lower plate. If a portion of the gel sticks to the top plate, it may be possible to loosen it by squirting water between the gel and plate. The result will be a very wet, but intact, gel that will require a longer drying time. Note that the gel will likely stretch and distort in the area that was “stuck,” which must be considered when subsequently interpreting data from that portion of the gel.
10. Expected PCR product sizes and allele frequencies must be considered when interpreting deletion data from gels. Results should be viewed with suspicion if either of these parameters don’t “match” between observed and expected. For example, amplification of locus A with a specific set of oligonucleotide primers is expected to produce six alleles with the following sizes and frequencies: A1 = 108 bp (0.10), A2 = 100 bp (0.005), A3 = 102 bp (0.030), A4 = 104 bp (0.10), A5 = 106 bp (0.040), and A6 = 108 bp (0.005). Therefore, one would expect to see the 102 bp and 106 bp alleles represented most frequently, followed by the other four alleles. If this is not the case, then an experimental artifact or some type of disequilibrium may be respon-

sible for the discrepancy. Bear in mind that allelic frequencies obtained using ethnically homogenous human populations (often stated in the description of the STRs) may not strictly apply to all populations. For example, allelic frequencies obtained from amplifying DNA from 100 Japanese individuals may not be the same as those obtained from 100 Caucasian or African-American individuals.

References

1. Knudson, A. G., Jr. (1971) Mutation and cancer: statistical study of retinoblastoma. *Proc. Natl. Acad. Sci. USA* **68**, 820–823.
2. Kaelin, W. G. and Maher, E. R. (1998) The VHL tumour-suppressor gene paradigm. *Trends Genet.* **14**, 423–426.
3. Sambrook, J., Fritsch, E. F., and Maniatis, T., eds. (1989) The polymerase chain reaction, in *Molecular Cloning: A Laboratory Manual. 2nd Ed.*) Cold Spring Harbor Laboratory Press, Cold Spring Harbor, NY, pp. 14.1–14.35.
4. Saiki, R. K. (1990) Amplification of Genomic DNA, in *PCR Protocols: A Guide to Methods and Applications* (Innis, M. A., Gelfand, D. H., Sninsky J. J., and White, T. J., eds.), Academic Press, Inc., New York, pp. 13–20.
5. Kramer, M. F. and Coen, D. M. (1995) The polymerase chain reaction, in *Current Protocols in Molecular Biology*. (Ausubel, F. M., Brent, R., Kingston, R. E., Moore, D. D., Seidman, J. G., Smith, J. A., and Struhl, K., eds.) John Wiley and Sons, New York, pp. 15.0.1–15.8.8.
6. Weber, J. L. (1989) Length polymorphisms in (dC-dA)_n(dG-dT)_n sequences using the polymerase chain reaction, in *Current Communications in Molecular Biology: Polymerase Chain Reaction* (Erich, H. A., Gibbs, R., and Kazazian, H. H., Jr., eds.), Cold Spring Harbor Laboratory Press, Cold Spring Harbor, NY, pp. 141–150.
7. Trybus, T. M., Burgess, A. C., Wojno, K. J., Glover, T. W., and Macoska, J. A. (1996) Distinct Areas of Allelic Loss on Chromosomal Regions 10p and 10q in Human Prostate Cancer. *Cancer Res.* **56**, 2263–2267.
8. Prasad, M. A., Wojno, K. J., and Macoska, J. A. (1998) Homozygous and frequent deletion of proximal 8p sequences in human prostate cancers: identification of a potential tumor suppressor gene site. *Genes Chromosomes Cancer* **23**, 255–262.
9. MacGrogan, D., Levy, A., Bostwick, D., Wagner, M., Wells, D., and Bookstein, R. (1994) Loss of chromosome arm 8p loci in prostate cancer: Mapping by quantitative allelic imbalance *Genes Chromosomes Cancer* **10**, 151–159.

Matrix Metalloproteinases and Their Inhibitors

Alexander Kugler, Paul Thelen, and Rolf-Hermann Ringert

1. Introduction

Matrix metalloproteinases (MMPs) are a group of 16 enzymes that are capable of degrading extracellular matrix components. Their catalytic function is dependent on a zinc ion in the active center. MMPs are separated in three groups: gelatinases (type IV-collagenases), stromelysins, and interstitial collagenases. Their physiological and pathological significance is to modulate the extracellular matrix—e. g., in embryogenesis, in the ovarian cycles, or in inflammatory diseases such as rheumatoid arthritis or fibrosis of the liver or kidney (1,2).

MMPs are secreted as inactive preenzymes. They are transformed to the active enzyme after cleaving off a N-terminal peptide. This regulation of MMP expression on the protein level is performed autocatalytically, by membrane-bound MT-MMPs or by external proteolytic activity such as the urokinase-plasminogene-activator system (3). Activation is counterbalanced, but can also be enhanced by multifunctional specific inhibitors—the tissue inhibitors of metalloproteinases (TIMPs). TIMPs reduce the proteolytic activities of MMPs, and four different varieties have been described. TIMPs have been detected by inverse zymography, Western blotting, and *in situ* hybridization. A high MMP expression and low TIMP expression have been correlated to invasiveness in cervical tumors (4). TIMPs also enhance the proliferation of tumor cells (5). High expression of TIMP-2 in the invasive area of breast tumors has been correlated with poor prognosis (6). In adenocarcinoma of the prostate, both MMP-2 and -9 have been detected, and poor prognosis has been significantly correlated to aneuploid carcinoma and MMP-9 activity (7). In addition, expression of MMPs was shown to correlate with tumor stage in renal cell carcinoma (RCC) (8).

In order to analyze the interactions involved in this highly regulated process of tumor invasion in RCC, mRNA levels of MMPs and TIMPs in normal and tumor tissue as well as in RCC-derived cell cultures were quantitated. Competitive quantitative reverse transcription polymerase chain reaction (cqRT-PCR) has been established for MMP-2, MMP-9, TIMP-3, and house-keeping gene β -actin. To describe the balance of activation and inhibition of MMP action, MT-MMP-1, MMP-2, and TIMP-2 simultaneously in multiplex-PCR were analyzed.

cqRT-PCR measures the absolute amount (copies or attomoles per μ g total cellular RNA) of a mRNA species by adding a known amount of a gene-specific competitor RNA to the RT-PCR. The merits of RT-PCR—i.e., the huge amplification potential, can also cause possible pitfalls such as false-positive amplicons. cqRT-PCR overcomes these problems with the added competitor RNA, which has amplification efficiencies equal to the target gene, rendering reliability and independence from PCR protocols restricted to the linear range of amplification (9). The use of a RNA competitor instead of only a DNA competitor solely in the PCR step of RT-PCR adds a control for reverse transcription efficiencies to this method. Thus, cqRT-PCR is the most preferred choice over relative RT-PCR, Northern blotting, and nuclease-protection assay for RNA quantitation.

Quantitative data obtained on the mRNA-level are solidified on the protein level by zymography and immunohistochemistry. In this chapter, we outline our methods for RNA extraction, construction of RNA competitors, reverse transcription, PCR, video-imaging densitometry of agarose gels, zymography, and reverse zymography.

1.1. RNA Extraction

When extracting total cellular RNA from tissue and cells, extreme care must be taken to inhibit RNA degradation by ribonucleases (RNases) which are released from intracellular compartmentations. This process includes the inhibition of ribonucleases during extraction and the extraction of RNA from proteins, including RNases and cell debris. Thus, tissue is frozen immediately after dissection and kept in liquid nitrogen until it is homogenized in the presence of the RNase inhibitor guanidinium isothiocyanate, followed by an extraction from a water-saturated phenol-chloroform-isoamylalcohol phase. All of the following procedures are carried out in commercially available RNase-free labware, solutions, and water. Total cellular RNA is extracted from tissue by acid guanidinium-isothiocyanate-phenol-chloroform-isoamylalcohol (10) and purified with the Qiagen RNeasy Mini Kit (11).

2. Materials

2.1. RNA Extraction from Frozen Tissue Up to 250 mg

1. Homogenization solution (**10**): 4 M guanidinium isothiocyanate, 25 mM sodium citrate.
2. Solution D: 0.5% sodium sarkosyl 0.1 M mercaptoethanol.
3. 2 M sodium acetate pH4 (Na-Ac).
4. Water-saturated phenol, chloroform, isoamylalcohol (125:24:1) (PCI).
5. Isopropanol, pure (IP).
6. RNeasy Mini Kit and (optional) RNase-free DNase Set (Qiagen).

2.2. Extraction of RNA from Cultured Cells and Small Amounts of Tissue

1. RNeasy Mini Kit, QIAshredder and (optional) RNase-free DNase Set (Qiagen).

2.3. Construction of Competitor cRNA Materials

1. Gene Amp[®] RT-PCR kit (Perkin Elmer, Weiterstadt, Germany).
2. Specific primers.
3. Platinum Taq DNA Polymerase High Fidelity (Gibco-BRL, Karlsruhe, Germany).
4. DNA cleanup kit (QIAquick PCR purification kit, Qiagen).
5. DNA gel-extraction kit (Qiaex II[®], Qiagen).
6. RNA transcription kit (MEGAscript[™] or MEGAshortscript[™], Ambion, Austin, TX).

2.4. RT-PCR

Gene-specific primers are used, and primer annealing temperatures accordingly. Competitor RNA is added in several dilutions (*see* **Fig. 1**).

2.5. Zymography

1. Separation buffer: 36 g Tris/200 mL H₂O pH 8.8.
2. Gelatin.
3. Ultrapure protogel (30% acrylamid, 0.8% bisacrylamid ratio 37.5:1).
4. SDS 10%.
5. Ammoniumpersulfat (100 mg in 2.5 mL H₂O).
6. TEMED.
7. Butanol.
8. Running buffer: SDS Tris glycine 1:10 (Novex[™]).
9. Top-buffer: 0.375 Tris-HCl, pH 6.8= 11.36 g Tris to 150 mL H₂O, adjust to pH 6.8 and bring to 250 mL with H₂O.
10. 5X: 0.4 M Tris-HCl pH 6.8, 20% glycerol 0.03%, 5% SDS bromophenol blue.
11. Triton X-100, 2.5%.
12. LSCB buffer 500, 1:10:500 mM Tris-HCl, 2 M NaCl, 50 mM, CaCl₂, 0.2% biglycine.

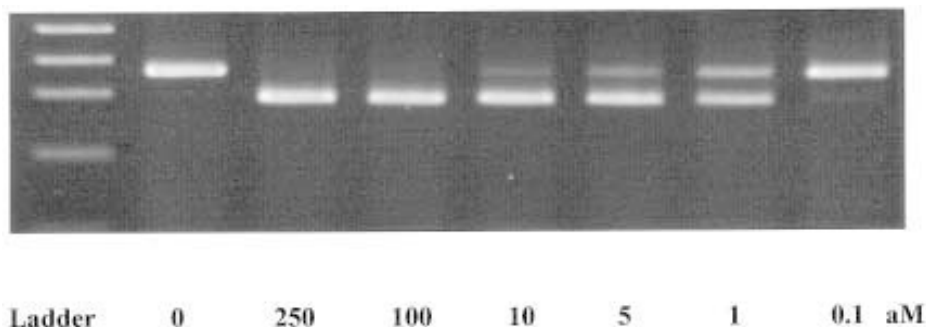


Fig. 1. cqRT-PCR for MMP-2 with MMP-2 competitor concentrations of 250; 100; 10; 5; 1; and 0.1 attomoles per μg tcRNA from RCC tissue. PCR products were separated on 2% agarose gel stained with ethidium bromide and subjected to densitometry. (see Note 2.)

13. Staining solutions: 0.5% Coomassie G250, 30% methanol, 10% acetic acid.
14. Destaining buffer: 30% methanol, 10% acetic acid.
15. Conservation buffer: 5% glycerol, 30% methanol.
16. 1-mm-wide 10 cm \times 10 cm gel-chambers.
17. Gel conservation.

2.6. Reverse Zymography

In addition to the materials listed in **Subheading 2.5.**, recombinant MMP-2 (0.134 mg/mL) is used.

3. Methods

3.1. RNA Extraction from Frozen Tissue

1. Frozen tissue chunks of up to 250 mg are homogenized from the frozen state in 4 mL Solution D optionally completed with three drops of Antifoam A (Sigma, Taufkirchen, Germany) using a tissue homogenizer (IKA, Germany) for 30 s.
2. Add 0.5 mL Na-Ac and mix well.
3. Add 5 mL PCL, shake or vortex vigorously, and hold on ice.
4. Centrifuge at 10,000g for 10 min with centrifuge brake off.
5. Collect aqueous supernatant carefully, leaving behind a liberal amount of inter-phase and phenol phase.
6. Mix supernatant into an aliquot of ice-cold IP and precipitate RNA at -20°C for 1 h.
7. Centrifuge at 5000g for 10 min, wash with 70% ethanol and dry RNA pellet.
8. Dissolve RNA in 100 μL H_2O and 350 μL RLT (provided in the Qiagen RNeasy Mini Kit), and follow the manufacturer's instructions with optional DNase treatment.

3.2. Small-Scale Extraction Protocol

1. Up to 10^7 cells or 30 mg of tissue pulverized on dry ice or under liquid nitrogen are suspended in 600 μL RLT and homogenized with a pestle (DSTROY-S, BIOzym, Hessischoldendorf, Germany) fitting in an Eppendorf cup.
2. The homogenate is run through QIAshredder and Rneasy Mini columns following the manufacturer's instructions with optional DNase treatment.
3. Quantitation and quality check of RNA is determined by OD_{260} in a spectrophotometer (GeneQuant II, Pharmacia, Freiburg, Germany). Eluted RNA from step 1.1 or 1.2 should be diluted (e.g., 1:100) in RNase-free water to yield OD readings exceeding 0.1 at 260 nm. An OD_{260} of 1.000 corresponds to 40 μg RNA/mL. Our RT-PCR applications require RNA concentrations of at least 0.25 $\mu\text{g}/\mu\text{L}$.
4. For larger series of samples, it may be worthwhile to apply the more sensitive, although more time-consuming measurements of RNA concentration in a fluorometer. Concentrations as low as 1 ng/mL can be measured and reproduced when RiboGreen[®] RNA Quantitation Kit (Molecular Probes) is used for calibration and measurements. Competitor RNA (*see Subheading 3.3.*), which is highly diluted when applied in an attomole range, should be quantified in all dilution steps by this highly sensitive method.
5. A straightforward way to estimate RNA purity provides the ratio $\text{OD}_{260}/\text{OD}_{280}$, i.e., the reading of RNA at 260 nm over the reading at 280 nm of contaminating proteins. This value should range between 1.8 and 2.1. In contrast to RNA quantitation, where water is the preferred solvent, the ratio $\text{OD}_{260}/\text{OD}_{280}$ should be measured in 10 mM Tris-HCl pH 7.5.
6. RNA integrity control and comparison of equal quantities of agarose gels. Several parallel RNA samples can be checked for integrity and equal quantities on agarose gels. RNA integrity is indicated by two prominent bands of 28S and 18S ribosomal RNA. A smear below 18S and/or a third band of much smaller size indicates degraded RNA, which is inappropriate for cqRT-PCR. An agarose gel can also verify photometric quantitation, especially when a video-imaging system (*see Subheading 2.4.*) is used for densitometry of RNA bands.
7. Cast 0.8% agarose gel in TAE-TE buffer (TAE supplemented with 40 mM Tris-HCl and 2 mM EDTA, both pH 8.0 (*12*)).
8. Dissolve 3 μg RNA in the same buffer. Heat to 70°C for 10 min and cool on wet ice for 5 min.
9. Add gel loading buffer (*12*) and load onto gel.
10. Run gel in TAE-TE at 5 V/cm.
11. Stain with ethidium bromide in water.

3.3. Construction of Competitor cRNA

Traditional molecular biology instruments such as restriction, ligation, and cloning into transcription vectors to generate the small deletions (or insertions) in gene sequences in order to yield competitor standards can be used. More

recently, an entirely PCR-based procedure for deletion and template generation for RNA transcription was applied (**13**). The design of a MMP-2 competitor RNA is outlined here (*see* **Note 3**; **Fig. 2**).

3.3.1. General Design

- A. A RT-PCR protocol is routinely run with MMP-2 FW-primer (black) and RV-primer (gray), which yield a 370 bp PCR-product.
- B. A deletion in this PCR product is introduced by a primer composite consisting of the usual RV-primer (gray) and a sequence (triple line), which primes a region 66 bp upstream of the RV binding site.
- C. In a further PCR, the shortened fragment is reamplified with two additional primer composites. The T7-FW primer attaches the T7 promoter region (dotted line) to the fragment for subsequent cRNA synthesis. The T₂₅ RV primer serves two purposes. The elongation renders efficient reverse transcription of the competitor RNA, and as the T₂₅ (dashed line) transcribes to an oligo-A tail of the competitor similar to mRNA, it can be primed with oligo-T primers.

3.3.2. Construction

1. Run routine RT-PCR (*see* **Subheading 3.4.**) to yield one single band of PCR product.
2. Clean up DNA with QIAquick.
3. Reamplify 100 ng purified PCR product with usual FW-primer and deletion primer.
4. Identify smaller band (as compared to usual PCR product) on an ethidium bromide-stained agarose gel and excise band under 366 nm UV light.
5. Extract DNA from agarose with QIAEX II^R.
6. Reamplify 100 ng-purified fragment with T7-FW primer and T₂₅ RV primer.
7. Clean up DNA with QIAquick.
8. Transcribe 100 ng purified DNA to RNA with MEGAscriptTM.
9. Quantify RNA, run RNA gel and identify one single RNA band.

3.4. cqRT-PCR

cqRT-PCR is run in the same manner as the usual RT-PCR protocol.

1. One cycle RT: 15 min. 42°C, 5 min 99°C, 5 min 5°C.
2. One initial cycle 2 min 95°C.
3. 35 cycles 1 min 94°C, 1 min 67°C, 1 min 72°C.
4. One final cycle 7 min 72°C.
5. Hold at 4°C.

Gels were visualized under UV and digitized. Densitometry was done using Herolab E.A.S.Y. Win 32 software. Densitometric intensities as log ratios of MMP-2 over competitor (log ratio target/competitor) were plotted against log competitor concentration (**13**). Computer-aided linear regression yielded the equivalence points—i.e., the calculated equilibrium of MMP-2 target and

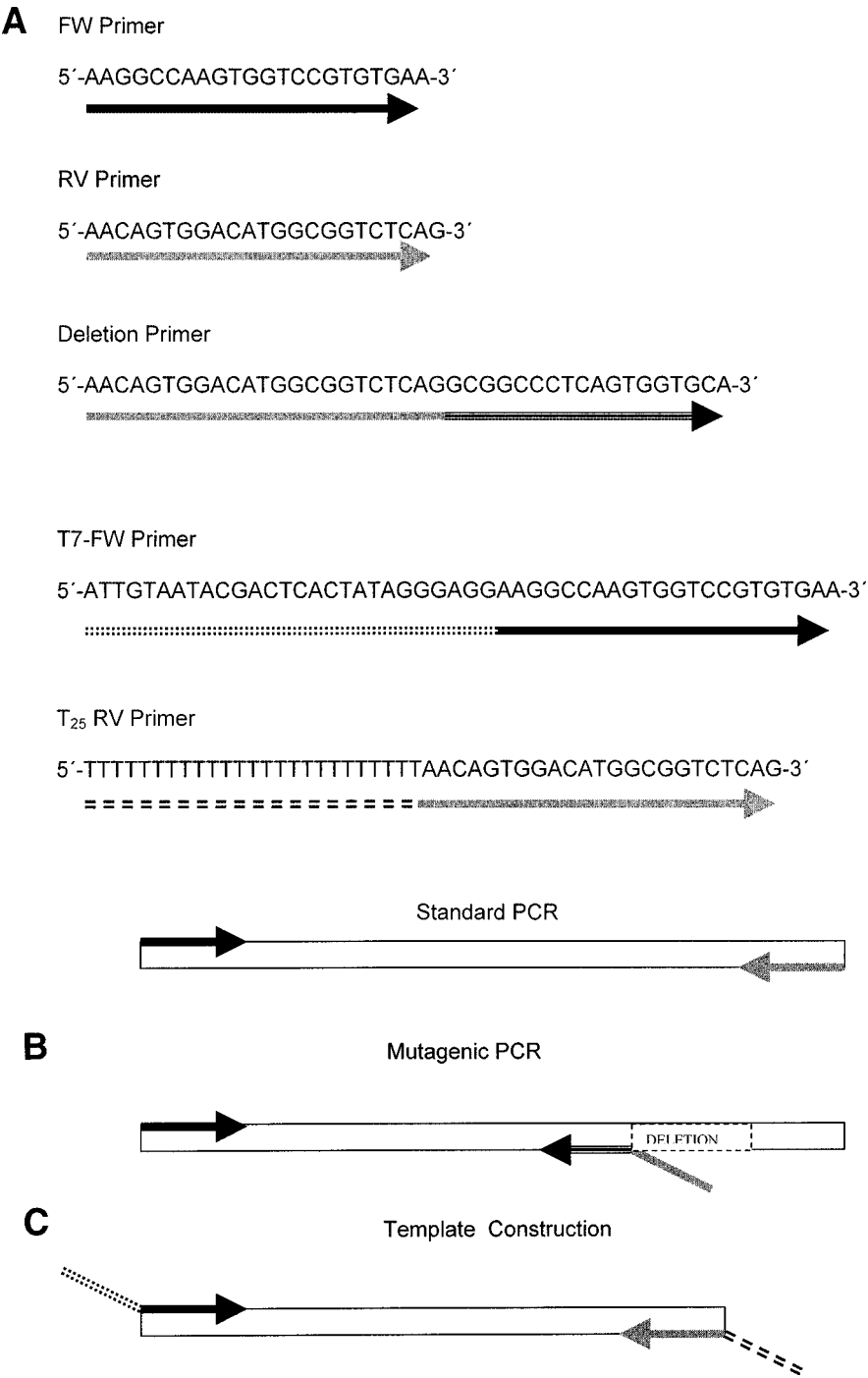


Fig. 2. (A) Standard PCR, (B) mutagenic PCR, (C) template construction.

cRNA competitor where log ratio MMP-2/competitor equals zero. Differences in molar ethidium bromide incorporation between target and competitor were corrected for according to Menzo et al. (14). The level of MMP-2 mRNA expression as determined in attomoles per μg tcRNA can then be compared between tumor and adjacent tissue or as absolute values in single samples. Accuracy can be highly increased when a coarse estimation of MMP-2 expression is first performed using only two different dilutions of competitor and then fine-tuned with several dilution steps in the vicinity of the estimated solution.

Once quantified precisely in cqRT-PCR, a key factor transcript can be included in a multiplex RT-PCR together with related factors such as TIMPs and MT-MMPs to yield results of interdependent relativity.

3.5. Zymography

3.5.1. Preparation of Samples

1. Subconfluent (80%) growth of tumor-cell culture in culture flasks.
2. Wash with PBS three times.
3. Serum-free medium for 24 h in incubator on the subconfluent cell cultures.
4. Harvest supernatant.

3.5.2. ANALYSIS OF MMP AND TIMP ACTIVITY ION THE SUPERNATANT OF TUMOR-CELL CULTURES

1. Add 2 g gelatin to 200 mL separation buffer.
2. For 4-5 gels in 10 × 10 cm plates fill 80% (lower phase) of the plate with the following mix:
 - a. Separation buffer (+gelatin): 20 mL.
 - b. Ultrapure protogel: 20 mL.
 - c. 10% SDS: 800 mL.
 - d. Ammonium persulphate: 400 mL (*see* Notes 4 and 5).
 - e. TEMED: 40 mL.
3. Polymerization of the gel for 1 h: Put butanol in the upper phase for this period of time.
4. After removal of butanol pour top-phase:
 - a. Top buffer: 30 mL.
 - b. Ultrapure protogel: 12.5 mL.
 - c. 10% SDS: 940 mL.
 - d. Ammonium peroxide: 700 mL.
 - e. TEMED: 70 mL.
5. Polymerization in running buffer overnight at 4°C.
6. Electrophoresis
 - a. Fill the chambers with 5 mL 5X and 20 mL supernatant.
 - b. Electrophoresis 120 V for 2–3 h (the first blue staining band should have run through the gel).

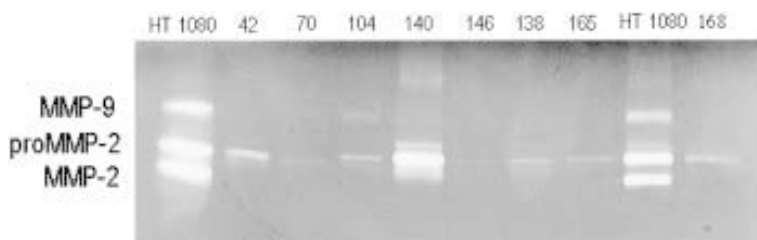


Fig. 3. Zymography of the supernatant of primary tumor-cell cultures derived from RCC tumor tissue. As a control, supernatant of HT 1080 tumor cells was used.

- c. After electrophoresis, the SDS is removed by soaking gels for 20 min each in buffer containing 50 mM/L Tris (pH 7.6), 10 mM/L CaCl_2 , and 2.5% Triton X-100.
- d. Protease activity was restored in the same buffer without Triton X-100 containing 0.01 M sodium azide, and the digestion reaction was performed at 37°C for 12 h (incubate the gel in LSCB buffer overnight at 37°C).
7. Staining
 - a. Staining of the gel for 3 h in Coomassie blue.
 - b. Destaining three to five times in destaining buffer each time for 20 min.
 - c. Conservation in conservation buffer for 20 min.
 - d. Sealing in cellophane overnight at room temperature (Novex DryEase™ Drying System).

The analysis of supernatant of primary cell cultures derived from RCC using this protocol revealed the gel shown in **Fig. 3** (see **Note 6**).

3.6. Reverse Zymography

1. Add 2 g gelatin to 200 mL separation buffer.
2. For 4–5 gels in 10 × 10 plates (1-mm wide) fill 80% (lower phase) of the plate with the following mix:
 - a. Separation buffer (+gelatin): 20 mL.
 - b. Ultrapure protogel: 20 mL.
 - b. 10% SDS: 800 mL.
 - c. rMMP-2, (0.134 mg/mL): 45 mL.
 - d. Ammonium persulfate: 400 mL.
 - e. TEMED: 40 mL.
 - f. Polymerization of the gel for 1 h. Put butanol in the upper phase for this period of time.
3. After removal of butanol pour top phase:
 - a. Top buffer: 30 mL.
 - b. Ultrapure protogel: 12.5 mL.
 - c. 10% SDS: 940 mL.

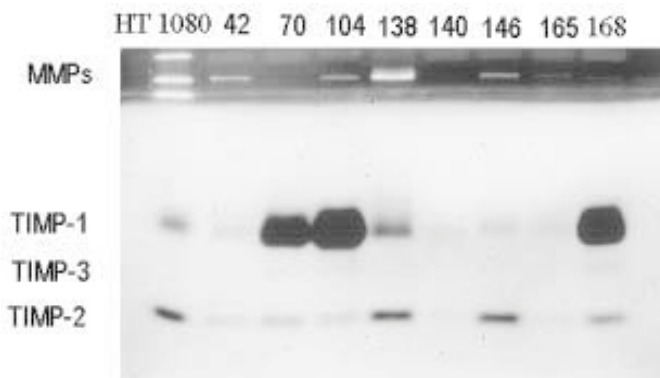


Fig. 4. Reverse zymography reveals activity of TIMP-1 and TIMP-2 in all samples. In addition, supernatant of culture 168 has an activity band at TIMP 3 level.

- d. Ammonium peroxide: 700 mL.
- e. TEMED 70 mL.
4. Polymerization in running buffer overnight 4°C.

Zymography and reverse zymography can also be performed in samples derived from fresh tumor tissue after protein isolation. The identical protocol can be used by replacing the tumor-culture

3.7. Conclusions

The methods presented here can precisely determine the expression status of key enzymes in RCC on the mRNA level, even from very moderately expressed transcripts. Future technologies will include microdissection with a more defined cellular origin of tissue, small-scale RNA extraction, sensitive single-step RT-PCR, and automated real-time quantitative PCR. All quantitation on the RNA level should be correlated to protein expression as in zymography, to proof the true biological role of the gene under investigation.

4. Notes

1. Although it is good laboratory praxis to run RNA on denaturing formaldehyde agarose gels (12) equally good results can be obtained with this less tedious method.
2. A series of different dilutions with defined concentrations of competitor RNA are spiked into a constant amount of cellular RNA and run according to the cycle protocol above. With decreasing competitor concentration the cellular target RNA has increasing access to all resources of RT-PCR. Thus, the target signal rises while the intensity of the competitor band decreases with decreasing concentrations of competitor RNA (see Fig. 1).

3. Once quantified precisely in cqRT-PCR a key factor transcript can be included in a multiplex RT-PCR together with related factors such as TIMPs and MT-MMPs to yield results of interdependent relativity.
4. Fill in ammonium persulphate and TEMED quickly and pour lower phase of the gel immediately afterwards (when adding 2 g gelatin to 200 mL separation buffer).
5. Fill in ammonium persulphate and TEMED quickly and pour upper phase immediately afterwards. Put in the combs (when adding upper phase of gel).
6. Zymography and reverse zymography (*see Fig. 4*) can also be performed in samples derived from fresh tumor tissue after protein isolation. The identical protocol can be used by replacing the tumor culture supernatant by the isolated protein.

References

1. Manicourt, D. H., Fujimoto, N., Obata, K., and Thonar, E. J. M. (1995) Levels of circulating collagenase, stromelysin-1, and tissue inhibitor of matrix metalloproteinase 1 in patients with rheumatoid arthritis. *Arthritis Rheum.* **38**, 1031–1039.
2. Milani, S., Herbst, H., Schuppan, D., Grappone, C., Pelligrini, G., Pinzani, M., Casini, A., Calabro, A., Ciancio, G., Stefanini, F., Burroughs, A. K., and Surrenti, C. (1994) Differential expression of matrix-metalloproteinase-1 and-2 Genes in normal and fibrotic liver. *Am. J. Pathol.* **144**, 528–537.
3. He, C., Wilhelm, S. M., Pentland, A. P., Marmer, B. L., Grant, G. A., Eisen, A. Z., and Goldberg, G. I. (1989) Tissue cooperation in a proteolytic cascade activating human interstitial collagenase. *Proc. Natl. Acad. Sci. USA* **86**, 2632–2636.
4. Nuovo, G. J., MacConnell, P. B., Simsir, A., Valea, F., French, D. L. (1995) Correlation of the in situ detection of polymerase chain reaction-amplified metalloproteinase complementary DNAs and their inhibitors with prognosis in cervical carcinomas. *Cancer Res.* **55**, 267–265.
5. Gilles, C., Polette, M., Piette, J., Munaut, C., Thompson, E. W., Birembaut, P., and Foidart, J. M. (1996) High level of MT-MMP expression is associated with invasiveness of cervical cancer cells. *Int. J. Cancer* **65**, 209–213.
6. Visscher, D. W., Hoyhtya, M., Ottosen, S. K., Liang, C. M., Sarkar, F. H., Crissman, J. D., and Fridman, R. (1994) Enhanced expression of tissue inhibitor of metalloproteinase-2 (TIMP-2) in the stroma of breast carcinoma correlates with tumor recurrence. *Int. J. Cancer* **59**, 339–344.
7. Hamdy, F. C., Fadlon, E. J., Cottam, D., Lawry, J., Thurrell, W., Silcocks, P. B., Anderson, J. B., Williams, J. L., and Rees, R. C. (1994) Matrix metalloproteinase 9 expression in primary human prostatic adenocarcinoma and benign prostatic hyperplasia. *Br. J. Cancer* **69**, 177.
8. Kugler, A., Hemmerlein, B., Thelen, P., Kallerhoff, M., Radzun, H. J., and Ringert, R.-H. (1998) Expression of metalloproteinase 2 and 9 and their inhibitors in renal cell carcinoma. *J. Urol.* **160**, 1914.

9. Morrison, C. and Gannon, F. (1994) The impact of the PCR plateau phase on quantitative PCR. *BBA* **1219**, 493.
10. Chomczynski, P. and Sacchi, N. (1987) Single-step method of RNA isolation by acid guanidinium thiocyanate-phenol-chloroform extraction. *Anal. Biochem.* **162**, 156.
11. Bonham, M. J. and Danielpour, D. (1996) Improved Purification and yields of RNA by Rneasy. *Biotechniques* **21**, 57.
12. Sambrook, J., Fritsch, E. F., and Maniatis, T. (1989) *Molecular Cloning: A Laboratory Manual*, Cold Spring Harbor Laboratory Press, Cold Spring Harbor, NY.
13. Riedy, M. C., Timm, E. A., and Steward, C. C. (1994) Quantitative RT-PCR for measuring gene expression. *Biotechniques* **18**, 70.
14. Menzo, S., Bagnarelli, P., Giacca, M., Manzin, A., Varaldo, P. E., and Clementi, M. (1992) Absolute quantitation of viremia in human immunodeficiency virus infection by competitive reverse transcription and polymerase chain reaction. *J. Clin. Microbiol.* **30**, 1752.

Purification of Growth Factor mRNA in Renal Tissues: *bFGF-2*, *FGF-2*, *TGF α* , and *EGFR*

Jack H. Mydlo

1. Introduction

Growth factors are polypeptides that induce cell mitogenicity, and thus play an important role in the etiology and progression of tumors (**1**). Fibroblast growth factors (FGF) constitute a family of structurally related polypeptides of 146 amino acids, which exhibit a wide spectrum of biologic activities, including angiogenesis or the formation of a vascular network. FGFs are mitogenic towards many mesodermal and ectodermal cell types, and can also induce and/or inhibit differentiation of cells (**2**). These heparin-binding factors are categorized as FGF-1 through FGF- 10. Acidic FGF, or FGF-1, is found mostly in brain and other neural tissues. Basic FGF, or FGF- 2, a protein of 18 kDa mw, is one of the most ubiquitous growth factors. It is found in numerous benign and cancerous human and animal tissues, including kidney, prostate, and bladder (**3–6**). In some cases it has also been demonstrated to have potential as a tumor marker (**7–11**). One group reported greater recovery of both FGF-2 protein and FGF-2 mRNA from renal-cancer tissue compared to equal amounts of normal renal tissue (**5**). Furthermore, when purified FGF-2 from renal cell carcinoma (RCC) is added exogenously to other established renal tumor-cell lines and endothelial cell lines, it demonstrates significant mitogenic activity (**6**). Thus, renal tumors may use FGF-2 in an autocrine manner to sustain themselves.

Another possible autocrine mechanism for this neoplasm was suggested when studies reported that there was a greater expression of transforming growth factor alpha (TGF α) and epidermal growth-factor expression in renal-cancer tissue than in normal benign renal tissue (**12–15**) (see **Fig. 1**).

Finally, many reports have been written concerning the association of obesity, diet, and hormones and the development of renal cancer. Several studies revealed an association of RCC and obesity (**16–20**). Since increased dietary estrogens have been found to induce renal tumors in the Syrian hamster, one possible mechanism to explain an obesity-related renal-cancer biology is that adipose tissue breaks down into triglycerides and cholesterol, the latter being a precursor for estrogen. However, another possible mechanism may involve FGF-2. Using the isolation and purification techniques described here, a report described a quantitatively and qualitatively greater expression of FGF-2 in adipose tissue compared to renal-cancer tissue, which in turn was greater than normal renal tissue (see **Fig. 2**) (**21**). Although FGF-2 is certainly only one of the many growth factors that affects renal-tumor biology, this finding may explain one piece of the puzzle of obesity-related tumor biology.

Although there are numerous assays used to detect FGF-2, such as *in situ* hybridization and RT-PCR, (described in other chapters in this book), heparin-sepharose chromatography remains a standard method for the isolation of FGF-2 from many tissues, especially renal. FGF-2 may play an integral role not only in the formation of normal kidney tissue—as it does for other benign tissues—but also in the etiology and perhaps the progression of renal-cancer neoplasm. Thus, the study of this growth factor and its inhibition may open new avenues of therapy for patients with this disease.

2. Materials

2.1. FGF Purification: Preparation of Tissues

1. Fresh renal tissues are obtained from surgical specimens.
2. Polytron/blender (Tekmar Industries, Cincinnati, OH).
3. Ultracentrifuge (Beckman J-21B).
4. 50 mM Tris-HCl, pH 7.6 (Sigma, St. Louis, MO).
5. 1.55 M NaCl.
6. 10 mM EDTA (GIBCO-BRL Laboratories, Grand Island, NY).
7. Ammonium sulfate.
8. Dialysis tubing (Fisher Scientific, Fairlawn, NJ).
9. Heparin-sepharose (Pharmacia, Piscataway, NJ).
10. 1.5 \times 8 cm elution affinity column and gradient pump (Pharmacia) (see **Fig. 3**).
11. Test tubes on ice, cold-room storage facility.
12. LKB Ultraspec 4050 spectrophotometer.

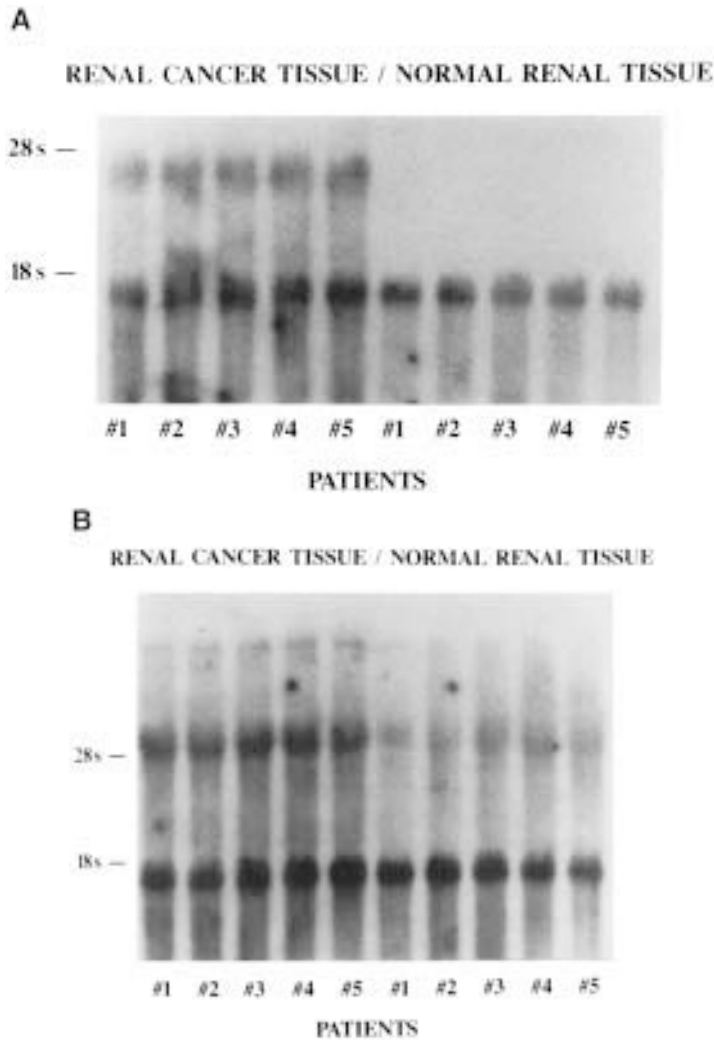


Fig. 1. Northern blot demonstrating greater expression of TGF α (**A**) and its receptor, EGFR, (**B**) in samples of RCC, compared to normal renal tissue. (Printed with permission, of the American Association of Cancer Research, Inc.)

- 13. Protein quantitation kit (Bio-Rad, Richmond, CA).
- 14. Liquid nitrogen.

2.2. Mitogenic Assay: Preparation of Cells

- 1. 3T3 BALB/c fibroblasts, Human umbilical-vein endothelial cells (HUVEC). (American Type Culture Collection, (ATCC), Rockville, MD) (22).

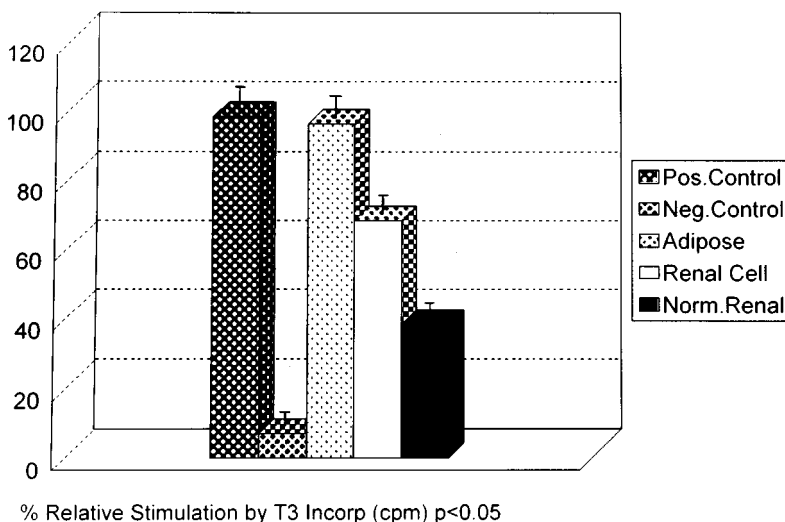


Fig. 2. Differences of FGF-2 recovery and activity in adipose tissue compared to equal amounts of renal cancer tissue and benign renal tissue. (Printed with permission of Williams & Wilkins).

2. Dulbecco's modified Eagle's medium, 0.4%, and 10% FCS (Sigma Chemical Co., St. Louis, MO).
3. 12-Well plates (Costar, Cambridge, MA).
4. Tritiated thymidine (New England Nuclear, Boston, MA).
5. Scintillation counter (Packard, model 3330).

2.3. Sodium Dodecyl Sulfate-Polyacrylamide Gel Electrophoresis

1. Distilled water.
2. Beta-mercaptoethanol (Sigma, St. Louis, MO).
3. 12.5% Sodium dodecyl sulfate (SDS) polyacrylamide gel (Fisher Scientific, Fairlawn, NJ).
4. 10X TBE: 108 g Tris-HCl, 55 g boric acid, and 40 mL of 0.5 M EDTA. (Make up to 1 L, autoclave, and leave at room temperature).
5. Ammonium persulfate 10% (1 g dissolved in 10 cc of distilled water and stored at -20°C).
6. Coomassie blue and silver staining kits (Bio-Rad) (24).
7. Gel electrophoresis kit and power supply (Bio-Rad).
8. Molecular weight standards (Gibco-BRL, Gaithersburg, MD).
9. Glycerol.
10. TEMED (N-tetramethylethylenediamine) (Sigma).
11. Formamide dye (Sigma).

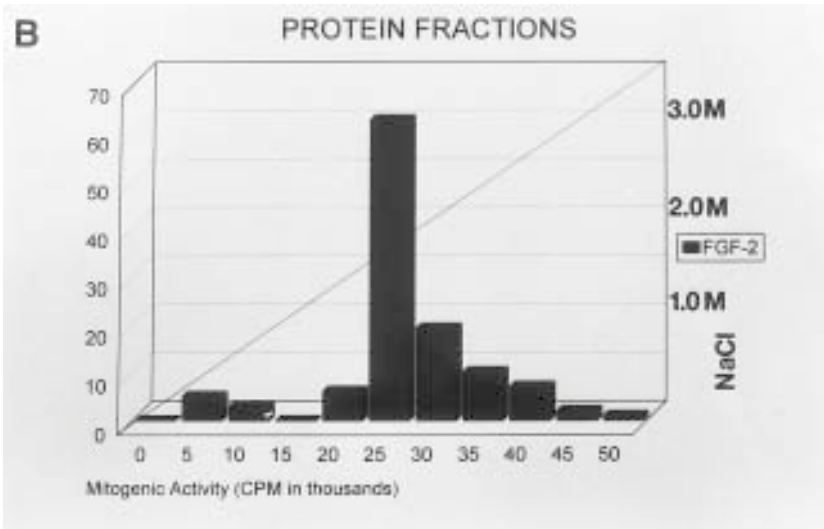


Fig. 3. (A) Typical heparin-sepharose affinity column apparatus used to purify FGF-2. (B) Graphic representation of FGF-2 elution profile from homogenated renal tissues. (Printed with permission of Williams & Wilkins.)

2.4. Western Blot

1. Polyclonal sera against FGF-2 (derived from placenta, Dr. Andrew Baird, Whittier Institute, La Jolla, CA).
2. Polyclonal sera against FGF-1 (derived from bovine brain tissue, Collaborative Research, Boston, MA).
3. Hoeffer Scientific Instruments Tank and Power Supply.
4. Latex gloves, tweezers.
5. Nitrocellulose paper (Schleicher and Schuell, Keene, NH).
6. 10% Carnation Instant Milk (CIM, Carnation Co., Los Angeles, CA).
7. Tris saline.
8. 0.05% Nonidet P-40 (NP-40).
9. I125 Protein A (New England Nuclear, Boston, MA).
10. Acidic and basic FGF controls (Collaborative Research).
11. Kodak XRAS film.
12. Gel dryer.

2.5. Northern Blot Analysis

2.5.1. RNA Extraction

1. May use Purescript RNA isolation kits (Gentra Systems, Research Triangle Park, NC).
2. Diethylpyrocarbonate (DEPC)-treated water: add 200 μ L of DEPC (Sigma, St. Louis, MO) to 1 L of water. Shake and incubate for 2–6 h at 37°C. Autoclave and shake again.
3. 10% sarcosine: add 250 mL of DEPC-treated water to 25 g of N-lauroyl sarcosine (Sigma), and filter through a 0.45 μ sterile filter system. Store at room temperature.
4. 0.75 *M* Citric acid: add 400 mL of DEPC-treated water to 78.75 g of citric acid, and then bring up vol to 500 mL.
5. 0.75 *M* sodium citrate, pH 7.0: add 400 mL of DEPC-treated water to 110 of sodium citrate, pH to 7.0 with 0.75 *M* citric acid, and bring up to 500 mL.
6. Denaturing solution: 4 *M* guanidinium thiocyanate, 25 *mM* sodium citrate, pH 7.0, 0.5% sarcosine. Add 117.2 mL of DEPC-treated water to a 100-g bottle of guanidinium thiocyanate (Fluka Chemicals, Ronkonkoma, NY). Add 10.5 mL of 10% sarcosine, 7.04 mL of 0.75 *M* sodium citrate, pH 7.0, swirl, and heat to dissolve.
7. Add 360 μ L of beta-mercaptoethanol (Sigma) to 50 mL of denaturing solution.
8. Water-saturated phenol, pH 6.6 at 4°C.
9. Chloroform (Sigma). Keep in a dark bottle at room temperature.
10. Isoamyl alcohol (Sigma). Keep at room temperature.
11. Isopropanol (Sigma).
12. 75% ethanol: add 25 mL of DEPC H₂O to 75 mL of absolute ethanol.
13. Glacial acetic acid (Fisher): Keep at room temperature.
14. 2 *M* sodium acetate: Add 15 mL of DEPC-treated water to 136 g of sodium acetate. Add glacial acetic acid until pH is 4.0. Add water to make 500 mL.
15. 10 mg/mL Yeast t-RNA (Boehringer Mannheim, Mannheim, Germany).

2.5.2. Preparation of Gel

1. Agarose (Fluka).
2. Casting mold for gel (Bio-Rad).
3. Tank and power supply (Bio-Rad).
4. Flasks, beakers, stirring rods (Fisher Scientific).
5. Eppendorf microfuges (Brinkman Instruments, Westbury, NY).
6. 1.7 mL siliconized microfuge tubes (PGC Scientific, Frederick, MD).
7. Automatic pipettors.
8. Isolation hood.
9. 37°C water bath.

2.5.3. Northern Hybridization

1. Use clone for FGF-2 consisting of a 1.4-kb (kb) *EcoRI* fragment derived from original BB2 bovine cDNA clone, ligated into the *EcoRI* site of pBR322. The 1.4-kb fragment begins approx 100 basepairs upstream of the initiating ATG for FGF-2. (Dr. Andrew Baird).
2. The FGF-1 cDNA is in the plasmid pJC3-5. This plasmid contains a 475-bp *NcoI-EcoRI* fragment that spans the human acidic FGF coding region (ATCC, Rockville, MD).
3. The cDNA probes for TGF α and EGFR were provided by Dr. Rik Deryk (Genentech, San Francisco, CA). The human TGF α probe consists of a 1400 basepair cDNA insert cloned into the *EcoRI* site of Sp65 in the antisense direction with respect to the Sp6 promoter.
4. The human EGF receptor probe consists of a 1-kb cDNA insert in the *EcoRI* site of pUC (Genentech).

3. Methods

3.1. FGF-2 Elution on Heparin-Sepharose Chromatography

3.1.1. Preparation of Renal-Tissue Homogenate

1. The tissue is quickly frozen in liquid nitrogen and stored at -20°C until ready to homogenize (*see Note 1*).
2. Homogenize in polytron blender at slow speed in extraction buffer consisting of 50 mM Tris-HCl, pH 7.6, 1.55 M NaCl, and 10 mM EDTA (Sigma Chemical Co.) at 4°C.
3. Following centrifugation for 60 min at 50,000g (Beckman J-21B), discard the pellet and bring up the supernatant to 25% saturation with ammonium sulfate at constant stirring at 4°C.
4. This is centrifuged for 30 min at 50,000g at 4°C.
5. Discard precipitate and increase supernatant saturation to 75% ammonium sulfate.
6. Centrifuge for another 30 min at 50,000g, discard supernatant, and reconstitute precipitate with 50 cc of 50 mM Tris-HCl buffer, pH 7.0, and 10 mM EDTA.
7. Dialyze overnight in dialysis tubing against 50 mM Tris-HCl at 4°C and pool the supernatants.

3.1.2. Preparation of the Heparin-sepharose Chromatography Column

1. Keep heparin-sepharose lightly settled; do not pack tightly.
2. Run 50 mM Tris-HCl buffer through first, then 3 M NaCl to rinse out any previous proteins, then gradually bring down to 0 M NaCl in 50 mM Tris-HCl buffer (*see* **Notes 2 and 3**).
3. Keep test-tube collector filled with ice; it may be preferable to place in cold room (*see* **Note 4**).

3.2. Preparation of the Mitogenic Assay

3.2.1. Preparation of Cells

1. 3T3 fibroblasts or HUVEC endothelial cells are established in culture, plating them on 12-well plates in Dulbecco's modified Eagle's medium (DME) with 10% FCS at 10,000 cells per well on day 1 and incubated at 37°C and 5% CO₂ (**22**).
2. These cells are then refed on day 2 with 0.4% FCS.
3. Day 3: 50 µL of the eluted fractions are added. 10% FCS and 0.4% FCS are used as positive and negative controls (*see* **Notes 5 and 6**).
4. Day 4: Add tritiated thymidine (4 mCi/mL., 6.7/mmol, NEN) to each well for 24 h.
5. Day 5: Wash cells with Hank's balanced salt solution (HBSS).
6. Remove unincorporated thymidine by adding cold 5% trichloroacetic acid (TCA) for 30 min followed by a 5-min 5% TCA wash.
7. Lyse the cells in 0.3 N NaOH for 1 h.
8. Add cells to 5 cc Hydroflour scintillation cocktail.
9. Measure incorporation using a Packard model 3330 scintillation counter.
10. 10% FCS and 0.4% FCS are used as positive and negative controls, respectively.

3.2.2. Protein Elution

1. Load supernatant onto the 1.5 × 8 cm heparin-sepharose column equilibrated with 50 mM Tris buffer at room temperature.
2. Perform elution at room temperature with a linear NaCl gradient from 0–3.0 M.
3. Protein elution is monitored by A₂₈₀.
4. Fractions are collected on ice at a rate of 1 mL/min, and tested for mitogenicity (*see* **Subheading 3.2.1., steps 1–10**).

3.2.3. Purification and Concentration of Protein

1. Final protein concentrations are determined using an LKB Ultraspec 4050 spectrophotometer at 280 nm, and then confirmed by the protein quantitation kit from Bio-Rad (**23**).
2. Be careful of the contaminating products from the beginning of the run. The non-heparin-binding proteins will elute first, at the lowest levels of NaCl concentration. Acidic FGF elutes at 0.9–1.1 M NaCl. Basic FGF elutes at 1.3–1.7 M NaCl.

3. Mitogenic fractions are pooled, dialyzed, and reloaded onto a second column, and this is repeated a third or fourth time until SDS/PAGE shows no impurities.
4. It is best to do the second, third, and sometimes fourth runs on separately prepared columns to avoid contamination from previous runs (**Fig. 1**) (*see Note 1*).
5. Concentrate by lyophilization, and prepare to load onto gel.

3.3. SDS/PAGE (14)

1. A 12.5% acrylamide gel is prepared with a 12- or 24-well sharks-tooth comb. For 80 cc of gel solution, use 52 mL of distilled water, 8 mL 10X TBE, 8 mL glycerol, and 12 cc of 80% acrylamide stock.
2. 40 μ L of TEMED and 300 μ L of 10% ammonium persulfate is added right before pouring the gel.
3. Prepare a 3% stacking gel to be placed on top of 12.5% gel, and add sharks-tooth comb.
4. Once the gel is polymerized, place at 4°C overnight along with 1 1/2 L of 1X TBE running buffer until ready to use.
5. Rinse gel off with 1X TBE to remove residual polyacrylamide (*see Note 6*).
6. 4-mL active fractions of 2 μ g/mL are dialyzed overnight against 50 mM Tris and lyophilized
7. Reconstitute with 25 μ L of distilled water, dilute with 1:1 with sample buffer containing beta-mercaptoethanol and SDS.
8. 10- μ L aliquots of sample containing 40 ng of protein and 5 μ L of formamide dye are electrophoresed on 12.5% gel at 40W for 5–6 h at 4°C (*see Notes 7 and 8*).
9. Use molecular weight standards on the far left or far right of the gel, and keep gel level.
10. Visualization of the bands is performed using silver staining and/or a double Coomassie blue/silver-staining technique. The silver-staining technique is much more sensitive, and thus should be used routinely to detect the small quantities of proteins (**24**).
11. 2-mm slices of unstained (native) gels are cut to confirm mitogenic activity (*see Note 9*).

3.4. Western Blot (15,16)

1. After SDS/PAGE, nitrocellulose transfer is performed at 0.6 A for 6 h using a Hoeffer Scientific Instruments tank and power supply (**25**). Place the nitrocellulose sheet directly on top of the gel without producing air bubbles. Never handle the nitrocellulose with bare hands, since it will retain even the smallest amount of proteins (*see Note 10*).
2. After the transfer, the nitrocellulose is then incubated with 10% Carnation Instant Milk (CIM) in Tris buffer overnight at 4°C and incubated with a 1:200 dilution of antisera in 10% CIM solution for 1 h (*see Note 11*).

3. Rinse nitrocellulose with 0.9% NaCl, 10 mM Tris HCl at pH 7.4, 0.05% Nonidet P-40 (NP-40), Tris saline, and expose to a 1:200 dilution of I125 Protein A in 10% for 1 h (**26**).
4. Final rinse using Tris saline containing 0.05% NP-40.
5. Air-dry nitrocellulose or use an 80°C gel dryer and expose to Kodak XARS film at -70°C for 2 d with intensifying screens (*see* **Note 10**).

3.5. Isolation of FGF-2 mRNA, Transforming Growth-Factor Alpha (TGF α), and Epidermal Growth Factor Receptor (EGFR) from Renal Tissue

3.5.1. Preparation of RNA Extraction (27**)**

1. Make sure all glassware is rendered nuclease free by overnight treatment at 180°C.
2. Similarly, stock solutions are treated for 20 min with 0.2% diethyl pyrocarbonate, and then boiled to remove traces of the reagent.
3. Fresh RCC tissue is quickly frozen in liquid nitrogen
4. Place 1 g of tissue in 5 cc of 4 M guanidine thiocyanate and homogenize with a polytron.
5. Add to the mixture 100 μ g/ μ L yeast tRNA as a carrier and vortex for 10 s.
6. Add 50 μ L of 2 M NaAc and mix well.
7. Add 500 μ L of water-saturated phenol and mix.
8. Add 100 μ L of chloroform/isoamylalcohol (49:1) and vortex well for 30-60 s while on ice, as described by Maniatis et al. (**16**).
9. Homogenate is centrifuged at 11,200g for 10 min at 4°C.
10. Supernatant is layered on a 4-mL cushion of 5.7 M cesium chloride and centrifuged at 32,000 rpm for 18 h at 20°C in a Beckman SW50 rotor.
11. Pellet is washed with 70% ethanol and resuspended in 100 μ L of diethylpyrocarbonate (DEPC)-treated water with brief heating in a water bath at 68°C.
12. Optical density is measured at 260/230 nm.
13. RNA samples are routinely stored as 70% ethanol suspension at pH 5 and -20°C.
14. Polyadenylated RNA (poly A+ mRNA) is obtained by running total RNA through an oligocellulose type 3 column (Collaborative Research), and then precipitated so that 10 μ g of poly A+ mRNA is injected into each well of a 1.5% agarose gel.
15. RNA is now ready for Northern-blot electrophoresis.

3.5.2. Preparation of Agarose Gel and Electrophoresis

1. Boil 1.5 g of agarose/10 mL of TBE (1X).
2. Cool to approx 50°C, and add 10 μ L of ethidium bromide/100 mL and 0.66 M formaldehyde.
3. Pour agarose into casting tray or minigel tray.
4. Place slim 1-mm comb. Allow to gel overnight at 5°C.
5. After setting, add 1X TBE solution to the gel tank and electrophorese RNA samples for 4 h at 100 V and room temperature with rapid recirculation of reservoir buffer (25 mM citrate, pH 3.5).
6. The gels are washed for at least 1 h in sterile 25% glycerol and scanned at 260 nm.

3.5.3. Northern Hybridization

1. After running RNA, transfer to Gene Screen Plus (NEN, Boston, MA) by electroblotting.
2. The probes are made radioactive by labeling with [α - ^{32}P]dCTP by random primer DNA synthesis (2×10^9 cpm/ μg of DNA) (28).
3. The filters are hybridized with ^{32}P -labeled cDNA probes in 50% formamide and 20% sodium dodecyl sulfate at 42°C for 24 h. Simultaneous hybridization with glyceraldehyde-3-phosphate dehydrogenase is performed for control.
4. Hybridization is performed at 42°C , and varied in time from 24–72 h. The filters are washed in 2X SSC for 10 min, in 2X SSC and 1% SDS at 65°C for 1 h, and finally in 0.1X SSC for 1 h.
5. Molecular weight estimation of the bands is obtained from the relative migration rates of the RNA ladder, placed at either end of the gel well.
6. The filters are air-dried, placed in a dryer, and exposed to Kodak XRAS film at -70°C for 48 h.

4. Notes

1. It is important to histologically determine which part of the kidney specimen is cancerous and which is benign before homogenization—especially to compare extraction of growth factors.
2. Make sure that subsequent runs on the heparin-sepharose column runs are made on separately prepared columns to avoid contamination.
3. The first eluants of the run are usually non-heparin-binding or minimally heparin-binding. It is important to make sure that the chromatography pump is calibrated to confirm adequate elution.
4. Always keep test tubes on ice, and soon after maintain ice tube rack in cold room. Combine all mitogenic fractions while in cold-room temperature to obtain optimal mitogenic response of growth factors, since they can denature in warmer temperatures.
5. Use an automatic pipette with disposable tips for each sample to be tested in triplicate, and use the mean value as your result.
6. Swirl 12-well plates to ensure uniform distribution of cells, samples, and tritiated thymidine.
7. Generously spray distilled water over and under polyacrylamide gel so that it will slide off the plastic holder intact and onto nitrocellulose transfer.
8. Be aware of cooling fans or air conditioners that can cause uneven temperatures on the gel, and therefore different migration rates.
9. It is best to confirm that the stained band you visualize on the gel is truly mitogenic. This can be done by running a parallel unstained or “native” gel and cut out the corresponding band for testing.
10. Always use plastic gloves or tweezers to handle nitrocellulose to avoid protein contamination.
11. While Western-blot analysis using antisera to FGF-1 and FGF-2 may confer homology of the isolated proteins, it is crucial to identify that the antisera is mitogenically inhibitory. This is done by adding 20 mg/mL of antisera to the wells and repeating the incorporation assay as in **Subheading 2.2.1., steps 1–5.**

References

1. Gospodarowicz, D., Neufeld, G., and Schweigerer, L. (1986) Fibroblast growth factor: a review. *Mol. Cell. Endocrinol.* **46**, 187–198.
2. Mydlo, J. H. and Macchia, R. J. (1992) growth factors in urologic tissues: detection, characterization, and clinical applications. *Urology* **40**, 491–498.
3. Mydlo, J. H. (1995) Growth factors and renal cancer: characterization and therapeutic implications. *World J. Urol.* **13**(6), 356–363.
4. Mydlo, J. H., Heston, W. D. W., and Fair, W. R. (1988) Characterization of a heparin-binding growth factor from adenocarcinoma of the kidney. *J. Urol.* **140**, 1575–1579.
5. Mydlo, J. H., Michaeli, J., Heston, W. D. W., and Fair, W. R. (1988) Expression of basic fibroblast growth factor mRNA in benign prostatic hyperplasia and carcinoma of the prostate. *Prostate* **13**, 241–247.
6. Mydlo, J. H., Zajac, J., and Macchia, R. J. (1993) Conditioned media from a renal carcinoma cell line demonstrates the presence of basic fibroblast growth factor. *J. Urol.* **150**, 997–1001.
7. Nguyen, M., Watanabe, H., Budson, A. E., Richie, J. P., Hayes, D. F., and Folkman, J. (1994) Elevated levels of an angiogenic peptide basic FGF in the urine of patients with a wide spectrum of cancers. *J. Natl. Cancer Inst.* **86**, 356–360.
8. Nanus, D. M., Schmitz-Drager, B. J., Motzer, R. J., Lee, A. C., Vlamis, V., Cordon-Cardo, C., Albino, A. P., and Reuter, V. E. (1993) Expression of basic FGF in primary human renal tumors and correlation with poor survival. *J. Natl. Cancer Inst.* **85**, 1597–1601.
9. Fujimoto, K., Ichimori, Y., Yamaguchi, H., Arai, K., Futami, T., Ozono, S., Hirao, Y., Kakizoe, T., Terada, M., and Okajima, E. (1995) Basic fibroblast growth factor as a candidate tumor marker for renal cell carcinoma *Jpn. J. Cancer Res.* **86**, 182–187.
10. Duensing, S., Grosse, J., and Atzpodien, J. (1995) Increased serum levels of basic fibroblast growth factor (bFGF) are associated with progressive lung metastases in advanced renal cell carcinoma patients. *Anticancer Res.* **15**, 2331–2333.
11. Emoto, N., Isozaki, O., Ohmura, E., Ito, F., Tsushima, T., Shizume, K., Demura, H., and Toma, H. (1994) Basic fibroblast growth factor (FGF-2) in renal cell carcinoma, which is indistinguishable from that in normal kidney, is involved in renal cell carcinoma growth. *J. Urol.* **152**, 1626–1631.
12. Lau, J. L. T., Fowler, J. E., Jr., and Ghosh, L. (1988) Epidermal growth factor in normal and neoplastic kidney and bladder. *J. Urol.* **139**, 170–174.
13. Ebert, T., Bander, N., Finstad, C., Ramsawak, R. D., and Old, L. J. (1990) Establishment and characterization of human renal cancer and normal kidney lines. *Cancer Res.* **50**, 5531–5536.
14. Gomella, L. G., Sargent, E. R., Wade, T. P., Anglard, P., Linehan, W. M., and Kasid, A. (1989) Expression of transforming growth factor alpha in human adult kidney. *Cancer Res.* **46**, 6972–6977.
15. Mydlo, J. H., Michaeli, J., Cordon-Cardo, C., Goldenberg, A., Heston, W. D. W., and Fair, W. R. (1989) Expression of transforming growth factor alpha and

- epidermal growth factor receptor mRNA in neoplastic and non-neoplastic renal tissue. *Cancer Res.* **49**, 3407–3411.
16. Moller, H., Mellemegaard, A., Lindvig, K., and Olsen, J. H. (1994) Obesity and cancer risk: a Danish record-linkage study. *Eur. J. Cancer* **30A**, 344.
 17. Lindblad, P., Wolk, A., Bergstrom, R., Persson, I., and Adami, H. O. (1994) The role of obesity and weight fluctuations in the etiology of renal cell cancer: a population-based case control study. *Cancer Epidemiol. Biomark. Prevent.* **3**, 631–638.
 18. Chow, W. H., McLaughlin, J. K., Mandel, J. S., Wacholder, S., Niwa, S., and Fraumeni, J. F., Jr. (1996) Obesity and risk of renal cell cancer. *Cancer Epidemiol. Biomark. Prevent.* **5**, 17–21.
 19. Li, J. J., Li, S. A., Oberley, T. D., and Parsons, J. A. (1995) Carcinogenic activities of various steroidal and nonsteroidal estrogens in the hamster kidney: relation to hormonal activity and cell proliferation. *Cancer Res.* **55**, 4347–4351.
 20. Mydlo, J. H., Kanter, J. L., Kral, J. G., and Macchia, R. J. (1999) Obesity, diet, and other factors in urological malignancies. A review. *Br. J. Urol.* **83(3)**, 225–234.
 21. Mydlo, J. H., Kral, J. G., and Macchia, R. J. (1998) Preliminary results comparing the recovery of basic fibroblast growth factor (fgf-2) in adipose tissue and benign and malignant renal tissue *J. Urol.* **159(6)**, 2159–2163.
 22. Maciag, T., Hoover, G. A., Stemerman, M. B., and Weinstein, R. (1981) Serial propagation of human endothelial cells in vitro. *J. Cell Biol.* **91**, 420–426.
 23. Bradford, M. A. (1976) A rapid and sensitive method for the quantitation of microgram quantities of protein utilizing the principle of protein dye binding. *Anal. Biochem.* **72**, 248–252.
 24. Dzandu, J. K., Deh, M. E., Barrett, D. L., and Wise, G. E. (1984) Detection of erythrocyte membrane proteins, sialoglycoproteins, lipids in the same polyacrylamide gel using a double-staining technique. *Proc. Natl. Acad. Sci. USA* **81**, 1733–1737.
 25. Towbin, H., Staehelin, T., and Gordon, J. (1979) Electrophoretic transfer of proteins from polyacrylamide gels to nitrocellulose sheets: procedure and some applications *Proc. Natl. Acad. Sci. USA* **76**, 4350–4356.
 26. Burnette, W. N. (1981) Western blotting: electrophoretic transfer of proteins from sodium dodecyl sulfate polyacrylamide gels to unmodified nitrocellulose and radiographic detection with antibody and radioiodinated protein A. *Anal. Biochem.* **112**, 195–203.
 27. Maniatis, T., Fritsch, E. F., and Sambrook, J. (1982) *Molecular Cloning: A Laboratory Manual*, Cold Spring Harbor Laboratory Press, Cold Spring Harbor, NY.
 28. Derynck, R., Goeddel, D. V., Ullrich, A., Gutterman, J. U., Williams, R. D., Bringman, T. S., and Berger, W. H. (1987) Synthesis of messenger RNA's for transforming growth factors α and β and the epidermal growth factor receptor by human tumors. *Cancer Res.* **47**, 707–711.

Laser-Capture Microdissection

Greg L. Griewe, Robert Dean, Wei Zhang, Isabella A. Sesterhenn, Shiv Srivastava, and Judd W. Moul

1. Introduction

Laser-capture microdissection is a recently discovered state-of-the-art method to obtain cells for genetic analysis. It is a one-step procedure that allows capture of selected cells under direct microscopic visualization.

Studies of genome as well as genetic expression in different cell types of normal tissue or in tumor tissues rely on the ability to obtain pure populations of cells for analysis. This can be particularly challenging when studying heterogeneous tumors, premalignant lesions, and small metastatic tumor foci. Contamination by normal cells can frustrate genetic analysis of a tumor. Although there are many published methods of microdissection (**1–5**), most require micromanipulation and can be tedious and imprecise. The advantage of laser-capture microdissection over other methods is its precision, speed, ease of use, and short learning curve. Laser-capture microdissection was developed at the National Institutes of Health, and in 1996 was subsequently developed as a commercial instrument by Arcturus Engineering (Mountain View, CA) (**6**).

The commercial system uses an inverted microscope equipped with an infrared laser as well as a video monitor and computer for storing images. The process of laser-capture microdissection is as follows (**Fig. 1**): 1. A thin, transparent film attached to a transparent cap is placed over a tissue section. 2. The tissue section is examined microscopically and the cells of interest are identified, then targeted. 3. The transfer film directly above the selected cells absorbs a pulsed, infrared laser beam. This melts the film and fuses it to the targeted cells. 4. The cap with transfer film and targeted cells is removed for processing. The cap is designed to fit a 0.5-mL Eppendorf tube. The currently avail-

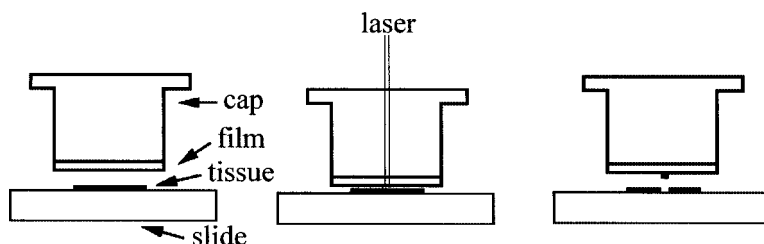


Fig. 1. Line drawing of laser-capture microdissection. 1. The slide is examined and cells are targeted. 2. The infrared laser is pulsed, fusing thermoplastic film to targeted cells. 3. The cap containing the thermoplastic film and targeted cells is removed for processing.

able commercial model allows focal polymer film melting in spots that range in size from 7.5–60 μ . Multiple targets may be selected per cap. Laser transfer spots can be overlapped to capture complicated microstructures. For example, the epithelial cells may be dissected from a single prostate gland in a focal prostate tumor, leaving behind stromal cells.

Laser-capture microdissection may be used on a variety of tissue preparations. The basic choices are paraffin-embedded and frozen-embedded tissues. It is important to match the tissue preparation method to the research goal. Paraffin-embedded tissue is readily available, durable, and provides excellent histology. Unfortunately, it contains relatively poor-quality nucleic acids, but is usable for recovery of short DNA fragments, which can be used by PCR-based assays. Frozen embedding is another way to preserve and stabilize specimens. In this method, the tissue is embedded in a viscous compound (e.g., optimum cutting temperature [OCT]) and is frozen on dry ice. The advantages of using frozen embedded tissue are faster processing time and good molecular recovery of both DNA and RNA. The drawback is its poorer and inconsistent histology. Another variable that markedly affects nucleic-acid quality is the fixation method. Prior to embedding, tissue must be fixed to preserve its morphology. Formalin fixation crosslinks nucleic acids and protein, making the molecules susceptible to shearing forces. The DNA extracted from formalin-fixed paraffin-embedded tissue is fragmented, which limits the size of PCR-derived amplicons (7). Although the DNA is fragmented, we have been able to routinely amplify fragments up to 200–300 base pairs (bp) in length. RNA is more labile than DNA, precluding its recovery from formalin-fixed, paraffin-embedded tissue. Frozen embedded tissue is the preferred preparation method for RNA, but has the limitations of less than optimal preservation of histological detail and more complicated storage and handling. Fragments of 800 bp for both DNA and RNA may be recovered from OCT-embedded tissue (8).

Applications of laser-capture microdissection to basic and clinical research are numerous. Any application that requires a selected population of cells or cell types may potentially benefit from laser-capture microdissection. Topics at a recent workshop (9) included genetic profiling, functional genomics, proteomics and protein markers, differential mRNA display, cDNA microarrays, and combination with immunohistochemistry techniques. The websites for the laser-capture microdissection group at NIH (9) and for Arcturus (10) provide a wealth of information and protocols. Most of the protocols outlined in this chapter are modified versions of protocols listed in these websites.

2. Materials

2.1. Paraffin Embedding

1. Paraffin wax (cat. no. 8889-501006, Oxford Labware, St. Louis, MO).
2. Glass slides (cat. no. 2951, Erie Scientific Co., Portsmouth, NH).

2.2. Frozen Embedding

1. Tissue-Tek® OCT (cat. no. 4583, Sakura Finetek USA, Torrance, CA).
2. Glass slides (cat. no. 2951, Erie Scientific Co., Portsmouth, NH).

2.3. Staining Protocol for LCM: Hematoxylin and Eosin

1. Xylenes (cat. no. 2377, Sigma, St. Louis, MO).
2. 100% ethanol (Warner-Graham Co., Cockeysville, MD).
3. Hematoxylin (cat. no. H-3401, Vector Laboratories, Inc., Burlingame, CA).
4. Eosin Y solution (cat. no. HT 110-1-32, Sigma, St. Louis, MO).

2.4. Staining Protocol for LCM: p53 Monoclonal Antibody (MAb)

1. Mouse MAb (cat. no. NCL-p53-801, Novacastra citric acid (cat. no. 201-069-1, Sigma, St. Louis, MO).
2. PBS buffer (Dulbecco's phosphate-buffered saline) (cat. no. 14190-144, Gibco Life Technologies, Grand Island, NY).
3. P53 Protein Laboratories, Newcastle-upon-Tyne, UK).
4. Fisher Superfrost®/Plus Microscope Slides (cat. no. 12-550-15, Fisher Scientific, Pittsburgh, PA).
5. Biotinylated Anti-Mouse IgG (cat. no. BA-2000, Vector Laboratories Inc., Burlingame, CA).
6. Horse serum (cat. no. 200-6050A6, Gibco Life Technologies, Grand Island, NY).
7. Vector® VIP (cat. no. SK-4600, Vector Laboratories Inc., Burlingame, CA).
8. VECTASTAIN® Elite ABC reagent (PK-6100, Vector Laboratories Inc, Burlingame, CA).

2.5. DNA Extraction

1. Proteinase K (cat. no. 2553-015, Gibco Life Technologies).
2. Tris-HCl (pH 8.0) (cat. no. 351-007-100, Quality Biological, Inc., Gaithersburg, MD).

3. 0.5 M EDTA (pH 8.0) (cat. no. 15575-020 Gibco Life Technologies).
4. Tween-20 (polyoxyethylene sorbitan monolaurate) (cat. no.170-6531, Bio-Rad, Hercules, CA).
5. Eppendorf 0.5-mL microcentrifuge tubes (part # 22 26 430-8, Brinkman Instruments, Westbury, NY).

2.6. RNA Extraction

1. RNAzol™ B (Cinna/BiotechX).
2. Chloroform (ACS grade) (cat. no. C-5312, Sigma, St. Louis, MO).
3. Isopropanol (ACS grade) (cat. no. I-0398, Sigma).
4. 75% ethanol (ACS grade).
5. Glycogen 20 µg/µL (cat. no. G-0885, Sigma).
6. Sodium acetate 2 M (pH 5.4) (S-7899, Sigma).
7. Eppendorf 0.5-mL microcentrifuge tubes. (part no. 22 26 430-8, Brinkman Instruments, Westbury, NY).
8. DEPC Water (cat. no. 351-068-060, Quality Biological Inc., Gaithersburg, MD).

3. Methods

3.1. Histological Preparation for LCM

3.1.1. Paraffin Embedding

3.1.1.1. FIXATION

Prior to paraffin embedding, tissue must be fixed to preserve cellular morphology and to prevent autolysis. The most common choices are formalin and 70% ethanol. Alcohol-based fixatives minimize crosslinking of nucleic acids with proteins, improving the recovery of nucleic acids. Alcohol-fixed specimens also transfer well by LCM. Recommended fixation time is 16–24 h for either formalin or alcohol-based methods. Fixation with ethanol is done at 4°C.

3.1.1.2. PROCESSING, EMBEDDING, AND TISSUE SECTIONING

1. After fixation, the tissue is processed with an automated tissue-processing machine. Processing may be done by a routine overnight or accelerated cycle. There is no difference in the quality of nucleic acids processed either way.
2. After the processing, the specimen is embedded in paraffin blocks, and then sectioned and mounted onto slides.
3. Cut sections on a clean microtome with a clean blade holder. It is important to clean the microtome knife or use a new disposable blade between different specimens to prevent carryover contamination from one specimen to another.
4. Float paraffin ribbons on 43°C to 44°C deionized water. It is important that this water does not contain adhesives.
5. Mount on plain glass slides (no charged coatings).
6. Air-dry the paraffinized sections overnight. Do not bake.

3.1.2. Frozen Embedding

3.1.2.1. EMBEDDING

1. Place an empty glass slide on dry ice for 1 min. It will remain on dry ice during the entire embedding procedure.
2. Place a small fresh tissue specimen on the slide, flush against the glass. The thickness of the specimen should be <4 mm.
3. Cover the specimen with OCT. Allow the medium to harden. The OCT will turn white when frozen.
4. Wrap the block in foil and store at -80°C until cutting.

3.1.2.2. CUTTING

1. Remove the block from the slide and attach it to the object disk (chuck) in the cryostat with OCT. The cutting surface should be as parallel as possible.
2. Allow the block to equilibrate to the cryostat temperature (-18°C to -20°C) for 15 min.
3. Cut 10- μ or thinner sections onto plain uncoated glass slides. If needed, the sections may be cut thinner or thicker.
4. Keep the slides on dry ice if they are to be microdissected that day; otherwise, store at -80°C until use.

3.1.3. Staining Protocol for LCM: Hematoxylin and Eosin

Frozen and paraffin-embedded tissue should be cut according to the guidelines and stained as soon as possible for best results. Begin with **step 1** for paraffin-embedded slides. Begin with **step 7** for frozen embedded slides. The length of hematoxylin and eosin Y staining used is tissue-dependent. Do not allow the sections to air-dry until the completion of staining to keep them from becoming too adherent to the slide, preventing LCM transfer. Staining procedures can harm the RNA. If the goal is to recover RNA, exposure to water must be minimized to avoid digestion by RNases.

1. Xylenes to deparaffinize the slides (5 min).
2. Xylenes (5 min).
3. 100% ethanol (30 s).
4. 100% ethanol (30 s).
5. 95% ethanol (30 s).
6. 70% ethanol (30 s).
7. Distilled water (30 s). Begin frozen embedded slides here, but expose to water for only 5 s.
8. Hematoxylin (10–30 s). This is tissue-dependent. The length of staining depends on the desired degree of contrast. This solution needs to be filtered before each use.
9. Distilled-water rinse.
10. Bluing reagent, 30 s or until differentiation. Filter this solution before each use.

11. 70% ethanol wash (30 s).
12. 5% ethanol wash (30 s).
13. Eosin Y (10–30 s). The length of time needed is tissue-dependent.
14. 95% ethanol wash (5 s).
15. 95% ethanol wash (5 s).
16. 100% ethanol wash (5 s).
17. Rinse with xylenes for 5 min (dehydrates section).
18. Shake off excess and blot the slide carefully with particle-free tissue.
19. Air-dry for 2–4 min. This allows the xylenes to evaporate completely.
20. Do not place a cover slip on the slide.

3.1.4. Staining Protocol for LCM: p53 Monoclonal Antibody

We use a modified version of the protocol distributed by Vector Laboratories. We use this protocol on archival paraffin-embedded prostate specimens.

1. Cut and mount sections on charged glass slides. (Charged slides are needed here).
2. Deparaffinize sections and dehydrate in 100% ethanol.
3. Place the sections in 1.5% hydrogen peroxide/methanol for 20 min (or use other appropriate endogenous peroxidase blocking procedure).
4. Wash the sections in PBS buffer (pH 7.5) for 1×5 min.
5. Place the sections in a plastic rack that will allow them to be immersed in buffer.
6. Prepare an adequate quantity of 0.01 M citrate buffer (pH 6.0), then cover the sections in buffer.
7. Heat the container of sections for 5 min in the microwave oven. Add sufficient distilled water to reimmerse the slides.
8. Repeat **step 5** two more times, then allow to stand at room temperature for 20 min.
9. Wash sections in PBS buffer for 2×5 min.
10. Place sections in diluted normal horse serum (1:100) for 20 min.
11. Cover sections with diluted primary antibody (1:40) for 1 h.
12. Wash in PBS buffer for 2×5 min.
13. Incubate sections in secondary antibody for 30 min. We use biotinylated horse antimouse antibody at 1:200 dilution.
14. Wash in PBS buffer for 2×5 min.
15. Incubate sections in VECTASTAIN Elite ABC reagent for 30 min.
16. Wash in PBS buffer for 2×5 min.
17. Incubate sections in Vector VIP or other suitable peroxidase substrate.
18. Wash in water for 2×5 min.
19. Counterstain with hematoxylin (if required), wash, and dehydrate. Do not place cover slip on slide.

3.2. Nucleic-Acid Extraction

DNA and RNA extraction protocols continue to be improved from laser-capture microdissected material. The difference in these protocols from stan-

standard protocols is chiefly one of scale. Typically, very small amounts of microdissected material are isolated.

3.2.1. DNA Extraction

1. Proteinase K buffer: 10 mM Tris-HCl (pH, 8.0), 1 mM EDTA and 1% Tween-20 with a final pH of 8.0. On a practical note, it is convenient to make a batch of 50–100 mL of this buffer prior to addition of proteinase K. Aliquot amount of buffer needed and add sufficient proteinase K to make a 0.04% solution. We use 50 μ L–100 μ L of proteinase K buffer per laser microdissected cap.
2. The cap is inserted into an Eppendorf tube allowing for a uniform 1 mm space between the cap and rim of tube. If the cap is fully or unevenly inserted leakage may occur.
3. Invert tube and shake to transfer buffer to cap surface.
4. Incubate overnight at 37°C in an air incubator.
5. Centrifuge tube at 7000g for 5 min.
6. Transfer contents to a new Eppendorf tube and heat at 95°C for 8 min to inactivate proteinase K.
7. Store the sample at 4°C until use as template for PCR reactions.
8. We have been able to reliably amplify p53 exons 5–8 (120–250 bp) using 5 μ L of extracted DNA template from archived formalin-fixed paraffin-embedded tissue. Because of better DNA quality from frozen embedded tissue, less template may be needed. It is prudent to save the original Eppendorf tube with LCM cap at 4°C should additional material be necessary.

3.2.2. RNA Extraction

We use a modified protocol based on the RNeasyTM B method (*II*). RNeasyTM B contains guanidinium thiocyanate and phenol.

1. Aliquot 200 μ L RNeasy B into an Eppendorf 0.5-mL tube.
2. After microdissection, affix the cap firmly to the tube.
3. Invert the tube and gently shake.
4. Store inverted on ice for 15 min.
5. Add 20 μ L of chloroform.
6. Vortex for 1 min.
7. Incubate on ice for 5 min.
8. Centrifuge at 7000g for 15 min at 4°C.
9. Collect the aqueous (upper) phase and transfer it to an Eppendorf tube. Discard the organic (lower) phase.
10. Add 2 μ L of 20 μ g/ μ L glycogen to the RNA solution.
11. Add an equal volume of isopropanol to the aqueous phase.
12. Vortex the alcohol/aqueous mixture for 15 s.

13. Store at -20°C overnight.
14. Centrifuge at 7000g for 15 min at 4°C .
15. Discard the isopropanol and wash with 75% ethanol (in DEPC water).
16. Centrifuge at 7000g for 8 min at 4°C .
17. Discard the supernatant (alcohol).
18. Allow the pellet to air-dry for 5 min.
19. Resuspend the pellet in 20 μL of DEPC water.
20. Store at -70°C until use.
21. DNase treatment (if needed)
 - a. Add 2 U DNase (certified RNase-free) per 20 μg RNA.
 - b. Incubate at 37°C for 20 min, then heat to 75°C for 10 min to inactivate DNase.
22. Reextraction (following DNase treatment)
 - a. Add 2 μL of 2 M sodium acetate (pH 5.4) and 50 μL ethanol.
 - b. Gently shake.
 - c. Store at -20°C overnight.
 - d. Centrifuge at 7000g for 15 min at 4°C .
 - e. Discard supernatant.
 - f. Allow pellet to air-dry for 10 min.
 - g. Resuspend pellet in 20 μL DEPC water.
 - h. Store at -70°C until use.

4. Notes

1. To ensure the successful transfer of cells with LCM, it is important that the bond between the targeted tissue and the polymer film is stronger than the bond between the tissue and the glass slide. To facilitate this, only uncharged slides should be used, as well as adhesive-free water in the microtome.
2. RNA preparations are often contaminated with genomic DNA. The presence of genomic DNA interferes in RT-PCR-based assays, specifically when primers are used within the exon of the gene.

References

1. Fearon, E. R., Hamilton, S. R., and Vogelstein, B. (1987) Clonal analysis of human colorectal tumors. *Science* **238**, 193.
2. Shibata, D. Hawes, D., Li, Z., Hernandez, A. M., Spruck, C. H., and Nichols, P. W. (1992) Specific genetic analysis of microscopic tissue after selective ultraviolet radiation fractionation and the polymerase chain reaction. *Am. J. Pathol.* **141**, 539–543.
3. Kovach, J. S., McGovern, R. M., Cassady, J. D., Swanson, S. K., Wold, L. E., and Vogelstein, B. (1991) Direct sequencing from touch preparations of human carcinomas: analysis of p53 mutations in breast carcinomas. *J. Natl. Cancer Inst.* **83**, 1004.
4. Emmert-Buck, M. R., Roth, M. J., Zhuang, Z., Campo, E., Rozhin, J., Sloane, B. F., Liotta, L. A., and Stetler-Stevenson, W. G. (1994) Increased gelatinase A (MMP-2) and cathepsin B activity in invasive tumor regions of human colon cancer samples. *Am. J. Pathol.* **145**, 1285–1290.

5. Becker, I., Becker, K. F., Rohrl, M. H., Minkus, G., Schutze, K., and Hofler, H. (1996), Single-cell mutation analysis of tumors from stained histologic slides. *Lab. Invest.* **75**, 801.
6. Emmert-Buck, M. R., Bonner, R. F., Smith, P. D., Chuaqui, R. F., Zhuang, Z., Goldstein, S. R., Weiss, R. A., and Liotta, L. A. (1996) Laser capture microdissection. *Science* **274**, 998–1001.
7. Wright, D. and Mannos, M. (1990) *PCR Protocols: A Guide to Methods and Applications* (Innis, M. A., ed.), Academic Press, San Diego, CA, pp. 153–158.
8. <http://dir.nichd.nih.gov/lcm/lcm.htm>.
9. Laser Capture Microdissection and Molecular Analysis of Normal Development and Pathology: Advances in Laser Capture Microdissection, June 15–16, 1999, sponsored by NIH and NICHD, Bethesda, MD.
10. <http://www.arctur.com>.
11. Chomczynski, P. (1989) *Cinna/Biotech* Bulletin No. 3.

Expression of *c-met* and WT-1

Leslie Kushner, Pui Yan Chiu, Peter Pinto, and Gary Hal Weiss

1. Introduction

Protooncogenes and tumor-suppressor genes are two types of genes associated with cancer development.

Protooncogenes are genes present in normal cells, the expression of which results in transformation when the sequence or level of expression is altered (1,2). Generally, protooncogenes are also highly expressed in tumors in a mutated or aberrantly regulated form. However, these genes are expressed in noncancerous tissue and are necessary for normal cellular function. A number of protooncogene protein products, like *c-met*, have been identified as specific growth factor receptors and, thereby have a direct role in normal cellular proliferation and differentiation.

Tumor suppressor genes are genes normally expressed, but when mutated in such a way as to abrogate function, or aberrantly expressed, tumorigenesis will occur. The normal function of such a gene, however, is *not* to prevent the development of a tumor. Like protooncogenes, tumor-suppressor genes are expressed in noncancerous tissue and are necessary for normal cellular function. A number of tumor-suppressor gene-protein products, like WT-1, have been identified as transcriptional regulators that play a direct role in normal cellular proliferation and differentiation.

Expression of these and other genes associated with tumors can be detected at the level of protein expression (translation) and at the level of messenger RNA expression (transcription). Altered transcription gives information about regulation of the gene. However, altered transcription may or may not result in differential expression of the protein, because protein expression may be either transcriptionally regulated, translationally

regulated, or both. Thus, in order to determine the mechanism of observed differences in protein levels, it is usually necessary to study expression of both the transcript (mRNA) and the encoded protein.

Steady-state levels of transcripts can be detected by either reverse transcriptase polymerase chain reaction (RT-PCR) or Northern analysis. While RT-PCR is more sensitive, Northern analysis is more specific and quantitative. Moreover, it may be difficult to detect transcripts from mutated genes, as may be present in certain tumors, by RT-PCR. However, Northern analysis will allow the detection of some transcripts with small deletions or sequence substitutions by altering the conditions of hybridization. On the other hand, alternative splice transcript variants of WT-1 can be distinguished by RT-PCR and not by Northern analysis.

Expression of the protein is usually detected and quantified by Western analysis. However, localization of the expression is accomplished by immunohistochemistry.

1. 1. *C-met*

C-met encodes a 190-kDa proprotein that is cleaved into the mature 170-kDa heterodimer, consisting of a 50-kDa α subunit and a 145-kDa β subunit linked by disulfide bonds (**Fig. 1**). The glycosylated heterodimeric protein is inserted in the cell membrane with the α subunit exposed on the extracellular surface, whereas the β subunit comprises the transmembrane moiety with extracellular, transmembrane, and intracellular domains (**3,4**). This protein belongs to the class of tyrosine kinase receptors with structural and functional features of a growth factor receptor. In fact, the *c-met* protein is the receptor for hepatocyte growth factor (HGF) (**5**).

Both HGF and *c-met* function in renal development. HGF is mitogenic (**6**) and morphogenic (**7**) for renal epithelial cells in vitro. HGF has been shown to stimulate differentiation of metanephric mesenchymal cells (**8**), which also express this growth factor (**9**). The *c-met* receptor protein is highly expressed in metanephric epithelium, as well as ureteric bud (**9**). In developing mouse kidney, HGF and *c-met* are highly expressed beginning at embryonic day 11.5, corresponding to the onset of tubulogenesis and branching morphogenesis (**10**). The role of HGF in nephrogenesis is demonstrated by experiments in which anti-HGF antibodies are shown to block condensation of metanephric mesenchyme and inhibit ureteric bud branching (**10**). However, renal development is not affected in transgenic mice lacking expression of HGF (**11**).

In the human adult, the *c-met* protooncogene product is highly expressed in renal epithelium (**12**). Mutations of the *c-met* gene have been associated with the development of hereditary papillary renal carcinomas (**13**). Greater than two-thirds of renal cell carcinomas (RCCs) have been shown to overexpress *c-met* (**14,15**).

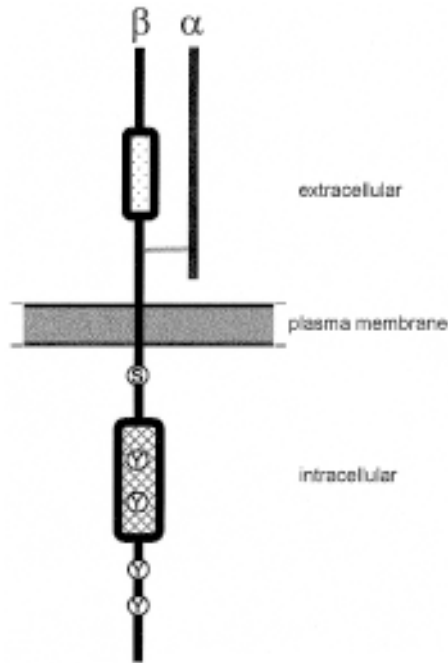


Fig.1. Schematic representation of the *c-met* protein. The extracellular α subunit is linked to the transmembrane β subunit by disulfide bonding (gray line). The extracellular portion of the β subunit contains a cysteine-rich region (stippled box) conserved within a family of related proteins (Met-related sequence [MRS]). The intracellular domain of the β subunit contains the tyrosine kinase (cross-hatched box). Two tyrosine (Y) residues within that region and a serine (S) residue close to the membrane regulate the kinase activity. Two tyrosine residues, c-terminal to the kinase, function in signal transduction.

1.2. WT-1

The gene encoding the WT-1 protein is composed of 10 exons (**Fig. 2**). There are two alternative splice sites that give rise to four different 55-kDa protein products, each of which contains four Cys-His zinc fingers characteristic of the DNA-binding region of transcriptional modulators (**16**). The -KTS splice variants of the WT-1 protein bind to a consensus sequence, in the promotor region of other genes, which also binds the EGR-1 nuclear protein (**17**). EGR-1 is a transcriptional activator expressed in response to mitogenic stimuli. The WT-1 protein inhibits EGR-1-induced transcription. This mechanism of transcriptional regulation appears to be important for expression of growth factors and other gene products. Other consensus sequences for DNA-binding of the WT-1 isoforms are being identified. In addition, there is evidence that the WT-1 protein has the capacity to dimerize (**18**).

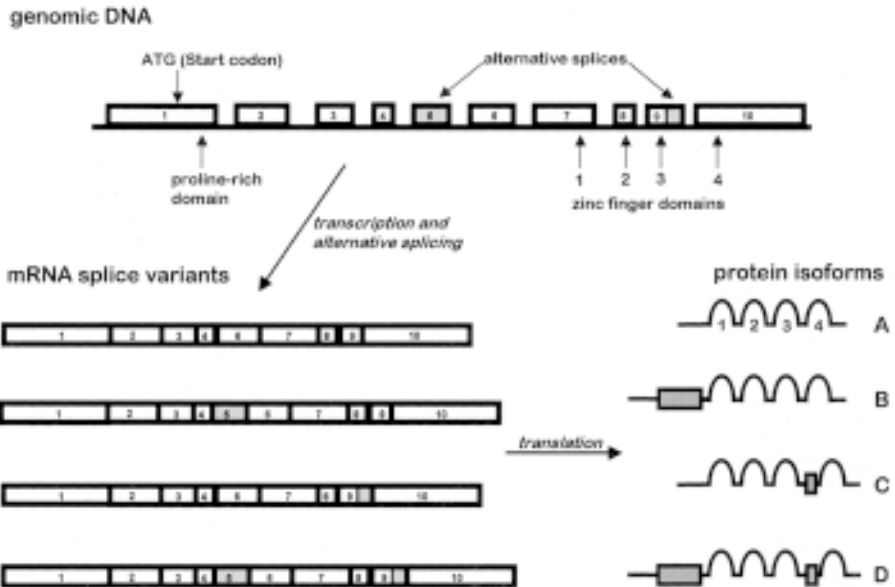


Fig. 2. Biosynthesis of the Wilms' Tumor protein (WT-1). The arrangement of exons and introns of the WT-1 gene is shown. Alternative RNA splicing can produce four different proteins. The four zinc fingers of the protein isoforms are indicated. Placement of additional amino-acid sequences in the resultant proteins is indicated by gray boxes.

Transcriptional inhibition of distinct target genes by WT-1 has been demonstrated. The transcription of the insulin-like growth factor II (IGF-II) (19), insulin-like growth-factor receptor-1 (IGFR-1) (20), platelet-derived growth factor A chain (PDGF-A) (21) and Pax-2 (22) genes are repressed by WT-1 binding to the promoter region of those genes. These genes are all overexpressed in Wilms' tumor. Thus, a lack of developmentally appropriate and tissue-specific transcriptional repression has been implicated as a potential mechanism of Wilms' tumorigenesis. WT-1 also represses the transcription of *bcl-2* (23), a protein that suppresses apoptotic cell death, a process necessary for normal renal development (24). In addition, there is evidence for direct interaction between the p53 and WT-1 proteins resulting in altered function of each protein (25).

During normal development, WT-1 gene expression is greatest in the developing urogenital tract (26). Transgenic mice lacking expression of WT-1 have a failure of kidney development (27), demonstrating the requirement of WT-1 expression for nephrogenesis. Mutations resulting in the absence or functional inactivation of the WT-1 protein are observed in a subset of people with genetic susceptibility to Wilms' tumor—the most common renal tumor of childhood—and in about 20% of sporadic human Wilms' tumors (28,29).

2. Materials

2.1. RNA Extraction

1. GIT buffer: 4 M guanidinium isothiocyanate, 25 mM sodium acetate, pH 7, 0.1 M β -mercaptoethanol.
2. CsCl buffer: 5.7 M CsCl, 25 mM sodium acetate, pH 7.
3. P/C solution: 25:24:1 (v/v/v) phenol/chloroform/isoamyl alcohol made with water-saturated phenol.
4. Chloroform.
5. 0.3 M sodium acetate, pH 5.2.
6. 100% ethanol, ice-cold.
7. 70% ethanol, ice-cold.
8. TE buffer: 10 mM Tris-HCl, 0.1 mM EDTA, pH 8.0.
9. 10 mL ultracentrifuge tubes.
10. Brinkmann Polytron homogenizer.
11. Ultracentrifuge.

2.2. Selection of Poly(A)+RNA

1. Oligo(dT) cellulose column: Oligo(dT) cellulose (Collaborative Research) is slurried in loading buffer B (item 4, below) and poured into a sterile disposable plastic column.
2. 0.1 M NaOH/5 mM EDTA.
3. Loading buffer A: 40 mM Tris-HCl, pH 7.4, 1 M NaCl, 1 mM EDTA, 0.1% SDS.
4. Loading Buffer B: 20 mM Tris-HCl, pH 7.4, 0.1 M NaCl, 1 mM EDTA, 0.1% SDS.
5. Elution buffer: 10 mM Tris-HCl, pH 7.4, 1 mM EDTA, 0.1% SDS.
6. 100% ethanol, ice-cold.
7. 70% ethanol, ice-cold.
8. 3 M sodium acetate, pH 5.2.
9. TE buffer: 10 mM Tris-HCl, 0.1 mM EDTA, pH 8.0.
10. Microcentrifuge tubes.
11. Microcentrifuge.

2.3. PCR

2.2.1. Reverse Transcription Reaction

1. Moloney murine leukemia virus (MMLV) reverse transcriptase.
2. RT buffer: 50 mM Tris-HCl, pH 8.3, 75 mM KCl, 3 mM $MgCl_2$, 20 mM dithiothreitol (DTT).
3. RNAsin.
4. 25 mM dNTP mix (made by mixing equal vol of 100 mM dATP, dCTP, dGTP, and dTTP).
5. Oligo(dT)₆.
6. 0.5 mL microcentrifuge or conical reaction tubes.

2.2.2. PCR Amplification

1. Mineral oil.
2. 10X PCR buffer: 500 mM KCl, 200 mM Tris-HCl (pH 8.4), 15 mM MgCl₂.
3. 0.5-mL thin-walled reaction tubes with flat caps.
4. Automated thermal cycler.
5. Bulk reaction mix: for each 1 mL, combine the following:
 - a. 100 μ L 10X PCR buffer.
 - b. 8 mL 25 mM dNTP mix (made by mixing equal vol of 100 mM dATP, dCTP, dGTP, and dTTP).
 - c. 5 μ L each oligonucleotide primer (20 μ M).
 - d. 5–10 μ L Taq DNA polymerase (5 U/ μ L).
 - e. Distilled water to 1000 μ L.

2.2.3. Agarose Gel Electrophoresis of DNA

1. Tris-borate buffer (TBE): 10.8 g Tris base, 5.5 g boric acid, 20 mL of 0.1 M EDTA, pH8.0, brought up to 1 L with distilled water.
2. Electrophoresis-grade agarose.
3. 6X loading buffer: 0.25% bromophenol blue, 0.25% xylene cyanol, 30% glycerol, 0.1 mg/mL ethidium bromide.
4. DNA molecular weight markers.
5. Horizontal gel electrophoresis apparatus.
6. Gel-casting platform.
7. Gel combs.
8. DC power supply.

2.3. Northern Analysis

2.3.1. Agarose Gel Electrophoresis of RNA

1. 10X borate-sulfate buffer, pH 8.2 (BBS): 30.92 g boric acid, 19.07 g sodium borate, 14.21 g sodium sulfate, 3.72 g EDTA, brought up to 1 L.
2. Electrophoresis-grade agarose.
3. 37% formaldehyde.
4. 5X loading buffer: 50% glycerol, 1 mM EDTA, pH 8.0, 0.25% bromophenol blue, 0.25% xylene cyanol.
5. "Cocktail": 50% formamide, 6% formaldehyde, 1X BBS, 1X loading buffer, 0.5 mg/mL ethidium bromide.
6. RNA molecular weight markers.
7. Horizontal gel electrophoresis apparatus.
8. Gel-casting platform.
9. Gel combs.
10. DC power supply.

2.3.2. Quantitation of Transcripts

1. 45 μ m Nytran (Schleicher and Schuell).
2. 10X SSC: 1.5 M NaCl, 0.15 M sodium citrate, pH 7.0.

3. Hybridization solution: 50% formamide, 2X Denhardt's solution, 5X SSC, 50 mM phosphate buffer (pH 6.8), 0.1% sodium dodecyl sulfate (SDS), 50 µg/mL salmon sperm DNA.
4. ³²P-labeled nucleic-acid probe for hybridization.
5. Stripping solution: 0.1X SSC, 0.5% sodium dodecyl sulfate.
6. Kodak X-AR film.
7. Film cassettes with intensifying screens.
8. Vacuum oven or UV crosslinker.
9. 42°C shaking water bath.

2.4. Western Analysis

2.4.1. Extraction of Protein

1. Homogenizing buffer: 50 mM Tris-HCl, pH 7.4, 1 mM EDTA, containing protease inhibitors.
2. Brinkmann Polytron homogenizer.

2.4.2. SDS-PAGE

1. Loading buffer: 62.5 mM Tris-HCl, 10% glycerol, 1% SDS, 0.05% bromophenol blue, 1% 2-mercaptoethanol.
2. Running buffer: 0.4 M glycine, 0.05 M Tris, 0.4% SDS.
3. Blotting buffer: 20% methanol, 25 mM Tris, 200 mM glycine.
4. 10X Tris-buffered saline (TBS), pH 7.6: 87.5 g NaCl, 60.5 g Tris base, brought up to 1 L and pH adjusted to 7.6.

2.4.3. Detection of Antigen

1. Blocking solution: 6% nonfat dry milk in 1X TBS.
2. Phosphate-buffered saline (PBS).
3. 10X TBS, pH 7.6.
4. Rabbit polyclonal primary antibody.
5. Goat antirabbit antibody conjugated to horseradish peroxidase.
6. ECL detection system (Amersham).

2.5. Immunohistochemical Staining

1. Plus slides (Fisher Scientific).
2. Xylene.
3. 100% ethanol.
4. PBS.
5. 1% H₂O₂ in PBS.
6. 0.5% trypsin in PBS.
7. Blocking solution: 5% goat serum/5% bovine serum albumin (BSA).
8. Rabbit polyclonal primary antibody.
9. Biotinylated secondary antibody (goat antirabbit).
10. Vectastain ABC kit (Biotin/Avidin System) Immunoperoxidase detection system (Vector Laboratories, Burlingame, CA).

11. Peroxidase substrate kit using DAB (diaminobenzidine tetrahydrochloride) as the chromogen to localize peroxidase in the tissue sections (Vector Laboratories, Burlingame, CA).
12. Mayer's modified hematoxylin.
13. Ammonia solution: 1.5% ammonium hydroxide/70% ethanol.

2.6. Primers

1. WT-1
WS7: 5'-ACGCCCTCGCACCATGCGGCGCAGTTCCCC-3'
WS12: 5'-CCTTTGGTGTCTTTTGAGCTGGTCTGAACG-3'
2. *c-met*
P1: 5'-AGATGAACGTGAACATGAAG-3'
P2: 5'-CTAATGAGTTGATCATCATAG-3'
3. β -actin
BAC1: 5'-CCTTCCTGGGCATGGAGTCCTG-3'
BAC2: 5'-GGAGCAATGATCTTGATCTTC-3'

2.7. Nucleic-Acid Probes

1. The 1.8-kb *Eco*R1 fragment of WT-1 was obtained from D. Housman, MIT. The 32 P-labeled DNA probe is made by random priming using standard techniques.
2. The Pmet5 probe for *c-met* is commercially available from the American Type Culture Collection. The *Eco*R1/*Hind*III fragment is nick-translated using standard techniques to produce a 32 P-labeled 500 bp probe.
3. 1B15 mRNA is detected with a 32 P-labeled antisense RNA probe synthesized from a pSP65 plasmid containing the specific 0.7-kb insert (30) using phage SP6 RNA polymerase.

2.8. Antibodies

1. Rabbit polyclonal antihuman WT-1 (C-19) (Santa Cruz Biotechnology).
2. Rabbit polyclonal antihuman cMet (C-28) (Santa Cruz Biotechnology).

3. Methods

There are four methods discussed: RT-PCR, Northern analysis, Western analysis, and immunohistochemistry. **Subheading 3.1** describes the extraction of RNA suitable for RT-PCR or Northern analysis.

3.1. Extraction of RNA

Total RNA can be extracted from renal tissue or cells grown in tissue culture using the guanidinium isothiocyanate method of Ullrich et al. (31).

1. Tissue, which had been flash-frozen in liquid nitrogen and stored at -70°C , is homogenized in GIT buffer (4 mL/g tissue) on ice, using a Brinkmann Polytron homogenizer.

2. The RNA is purified by cesium chloride gradient centrifugation. Each tissue homogenate (4 mL) is layered over 4 mL of CsCl buffer in a 10-mL ultracentrifuge tube. The tubes are centrifuged overnight (18–21 h) at 179,000g at 20°C.
3. The gradient is gently removed, leaving the RNA pellet, which is resuspended in 0.3 M sodium acetate, pH 5.2, and transferred to a microfuge tube.
4. The aqueous solution of RNA is further purified by extraction with an equal volume of P/C solution. The phenol is removed from the aqueous phase (which contains the RNA) by extraction with an equal volume of chloroform. The RNA is precipitated by the addition of 2.5 volumes of ice-cold 100% ethanol. The RNA may be stored as a precipitate under ethanol at –20°C.
5. The precipitate is spun down and rinsed with 70% ice-cold ethanol, and the ethanol is removed by centrifugation followed by air-drying the remaining pellet. The pellet is resuspended in water or TE buffer.

3.2. Selection of Poly(A+)RNA

This method takes advantage of the poly(A+) tail on most mRNAs (32).

1. The final packed oligo (dT)cellulose column is washed with 3 mL of 0.1 M NaOH/ 5 mM EDTA and then washed with water until the pH of the eluate is less than 8.
2. The total RNA (up to 10 mg/500 µL) is denatured at 65°C for 5 min and cooled to room temperature for 2 min.
3. The denatured total RNA is applied to the column, followed by 500 µL loading buffer A, and the eluate is collected. The eluate is reapplied to the column twice more to maximize retention of poly (A+) RNA.
4. The column is washed with 5 mL loading buffer B. Eluate collected contains RNA that is not poly (A+), and may be discarded or collected.
5. The column is washed with 1.5 mL of elution buffer. The eluate collected contains poly (A+) RNA and is retained on ice.
6. Poly (A+) is precipitated by the addition of one-tenth volume of 3 M sodium acetate and 2.5 volumes of 100% ice-cold ethanol, which is placed on dry ice for 30 min or at –20°C overnight.
7. The precipitate is spun down and rinsed with 70% ice-cold ethanol, and the ethanol is removed by centrifugation followed by air-drying the remaining pellet. The pellet is resuspended in water or TE buffer and stored at –70°C.

3.3. RT-PCR

3.3.1. Reverse Transcription

1. 50–500 ng mRNA (or 1–5 µg total RNA) is reverse transcribed using 200 U of MMLV reverse transcriptase in RT buffer containing 6.5 U RNasin, 1 mM dNTPs, and 1 nmol oligo(dT)₆ in a 20-µL reaction vol.
2. Reactions are incubated at 37°C for 60 min.
3. Reactions are inactivated at 90°C for 2 min.
4. cDNA may be stored at –70°C until use.

3.3.2. PCR Amplification

1. Add 99 μL of “Bulk Mix” to each reaction tube.
2. Add template cDNA (1 μL).
3. Layer 50 μL of light mineral oil above the mix.
4. Mix by flicking the tubes, pulse-spin, and transfer to PCR thermal cycler.
5. The amplification conditions are as follows:
 - a. *c-met* is amplified using primers P1 and P2 under the following conditions:
 - i. 1 cycle of 94°C for 1 min, 48°C for 30 s.
 - ii. 45 cycles of 48°C for 2 min, 72°C for 2 min.
 - b. WT-1 is amplified using primers WS7 and WS12 under the following conditions:
 - i. 1 cycle of 94°C for 3 min, 56°C for 30 s.
 - ii. 30 cycles of 56°C for 2 min, 72°C for 10 min.
 - c. β -actin is amplified using primers BAC1 and BAC2 under the following conditions:
 - i. 1 cycle of 94°C for 1 min, 57°C for 30 s.
 - ii. 26 cycles of 57°C for 1 min, 72°C for 2 min, 94°C for 1 min.
 - iii. 1 cycle of 57°C for 1 min, 72°C for 5 min.

3.3.3. Agarose Gel Electrophoresis

1. The 1.5% agarose gel in 0.5X TBE buffer is prepared in advance. 1.5 g of electrophoresis-quality agarose is added to 100 mL of 0.5X TBE buffer and heated with stirring until dissolved. Once cool to the touch, the solution is poured into a gel cast and a comb is applied. The cast gel is allowed to set and dry for approx 1 h before the edge tape and comb are removed.
2. The cast gel is placed in a horizontal gel electrophoresis apparatus and covered with 0.5X TBE buffer to approx 2 mm above the surface of the gel.
3. Equal aliquots of DNA in small volumes of loading buffer are added to the wells. One well is for loading buffer containing DNA markers. The DNA is electrophoresed at constant voltage (1–5 V/cm of gel) until the bromophenol blue dye has migrated a distance sufficient for separation of the DNA fragments.
4. The DNA can be visualized by placing the gel on a UV light source, and the gel can be photographed.
5. The WT-1 and/or *c-met* signal can be quantified relative to the β -actin signal in the same samples by scanning densitometry after Southern blotting and probing gels with ^{32}P -labeled DNA probes.

3.4. Northern Analysis

3.4.1. Agarose Gel Electrophoresis

1. The 1.2% agarose—4 M formaldehyde gel in BBS buffer (pH 8.2) is prepared in advance. 1.2 g of electrophoresis-quality agarose is added to 10 mL of 10X borate-sulfate buffer, (pH 8.2) and heated with stirring until dissolved. Once cool to the touch, formaldehyde is added to a final concentration of 4 M and the solu-

tion is brought to a volume of 100 mL with distilled water. The solution is poured into a gel cast and comb applied. The cast gel is allowed to set and dry for approx 1 h before the edge tape and comb are removed.

2. The cast gel is placed in a horizontal gel electrophoresis apparatus and covered with BBS buffer to approx 2 mm above the surface of the gel.
3. Equal aliquots of total tissue RNA (20 μ g/lane) in small vol of “cocktail” are denatured at 65°C for 5 min, cooled, and added to the wells. One well is for a “cocktail” containing RNA markers. The RNA is electrophoresed at constant voltage (approx 60 mA) until bromophenol blue dye runs close to the end of the gel.

3.4.2. Detection and Quantitation of Transcripts

1. RNA is transferred from the gel to a 45- μ m Nytran membrane (Schleicher and Schuell) by overnight capillary blotting in 10X SSC.
2. Filters are rinsed in 2X SSC and baked at 80°C under vacuum for 2 h or crosslinked to the membrane by ultraviolet light at 12 kJ/cm² for 30 s.
3. Filters are prehybridized at 42°C in hybridization solution for 2–4 h.
4. The appropriate ³²P-labeled probe (1–4 \times 10⁶ dpm/mL) is added to the hybridization solution and the filter is hybridized at 42°C for 16–24 h.
5. Blots are washed twice in 2X SSC and 0.1% sodium dodecyl sulfate (SDS) for 30 min at 42°C, exposed to Kodak XAR-5 film at –70°C, and developed.
6. Bands on the autoradiogram are quantified by scanning densitometry. *C-met* transcripts are detectable at 9 kb, *WT-1* transcripts at 3 kb, and *1B15* transcripts at 1 kb.
7. Blots can be stripped by boiling in stripping solution, in order to rehybridize to a different probe.
8. Levels of mRNA expression are compared to that of *1B15*—a constitutively produced mRNA (30)—and expressed as a ratio of the two values.
9. **Figure 3** shows Northern analytical detection of *WT-1* transcripts compared to *1B15* in the same kidney specimens.

3.5. Western Analysis

3.5.1. Preparation of Protein

1. Tissue is flash-frozen in liquid nitrogen and stored at –70°C.
2. Frozen tissue is homogenized in homogenizing solution using a Brinkmann Polytron.
3. The insoluble material is pelleted by centrifugation at 100,000g for 30 min.

3.5.2. SDS-PAGE

1. 20–50 μ g proteins are solubilized in loading buffer and separated on SDS-10% PAGE in 2X running buffer containing 0.4 M glycine, 0.05 M Tris, and 0.4% SDS.
2. Transfer is to Immobilon-P (Millipore) in ice-cold blotting buffer containing 20% methanol, 25 mM Tris, and 200 mM glycine at < 200mA for 1 h.
3. Membranes are blocked in TBS + 5% nonfat dry milk at room temperature for 1h.

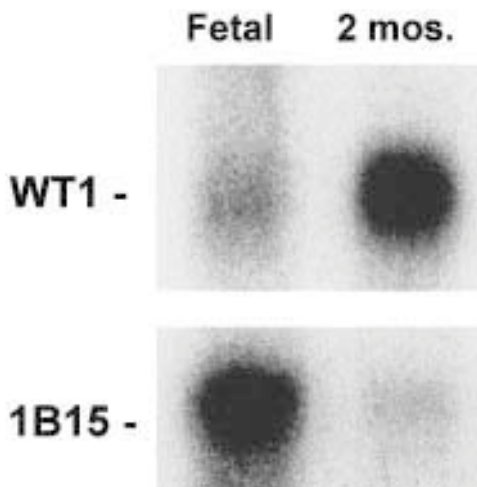


Fig. 3. Representative Northern analysis of WT-1 in developing kidney. Total RNA was extracted from kidney specimens and hybridized to a 1.8-kb *Eco*R1 fragment of WT-1 cDNA probe or cRNA for constitutively produced 1B15, as noted in the figure.

3.5.3. Detection

1. Filters are incubated for 1 h with primary antibody diluted in blocking solution.
2. Filters are rinsed in PBS and incubated for 30 min with secondary antibody (goat antirabbit) coupled to horseradish peroxidase, 1/10,000 dilution in blocking solution.
3. Detection is by enhanced chemiluminescence (ECL) system (Amersham) and autoradiography.

3.6. Immunohistochemistry

1. Tissue is harvested, fixed in 10% phosphate-buffered formalin, and embedded in paraffin.
2. Sections (4- μ m thick) are cut and mounted onto plus slides (Fisher Scientific).
3. Slides are deparaffinized with xylene and rehydrated with graded ethanol by dipping for 30 s each in the following: xylene (2X), 50% ethanol/50% xylene, 100% ethanol (3X), 95% ethanol.
4. Slides are washed three times for 5 min in 1X PBS.
5. Slides are incubated for 30 min at room temperature in 1% H_2O_2 to quench endogenous peroxidase, and then washed three times for 5 min in 1X PBS.
6. Slides are incubated for 10 min in 0.5% trypsin in PBS at 37°C and then washed three times for 5 min in 1X PBS.
7. Slides are incubated in 5% goat serum and 5% BSA (blocking solution) for 1 h in a moist chamber to block nonspecific binding.
8. Slides are incubated at 4°C for 18 h with diluted (1:1000 to 1:200) primary antibody and then washed three times for 5 min in 1X PBS.

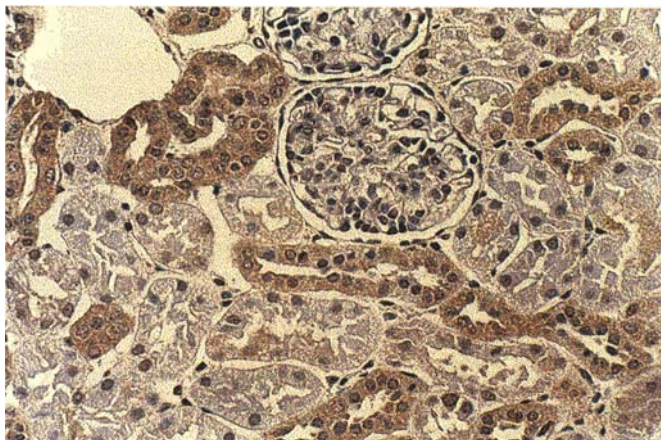


Fig. 4. Immunohistochemical detection of *c-met* in kidney. Formalin-fixed, paraffin-embedded kidney sections (4 μ m) were processed and stained as described in the text. Note that tubule epithelial cells expressing the *c-met* protein on the membrane stain brown.

9. Slides are incubated for 1 h in a moist chamber with biotinylated secondary antibody (goat antirabbit) and then washed three times for 5 min in 1X PBS.
10. Slides are then incubated for 30 min in ABC solution (prepared 30 min before use. ABC consists of avidin, biotinylated horseradish peroxidase H, and buffer; 5 mL of 1X PBS, 1 drop of A (avidin DH), 1 drop of B (biotinylated horseradish peroxidase H). Slides are washed three times for 5 min in 1X PBS.
11. Slides are incubated in 5 mg/mL DAB for 3–6 min.
12. Slides are rinsed in distilled water for 5–10 min, counterstained with Mayer's modified hematoxylin, and washed in distilled water. Then they are dipped in ammonia solution for 1 min and washed in distilled water.
13. To dehydrate, slides are dipped in 95% ethanol, 100% ethanol (2X), 50% ethanol/50% xylene, and xylene (2X).
14. Slides are covered with a coverslip and viewed by light microscopy.
15. **Figure 4** shows a representative slide of immunohistochemical detection of *c-met* in kidney.

4. NOTES

1. Small quantities of contaminant nucleic acids in the laboratory environment can result in undesirable products of PCR reactions and anomalous results. Special precautions must be taken to prevent such contamination. These precautions include (a) performing PCR procedures in a designated area separate from

processing of PCR products; (b) using separate pipets and reagents reserved for PCR reactions; (c) using aerosol-resistant pipet tips; (d) including negative controls (without template DNA).

2. All methods that utilize RNA must include precautions to exclude or inactivate ribonucleases (RNase). RNA is particularly sensitive to RNase activity, which is ubiquitous. These precautions include (a) wearing latex gloves to protect work from RNase in sloughed epithelial cells; (b) using water (and other aqueous solutions, except Tris-based buffers) that had been pretreated with 0.1% diethylpyrocarbonate (DEPC) and autoclaved; (c) microfiltration of solutions through a 22- μ m filter if DEPC pretreatment and/or autoclaving is unsuitable; (d) use disposables where appropriate and DEPC-treat and autoclave nondisposables when possible; (e) use separate reagents reserved for use in procedures utilizing RNA; (f) work in a designated area away from experiments involving tissue processing or culturing.
3. Several methods exist for the extraction of RNA suitable for Northern analysis. An equally satisfactory method is the guanidinium isothiocyanate-phenol/chloroform extraction method of Chomczynski and Sacchi (33). Both methods result in high-yield and intact mRNA, which comprises approx 2% of the RNA extracted. The main criteria for selecting a suitable method are ease of use, yield, and quality of RNA. Yield is determined by measuring the conc. of RNA in aqueous solution by UV spectrophotometric *A* at a wavelength of 260 nm. Quality of RNA is determined empirically by the sharpness of the bands on the final autoradiogram. RNA that has degraded will give an autoradiographic band that trails toward smaller size. An important consideration is the quality of the guanidinium isothiocyanate. This compound has a short shelf-life, and should not be used if it is yellowish in color and/or strong-smelling. The working solution should not be kept more than 1 d. Phenol, used in the extraction, should be colorless. Phenol which is pinkish in color should be discarded.
4. The successful extraction of poly(A+)RNA can be monitored in several ways. The column eluate can pass through a flowthrough spectrophotometer and *A* at 260 nm measured. This would allow one to capture only that small volume of eluate containing poly(A+)RNA. Alternatively, small fractions can be collected and the presence of RNA in the eluate can be determined by ethidium bromide-stained bands on an agarose gel following electrophoresis. The simplest procedure is to precipitate the entire pooled eluate and determine the concentration of RNA in the final aqueous solution by its absorbance at 260 nm.
5. Ribosomal RNA can be visualized in the electrophoresed gel, during Northern analysis, by placing over or under a source of UV light.
6. The radiolabeled probe used to detect specific sequences of nucleic acid in a gel following agarose-gel electrophoresis should be of high specific radioactivity. For that reason, the percentage of incorporation of the ³²P-labeled NTP should be determined. Probes with less than 60% incorporation of radiolabel are likely to give a weak signal on the resultant autoradiogram. Such low incorporation of label suggests a problem with the reaction.

7. ^{32}P -labeled materials must be handled with the proper caution. All work utilizing ^{32}P -labeled materials should be performed behind an acrylic screen. Gloves, protective eyewear, and a radioactivity detection badge should be worn. The area and all nondisposable equipment should be monitored for radioactivity after completion of work. Personnel should be trained in safe handling of radioactive materials.
8. Detection of the 1B15 transcript is utilized for normalization to correct for loading errors. Several different normalization transcripts may be used for this purpose. Care must be taken to use a transcript that does not vary with the experimental procedure.
9. The optimal conc. of MgCl_2 in the PCR buffer must be determined empirically for each template primer pair.
10. The 55-kDa WT-1 protein is detected as a single-band by Western analysis.
11. The 170-kDa heterodimer and the 145 kDa b subunit of *c-met* are detectable by Western analysis.
12. The dilution of primary antibody is determined empirically. Recommended dilutions are 1:200–1:1000. Generally, a span of dilutions is tested to determine which conc. yields the greatest specificity with the lowest background staining.

References

1. Takeya, T. and Hanafusa, H. (1983) Structure and sequence of cellular gene homologous to the RSV src gene and the mechanism for generating the transforming virus. *Cell* **32**, 881–890.
2. Blair, D. G., Oskarsson, M., Wood, T. G., McClements, W. L., Fischinger, P. J., and Vande Woude, G. F. (1981) Activation of the transforming potential of a normal cell sequence, a model for oncogenesis. *Science* **212**, 941–943.
3. Giordano, S., Ponzetto, C., DiRenzo, M. F., Cooper, C. S., and Comoglio, P. M. (1989) Tyrosine kinase receptor indistinguishable from the *c-met* protein. *Nature* **339**, 155–156.
4. Giordano, S., DiRenzo, M. F., Narsimhan, R., Cooper, C. S., Rosa, C., and Comoglio, P. M. (1989) Biosynthesis of the protein encoded by the *c-met* proto-oncogene. *Oncogene* **4**, 1383–1388.
5. Bottaro, D. P., Rubin, J. S., Faletto, D. L., Chan, A. M.-L., Kmieciak, T. E., Van de Woude, G. F., and Aaronson, S. A. (1991) Identification of the hepatocyte growth factor receptor as the *c-met* proto-oncogene product. *Science* **251**, 802–804.
6. Ishibashi, K., Sasaki, S., Sakamoto, H., Nakamura, Y., Hata, T., Nakamura, T., and Marumo, F. (1992) Hepatocyte growth factor is a paracrine factor for renal epithelial cells, stimulation of DNA synthesis and NA,K-ATPase activity. *Biochem. Biophys. Res. Commun.* **182**, 960–965.
7. Montesano, R., Matsumoto, K., Nakamura, T., and Orci, L. (1991) Identification of a fibroblast-derived epithelial morphogen as hepatocyte growth factor. *Cell* **67**, 901–908.
8. Karp, S. L., Ortiz-Arduan, A., Li, S., and Neilson, E. G. (1994) Epithelial differentiation of metanephric mesenchymal cells after stimulation with hepatocyte growth factor or embryonic spinal cord. *Proc. Natl. Acad. Sci. USA* **91**, 5286–5290.

9. Sonnenberg, E., Meyer, D., Weidner, K. M., and Birchmeier, C. (1993) Scatter factor/hepatocyte growth factor and its receptor, the c-met tyrosine kinase, can mediate a signal exchange between mesenchyme and epithelia during mouse development. *J. Cell. Biol.* **123**, 223–235.
10. Santos, O. F. P., Barros, E. J. G., Yang, X.-M., Matsumoto, K., Nakamura, T., Park, M., and Nigam, S. K. (1994) Involvement of hepatocyte growth factor in kidney development. *Dev. Biol.* **163**, 525–529.
11. Schmidt, C., Bladt, F., Goedecke, S., Brinkmann, V., Zschiesche, W., Sharpe, M., Gherardi, E., and Birchmeier, C. (1995) Scatter factor/hepatocyte growth factor is essential for liver development. *Nature* **373**, 699–702.
12. DiRenzo, M. F., Narsimhan, R. P., Olivero, M., Bretti, S., Giordano, S., Medico, E., Gaglia, P., Zora, P., and Comoglio, P. M. (1991) Expression of the Met/HGF receptor in normal and neoplastic human tissues. *Oncogene* **6**, 1997–2003.
13. Schmidt, L., Duh, F.-M., Chen, F., Kishida, T., Glenn, G., Choyke, P., et al. (1997) Germline and somatic mutations in the tyrosine kinase domain of the MET proto-oncogene in papillary renal carcinomas. *Nat. Genet.* **16**, 68–73.
14. Natali, P. G., Prat, M., Nicotra, M. R., Bigotti, A., Olivero, M., Comoglio, P. M., and DiRenzo, M. F. (1996) Overexpression of the met/HGF receptor in renal cell carcinomas. *Int. J. Cancer* **69**, 212–217.
15. Pisters, L. L., El-Naggar, A. D., Luo, W., Malpica, A. and Lin, S.-H. (1997) C-met proto-oncogene expression in benign and malignant human renal tissues. *J. Urol.* **158**, 724–728.
16. Haber, D. A., Sohn, R. L., Buckler, A. J., Pelletier, J., Call, K. M., and Housman D. (1991) Alternative splicing and genomic structure of Wilms' tumor gene WT-1. *Proc. Natl. Acad. Sci. USA* **86**, 9618–9622.
17. Rauscher, F. J. III, Morris, J. F., Tournay, O. E., Cook D. and Curran, T. (1990) Binding of the Wilms' tumor locus zinc finger protein to the EGR-1 consensus sequence. *Science* **250**, 1259–1262.
18. Reddy, J. C., Morris, J. C., Wang, J., English, M. A., Haber, D. A., Shi, Y. and Licht, J. D. (1995) WT-1 mediated transcriptional activation is inhibited by dominant negative mutant proteins. *J. Biol. Chem.* **270**, 10,878–10,884.
19. Drummond, I. A., Madden, S. L., Rohwer-Nutter, P., Bell, G. I., Sukhatme, V. K., and Rauscher, F. J. (1992) Repression of the insulin-like growth factor-II gene by Wilms' tumor suppressor WT-1. *Science* **257**, 674–678.
20. Werner, H., Re, G. G., Drummond, I. A., Sukhatme, V. P., Rauscher, F. J. 3d, Sens, D. A., Garvin, A. J., LeRoith, D., and Roberts, C. T. Jr. (1993) Increased expression of the insulin like growth factor 1 receptor gene, IGF1R, in Wilms' tumor is correlated with modulation of IGF1R promoter activity by the WT-1 Wilms' tumor gene product. *Proc. Natl. Acad. Sci. USA* **90**, 5828–5832.
21. Wang, Z. Y., Madden, S. L., Deuel, T. F., and Rauscher III, F. J. (1992) The Wilms' tumor gene product, WT-1 represses transcription of the platelet derived growth factor A-chain gene. *J. Biol. Chem.* **267**, 21,999–22,002.
22. Ryan, G., Steele-Perkins, V., and Morris, J. F., Rauscher, F. J. III, and Dressler, G. R. (1995) Repression of Pax-2 by WT-1 during normal kidney development. *Development* **121**, 867–875.

23. Hewitt, S. M., Hamada, S., McDonnell, T. J., Rauscher, F. J., and Saunders, G. F. (1995) Regulation of the proto-oncogenes *bc1-2* and *c-myc* by the Wilms' tumor suppressor gene *WT1*. *Cancer Res.* **55**, 5386–5389.
24. Koseki, C., Herzlinger, D., and Al-Awqati, Q. (1992) Apoptosis in metanephric development. *J. Cell. Biol.* **119**, 1327–1333.
25. Maheswaran, S., Park, S., Bernard, A., Morris, J. F., Raucher, F. J., Hill, D. E. ; and Haber, D. A. (1993) Physical and functional interaction between *WT-1* and *p53* proteins. *Proc. Natl. Acad. Sci. USA* **90**, 5100–5104.
26. Pritchard-Jones, K., Fleming, S., Davidson, D., et al. (1990) The candidate Wilms' tumour gene is involved in genitourinary development. *Nature* **346**, 194–197.
27. Kreidberg, J. A., Sariola, H., Loring, J. M., Maeda, M., Pelletier, J., Housman, D., and Haenisch, R. (1993) *WT-1* is required for early kidney development. *Cell* **74**, 679–691.
28. Haber, D. and Housman, D. (1992) The genetics of Wilms' tumor. *Adv. Cancer. Res.* **59**, 41–68.
29. Haber, D. A., Park, P., Maheswaran, S., Englert, C., Re, G. G., Hazen-Martin, D. J., Sens, D., and Garvin, A. J. (1993) *WT-1* -mediated growth suppression of Wilms' tumor cells expressing a *WT-1* splicing variant. *Science* **262**, 2057–2059.
30. Danielson, P. E., Forss-Petter, S., Brow, M. A., Calavetta, L., Douglass, J., Milner, R. J. and Sutcliffe, J. G. (1988) *p1B15*: a cDNA clone of the rat mRNA encoding cyclophilin. *DNA* **7**, 261–267.
31. Ullrich, A., Shine, J., Chirgwin, J., Pictet, R., Tiscer, E., Rutter, W. J., and Goodman, H. M. (1977) Rat insulin genes: construction of plasmids containing the coding sequences. *Science* **196**, 1313–1319.
32. Aviv, H. and Leder, P. (1972) Purification of biologically active globin messenger RNA by chromatography on oligothymidylic acid-cellulose. *Proc. Natl. Acad. Sci. USA* **69**, 1408–1421.
33. Chomczynski, P. and Sacchi, N. (1987) Single-step method of RNA isolation by acid guanidiniumthiocyanate-phenol-chloroform extraction. *Anal. Biochem.* **162**, 156–159.

Molecular Analysis of the von Hippel-Lindau Disease Gene

Allen Chernoff, Viera Kasparcova, W. Marston Linehan,
and Catherine A. Stolle

1. Introduction

Von Hippel-Lindau (VHL) disease is an autosomal dominant disorder that predisposes the affected individual to develop characteristic tumors. These include CNS hemangioblastoma, retinal angiomas, endolymphatic sac tumors, pancreatic cysts and tumors, epididymal cystadenomas, pheochromocytomas, renal cysts, and clear-cell renal carcinoma. The VHL gene was localized to 3p25 and then isolated by Latif et al. (1). The gene contains three exons with an open reading frame of 852 nucleotides, which encode a predicted protein of 284 amino acids. The VHL protein is believed to have several functions. It is involved in transcription regulation through its inhibition of elongation by binding to the *B* and *C* subunits of elongin. Mutations of VHL allow the *B* and *C* subunits to bind with the *A* subunit. This complex then overcomes “pausing” of RNA polymerase during mRNA transcription (2,3). Several studies suggest that the VHL protein is also involved in regulation of hypoxia—inducible transcripts, particularly vascular endothelial growth factor (VEGF), by altering mRNA stability (4,5). Therefore, VHL gene mutations permit the overexpression of VEGF under normoxic conditions, which leads to the angiogenesis believed to be required for tumor growth. The VHL-elongin BC complex (VBC) also binds two other proteins—CUL2 and Rbx1—in a complex that has structural similarity to other E3 ubiquitin ligase complexes (6). Such complexes mediate the degradation of cell-cycle regulatory proteins. The VCB complex may function as a tumor suppressor by mediating the degradation of cell-cycle-specific proteins. In accordance with Knudson’s model, VHL appears to func-

tion as a tumor-suppressor gene. Tory et al. (7) found 3p loss of heterozygosity (LOH) in 11 RCCs, a pheochromocytoma, and a hemangioblastoma from patients with VHL. In five patients where the parental origin of 3p was known, the 3p loss was shown to be of the unaffected parent. It therefore appears that the inactivation of both copies of the VHL gene is a necessary step for tumorigenesis in these patients.

The loss of VHL gene function has also been studied in sporadic RCC. Studies have repeatedly shown a high incidence of VHL LOH in sporadic clear-cell RCC. Brooks et al. (8), reported LOH in 85% of clear-cell RCC studied—Herman et al. (9) found that 19% of sporadic tumors studied had hypermethylation of the VHL gene—another mechanism for VHL gene inactivation. When the data of this study was combined with previous studies by Gnarra et al. (10), the number of clear-cell tumors found with inactivation of VHL was 88%. Clearly, understanding VHL gene function and its relationship to VHL disease may lead to a better understanding of sporadic RCC.

There is now growing evidence of the existence of a genotype/phenotype correlation with VHL mutations. Glenn et al. (11) reported on a family where 57% of those affected had pheochromocytomas and no affected family members developed RCCs or pancreatic cysts. Ninety-eight percent of patients with pheochromocytomas have as their germline mutation a missense mutation. Families with missense mutations at codon 167 are particularly at risk for pheochromocytomas and RCC. We have also recently noticed a possible correlation between the extant and severity of renal involvement and the site and/or size of the deletion found where complete deletions have a more attenuated phenotype than those with smaller deletions (unpublished observations).

Since the VHL gene has been identified methods for determining germline mutations have been improving. Different laboratories have reported different percentages of germline mutation detection ranging from 39–80%. Recently Stolle et al. (12) reported a 100% detection rate of VHL germline mutations by using different techniques for different types of germline mutations. As deletions, whole-gene or partial, account for 28% of all cases, screening begins with a search for these mutations. This is done via quantitative Southern-blot analysis of *EcoRI* and *AseI*-digested genomic DNA hybridized to the g7 probe (to detect digestion products of the VHL gene) and the human beta globin gene probe (as an internal standard for gene-copy number). A mutation-scanning method such as Conformation-Sensitive Gel Electrophoresis (CGSE) may be used to identify PCR products containing mismatched bases in heteroduplex DNA, to determine specific mutation exons exhibiting shifted bands must be sequenced. Point mutations in the VHL gene are detected by DNA sequence analysis of PCR amplified products of exons 1–3.

The following procedures describe extraction of genomic DNA from whole blood, quantitative Southern-blot analysis, mutation scanning by CSGE, and DNA sequence analysis of PCR amplified genomic DNA. For the most part, this involves the use of standard molecular biologic techniques and manufacturer's reagents or kits. For steps performed with reagent kits, the source of the kit is identified and the method briefly described, but the reader is referred to the manufacturer's instructions for a complete description of the procedure. A more in-depth treatment of routine molecular biological techniques may be found in any of a number of excellent laboratory manuals (*13,14*).

2. Materials

2.1. Extraction of High Molecular Weight Genomic DNA

1. Purogene DNA Isolation kit (Gentra Systems, Inc.):
 - a. RBC (red-blood-cell) lysis solution.
 - b. Cell lysis solution.
 - c. Protein precipitation solution.
 - d. DNA hydration solution.
 - e. RNase A solution (4 mg/mL, >30 U/mg). Store at 4°C.
2. Isopropanol (2-propanol).
3. 70% ethanol.
4. 1.5-mL Eppendorf tubes.
5. 15-mL disposable test tubes (Falcon).
6. Vortex mixer.
7. Microfuge and clinical centrifuge.
8. 37°C Water bath.

2.2. Southern-Blot Analysis

2.2.1. Restriction Enzyme Digestion

1. *Eco*RI (20 U/μL) and *Ase*I (10 U/μL) restriction endonuclease (New England Biolabs). Store at -20°C.
2. 10X Restriction enzyme buffer (NEB buffer 3). Store at -20°C.
3. 10X Stop/gel loading buffer: 50% glycerol, 25 mM EDTA, pH 7.5, 0.25% bromophenol blue, 0.25% xylene cyanol.
4. Thin-walled 0.6 mL polypropylene PCR tubes (Corning).
5. 37°C water bath.
6. Microfuge.

2.2.2. Agarose-Gel Electrophoresis

1. 1X TAE electrophoresis buffer: 0.04 M Tris acetate, pH 8.0, 1 mM EDTA. Make as 10X stock solution. Store at room temperature.
2. DNA size marker: Lambda *Hind*III digest (New England Biolabs).
3. Agarose (Sigma).

4. Stirring hot plate.
5. Horizontal gel-electrophoresis apparatus (20 cm × 20 cm gel casting tray and 30-well comb).
6. Power supply.
7. Thermometer.

2.2.3. Quantitative Southern Blotting

1. Ethidium bromide solution: 1 µg/mL.
2. Denaturing solution: 0.5 M NaOH, 1.5 M NaCl.
3. Neutralization solution: 1.0 M Tris-HCl, pH 7.4, 1.5 M NaCl.
4. 20X SSC: 3 M NaCl, 0.3 M sodium citrate, pH 7.0.
5. Supported nitrocellulose (Nitropure, Micron Separations, Inc.).
6. Soaking trays and gel lifter.
7. Transfer tray and plastic plate.
8. Whatman 3MM paper.
9. Paper towels.
10. Parafilm or plastic wrap.
11. Platform shaker.
12. Marking pen.
13. UV crosslinker (Stratagene) or vacuum oven.

2.2.4. Random Primer Labeling

1. Rad Prime Labeling kit (Gibco-BRL).
2. ³²P dCTP (3000 Ci/mmol; 10 mCi/mL; New England Nuclear).
3. 25-ng probe DNA.
4. TE buffer: 10 mM Tris-HCl, pH 7.4, 1 mM EDTA.
5. 0.5 M NaH₂PO₄.
6. 70% ethanol.
7. 1.5-mL Eppendorf tubes.
8. Nick columns (Pharmacia).
9. Scintillation fluid and vials; scintillation counter.
10. Boiling water bath.
11. Microfuge.
12. Plexiglas shielding for radioactivity.
13. DE-81 filters (Whatman).

2.2.5. Prehybridization and Hybridization

1. Formamide (Boehringer Mannheim).
2. Salmon-sperm DNA: 10 mg/mL (U.S. Biochemical).
3. 0.5 M Na₂EDTA (Gibco-BRL).
4. 1 M HEPES buffer (Gibco-BRL).
5. 10% Bovine serum albumin (BSA) (Sigma).
6. 5% Sodium pyrophosphate (Sigma).
7. 2% Ficoll/2% polyvinylpyrrolidone (Sigma).

8. 20X SSC: 3 M NaCl, 0.3 M sodium citrate, pH 7.0. Store at room temperature. (BioWhittaker).
9. 10% Sodium dodecyl sulfate (SDS) (Sigma).
10. Hybridization oven and tubes.
11. Plexiglas shielding for radioactivity.

2.2.6. Washing and Exposure

1. 20X SSC: 3 M NaCl, 0.3 M sodium citrate, pH 7.0. Store at room temperature. (BioWhittaker).
2. 10% sodium dodecyl sulfate (SDS) (Sigma).
3. 2% Ficoll/2% PVP.
4. Wash solution #1: 2X SSC, 0.1% SDS, 0.02% Ficoll/PVP.
5. Wash solution #2: 0.2X SSC, 0.1% SDS.
6. Wash solution #3: 0.2X SSC.
7. Hybridization oven and tubes.
8. Filter tweezers (Millipore).
9. Radioactive waste containers.
10. Water bath.
11. Paper towels.
12. Whatman 3MM paper.
13. 37°C Drying oven.
14. X-ray film (X-OMAT AR, Kodak).
15. Film cassettes with intensifying screens (Kodak).
16. -70°C Freezer.
17. Automatic film developer.

2.3. PCR

1. 10X PCR buffer: 15 mM MgCl₂, 500 mM KCl, 100 mM Tris-HCl, pH 8.3, 0.01% (w/v) gelatin. Store at -20°C.
2. Deoxynucleoside triphosphates (dNTP): 10 mM each of dATP, dCTP, dGTP, and dTTP. Make from equal amount of 100 mM stock dNTPs (Pharmacia) and store aliquots at -20°C. Avoid excessive freezing and thawing.
3. Oligonucleotide primers (*see Table 1*). Stock solutions of primers are stored at -20°C. Each primer is diluted with water at 10 μM.
4. *Taq* DNA polymerase (5 U/μL). Store at -20°C.
5. Dimethyl sulfoxide (DMSO) (Sigma).
6. 1% Gelatin (Sigma). Autoclave and store at room temperature.
7. Mineral oil (Sigma).
8. Thin-walled 0.6 mL polypropylene PCR tubes (Corning).
9. Agarose (Sigma): 1% (w/v) solution of agarose in 1X TBE buffer containing 1 μg/mL ethidium bromide.
10. 1X TBE electrophoresis buffer: 0.89 M Tris-HCl, 0.89 M boric acid, 0.02 M EDTA, pH 8.0. Make as 10X stock solution. Store at room temperature.
11. 10X Gel-loading buffer: 50% glycerol, 0.1% (w/v) bromophenol blue, 0.1% (w/v) xylene cyanole.

Table 1
Primer Sequences and PCR Conditions Used for the Detection of Mutations in VHL Gene

VHL exon	Primer sequence, 5'-3'	Product size, bp	PCR conditions ^a
Exon 1	1F: CGAAGAGTACGGCCCTGAAGAAGAC 1R: CAGTACCCTGGATGTGTCCTGCCTC	410	94°C: 1 min 65°C: 1 min 72°C: 1 min 35 cycles
Exon 2	2F: AGACGAGGTTTCACCACGTTAGC 2R: GTGTCTATCCTGTACTTACCAC	333	94°C: 30 s 60°C: 30 s 72°C: 30 s 30 cycles
Exon 3	3F: CACACTGCCACATACATGCACTC 3R: TACCATCAAAAGCTGAGATGAAACAGTGTAAGT	375	94°C: 1 min 65°C: 1 min 72°C: 1 min 35 cycles

^aFor all PCR reactions initial denaturation 94°C : 6 min and final extension 72°C: 10 min is performed.

12. QIAquick PCR purification kit (Qiagen).
13. DNA size marker: PhiX174 *Hae*III digest.
14. Thermal cycler (e.g., Hybaid Omn-E, Hybaid Ltd.).
15. Agarose-gel electrophoresis apparatus (e.g., Horizon 11-14, Gibco-BRL).
16. UV transilluminator.

2.4. Conformation-Sensitive Gel Electrophoresis (CSGE)

1. 40% acrylamide solution (Gene Mate). Store in dark at 4°C.
2. 1,4-Bis(acryloyl)piperazine (Fluka). Store at 4°C.
3. Ethylene glycol (Sigma).
4. Formamide (Gibco-BRL). Deionize formamide by mixing 100 mL of formamide with 10 g of mixed bed resins (Sigma) for 1 h. Filter mixture through Whatman 3MM filter to remove mixed bed resins. Aliquot formamide in 15-mL tubes. Store at -20°C for up to 1 mo.
5. Ammonium persulfate: 10% (w/v) solution in deionized water. Make fresh daily.
6. N,N,N',N'-tetramethylethylenediamine (TEMED). Store in dark at 4°C.
7. 0.5X TTE electrophoresis buffer: 44.5 mM Tris, 7.5 mM taurine, 0.25 mM EDTA, pH 9.0. Make as 20X stock solution. Store at room temperature.
8. 6X Gel-loading buffer: 30% glycerol, 25% bromophenol blue, 0.25% xylene cyanol.
9. Ethidium bromide solution: 1 mg/L ethidium bromide in 0.5X TTE buffer. Make using 10 mg/mL stock ethidium bromide. Store at room temperature, either in dark or a brown glass bottle.

10. Tray for ethidium bromide staining.
11. Whatman 3MM paper.
12. Polyacrylamide gel electrophoresis apparatus (e.g., BioMax STS-451 DNA Sequencing Unit, KSIS/IBI).
13. Power supply.
14. UV transilluminator.
15. Polaroid camera.

2.5. Sequencing

2.5.1. Purification of Template DNA

1. QIAquick PCR Purification kit (Qiagen).
2. 96–100% ethanol.
3. 1.5 mL Eppendorf tubes.
4. Microcentrifuge.

2.5.2. Cycle Sequencing of PCR Fragments

1. BigDye Terminator Cycle Sequencing Ready Reaction kit (PE Applied Biosystems).
2. Oligonucleotide primers (*see Table 1*). Prepare 1 μM solution from 10 μM by diluting with water.
3. Mineral oil (Sigma).
4. Thin-walled polypropylene 0.6 mL PCR tubes (Corning).
5. Thermal cycler (e.g., Perkin-Elmer Cetus DNA thermal cycler).

2.5.3. Purification of Sequencing Reaction Products

1. CENTRI-SEP Columns (Princeton Separations).
2. Microcentrifuge.

3. Methods

3.1. Extraction of High-Molecular-Weight Genomic DNA

DNA may be extracted from nucleated cells by a variety of methods with either homemade reagents or commercially available kits. We routinely use the Puregene DNA Isolation kit (Gentra Systems, Inc.), which is based on a salting-out procedure described previously (*15–17*). The procedure for isolating genomic DNA from whole blood is described in **Subheading 3.1.1**. Slight modifications of the procedure may be used to isolate DNA from cultured cells or tissues using protocols supplied by the manufacturer.

3.1.1. Cell Lysis

1. Add 3 mL of whole blood to 9 mL of RBC lysis Solution in a 15-mL tube. Invert to mix and incubate for 10 min at room temperature (*see Note 1*). Caution: Human blood may contain infectious agents. Use universal precautions (*see Note 2*).

2. Centrifuge at room temperature for 10 min at 2000g. Remove supernatant, leaving behind the visible white-cell pellet and 0.1–0.2 mL of residual liquid.
3. Vortex the tube vigorously to resuspend the white blood cells.
4. Add 3 mL of cell lysis solution and pipet up and down to lyse the cells.

3.1.2. RNase A Treatment

1. Add 15 μ L of RNase A Solution to the cell lysate.
2. Mix by inverting the tube 25 times and incubate at 37°C for 15 min.

3.1.3. Protein Precipitation

1. Add 1 mL of protein precipitation solution to the RNase-treated cell lysate.
2. Vortex vigorously at high speed for 10–20 s.
3. Centrifuge at 2000g for 10 min at room temperature. The precipitated proteins will form a tight, dark-brown pellet. If the protein pellet is not tight, repeat **steps 2 and 3**.

3.1.4. DNA Precipitation

1. Pipet the supernatant containing the DNA into a clean 15-mL tube containing 3 mL of isopropanol.
2. Mix by inverting 50 times until the white threads of DNA form a visible clump.
3. Centrifuge at 2000g for 5 min to pellet the DNA.
4. Pour off the supernatant and add 5 mL of 70% ethanol. Invert the tube several times to wash the DNA pellet.
5. Centrifuge at 2000g for 5 min. Carefully pour off the ethanol.
6. Allow the DNA pellet to air-dry for 20 min.

3.1.5. DNA Hydration

1. Add 200 μ L of DNA hydration solution to the tube. Transfer the DNA pellet and solution to a clean 1.5-mL Eppendorf tube.
2. Allow the DNA to rehydrate overnight at 37°C while rotating the tube.
3. Store rehydrated DNA at 2–8°C.

3.1.6. Concentration of DNA Determined by OD_{260/280}

1. Determine the OD at 260 and 280 nm of a 200-fold dilution of the DNA in dH₂O using a UV spectrophotometer.
2. Calculate the concentration of DNA as follows:

$$\text{DNA conc. } (\mu\text{g}/\mu\text{L}) = (\text{OD}_{260} \times 50 \mu\text{g}/\mu\text{L} \times \text{dilution factor}) / 1000 \mu\text{L}/\text{mL}$$

With a dilution factor of 200 (i.e., 5 μ L in 1 mL), this formula reduces to DNA conc. ($\mu\text{g}/\mu\text{L}$) = $\text{OD}_{260} \times 10$

NB: For quantitative Southern-blot analysis, the DNA concentration should be between 0.25 and 1.0 $\mu\text{g}/\mu\text{L}$.

3. The purity of the DNA solution can be determined from the OD 260/280 ratio. A value between 1.7 and 2.0 is acceptable. A ratio less than 1.7 indicates that DNA sample is contaminated by UV-absorbing material (i.e., protein) that may interfere with subsequent steps.

3.2. Quantitative Southern Blot Analysis

Southern-blot analysis is a technique whereby high molecular weight genomic DNA is digested, electrophoresed on an agarose gel to separate the fragments by size, transferred by capillary action, and fixed to a solid support, hybridized to a labeled probe complementary to the gene of interest, and then visualized as a band of predictable size on an X-ray film. Quantitative Southern blotting incorporates the use of a second probe specific for another two-allele gene that is used as an internal standard for DNA loading.

The steps involved in quantitative Southern-blot analysis include restriction-enzyme digestion of genomic DNA, agarose-gel electrophoresis of the digestion products, denaturation and renaturation of the DNA in the gel, transfer of the DNA to a nitrocellulose or nylon filter by capillary action, preparation of the labeled probe, prehybridization and hybridization of the filter, washing of the filter, exposure and development of the X-ray film, and interpretation of the results.

3.2.1. Restriction-Enzyme Digestion of Genomic DNA

1. Label 0.6-mL reaction tubes.
2. Organize the DNA samples to be used (*see Note 3*).
3. Thaw the 10X restriction enzyme reaction buffer and place on ice. Place enzymes on ice or, preferably, in a benchtop cooler (Stratacooler, Stratagene).
4. Based on the concentration of the genomic DNA in each sample, calculate the volume (x μ L) of DNA needed to equal 5 μ g per reaction; determine the amount of dH₂O (y μ L) needed per reaction to make up the total volume of the reaction (*see Note 4*).
5. Pipet reagents into the reaction tubes in the following order:

1. dH ₂ O	vol as calculated	y μ L
2. 10X buffer	1/10th total reaction vol	2 μ L
3. 5 μ g of DNA	vol as calculated	x μ L
4. enzyme (<i>see Note 5</i>)	0.5 μ L <i>Eco</i> RI + 1 μ L <i>Ase</i> I	1.5 μ L
Total volume		20 μ L

6. Cap tube and mix sample thoroughly by tapping the tube with your finger. Do NOT vortex tubes containing genomic DNA.
7. Spin tubes briefly in microfuge (5 s) to force liquid to the bottom.
8. Place reaction tubes at 37°C and incubate for at least 4 h and, preferably overnight.
9. Stop reaction by adding 2 μ L of 10X stop/gel loading buffer.

3.2.2. Agarose-Gel Electrophoresis

Agarose-gel electrophoresis is used to separate DNA fragments by size. DNA is negatively charged, and small fragments will migrate through the gel

more rapidly than large fragments. The rate of migration of DNA fragments through the gel is proportional to the current applied at relatively low voltages. However, voltages should not exceed 5 V/cm of gel.

1. Prepare the gel-casting tray. With some horizontal gel-electrophoresis apparatus, the gel-casting tray is open at either end and must be taped to keep molten agarose in the tray. (Ordinary laboratory tape or autoclave tape works well for this purpose.) Other types of apparatus use tightly fitting plastic dams during casting of the gel that will be removed prior to electrophoresis.
2. Place a sample well comb in place in the gel-casting tray. We typically use a 30-well comb on a 20 × 20-cm gel tray.
3. Prepare 200 mL of a 1% solution of agarose in 1X TAE buffer. Heat to boiling while stirring with a magnetic spin bar on a stirring hot plate (*see Note 6*).
4. Place a thermometer in the solution and cool to 65–70°C while stirring.
5. Pour the solution into the prepared gel-casting tray and allow the agarose to harden into a gel for at least 1 h.
6. Remove the tape or plastic dams from both ends of the gel-casting tray. Place the tray containing the gel in the electrophoresis chamber with sufficient 1X TAE buffer to cover the gel to a depth of 2–5 mm above the gel surface.
7. Slowly remove the sample comb from the gel by pulling straight upward on the comb.
8. Load the samples in a predetermined order. Positive and negative controls should be run on each gel. Also load 0.5 µg of *Hind*III digested lambda phage DNA as a molecular weight marker.
9. Run the gel at constant voltage of 60 V for 21 h.

3.2.3. Quantitative Southern Blotting

The DNA fragments in the agarose gel will be transferred to a supported nitrocellulose filter as single-stranded DNA molecules so that the DNA fragments will be available to hybridize with a radiolabeled DNA probe of complimentary sequence. After the transfer, the DNA strands will be “fixed” to the nitrocellulose by baking or UV crosslinking.

1. Slide the gel gently off the gel-casting tray into a tray containing 1 µg/µL solution of ethidium bromide (EtBr). Rotate on a platform shaker for 20 min to stain the gel. Pour off the EtBr. Destain in H₂O for 20 min with shaking. Caution: Ethidium bromide is a carcinogen. Always wear gloves when working with EtBr.
2. Visualize the DNA in the ethidium bromide-stained gel by placing the gel on a UV transilluminator (*see Note 7*). Caution: UV light is damaging to eyes. Wear UV protective glasses or face shield when using the UV light.
3. Trim away portions of the gel that do not contain DNA fragments of interest. Measure the size of the remaining gel.
4. Place the gel in a tray with enough denaturing solution so that the gel can float freely. Rotate on a platform shaker vigorously enough to keep gel suspended in the solution. Denature for 45 min.

5. Pour off the denaturation solution. Rinse the gel briefly with deionized water. Add a sufficient volume of neutralization buffer to the tray to suspend the gel. Shake gels gently for 20 min.
6. Pour off the neutralization buffer and replace with fresh neutralization buffer. Shake gently for another 20 min.
7. Cut a piece of reinforced nitrocellulose to match the size of the gel. With a black Sharpie marker, note on each filter the gel number, enzyme/probe combination, or other identifying information you will need. Wear gloves while handling the nitrocellulose.
8. Fill a transfer tray with 20X SSC. Cut a piece of Whatman 3MM filter paper to cover the transfer bed.
9. Lay the cut Whatman 3MM filter on the transfer bed and wet with 20X SSC. Press out air bubbles with a gloved hand or roll out bubbles with a plastic rod or pipet.
10. Place gel pieces on the transfer bed on top of the Whatman filter. Lightly push out air bubbles that may be trapped under the gel, but do not press on gel, because this will distort the bands on the final autoradiogram.
11. Cover the area of the Whatman filter bordering the gel with parafilm or plastic wrap so that subsequent layers of absorbent paper placed on top of the gel cannot touch the Whatman paper.
12. Place a nitrocellulose filter on top of the gel.
13. Place two pieces of Whatman 3MM filter paper cut to the same size on top of the nitrocellulose filter. Dampen the top of the Whatman paper with 20X SSC. Press lightly to ensure that good contact is made between the nitrocellulose filter and the Whatman paper.
14. Place approx 3 in. of paper towels on top of Whatman filter. It may be necessary to cut the paper towels to approximately fit the top of the gel.
15. Place a plastic plate on top of paper towels, cover the transfer tray with plastic wrap to prevent evaporation of the 20X SSC, and place small weight on top of this. The weight should ensure even contact of the paper towels with the Whatman paper, but should not be heavy enough to press and distort the gel.
16. Allow transfer to take place overnight at room temperature.
17. The next morning, disassemble the blot. Carefully peel the nitrocellulose filter off the gel and place DNA side up in a shallow tray with just enough 6X SSC to cover the filter. Gently rub the filter with a gloved hand to remove adhering particles of agarose. Drain the filter of excess fluid and allow to air-dry (10–20 min) DNA side up, on a piece of absorbant paper. Discard the gel, parafilm, and Whatman paper pad.
18. Fix the DNA to the nitrocellulose filter either by baking at 80°C for 2 h under vacuum or by UV crosslinking (Stratalinker, Stratagene).

3.2.4. Random Primer Labeling

DNA fragments complementary to the VHL (*g7; 1*) and human beta globin (*12*) genes will be random primer labeled with ^{32}P dCTP. The probe DNA is

first heated to boiling and then mixed with a reaction buffer containing short primers of random sequence that anneal to the single-stranded probe DNA. The Klenow fragment then extends the primed fragment, incorporating nucleotide triphosphates in the reaction mixture—one of which (dCTP) is radioactive labeled.

1. Label a 1.5-mL Eppendorf tube for each reaction.
2. Thaw probe DNA, 10X buffer, and dNTPs. Place on ice with Klenow fragment.
3. Pipet probe DNA (25 ng) into a 1.5-mL Eppendorf tube containing dH₂O. The total volume of probe and dH₂O is 22 μ L.
4. Heat for 5 min in a boiling water bath. Cool on ice.
5. To the reaction tube on ice, add 1 μ L each of the nonradioactive nucleotides (i.e., dATP, dGTP, and dTTP) and 20 μ L of the random primer/buffer mix.
6. Place the reaction tubes and ice bucket behind 1/4 in. Plexiglas shielding and add 5 μ L of [³²P]dCTP (3000 Ci/mmol; 10 mCi/mL; NEN). Caution: Radioisotopes emit potentially harmful radiation. Wear gloves and protective clothing, and use appropriate shielding when working with radioisotopes.
7. Mix sample briefly; microfuge for 5 s.
8. Add 1 μ L of Klenow fragment and mix gently; microfuge for 5 s.
9. Place tubes in a Plexiglas container and leave at 37°C for 30 min.
10. Add 5 μ L of Stop buffer.
11. The probe may be used directly, or unincorporated nucleotides may be removed by using Nick columns (Pharmacia) as described:
 - a. Remove cap from top of column and pour off excess liquid.
 - b. Remove bottom plug.
 - c. Fill column to the top with TE buffer and let drain by gravity.
 - d. Add 55 μ L sample and allow to enter gel bed.
 - e. Add 350 μ L TE buffer and collect outflow in Eppendorf tube. Discard in radioactive waste.
 - f. Add 400 μ L TE buffer and collect probe in 1.5-mL Eppendorf tube.
 - g. Discard column in radioactive waste.
12. Determine the specific activity of the probe by counting 2 μ L of sample in a scintillation counter. Specific activity (cpm/ μ g) = cpm \times 200/0.025 μ g. The specific activity of the probes should be $>1 \times 10^9$ cpm/ μ g.
13. Cap the tube containing the labeled probe tightly, using an Eppendorf tube clamp, and heat the probe in a boiling water bath for 10 min.
14. Place boiled probe on ice.

3.2.5. Prehybridization and Hybridization of Nitrocellulose Filters

Prior to hybridization, prehybridization is necessary to prevent the probe DNA from nonspecifically binding to the nitrocellulose filter. The prehybridization buffer contains nonhuman (salmon-sperm) DNA and other reagents that will bind to those parts of the filter that have not already bound DNA, and thus prevent nonspecific binding of the probe.

1. Prepare deionized formamide by adding 6 g of mixed bed resin (Sigma) to 60 mL of formamide (Boehringer Mannheim). Stir at room temperature for 1 h. Filter formamide through Whatman filter paper to remove resin. Add 0.165 g NaH_2PO_4 and adjust pH to 6.8 with NaOH or HCl. Deionize formamide fresh the day of use.
2. Prepare prehybridization/hybridization buffer as follows:

Chemical	Final conc.	Vol/100 mL
20X SSC	3X	15 mL
0.5 M Na_2EDTA	1 mM	0.2 mL
1 M HEPES	10 mM	1 mL
10% BSA	0.2%	2 mL
2% Ficoll, 2% PVP	0.2%	10 mL
5% Na pyrophosphate	0.05%	1 mL
10% SDS	0.1%	1 mL
Salmon-sperm DNA	100 $\mu\text{g}/\mu\text{L}$	2 mL
Deionized formamide	50%	50 mL

Mix all chemicals except formamide together, and warm to 37°C to ensure that SDS and salmon-sperm DNA are in solution. Add deionized formamide. Centrifuge at 1000g for 10 min in 50 mL conical screw-cap tubes (Corning) to remove insoluble and/or gelatinous material. Pipet off 45 mL of prehybridization buffer to a fresh tube, leaving pelleted material in bottom of tube. Prepare prehybridization/hybridization buffer fresh the day of use.

3. Place filters in a hybridization tube with DNA side facing inward. If the filter is so wide that the edges overlap, use a plastic mesh to ensure that prehybridization/hybridization solution can flow freely over the filter (*see Note 8*).
4. Add enough prehybridization/hybridization buffer to the tube to coat the filter with a thin film of solution (approx 20 mL). Screw the cap onto the tube.
5. Place the tube with filter in the hybridization oven at 42°C and rotate for 3 h.
6. After the 3-h prehybridization step, pipet the denatured and chilled probes directly into the prehybridization/hybridization solution in the tubes. This step should be performed behind Plexiglas shielding in an area designated for radioactive work.
7. Recap the hybridization tube and return it to the hybridization oven. Rotate overnight at 42°C.

3.2.6. Washing and Exposing Filters

After the hybridization, the filters are washed with buffers of increasing stringency to remove nonspecifically bound probe. The stringency of a wash is increased by gradually lowering the salt concentration and raising the temperature of the wash.

1. Heat washes 1 and 2 to 42°C.
2. Remove the cap of the hybridization tube and pour the hybridization fluid containing the probe into a radioactive liquid-waste container. Pour about 50 mL of wash 1 into the tube and recap. Rotate the tube to wash the tube and nitrocel-

lulose filter. Discard liquid into radioactive waste. Pour 50 mL of wash 1 into the tube and rotate in a hybridization oven at 42°C for 20 min. Discard wash down a drain designated for disposal of low levels of radioactivity. Repeat this wash twice more. Do not allow filters to dry, since this may cause background on the X-ray film.

3. Add 50 mL of prewarmed wash 2 to the tube. Rotate in the hybridization oven at 42°C for 30 min. Discard wash.
4. Add 50 mL of fresh wash 2 to the tube. Rotate in the hybridization oven at 52°C for 30 min. Discard wash.
5. Add 50 mL of fresh wash 2. Rotate at 65°C for 30 min. Discard wash.
6. Rinse with wash 3 three times (15 s to 5.0 min) at room temperature.
7. Remove filters from the tube using filter forceps (Millipore). Blot filters on paper towels and air-dry at room temperature for approx 3 h. Bake filters in a 37°C oven until bone-dry (about 30 min). Any dampness in the filter will result in the filter sticking to the emulsion of the X-ray film.
8. Either tape the filter to a piece of paper cut to fit the interior of a film cassette or tape the filter directly to the intensifying screen of the film cassette.
9. In a dark room, place a piece of X-ray film over the filter and tightly close the cassette.
10. Place cassettes in -70°C freezer overnight.
11. The next morning, remove the cassette from the freezer and develop the film. Place another piece of X-ray film in the cassette.
12. Return cassettes to -70°C. Review of the just-developed films will determine when the next film will be developed. Generally the second film is developed after 2–3 d of exposure.

3.2.7. Interpretation of Southern Blots for Deletions in the VHL Gene

Patients with a partial deletion of the VHL gene exhibit an abnormal band (migrating either below or above the normal 9.7-kb VHL gene fragment) on Southern blot analysis with the g7 probe (*see Fig. 1, lanes 2 and 6*). Patients with a complete deletion of one VHL allele exhibit a 9.7-kb VHL band of reduced intensity (*see Fig. 1, lane 7*) compared to controls (*see Fig. 1, lanes 1, 3–5, and 8*) when equal amounts of DNA are loaded on the gel, as determined by the equal intensities of the 4-kb beta globin band in each lane.

3.3. PCR

The polymerase chain reaction (PCR) is used to amplify a specific segment of DNA using oligonucleotide primers (*18*). Three PCR reactions are used to amplify exon 1 (NT 300–553 plus 30 bp 3' of exon 1), exon 2 (NT 554–676 plus 30 bp 5' and 3' of exon 2) and exon 3 (NT 677 to the stop codon at NT 855 plus 30 bp 5' of exon 3) of VHL gene (*see Note 9*). Nucleotides are numbered according to (*1*) (GenBank accession number L15409) in which the first nucleotide of the coding sequence is 214.

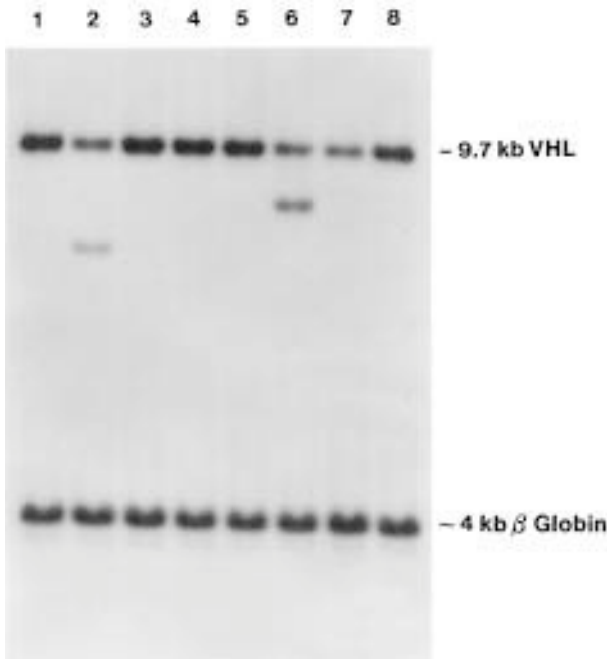


Fig. 1. Quantitative Southern blot analysis to detect partial or complete deletions of the VHL gene.

1. Prepare enough of each PCR mastermix (*see Table 2*) for the number of samples to be amplified plus one extra. Aliquot 45 μ L of each master mix into appropriately labeled 0.6-mL tubes (*see Note 10*).
2. Dilute the genomic DNA to be amplified to a concentration of 100 ng/ μ L and add 3 μ L of the DNA solution to the tubes containing master PCR mixes for VHL exons 1–3. Vortex and spin briefly.
3. Overlay each reaction mix with two drops of mineral oil.
4. Prepare *Taq* polymerase mix (*see Table 2*) and keep on ice until needed.
5. Place the tubes in the thermal cycler, and start cycling program. For PCR conditions, *see Table 1* (*see Note 11*).
6. During the initial denaturation step (94°C for 6 min) add 2 μ L of *Taq* polymerase mix into each tube by inserting pipet tip through mineral-oil layer and ejecting into aqueous layer (“hot start” reaction).
7. When PCR is finished, check for satisfactory amplification on a 1% agarose gel containing ethidium bromide to ensure that a single product of the correct size and adequate concentration has been generated. Include a suitable size marker—e.g., *PhiX174 HaeIII* digest. Use UV transilluminator to visualize the bands (*see Note 12*).
8. PCR reaction can be used immediately for DNA heteroduplex formation and CSGE analysis, or stored at 4°C overnight, or at –20°C for several mo.

Table 2
Master PCR Mixes: Reagent Volumes/Sample

Reagent	Exon 1, μL	Exon 2, μL	Exon 3, μL
10X PCR buffer (15 mM MgCl_2)	4.80	4.8	4.80
10 μM Forward primer	1.25	2.5	1.25
10 μM Reverse primer	1.25	2.5	1.25
10 mM dNTPs	1.00	1.0	1.00
DMSO	5.00	—	—
1% gelatin	—	—	0.50
Deionized water	31.7	34.2	36.2

3.4. Conformation-Sensitive Gel Electrophoresis (CSGE)

Several techniques have been developed to scan DNA sequences for single-base changes (for review, *see* Cotton, [19]). We use Conformation-Sensitive Gel Electrophoresis (CSGE) for the detection of mutations in the VHL gene. Using CSGE, DNA heteroduplexes containing one strand of wild-type and one strand of mutated DNA are separated from homoduplex bands containing two normal alleles (20). Mildly denaturing solvents (ethylene glycol, formamide) are used to induce bends in the double helix containing single-base mismatches, thereby retarding heteroduplex bands on the gel compared to homoduplex bands. One or two “shifted” heteroduplex bands are usually seen on a CSGE gel with samples containing a mutation (*see* Note 13). The bands are detected on the gel after ethidium bromide-staining, which obviates the need for radioactivity commonly used with SSCP gels (19,20).

1. Form heteroduplexes by incubating PCR product in 0.6-mL thin-walled tubes at 98°C for 5 min, cool to 68°C, and incubate for 30 min. This is best done using a thermal cycler.
2. Wash glass plates of the sequencing apparatus (e.g., BioMax STS-45i DNA Sequencing Unit, KSIS/IBI) with hot tap water, and rinse with deionized water and ethanol, wiping with lint-free paper tissue (*see* Note 14).
3. Assemble the glass plates with spacers for casting the gel.
4. Prepare acrylamide gel solution. For a gel of 43 cm \times 36 cm \times 1 mm (BioMax STS-45i DNA Sequencing Unit, KSIS/IBI) prepare 175 mL solution by mixing the following:

40% acryl:BAP (99:1) solution (<i>see</i> Note 15)	43.75 mL
20X TTE buffer	4.375 mL
Deionized formamide	26.25 mL
Ethylene glycol	17.5 mL
Deionized water	81.275 mL
TEMED	0.1 mL
10% ammonium persulfate solution	1.75 mL

Table 3
Taq Polymerase Mix: Reagent Volumes/Sample

Reagent	Volume, μL
Taq polymerase (5 U/ μL)	0.25
10X PCR buffer (15 mM MgCl_2)	0.20
Deionized water	1.55

Caution: Acrylamide is a potent neurotoxin. Always wear gloves when working with acrylamide.

5. Pour acrylamide gel solution between the plates and insert comb. Allow gel to polymerize horizontally at room temperature for at least 1 h.
6. After polymerization of the gel is complete, remove the comb and the bottom spacer.
7. Attach plates to the electrophoresis apparatus.
8. Fill upper and lower reservoir of apparatus with 0.5X TTE buffer.
9. Remove air bubbles trapped between the plates at the bottom of the gel and rinse wells thoroughly.
10. Prerun the gel at 400 V for approx 15 min.
11. While the gel is prerunning, mix 2 μL of each PCR product with 0.5 μL of gel-loading buffer (*see* **Notes 16** and **17**).
12. After the prerun, rinse wells again. Quickly load the samples and size marker to prevent diffusion of samples in the wells (*see* **Note 18**).
13. Run the gel at 400 V for 18 h.
14. When the electrophoresis has finished, detach gel plates from electrophoresis apparatus. Carefully pry apart the plates, taking care to leave the gel attached to one.
15. Stain gel attached to plate for 10 min in EtBr solution in a tray by pouring just enough staining solution on the gel to cover it completely. Destain the gel for 10 min with deionized water using the same method. Pour water off the gel.
16. Cut a piece from a sheet of Whatman 3MM paper at least as large as the gel and apply to the gel (adherent to the plate). Make sure with that the gel is in contact with the paper sheet.
17. Carefully peel gel away from the glass plate by lifting the paper sheet from one side. The gel will adhere to the paper. Put the gel on a disposable underpad (gel side up).
18. Visualize the bands on the gel with a handheld UV lamp. Cut the relevant portion of the gel and transfer on a UV transilluminator (gel side down). Wet the paper sheet adhered to the gel with water and carefully remove from the gel.
19. Photograph the gel.

3.4.1. Interpretation of CSGE Gels for Mutation Detection

DNA heteroduplexes containing one strand of wild-type and one strand of mutated DNA are retarded on CSGE gels (*see* **Fig. 2, lanes 4, 7, and 10**) compared to homoduplex bands made of perfect match of two normal alleles (*see* **Fig. 2, remaining lanes**). The presence of a shifted band(s) on CSGE gel



Fig. 2. Conformation-Sensitive Gel Electrophoresis (CSGE) to scan for point mutations in exons 1-3 of the VHL gene.

therefore indicate the presence of a mismatched base (mutation or polymorphism) in a given exon (*see Note 22*). To determine the precise nature of the mutations (or polymorphisms), exons exhibiting shifted band(s) must be sequenced.

3.5. DNA Sequencing

After gene scanning by CSGE, it is necessary to sequence one exon (to identify the mutation) or all three exons (to exclude the presence of mutation) in the VHL gene. Direct sequencing of PCR products using the dideoxy chain-termination procedure developed by Sanger et al. (**21**) is now the most commonly used method for defining specific mutations. The protocol described here is based on the BigDye terminator cycle sequencing system, and can be used to prepare sequencing reactions for automated sequence analysis on the ABI 373A or 377 fluorescent sequencer (Perkin-Elmer). Use of the 373A or 377 sequencer and the relevant software is described in detail in the manufacturer's manual, and is beyond the scope of this chapter.

The steps involved in sequencing include purification of template DNA (PCR products), cycle sequencing, and purification of sequencing reaction products.

3.5.1. Purification of Template DNA

The PCR product must be purified in order to remove the oligonucleotides and dNTPs that would otherwise interfere with the sequencing reaction. For this purpose we use the QIAquick PCR Purification kit (Qiagen), following the manufacturer's instructions (*see Note 19*).

1. Add 5 vol of buffer PB to 1 vol of the PCR reaction and mix. It is not necessary to remove mineral oil.
2. Place a QIAquick spin column in a provided 2-mL collection tube. To bind DNA, apply the sample to the QIAquick column and centrifuge for 30–60 s.
3. Discard flowthrough and place the QIAquick column back into the same tube. To wash, add 0.75 mL buffer PE to the QIAquick column and centrifuge for 30–60 s.
4. Discard flowthrough and place the QIAquick column back in the same tube. Centrifuge the column for an additional 1 min at maximum speed.
5. Place QIAquick column in a clean 1.5-mL tube. To elute DNA, add 50 μ L H₂O to the center of the QIAquick membrane and centrifuge the column for 1 min. Store DNA at -20°C .

3.5.2. BigDye Terminator Cycle Sequencing of PCR Fragments

The sequencing reactions are performed using the BigDye Terminator Sequencing Ready Reaction kit (Perkin-Elmer) according to the manufacturer's instructions. The primers used for the sequencing of VHL exons are the same as those used for the PCR reaction.

1. For each sequencing reaction, add the following reagents to a 0.6-mL thin-walled tube:
 - a. Template (PCR product) 20–30 ng (*see Note 20*).
 - b. Primer (1 μM) 3.2 μL
 - c. BigDye terminator Ready Reaction Mix 4.0 μL .
 - d. Deionized water up to 20 μL
2. Mix well and spin briefly.
3. Overlay the reaction mixture with 1 drop of mineral oil.
4. Place the tubes in thermal cycler and run the following program (*see Note 21*): 25 cycles of 96°C 30 s, 50°C 15 s, and 60°C 4 min.
5. Sequencing reactions can be purified immediately or stored at -20°C .

3.5.3. Purification of Sequencing Reaction Products

After cycle sequencing, the huge excess of fluorescent dye terminators used to drive the reaction must be efficiently removed for good quality electrophoretic separation of the termination products and effective analysis of the initial 50 bases after the primer. For this purpose, we use the CENTRI-SEP Columns (Princeton Separations), following the manufacturer's instructions.

1. Hydrate the dry gel in the spin column by adding 0.80 mL of water. Cap the column and mix by shaking and inverting the column. Let sit at room temperature for at least 1 h.
2. Remove air bubbles from the column gel by inverting and sharply tapping the column. Stand the column up and allow the gel to settle.
3. Remove the column cap and plug and allow excess column fluid to drain (by gravity) into a 2 mL wash tube. Discard the fluid.

4. Spin the column and wash tube in a variable speed centrifuge at 750g for 2 min to remove the interstitial fluid.
5. Transfer 20 μ L of completed BigDye deoxy terminator reaction mixture onto the center of the gel bed without disturbing the gel surface.
6. Place the column into the 1.5-mL sample collection tube and place both into the rotor. The highest point of the gel media in the column should point toward the outside of the rotor. Spin at 750g for 2 min.
7. Dry the purified sample collected in the bottom of the sample collection tube in a vacuum centrifuge without applying heat. At this point, the sample may be submitted to the DNA Sequencing Core Laboratory or stored at -20°C .

3.5.4 Interpretation of DNA Sequencing Gels for Point Mutation Detection

The typical result of fluorescent sequencing analysis is a chromatogram consisting of colored peaks (*see Fig. 3*). The area under the peak represents the strength of the signal and the peak color is specific for the base at each position (T-red, A-green, C-blue, and G-black). The software assigns N if the position is ambiguous. Visual pattern recognition is very efficient for mutation detection. Peak profiles are irregular but highly consistent for given sequence. A portion of the normal sequence for exon 1 of the VHL gene is presented in **Fig. 3A**. A frame-shift mutation gives a characteristic profile with two bases at every position after the mutation. An example of frame-shift mutation in the same region of exon 1 is presented in **Fig. 3B**. A single base substitution can be recognized by the appearance of two colored peaks (two bases) at a given position. Signal strength of the normal base at this position is reduced in most cases. An example of a single base substitution in the same region of exon 1 is presented in **Fig. 3C**.

To determine whether an observed mutation has been reported previously, refer to the VHL mutation database on the internet at www.umd.necker.fr:2005/. Previously unreported mutations may be evaluated for their potential to cause disease as described in Cotton and Scriver (22).

4. Notes

1. To reduce degradation of DNA, blood samples should be collected in purple-topped tubes containing EDTA anticoagulant and stored at $2-8^{\circ}\text{C}$ for not more than 5 d prior to DNA isolation procedures. Yellow top (ACD anticoagulant) tubes can also be used. Avoid using green-top (heparin anticoagulant) tubes. Heparin can inhibit some restriction enzymes.
2. Human blood may contain infectious agents such as HIV, hepatitis B, or hepatitis C. Therefore, universal precautions should be used at all times during this procedure. Workers should use suitable barrier protection, including gloves, lab coats, and face shields. Since isolated DNA may also contain blood-borne pathogens, effective barrier protection should be used during all stages of this procedure.
3. High-molecular-weight genomic DNA in solution in either dH_2O or TE buffer is required for restriction enzyme digestion. Samples that have been frozen for long-

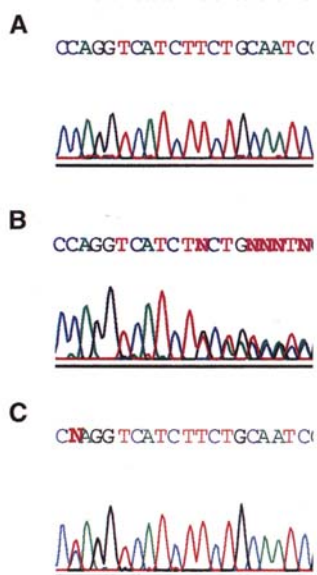


Fig. 3. DNA sequence analysis to identify point mutations in the VHL gene.

term storage need to be rotated overnight at 37°C before use. If the DNA has become partially degraded, or if it is not uniformly in solution, it is unlikely that a reliable result will be obtained. To test whether a sample is degraded, 1 µg of undigested DNA can be run on a 1% agarose minigel. A degraded sample will show a smear after electrophoresis and staining with EtBr whereas an intact sample will not migrate any further than the 23-kb *Hind*III digested lambda DNA marker. To determine whether the DNA is in solution, rock the microcentrifuge tube slowly in the light. A sample that is in solution will contain no obvious clumps of “gelatinous”-appearing material. Pipetting the sample with a pipetman will produce a smooth stream of viscous solution if it is either pulled up into or expelled from the pipet tip.

4. The volume of the reaction is limited by the volume of the agarose gel sample well. We use a 30-tooth sample comb that has a maximum loading volume of 40 µL. Typical reaction volumes are 20 µL.
5. The amount of enzyme added (10 U) is intended to be a twofold molar excess to ensure complete digestion of the DNA. However, the amount of enzyme must not exceed 10% of the reaction volume—otherwise the glycerol in the enzyme storage buffer will inhibit the digestion.

6. The agarose used for Southern blots should be low electroendoosmosis (EEO) agarose. Sigma markets a product specificity for molecular biology (catalog #A-6013).
7. Visualizing the DNA in the ethidium bromide-stained gel is not essential to the procedure, but it does provide information about the success of the procedure up to that point in case you have to troubleshoot a failed blot. You may wish to photograph the gel using a Polaroid camera or digital camera as a permanent record.
8. If a hybridization oven is not available, prehybridization and hybridization may be performed in heat-sealed plastic bags (seal-a-meal bags) as described in Sambrook et al. (13).
9. The first 86 nucleotides of exon 1 are not routinely amplified, since few mutations have been reported in this region. The region may be amplified using the following primers:
 - a. K54:GAAATACAGTAACGAGTTGGCCTAGC
 - b. RD101:CCCAGCTGGGTCTGGGCCTAAGCGCCGGGC
10. Include a sample from a known normal individual and “no DNA” control. It is highly recommended to include a sample or samples from known mutants as well. “Normal” and “mutant” samples will be used for quality control of CSGE analysis.
11. The PCR thermal cycling parameters have been determined with a standard 0.6-mL microcentrifuge tubes (Corning) in Hybaid Omn-E thermal cycler (Hybaid Limited) using the “Simulated Tube” control option. The conditions may need to be adjusted if other tubes, machines and/or control options are used.
12. Standard agarose-gel electrophoresis apparatus (e.g., Horizon 11-14, Gibco-BRL) can be used to check 8- μ L aliquots of PCR products for good amplification.
13. If the mutation is an insertion or deletion, four bands can be observed on CSGE gel (two homoduplex and two heteroduplex bands).
14. Standard sequencing apparatus with spacers 0.8–1.0-mm-thick and a flat-toothed comb can be used. If spacers and comb of this thickness is not provided with apparatus, they can be custom-made by OWL Scientific. Bottom spacer is required.
15. Prepare 40% acryl:BAP (99:1) solution by mixing the following:
 - a. 40% acrylamide 100 mL
 - b. BAP 0.404 g
 - c. Deionized water 1 mLStore at 4°C for up to 1 mo.
16. The PCR reaction should be robust enough so that 2 μ L of PCR product can be easily seen after ethidium bromide staining. We recommend the concentration of PCR product to be at least 10 ng/ μ L. If the concentration is lower, up to 6 μ L of PCR product can be loaded on the gel.
17. For each exon, a sample from a known normal individual and a known mutant should be included also.
18. It is convenient to load 6–12 samples at a time and let the gel run for 5–10 min between each loading.
19. Alternatively, other kits such as Wizard™ PCR Preps DNA Purification System (Promega) or High Pure Product Purification Kit (Boehringer Mannheim) can be used.

20. The concentration of PCR products can be estimated from agarose gel comparing the intensity of PCR product with the intensity of known amount of DNA marker.
21. These conditions work very well on Perkin-Elmer DNA thermal cycler using the standard 0.6-mL microcentrifuge tubes (Corning). They may need to be adjusted if other tubes and/or machines are used.
22. For polymorphisms reported for VHL gene, see Whaley et al. (22).

References

1. Latif, F., Tory, K., Gnarra, J., Yao, M., Duh, F. M., Orcutt, M. L., et al. (1993) Identification of the von Hippel-Lindau disease tumor suppressor gene. *Science* **260**, 1317–1320.
2. Duan, D. R., Pause, A., Burgess, W. H., Aso, T., Chen, D. Y. T., Garrett, K. P., Conoway, R. C., Conoway, J. W., Linehan, W. M., and Klausner, R. D. (1995) Inhibition of transcription elongation by the VHL tumor suppressor protein. *Science* **269**, 1402–1406.
3. Kibel, A., Iliopoulos, O., DeCaprio, J. A., and Kaelin, W. G., Jr. (1995) Binding of the von Hippel-Lindau tumor suppressor protein to elongin B and C. *Science* **269**, 1444–1446.
4. Gnarra, J. R., Zhou, S., Merrill, M. J., Wagner, J. R., Krumm, A., Papavassiliou, E., Oldfield, E. H., Klausner, J. D., and Linehan, W. M. (1996) Post-transcriptional regulation of vascular endothelial growth factor mRNA by the product of the VHL tumor suppressor gene. *Proc. Natl. Acad. Sci. USA* **93**, 10589–10594.
5. Iliopoulos, O., Ohh, M., Kaelin, W. G. Jr. (1998) pVHL 19 is a biologically active product of the von Hippel-Lindau gene arising from internal translation initiation. *Proc. Natl. Acad. Sci. USA* **95**(20), 11,661–11,666.
6. Kamura, T., Koepp, D. M., Conrad, M. N., Skowyra, D., Moreland, R. J., Iliopoulos, O., Lane, W. S., Kaelin, W. G., Jr., Elledge, S. J., Conoway, R. C., Harper, J. W., and Conoway, J. W. (1999) Rbx 1, a component of the VHL tumor suppressor complex and SCF ubiquitin ligase. *Science* **284**, 657–661.
7. Tory, K., Brauch, H., Linehan, W. M., Barba, D., Oldfield, E., Filling-Katz, M., Seizinger, B., Nakamura, Y., White, R., Marshall, F. F., Lerman, M. I., and Zbar, B. (1989) Specific genetic change in tumors associated with von Hippel-Lindau disease. *J. Natl. Cancer Inst.* **81**, 1097–1101.
8. Brooks, J. D., Bova, G. S., Marshall, F. F., and Isaacs, W. B. (1993) Tumor suppressor gene allelic loss in renal cancers. *J. Urol.* **150**, 1278–1283.
9. Herman, J. G., Latif, F., Weng, Y., Linehan, W. M., Lerman, M. I., Zbar, B., Duan, D. S., Gnarra, J. R., and Baylin, S. B. (1994) Silencing of the VHL tumor suppressor gene by DNA methylation in renal carcinoma. *Proc. Natl. Acad. Sci. USA* **91**(21), 9700–9704.
10. Gnarra, J. R., Tory, K., Weng, Y., Schmidt, L., Wei, M. H., Latif, F., Liu, S., Chen, F., Duh, F. M., Lubensky, I., Duan, D. S., Florence, C., Pozatti, R., Walther, M. M., Bander, N. H., Grossman, H. B., Brauch, H., Isaacs, W. B., Lerman, M. I., Zbar, B., and Linehan, W. M. (1994) Mutations of the VHL suppressor gene in renal cell carcinoma. *Nat. Genet.* **7**, 85–90.

11. Glenn, G. M., Daniel, L. N., Choyke, P., Linehan, W. M., Oldfield, E., Gorin, M., Hosoe, S., Latif, F., Weiss, G., Walther, M., Lerman, M. I., and Zbar, B. (1991) von Hippel-Lindau disease: distinct phenotypes suggest more than one mutant allele at the VHL locus. *Hum. Genet.* **87**, 207–210.
12. Stolle, C. A., Payne, M. S., Benz, E. J., Jr. (1987) Equal stabilities of normal β -globin and non-translatable beta 0-39 thalassemic transcripts in cell-free extracts. *Blood* **70**, 293–300.
13. Sambrook, J., Fritsch, E. F., and Maniatis, T. (1989) *Molecular Cloning: A Laboratory Manual*, 2nd ed., Cold Spring Harbor Laboratory Press, Cold Spring Harbor, NY.
14. Ausubel, F. M., Brent, R., Kingston, R. E., Moore, D. D., Seidman, J. G., Smith, J. A., and Struhl, K. (1999) *Current Protocols in Molecular Biology*, John Wiley & Sons, New York.
15. Davis, R. W. (1980) Rapid DNA isolation for enzymatic and hybridization analysis. *Methods Enzymol.* **65**, 404–411.
16. Buffone, G. J. (1985) Isolation of DNA from biological specimens without extraction with phenol. *Clin. Chem.* **31**, 164–165.
17. Miller, S. A., Dykes, D. D., and Polesky, H. F. (1988) A simple salting out procedure for extracting DNA from human nucleated cells. *Nucleic Acids Res.* **16**, 1215.
18. Saiki, R. K., Scharf, S., Faloona, F., Mullis, K. B., Horn, G. T., Erlich, H. A., and Arnheim, N. (1985) Enzymatic amplification of β -globin genomic sequences and restriction site analysis for diagnosis of sickle cell anemia. *Science* **230**, 1350–1354.
19. Cotton, R. G. H. (1993) Current methods of mutation detection. *Mutat. Res.* **285**, 125–144.
20. Ganguly, A., Rock, M. J., and Prockop, D. J. (1993) Conformation-sensitive gel electrophoresis for rapid detection of single-base difference in double-stranded PCR products and DNA fragments: evidence for solvent-induced bends in DNA heteroduplexes. *Proc. Natl. Acad. Sci. USA* **90**, 10325–10329.
21. Sanger, F., Nicklen, S., and Coulson, A. R. (1977) DNA sequencing with chain terminating inhibitors. *Proc. Natl. Acad. Sci. USA* **74**, 5463–5467.
22. Cotton, R. G. H. and Scriver, C. R. (1998) Proof of “disease causing” mutation. *Hum. Mutat.* **12**, 1–3.
23. Whaley, J. M., Naglich, J., Gelbert, L., Hsia, Y. E., Lamiell, J. M., Green, J. S., Collins, D., Neumann, H. P. H., Laidlaw, J., Li, F. P., Klein-Szanto, A. J. P., Seizinger, B. R., Kley, N. (1994) Germ-line mutations in the von Hippel-Lindau tumor suppressor gene are similar to somatic von Hippel-Lindau aberrations in sporadic renal cell carcinoma. *Am. J. Genet.* **55**, 1092–1102.

Experimental Models and Methods in Antibody Targeting of Renal Cell Carcinoma

Robert L. Vessella, D. Scott Wilbur, Kent Buhler, and Paul H. Lange

1. Introduction

Metastatic renal cell carcinoma (RCC) is incurable and there are few treatment options that assure even a short prolongation in survival. It is the most common malignancy of the adult kidney and accounts for approximately 12,000 deaths per year (1). Due to a lack of diagnostic markers for early detection and the infrequency of notable symptoms early in the disease process, about one third of patients present with known metastatic disease. However, the staging of RCC is an inaccurate science and in 40% of those patients where a nephrectomy is the treatment choice for presumed organ-confined disease, metastases become evident within about 1 yr (2). For reasons that are poorly understood, metastatic RCC has remained relatively resistant to chemotherapy, biological response modifiers and cellular immunotherapy—although, glimpses of encouragement have appeared in numerous studies. These are discussed in great depth throughout the accompanying chapters.

One course of treatment for primary and metastatic RCC that has high theoretical appeal is the infusion of radiolabeled monoclonal antibodies (mAbs) or similar recombinant constructs that would “search out and destroy” metastatic sites in a highly selective manner. mAbs preferentially reactive with tumor cells could theoretically overcome the disadvantages of chemotherapies by sparing normal tissues/organs and bypassing the mechanisms associated with drug-resistance. This approach also overcomes the disadvantages of biological response modifiers in not relying on an intact host immune system. It has advantages over the infusion of “activated” immune cells in that numerous

studies have demonstrated an ability of the antibodies to specifically localize at the site of the tumor whereas specific tumor targeting has been difficult to achieve using infused natural killer or activated immune cells. Finally, the options exist to customize the type of radiotherapy delivered by the mAb; one could potentially select a radioimmune conjugate ideally suited for micrometastases (e.g., an alpha particle emitting radionuclide) or one better suited for masses greater than 0.5 cc (e.g., a beta-particle-emitting radionuclide).

With such theoretical advantages, why hasn't the radiolabeled mAb approach tendered a cure for metastatic RCC? Despite encouraging progress over the past two decades in the field overall, there remain a few limitations revealed through the animal model studies and clinical trials conducted to date. One of the greatest limitations that appear to now be solved was the tendency for the patient to mount an anti-mouse antibody response thereby negating subsequent infusions of the mouse mAb. With significant advances in recombinant technologies, the infused radio-immune conjugates can now appear more "human-like" or "stealth-like."

A second noted limitation of radioimmunotherapy was the overall low accumulation of radiolabeled antibody, albeit specific, at the tumor sites. This has proven to be a more difficult hurdle to overcome. In the few radioimmunotherapy clinical trials conducted to date, the percent injected dose per gram has ranged from approx 0.003% ID/g to 0.1% ID/g. Although the upper range of these values is far better than observed overall in radioimmunotherapy trials of other tumor types, improvements are still needed to be curative. Novel delivery approaches, such as those experimentally described herein, should enhance the accumulation of radionuclide at the tumor site in patients.

The third limitation is in the availability of suitable radionuclides for these targeted studies. Beta-emitting isotopes, such as iodine I-131 and Y-90 deliver most of their energy many cell diameters from the targeted cell. In larger tumor masses, this can be quite effective because of the cross-over pattern of distribution, but in targeting small metastatic foci, most of the energy is distributed to the surrounding tissue, not to the tumor cells. As previously noted, the alpha-particle emitting radionuclides are ideal for destroying these small tumor masses because the energy is delivered to the targeted cell. However, the availability of alpha-particle emitting radionuclides for testing in preclinical models is extremely limited. Fortunately, as interest in these radionuclides is increasing, at least a few centers, including our own, are reconfiguring their radionuclide generating systems to produce alpha-particle emitters for testing in tumor targeting models.

The authors of this chapter have had a long history in the study of radiolabeled mAbs for the imaging and therapy of primary and metastatic RCC. This chapter will summarize some of that experience. Over the past several years

we have focused attention on improving the accumulation of the radionuclide at the site of the tumor, with a particular emphasis on treatment of small metastatic foci. One approach that has shown considerable promise is referred to as pretargeting. The advantages are higher accumulation of radiolabel at the tumor site and very low levels of radiolabel in normal organs.

2. Materials

2.1. Purifying mAbs

1. Ascites.
2. 100% (w/v) saturated NH_4SO_4 solution.
3. 20 mM Sodium phosphate, pH 6.9.
4. Dialysis Tubing, MWCO 12-15 kDa.
5. 1 mL Hitrap Protein G Sepharose Column (Pharmacia Biotech, Piscataway, NJ).
6. High Pressure Liquid Chromatography (HPLC) System or UV spectrometer.
7. 100 mM Glycine HCl, pH 2.5.
8. 1.5 M Tris-HCl, pH 8.0.
9. 1X Phosphate-buffered saline (PBS): 6 mM KH_2PO_4 , 24 mM Na_2HPO_4 , 120 mM NaCl, pH 7.4.
10. 0.22 μm syringe filter.
11. Bicinchoninic Acid (BCA) Protein Assay Reagents, PIERCE, Rockford, IL.
12. Bovine serum albumin (BSA) standards.
13. 96 well micro-EIA/RIA assay plates.
14. Sodium dodecyl sulfate polyacrylamide gel electrophoresis (SDS-PAGE) Mini-gel apparatus, SDS-PAGE gradient gels, 4–15%.

2.2. Production of $F(ab')_2$ and Fab' Fragments from Purified mAb

2.2.1. Production of $F(ab')_2$ Fragments

1. Purified mAb.
2. Porcine pepsin.
3. 0.01M HCl.
4. 10 M Sodium acetate, pH 2.5.
5. pH paper.
6. 37°C incubator or hybridization oven.
7. 1.5 M Tris-HCl, pH 8.8.
8. 20 mM Sodium phosphate, pH 6.8.
9. Millipore Ultra-15 Centrifuge Filters (Bedford, MA).
10. Sephadex G-200 Resin, Pharmacia Biotech (Piscataway, NJ).
11. Column and fittings, 2 × 75 cm.

2.2.2. Production of mAb A6H Fab' Fragments from $F(ab')_2$ Fragments

1. Purified A6H $F(ab')_2$.
2. 100 mM DTT in 20 mM sodium phosphate, pH 6.8.
3. Sephadex G-25 size exclusion column (PD-10).

4. 20 mM sodium phosphate, pH 6.8, containing 1 mM EDTA.
5. HPLC system with size exclusion column and UV detector.
6. UV spectrometer.
7. SDS-PAGE mini-gel apparatus, SDS-PAGE gradient gels, 4–15%.

2.3. Production of A6H Fab'-S-Biotin

1. Purified A6H Fab'.
2. Biotin-maleimide.
3. 20 mM sodium phosphate, pH 6.8.
4. Centricon-30 ultracentrifugation filters.
5. HPLC system with size-exclusion column and UV detector.
6. UV spectrometer.
7. SDS-PAGE mini-gel apparatus, SDS-PAGE gradient gels, 4–15%.

2.3.1. Determination of Number of Biotin Molecules Conjugated to A6H Fab'

1. 4'-Hydroxyazobenzene-2-carboxylic acid (HABA).
2. 1 mg/mL avidin solution in PBS.
3. 50 mM sodium phosphate, 0.9% NaCl, pH 6.0.
4. 10 mM HABA in 10 mM NaOH.
5. UV spectrophotometer measuring at 500 nm.

2.4. Succinylation of Streptavidin

1. 5.4 mg/mL solution of recombinant streptavidin in PBS.
2. 50 mM NaHCO₃ buffer, pH 8.5.
3. 4.75 mg/mL succinyl anhydride in dimethyl sulfoxide (DMSO).
4. Centricon-30 ultracentrifuge filter.
5. HPLC with size-exclusion column.
6. UV measuring at 280 nm.

2.5. Production of A6H Fab'-Streptavidin Conjugates

1. Purified A6H F(ab')₂.
2. Recombinant streptavidin in PBS, pH 7.2.
3. Succinimidyl 4-(*N*-maleimido-methyl)cyclohexane-1-carboxylate (SMCC, Pierce) in DMSO at 10 mg/mL.
4. PBS, pH 6.0.
5. 100 mM DTT in 20 mM sodium phosphate, pH 6.8.
6. Sephadex G-25 size-exclusion column (PD-10).
7. 20 mM sodium phosphate, pH 6.8, containing 1 mM EDTA.
8. Centricon-30 ultracentrifuge filters.
9. Gel electrophoresis system.
10. HPLC System with size exclusion column and UV detector.
11. UV spectrometer.
12. SDS-PAGE mini-gel apparatus, SDS-PAGE gradient gels, 4–15%.

2.6. Radioiodination of A6H F(ab')₂, A6H-S-Biotin, and Streptavidin

1. Personal protective clothing as required by institution for work with radioactive isotopes, should include, but not limited to: lab coat, Tyvek sleeve protectors, gloves, protective eyewear, mask, and shoe covers.
2. Radioactive monitoring devices—including personal monitoring equipment.
3. Absorbent underpads.
4. Shielding when/where possible, e.g., lead pigs to hold load syringes.
5. Radioiodinations must be conducted in a fume hood inside of a container in which the effluents pass through a charcoal filter.
6. Radioiodine as sodium salt in 0.1 *N* NaOH solution.
7. 1 mg/mL solution of chloramine-T in water.
8. 10 mg/mL sodium metabisulfite in water.
9. Size-exclusion column—NAP-10.
10. HPLC with radioactivity detector.
11. Dose calibrator to quantify radioactivity.
12. Radioactive sharps container and radioactive disposal containers.

2.7. Radioiodination of Stannylbenzoate Biotin Derivatives

1. Protective clothing and equipment as listed in **Subheading 2.6., item 1.**
2. Solution of biotin derivative containing trioxadiazine linker and benzoylstannane/benzoyliodide in methanol containing 1% acetic acid.
3. Radioiodine as sodium salt in 0.1 *N* NaOH solution.
4. 1 mg/mL solution of *N*-chlorosuccinimide in methanol.
5. 1 mg/mL sodium bisulfite in water.
6. HPLC with radioactivity detector and valve to isolate radioactivity.
7. Dose calibrator to quantify radioactivity.
8. Radioactive sharps container and radioactive disposal containers.

2.8. In Vitro Cell Immunoassay

1. Personal protective equipment and clothing as required for working with radioisotopes.
2. Antigen positive RCC cells, growing in log phase; aliquots in sterile microcentrifuge tubes.
3. Sterile 1X PBS.
4. Radiolabeled immunoconjugate (*see Subheadings 2.6. and 3.6.*).
5. Test tube rotator.
6. Access to gamma counter normalized for radioisotope being used, e.g., Wallac 1480 gamma counter.
7. Microtube centrifuge.

2.9. Establishment of RCC Xenografts

2.9.1. RCC Tumor Bit Preparation

1. 35 × 10 mm petridishes.
2. Gentimycin-HCl injectable 40 mg/mL.

3. Sterile 1X PBS.
4. Surgical instrument set (*see Subheading 2.9.2., item 12*).

2.9.2. Implantation Surgery

1. Balb/C nu/nu mice, male, 4–6 wk old at time of surgery.
2. Clean room apparel—hair cover, gown, mask, and shoecovers.
3. Approved biological safety cabinet or laminar flow hood.
4. Sterile gloves.
5. Sterilized surgery board.
6. Anesthetic—ketamine/xylazine mix: 6.5 mg/0.44 mg/mL diluted into 0.9% sterile normal saline; stocks: ketamine-HCl injectable 100 mg/mL, xylazine-HCl injectable 20 mg/mL.
7. Sterile syringes: 1 and 3 cc sizes.
8. Sterile 26 gauge needles.
9. Betadine surgical scrub solution.
10. 70% Isopropanol.
11. Sterile 2 × 2 gauze.
12. Surgical instrument set that contains: 2-pairs of microdissecting scissors, 4–0.8 mm point fine serrated forceps, 1–9.0 mm wound clip applicator with wound clips, and 1–9.0 mm wound clip remover.
13. Dry glass bead sterilizer.
14. Clean sterile cage.

2.10. Injection of Mice Bearing RCC Xenografts with Radiolabeled Conjugates

1. Personal protective clothing as required by institution for work with radioactive isotopes, should include, but not limited to: lab coat, Tyvek sleeve protectors, gloves, protective eyewear, mask, and shoe covers.
2. Radioactive monitoring devices—including personal monitoring equipment.
3. Absorbent underpads.
4. Shielding when/where possible, e.g., lead cylinders to hold syringes.
5. Mice bearing RCC xenografts of required size.
6. Biotin-free test diet (if required).
7. Isotopic injectate.
8. Sterile 0.9% normal saline or 1X PBS.
9. Sterile 0.5 cc, 28 gauge cemented needle insulin syringes.
10. Balance—accurate to ± 0.001 g.
11. Ketamine/xylazine anesthetic mix.
12. Sterile 3 cc syringes.
13. Sterile 26 gauge needles.
14. Ear notcher.
15. Sterile 2 × 2 gauze.
16. Broome- style rodent restrainer (if required).
17. Radioactive sharps container and radioactive disposal containers.

2.11. Biodistribution of Mice Bearing RCC Xenografts

1. Personal protective clothing and equipment as required to work with radioactive materials.
2. Absorbent underpads.
3. Dissection board.
4. Sterile 0.3 cc syringes with 26 gauge needles.
5. 0.5 cc insulin syringes with cemented 28 gauge needles.
6. Microdissecting scissors, 1.0 mm rat-tooth forceps, 1.0 mm serrated forceps.
7. Anesthesia—ketamine/xylazine mix.
8. 12 × 75 mm polypropylene or polystyrene test tubes.
9. Absorbent paper.
10. Balance—accurate to ± 0.001 g.
10. 10% Normal Buffered Formalin—10% Formaldehyde in 1xPBS.
11. Gamma counter, e.g., Wallac 1480 gamma counter.
12. Computer with a spreadsheet program, e.g., Excel 97 for Windows.

3. Methods

3.1. Purification of Monoclonal Antibodies from Ascites

1. Ascites is clarified by incubation of the fluid at 37°C for 1 h.
2. The ascites is centrifuged at 100,000g for 25 min, the resulting pellet discarded.
3. The supernatant is then mixed 1:1 with a 100% (w/v) saturated solution of $(\text{NH}_4)_2\text{SO}_4$ of the period of approx 1–2 h. This mixture is slowly mixed for an additional 45 min, then allowed to sit at 4°C overnight.
4. The precipitate is collected by centrifugation, and then resuspended in a minimum volume of 20 mM sodium phosphate, pH 6.9, and dialyzed against this buffer at 4°C for 12 h, three buffer changes.
5. 2 mL aliquots are loaded onto a Hitrap Protein G Sepharose Column (Pharmacia), on a Gilson HPLC System, equilibrated with 20 mM sodium phosphate, pH 6.9.
6. Column is washed with 7–10 column volumes until absorbance base line (280 nm) has decrease to less than 0.050.
7. mAb is eluted from the column using 100 mM Glycine HCL, pH 2.5.
8. Elute is immediately neutralized by addition of 1/10th volume 1.5 M Tris-HCl, pH 8.0.
9. All eluted fractions are collected and pooled.
10. mAb is dialyzed against 1 × PBS at 4°C for 12 h, 3 buffer changes.
11. mAb is sterile filtered through a 0.22- μm syringe filter.
12. mAb is quantitated by BCA microplate assay against albumin standards.
13. mAb concentration is adjusted, if necessary.
14. mAb is quality controlled by ELISA, HPLC (sizing column), and SDS-PAGE (reduced and non-reduced conditions).
15. mAb is aliquoted and stored until use at –80°C.

3.2. Production of $F(ab')_2$ and Fab' Fragments from Purified mAb

3.2.1. Production of $F(ab')_2$ Fragments

For production of $F(ab')_2$ fragments, a low scale test run is performed to test varying stoichiometric ratios of mAb to pepsin—encompassing the range of 1:5–1:80. This test run is performed as outlined using time points of 4, 14 and 24 h to assess the digestion of mAb to $F(ab')_2$. The samples are taken, neutralized with 5X reducing SDS-PAGE sample buffer and evaluated on 4–15% SDS gradient gels. The mAb-to-pepsin ratio that produces $F(ab')_2$ without further enzymatic degradation is chosen. Whole mAb that is uncleaved can be recovered and digested again.

1. mAb is adjusted to a concentration of 5 mg/mL.
2. The pepsin solution (0.5 mg/mL in 0.01 M HCl) is made fresh.
3. mAb solution is adjusted to 100 mM sodium acetate using 10 M sodium acetate, pH 2.5.
4. mAb and pepsin are combined at predetermined stoichiometric ratio; pH of digestion mixture should be less than 4.0 as spotted on pH paper.
5. mAb digestion mixture is placed at 37°C, gently shaking for predetermined time point.
6. Reaction is terminated by addition of 1/20th vol of 1.5 M Tris-HCl, pH 8.8.
7. Reaction solution is then dialyzed against 20 mM sodium phosphate at 4°C for 12 h, one buffer change.
8. This reaction mixture is then passed over a Protein G column (*see Subheading 3.1., step 5*), but the flowthrough is collected.
9. The flow through is then dialyzed against 20 mM sodium phosphate, pH 6.8, at 4°C for 12 h, three buffer changes.
10. The solution is then concentrated to a volume of approx 5 mL using a Ultra-15 centrifuge filter.
11. The concentrated solution is then loaded onto a Sephadex G-200 column (2 × 75 cm), equilibrated with a running buffer of 20 mM sodium phosphate, pH 6.8, with a flow rate of 1.5 mL/min.
12. 3 mL fractions are collected (OD monitored at 280 nm), and samples from each protein containing fraction are evaluated by reduced SDS-PAGE.
13. $F(ab')_2$ containing fractions are combined and concentrated using a Ultra-15 centrifuge filter.
14. Protein concentration is confirmed by BCA assay.
15. Purified $F(ab')_2$ is sterile filtered through a 0.22 µm syringe filter and aliquoted for storage at -80°C.
16. Purified $F(ab')_2$ is quality controlled by ELISA, HPLC (sizing column), and SDS-PAGE (reduced and nonreduced conditions).

3.2.2. Production of A6H Fab' Fragments from $F(ab')_2$ Fragments

For antibody $F(ab')_2$ fragments that have not previously been cleaved to Fab' fragments, initial studies using varying quantities of DTT and varying incuba-

tion times are evaluated using HPLC. The following conditions are used for A6H F(ab')₂.

1. 150 μ L of the A6H F(ab')₂ is aliquoted into a reaction vessel
2. To that solution is added 6 μ L of the DTT solution
3. The resultant solution is incubated at room temperature for 1 h.
4. The progress of reaction is followed by size exclusion HPLC.
5. Once complete by HPLC (i.e., 1 h), the reaction solution is placed on a Sephadex G-25 column (PD-10) and eluted with sodium phosphate, 1 mL fractions are collected.
6. The Fab' is collected in fractions 3 and 4. Those fractions are combined.
7. The concentration of Fab' is determined by UV at 280 nm (0.1% solution—estimated absorbance of 1.15)
8. Protein recovery is 95%.

3.3. Production of A6H Fab'-S-Biotin

1. Biotin-maleimide can be purchased (e.g., biotin-BMCC, Pierce; or biotin-maleimide, Sigma) or a custom derivative can be prepared (3).
2. A 1.8 mL of a 0.9 mg/mL solution of A6H Fab is aliquoted into a reaction vial.
3. To that vial is added 50 equivalents of the biotin-maleimide in 100 μ L of 20 mM sodium phosphate, pH 6.8. (See Note 1.)
4. The reaction is allowed to run for 30 min.
5. The reaction mixture is then placed in a Centricon-30 ultracentrifugation filter and centrifuged at 1750g for 15 min to concentrate to 100 μ L vol.
6. The filter retentate is rinsed 4 times with 500 μ L phosphate buffer each rinse.
7. The concentration of Fab'-S-biotin is estimated by UV absorbance at 280 nm.
8. Protein recovery is >90%.

3.3.1. Determination of Number of Biotin Molecules Conjugated to A6H Fab'

The number of biotin molecules on the Fab' is determined by measuring the decrease in absorbance at 500 nm for a solution containing avidin and HABA after the biotinylated Fab' is added. The HABA method used is adapted from a Pierce biotinylation kit (#21430).

1. A 1-mL aliquot of avidin solution is placed in a vial.
2. To that solution is added 0.94 mL of PBS, then 60 μ L of 10 mM HABA in 10 mM NaOH.
3. The UV absorbance at 500 nm is measured for 900 μ L of the avidin/HABA solution
4. 100 μ L of the diluted Fab' is added
5. After 1 min, the absorbance is again measured.
6. The number of biotin molecules is determined from the equation: no. = (A/3400)/B, where A = [0.9((A₅₀₀ of HABA/avidin solution) – A₅₀₀ of HABA/avidin/Fab' solution)]; and B = sample molar concentration

3.4. Succinylation of Streptavidin

Succinylation of streptavidin is conducted to diminish the propensity of this protein to accumulate in kidneys (4).

1. A 185 μL quantity of a 5.4-mg/mL solution of recombinant streptavidin is aliquoted into a vial.
2. To the streptavidin solution is added 370 μL of 50 mM NaHCO_3 buffer, pH 8.5.
3. A 95- μg quantity of succinyl anhydride in 20 μL DMSO is added and the mixture is stirred for 30 min at room temperature.
4. The contents of the reaction vial are transferred to a Centricon-30 ultracentrifugation filter and concentrated to 50 μL .
5. The concentrated streptavidin is washed six times with 500 μL PBS, concentrating to 50 μL each time.
6. Protein recovery is 88%.
7. Recovered succinylated streptavidin is analyzed by immunoelectrophoresis (IEF) to make sure the pI is below 4.

3.5. Production of A6H Fab'-Streptavidin Conjugates

Preparation of A6H Fab'-streptavidin conjugates involves modification of native streptavidin to introduce maleimide groups and separate preparation of Fab'-SH for crosslinking. The reaction conditions outlined should be considered preliminary. Optimization of this experimental procedure is currently being conducted.

3.5.1. Production of A6H Fab'-SH

1. A quantity of A6H Fab' is prepared by DTT reduction as described in **Subheading 3.2.2., steps 1–8**.
2. Production of SMCC-modified streptavidin:
 - a. A 100- μL aliquot of 10-mg/mL streptavidin in PBS, pH 7.2 is placed in a vial (see **Note 2**).
 - b. To the vial is added 10 μL of a 10 mg/mL solution of SMCC in DMSO.
 - c. After 30 min, the reaction mixture is run over a PD-10 column that is pre-equilibrated with PBS, pH 6.0.
 - d. The protein fractions are combined (determine by UV).

3.5.2. Production of A6H Fab'-Streptavidin Conjugates

1. Approximately one-third of streptavidin-SMCC adduct is added to 2/3 of A6H Fab'-SH.
2. That mixture is placed in a Centricon-30 and concentrated to approx. 200 μL volume.
3. After 1 h, the reaction mixture is purified by size exclusion HPLC.
4. The mono-Fab'-streptavidin is separated from the DI-Fab'-streptavidin and any unreacted starting materials.
5. The desired mono-Fab'-streptavidin and/or di-Fab'-streptavidin are concentrated and stored in the refrigerator before use.

3.6. Radioiodination of A6H F(ab')₂, A6H Fab'-S-Biotin, A6H Fab'-Streptavidin, and Streptavidin

Similar radioiodination methods are used for the four proteins listed (*see Note 3*). A general radioiodination method is provided as follows:

1. All personnel must wear appropriate protective clothing as required to work with radioactive materials.
2. Cover work area with absorbent underpads.
3. A 0.5–2 μL aliquot of Na^{125}I or Na^{131}I in 0.1 *N* NaOH is added to 25 μL of sodium phosphate (0.5 *M*, pH 7.4) in a reaction vial.
4. To that vial is added the quantity of protein to label (0.050–1.0 mg) in 100–150 mL 0.5 *M* sodium phosphate, pH 7.4.
5. A 20–25 μL aliquot of a 1-mg/mL solution of chloramine-T in water.
6. The reaction is quenched after 5 min with an addition of 2–3 μL of a 10-mg/mL aqueous solution of sodium metabisulfite.
7. The radioiodinated protein is placed on a Sephadex G-25 column (NAP-10) and eluted with 0.9% saline.
8. The protein containing fractions (determined by UV) are combined.
9. The amount of radioactivity with the protein is determined in a dose calibrator.
10. The amount of protein present is determined by UV analysis at 280 nm.
11. The specific activity (mCi/mg) is determined by dividing the amount of radioactivity by the amount of protein.
12. The radiochemical purity is determined by instant thin layer chromatography (ITLC) (eluting 80% MeOH/H₂O), denatured protein at the origin and free radioiodide at the solvent front. Alternatively, the purity may be assessed by size exclusion HPLC.
13. The radiochemical yield is calculated based on amount of activity used in the labeling and the amount of radioactivity on the protein.
14. For antibody preparations, the immunoreactivity is determined as defined in **Subheading 3.8**.

3.7. Radioiodination of Biotin Derivatives

Biotin derivatives that can be radioiodinated have not been readily available from commercial sources, but they can be synthesized using literature procedures (5). An important aspect for *in vivo* application is incorporation of functional groups that block degradation by the enzyme biotinidase (6).

1. A 50- μL aliquot of a 1-mg/mL solution of the biotin derivative is added to a vial.
2. To that vial is added 1–5 μL of a Na^{125}I or Na^{131}I solution in 0.1 NaOH.
3. To that mixture is added 10 μL of a 1-mg/mL solution of *N*-chlorosuccinimide in methanol.
4. After 2 min, 10 μL of a 1-mg/mL solution of sodium metabisulfite solution is added to the reaction vial.
5. The reaction mixture is drawn into a syringe and injected onto an HPLC column for purification.

6. The radioiodinated biotin derivative is obtained from the HPLC effluent (retention time predetermined by a stable iodine standard).
7. The non-aqueous portion of the collected solvent mixture is removed under a stream of nitrogen (escaping gases pass through a charcoal-filled syringe).
8. Purity of the isolated radioiodinated biotin derivative is determined by reinjection on the HPLC.
9. The radioiodinated derivative is stored in the refrigerator until used. Studies of stability with time are performed by injection of aliquots onto the HPLC at various storage times.
10. The sample is sterile filtered prior to using for animal studies.

3.8. In Vitro Cell Immunoassay

1. Antigen positive RCC cells (growing in log phase) are shaken (not trypsinized) from tissue culture flasks—washed, resuspended in 1X PBS with 1% BSA, and counted.
2. A final cell suspension of 2×10^6 viable cells/mL is prepared and a 1-mL aliquot in duplicate is used for each determination.
3. Add $2\text{--}4 \times 10^5$ counts of radiolabeled immunoconjugate to each aliquot.
4. Cells are incubated for 1 h at room temperature on a test tube rotator.
5. Following incubation, total activity per aliquot is quantitated on a Wallac 1480 gamma counter.
6. Cell aliquots are pelleted by centrifugation (100g) for 10 min.
7. Supernatant is decanted and discarded; cells are resuspended in 1 mL of 1X PBS.
8. Cell aliquots are then recounted.
9. Retained counts are expressed as a percentage of total counts added. For example, immunoreactivities for radiolabeled whole mAb of less than 50% are not used.

3.9. Establishment of RCC Xenografts

RCC xenografts are serially passaged in Balb/C nu/nu male mice, 4–6 wk of age; RCC xenografts were previously established from fresh surgical specimens. All procedures described were done with the approval of the University of Washington's Institutional Animal Care and Use Committee (IACUC) and following NIH guidelines. Animals are housed in micro-isolator cages on suitable bedding, and are given a standard irradiated rodent chow and sterilized water *ad libitum*.

3.9.1. Tumor Bit Preparation

1. Dissect, using aseptic technique (*see Subheading 4.2.5.2., item 3*), RCC tumor from donor animal (xenograft should be approx $300\text{--}500\text{ mm}^3$ in size).
2. Place in small Petri dish with 5–10 mL of 1X PBS.
3. Cut tumor into bits of implantable size (approx 25 mm^3).
4. Suspend tumor bits in new Petri dish with 1X PBS containing Gentamycin (4 mg/mL) for at least 10 minutes prior to implantation.

3.9.2. Implantation Surgery

1. Animals to be implanted are restrained and injected ip, using a 3 cc syringe with a 26-gauge needle, with the anesthetic mix—70 mg ketamine/5.3 mg xylazine/kg body weight; approx 0.2–0.3 mL of anesthetic mix for an average size mouse (approx 20–25 g). Animals will be assessed for proper levels of anesthesia by stimulation of the leg reflex by lightly squeezing the foot. For any observed sensitivity or pain, additional anesthesia will be titrated accordingly.
2. Position anesthetized animal lying on its left side.
3. Prepare surgical site on animal:
 - a. Saturate 2 × 2 gauze with Betadine solution and scrub entire side of animal. Wait 2 min.
 - b. Wet 2 × 2 gauze with 70% isopropanol and wipe area once.
4. Using sterile tissue forceps and sterile scissors, make a 2.0-mm incision distal to the right shoulder blade.
5. Using the scissors, insert them closed into this opening and develop/tunnel a pocket between the skin and superficial fascia by opening the scissors slightly once or twice.
6. Using a second pair of sterile tissue forceps, place a previously prepared tumor bit into the pocket just created under skin.
7. Close the incision by retracting slightly with tissue forceps at base of the incision, clipping the skin incision with one 9 mm wound clip.
8. Place animal into a clean cage and monitor until fully recovered.
9. Remove 9 mm wound clip 7–14 d postsurgery.
10. Monitor animals daily for health, estimation of tumor volume, and for ulceration of tumors.

3.10. Isotopic Injection of RCC Xenografts

1. All personnel must wear appropriate protective clothing as required to work with radioactive materials.
2. Cover work area with absorbent underpads.
3. RCC xenografts for biodistribution studies are allowed to grow to approx 100–300 mm³. Growth to this volume usually takes from 4 to 6 wk postimplantation.
4. Animals (per study design) are placed upon biotin-free test diet 7 d prior to initial injection.
5. Study injectates are quantified and diluted to be delivered in an injection volume of approx 100 µL, but no greater than 200 µL/injection.
6. Each individual isotopic dose (only one dose per syringe) is loaded into a 0.5 cc, 28-gauge cemented needle insulin syringe.
7. Each loaded syringe is identified and weighed to 0.001 g accuracy.
8. Animals anesthetized as described in **Subheading 3.9.2., step 1**, randomized into the appropriate study/treatment groups.
9. Animals are permanently notched on the ear with a permanent animal number for identification.

10. Animals are injected intravenously with their isotopic dose via the lateral tail vein; following the injection, pressure is placed upon the injection site using 2×2 gauze for 30–45 s until bleeding stops.
11. Each empty syringe is identified and weighed to 0.001 g accuracy.
12. Animals are returned to clean cages and monitored until fully recovered.
13. The above procedure can be performed without using anesthesia by placing animals in an appropriate rodent restrainer that allows free access to the tail.
14. From each animal injectate preparation remove 1 μ L and add to 1 mL of water as an internal counting standard.

3.11. Biodistribution of Mice Bearing RCC Xenografts (see Note 4)

1. All personnel must wear appropriate protective clothing as required to work with radioactive materials.
2. Cover work area with absorbent underpads.
3. Anesthetize animals as described in **Subheading 3.9.2., step 1**.
4. Immediately prior to euthanasia, draw approx 0.5 mL of blood via cardiac puncture.
5. Kill animal using cervical dislocation or other IACUC-approved method.
6. Pin out animal, ventral side up, on dissecting board.
7. Incise ventral side of animal from anus to neck.
8. Tap urine (if present) using a 0.5-cc insulin syringe.
9. Dissect out tissues of interest in a logical step-wise fashion including, but not limited to: RCC tumor, muscle (quadriceps), intestine (approx 700 mg), liver, kidney, spleen, stomach, lung, neck (submaxilar tissue—to include thyroid), and the tail.
10. Blot each tissue as it is extracted to remove blood.
11. Place each tissue in a tared, appropriately labeled 12×75 mm test tube and weight to 0.001 g accuracy.
12. Post collection of all tissues—place approx 1 mL 10% neutral buffered formalin (NBF) in each tube to prevent putrefaction.
13. Count all tissues and internal counting standards on gamma Counter.
14. Using a biodistribution worksheet in a spreadsheet program—we calculate percent injected dose per gram of tissue, tissue-to-blood ratios, μ Ci/g, μ g injectate/gram, mg injectate/organ, and ratios of injectates where applicable.

3.12. Results

3.12.1. Historical Development of RCC Xenograft Models, Monoclonal Antibody A6H, and Biodistribution Efficacy

Our work on the targeting of RCC with radiolabeled Mabs began in the early 1980's. Much of this early work using direct labeling of mAbs with radionuclides of iodine has been published (7–9). Briefly, we developed a series of RCC reactive Mabs and tested these in biodistribution studies against a panel of RCC xenografts. The RCC xenografts in athymic (BALB/c nu/nu) mice had been established from subcutaneously implanted surgical specimens and are serially passaged. From these biodistribution efforts we selected one mAb, designated A6H (10) as the best for

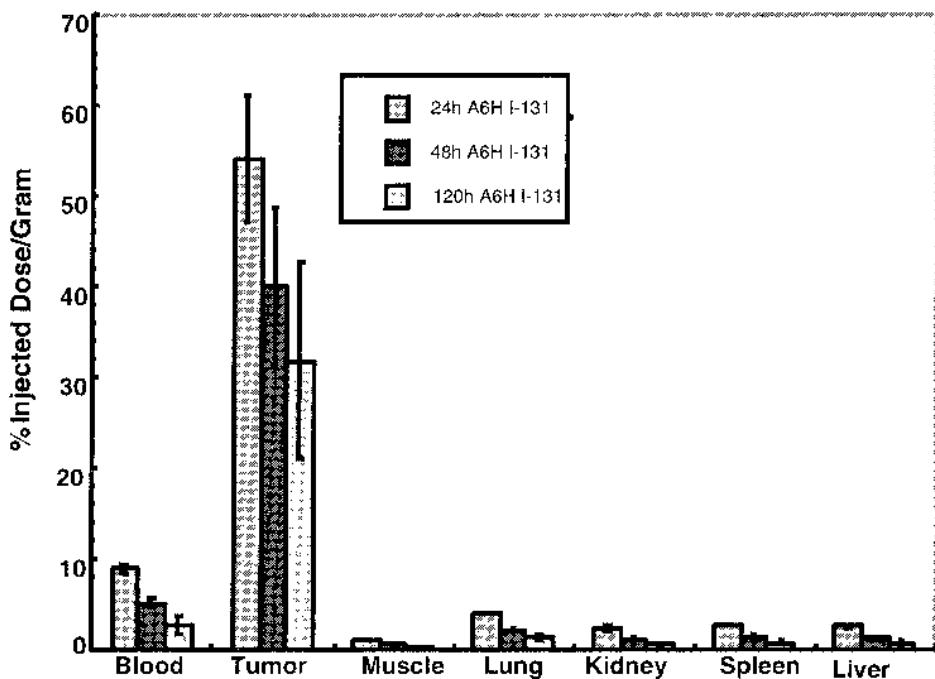


Fig. 1. A6H directly labeled with ^{131}I in athymic mice bearing TK-82 xenografts at 24, 48, and 120 h postinjection.

future studies of RCC targeting in the pre-clinical xenograft models and in clinical trials. A6H is an IgG₁ murine monoclonal that exhibits exceptionally good targeting of RCC. The best combination was A6H and the RCC xenograft designated TK-82, although A6H was able to target all of the RCC xenografts well. We were consistently able to target and detect, by radioimmunosciintigraphy, RCC xenografts of less than 30 mg implanted beneath the renal capsule. A recent example of the biodistribution of directly labeled A6H with ^{131}I in athymic mice bearing a subcutaneous TK-82 xenograft is shown in **Fig. 1**. These results demonstrated that directly labeled A6H targeted primary subcutaneous xenografts with high specificity and with a high percent injected dose per gram. Subsequently we demonstrated an ability to successfully treat subcutaneous xenografts with ^{131}I -labeled A6H (8,9,11–13).

3.12.2. Developing a More Attractive Targeting System for Metastatic Disease

Shortly thereafter we began a new research initiative aimed toward the targeting and treatment of metastatic RCC. In contrast to the earlier work, this

project was focused heavily towards treatment rather than imaging. This led us to consider the use of alpha-particle emitting radionuclides (14-17). Only two alpha-particle emitting radionuclides, At-211 ($t_{1/2} = 7.2$ h) and Bi-213 ($t_{1/2} = 46$ min) appeared to be reasonable candidates (18) for this application, and the half-life of Bi-213 was considered too short for practical use in future clinical trials.

3.12.3. Directly Labeled A6H F(ab')₂ As Precursor Study of Alpha-Particle-Emitting Radionuclide Labeling

Our interest in targeting RCC metastases with the alpha-particle emitting radionuclide At-211 led us to consider using directly labeled A6H and its fragments. Early studies had shown that astatine could not be labeled directly to antibodies, so it had to be attached to a small pendant group, *p*-astatobenzoate *N*-succinimidyl ester, also referred to as the PAB reagent (20), or its meta-substitution counterpart (21). Previous studies with At-211 labeled intact antibodies indicated that the blood clearance was too slow for its application. Therefore, we decide to begin the studies in RCC with PAB labeled A6H F(ab')₂. Prior to conducting studies with At-211, we prepared the F(ab')₂ labeling with the same reagent with a radionuclide of iodine attached. This labeling reagent, is referred to as the PIB reagent (22). The PIB labeled A6H F(ab')₂ was coinjected with the directly labeled (chloramine-T, I-131) A6H F(ab')₂ into athymic mice bearing TK-82 RCC xenografts, and their distributions were evaluated at 4, 24, and 48 h post injection. No significant difference was observed in any tissue except stomach and neck (thyroid) between the PIB-labeled F(ab')₂ and Chloramine-T labeled F(ab')₂. This gave us confidence that we should proceed with the At-211 studies.

The initial At-211 study conducted in RCC was co-injection of At-211 PAB labeled A6H F(ab')₂ with I-125 PIB labeled A6H F(ab')₂ to assess the biodistribution and to compare the stability of the At-211 label with the I-125 label (23). The results of At-211 labeled A6H F(ab')₂ distribution revealed that the blood levels were similar (at 4 and 19/24 h) but the tumor uptake was only half that observed in the previous radio-iodine studies. Even though the At-211 label was stable to degradation, the target-to-non-target tissue ratios were not as high as desired for treatment of RCC metastases.

We then investigated whether directly labeled A6H Fab' in the TK-82 RCC xenograft model would improve the tumor targeting and blood clearance characteristics over the F(ab')₂ fragments. A6H Fab' was labeled with another conjugation molecule, termed IPEM (iodophenethylmaleimide), which is reactive with sulfhydryl groups (24) and compared with coinjected Fab' that was labeled using the chloramine-T method. It was clear from the data obtained that the concentrations of radioactivity in lung and kidney at the early timepoints would not be acceptable. Furthermore, we also demonstrated that

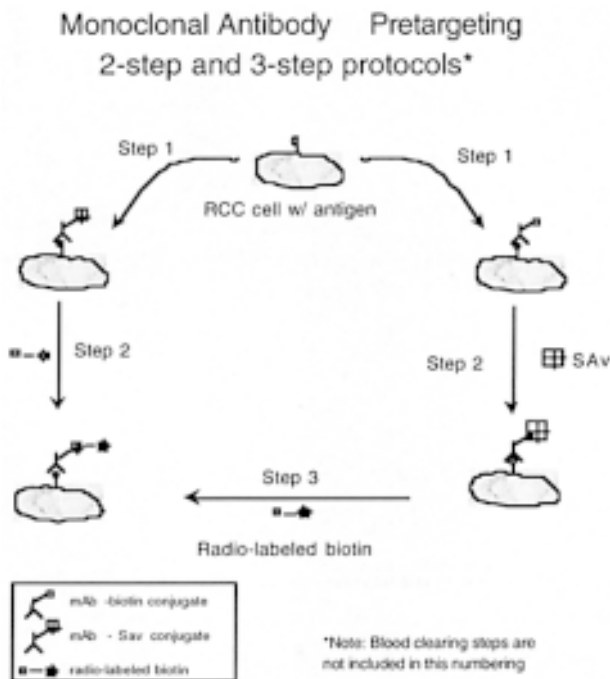


Fig. 2. Schematic of antibody-based pretargeting (two- and three-steps) protocols.

conjugation of the PAB-At-211 to Fab' fragments resulted in the release of At-211, which were problematic (25). Therefore, we looked for another approach that would allow rapid delivery of At-211 to metastatic RCC cells, but also cleared rapidly from blood and other tissues.

3.12.4. The Pretargeting Approach

The approach that we chose is termed pretargeting (26,27). In the pretargeting approach, we could use the very good tumor targeting of A6H but deliver the radionuclide on another molecule that had very different pharmacokinetics from that of the antibody. Two major advantages of this approach are that short half-lived radionuclides (such as At-211 and Bi-213) can be used, and large quantities of antibody can be administered so that a more homogeneous distribution within the tumor can be obtained. A schematic of the pretargeting approach is provided in **Fig. 2**. Note that there is the option of using a 2-step or a three-step approach (28).

The data obtained from the tumor targeting and tissue distribution of A6H Fab' suggested that we could use the Fab' as the targeting agent if the biotin was placed on the same sulfhydryl group(s) as the IPeM. To begin our pre-

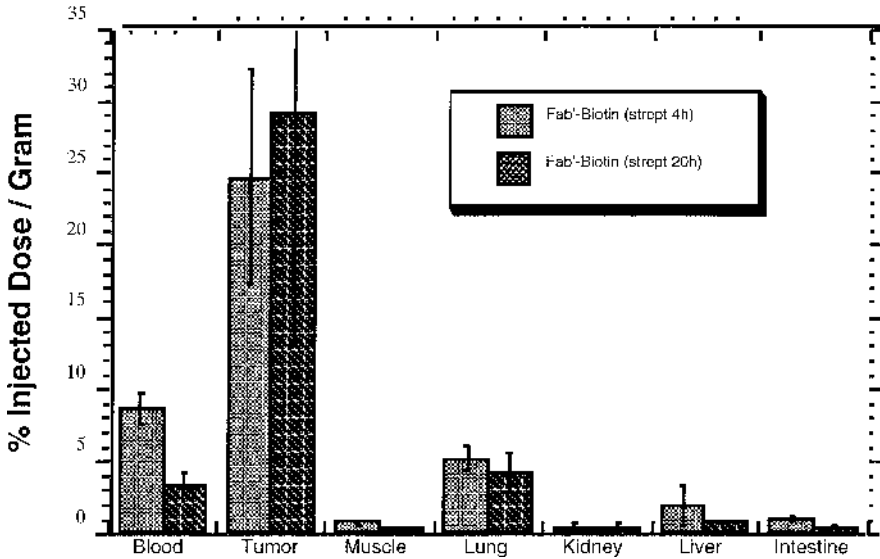


Fig. 3. Distribution of biotinylated A6H Fab' in athymic mice bearing TK-82 xenografts at 24 h postinjection with streptavidin administered 4 or 20 h post injection.

targeting studies, a biodistribution of biotinylated A6H Fab' was conducted and the results confirmed the good tumor targeting and rapid blood clearance (3). When the Fab' was chosen, our initial studies in pretargeting were focused on evaluation of the three-step approach as it was thought that this method would be the easiest to implement. In the three-step approach, A6H Fab'-biotin was injected, allowed to localize to tumor and cleared from nontarget tissues. Following this period of antibody clearance from nontargeted tissues, streptavidin was injected and allowed to localize to the biotinylated Fab' in the xenograft. However, it was unclear at what time point to inject the streptavidin. Therefore, a study was conducted where the streptavidin was injected at 4 or 20 h post injection of the biotinylated Fab'. As **Fig. 3** shows, good tumor targeting of the antibody was obtained with both approaches, but blood clearance was best if the streptavidin was administered 20 h after the antibody.

Another important, and limiting factor became apparent quite early in our studies. It was observed that good targeting of streptavidin to the biotinylated antibody in tumor xenografts was obtained only when the animals were placed on a biotin free diet (start 7 d prior to beginning of experiment). This is shown clearly in the results obtained for streptavidin shown in **Fig. 4**. Importantly, in this experiment and in all subsequent experiments, dual label studies have indicated that each biotinylated antibody localized in the tumor xenograft

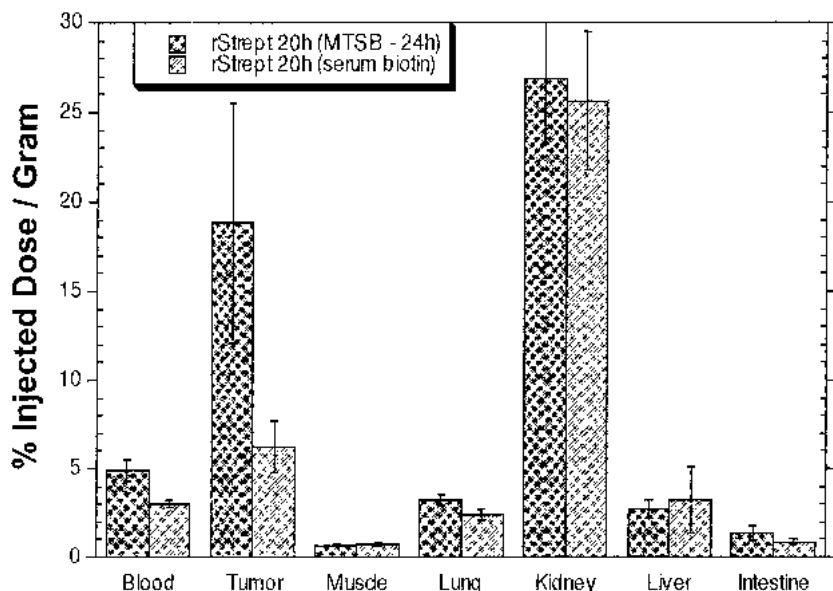


Fig. 4. Distribution of recombinant streptavidin in athymic mice bearing TK-82 xenografts at 24 h postinjection of biotinylated A6H Fab', with/without biotin-free diets.

has a streptavidin molecule associated with it when the mice are on biotin-free diets.

The data obtained in **Fig. 4** also pointed out the high concentration of streptavidin that localized in the kidney (29). We evaluated a number of streptavidin mutants and found that all of them localized to kidney. Data obtained by other investigators indicated that the kidney localization of streptavidin can result in uptake of radiolabeled biotin causing a higher dose to that organ. This fact combined with at least some of our data that supported the use of streptavidin as the carrier of radioactivity, prompted us to investigate methods to reduce or eliminate kidney localization. Indeed, we found that succinylation of streptavidin decreased the kidney localization in our pretargeting studies while retaining the tumor targeting (4). Bio-distribution data that support this hypothesis is shown in **Fig. 5** (note the tumor and kidney concentrations).

Presently studies of pretargeting RCC are focused on the development of A6H Fab'-streptavidin conjugates and new biotin derivatives for carrying the radionuclide (30). Chemical crosslinking of Fab' with modified streptavidin has yielded conjugates that contain one and two Fab' per streptavidin. These conjugates are easily purified by size exclusion HPLC and their *in vivo* distributions will be studied. These new compounds will be evaluated in the two step pretargeting protocols.

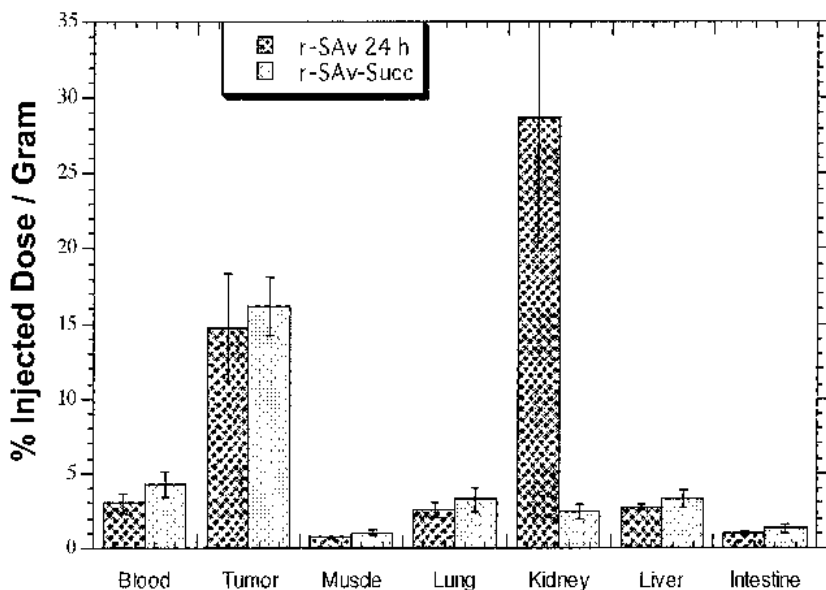


Fig. 5. Distribution of succinylated streptavidin vs streptavidin in athymic mice bearing TK-82 xenografts at 24 h postinjection of biotinylated A6H Fab'.

3.12.5. The Biotinidase Issue

Our studies to optimize the structure of radiolabeled biotin derivatives have demonstrated that they must be designed in a manner that blocks the cleavage of biotin by the serum enzyme, biotinidase (31,32). Other investigators, and we demonstrated that an *N*-methyl biotinamide functionality completely blocks the action of biotinidase (33). We have prepared and labeled new biotin derivatives containing the *N*-methyl group for labeling with I-131 and At-211 [unpublished results] and with radiometals such as In-111, Y-90 and Bi-213 (34). However, more recently we have found that the *N*-methyl moiety greatly increases the rate of dissociation of biotin derivatives from streptavidin (unpublished results). Continuing studies have provided data that suggests there are biotin derivatives that block biotinidase cleavage, but do not adversely affect the binding affinity of the biotin derivative with streptavidin. New biotin reagents are being prepared which can be radiolabeled with the alpha-emitting radionuclides At-211 and Bi-213. These compounds will be tested soon in the two and three-step pretargeting protocols. Once the reagents, the quantities to administer, and the timing of the administrations are optimized, we plan to investigate therapy of RCC with alpha-particle emitting radionuclides using the pretargeting method.

3.13. Conclusions

The ability to specifically target tumors with mAbs has considerable appeal and is theoretically within the realms of our biotechnology skills of today. These antibodies can be molecularly “tuned” to be of cytotoxic nature themselves or cytotoxic upon interaction with monocytes utilizing the antibody-dependent cellular cytotoxicity pathway. Alternatively, these mAbs can be conjugated to cytotoxic drugs or as illustrated herein, to radionuclides. We find the radionuclide approach to be highly attractive because it can be customized to allow eradication of neighboring tumor cells in macroscopic masses or optimized for micrometastases using alpha-particle emitting radioisotopes.

For effective therapy of micrometastases, the entire radioimmunotherapy system needs to be designed for optimal delivery of the radionuclide to the tumor with minimal exposure of normal cells to the radiation. We have provided herein a stepwise progression of our efforts to design the best method of antibody and alpha-particle emitting radionuclide delivery—beginning with the first generation of directly labeled antibody to that of antibody fragments and most recently evaluating the two- and three- step pretargeting approach. Since we are strong believers that short-lived alpha-particles are the ideal manner in which to eliminate micrometastatic disease the two- and three-step delivery approaches are much more attractive than direct labeling because of the long biological half-lives of antibodies.

Having settled upon either the two- or three-step approach for delivery of the alpha-particle emitting radiotherapy, the choice of which radionuclide to select for use was made more difficult because of limited material for study. Although a few alpha-particle emitting radionuclides are currently available (e.g., Bi-212, Bi-213) their physical properties are not ideally suited for tumor targeting in our opinion due to their very short half-life (60.6 and 45.6 min, respectively). Obviously, the choice of radionuclide depends upon its physical properties as well as on its potential availability in sufficient amounts for clinical use. With these considerations in mind, one of the most attractive alpha-particle emitting radionuclides is astatine-211 ($t_{1/2} = 7.2$ h), which can be produced on a cyclotron with an alpha-particle beam irradiation of bismuth metal. Our efforts over the past couple of years have been directed toward the eventual use of At-211 in a two- or three-step targeting approach and, as mentioned, the cyclotron at the University of Washington is being upgraded to produce clinical level quantities.

In summary, the field of antibody based radioimmunotherapy is undergoing a serious second look after near abandonment a decade ago. One of the most serious limitations of the initial series of studies—that of a human anti-mouse antibody response—can be nearly eliminated with new advances in

molecular engineering. Novel methods of delivery, such as those described herein, can result in theoretically sufficient levels of radionuclides at the tumor site to provide a high therapeutic index. This is especially promising when one calculates the lethality of alpha-emitting radionuclides. As such, efforts are underway at a number of centers to produce research and clinical levels of these alpha-emitting radionuclides for study. These combined advances have taken more than 15 years to materialize but the promise of being able to eliminate micrometastatic disease by radioimmunotherapy is more real today than at any time in the past. We continue to believe that micrometastatic RCC is ideally suited biologically and clinically for radioimmunotherapy trials.

4. Notes

1. Biotinylation of A6H Fab'. It should be noted that addition of biotin moieties to antibodies can diminish or even completely eliminate the antibody's ability to bind with its antigen. Therefore, prior to conducting in vivo evaluations of biotinylated antibodies, it is imperative that varying levels of biotinylation be conducted on the antibody and (after radiolabeling), the immunoreactivity for each biotinylated antibody prep should be checked. This process will provide information on the optimal loading of biotin on the antibody being used, and what the ratio of reagents should be to obtain that loading.
2. Preparation of A6H Fab'-streptavidin conjugates. It should be noted it is important that the pH used when conjugating SMCC to streptavidin remain near neutral (pH 7–7.2) otherwise conjugation with the lysine amines can give too many SMCC conjugates, and lysine amines may react with conjugated maleimides. Both situations can result in aggregation (crosslinking) of the streptavidin.
3. Radioiodinated biotin derivatives. We have found that the highest yields of radioiodinated biotin derivatives are obtained when the stannylbenzoate derivative of biotin is purified by HPLC just prior to the radioiodination step.
4. Biodistribution. There are four general problems that can arise in the process of performing biodistribution studies: (a) insufficient numbers of animals bearing adequate size xenografts for analysis, (b) considerable size variation of xenografts, (c) antibody conjugates failing the cell immunoassay, and (d) injectates aggregating or sticking to the injection syringe.
 - a. The problem in item 1 can be addressed by adequate characterization of the human xenograft line of interest. Take-rates (percent of animals that have positive tumor growth) must be considered when planning a study. The first important point is to set up adequate numbers based upon the historic positive take-rate of the line. If more than the anticipated numbers of animals show tumor growth, they can subsequently be added to the study, either by adding them to the existing study groups thereby increasing the N , adding an extra timepoint, or by having an alternative treatment group of interest planned. In the case of serially passaged xenografts, we most often divert extra animals to

the maintenance of the xenograft line. You can also employ methods that can help raise the take rate. For example, coating the tumor bit with Matrigel (a liquid collagen extract that solidifies at body temperature [Collaborative Bio-medical Products, Bedford, MA]) or suspending the cells for injection in Matrigel can raise the positive take-rate of the xenografts.

- b. Another common problem arises when the tumors show considerable size variation at the time planned for immunoconjugate injection. This problem can often be overcome by implanting smaller tumor bits or lower cell numbers—this will increase the time from implantation to injection of the immunoconjugate, but will often result in the xenografts being more uniform in size, hence better data due to smaller variances.
- c. Sometimes, prior to injection, the immunoconjugate preparation will have poor cell immuno-reactivity results. Antigen expression is often cell cycle dependent. It is important to test the cell line to be used for the cell-binding studies for this possible variable prior to engaging in biodistribution studies. In addition, adequate radiolabeled controls, even though they may not be injected, will help interpret results. Keep in mind that intact, whole mAbs generally have greater immunoreactivities than antibody fragments. If using antibody fragments, a control comparison to the immunoreactivity of the intact mAb may help determine if the preparation is suitable for injection. Likewise, use of a non-antigen producing cell line is recommended as another control since it will help determine if you are experiencing high non-specific cell binding. Of course, poor cell binding is most likely due to damage during preparation or radiolabeling of the immunoconjugate. It is our practice to have additional reagents on hand so a repeat radiolabeling can be performed the same day in case an immunoconjugate does not pass the cell binding-quality control.
- d. Many radioimmunoconjugates, when prepared for injection can form aggregates or stick to the sides of the injection syringe. To determine if the preparation has stuck to the injection syringe, we always will test load a syringe, measure the activity in a radiodosimeter, and subsequently expel the injectate and remeasure the empty syringe—retention of high activity indicates a problem. This is usually due to inadequate protein levels in the buffer and can often be overcome by the addition of a carrier protein such as BSA following the labeling reaction.

Acknowledgments

The authors thank Donald K Hamlin and Janna Quinn for their excellent technical assistance. These studies were funded by the Department of Veteran's Affairs and the Department of Energy, Medical Applications and Biophysical Research Division, Office of Health and Environmental Research, under grants DE-FGO[^]-95-ER62029 and DE-FG)#-98ER62572.

References

1. Mulders, P., Figlin, R., DeKernion, J. B., Wilttrout, R., Linehan, M., Parkinson, D., DeWolf, W., and Belldgrun, A. (1997) Renal cell carcinoma: recent progress and future directions. *Cancer Res.* **57**, 5189–5195.
2. DeKernion, J. B. (1997) Renal tumors, in *Campbell's Urology* (Walsh, P. C., Gittes, R. F., Perlmutter, A. D., et al., eds.), Saunders Press, Philadelphia, pp. 1294–1342.
3. Wilbur, D. S., Hamlin, D. K., Vessella, R. L., Stray, J. E., Buhler, K. R., Stayton, P. S., Klumb, L. A., Pathare, P. M., and Weerawarna, S. A. (1996) Antibody fragments in tumor pretargeting. Evaluation of biotinylated fab' colocalization with recombinant streptavidin and avidin. *Bioconjug. Chem.* **7**, 689–702.
4. Wilbur, D. S., Hamlin, D. K., Buhler, K. R., Pathare, P. M., Vessella, R. L., Stayton, P. S., and To, R. (1998) Streptavidin in antibody pretargeting. 2. Evaluation of methods for decreasing localization of streptavidin to kidney while retaining its tumor binding capacity. *Bioconjug. Chem.* **9**, 322–330.
5. Wilbur, D. S., Hamlin, D. K., Pathare, P. M., and Weerawarna, S. A. (1997) Biotin reagents for antibody pretargeting. Synthesis, radioiodination, and in vitro evaluation of water soluble, biotinidase resistant biotin derivatives. *Bioconjug. Chem.* **8**, 572–584.
6. Hymes, J., Fleischhauer, K., and Wolf, B. (1997) Biotinidase in serum and tissues. *Methods Enzymol.* **279**, 422–434.
7. Chiou, R. K., Vessella, R. L., Elson, M. K., Clayman, R. V., Gonzalez-Campoy, J., Klicka, M. J., Shafer, R. B., and Lange, P. H. (1985) Localization of human renal cell carcinoma xenografts with a tumor-preferential monoclonal antibody. *Cancer Res.* **45**, 6140–6146.
8. Vessella, R. L., Alvarez, V., Chiou, R. K., Rodwell, J., Elson, M. K., Palme, D. F., Shafer, R. B., and Lange, P. H. (1987) Radioimmunoscinigraphy and radioimmunotherapy of renal cell carcinoma xenografts. *Natl. Cancer Inst. Monogr.* **3**, 159–167.
9. Vessella, R. L., Lange, P. H., Palme, D. F., Chiou, R. K., Elson, M. K., and Wessels, B. W. (1988) Radioiodinated monoclonal antibodies in the imaging and treatment of human renal cell carcinoma xenografts in nude mice. *Targeted Diagn. Ther.* **1**, 245–282.
10. Vessella, R. L., Moon, T. D., Chiou, R. K., Nowak, J. A., Arfman, E. W., Palme, D. F., Peterson, G. A., and Lange, P. H. (1985) Monoclonal antibodies to human renal cell carcinoma: recognition of shared and restricted tissue antigens. *Cancer Res.* **45**, 6131–6139.
11. Wessels, B. W., Vessella, R. L., Palme, D. F., Berkopec, J. M., Smith, G. K., and Bradley, E. W. (1989) Radiobiological comparison of external beam irradiation and radioimmunotherapy in renal cell carcinoma xenografts. *Int. J. Radiat. Oncol. Biol. Phys.* **17**, 1257–1263.
12. Palme, D. F., Berkopec, J. M., Elson, M. K., Wessels, B. W., Lange, P. H., and Vessella, R. L. (1991) Dosimetry and pharmacokinetics of monoclonal antibody A6H with human renal cell carcinoma xenografts: single dose study. *Int. J. Rad. Appl. Instrum. [B]* **18**, 527–537.

13. Vessella, R. L. (1991) Radioimmunoconjugates in renal cell carcinoma, in *Immunotherapy of Renal Cell Carcinoma* (Debruyne, F. M. J., Bukowski, R. M., Pontes, J. E., and de Mulder, P. H. M., eds.), Springer-Verlag, Heidelberg, pp. 38–46.
14. Bloomer, W. D., McLaughlin, W. H., Adelstein, S. J., and Wolf, A. P. (1984) Therapeutic applications of auger and alpha emitting radionuclides. *Strahlentherapie* **160**, 755–757.
15. Macklis, R. M., Kinsey, B. M., Kassis, A. I., Ferrara, J. L. M., Atcher, R. W., Hines, J. J., Coleman, C. N., Adelstein, S. J., and Burakoff, S. J. (1988) Radioimmunotherapy with alpha-particle-emitting immunoconjugates. *Science* **240**, 1024–1026.
16. Wilbur, D. S. (1991) Potential use of alpha emitting radionuclides in the treatment of cancer. *Antibody Immunoconjug. Radiopharm.* **4**, 85–97.
17. Zalutsky, M. R. and Bigner, D. D. Radioimmunotherapy with a-particle emitting radioimmunoconjugates. *Acta Oncol.* **35**, 373–379.
18. Feinendegen, L. E. and McCombie, R. (1997) Alphasemitters for medical therapy—workshop of the United States Department of Energy. *Radiat. Res.* **148**, 195–201.
19. Visser, G. W. M., Diemer, E. L., and Kaspersen, F. M. (1981) The nature of the astatine-protein bond. *Int. J. Appl. Rad. Isot.* **32**, 905–912.
20. Wilbur, D. S., Hyalarides, M. D., and Fritzberg, A. R. (1989) Reactions of Organometallic Compounds with Astatine-211. Application of protein labeling. *Radiochim. Acta* **47**, 137–142.
21. Zalutsky, M. R. and Narula, A. S. (1988) Astatination of proteins using an N-succinimidyl Tri-n-butylastannyl benzoate intermediate. *Appl. Radiat. Isot.* **39**, 227–232.
22. Wilbur, D. S., Hadley, S. W., Hyalarides, M. D., Abrams, P. G., Beaumier, P. A., Morgan, A. C., Reno, J. M., and Fritzberg, A. R. (1989) Development of a Stable Radioiodinating Reagent to Label Monoclonal Antibodies for Radiotherapy of Cancer. *J. Nucl. Med.* **30**, 216–226.
23. Wilbur, D. S., Vessella, R. L., Stray, J. E., Goffe, D. K., Blouke, K. A., and Atcher, R. W. (1993) Preparation and evaluation of PARA-[²¹¹At]Astatobenzoyl labeled antirenal cell carcinoma antibody A6H F(ab')₂. In vivo distribution comparison with PARA-[¹²⁵I]Iodobenzoyl labeled A6H F(ab')₂. *Int. J. Radiat. Appl. Instrum. [B]* **20**, 917–927.
24. Hyalarides, M. D., Wilbur, D. S., Reed, M. W., Hadley, S. W., Schroeder, J. R., and Grant, L. M. (1991) Preparation and in vivo evaluation of an N-(p-[¹²⁵I]iodophenethyl)maleimide-antibody conjugate. *Bioconjug. Chem.* **2**, 435–440.
25. Hadley, S. W., Wilbur, D. S., Gray, M. A., and Atcher, R. W. Astatine-211 labeling of an antimelanoma antibody and its Fab fragment using N-succinimidyl p-[²¹¹At]astatobenzoate: comparisons in vivo with the p-[¹²⁵I]iodobenzoyl conjugate. *Bioconjug. Chem.* **2**, 171–179.
26. Hnatowich, D. J., Virzi, F., and Rusckowski, M. (1987) Investigations of avidin and biotin for imaging applications. *J. Nucl. Med.* **28**, 1294–1302.
27. Paganelli, G., Pervez, S., Siccardi, A. G., Rowlinson, G., Deleide, G., Chiolerio, F., Malcovati, M., Scassellati, G. A., and Epenetos, A. A. (1990) Intraperitoneal

- radio-localization of tumors pre-targeted by biotinylated monoclonal antibodies. *Int. J. Cancer* **45**, 1184–1189.
28. Paganelli, G., Malcovati, M., and Fazio, F. (1991) Monoclonal antibody pre-targeting techniques for tumour localization; the avidin-biotin system. International workshop on techniques for the avidin-biotin system. International Workshop on Techniques for Amplification of Tumour Targeting. *Nucl. Med. Commun.* **9**, 211–234.
 29. Wilbur, D. S., Stayton, P. S., To, R., Buhler, K. R., Klumb, L. A., Hamlin, D. K., Stray, J. E., and Vessella, R. L. (1998) Streptavidin in antibody pretargeting. Comparison of a recombinant streptavidin with two streptavidin mutant proteins and two commercially available streptavidin proteins. *Bioconjug. Chem.* **9**, 100–107.
 30. Wilbur, D. S., Pathare, P. M., Hamlin, D. K., Stayton, P. S., To, R., Klumb, L. A., Buhler, K. R., and Vessella, R. L. (1999) Development of new biotin/streptavidin reagents for pretargeting. *Biomol. Eng.* **16**, 113–118.
 31. Hymes, J. and Wolf, B. (1996) Biotinidase and its roles in biotin metabolism. *Clin. Chim. Acta* **255**, 1–11.
 32. Pispa, J. (1965) Animal biotinidase. *Ann. Med. Exp. Biol. Fenn. (Suppl. 5)* **43**, 1–39.
 33. Wilbur, D. S., Pathare, P. M., Hamlin, D. K., Buhler, K. R., and Vessella, R. L. (1998) Biotin reagents for antibody pretargeting. 3. Synthesis, radioiodination, and evaluation of biotinylated starburst dendrimers. *Bioconjug. Chem.* **9**, 813–825.
 34. Pathare, P. M., Hamlin, D. K., Wilbur, D. S., Brechbiel, M. W., and Bray, L. A. (1998) Synthesis and radiolabeling of a biotin-CHX-B chelate for Bi-213. *J. Labelled Comput. Radiopharm.* **41**, 595–603.

Orthotopic Model of Renal Cell Carcinoma

David M. Nanus and Dov Engelstein

1. Introduction

1.1. Renal Cancer Cell Lines

A human renal cancer was first established in continuous culture in 1962. Currently, there are well over 100 different characterized renal cancer cell lines derived from both primary and metastatic renal cell carcinomas (RCCs) (1–3). The biological phenotype of cultured renal cancer cells typically includes a sustained and essentially unlimited growth capacity, a lack of contact inhibition and anchorage dependence, a capacity to form tumors in athymic mice, and an aneuploid karyotype including nonrandom chromosomal abnormalities (1,2). The antigenic phenotype of RCCs as determined by monoclonal antibodies (mAbs) generated against cell-surface glycoproteins, glycolipids, and blood-group antigens of renal cancers provide a series of phenotypic markers which characterize these tumors (4–6). Many of these mAbs also react with the proximal tubule portion of the human nephron, confirming earlier studies indicating that >90% of renal cancers derive from epithelial cells of the proximal tubule (7,8). While established RCC cell lines have frequently been analyzed for molecular defects, their greatest utility has been to screen combinations of chemotherapeutic and biologic agents for antiproliferative activity (9–12). Short-term cultures of renal cancer cells derived from fresh tumor specimens have similarly been used to screen drugs (13), but inhibitory effects in vitro have not been shown to predict a response in vivo (i.e., in human patients).

1.2. Renal Cancer Tumor Models

An ideal renal-tumor model should arise spontaneously, and should have the histological characteristics of an adenocarcinoma, a predictable growth rate,

the capacity to metastasize, and the ability to grow and metastasize without hormonal dependence—as is the case in the majority of human renal cancers. Models, that fit many of these criteria are available for study such as the murine renal adenocarcinoma system (RENCA) or the Eker rat (14). The advantage of these models is the ability to study the antitumor effect of biologic therapies that rely on the immune system to induce tumor regression (15,16). A major disadvantage is that these strains often require experience for use, and they will not measure the effects of antitumor agents that directly inhibit cell growth and tumorigenicity of human renal carcinoma cells.

1.3. Renal Cancer Xenograft Models

Renal cancer xenografts in athymic mice, in which the tumor cells are injected into the flank of the animal, have frequently been used to determine drug sensitivities and their potential for clinical applicability (11,17,18). Systemic drug administration is typically done intraperitoneally, and such studies are designed to simulate systemic administration of drug to treat a renal tumor in human patients. However, this model is not representative of the human disease, since renal cancer cells rarely metastasize to the skin, and renal cancer cells injected into the flank of athymic mice do not metastasize to other organs. Fidler and colleagues noted that renal cancer cells implanted into murine organs other than the kidney do not metastasize (19,20), and subsequently developed a model of orthotopic injection of renal cancer cells directly into a renal subcapsule (21). In this model, renal cancer metastases that possessed greater metastatic potential (22) and a greater invasive potential (23) than the parental cells were isolated. Others—including our laboratory have also developed similar orthotopic models of renal cancer using established human renal cancer cell lines.

The orthotopic model of human renal cancer is often used to assess the antitumor effect of systemically administered antitumor agents, or to assess growth-inhibitory effects and antimetastatic activity of various cytokines in vivo or by overexpression of a specific gene in renal cancer cells (24). Technological advances in the delivery of genes into mammalian cells have facilitated studies into the feasibility of introducing cytokine genes into human tumor cells as a form of antitumor therapy (25). The fact that immunologic therapies can induce tumor regression in advanced RCC has made RCC an attractive model in which to explore the effects of gene transfer. Genes that express interleukin-2, interferon α , and interferon γ have been successfully introduced into RCC cell lines (26,27). Local tumor formation following sc injection into athymic mice of tumor cells expressing these cytokines is significantly inhibited (26,27). Cytokine genes have also been introduced into cultured tumor cells derived from primary nephrectomy specimens (28).

One limitation with this model— as compared to a xenograft tumor in the flank of the animal which can easily be monitored— is the need to sacrifice the animal in order to assess tumor formation or tumor size of cells implanted into the kidney. Newer imaging techniques now make it possible to image an orthotopically implanted renal tumor in small animals, such as a athymic mice, without sacrificing the animal. We have used MRI to image a renal tumor growing in a mouse. As illustrated in **Fig. 1**, the tumor implanted into the kidney can easily be imaged 4 wk after implantation. Animals can be imaged serially to assess time to tumor formation, or following therapy, to accurately determine the antitumor effect of a systemically administered drug.

2. Materials

2.1. Renal Cancer Cells and Preparation

1. Renal cancer cells from an established cell line in the logarithmic phase of cell growth (70–80% confluent flasks).
2. Trypsin.
3. Minimal essential media (MEM) with 10% fetal calf serum (FCS).
4. MEM without FCS (serum-free media).

2.2. Anesthesia

1. 4–6-wk-old Swiss *nu/nu* mice.
2. Parasympatholytic agent (e.g., atropine 0.05 mg/kg body wt).
3. General anesthetic solution (e.g., tribromoethanol (Avertin), pentobarbital sodium or ketamine + xylazine).
4. Analgesic (e.g., butorphanol).
5. 1-cc syringe with 27-gauge needle.

2.3. Surgical Supplies

1. Suture materials (e.g., chromic catgut or vycril).
2. Surgical scissors, forceps, and scalpel.
3. Alcohol wipes or Betadine swabs.
4. Disinfectant solutions (e.g., sodium hypochlorite or quaternary ammonium compound + gentaraldehyde).
5. 9-mm autoclip wound applier and 9-mm MiKon autoclips, stainless-steel.
6. 10% buffered formalin solution.

3. Methods

3.1. Cell Preparation

1. Trypsinize cultured cells, spin, and wash twice with MEM without FCS.
2. Prepare the desirable concentration(s) of cells for subcapsular injection, e.g., 2×10^6 cells/ 0.1 mL MEM; 2×10^6 cells/ 0.2 mL serum-free media.



Fig. 1. Magnetic resonance imaging of mouse orthotopically implanted with renal cancer cells. The image is a coronal view of a mouse obtained on a 4.7T imaging system. The slice thickness is 1 mm and the in-plane resolution of 150×300 U. The image shows a normal kidney on the right side and a kidney implanted with renal cancer cells on the left side 4 wk after implantation. Note that tumor replaces kidney and extends outside of renal capsule.

3. Cells are kept in a 15-mL centrifuge tube. Keep cells at room temperature, or place cell suspension on ice until further use.
4. Prior to injecting the cells into the animal, gently resuspend the cells in the media and transfer to the 1-cc syringe.

3.2. Anesthesia

1. Weigh animals as injectable agents are administered on a per body-wt basis.
2. Inject parasympatholytic agent (e.g., atropine 0.05 mg/kg body wt) subcutaneously 15–30 min prior to general anesthesia.
3. Inject general anesthetic (*see Note 4* for recommendations).
4. Monitor animal for depth of anesthesia. When anesthesia is obtained (usually within 3–5 min), proceed with surgery.

3.3. Animal Surgery

1. Place the animal supine on its stomach, exposing the back for bilateral renal approach, or in a lateral position for a unilateral renal approach.

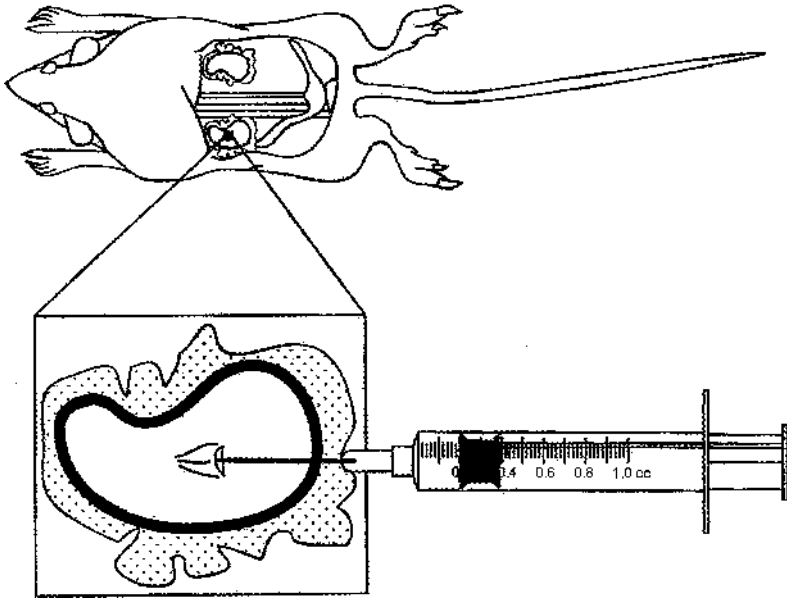


Fig. 2. Orthotopic injection of renal cancer cells into mouse kidney. Diagram of surgically exposed kidney (bilateral approach) with injection beneath kidney capsule in mid-kidney.

2. Scrub the back and flank with alcohol or betadine swab. Repeat two or three times.
3. Use scalpel to incise the skin longitudinally for about 1.5 cm, either in the midline (for bilateral renal approach) or paravertebrally (for unilateral renal approach). Carefully separate muscular layers by blunt and sharp dissection. Expose the kidney and clear perirenal fat off the injection site, typically the lower pole (*see Fig. 2*).
4. Using the 1-cc syringe containing the cell suspension, carefully insert the 27-gauge needle just below the renal capsule and advance it cranially 2–3 mm. Inject the well-suspended tumor cells.
5. Place a cotton-tipped applicator over the injection site for approx 1 min to prevent spillage of tumor cells. Lack of significant bleeding or extrarenal leakage are criteria for a successful injection.
6. Suture the muscular layers using chromic catgut or vycril. Approximate the skin wound and close using 9-mm autoclip wound applier with three or four steel autoclips.
7. Monitor recovery of animals from anesthesia until they are fully awake and ambulatory.

3.4. Postoperative Care

1. Animals are returned to their cages when they recover postoperatively.
2. Animals should be observed 4–6 h postoperatively and daily for at least 2–3 d.

3. The use of analgesics should be considered if animals exhibit signs of pain such as decreased ambulation or decreased oral intake. An analgesic such as butorphanol (1–5 mg/kg body wt, subcutaneously every 4 h) may be administered until the animal recovers.

3.5. Animal Sacrifice

1. Mice to be sacrificed are treated by overdosage of pentobarbital sodium (e.g., at an ip dosage >100 mg/kg body wt) or CO₂ inhalation in a closed cage.
2. Injected mice may be sacrificed according to the specific study plan (e.g., at 2, 3, and 4 wk following injection of cells).
3. The kidney containing the tumor is removed, measured, weighed, and placed in 10% buffered formalin solution. The contralateral uninjected kidney is similarly analyzed for comparison.
4. Liver or mesenteric mass are also measured, weighed and fixed in 10% buffered formalin solution.
5. Histologic analysis of representative tumors should confirm the presence of carcinoma.

4. Notes

1. Immortal renal cancer cell lines are used. These cell lines can be established by researchers through culturing of renal cancer cells obtained from nephrectomy specimens under sterile conditions as previously described (2,29). Approximately 10% of cultured tumors will result in an immortal cell line. Alternatively, an established cell line can be obtained from the American Type Culture Collection (ATCC) or other investigators.
2. Cells should be prepared using sterile techniques as close to the time of surgery as possible to minimize cell death. Place cells in 1–2 mL of trypsin for the shortest time necessary for the cells to dissociate, and immediately add a small amount of MEM containing 10% FCS to inactivate the trypsin. Following initial centrifugation (140g for 5 min), the trypsin is discarded and the cells are gently suspended in MEM without FCS. It is important to gently pipet up and down repeatedly in order to obtain a single-cell suspension and to decrease cell clumping. Cells are again centrifuged and resuspended in MEM at a fixed vol (usually 10 mL). Cell number is determined, and the number of cells necessary for $n + 2$ injections is placed in a new 15-mL sterile plastic tube and centrifuged. The supernatant is discarded, and the cell pellet is resuspended in the correct volume for the planned experiment. Cells may be kept at room temperature, or on ice for transport to the animal facility. Prior to administration, cells are transferred to the 1-cc syringe.
3. Four-to-six-wk-old Swiss female *nu/nu* mice are the preferred animals. Males can also be used. The number of animals needed will depend on the experimental design. Typically, 10 animals are used per treatment arm in order to attain statistically valid results. This will take into consideration variability in tumor growth and potential death of one or two animals from other causes such as infection.

4. Small differences in body wt may reflect a large difference in the amount of drug administered. Anesthetic agents are always given “to effect.” This term indicates that sufficient anesthetic has been administered to achieve the depth of anesthesia appropriate for the surgical procedure to be conducted. Reflexes—including toe or ear pinch—should be obtunded prior to beginning of the procedure. The depth of anesthesia must be monitored frequently (approx every 5–10 min) using appropriate methods during the procedure or experiment.

There are several ways to achieve effective general anesthesia in mice. An ip injection is the recommended route for administration of the anesthetic solution. Commonly used anesthetics include pentobarbital sodium 40–60 mg/kg body wt, ketamine 85–100 mg/kg + xylazine 3–10 mg/kg body wt, and 2.5% tribromoethanol (Avertin) at a conc. of 0.01 mL of stock solution per g body wt at the dose of 0.015–0.016 mL/kg body wt (typically 0.5 mL/mouse, approx 33 g body wt). The choice of anesthetic will depend on the recommendation of the animal facility of each institution.

5. Athymic mice are maintained in a sterile environment. Major survival surgery is typically performed in a hood in the room where the mice are kept, or in a separate surgical suite. Although specialized surgical facilities are not required, the importance of utilizing aseptic techniques should not be underestimated. This will reduce postsurgical complications (e.g., infections and wound dehiscence), improve animal survival rates, and accelerate return of basal physiological functions that were present in the animal prior to surgery. The area in which surgery will be done should be cleaned and disinfected with sodium hypochlorite solution (1:20 dilution of bleach in water) or 10% quaternary ammonium compound + 2.5% gentaraldehyde (1:100 dilution in water or alcohol). Surgical instruments should be sterilized, typically using an autoclave. Steel autoclips are removed approx 10 d following surgery.

Acknowledgments

The authors thank Dr. Ehud Lebel, Head, Committee of Animal Research, Rabin Medical Center (Beilinson Campus), Petach Tikva, Israel, and Dr. Naam Kriv, Head, laboratory and animal facilities, Sackler School of Medicine, Tel-Aviv University, Israel, for helpful comments, Dr. Jason Koutcher, Memorial Sloan-Kettering Cancer Center for **Fig. 1**, and Irena Soroker, Rabin Medical Center (Beilinson Campus), Petach Tikva, Israel, for **Fig. 2**.

References

1. Ebert, T. and Bander, N. H. (1989) Kidney-derived cell lines. *Semin. Urol.* **7**, 247–251.
2. Ebert, T., Bander, N. H., Finstad, C. L., Ramsawak, R. D. and Old, L. J. (1990) Establishment and characterization of human renal cancer and normal kidney cell lines. *Cancer Res.* **50**, 5531–5536.

3. Anglard, P., Trahan, E., Liu, Latif, F., Merino, M. J., Lerman, M. I., Zbar, B., and Linehan, W. M. (1992) Molecular and cellular characterization of human renal cell carcinoma cell lines. *Cancer Res.* **52**, 348–356.
4. Finstad, C. L., Cordon Cardo, C., Bander, N. H., Whitmore, W. F., Melamed, M. R., and Old, L. J. (1985) Specificity analysis of mouse monoclonal antibodies defining cell surface antigens of human renal cancer. *Proc. Natl. Acad. Sci. USA* **82**, 2955–2959.
5. Cordon Cardo, C., Reuter, V. E., Finstad, C. L., Sheinfeld, J., Lloyd, K. O., Fair, W. R., and Melamed, M. R. (1989) Blood group-related antigens in human kidney: modulation of Lewis determinants in renal cell carcinoma. *Cancer Res.* **49**, 212–218.
6. Vessella, R. L., Moon, T. D., Chiou, R. K., Nowak, J. A., Arfman, E. W., Palme, D. F., Peterson, G. A., and Lang, P. H. (1985) Monoclonal antibodies to human renal cell carcinoma: recognition of shared and restricted tissue antigens. *Cancer Res.* **45**, 6131–6139.
7. Bander, N. H., Cordon Cardo, C., Finstad, C. L., Whitmore, W. F. Jr., Vaughan, E. D. Jr., Oettgen, H. F., Melamed, M., and Old, L. J. (1985) Immunohistologic dissection of the human kidney using monoclonal antibodies. *J. Urol.* **133**, 502–505.
8. Cordon Cardo, C., Finstad, C. L., Bander, N. H., and Melamed, M. R. (1987) Immunoanatomic distribution of cytostructural and tissue-associated antigens in the human urinary tract. *Am. J. Pathol.* **126**, 269–284.
9. Lai, T., Ferro, M. A., Kaisary, A. V., Smith, P. J., and Symes, M. O. (1989) Testing the chemosensitivity of renal carcinoma in vitro. *Br. J. Urol.* **64**, 25–29.
10. Nygren, P. and Larsson, R. (1991) Differential in vitro sensitivity of human tumor and normal cells to chemotherapeutic agents and resistance modulators. *Int. J. Cancer* **48**, 598–604.
11. Nanus, D. M., Pfeffer, L. M., Bander, N. H., Bahri, S., and Albino, A. P. (1990) Antiproliferative and antitumor effects of alpha interferon in renal cell carcinomas: correlation with the expression of a kidney associated differentiation glycoprotein. *Cancer Res.* **50**, 4190–4194.
12. Safrit, J. T., Belldegrun, A., and Bonavida, B. (1993) Sensitivity of human renal cell carcinoma lines to TNF, adriamycin, and combinations: role of TNF mRNA induction in overcoming resistance. *J. Urol.* **149**, 1202–1208.
13. Mickisch, G., Fajta, S., Keilhauer, G., Schlick, E., Tschada, R., and Alken, P. (1990) Chemosensitivity testing of primary human renal cell carcinoma by a tetrazolium based microculture assay. *Urol. Res.* **18**, 131–136.
14. Nanus, D. M. and Walker, C. L. (1997) Experimental models of renal cancer, in *Principles and Practice of Genitourinary Oncology* (Raghavan, D., Scher, H. I., Leibel, S. A., and Lange, P., eds.), Lippincott-Raven, Philadelphia, PA, pp. 779–786.
15. Sayers, T. J., Wiltout, T. A., McCormick, K., Husted, C., and Wiltout, R. H. (1990) Antitumor effects of alpha-interferon and gamma-interferon on a murine renal cancer (Renca) in vitro and in vivo. *Cancer Res.* **50**, 5414–5420.
16. Wigginton, J. M., Komschlies, K. L., Back, T. C., Franco, J. L., Brunda, M. J., and Wiltout, R. H. (1996) Administration of interleukin 12 with pulse interleukin 2 and the rapid and complete eradication of murine renal carcinoma. *JNCI* **88**, 38–43.

17. Beniers, A. J., Peelen, W. P., Hendriks, B. T., Schalken, J. A., Romijn, J. C., and Debruyne, F. M. (1988) In vitro antiproliferative efficacy of interferon-alpha, -gamma and tumor necrosis factor on two human renal tumor xenografts. *Urol. Res.* **16**, 309–314.
18. Baselga, J. and Dmitrovsky, E. (1993) Human teratocarcinomas and retinoic acid-mediated tumor differentiation, In *Retinoids in Oncology* (Hong, W. K. and Lotan, R., eds.), Marcel Dekker, Inc., New York, NY, pp. 285–298.
19. Naito, S., von Eschenbach, A. C., Giavazzi, R., and Fidler, I. J. (1986) Growth and metastases of tumor cells isolated from a human renal cell carcinoma implanted into different organs of nude mice. *Cancer Res.* **46**, 4109–4225.
20. Naito, S., von Eschenbach, A. C., and Fidler, I. J. (1987) Different growth pattern and biologic behavior of human renal cell carcinoma implanted into different organs of nude mice. *J. Natl. Cancer Inst.* **78**, 377–385.
21. Fidler, I. J., Naito, S., and Pathak, S. (1990) Orthotopic implantation is essential for the selection, growth, and metastasis of human renal cell cancer in nude mice. *Cancer Metastasis. Rev.* **9**, 149–165.
22. Naito, S., Walker, S. M., and Fidler, I. J. (1989) In vivo selection of human renal cell carcinoma cells with high metastatic potential in nude mice. *Clin. Exp. Metastasis* **7**, 381–389.
23. Saiki, I., Naito, S., Yoneda, J., Azuma, I., Price, J. E., and Fidler, I. J. (1991) Characterization of the invasive and metastatic phenotype in human renal cell carcinoma. *Clin. Exp. Metastasis* **9**, 551–566.
24. Fidler, I. J. (1992) The biology of renal cancer metastasis. *Semin. Urol.* **10**, 3–11.
25. Mulligan, R. C. (1993) The basic science of gene therapy. *Science* **260**, 926–932.
26. Gastl, G., Finstad, C. L., Guarini, A., Bosl, G., Gilboa, E., Bander, N. H., and Gansbacher, B. (1992) Retroviral vector-mediated lymphokine gene transfer into human renal cancer cells. *Cancer Res.* **52**, 6229–6236.
27. Belldgrun, A., Tso, C. L., Sakata, T., Duckett, T., Brunda, M. J., Barsky, S. H., Chai, J., Kaboo, R., Lavey, R. S., and McBride, W. H. (1993) Human renal carcinoma line transfected with interleukin-2 and/or interferon alpha gene(s): implications for live cancer vaccines. *J. Natl. Cancer Inst.* **85**, 207–217.
28. Schendel, D. J., and Gansbacher, B. (1993) Tumor-specific lysis of human renal cell carcinomas by tumor-infiltrating lymphocytes: modulation of recognition through retroviral transduction of tumor cells with interleukin 2 complementary DNA and exogenous alpha interferon treatment. *Cancer Res.* **53**, 4020–4025.
29. Schattka, S., Decken, K., Schmitz-Drager, B., Ackermann, R., and Ebert, T. (1994) Establishment and characterization of human renal cancer cell lines and autologous normal kidney short term cultures. *Invest. Urol.* **5**, 35–41.

Murine Animal Model

**Nobuyasu Nishisaka, Philo Morse, Richard F. Jones,
Ching Y. Wang, and Gabriel P. Haas**

1. Introduction

Experimental animal models are available for the development of new treatment. Murine animal models have particular advantages for comparative study to evaluate the efficacy and safety of different treatment modalities because many mice can be treated at the same time with easy handling. Among several experimental models, murine renal carcinoma (Renca), which arises spontaneously in Balb/c mice, is the most frequently used for the assessment of chemotherapy, immunotherapy, and radiotherapy. Renca cells readily establish tumors in isogenic mice, producing histologically proven adenocarcinoma with a predictable growth rate to mimic the clinical situation for orthotopic growth and metastasis in a reasonable time frame. Because of its poor immunogenicity and its responsiveness to immunotherapy, the number of studies using cytokine gene-modified tumor vaccines—such as interferon-alpha or interleukin-2—in the Renca system is growing. Therefore, Renca experiments greatly contribute to the analysis of the mechanisms of antitumor immune response. In this chapter, we describe several experimental systems using this Renca model.

2. Materials

2.1. *Implantation of Tumor Cells*

2.1.1. *Preparation of Renca Cell Suspension*

1. Complete RPMI-1640 medium: RPMI-1640, 10% heat-inactivated fetal calf serum (FCS), 2 mM L-glutamine, 2 mg/mL sodium bicarbonate, 1 mM sodium pyruvate, 0.1 mM MEM nonessential amino acids, 10 mM HEPES buffer solution, 50 U/mL penicillin, 50 µg/mL streptomycin.

2. 25 cm² tissue-culture flasks.
3. Phosphate-buffered saline (PBS).
4. 0.53 mM ethylenediaminetetraacetic acid (EDTA).
5. 0.9% (w/v) NaCl.

2.1.2. Subcutaneous Injection

1. 70% ethanol.
2. 1.0-mL syringe with 26-gauge needle.

2.1.3. Intravenous Injection

1. Warming box or 45°C water bath.
2. Glass beaker with lead donut or mouse holder.
3. 70% ethanol.
4. 0.9% NaCl.
5. 0.5-mL syringe with 27-gauge needle.

2.1.4. Renal Subcapsular Injection

1. 70% ethanol.
2. 5 mg/mL pentobarbital (commercial pentobarbital solution is diluted with 10% ethanol or 0.9% NaCl).
3. 1.0-mL syringe with 26-gauge needle.
4. Sterile scissors.
5. Sterile forceps
6. 0.5-mL syringe with 27-gauge needle
7. 50- or 100- μ L Hamilton syringes.
8. Suture forceps.
9. 4-0 chromic catgut.

2.2. Carcinogen-Induced Renal Cell Carcinoma (RCC) Model

1. 2.5% streptozocin in 0.9% NaCl.
2. CBA/H/T6J mouse.
3. Glass beaker with lead donut or mouse holder.
4. 70% ethanol.
5. 0.5-mL syringe with 27-gauge needle.

2.3. Tumor Growth Assessment

2.3.1. Measurement of Tumor Volume

1. Outside Vernier calipers.

2.3.2. Enumeration of Lung-Tumor Nodules

1. Scissors.
2. Forceps.
3. 5-mL syringe with 18-gauge needle.
4. India ink solution (for 100 mL): 85 mL distilled water, 2 drops ammonium hydroxide, and 15 mL India ink.

5. Water.
6. Feketes solution (for 100 mL): 64 mL ethanol, 23 mL distilled water, 7.6 mL formaldehyde, and 4.4 mL glacial acetic acid.
7. 10% formaldehyde in PBS.

2.4. Oral Administration of Antitumor Agents

1. Gavage tube.

2.5. Depletion of Immune Cells In Vivo

2.5.1. Natural Killer (NK) Cell Depletion

1. Anti-asialo GM1 (Wako, Osaka, Japan).
2. Anti-NK1.1 (hybridoma PK 136; ATCC HB 191).

2.5.2. CD4 T-Cell Depletion

1. Hybridoma GK 1.5 (ATCC; TIB 207).

2.5.3. CD8 T-Cell Depletion

1. Hybridoma 2.43 or hybridoma 53-6.72 (ATCC; TIB 105).

2.5.4. Macrophage Depletion

1. Hybridoma MH-S (ATCC; CRL 2019).

2.5.5. Preparation of Antibodies

2.5.5.1. GENERATION FROM ASCITES

1. Balb/c mouse or nude mouse.
2. Pristane (2,6,10,14-tetramethylpentadecane).
3. 1.0-mL syringe with 26-gauge needle.

2.5.5.2. GENERATION FROM SUPERNATANT OF HYBRIDOMA CELLS (PRECIPITATION BY AMMONIUM SULFATE)

1. 100% saturated ammonium sulfate (pH 7.3).
2. PBS.
3. Sephadex G-200.

2.6. Radiation

2.6.1. Radiation of Cultured Cells

1. Phillips MGC30 X-ray machine

2.6.2. Radiation of Local Tumor

1. Phillips MGC30 X-ray machine.
2. Machlett Collimaster M collimator.
3. Mouse holder.

2.7. Vaccination

1. Complete RPMI-1640 medium.
2. PBS.
3. 0.53 mM EDTA.

3. Methods

3.1. Implantation of Tumor cells

There are several different methods for implantation of tumor cells, which are used according to the purpose of the study model. Subcutaneous implantation is the most frequently used technique, because tumor growth is visible and the efficacy of desired drugs can be easily estimated. Intravenous injection via the tail vein is also frequently used, because it can be easily performed and yields reproducible lung metastasis. Intrarenal injection or subcapsular implantation is used as an orthotopic tumor model that reflects human RCC. Finally, intrasplenic injection of Renca cells yields liver metastasis.

3.1.1. Preparation for Renca Cell Suspension

1. Maintain Renca cells in vitro with complete RPMI-1640 medium (CM) in 25 cm² tissue-culture flask.
2. Discard old medium and wash cells once with PBS.
3. Add 1 mL of 0.53 mM EDTA and incubate at 37°C for 2–5 min to detach the cells.
4. Add 1 mL of CM to the plate and suspend the cells by pipetting.
5. Centrifuge the suspension at 250g for 5 min.
6. Discard supernatant and resuspend the cells in ice-cold PBS.
7. Centrifuge at 250g for 5 min.
8. Discard supernatant and suspend the cells in 0.9% NaCl.
9. Keep the cells at 4°C.

3.1.2. Subcutaneous Injection

1. Disinfect the right flank of mouse with 70% ethanol.
2. Administer a sc injection of 5×10^5 cells in 200 μ L of normal saline using 26-gauge needle to the disinfected area (*see Note 1*).

3.1.3. Intravenous Injection

1. Put mice in a warming box, or warm the tail of mouse directly with hot water at 45°C to dilate tail vein.
2. Put the mouse in a mouse holder.
3. Disinfect the tail with 70% ethanol.
4. Inject 1×10^5 cells in 200 μ L of normal saline using 27-gauge needle into either lateral tail vein.

3.1.4. Renal Subcapsular Injection (see **Notes 2–4**)

1. Disinfect the abdomen with 70% ethanol and inject, intraperitoneally, 200 μ L of 5 mg/mL pentobarbital using a 26-gauge needle to anesthetize the mouse.
2. Incise 1 cm of a right flank skin and separate the sc tissue.
3. Incise muscles along the skin incision to expose the right kidney through a right-flank incision.
4. Inject 1×10^5 cells in 40- μ L of normal saline into renal capsule using a 27-gauge needle.

3.2. Carcinogen-Induced RCC Model

A number of chemicals induce RCC in the mouse, including dimethylnitrosamine, N-nitrosomethylurea, N-nitrosoethylurea, cycasin, basic lead acetate, 2-acetylaminofluorene and Tris(2,3-dibromopropyl)phosphate. However, only a few such chemicals produce an incidence of renal cell tumor sufficiently high for experimental purposes. Yet the administration of a single dose of streptozocin has been demonstrated to induce a high incidence of renal-cell tumor. The procedure, adapted from Hard (2), is described in **steps 1–3**:

1. Prepare a fresh 2.5% streptozocin solution in normal saline.
2. Inject 250 mg/kg of streptozocin into the tail vein of a female CBA/H/T6J mouse (Jackson Laboratories, Bar Harbor, ME), as described in **Subheading 3.1.3., step 4** (see **Note 5**).
3. RCCs begin to appear at approx 20 wk (see **Note 6**).

3.3. Tumor Growth Assessment

3.3.1. Measurement of Tumor Volume (see **Notes 7–9**)

Tumor size is measured with a caliper, and the volume is determined as follows:

1. Tumor volume (cm^3) = $0.52 \times (\text{length}) \times (\text{width})^2$
2. Excise the tumor surgically and determine its weight.

3.3.2. Enumeration of Lung-Tumor Metastases (3)

1. Open the chest cavity and expose the trachea.
2. Inject India ink into both lungs through trachea with a 18-gauge needle until the entire lungs are filled.
3. Remove both lungs along with the heart and rinse with water.
4. Fix lungs in Feketes solution for 5 min and store in 10% formalin solution.
5. Count white tumor nodules in all lung lobes (see **Note 10**).

3.4. Administration of Antitumor Agents

When the efficacy of antitumor agents is evaluated in the Renca model, agents are administered intravenously, intraperitoneally, or orally. The method

of iv and ip injection can be done as previously described. Here we describe oral administration (4):

1. Hold a mouse with one hand. Hold the tail with the last two fingers and catch the neck with thumb and index finger.
2. Insert a gavage tube into the stomach.
3. Inject antitumor agents gently into the stomach.

3.5. Depletion of Immune Cells In Vivo

For the past several decades, immunotherapy using interferon-alpha and/or interleukin-2 has been the main clinical management strategy for advanced RCC. A variety of cytokines for RCC treatment have been investigated as the techniques for gene therapy have advanced. Frequently, those studies use in vivo depletion of NK cells, T cells, or macrophages to investigate mechanisms of host antitumor immunity response. Here we describe the procedure for depletion of immune cells:

3.5.1. NK Cell Depletion

3.5.1.1. ANTI-ASIALO GM1 (SEE SUBHEADING 3.5.6.)

1. Dilute anti-asialo GM1 (1 mg/mL, Wako Chemical Co., Tokyo, Japan) 10 times with PBS.
2. Administer an injection (i.p.) as described in **Subheading 3.1.4., step 1**.

3.5.1.2. ANTI-NK 1.1. (SEE SUBHEADINGS 3.5.5. AND 3.5.6)

1. Hybridoma PK 136 (ATCC; HB191) antibody.
2. Administer an injection (i.p.) as described in **Subheading 3.1.4., step 1**.

3.5.2. CD4⁺ T-cell Depletion (see Subheadings 3.5.5. and 3.5.6.)

3.5.3. CD8⁺ T-cell Depletion (see Subheadings 3.5.5. and 3.5.6.)

3.5.4. Macrophage Depletion (see Subheadings 3.5.5. and 3.5.6.)

3.5.5. Preparation of Antibodies

3.5.5.1. GENERATION FROM ASCITES FLUID

1. Inject 0.5 mL of pristane i.p. (2,6,10,14-tetramethylpentadecane) into balb/c mice at 14 and 7 d prior to injection of hybridoma cells (see **Note 11**).
2. On day 0, inject 1×10^7 of hybridoma cells i.p. into mice.
3. Ascites of mice can be harvested after 2 wk and collected consecutively every 2–3 d (see **Note 12**) afterward.
4. Centrifuge the ascites at 350g at room temperature for 10 min (see **Note 13**).
5. Inject, 100–200 μ L of the supernatant intraperitoneally into experimental mice for depletion test each time.

3.5.5.2. GENERATION FROM SUPERNATANT OF HYBRIDOMA CELLS (AMMONIUM SULFATE PRECIPITATION)

1. Harvest culture supernatant from hybridoma cells.
2. Centrifuge at 250g for 20 min (*see Note 14*).
3. Add saturated ammonium sulfate (pH 7.3) to the supernatant until the solution reaches 45% saturation.
4. Keep the suspension overnight at 4°C. Precipitates are collected after centrifugation.
5. Dissolve pellet in PBS.
6. Place solution in dialysis tubing and dialyze against PBS for 24 h.
7. Further concentrate the antibody by placing the dialysis tubing in Sephadex G-200.
8. Determine the concentration of mouse IgG by enzyme-linked immunosorbent (ELISA) assay.

3.5.6. In Vivo Depletion Test Model

Basically, immune cells can be depleted by the administration of antibody prior to or after tumor implantation (*see Note 15*). An example of the use of antibody depletion in a model of cytokine gene-modified tumor-cell vaccination is described here:

Day-1: Injection of antibodies.

Day 0: iv injection of tumor cells.

Day 1: Injection of antibodies (just before treatment) and then vaccination.

Day 6: Injection of antibodies.

Day 7: Injection of antibodies (just before treatment) and then 2nd vaccination.

Day 13: Injection of antibodies.

Day 14: Injection of antibodies (just before treatment) and then 3rd vaccination.

Day 21: Sacrifice and count lung-tumor nodules.

3.6. Radiation

X-irradiation for the treatment of murine cancers has been used extensively in the past, and it has found renewed interest since the observation of synergistic interaction between radiation and cytokine therapy (5). Radiation is also used to inactivate tumor cells prepared for vaccination.

3.6.1. Radiation of Cultured Cells

1. Harvest and prepare Renca cells as described above.
2. Suspend the cells in 10–20 mL of fresh media.
3. Irradiate cells on ice with 3000–5000 rad.
4. Pellet and resuspend the cells in appropriate vol of PBS.

3.6.2. Radiation of Local Tumor

1. Immobilized mice are placed prone in lucite jigs (*see Note 16*).
2. Jigs are then placed in an aluminum frame at 15 cm from the X-ray tube (*see Note 17*).

3. A 6.4-mm-thick lead shielding is used to cover areas that do not require shielding. The shield is supported by posts on four corners of the frame (*see Note 18*).
4. Irradiated mice with appropriate dose (*see Note 19*).

3.7. Vaccination

Vaccine therapy for cancer is based on the premise that tumor-associated antigens (TAAs) can be recognized by host immune cells to activate antitumor immunity. However, specific TAAs have not been identified in RCC. Therefore, whole tumor cells are used as immunogens. The efficacy of tumor-cell vaccine can be enhanced by modifying the cells to produce immunostimulatory cytokines. Two models are available: prophylactic effect, in which vaccinations precede the challenge of tumor cells, and therapeutic effect, in which vaccinations are used in hosts bearing established tumors.

3.7.1. Preparation of Cytokine Gene-Modified Tumor Cells

The desired cytokine genes are introduced into tumor cells by plasmid- or viral-expression vectors. Secretion of cytokines can be determined using ELISA kits available from commercial sources or by bioassays using cytokine-dependent cells. Media of cytokine-producing Renca cells cultured for 48 h can be used for the bioassay of the cytokine of interest. For vaccination, cytokine gene-modified tumor cells are irradiated in order to eliminate their proliferative ability while retaining the production of cytokines. This treatment also maintains the stability of tumor antigens. Here we describe the handling of cytokine gene-modified Renca cells:

1. Culture cytokine-producing Renca cells until subconfluent condition.
2. Prepare cell suspension in ice-cold CM as described in **Subheading 3.1.1**.
3. Pipet 1×10^6 cells in 5 mL of CM into a 25-cm² culture flask.
4. Place the flask on ice and irradiated with 5,000 rads.
5. Transfer cells to a centrifuge tube and centrifuge at 250g at 4°C for 5 min.
6. Discard supernatant and suspend the cells in normal saline.
7. Maintain the cells at 4°C until injection.

3.7.2. Prevaccination Model

1. Inject 200 μ L normal saline containing 1×10^6 of irradiated cytokine gene-modified Renca cells sc into the left flank at days 21, 14, and 7 prior to tumor implantation.
2. To evaluate tumor growth at the injection site, inject, 1×10^6 of wild-type Renca cells sc in 200 μ L normal saline into the right flank on day 0. Measure the length and width of tumor every 3–4 d.
3. To evaluate tumor growth in the lung, inject 1×10^5 of wild-type Renca cells in 200 μ L normal saline into the tail vein on day 0. Sacrifice mice on day 21 and count the number of lung-tumor nodules.

3.7.3. Postvaccination Model

3.7.3.1. SUBCUTANEOUS TUMOR

1. Inoculate 1×10^6 of wild type Renca cells in 200 μL normal saline into the right flank.
2. Start vaccinations when tumors reach 5–10 mm in the largest dimension (about 8–10 d after injection). Vaccinations are performed once a week for 3 wk each time with 3×10^6 of irradiated cytokine gene-modified Renca cells in 200 μL normal saline into the opposite flank.
3. Measure the length and width of tumor every 3–4 d to monitor growth.

3.7.3.2. LUNG TUMOR

1. Inject 1×10^5 of wild-type Renca cells in 200 μL normal saline into the right flank on day 0.
2. Vaccination with 3×10^6 of irradiated cytokine gene-modified Renca cells in 200 μL normal saline into the left flank on days 1, 7, and 14.
3. Sacrifice mice on day 21 and count the number of lung-tumor nodules.

4. Notes

1. When withdrawing cells for injection, the cells must be loosened by gently tapping the tube to evenly suspend the cells.
2. It is convenient to use a Hamilton syringe equipped with a push-button dispenser to accurately deliver replicate small volumes. When the cell sample is injected into the subcapsular cavity, swelling can be seen.
3. The needle should penetrate through the renal cortex once to reach subcapsular cavity to prevent leakage of cell samples to the surrounding tissue.
4. With this model, metastasis to regional lymph nodes often occurs.
5. Female mice are usually chosen, since streptozocin is less toxic in female mice than in males.
6. The tumors are invariably multiple, and usually originate in the outermost zone of the kidney parenchyma.
7. To measure a tumor, wet fur with 70% ethanol to make it easier to find tumor margins.
8. When 5×10^5 of Renca cells are injected subcutaneously, tumors usually become palpable within 7 d.
9. When 5×10^5 of Renca cells are injected subcutaneously, tumors are usually 7–8 cm^3 by 28 d following the formula in **Subheading 3.3.1**.
10. An iv injection of 5×10^5 Renca cells typically yeilds 200–300 lung nodules at 21 d after injection.
11. When nude mice are used for generation of ascites, injection of pristane is not always necessary.
12. Four to eight mL of ascites usually can be collected.
13. If removal of fibrin is necessary, centrifuge at 10,000g for 30 min at 4°C.
14. When storage of supernatant is desired, store at 4°C.

15. Analysis of splenocytes by flow cytometry shows that administration of antibodies completely depletes splenic population almost immediately after injection of antibody. The depletion remains complete for 2 wk, after which the T-cell subsets gradually recover (6).
16. Lucite jigs are a modification of the design by Travis et al. (7).
17. The aluminum frame is designed so that three animals can be irradiated at once.
18. The lead shields have holes cut for the irradiation of appropriate regions.
19. When bilateral lung irradiation is performed, 300 rad gives sublethal irradiation.

References

1. Rangel, M. C. and Pontes, J. E. (1989) Animal models of renal cell carcinoma. *Semin. Urol.* **7**, 237–246.
2. Hard, G. C. (1985) Identification of a high-frequency model for renal carcinoma by the induction of renal tumors in the mouse with a single dose of streptozotocin. *Cancer Res.* **45**, 703–708.
3. Wexler, H. (1966) Accurate identification of experimental pulmonary metastases. *J. Natl. Cancer Inst.* **36**, 641–645.
4. Nishisaka, N., Maini, A., Kinoshita, Y., Yasumoto, R., Kishimoto, T., Jones, R. F., Morse, F., Hillman, G. G., Wang, C. Y., and Haas, G. P. (1999) Immunotherapy for lung metastases of murine renal cell carcinoma: synergy between radiation and cytokine-producing tumor vaccines. *J. Immunother.* **22**, 308–314.
5. Dybal, E. J., Haas, G. P., Maughan, R. L., Sud, S., Pontes, J. E., and Hillman, G. G. (1992) Synergy of radiation therapy and immunotherapy in murine renal cell carcinoma. *J. Urol.* **148**, 1331–1337.
6. Udono, H., Levey, D. L., and Srivastava, P. K. (1994) Cellular requirements for tumor-specific immunity elicited by heat shock proteins: tumor rejection antigen gp96 primes CD8+ T cells in vivo. *Proc. Natl. Acad. Sci. USA* **91**, 3077–3081.
7. Travis, E. L., Parkins, C. S., Holmes, S. J., and Down, J. D. (1982) Effect of misonidazole on radiation injury to mouse spinal cord. *Br. J. Cancer* **45**, 469–473.

Angiogenesis Assays

Jack H. Mydlo

1. Introduction

Angiogenesis—the formation of a vascular network—is essential for the support of a developing tumor when simple diffusion of nutrients is impossible. The ability of a solid tumor to achieve metabolic needs beyond simple diffusion is dependent on the development of this neovascular network. The process of angiogenesis lets the tumor become self-sufficient to grow, and also gives it the ability to metastasize. Growth factors added to human-vein endothelial cells in culture may demonstrate tubularization of cells, but this does not necessarily imply angiogenesis. True *in vivo* angiogenesis means not only the mobilization of endothelial cells, but the degradation of the matrix and the formation of vessel sprouts in a network that can transport red blood cells (RBCs).

Although the rabbit cornea assay may be expensive and somewhat cumbersome, it still is an effective way to demonstrate angiogenesis (1). Subsequent assays, such as the chorioallantoic membrane (CAM) assay, the disc angiogenesis system (DAS), and the radiolabeled RBC assay, may be more efficient for the investigator (2–7).

In many tumors—such as breast, prostate, and colon—the quantitation of microvessel density (MVD), a measure of neovascularity, has shown some predictive value in clinical outcome. Even in renal cancers, the hypovascular papillary adenocarcinoma does not behave as aggressively as the more hypervascular clear-cell adenocarcinoma (8). Although there are many other prognostic variables that may influence renal tumor biology—such as cytokeratin content and nuclear morphology—quantitation of microvessel density may become another important parameter in assessing the aggressive nature of this disease (9–13).

Since many growth factors induce angiogenesis, these assays can help to determine the antiangiogenic potential of certain inhibitors, which may be utilized in therapeutic approaches (14–23). These are described in another chapter.

2. Materials

2.1. Rabbit Cornea Assay

2.1.1. Preparation of Rabbits

1. New Zealand White adult rabbits.
2. Phenobarbital (Sigma, St. Louis, MO).
3. Ophthalmic lid retractor.
4. 1- and 5-cc syringes with 26-gauge needles.

2.1.2. Preparation and Insertion of Tissue Plug

1. No. 11 surgical blade.
2. Punch dermatome.
3. Zeiss stereomicroscope.

2.1.3. Enucleation and Fixation of Eyes

1. Spoon.
2. Phosphate-buffered formalin (Fisher Scientific, Fairlawn, NJ).
3. Slit lamp.
4. Zeiss microscope 16X.

2.2. Chorioallantoic Membrane (CAM) Assay

2.2.1. Preparation of Eggs

1. Fertilized chick eggs (SPAFAS, Norwich, CT).
2. Cardboard egg crates.
3. Incubator at 37°C and 3% CO₂.
4. Petri dishes with covers (105-mm diameter, Falcon).
5. Thermometer.

2.2.2. Preparation of Methylcellulose Plugs with Samples

1. 0.1% liquid methylcellulose (Gibco-BRL, Grand Island, NY).
2. Teflon rods for pedestals.
3. Camera with macro lens and grid, tripod, or vertical holder; ASA 400 film.
4. Petri dishes with covers, 105-mm diameter (Fisher Scientific) model glue.
5. 1-cc tuberculin syringe with 26-gauge needle as applicator of sample; tweezers.

2.3. Disc Angiogenesis System (DAS)

2.3.1. Preparation of Rat

1. Male Sprague-Dawley rats, 4–5 mo old (Charles River Laboratories, Wilmington, MA).
2. Phenobarbital for im injection.

3. Animal hair shaver for shaving back of rat.
4. 3–0 and 4–0 vicryl sutures, scissors, scalpels, needle holders.
5. Ethanol (Gibco-BRL).
6. Sterile hood.

2.3.2. Preparation of Disc for Implantation

1. Polyvinyl alcohol sponges (13-mm in diameter and 2-mm-thick, Fisher Scientific, Fairlawn, NJ).
2. Millipore filters (Type HA with 0.45 μm pore size, Gibco-BRL).
3. Sterile agarose (Sigma).
4. Hank's balanced salt solution (HBSS) (Sigma).
5. Wooden dowel to apply melted steile agarose to inside hole of disc.
6. 1-cc tuberculin syringe with 26-gauge needle to apply tested contents to disc.
7. Millipore glue No. 1 (Gibco-BRL).
8. Scapel, staple gun (U.S. Surgical).

2.3.3. Removal and Preparation of Disc for Evaluation

1. 10% neutral formalin.
2. Paraffin.
3. Samples of rat kidney, aorta, and adipose tissue for controls of collagen IV staining.
4. Microscope slides treated with 3-aminopropyltriethoxysilane (Sigma).
5. Zeiss microscope with calibrated eyepiece micrometer (Spencer ocular micrometer).
6. Polyclonal rabbit anti-mouse collagen type IV antibody (Collaborative Research, Boston, MA).
7. Biotinylated goat anti-rabbit IgG, avidin-biotin-peroxide complex (Vector Labs, Burlingame, CA).

2.4. Radiolabeled RBC Assay

2.4.1. Preparation of Mice

1. Female Balb/c mice, 8 wk old (Charles River Laboratories).
2. Phenobarbital (Sigma, St. Louis, MO).
3. Mouse holder.

2.4.2. Preparation of Tumor Suspension for Inoculation

1. RC-29 renal-cancer cells (American Type Culture Collection, Rockville, MD).
2. Dulbecco's minimal essential medium (Sigma).
3. Sterile 1.2% sodium alginate (Allepro, Rockland, MA).
4. 80 mM CaCl_2 .
5. 0.15 M NaCl.
6. 1% ethylenediaminetetraacetic acid (EDTA).
7. 1-cc tuberculin syringe with 21-gauge needle to give sc injections along peritoneum.
8. ^{51}Cr -labeled mouse RBCs.

2.4.3. Evaluation of Alginate Pellets for Radiolabeled Pooling

1. Scalpel to excise alginate pellets.
2. Weigh scale (Fisher Scientific).
3. LKB gamma counter.
4. Dissecting microscope (Olympus Inc., Culver, CA).

2.5. Microvessel Density (MVD) Assay

2.5.1. Preparation of Tissue Sections

1. Histological confirmation of renal-cancer tissue compared to normal renal tissues.
2. 10% neutral buffered formalin.
3. Paraffin (Gibco-BRL).
4. Poly-L-lysine coated slides.
5. Graded ethanols (Gibco-BRL).
6. 0.3% H₂O₂.
7. 5% normal goat serum (Dako, Santa Barbara, CA).
8. Polyclonal rabbit antibodies to Factor VIII, or PECAM-1/CD-31 (Dako).
9. Biotinylated goat antibodies to rabbit immunoglobulins (Vector Laboratories).
10. 1% EDTA, prostaglandin E1, 3-aminopropyltriethoxysilane (Sigma).
11. Avidin-biotin-peroxidase complex (Vector Laboratories).
12. 3,3'-diaminobenzidine (Sigma).
13. Methyl green (Polysciences).
14. 0.01% nickel chloride (Polysciences).
15. Computer-assisted image analysis system (video camera with external image controller, Dage-MTI CCD72, Michigan City, IN) coupled to a compound microscope (Nikon, Garden City, NY) with computer and digitizing frame grab software (Matrox Electronics, Dorval, Québec).

3. Methods

3.1. Rabbit Cornea Assay

3.1.1. Preparation of Rabbit for Tumor Injection

1. Place rabbit in rabbit holder after injection of i.m. 5 mg phenobarbital.
2. Once there is adequate sedation, use ophthalmic lid retractor to get exposure of eye.
3. A #11 surgical blade is used to create a corneal pocket midway between the limbus and pupil center (*see Note 1*).
4. A punch dermatome is used to obtain 1-mm spherical plugs of fresh renal tumor.
5. Use tweezers to place tumor plug into corneal pocket (*see Notes 2 and 3*).
6. Document vessel growth with Zeiss stereomicroscope on days 1, 3, 7, and 21 using a slit lamp. The following scale can be used to quantitate vessels (*see Fig. 1A and B*).

0 = No vessels seen.

1 = 1–2 vessels seen at the limbus, less than 1 mm in length.

2 = 3–4 vessels seen at the limbus, greater than 1 mm in length.

3 = Several vessels approaching tumor implant site.

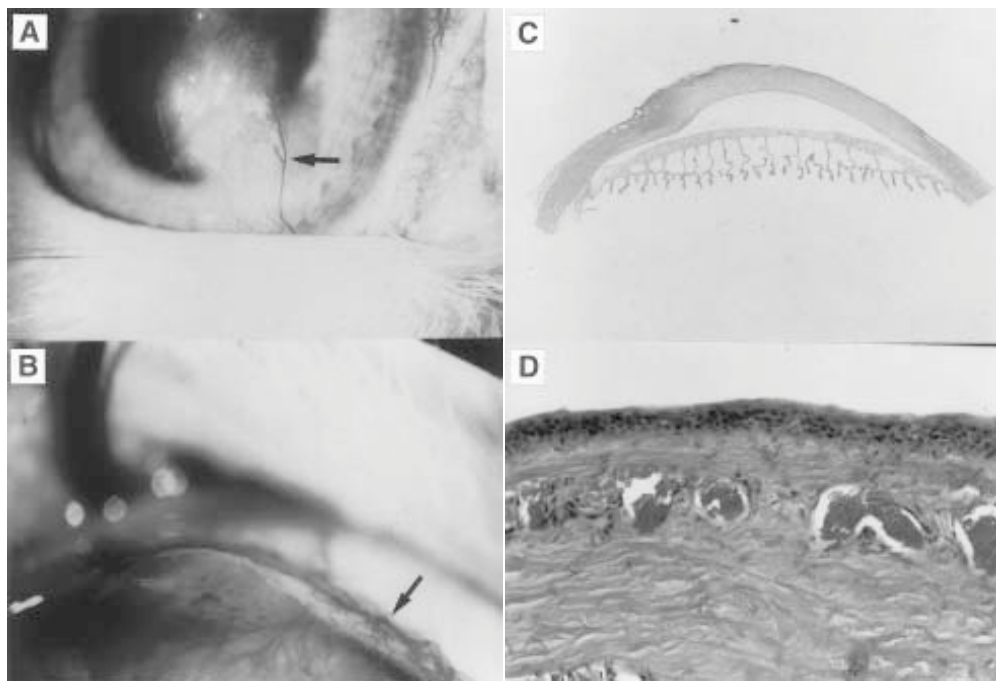


Fig. 1. Rabbit cornea demonstrates neovascularity starting at limbus (A) and growing toward implant (B). (C,D) Histological section of rabbit cornea demonstrating neovascularity. (Printed with permission of Elsevier Publishing.)

3.1.2. Fixing and Staining of Corneas

1. Rabbits are killed on day 42, and eyes are enucleated (*see Note 4*).
2. The eyes are fixed in phosphate-buffered formalin.
3. Corneal sections are obtained.
4. Staining is done with hematoxylin and eosin (*see Fig. 1C and D*).
5. Microscopic readings are done in triplicate, and the averages are taken.

3.2. Chorioallantoic Membrane (CAM) Assay

3.2.1. Preparation of Fertilized Eggs

1. Fertilized chick eggs are incubated at 37°C and 3% CO₂ for 3 d on egg crates (*see Note 5*).
2. Gently roll eggs periodically. Do not let them incubate in same position for all 3 d.
3. The eggs are then cracked and placed on 100 × 20-mm Petri dishes on day 3. Gently tap the top of the egg until it cracks, remove some of the eggshell with tweezers to create an opening, and pour the intact yolk onto the Petri dish (*see Notes 6 and 7*).

3.2.2. Preparation of Methylcellulose Test Substances

1. Use 1–2 μg of purified growth factor injected into 10 μL of liquid methylcellulose resting on Teflon pedestals and let dry for 1 h.
2. These pedestals are 3–4 mm in diameter and 2 cm high. One end is glued onto a Petri dish, and the other end is used to hold the methylcellulose. Up to 25 pedestals can be glued onto a Petri dish and act as a reusable applicator.
3. Place dried pellets on the CAM on day 6 of developing embryo (*see Note 8*).
4. Photograph CAM using a grid on camera to quantitate vessels. Camera must be on a tripod or straight holder, with a macro lens. Always use an empty pellet of methylcellulose as a control, since the inflammatory reaction can sometimes be mistaken for an angiogenic response (*see Fig. 2*).

3.3. Disc Angiogenesis System (DAS)

3.3.1. Preparation of Rat

1. Anesthetize male Sprague-Dawley rats 4–5 mo of age while in rat holder.
2. Backs of anesthetized rats are shaved and cleaned with ethanol while under a sterile hood.
3. A 20-mm incision is made with subsequent lateral tunnels for disc implantation (for positive and negative controls and test samples). The incision is then closed with staples.

3.3.2. Preparation of Disc

1. Discs of polyvinyl alcohol sponges 13 mm in diameter and 2-mm-thick are used, which will be covered on both flat sides by Millipore filters using Millipore glue.
2. A 3-mm core is cut from the center of the disc with a skin biopsy punch.
3. Melted sterile agarose (1% gel temperature 36°C, melting temperature 87°C; Sigma) is applied to the inside hole of the disc.
4. After the agarose has solidified, the lower Millipore filter—0.45 μm pore size, type HA—is attached to one side of the disc with Millipore glue.
5. Impregnate core plug with 20 μL of angiogenic growth factor to be tested, and then reinsert into the disc center.
6. The upper Millipore filter is glued to the upper side of the disc.
7. The disc is placed in sterile HBSS in a Petri dish until ready for implantation into the rat.
8. Positive controls may be 50 μg of prostaglandin E1 (Sigma). Negative controls may be 20 μL Hank's balanced salt solution (HBSS). Samples may be purified growth factor or 104 tumor cells suspended in 20 μL of HBSS.

3.3.3. Removal and Interpretation of Disc Results

1. Discs are removed after 14 d and one Millipore filter is detached with a scalpel. They are fixed in 10% neutral formalin for 48 h, dehydrated, and embedded in paraffin.
2. 6- μm -thick sections are mounted on microscope slides treated with 3-aminopropyltriethoxy-silane.
3. Controls used are rat kidney, aorta, and adipose tissue for collagen-staining technique.

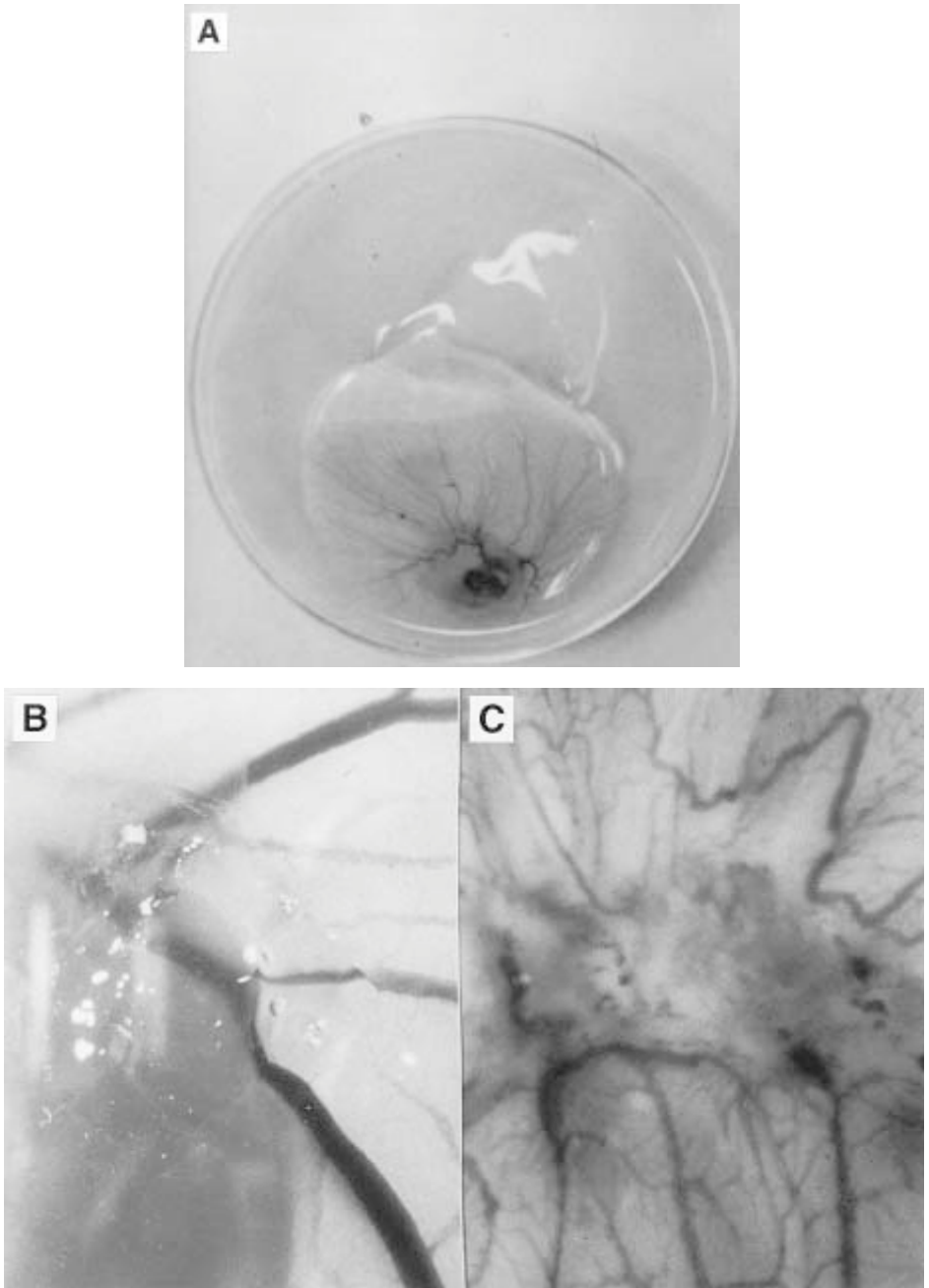


Fig. 2. (A) Chorioallantoic membrane (CAM) assays consists of placing fertilized chick egg in Petri dish. Negative control (B) and positive angiogenic response of sample tested (C). (Printed with permission of Williams & Wilkins.)

4. Quantitation of vessel growth consists of dividing each disc into eight equal sectors and measuring the radial distance between the most central vessel and disc rim.

3.4. Radiolabeled RBC and Hemoglobin Measurements

3.4.1. Preparation of Mice

1. Female Balb/c mice, approx 8 wk old (Charles River Laboratories) are used.
2. Mice are given s.c. injections along the peritoneal midline of 0.1–0.2 mL alginate-entrapped cells and alginate beads without cells as controls as to form a pellet of beads.
3. In 1–2 wk, the mice are given iv injections of ^{51}Cr -labeled mouse RBC, and then the animals are killed 1 h later by cervical dislocation.

3.4.2 Preparation of Tumor Suspension

1. Tumor cells to be tested are washed, counted, and resuspended in Dulbecco's minimal essential medium. This suspension of cells is mixed with sterile 1.2% sodium alginate (Allepro) for a final concentration of $1-5 \times (10)^6$ cells/mL in 0.8% sodium alginate (0.8% alginate in 0.15 M NaCl as control).
2. These mixtures are pumped through a spray nozzle into a bath of 80 mM CaCl_2 . Calcium alginate beads containing cells or calcium alginate control beads are washed three times in 0.15 M NaCl.
3. The number of entrapped cells are determined by mixing 1% EDTA in 0.15 M NaCl (1:1) with beads containing cells. The beads are dissolved by this method, and cells are counted with trypan blue to assess viability.

3.4.3. Evaluation of Alginate Pellets

1. One hour after mice have been given i.v. radiolabeled ^{51}Cr RBCs, the mice are sacrificed by cervical dislocation.
2. The alginate pellets that were injected subcutaneously and now contain induced blood vessels are now excised, weighed, and counted on a LKB gamma counter.
3. The pellets may also be crushed in water and the Drabkin and Austin assay may be used to quantitate the amount of hemoglobin (24).

3.5. Staining for Microvessel Density (MVD)

3.5.1. Preparation of Slides

1. Sections of 5- μ thickness are mounted on coated slides and dried at room temperature.
2. Slides are deparaffinized in three changes of Histoclear (National Diagnostics, Manville, NJ) and rehydrated through three 1-min changes of 100% ethanol, followed by two changes each of 95% and 75% ethanol, respectively.
3. Tissues are blocked for 20 min in 0.2% Tween-20 and 10 min in 3% BSA in PBS.
4. Slides of tissues are then stained with either polyclonal rabbit antibodies to PECAM-1/CD-31, an endothelial cell transmembrane molecule, or with antibody against Factor VIII-related antigen. This is done in 3% BSA in 0.01 M phosphate buffered solution overnight at room temperature (see **Note 9**).

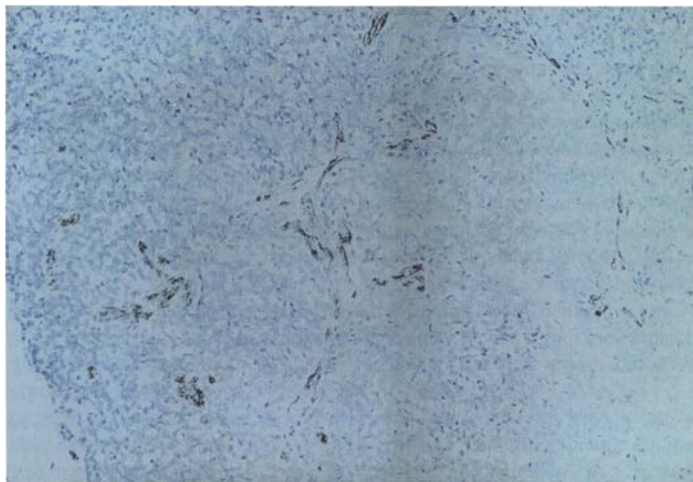


Fig. 3. Microvessel density is demonstrated by increased staining with PECAM-1/CD-31 antibody. (Printed with permission of A. G. Karger.)

5. After rinsing with PBS, the slides are incubated with biotinylated goat immunoglobulins to the rabbit antibodies for 30 min.
6. After washing, an avidin-biotin-peroxidase complex is applied to the sections (Vector Labs).
7. The slides are then developed with 0.5 mg/mL 3,3'-diaminobenzidine (DAB, Sigma, St. Louis, MO) and 0.1% H_2O_2 and 0.02% $NiCl_2$ in 0.05 M Tris-HCl buffer (pH 7.6).
8. Slides are then incubated for 5 min at 37°C, rinsed, lightly counterstained with 2% methyl green (Sigma), dehydrated, and mounted for imaging.
9. The cellular analysis system (CAS-200) is used to quantify the amount of MVD by measuring the optical density of CD-31 or Factor VIII by spectral analysis (expressed as vessels per millimeter squared (vv/mm²) (see **Note 10** and **Fig. 3**).

4. Notes

1. Use sham pockets in same rabbit eye as well as contralateral eye for controls.
2. Use care in handling tumor plugs, since excessive pressure may induce tissue necrosis.
3. Perform experiment promptly, because this could affect neovascular induction. Contralateral slits serve as controls. Slit-lamp examinations can be performed with a Zeiss stereomicroscope at 16x.
4. Enucleation of rabbit eyes can be performed with a simple teaspoon.

5. Use at least three dozen eggs on egg crates, as there are up to 10% of fertilized eggs that do not develop embryologically. Rotate them periodically.
6. Make sure that fertilized egg yolks are intact when poured onto the Petri dish; otherwise they will not develop embryologically.
7. Some embryos develop more quickly than usual, and may develop enough bulk to lift off the top cover of the Petri dish. Once the embryo comes into contact with the top cover, it rarely continues to develop normally.
8. Always use a control methylcellulose plug without any sample, since they may produce an inflammatory response which may be mistaken for angiogenesis.
9. Assessment of MVD may differ depending upon the use of antibody for CD-31 vs. CD-34 or Factor VIII. Always use control to assess the intensity of the staining with each antibody.
10. Although the computer image analysis system can be quite expensive, one can do manual counting of the stains in triplicate and thus take the average value.

References

1. Bard, R. H., Mydlo, J. H., and Freed, S. Z. (1986) Detection of tumor angiogenesis factor in adenocarcinoma of the kidney. *Urology* **27**, 447–450.
2. Preminger, G. M., Koch, W. E., Fried, F. A., and Mandell, J. (1980) Utilization of the chick chorioallantoic membrane for in vitro growth of the embryonic murine kidney. *Am. J. Anat.* **159**, 17–21.
3. Mydlo, J. H., Heston, W. D. W., and Fair, W. R. (1988) Characterization of a heparin-binding growth factor from adenocarcinoma of the kidney. *J. Urol.* **140**, 1575–1579.
4. Mydlo, J. H., Kral, J. G., and Macchia, R. J. (1998) Preliminary results comparing the recovery of basic fibroblast growth factor (FGF-2) in adipose tissue and benign and malignant renal tissue. *J. Urol.* **159**(6), 2159–2163.
5. Robertson, N. E., Discafani, C. M., Downs, E. C., Hailey, J. A., Sarre, O., Runkle, R. L., Popper, T. L., and Plunkett, M. L. (1991) A quantitative in vivo mouse model used to assay inhibitors of tumor-induced angiogenesis. *Cancer Res.* **51**, 1339–1344.
6. Nelson, M. J., Conley, F. K., and Fajardo, L. F. (1993) Application of the disc angiogenesis system to tumor induced neovascularization. *Exp. Mol. Pathol.* **58**, 105–113.
7. Nguyen, M., Shing, Y., and Folkman, J. (1994) Quantitation of angiogenesis and antiangio-genesis in the chick embryo chorioallantoic membrane. *Microvasc. Res.* **47**, 31–38.
8. Mydlo, J. H. and Bard, R. (1987) An analysis of papillary adenocarcinoma of the kidney. *Urology* **30**, 529–534.
9. Folkman, J. (1985) Tumor angiogenesis. *Adv. Cancer Res.* **43**, 175–203.
10. Kowalski, J., Kwan, H. H., Prionas, S. D., Allison, S. C., and Fajardo, L. F. (1992) Characterization and applications of the disc angiogenesis system. *Exp. Mol. Pathol.* **56**, 1–19.
11. Bigler, S.A., Deering, R.E., and Brawer M.K. (1993) Comparison of microscopic vascularity in benign and malignant prostate tissue. *Hum. Pathol.* **24**, 220–226.

12. Deering, R. E., Bigler S. A., Brown, M., and Brawer, M. K. (1995) *Microvasculature in Benign Prostatic Hyperplasia* **26**, 111–115.
13. Mydlo, J. H., Kral, J. G., Volpe, M. A., Axiotis, C., Macchia, R. J., and Pertschuk, L. P. (1998) An analysis of microvessel density, androgen receptor, p53 and HER-2/neu expression and Gleason score in prostate cancer: preliminary results and therapeutic implications. *Eur. Urol.* **34**, 426–432.
14. Hayek, A., Culler, F. L., Beattie, G. M., Lopez, A. D., Cuevas, P., and Baird, A. (1987) An in vivo model for the study of angiogenic effects of basic fibroblast growth factor. *Biochem. Biophys. Res. Commun.* **147**, 876–880.
15. Mydlo, J. H., Kanter, J. L., Kral, J. G., and Macchia, R. J. (1999) Obesity, diet, and other factors in urological malignancies. A review. *Br. J. Urol.* **83(3)**, 225–234.
16. Moller, H., Mellemegaard, A., Lindvig, K., and Olsen, J.H. (1994) Obesity and cancer risk: a Danish record-linkage study. *Eur. J. Cancer* **30A**, 344.
17. Lindblad, P. Wolk, A. Bergstrom, R. Persson, I., and Adami, H. O. (1994) The role of obesity and weight fluctuations in the etiology of renal cell cancer: a population-based case control study. *Cancer Epidemiol. Biomark Prevent* **3**, 631–636.
18. Li, J. J., Li, S. A., Oberley, T. D., and Parsons, J. A. (1995) Carcinogenic activities of various steroidal and nonsteroidal estrogens in the hamster kidney: relation to hormonal activity and cell proliferation. *Cancer Res.* **55**, 4347–4351.
19. Chow, W. H., McLaughlin, J. K., Mandel, J. S., Wacholder, S., Niwa, S., and Fraumeni, J. F., Jr. (1996) Obesity and risk of renal cell cancer. *Cancer Epidemiol. Biomark. Prevent.* **5**, 17–21.
20. Cordon-Cardo, C., Finstad, C., Bander, N. H., and Melamed, M. R. (1987) Immunoanatomic distribution of cytostructural and tissue-associated antigens in the human urinary tract. *Am. J. Pathol.* **126**, 269–284.
21. Mydlo, J. H. and Fair, W. R. (1988) *Growth Factors and Angiogenesis in Urology. AUA Update Series* Vol. 7, Lesson 39.
22. Maciag, T., Hoover, G. A., Stemerman, M. B., and Weinstein, R. (1981) Serial propagation of human endothelial cells in vitro. *J. Cell. Biol.* **91**, 420–426.
23. Moscatelli, D., Presta, M., and Rifkin, D. B. (1986) Purification of a factor from human placenta that stimulates capillary endothelial cell protease production, DNA synthesis, and migration. *Proc. Natl. Acad. Sci. USA* **83**, 2091–2098.
24. Drabkin, D. L. and Austin, J. H. (1982) Spectrophotometric constants for common hemoglobin derivatives in human, dog, and rabbit blood. *J. Biol. Chem.* **98**, 719–733.

Antiangiogenic Approaches to Renal Cell Carcinoma

Assays for Inhibitors and Clinical Trials

Steven C. Campbell, Frank K. Reiher, and Norman D. Smith, Jr.

1. Introduction

Angiogenesis—the formation of new blood vessels from preexisting ones—is a complex process regulated by a number of soluble factors as well as important interactions between endothelial cells, extracellular matrix components, and adjacent cells (*1–5*). Activation of the endothelial cell, which occurs when the balance between proangiogenic and antiangiogenic signals within a given microenvironment tilts in a positive direction, leads initially to increased expression of proteases, allowing the endothelial cell to mobilize itself and release inducers sequestered within the matrix (*1,6,7*). This is followed by endothelial-cell proliferation and migration and culminates in reorganization of the endothelial cell plexus to form tubules and eventually capillary structures that can conduct blood. Most proangiogenic factors—such as VEGF and basic fibroblast growth factor (bFGF)—are peptide growth factors that bind to transmembrane-receptor tyrosine kinases on the surface of the endothelial cell, initiating intracellular transduction pathways resulting in cellular activation (*8,9*). Other important angiogenic factors—the angiopoietins—further modulate this process by stabilizing or destabilizing interactions between small blood vessels and adjacent pericytes (*10*). Expression of angiopoietin 2 results in dissociation of pericytes, which can lead to endothelial-cell activation or vascular regression, depending on whether angioiductive or angioinhibitory signals predominate (*10,11*). In contrast, angiopoietin 1 stabilizes interactions with pericytes and promotes vascular quiescence (*10,12*). Proangiogenic factors can be produced directly by tumor cells, activated cells of the immune

system such as lymphocytes or macrophages, or stromal elements such as fibroblasts, or they can be released from the extracellular matrix by proteases—a well-characterized mechanism of bFGF activation (1,7,13,14).

The importance of angiogenesis in tumor biology is now well established, based on over three decades of experimentation from a multitude of laboratories, and confirming many of the hypotheses of Dr. Judah Folkman, long recognized as the leader of this field (2,3). Several lines of evidence have now converged to support the central thesis that tumors must induce the ingrowth of blood vessels to provide themselves with nutrients and oxygen required for progressive growth, and to obtain access to the bloodstream, an essential step in the metastatic cascade. An important role for angiogenesis in tumor progression is demonstrated by observations of tumor development in transgenic mice predisposed to malignancy and in human breast and cervical cancer. These studies have shown that the acquisition of an angiogenic phenotype occurs early, at the hyperplastic or carcinoma *in situ* stage, and represents an important determinant of which premalignant lesions will progress to frank malignancy (7). Numerous reports have confirmed that increased expression of proangiogenic substances promotes tumor growth and metastasis in relevant animal models, while antiangiogenic agents have the opposite effect (1,3). Studies of microvessel density have shown direct correlation with advanced pathologic features and compromised clinical outcomes for a wide variety of malignancies (15–18). Taken together, this extensive database argues in favor of an important role for angiogenesis in tumor progression and metastasis, and suggests that blocking angiogenesis may prove useful for the chemoprevention and treatment of cancer.

The list of agents that can block angiogenesis is now quite extensive and includes both naturally produced and exogenous substances (Table 1). Endogenous inhibitors include the interferons (19), thrombospondins 1 and 2 (20,21), and certain interleukins (22–24), in addition to encrypted molecules such as angiostatin (25) and endostatin (26,27), which represent fragments of plasminogen and collagen XVIII, respectively. Expression of endogenous inhibitors by normal tissues contributes to vascular quiescence, and in many tissue types, downregulation of inhibitor plays a key role in the switch to an angiogenic phenotype during tumor development (1). Fibrosarcoma, glioblastoma, and bladder cancer are examples of tumors for which downregulation of endogenous inhibitors contributes to the development of neovascularity (1,28–30). In these systems, replacement of the naturally produced inhibitor may have specificity for blocking tumor progression, and such inhibitors are also appealing because they are likely to be well tolerated. The diversity of antiangiogenic substances is now quite impressive, as angioinhibitory compounds have been identified from other natural sources such as fungal cultures (31), shark cartilage

Table 1
Examples of Angioinhibitory Substances

Endogenous substances

- Interferons α -, β -, and γ - and interferon-inducible protein 10 (IP-10) (19)
- Thrombospondins 1 and 2 (20,21)
- Pigmented epithelial-derived factor (PEDF) (91)
- Interleukins 1, 4, and 12 (22–24)
- Platelet factor 4 (101)
- Encrypted molecules such as angiostatin and endostatin (26,27,89)

Anticancer treatments

- Chemotherapeutic agents: bleomycin, methotrexate, and paclitaxel (42–44,102)
- Radiotherapy and hyperthermia (45,103)
- Antiestrogens such as tamoxifen (104)
- Retinoids (34)

Antibiotics

- TNP-470 (31)
- Linomide (41)
- Suramin (105)

Factors that affect matrix interactions

- Protease inhibitors (106,107)
- Antibodies to $\alpha v \beta 3$ and $\alpha v \beta 5$ integrins (108)
- Inhibitors of collagen synthesis (109)

VEGF-targeted approaches

- MAbs against VEGF (110,111)
- Antisense oligonucleotides or expression constructs against VEGF (118)
- Soluble VEGF receptors (112,113)
- VEGF receptor-signaling antagonists (SU5416) (114)

Miscellaneous

- Aspirin and cyclooxygenase-2 inhibitors (37,45)
 - Captopril (38)
 - Thalidomide (39)
 - Genestein and other soy products (36)
 - Vitamin D₃ analogues (35)
 - Squalamine (derived from shark cartilage) (32,115)
 - Contortrostatin (snake-venom disintegrin) (116)
-

(32), snake venom (33), or constituents of a normal, healthy diet such as retinoids (34), vitamin D analogues (35), or soy products (36). In addition, several drugs developed for other purposes, such as aspirin (37), captopril (38), thalidomide (39), and certain antibiotics (40,41), have been found to yield antiangiogenic effects as an unexpected dividend, and many conventional anticancer treatments are now known to be angioinhibitory, which may contribute to their efficacy (42–45).

A hypervascular pattern on renal angiogram is common for most clear-cell renal cell carcinomas (RCCs) of the kidney, and, until the advent of noninvasive imaging in the past 2–3 decades, was often relied on for diagnostic purposes (46). This pattern can be quite striking, reflecting the markedly increased number of vessels within such tumors as well as qualitative differences in vessel structure and configuration (**Fig. 1**).

Nevertheless, studies of microvessel density (MVD) in RCC have been conflicting, as some investigators have found a correlation with clinical outcomes while others report no such association. In general, there has been a scarcity of studies of MVD in this disease, perhaps reflecting the fact that the kidney is a highly vascular organ at baseline, making detection of increased MVD within tumors more difficult. Two studies focusing on patients with organ-confined RCC (stages T1 and T2) have reported significantly improved survival for patients with low MVD, and in both MVD proved to be an independent predictive factor on multivariate analysis (47,48). In contrast, Gelb and colleagues reported no association between MVD and survival for 52 patients with organ-confined RCC, and an inverse relationship between these parameters has also been described (49,50). Small numbers of patients and methodological considerations may have contributed to these divergent results. Immunohistochemical techniques and choice of antibodies can influence the sensitivity and specificity for the detection of microvasculature, and interpretation of stained sections can also vary considerably for investigators without dedicated training in this field (51,52).

The best evidence in favor of an important role for angiogenesis in the biology of RCC comes from *in vivo* studies examining the effect of proangiogenic or antiangiogenic substances on tumor growth and metastasis. These studies have used either the Renca or xenograft models of RCC, in which human RCC cells are implanted orthotopically into immune-deficient mice. Increased expression of the proangiogenic molecule bFGF increased the number of metastases to the lymph nodes or liver by greater than 10-fold (53), while a multitude of antiangiogenic agents, including endostatin (54), IL-12 (55), and TNP-470 (56–58) blocked tumor growth and/or metastases in these experimental models. Vitamin D3 analogs (59), genistein (60), captopril (61), and certain chemotherapeutic agents such as bleomycin (62)—all of which are known to have pleiotropic effects including antiangiogenic properties—also blocked tumor growth in these models. The observation of reduced MVD within tumors in mice treated with some of these agents suggests that their antiangiogenic properties may have contributed substantially to their efficacy (59,62).

Several proangiogenic molecules are expressed at increased levels in RCC when compared to the normal kidney (**Table 2**). Of these factors, the data in favor of VEGF as the primary physiologic inducer for RCC is most convincing.

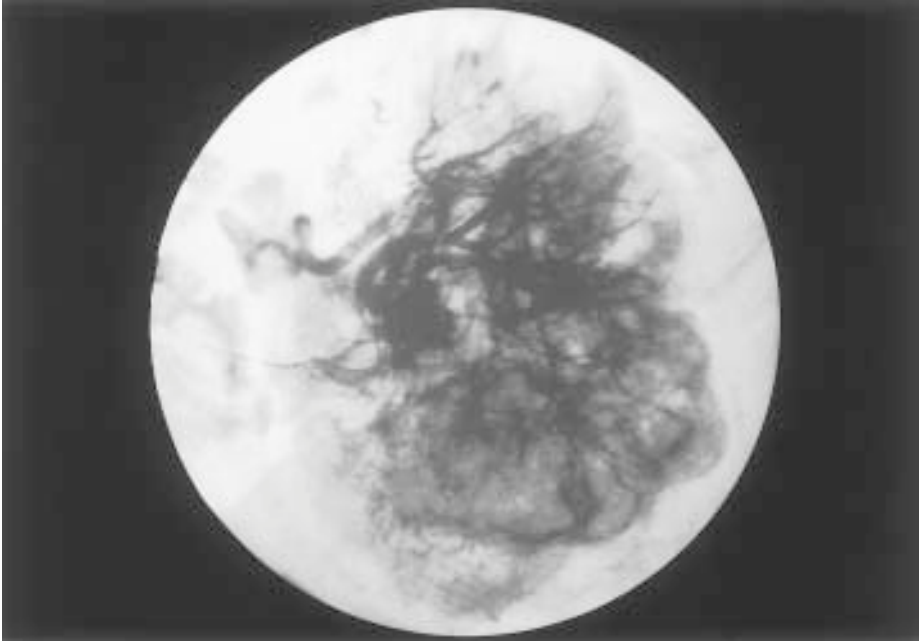


Fig. 1. Left renal angiogram illustrating marked hypervascularity associated with a clear-cell RCC of the kidney.

Table 2
Proangiogenic Molecules Expressed in RCC

VEGF (63,64,66)
bFGF (72,73,117)
Placental growth factor (63)
TGF- α and TGF- β -1 (76)
Angiogenin (77)
Scatter factor (78,79)
Thymidine phosphorylase (80)
Matrix metalloproteinases (84)

Increased levels of transcript for VEGF have been found in most hypervascular RCCs, while their less common hypovascular counterparts have demonstrated low expression of this molecule (63,64). Functional relevance of VEGF is also supported by in vitro data showing that neutralizing antibodies to VEGF can block the angiogenic activity of conditioned media derived from RCC cells (65). In addition, VEGF levels in the serum of patients with RCC are elevated

when compared to normal controls, and a correlation with tumor stage and tumor status has been observed (66). Interestingly, a correlation between certain patterns of VEGF isoform expression and MVD has also been reported. Tumors expressing all three of the VEGF isoforms 121, 165, and 189 amino acids in length were found to be more vascular, and a correlation with advanced stage was described (67).

Regulation of VEGF expression by the VHL tumor-suppressor gene is well established, as it has been shown that overexpression of the wild-type VHL gene product downregulates the expression of VEGF at both the transcriptional and posttranscriptional levels (68,69). The current literature demonstrates that loss or inactivation of wild-type VHL, which commonly occurs in clear-cell RCC, leads to dysregulated expression of VEGF, contributing to tumor neovascularity. As such, this represents an excellent example of the regulation of angiogenesis by genetic alterations—a theme originally developed by Bouck and colleagues (1). However, the story may not be quite so straightforward, as others have reported high levels of expression of VEGF by normal renal tubular cells, which would argue against modulation of VEGF as the primary factor leading to the switch to an angiogenic phenotype during the development of RCC (70,71). In turn, this would suggest that other factors, such as downregulation of endogenous inhibitors, may also regulate this process.

Several studies also suggest a potential role for bFGF in the stimulation of neovascularity by RCC. Elevated serum levels of bFGF have been found in patients with RCC and correlation with stage and grade has been reported (72,73). In addition, Nanus and colleagues reported increased cytoplasmic and extracellular staining for bFGF in RCC when compared to the normal kidney, and found that tumors staining positive for cytoplasmic bFGF were associated with a 3.5-fold increased rate of death resulting from disease (74). Other data suggest that stromal/epithelial interactions may contribute to the regulation of bFGF expression in RCC. Singh and colleagues showed that human RCC cells grown in mice expressed markedly increased levels of bFGF and neovascularity when implanted into the kidney, but not when grown subcutaneously (75). Extracellular stores of bFGF may contribute substantially to the pathogenesis of this disease, as they can be released from their sequestered form by proteases expressed during tumor invasion.

A multitude of other proangiogenic substances are also expressed at increased levels in RCC, and may contribute to neovascularity, although in most cases the evidence is still circumstantial. Placental growth factor, a member of a family of inducers that includes VEGF, is expressed primarily in hypervascular RCCs, suggesting that it may play a functional role (63). Increased serum levels of TGF β 1 (76), angiogenin (77) and scatter factor (also known as hepatocyte growth factor) (78,79) and enhanced staining for thymi-

dine phosphorylase, a proangiogenic enzyme, have been reported in RCC, and a correlation with MVD, tumor grade and stage, and survival has been observed in some instances, suggesting physiologic relevance (80). The available data on TGF α and TGF β 1 expression and their significance in the tumor biology of RCC is reviewed in Chapter 10.

1.1. Endogenous Inhibitors and RCC

Using both the endothelial cell migration and the rat corneal neovascularization assays, we recently explored the potential role of endogenous inhibitors in the regulation of angiogenesis in RCC (71). We found that conditioned media from normal renal tubular cells was weakly angioinhibitory, in contrast to conditioned media from RCC cells, which was strongly proangiogenic. Significantly increased levels of thrombospondin-1 (TSP-1), a 450-kDa extracellular matrix glycoprotein with potent antiangiogenic effects, were secreted by normal renal tubular cells as compared to cancer cells (71). Furthermore, a functional effect was demonstrated, as neutralizing antibodies to TSP-1 completely blocked the antiangiogenic activity of conditioned media derived from normal renal tubular cells (Fig. 2). Our data indicate that downregulation of the secretion of TSP-1 may contribute to the angiogenic switch in RCC. Interestingly, we found similar levels of intracellular TSP-1 in both normal renal tubular and RCC cells, suggesting that defective posttranslational processing and/or secretion of TSP-1 may occur in RCC (71). Defective processing and secretion of fibronectin and other matrix components has also been described in RCC, suggesting a common defect in this important cellular pathway (86,87). Further studies will be required to determine the role of TSP-1 in vivo; it should be emphasized that our data are derived primarily from in vitro models.

1.2. Antiangiogenic Approaches to RCC

Novel approaches are greatly needed for the management of patients with metastatic RCC, given the poor response rates associated with conventional forms of systemic therapy. Antiangiogenic strategies are particularly appealing for this malignancy because of its highly vascular nature, and offer several distinct advantages over cytotoxic therapies (1). Since antiangiogenic agents are not genotoxic and target the genetically stable endothelial cells rather than the tumor cells, induction of tumor resistance and secondary malignancies should be much less common. Side effects should also be reduced, given the unique mechanism of action and the fact that most other vascular beds are quiescent in adults and not significantly disturbed by angioinhibitory therapy (1). Experimental models suggest that morbidity should be primarily limited to delayed wound healing and female infertility. Thus far, results in these model

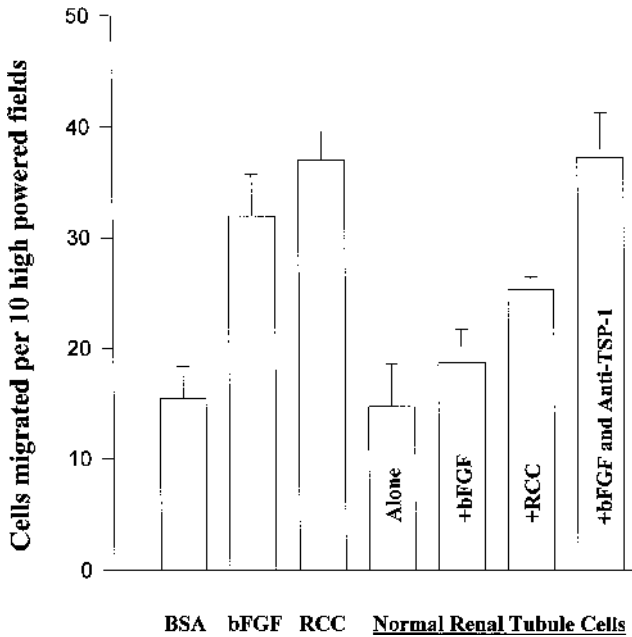


Fig. 2. Endothelial-cell migration assay of conditioned media (CM) derived from normal renal tubular cells and RCC cell lines. CM from normal renal tubular cells does not stimulate migration and partially inhibits migration induced by bFGF and CM from RCC cells. In the presence of neutralizing antibody to TSP-1, which had no effect when tested alone, CM from normal renal tubular cells is no longer inhibitory, demonstrating a functional role for this inhibitor. These results were confirmed in the corneal neovascularization assay (71).

systems have been very encouraging, as antiangiogenic agents such as angiostatin and endostatin have held tumors in a dormant state for prolonged periods of time, and in some cases complete remission of disease has been achieved (26,88,89). Although clinical evaluation of antiangiogenic agents is still in its infancy, some definite successes have been reported. Interferon alpha has proven to be very effective for the management of life-threatening pediatric hemangiomas, and improved response rates have been reported for some adult cancers, such as squamous-cell carcinoma of the skin and cervix (3,27,90). Hopes are high for the most recent generation of antiangiogenic agents, many of which are orders of magnitude more potent than their predecessors (91). Purified, active preparations of endostatin are now available, which entered clinical trials in the autumn of 1999.

Prior studies suggest that metastatic RCC, which is notoriously chemoresistant, may be susceptible to antiangiogenic therapies (92,93). Interferon alpha,

which is commonly used along with IL-2 to treat this patient population, has yielded 15–20% response rates, even when tested as monotherapy (92,93). However, the contribution of interferon's antiangiogenic effects relative to its immunological effects has not been established. Motzer and colleagues reported a 30% response rate for 43 patients treated with interferon alpha in combination with another antiangiogenic agent, 13-*cis* retinoic acid, but again, both agents have pleiotropic effects and their mechanism of action in this setting has not been defined (94). In a more focused approach, TNP-470 yielded one partial response and six patients with stabilization of disease among 20 patients with metastatic RCC (95). Oral linomide, an antibiotic with antiangiogenic effects, has been tested in two recent European Organization for Research and Treatment of Cancer (EORTC) studies, demonstrating limited efficacy (96,97). Thirty percent of patients experienced stabilization of disease, but there were no partial or complete responders, and therapy was poorly tolerated, with 40% of patients requiring dose reduction or withdrawal from therapy.

Ongoing antiangiogenic protocols for the management of advanced RCC are using IL-12, thalidomide, squalamine, TNP-470, bryostatin, a matrix metalloproteinase inhibitor, and monoclonal antibodies to VEGF. Information about these studies, including study sites and inclusion criteria, can be obtained on the website for the Kidney Cancer Association (www.nkca.org) and the National Cancer Institute (<http://cancertrials.nci.nih.gov>). Future studies will test endostatin, angiostatin, and a variety of innovative approaches to target VEGF, which appears to be the primary inducer in this cancer.

Our institution will soon be initiating a protocol designed to generate angiostatin *in vivo*, obviating the need for *ex vivo* production, which has proven to be very challenging. Proper tertiary folding of angiostatin—which represents an internal domain of plasminogen and plasmin—is required for its activity, and has been difficult to reproduce *in vitro*. Soff and colleagues, who are spearheading this effort, have shown that plasmin can cleave itself to yield active angiostatin, and this process can be accelerated in the presence of sulfhydryl donors (98). Patients will thus be treated with urokinase or tissue plasminogen activator (TPA) to generate plasmin, along with a sulfhydryl donor such as captopril. The levels of angiostatin and immunologically related proteins in the serum will be monitored by Western blot, as they may represent a surrogate marker of activity. Experiments in animal tumor models and limited clinical experience with other cancers have demonstrated activity with this protocol, which takes advantage of commonly used medications and should be well-tolerated.

It is important to maintain a proper perspective about such novel forms of therapy, especially given the refractory nature of RCC. Most likely, antiangiogenic therapies will need to be integrated with conventional treat-

ments such as chemotherapy or immunotherapy to optimize results. There is a strong theoretical basis for doing so, as antiangiogenic agents have proven to be synergistic with cytotoxic therapies in animal models (**99,100**). The focus thus far has naturally been on patients with metastatic disease, but the rationale for using antiangiogenic therapy for adjuvant (patients with high-risk disease after surgery) or chemopreventative (patients with VHL disease or known gene mutations) purposes may be even stronger.

Antiangiogenic therapy appears to be particularly well-suited for the management of RCC, one of the most vascular of malignancies. Improved knowledge of the factors regulating angiogenesis in this cancer, including the role of endogenous inhibitors, should suggest new and improved ways to block the tumor vasculature. Integration of antiangiogenic approaches with conventional forms of therapy will most likely be required to optimize outcomes for patients with or at risk for recurrence of RCC.

2. Materials

2.1. Preparation of Conditioned Media and Pellets for Use in the Corneal Neovascularization Assay

A variety of substances including tissue fragments, cell extracts, or conditioned media can be investigated, but we prefer conditioned media that has been concentrated and dialyzed, as its angiogenic activity is more readily quantifiable for comparative purposes (**29,82**).

1. We grow 2–3 100-mm plates of cells to near confluence.
2. Rinse three times with phosphate-buffered saline (PBS), incubate in DME without serum for 8 h to remove adsorbed growth factors.
3. Incubate in fresh DME without serum for 48–72 h.
4. Viability of the cells is confirmed and the conditioned media is harvested and concentrated and dialyzed into PBS by filter centrifugation using an Ultrafree filter device with a nominal molecular weight exclusion of M_r 5000 (Millipore, Bedford, MA).
5. Concentration of 50–100-fold is readily obtained, and facilitates subsequent assay of the media.
6. Conditioned media or other test substances are mixed 1-1 with poly-2-hydroxyethylmethacrylate (Hydron, Interferon Sciences, New Brunswick, NJ), a slow-release noninflammatory polymer, which is prepared as a 12% solution (w/v) in absolute ethanol.
7. Ten μ L of the above mix in **step 6** is pipetted onto the surface of a sterile 3.2-mm-diameter Teflon peg (Du Pont, Wilmington, DE).
8. Mix is allowed to solidify over 2 h in a sterile environment.
9. This yields a 2.0–2.5-mm-diameter disk that can be stored at 4°C for later use in the assay.

3. Methods

The switch from an antiangiogenic to an angiogenic phenotype during tumor development can result from increased expression of proangiogenic substances or downregulation of endogenous inhibitors, or a combination of both mechanisms (1,7). The identification and characterization of endogenous inhibitors produced by various organ systems represents an important priority, as such inhibitors may provide increased efficacy for blocking the growth of tumors derived from that organ, and are likely to be well-tolerated. A wide variety of both in vitro and in vivo assays can be used to assess for angioinhibitory activity, with each presenting distinct advantages or disadvantages in terms of technical expertise required, reliability, cost, temporal characteristics, and ability to quantify relative levels of inhibitory activity (81). The chorioallantoic membrane assay (described in detail in Chapter 17) and chronic transparent chambers such as the dorsal skin chamber and cranial windows in rodents are commonly used, as they provide reliable in vivo assessment of angiogenic activity, but the technical expertise required to conduct these assays is substantial, and quantification of relative angiogenic activities in various samples is difficult (81). We will focus on the endothelial-cell migration and corneal neovascularization assays, as we have found them to be most useful in our studies (29,82).

3.1. Endothelial Cell Migration Assay

We have used the endothelial-cell migration assay for in vitro assessment of angiogenic activity, as it most closely reflects in vivo angiogenic responses and provides useful quantitative information about relative levels of inhibitors or inducers in various samples (29,82). In addition, this assay is relatively inexpensive and animals are not required—practical considerations that contribute to its general utility.

1. Migrations are performed in a modified Boyden chamber using cultured endothelial cells.
2. The selection and condition of the endothelial cells is of critical importance. Important considerations include the source (large vs small vessel), general health and passage in culture, profile of receptor expression, and responsiveness to various growth factors or inhibitors. We have found that the levels of expression of CD36—the receptor for thrombospondin-1, a potent antiangiogenic molecule—can vary considerably depending on culture conditions, passage number, and cell type, ranging between high levels expressed by bovine capillary endothelial cells to undetectable levels expressed by human umbilical-vein endothelial cells (83). Early passage and nontransformed cells should be used, and receptor levels should be assessed if there is any question about responsiveness to various angiogenic mediators.

3. Endothelial cells are grown to confluence and then harvested with trypsin and plated in the lower wells of the chamber, and covered with a gelatinized membrane (5- μ m pore size, Nucleopore Corp., Pleasanton, CA). A single-cell suspension is essential, but is often difficult to achieve depending on the cell type and condition. One helpful maneuver is to gently pass the harvested cells several times through a small-caliber pipet tip to disperse any remaining clusters of cells. The chamber is everted and incubated for 1.5 h at 37°C to facilitate attachment of the cells to the undersurface of the membrane.
4. Conditioned media is then diluted (final concentration = 10–20 μ g/mL) into DME with 0.1% BSA, placed into the upper wells of the chamber, and incubated for 4 h at 37°C.
5. The filters are stained with Diff-Quick stain (American Scientific Products, McGaw Park, IL) and mounted on a glass slide with Permount (Fisher Scientific, Fairlawn, NJ).
6. The number of cells migrating to the top surface of the membrane per 10-high powered fields (100X) are counted. The upper surface of the membrane is readily recognized, since the outlines of the pores are only distinctly visualized on this side.
7. Negative and positive controls include DME with 0.1% BSA and bFGF at 10–20 ng/mL, respectively.
8. To test for inhibition of migration, a test substance or media is mixed at various concentrations with known inducers such as bFGF, VEGF, or conditioned media from cancer cells, and the effect on migration is measured.
9. The migration assay can also be used to determine the functional significance of angiogenic mediators and to quantify angiogenic activity (81,82). The functional relevance of putative inducers or inhibitors is assessed using neutralizing antibodies (typically at 30 μ g/mL, although a titration is preferred to establish an effective concentration). To quantify inductive activity the ED₅₀ (concentration at which half maximal induction occurs) is determined by testing the media at a wide range of concentrations to establish a dose-response curve. This should be performed in the presence of neutralizing antibodies to any functional inhibitors present within the media to reveal the total inductive activity. Similarly, any functional inducers should be blocked to reveal the total inhibitory activity, which can then be titrated to establish the ED₅₀ for inhibition of bFGF-induced migration.

3.2. Corneal Neovascularization Assay

The rat corneal neovascularization assay has been used extensively for in vivo evaluation of angiogenic activity. This assay requires animals, is relatively expensive, takes 8–9 days to conduct, and requires considerable technical expertise. It is best reserved for qualitative evaluation of activity—e.g. to determine whether a given sample is proangiogenic or antiangiogenic in an in vivo setting—and we have used it primarily for confirmation of results derived from the endothelial-cell migration assay (81,82).

1. Inbred F344 rats are anesthetized with metaphane in preparation for formation of a corneal pocket.
2. The eyes are gently proptosed and secured by grasping the lateral skin around the eye with a nontraumatic hemostat.
3. A dissecting microscope is used to facilitate dissection.
4. Local anesthetic is administered (AK-Taine eyedrops) and a 1.5-mm incision is made near the center of the cornea using an 11 blade. The incision should extend to a depth of 1.0 mm, which will be into but not through the stroma of the cornea. The scalpel tip is used to further define the edges of the incision, and an autoclaved, curved iris spatula (1.5 mm in width and 5.0 mm in length) is inserted under one edge and gently rocked and advanced to bluntly develop the corneal pocket.
5. A fragment of the pellet (approximately one-third of the disk) is placed into the pocket using a fine forceps, and the eye is covered with erythromycin ointment.
6. After 1 wk the animals are sacrificed and the eyes are perfused with black ink and harvested for analysis. First, the animals are anesthetized with pentobarbital and metaphane, and a thoracotomy is performed. The left ventricle is catheterized with a 22g Angiocath and the right atrium or superior vena cava is opened to exsanguinate the animal. The circulatory system is then gently flushed with 20–40 cc of PBS followed by 20 cc of India ink.
7. The eyes are enucleated and stored in formalin overnight at 4°C.
8. The following day the corneas are dissected free of adjacent structures, and the iris is removed by gently rubbing the cornea against a paper towel.
9. The cornea is examined under the dissecting microscope, and a photocopy can be made.
10. Ingrowth of vessels from the limbic region into the pellet is considered a positive response.
11. Quantitative analysis of the neovascular response can be performed by measuring the length and number of induced vessels in a systematic manner, but its use for comparative purposes has been debated, and this is clearly not a strength of the assay (82,85).
12. As with the migration assay, inhibition can be assessed by mixing a test sample or conditioned media with a known inducer, and the functional relevance of angiogenic mediators can be evaluated through the use of neutralizing antibodies.

4. Notes

1. Infection of the cultures must be avoided, as many bacterial products such as lipopolysaccharide (LPS) have angiogenic activity. Dialysis or filter centrifugation will inevitably result in a loss of small molecules, which in some cases can have angiogenic activity. If this is a major concern, the media can be tested directly, before concentration and dialysis.
2. Tissue fragments or more sophisticated culture techniques will be required to assess the effects of stromal-epithelial interactions and tumor-infiltrating immune cells on the net angiogenic activity in a given tissue or tumor type.

3. A minimal but effective concentration of inducer should be used when testing for inhibition, as excess inducer can make it difficult to detect antiangiogenic activity. When inhibition of migration is observed, a direct toxic effect on the endothelial cells should be excluded by trypan blue staining of cells treated in a parallel experiment.
4. Neutralizing antibodies should be dialyzed into PBS by filter centrifugation to remove any proangiogenic or inhibitory contaminants, and the specificity and efficacy of each antibody must be confirmed by testing against a panel of known angiogenic mediators.
5. Care should be taken to keep the corneal pocket at least 1.0 mm away from the limbus to avoid false-positive results, which can also occur if the pocket extends too deep into the substance of the cornea. Other common sources of false positives are infection or inflammation, which can develop if extensive or awkward dissection is performed. The initial incision into the cornea is extremely important, as it facilitates all subsequent steps involved in creating the pocket. A new scalpel should be used. The iris spatula should be resharpener before each session, and all instruments should be autoclaved before use. When perfusing the animals with saline or ink, one must proceed gently to avoid rupturing the fragile capillary beds in the nasal region, or they will become the path of least resistance, making it more difficult to adequately perfuse the corneas. In addition, many of the caveats about neutralizing antibodies and experimental controls necessary for reliable conduct of the migration assay also apply to the corneal assay.

References

1. Bouck, N., Stellmach, V., and Hsu, S. C. (1996) How tumors become angiogenic. *Adv. Cancer Res.* **69**, 135–174.
2. Folkman, J. (1995) Angiogenesis in cancer, vascular, rheumatoid and other disease. *Nat. Med.* **1**(1), 27–31.
3. Folkman, J. (1995) Tumor Angiogenesis, in *Tumor Angiogenesis* (Mendelson, J., Howley, P. M., Israel, M. A., Liotta, L. A., eds.), W.B. Saunders, Philadelphia, pp. 206–232.
4. Varner, J. A. and Cheresh, D. A. (1996) Tumor angiogenesis and the role of vascular cell integrin $\alpha\beta 3$. *Important Adv. Oncol.* 69–87.
5. Carmeliet, P., Lampugnani, M. G., Moons, L., Breviario, F., Compernelle, V., Bono, F., et al. (1999) Targeted deficiency or cytosolic truncation of the VE-cadherin gene in mice impairs VEGF-mediated endothelial survival and angiogenesis. *Cell* **98**(2), 147–157.
6. Polverini, P. J. (1995) The pathophysiology of angiogenesis. *Crit. Rev. Oral Biol. Med.* **6**(3), 230–247.
7. Hanahan, D. and Folkman, J. (1996) Patterns and emerging mechanisms of the angiogenic switch during tumorigenesis. *Cell* **86**(3), 353–364.
8. Bussolino, F., Albini, A., Camussi, G., Presta, M., Viglietto, G., Ziche, M., et al. (1996) Role of soluble mediators in angiogenesis. *Eur. J. Cancer* **32A**(14), 2401–2412.

9. Ferrara, N. (1996) Vascular endothelial growth factor. *Eur. J. Cancer* **32A(14)**, 2413–2422.
10. Hanahan, D. (1997) Signaling vascular morphogenesis and maintenance. *Science* **277(5322)**, 48–50.
11. Maisonpierre, P. C., Suri, C., Jones, P. F., Bartunkova, S., Wiegand, S. J., Radziejewski, C., et al. (1997) Angiopoietin-2, a natural antagonist for Tie2 that disrupts in vivo angiogenesis. *Science* **277(5322)**, 55–60.
12. Suri, C., Jones, P. F., Patan, S., Bartunkova, S., Maisonpierre, P. C., Davis, S., et al. (1996) Requisite role of angiopoietin-1, a ligand for the TIE2 receptor, during embryonic angiogenesis. *Cell* **87(7)**, 1171–1180.
13. Folkman, J., Klagsbrun, M., Sasse, J., Wadzinski, M., Ingber, D., and Vlodavsky, I. (1988) A heparin-binding angiogenic protein-basic fibroblast growth factor is stored within basement membrane. *Am. J. Pathol.* **130(2)**, 393–400.
14. Sunderkotter, C., Goebeler, M., Schulze-Osthoff, K., Bhardwaj, R., and Sorg, C. (1991) Macrophage-derived angiogenesis factors. *Pharmacol. Ther.* **51(2)**, 195–216.
15. Takebayashi, Y., Aklyama, S., Yamada, K., Akiba, S., and Aikou, T. (1996) Angiogenesis as an unfavorable prognostic factor in human colorectal carcinoma. *Cancer* **78(2)**, 226–231.
16. Gasparini, G. (1996) Clinical significance of the determination of angiogenesis in human breast cancer: update of the biological background and overview of the Vicenza studies. *Eur. J. Cancer* **32A(14)**, 2485–2493.
17. Weidner, N., Semple, J. P., Welch, W. R., and Folkman, J. (1991) Tumor angiogenesis and metastasis-correlation in invasive breast carcinoma. *N. Engl. J. Med.* **324(1)**, 1–8.
18. Craft, P. S. and Harris, A. L. (1994) Clinical prognostic significance of tumour angiogenesis. *Ann. Oncol.* **5(4)**, 305–311.
19. Sidky, Y. A. and Borden, E. C. (1987) Inhibition of angiogenesis by interferons: effects on tumor- and lymphocyte-induced vascular responses. *Cancer Res.* **47(19)**, 5155–5161.
20. Volpert, O. V., Tolsma, S. S., Pellerin, S., Feige, J. J., Chen, H., Mosher, D. F., et al. (1995) Inhibition of angiogenesis by thrombospondin-2. *Biochem. Biophys. Res. Commun.* **217(1)**, 326–332.
21. Good, D. J., Polverini, P. J., Rastinejad, F., Le Beau, M. M., Lemons, R. S., Frazier, W. A., et al. (1990) A tumor suppressor-dependent inhibitor of angiogenesis is immunologically and functionally indistinguishable from a fragment of thrombospondin. *Proc. Natl. Acad. Sci. USA*, **87(17)**, 6624–6628.
22. Cozzolino, F., Torcia, M., Aldinucci, D., Ziche, M., Almerigogna, F., Bani, D., et al. (1990) Interleukin 1 is an autocrine regulator of human endothelial cell growth. *Proc. Natl. Acad. Sci. USA* **87(17)**, 6487–6491.
23. Voest, E. E., Kenyon, B. M., O'Reilly, M. S., Truitt, G., D'Amato, R. J., and Folkman, J. (1995) Inhibition of angiogenesis in vivo by interleukin 12. *J. Natl. Cancer Inst.* **87(8)**, 581–586.
24. Volpert, O. V., Fong, T., Koch, A. E., Peterson, J. D., Waltenbaugh, C., Tepper, R. I., et al. (1998) Inhibition of angiogenesis by interleukin 4. *J. Exp. Med.* **188(6)**, 1039–1046.

25. O'Reilly, M. S., Holmgren, L., Shing, Y., Chen, C., Rosenthal, R. A., Moses, M., et al. (1994) Angiostatin: a novel angiogenesis inhibitor that mediates the suppression of metastases by a Lewis lung carcinoma. *Cell* **79**(2), 315–328.
26. Boehm, T., Folkman, J., Browder, T., and O'Reilly, M. S. (1997) Antiangiogenic therapy of experimental cancer does not induce acquired drug resistance. *Nature* **390**(6658), 404–407.
27. O'Reilly, M. S., Boehm, T., Shing, Y., Fukai, N., Vasios, G., Lane, W. S., et al. (1997) Endostatin: an endogenous inhibitor of angiogenesis and tumor growth. *Cell* **88**(2), 277–285.
28. Volpert, O. V., Dameron, K. M., and Bouck, N. (1997) Sequential development of an angiogenic phenotype by human fibroblasts progressing to tumorigenicity. *Oncogene* **14**(12), 1495–1502.
29. Campbell, S. C., Volpert, O. V., Ivanovich, M., and Bouck, N. P. (1998) Molecular mediators of angiogenesis in bladder cancer. *Cancer Res.* **58**(6), 1298–1304.
30. Hsu, S. C., Volpert, O. V., Steck, P. A., Mikkelsen, T., Polverini, P. J., Rao, S., et al. (1996) Inhibition of angiogenesis in human glioblastomas by chromosome 10 induction of thrombospondin-1. *Cancer Res.* **56**(24), 5684–5691.
31. Kusaka, M., Sudo, K., Fujita, T., Marui, S., Itoh, F., Ingber, D., et al. (1991) Potent anti-angiogenic action of AGM-1470: comparison to the fumagillin parent. *Biochem. Biophys. Res. Commun.* **174**(3), 1070–1076.
32. Sills, A. K., Jr., Williams, J. I., Tyler, B. M., Epstein, D. S., Sipos, E. P., Davis, J. D., et al. (1998) Squalamine inhibits angiogenesis and solid tumor growth in vivo and perturbs embryonic vasculature. *Cancer Res.* **58**(13), 2784–2792.
33. Zhou, O., Arnold, C., and Ritter, M. R. (1998) Contortrostatin, a snake venom disintegrin, is an inhibitor of angiogenesis, in *Angiogenesis and Cancer* (Folkman, J. and Klagsbrun, M., eds.), AACR Special Conference in Cancer Research, (abstract) pp. B74.
34. Lingen, M. W., Polverini, P. J., and Bouck, N. P. (1996) Retinoic acid induces cells cultured from oral squamous cell carcinomas to become anti-angiogenic. *Am. J. Pathol.* **149**(1), 247–258.
35. Oikawa, T., Hirotani, K., Ogasawara, H., Katayama, T., Nakamura, O., Iwaguchi, T., et al. (1990) Inhibition of angiogenesis by vitamin D3 analogues [published erratum appears in *Eur. J. Pharmacol.* 1990 Jul 17; **182**(3), 616]. *Eur. J. Pharmacol.* **178**(2), 247–250.
36. Fotsis, T., Pepper, M., Adlercreutz, H., Fleischmann, G., Hase, T., Montesano, R., et al. (1993) Genistein, a dietary-derived inhibitor of in vitro angiogenesis. *Proc. Natl. Acad. Sci. USA*, **90**(7), 2690–2694.
37. Peterson, H. I. (1986) Tumor angiogenesis inhibition by prostaglandin synthetase inhibitors. *Anticancer Res.* **6**(2), 251–253.
38. Volpert, O. V., Ward, W. F., Lingen, M. W., Chesler, L., Solt, D. B., Johnson, M. D., et al. (1996) Captopril inhibits angiogenesis and slows the growth of experimental tumors in rats. *J. Clin. Invest.* **98**(3), 671–679.
39. D'Amato, R. J., Loughnan, M. S., Flynn, E., and Folkman, J. (1994) Thalidomide is an inhibitor of angiogenesis. *Proc. Natl. Acad. Sci. USA* **91**(9), 4082–4085.

40. Tamargo, R. J., Bok, R. A., and Brem, H. (1991) Angiogenesis inhibition by minocycline. *Cancer Res.* **51**(2), 672–675.
41. Vukanovic, J., Passaniti, A., Hirata, T., Traystman, R. J., Hartley-Asp, B., and Isaacs, J. T. (1993) Antiangiogenic effects of the quinoline-3-carboxamide linomide. *Cancer Res.* **53**(8), 1833–1837.
42. Oikawa, T., Hirotani, K., Ogasawara, H., Katayama, T., Ashino-Fuse, H., Shimamura, M., et al. (1990) Inhibition of angiogenesis by bleomycin and its copper complex. *Chem. Pharm. Bull. (Tokyo)* **38**(6), 1790–1792.
43. Burt, H. M., Jackson, J. K., Bains, S. K., Liggins, R. T., Oktaba, A. M., Arsenault, A. L., et al. (1995) Controlled delivery of taxol from microspheres composed of a blend of ethylene-vinyl acetate copolymer and poly (d,l-lactic acid). *Cancer Lett.* **88**(1), 73–79.
44. Klauber, N., Parangi, S., Flynn, E., Hamel, E., and D'Amato, R. J. (1997) Inhibition of angiogenesis and breast cancer in mice by the microtubule inhibitors 2-methoxyestradiol and taxol. *Cancer Res.* **57**(1), 81–86.
45. Milas, L., Hunter, N., Furuta, Y., Nishiguchi, I., and Runkel, S. (1991) Antitumour effects of indomethacin alone and in combination with radiotherapy: role of inhibition of tumour angiogenesis. *Int. J. Radiat. Biol.* **60**(1–2), 65–70.
46. Lang, E. K. (1973) Proceedings: arteriography in the diagnosis and staging of hypernephromas. *Cancer* **32**(5), 1043–1052.
47. Yoshino, S., Kato, M., and Okada, K. (1995) Prognostic significance of microvessel count in low stage renal cell carcinoma. *Int. J. Urol.* **2**(3), 156–160.
48. Nativ, O., Sabo, E., Reiss, A., Wald, M., Madjar, S., and Moskovitz, B. (1998) Clinical significance of tumor angiogenesis in patients with localized renal cell carcinoma. *Urology* **51**(5), 693–696.
49. Delahunt, B., Bethwaite, P. B., and Thornton, A. (1997) Prognostic significance of microscopic vascularity for clear cell renal cell carcinoma. *Br. J. Urol.* **80**(3), 401–404.
50. Gelb, A. B., Sudilovsky, D., Wu, C. D., Weiss, L. M., and Medeiros, L. J. (1997) Appraisal of intratumoral microvessel density, MIB-1 score, DNA content, and p53 protein expression as prognostic indicators in patients with locally confined renal cell carcinoma. *Cancer* **80**(9), 1768–1775.
51. Vermeulen, P. B., Gasparini, G., Fox, S. B., Toi, M., Martin, L., McCulloch, P., et al. (1996) Quantification of angiogenesis in solid human tumours: an international consensus on the methodology and criteria of evaluation. *Eur. J. Cancer* **32A**(14), 2474–2484.
52. Weidner, N. (1995) Current pathologic methods for measuring intratumoral microvessel density within breast carcinoma and other solid tumors. *Breast Cancer Res. Treat.* **36**(2), 169–180.
53. Miyake, H., Hara, I., Yoshimura, K., Eto, H., Arakawa, S., Wada, S., et al. (1996) Introduction of basic fibroblast growth factor gene into mouse renal cell carcinoma cell line enhances its metastatic potential. *Cancer Res.* **56**(10), 2440–2445.

54. Dhanabal, M., Ramchandran, R., Volk, R., Stillman, I.E., Lombardo, M., Iruela-Arispe, M. L., et al. (1999) Endostatin: yeast production, mutants, and antitumor effect in renal cell carcinoma. *Cancer Res.* **59**(1), 189–197.
55. Tan, J., Newton, C. A., Djeu, J. Y., Gutsch, D. E., Chang, A. E., Yang, N. S., et al. (1996) Injection of complementary DNA encoding interleukin-12 inhibits tumor establishment at a distant site in a murine renal carcinoma model. *Cancer Res.* **56**(15), 3399–3403.
56. Fujioka, T., Hasegawa, M., Ogiu, K., Matsushita, Y., Sato, M., and Kubo, T. (1996) Antitumor effects of angiogenesis inhibitor O-(chloroacetyl-carbamoyl) fumagillol (TNP-470) against murine renal cell carcinoma. *J. Urol.* **155**(5), 1775–1778.
57. Morita, T., Shinohara, N., and Tokue, A. (1994) Antitumour effect of a synthetic analogue of fumagillin on murine renal carcinoma. *Br. J. Urol.* **74**(4), 416–421.
58. Choi, H. R., Kim, S. C., Moon, W.-C. (1995) Inhibition of tumor growth and metastasis of renal cell carcinoma by angiogenesis inhibitor TNP-470. *Proc. Am. Urol. Assoc. (Suppl.)* **153**, 402A.
59. Fujioka, T., Hasegawa, M., Ishikura, K., Matsushita, Y., Sato, M., and Tanji, S. (1998) Inhibition of tumor growth and angiogenesis by vitamin D3 agents in murine renal cell carcinoma. *J. Urol.* **160**(1), 247–251.
60. Yanase, M., Sasamura, H., Takahashi, A., Miyao N., Masumori, N., Shigyo, M., Oda, T., Tsukamoto, T. (1997) Genistein inhibits the growth and expression of angiogenic factors in human renal cell carcinoma. *Br. J. Urol.*(Suppl. 2), **80**, 486.
61. Hii, S.I., Nicol, D. L., Gotley, D. C., Thompson, L. C., Green, M. K., and Jonsson, J. R. (1998) Captopril inhibits tumour growth in a xenograft model of human renal cell carcinoma. *Br. J. Cancer* **77**(6), 880–883.
62. Schirner, M., Hoffmann, J., Menrad, A., and Schneider, M. R. (1998) Antiangiogenic chemotherapeutic agents: characterization in comparison to their tumor growth inhibition in human renal cell carcinoma models. *Clin. Cancer Res.* **4**(5), 1331–1336.
63. Takahashi, A., Sasaki, H., Kim, S. J., Tobisu, K., Kakizoe, T., Tsukamoto, T., et al. (1994) Markedly increased amounts of messenger RNAs for vascular endothelial growth factor and placenta growth factor in renal cell carcinoma associated with angiogenesis. *Cancer Res.* **54**(15), 4233–4237.
64. Brown, L. F., Berse, B., Jackman, R. W., Tognazzi, K., Manseau, E. J., Dvorak, H. F., et al. (1993) Increased expression of vascular permeability factor (vascular endothelial growth factor) and its receptors in kidney and bladder carcinomas. *Am. J. Pathol.* **143**(5), 1255–1262.
65. Siemeister, G., Weindel, K., Mohrs, K., Barleon, B., Martiny-Baron, G., and Marme, D. (1996) Reversion of deregulated expression of vascular endothelial growth factor in human renal carcinoma cells by von Hippel-Lindau tumor suppressor protein. *Cancer Res.* **56**(10), 2299–2301.
66. Tsuchiya, N., Sato, K., Ogawa, O., Sasaki, R., Shimoda, N., Sato, S., Kato, T., (1998) Elevated vascular endothelial growth factor (vegf) and normal level of basic fibroblast growth factor (bFGF) in the sera of patients with renal cell carcinoma. *J. Urol. (Suppl.)* **159**, No.5, 188.

67. Tomisawa, M., Tokunaga, T., Oshika, Y., Tsuchida, T., Fukushima, Y., Sato, H., et al. (1999) Expression pattern of vascular endothelial growth factor isoform is closely correlated with tumour stage and vascularisation in renal cell carcinoma. *Eur. J. Cancer* **35(1)**, 133–137.
68. Gnarra, J. R., Zhou, S., Merrill, M. J., Wagner, J. R., Krumm, A., Papavassiliou, E., et al. (1996) Post-transcriptional regulation of vascular endothelial growth factor mRNA by the product of the VHL tumor suppressor gene. *Proc. Natl. Acad. Sci. USA* **93(20)**, 10589–10594.
69. Iliopoulos, O., Levy, A. P., Jiang, C., Kaelin, W. G., Jr., and Goldberg, M. A. (1996) Negative regulation of hypoxia-inducible genes by the von Hippel-Lindau protein. *Proc. Natl. Acad. Sci. USA* **93(20)**, 10595–10599.
70. Steinberg, A. P., Chevrette, M., Duguid, W. P., Guy, L. Tanguay, S. (1998) VEGF expression in renal cell carcinoma. *J. Urol. (Suppl.)* **159, No.5**, 193.
71. Smith, N. D., Ivanovich, M., Bouck, N., and Campbell, S. C. (1999) Molecular mediators of angiogenesis in renal cell carcinoma. *J. Urol. (Suppl.)* **161(4)**, 137.
72. Fujimoto, K., Ichimori, Y., Kakizoe, T., Okajima, E., Sakamoto, H., Sugimura, T., et al. (1991) Increased serum levels of basic fibroblast growth factor in patients with renal cell carcinoma. *Biochem. Biophys. Res. Commun.* **180(1)**, 386–392.
73. Duensing, S., Grosse, J., and Atzpodien, J. (1995) Increased serum levels of basic fibroblast growth factor (bFGF) are associated with progressive lung metastases in advanced renal cell carcinoma patients. *Anticancer Res.* **15(5B)**, 2331–2333.
74. Nanus, D. M., Leung, A., Hutchinson, B., Brown, K. T., Lotan, R., Reuter, V. E., Motzer, R. J. (1997) Analysis of retinoid acid receptor beta (rar-beta) expression, angiogenesis and apoptosis in tumor specimens from patients with renal cell carcinoma treated with interferon alfa-2A and 13-CIS-retinoic acid: correlation with response. *J. Urol.* **157, No. 4**, 277.
75. Singh, R. K., Bucana, C. D., Gutman, M., Fan, D., Wilson, M. R., and Fidler, I. J. (1994) Organ site-dependent expression of basic fibroblast growth factor in human renal cell carcinoma cells. *Am. J. Pathol.* **145(2)**, 365–374.
76. Wunderlich, H., Steiner, T., Junker, U., Knofel, B., Schlichter, A., and Schubert, J. (1997) Serum transforming growth factor-beta1 in patients with renal cell carcinoma. *J. Urol.* **157(5)**, 1602–1603.
77. Petri, E., Feil, G., Wechsel, H. W., Bichler, and K.-H., (1997) Induction of angiogenesis in renal cell carcinoma (RCC)? Investigation of regulatory cytokines and control mechanism in vivo and in vitro. *J. Urol. (Suppl.)* **157, No. 4**, 377.
78. Petri, E., Wechsel, H. W., Feil, G., and Bichler, K.-H. (1997) Systemic elevation and implication for physiology of hepatocyte growth factor/scatter factor (HGF/SF) in renal cell carcinoma (RCC). *J. Urol. (Suppl.)* **157, No. 4**, 377.
79. Kano, M., Horie, S., Nakamura, K., Okui, N., and Kawabe, K. (1995) Quantification of hepatocyte growth factor (HGF) gene expression in renal cell carcinoma (RCC). *Proc. Am. Urol. Assoc. (Suppl.)* **153**, 496A.
80. Imazano, Y., Takebayashi, Y., Nishiyama, K., Akiba, S., Miyadera, K., Yamada, Y., et al. (1997) Correlation between thymidine phosphorylase expression and prognosis in human renal cell carcinoma. *J. Clin. Oncol.* **15(7)**, 2570–2578.

81. Jain, R. K., Schlenger, K., Hockel, M., and Yuan, F. (1997) Quantitative angiogenesis assays: progress and problems. *Nat. Med.* **3**(11), 1203–1208.
82. Polverini, P. J., Bouck, N. P., and Rastinejad, F. (1991) Assay and purification of naturally occurring inhibitor of angiogenesis. *Methods Enzymol.* **198**, 440–450.
83. Dawson, D. W., Pearce, S. F., Zhong, R., Silverstein, R. L., Frazier, W. A., and Bouck, N. P. (1997) CD36 mediates the in vitro inhibitory effects of thrombospondin-1 on endothelial cells. *J. Cell Biol.* **138**(3), 707–717.
84. Kugler, A., Hemmerlein, B., Thelen, P., Kallerhoff, M., Radzun, H. J., and Ringert, R. H. (1998) Expression of metalloproteinase 2 and 9 and their inhibitors in renal cell carcinoma. *J. Urol.* **160**(5), 1914–1918.
85. Sholley, M. M., Ferguson, G. P., Seibel, H. R., Montour, J. L., and Wilson, J. D. (1984) Mechanisms of neovascularization. Vascular sprouting can occur without proliferation of endothelial cells. *Lab. Invest.* **51**(6), 624–634.
86. Lieubeau-Teillet, B., Rak, J., Jothy, S., Iliopoulos, O., Kaelin, W., and Kerbel, R. S. (1998) von Hippel-Lindau gene-mediated growth suppression and induction of differentiation in renal cell carcinoma cells grown as multicellular tumor spheroids. *Cancer Res.* **58**(21), 4957–4962.
87. Gorospe, M., Egan, J. M., Zbar, B., Lerman, M., Geil, L., Kuzmin, I., et al. (1999) Protective function of von Hippel-Lindau protein against impaired protein processing in renal carcinoma cells. *Mol. Cell Biol.* **19**(2), 1289–1300.
88. Holmgren, L., O'Reilly, M. S., and Folkman, J. (1995) Dormancy of micrometastases: balanced proliferation and apoptosis in the presence of angiogenesis suppression. *Nat. Med.* **1**(2), 149–153.
89. O'Reilly, M. S., Holmgren, L., Chen, C., and Folkman, J. (1996) Angiostatin induces and sustains dormancy of human primary tumors in mice. *Nat. Med.* **2**(6), 689–692.
90. Lippman, S. M., Parkinson, D. R., Itri, L. M., Weber, R. S., Schantz, S. P., Ota, D. M., et al. (1992) 13-cis-retinoic acid and interferon alpha-2a: effective combination therapy for advanced squamous cell carcinoma of the skin. *J. Natl. Cancer Inst.* **84**(4), 235–241.
91. Dawson, D. W., Volpert, O. V., Gillis, P., Crawford, S. E., Xu, H., Benedict, W., et al. (1999) Pigment epithelium-derived factor: a potent inhibitor of angiogenesis. *Science* **285**(5425), 245–248.
92. Taneja, S. S., Pierce, W., Figlin, R., and Belldgrun, A. (1994) Management of disseminated kidney cancer. *Urol. Clin. N. Am.* **21**(4), 625–637.
93. Figlin, R. A. (1999) Renal cell carcinoma: management of advanced disease. *J. Urol.* **161**(2), 381–387.
94. Motzer, R. J., Schwartz, L., Law, T. M., Murphy, B. A., Hoffman, A. D., Albino, A. P., et al. (1995) Interferon alfa-2a and 13-cis-retinoic acid in renal cell carcinoma: antitumor activity in a phase II trial and interactions in vitro. *J. Clin. Oncol.* **13**(8), 1950–1957.
95. Stadler, W. M., Shapiro, C. L., Sosmann, J., Clark, J., Vogelzang, N. J., and Kuzel, T. (1998) A Multi-Institutional Study of the Angiogenesis Inhibitor TNP-470 in Metastatic Renal Cell Carcinoma (RCC). *Proc. Am. Soc. Clin. Oncol.* **17**, 310A.

96. Pawinski, A., van Oosterom, A. T., de Wit, R., Fossa, S., Croles, J., Svedberg, A., et al. (1997) An EORTC phase II study of the efficacy and safety of linomide in the treatment of advanced renal cell carcinoma. *Eur. J. Cancer* **33(3)**, 496–499.
97. de Wit, R., Pawinsky, A., Stoter, G., van Oosterom, A. T., Fossa, S. D., Paridaens, R., et al. (1997) EORTC phase II study of daily oral linomide in metastatic renal cell carcinoma patients with good prognostic factors. *Eur. J. Cancer* **33(3)**, 493–495.
98. Gately, S., Twardowski, P., Stack, M. S., Cundiff, D. L., Grella, D., Castellino, F. J., et al. (1997) The mechanism of cancer-mediated conversion of plasminogen to the angiogenesis inhibitor angiostatin. *Proc. Natl. Acad. Sci. USA* **94(20)**, 10,868–10,872.
99. Teicher, B. A., Sotomayor, E. A., and Huang, Z. D. (1992) Antiangiogenic agents potentiate cytotoxic cancer therapies against primary and metastatic disease. *Cancer Res.* **52(23)**, 6702–6704.
100. Teicher, B. A., Holden, S. A., Ara, G., Sotomayor, E. A., Huang, Z. D., Chen, Y. N., et al. (1994) Potentiation of cytotoxic cancer therapies by TNP-470 alone and with other anti-angiogenic agents. *Int. J. Cancer* **57(6)**, 920–925.
101. Maione, T. E., Gray, G. S., Petro, J., Hunt, A. J., Donner, A. L., Bauer, S. I., et al. (1990) Inhibition of angiogenesis by recombinant human platelet factor-4 and related peptides. *Science* **247(4938)**, 77–79.
102. Hirata, S., Matsubara, T., Saura, R., Tateishi, H., and Hirohata, K. (1989) Inhibition of in vitro vascular endothelial cell proliferation and in vivo neovascularization by low-dose methotrexate. *Arthritis Rheum.* **32(9)**, 1065–1073.
103. Fajardo, L. F., Prionas, S. D., Kowalski, J., and Kwan, H. H. (1988) Hyperthermia inhibits angiogenesis. *Radiat. Res.* **114(2)**, 297–306.
104. Gagliardi, A. and Collins, D. C. (1993) Inhibition of angiogenesis by antiestrogens. *Cancer Res.* **53(3)**, 533–535.
105. Stein, C. A. (1993) Suramin: a novel antineoplastic agent with multiple potential mechanisms of action. *Cancer Res.* **53**, 2239–2248.
106. Twardowski, P. and Gradishar, W. J. (1997) Clinical trials of antiangiogenic agents. *Curr. Opin. Oncol.* **9(6)**, 584–589.
107. Pluda, J. M. (1997) Tumor-associated angiogenesis: mechanisms, clinical implications, and therapeutic strategies. *Semin. Oncol.* **24(2)**, 203–218.
108. Brooks, P. C., Montgomery, A. M., Rosenfeld, M., Reisfeld, R. A., Hu, T., Klier, G., et al. (1994) Integrin alpha v beta 3 antagonists promote tumor regression by inducing apoptosis of angiogenic blood vessels. *Cell* **79(7)**, 1157–1164.
109. Ingber, D. and Folkman, J. (1988) Inhibition of angiogenesis through modulation of collagen metabolism. *Lab Invest.* **59(1)**, 44–51.
110. Kim, K. J., Li, B., Winer, J., Armanini, M., Gillett, N., Phillips, H. S., et al. (1993) Inhibition of vascular endothelial growth factor-induced angiogenesis suppresses tumour growth in vivo. *Nature* **362(6423)**, 841–844.
111. Claffey, K. P., Brown, L. F., del Aguila, L. F., Tognazzi, K., Yeo, K. T., Manseau, E. J., et al. (1996) Expression of vascular permeability factor/vascular endothelial growth factor by melanoma cells increases tumor growth, angiogenesis, and experimental metastasis. *Cancer Res.* **56(1)**, 172–181.

112. Goldman, C. K., Kendall, R. L., Cabrera, G., Soroceanu, L., Heike, Y., Gillespie, G. Y., et al. (1998) Paracrine expression of a native soluble vascular endothelial growth factor receptor inhibits tumor growth, metastasis, and mortality rate. *Proc. Natl. Acad. Sci. USA* **95**(15), 8795–8800.
113. Lin, P., Sankar, S., Shan, S., Dewhirst, M. W., Polverini, P. J., Quinn, T. Q., et al. (1998) Inhibition of tumor growth by targeting tumor endothelium using a soluble vascular endothelial growth factor receptor. *Cell Growth Differ.* **9**(1), 49–58.
114. Vajkoczy, P., Menger, M. D., and Vollmar, B. (1998) Effect of the Flk-1 antagonist SU5416 on tumor growth, angiogenesis and microhemodynamics (abstract). *Proc. Am. Assoc. Cancer Res.* **39**, 96.
115. Dupont, E., Alaoui-Jamal, M., and Wang, T. (1998) Angiostatic and antitumoral activity of AE-914 (Neovastat), a molecular fraction derived from shark cartilage (abstract). *Proc. Am. Assoc. Cancer Res.* **38**, 227.
116. Nasuda, S., Hayasha, H., and Arakis, S. (1998) Two vascular apoptosis inducing proteins from a snake venom are members of the metalloproteinase/disintegrin family. *Eur. J. Biochem.* **253**, 36–41.
117. Nanus, D. M., Schmitz-Drager, B. J., Motzer, R. J., Lee, A. C., Vlamis, V., Cordon-Cardo, C., et al. (1993) Expression of basic fibroblast growth factor in primary human renal tumors: correlation with poor survival. *J. Natl. Cancer Inst.* **85**(19), 1597–1599.
118. Cheng, S. Y., Huang, H. J., Nagane, M., et al. (1998) Suppression of glioblastoma angiogenicity and tumorigenicity by inhibition of endogenous expression of vascular endothelial growth factor. *Proc. Natl. Acad. Sci. USA* **93**, 8502–8507.

Interferon Alpha, GM-CSF–Activated T Cells, and IL-6 in Renal Cell Carcinoma

Belur Patel and Arie Belldegrun

1. Introduction

Treatment of renal cell carcinoma (RCC) has historically involved surgical removal of the primary tumor when localized, but when presented with metastatic disease the options have been limited. Approximately 30% of patients present with metastatic disease implicating a generally poor prognosis. The most significant advances have occurred in the area of immunotherapy as treatment for metastatic disease. This is because RCC is generally resistant to chemotherapy and radiation. One of the major successes of immunotherapy has been with interleukin-2 (IL-2). Initial IL-2 therapy proved difficult due to the significant administrative and side effect problems that occurred. This led to numerous variations in dose scheduling and delivery to identify an optimal beneficial way of administering IL-2. In addition, investigation also led to other immunotherapy agents such as interferon and cellular therapy.

We have worked extensively with various forms of immunotherapy involved with the treatment of RCC, and present some of the protocols developed for this purpose. Some of the basic techniques are those commonly used in cell culture preparation and will not be described in detail.

2. Materials

Materials used in the various sections are fairly standard and can be substituted to perform the technique. The materials listed for each section are those that we used in our laboratory to obtain the desired results, in addition to standard cell and tissue culturing techniques.

2.1. Tumor-Infiltrating Lymphocyte Preparation

1. Hank's balanced salt solution (HBSS).
2. 0.01% Hyaluronidase type V.

3. 0.1% Collagenase type IV.
4. 0.002% Deoxyribonuclease type I (Sigma Chemical Co., St. Louis, MO).
5. Ficoll-Hypaque gradient (LSM, Litton Bionetics, Kensington, MD).
6. Serum-free medium.
7. Human serum albumin.
8. Cell harvester (Stericell System, E. I. DuPont de Nemours and Co., Wilmington, DE).

2.2. GM-CSF Activated T Cells

1. Granulocyte-macrophage colony-stimulating factor.
2. Staining buffer: 1X PBS without calcium and magnesium plus 2% fetal calf serum (FCS) and 0.1% sodium azide, pH 7.3.

2.3. Interleukin-6

1. Complete media (CM):
 - a. For preparation of cell culture from resected tumors (*see Subheading 3.3.2.*): RPMI-1640, 10% FCS, penicillin and streptomycin antibiotic, fungizone (antifungal), and glutamine.
 - b. For measurement of IL-6 levels by B9 bioassay (*see Subheading 3.3.7.*): RPMI-1640, 10% FCS, glutamine, penicillin, streptomycin, 2-mercaptoethanol, and 20 hybridoma growth factor U/mL rIL-6.
2. Recombinant interleukin-6.
3. Recombinant tumor necrosis factor.
4. Recombinant Interferon- γ .
5. Polyclonal goat anti-human IL-6.
6. Biotinylated anti-goat IgG.
7. Peroxidase-conjugated streptavidin.

2.4. Interferon- α

1. Interleukin-2 plasmid.
2. Interferon- α plasmid.
3. Restriction enzymes, NotI, PstI and EcoRI.
4. Vector pGEM3 Sra.neo.
5. G418.
6. Fluorescein isothiocyanate labeled goat anti-mouse antiserum.

3. Methods

Tumor-infiltrating lymphocytes (TIL) are found in large numbers in RCC and have demonstrated efficacy in causing tumor regression. We have also isolated and evaluated the possible improvement in the efficacy of TIL by implementing a select subpopulation of these cells (**I**). This subpopulation consists of CD8(+) TIL which consist of cytotoxic cells capable of mediating immunological destruction of tumor cells. Clinical results demonstrated a complete response in 9.1% of patients and a partial response in 25.5%, with a 65% 1 yr actuarial survival and 43% at 2 yr from the time of nephrectomy.

In this section we describe our method of obtaining and developing TIL for therapeutic use, therefore all techniques require strict adherence to sterile preparation.

3.1. Tumor-Infiltrating Lymphocyte

3.1.1. Tissue Preparation

1. Obtain tumor tissue from resected RCC specimens under sterile conditions.
2. Transport tumor in Hank's balanced salt solution (HBSS).
3. Remove any necrotic, fatty, and normal tissue.
4. Mince remaining tissue into small pieces using surgical blades.
5. Weigh approx 25–50 g of the tissue.

3.1.2. Cell Suspension Preparation

1. Place chopped tissue in a flask containing RPMI-1640 (Biofluids, Rockville, MD) with no serum for digestion.
2. To the flask also add:
 - a. 0.01% hyaluronidase type V (1500 U/g).
 - b. 0.1% collagenase type IV (163–230 U/g).
 - c. 0.002% deoxyribonuclease type I (100 U/mg).
3. Mechanically stir for 16–24 h.
4. Filter through sterile steel mesh.
5. Wash twice with HBSS without calcium or magnesium.
6. Separate on differential Ficoll-Hypaque gradient at 900g for 20 min.

3.1.3. Growth of TIL Cell Suspension

1. Wash three suspension three times in cold phosphate-buffered saline (PBS).
2. Separate over a Histopaque 1077 layer (Sigma) at 450g for 35 min to concentrate the viable cells.
3. Wash the cell suspension three times again in PBS.
4. Resuspend cells in 75 mL serum-free media (AIM-V) (Gibco, Chagrin Falls, OH) in standard culture flasks with 400 U/mL of recombinant IL-2 (rIL-2).
5. Incubate flasks at 37°C in 5% CO₂ for approximately 8–10 d. (After 3–4 d you should notice lymphoid cells with progressively decreasing tumor cells.)
6. Harvest the cells from the flasks by gentle shaking and pipetting and then count, use approx $2.5\text{--}5 \times 10^5$ cells/mL.
7. Transfer cells to sterile gas bags and allowed to proliferate.
8. Maintain cells at the above concentration for 3–4 wk, changing media (AIM-V) as needed by checking cells every 2–3 d.
9. Media is supplemented with 1200 U of rIL-2 during each media change.
10. Incubate at 37°C, 5% CO₂, and 95% humidity.

3.1.4. Preparation for Patient Administration

1. Final cell preparation completed by harvesting $1 \times 10^9\text{--}10^6$ cells/mL.
2. Wash cells with 0.9% sterile injectable normal saline (NaCl).
3. Resuspend cells in approx 200 mL of NaCl with 5% human serum albumin and 75,000 U rIL-2.

4. Primed TIL were harvested using the Stericell System (E. I. DuPont de Nemours and Co., Wilmington, DE).
5. Cells are now ready for infusion into patients over 60–90 min.

3.1.5. Preparation of CD8(+) TIL

The initial preparation of TIL is the same as before.

1. Analyze cells with a fluorescence cell sorter until 20% of the cells are CD8(+).
2. Collect 5×10^6 TIL and incubate in tissue culture flasks coated with anti-CD8 mAb. (CELLector CD8 culture flask, Applied Immune Science, Santa Clara, CA).
3. Incubate for 1 h at 37°C, 5% CO₂, and 95% humidity.
4. Wash flasks with PBS and then place culture media.
5. After 2–5 d, bound CD8(+) TIL detach and are collected and harvested as for TIL cell suspension.

Both populations of TIL are grown in sterile gas-permeable bags and are expanded to a concentration of 1×10^9 – 10^{10} cells/mL. These cells are then ready to be transferred to the patient intravenously.

3.1.6. Transfer of TIL to Patients

The preparation of TIL usually requires 4–6 wk and is sufficient time for the patient to recover from surgery.

On the initiation of treatment patients are placed on a protocol consisting of administration of IL-2 and interferon- α -2a (IFN).

1. On d 1–4 each patient received 2×10^6 U/m² on a continuous infusion basis (96 h).
2. IFN was given on days 1 and 4 at a dose of 6×10^6 U/m², intramuscularly, in the evening.
3. TIL were administered intravenously 1 h after the first dose of IL-2 over 60–90 min.
4. Additional medications administered:
 - a. Acetaminophen 650 mg orally every 4 h for temperatures over 38.5°C.
 - b. Indomethacin 25–50 mg orally 30 min after IFN administration.
 - c. Diphenhydramine 25–50 mg orally for rash or pruritis.
 - d. Dephenozylate hydrochloride with atropine sulfate 2.5–5 mg orally for diarrhea.
 - e. Perchloroperazine 10 mg orally for nausea and vomiting.
5. Patients with progressive disease are eligible to receive additional treatment.

3.1.6.1. ALTERNATIVE PROTOCOL

We have also prepared primed TIL cells with low-dose rIL-2 after in vivo priming with IFN.

1. Prior to surgery patients receive 3 million U/m², injected subcutaneously daily for 5 d prior to surgery.
2. A 2-d rest period prior to the actual surgery to allow maximum MHC expression.
3. The TIL cells are generated as before.
4. Supplement cell cultures with 400 U rIL-2 instead of 1200 U.
5. Treatment of patients is the same as described before.

3.2. Granulocyte-Macrophage Colony Stimulating Factor (GM-CSF) Activated T Cells

Granulocyte-macrophage colony-stimulating factor (GM-CSF) is a multilineage glycoprotein cytokine synthesized by a variety of cell types, such as T and B lymphocytes, macrophages, and endothelial cells. Certain solid tumors are also known to express GM-CSF and we have also shown that TIL from RCC releases a wide array of cytokines, including GM-CSF (2). In vitro and in vivo studies demonstrated that GM-CSF is a potent growth factor involved in the host defense mechanisms activating macrophages, which can be nonspecifically cytotoxic for tumor cells in an MHC-independent fashion (3). Specific antitumor immunity has been shown after vaccination with irradiated cells engineered to secrete murine GM-CSF, and secretion of this cytokine upon autologous tumor correlates positively with clinical response in TIL immunotherapy in melanoma patients (4). In addition, GM-CSF can stimulate proliferation or function of T-cell lines, and acts synergistically with IL-2 on peripheral lymphocytes inducing a highly effective cytotoxic cell population (5). In view of some of the cytotoxicity potential of GM-CSF we investigated its role on TIL from RCC and demonstrated remarkable modulatory effects on growth, expansion, proliferation, and in vitro cytolytic activity in the presence of optimal IL-2 doses (6). These results demonstrate the potential significant clinical benefit of GM-CSF in treatment of RCC. The method we implemented is outlined as follows using the optimal and most effective IL-2 dose.

3.2.1. TIL Preparation and Culture Conditions

The generation of TIL cells is conducted in the standard method outlined previously using primary resected RCC tumors with similar culture growth condition.

The difference in the method was related to the variation in IL-2 concentrations. Single-cell suspensions were propagated either alone or with 8, 40, and 400 U/mL (400 U/mL equals 1000 cetus U/mL or 6000 IU/mL).

Passage cells as needed to maintain a concentration of 1×10^6 to 1.5×10^6 TIL/mL.

3.2.2. Proliferation

[^3H]-thymidine-uptake assays were performed to assess the TIL proliferation.

1. Place approximately 5×10^4 TIL per well in 96-well, flat-bottom microtiter plates.
2. Grow in 100 μL of complete media supplemented with GM-CSF and/or IL-2. (IL-2 dose 400U/mL with 500 or 1000 nmol/mL of GM-CSF).
3. Pulse wells with 0.5 μCi [^3H]Tdr for 24 h.
4. Harvest cells using a PHD cell harvester and measure using a liquid scintillation counter.

3.2.3. Phenotypic Analysis

A phenotypic analysis is performed several days prior to functional assay using a two-color fluorescence.

1. Suspend approximately 5×10^5 TIL in 50 μL of staining buffer (1 \times PBS without calcium and magnesium plus 2% FCS and 0.1% sodium azide, pH 7.3).
2. Incubate with 10 μL of antibody for 30 min at 4°C.
3. Wash cells twice and fix using 1% formaldehyde.
4. Resuspend in 0.5 mL of staining buffer and measure cell surface antigens using flow cytometry.

3.2.4. Cytotoxic Assay

The activity of the GM-CSF TIL can be determined by the cytolytic activity using chromium-release assay. The TIL can be tested against autologous tumor or other tumor cell lines such as TU59, K562, and daudi cells.

1. Label 5×10^7 targets in a volume of 2 mL with 200 μCi of ^{51}Cr .
2. Incubate for 1 h at 37°C and wash three times.
3. Plate 5×10^3 targets in triplicates in a 96-well, round-bottom microtiter plate with appropriate number of effectors at several effector-target (E/T) ratios (total volume 0.2 mL). (E/T ratios used were 40:1, 20:1, 10:1, and 5:1.)
4. Incubate for 4 h and centrifuge plates for 3 min at 72g.
5. Harvest 100 μL of the supernatant and count activity on a gamma counter.
6. Specific lysis can be determined by:

$$\frac{\text{Experimental counts} - \text{spontaneous counts}}{\text{Total counts} - \text{spontaneous counts}} \times 100$$

Cytotoxicity is expressed as lytic units (LU) per 1×10^6 cells. One lytic unit is defined as the number of effector cells needed to lyse 30% of 5×10^3 target cells.

3.3. Interleukin-6

Interleukin-6 (IL-6) is a pleiotropic cytokine that plays an important part in the regulatory pathways controlling cellular growth and differentiation (7). Production of IL-6 has been demonstrated in numerous tumors and is thought to contribute to the development of tumors. Some of the actions of IL-6 include the stimulation and production of elements that induce fever, constitutive symptoms, activation of osteoclasts, and stimulation of blood stem cells.

RCC is known to be associated with paraneoplastic symptoms such as fever, erythropoiesis, hypercalcemia, and elevation of acute-phase reactants. The pathogenic mechanism for these symptoms associated with renal cell carcinoma are not completely understood. Since IL-6 has an effect on causing some of the symptoms, we have examined the association of IL-6 and RCC, including RCC tumor-infiltrating lymphocytes. Initial results from our laboratories demonstrated that IL-6 enhanced the growth of RCC-derived TIL grown in the

presence of IL-2 (8). Further characterization of the effects of IL-6 on RCC showed that IL-6 enhanced the growth and proliferative response of renal cell tumor lines in vitro. The enhanced production was noted in the presence of tumor necrosis factor- α (TNF- α) with synergistic effects seen with interferon- γ (INF- γ) (9). The growth effects of IL-6 on tumors suggests a specific autocrine function in cancer growth that can be applied in a clinical setting. The method for evaluation is outlined in this section.

3.3.1. RCC Lines

1. R4, R6, and R11 (Dr. Hans Stotter, Bethesda, MD).
2. SK28, SK29, and SK39 (Dr. N. Bender, New York, NY).
3. J80 (Dr. Sidney Golub, Los Angeles, CA).
4. TL2, TL9, and 444 from RCC nephrectomy specimens.

3.3.2. Preparation of Cell Culture from Resected Tumors

1. Obtain approximately 1–2 cm² of tumor.
2. Mince tumor, trypsinize and place on culture plates.
3. Use culture media of complete media (CM; *see Subheading 2.3., item 1a*).
4. Allow tumor cells to passage 10–15 times.
5. Remove fibroblasts as necessary.

3.3.3. Recombinant Cytokines and Monoclonal Antibodies

1. Recombinant IL-6 (rIL-6) provided by Immunex Corp. (Seattle, WA).
2. Recombinant tumor necrosis factor- α (TNF- α) provided by Cetus Corp. (Emeryville, CA).
3. Recombinant IFN- γ provided by Amgen, Inc. (Thousand Oaks, CA).
4. Monoclonal antibody (mAb) to IL-6 from Collaborative Research Inc. (Bedford, MA).
5. Use MOPC 21 mAb as control (Organon, Teknika, West Chester, PA).

3.3.4. RNA Extraction

1. Obtain tumor specimen from nephrectomy and freeze in liquid nitrogen.
2. Mechanically pulverize tissue.
3. Lyse samples in guanidine isothiocyanate.
4. Ultrafugation through a caesium chloride gradient for 16 h.
5. Isolate RNA fraction with ethanol precipitation and store in ribonuclease-free water at -70°C if needed or extract RNA using miniprep method.
6. Suspend approximately 10^7 cells and wash in 1 mL ice-cold Tris-saline (25 mM Tris, pH 7.4, 130 mM NaCl, 5 mM KCl).
7. Centrifuge and resuspend cells in 400 μL Tris/saline and 100 μL NDD buffer). (NDD buffer: 1% Nonidet P-40, 0.5% sodium deoxycholate, and 0.01% dextran sulfate in Tris-saline).
8. Centrifuge and extract supernatant.
9. Add supernatant to 25 μL 20% sodium dodecyl sulfate (SDS) and 15 μL 5M NaCl.
10. Further extract RNA with a 1:1 mixture of phenol (chloroform: amyl alcohol at 24:1).

11. Transfer aqueous layer to 1 mL 100% ethanol and precipitate at -20°C for 30 min.
12. Centrifuge to yield a pellet and wash pellet with 70% ethanol.
13. Dry and resuspend in ribonuclease-free water at -70°C .
14. RNA concentrations measured by spectrophotometry at 260 nm.
15. Isolate polyadenylated RNA using a column (Poly(A) Quik Kit, Stratagene, La Jolla, CA).

3.3.5. Northern Blot Analysis for Expression of IL-6

1. Size fractionate 10 μg of RNA on 1% agarose gel containing 6% formaldehyde.
2. Transfer onto nylon membranes (Sure Blot, Oncor, Gaithersburg, MD).
3. Bake membrane under vacuum at 80°C for 3 h.
4. Prehybridize for 8–12 h at 42°C .
5. Hybridize with ^{32}P -labeled probe for 16 h at 42°C in 50% formaldehyde, 2X standard saline citrate, 5X Denhardt's, solution, 0.1% SDS, 10% dextran sulfate, and 20 $\mu\text{g}/\text{mL}$ sheared and denatured salmon sperm DNA.
6. Wash membranes to a stringency of 0.1X SSC at 65°C and expose to X-omat AR film (Eastman-Kodak, Rochester, NY) at -70°C with intensifying screens.
7. Measure intensity of signals using densitometry.
8. Confirmation of quality and equivalent of RNA can be confirmed by ethidium bromide stain. For confirming similar amounts are loaded the β -actin band of hybridization can be used.
9. Blots are sequentially hybridized with ^{32}P -labeled IL-6 and β -actin probes.
10. Fold stimulation (mRNA expression index) calculated as follows:

$$\frac{\text{IL-6 (experimental conditions)}/\text{IL-6 (control)}}{\beta\text{-actin (experimental conditions)}/\beta\text{-actin (control)}}$$

3.3.6. cDNA Probes

1. Human IL-6 (1.2×10^3 bases, 1.2kb *Xho*I) and β -actin (0.7 kb, *Eco*RI-*Bam*HI) probes.
2. Label probes with [^{32}P]CTP by random priming (specific activity of $(2-5) \times 10^8$ cpm/ μg).

3.3.7. Measurement of IL-6 Levels by B9 Bioassay

IL-6 levels were detected by [^3H]dt uptake assay using the IL-6-dependent cell line, B9. B9 is a subclone of the murine B cell hybridoma, which proliferates only in the presence of IL-6 (as little as 1 pg/mL).

1. Maintain B9 cell line in CM (1U = amount causing half maximal B9 cell proliferation; see **Subheading 2.3., item 1b**).
2. Supernatants were used for analysis and can be stored at -70°C .
3. Place triplicate samples in 96-well, flat-bottom plates.
4. Serially dilute samples over 10 dilutions.
5. Wash B9 cells with PBS and seed 2×10^3 cells/well.

6. Incubate at 37°C in 5% CO₂ for 72 h.
7. Pulse wells with 0.5 mCi [³H]dt for 6 h.
8. Harvest cells on a PHD cell harvester (Cambridge Technology Inc., Cambridge, MA).
9. Measure radioactivity on a beta counter.
10. Known concentration of IL-6 used as standards.

3.3.8. Immunoperoxidase Staining

1. Cytocentrifuge cells onto glass slides and air-dry.
2. Fix slides with 2% paraformaldehyde at room temperature (RT) for 20 min.
3. Wash with PBS and permeabilize with 0.1% saponin for 20 min.
4. Place in 3% hydrogen peroxidase to remove endogenous peroxidase.
5. Block with normal rabbit serum.
6. Add a 1:20 dilution of polyclonal goat anti-human IL-6 (Collaborative Research Inc., Bedford, MA), incubate at RT for 1 h.
7. Wash with PBS and apply biotinylated rabbit anti-goat IgG for 20 min.
8. Wash with PBS and treat with peroxidase-conjugated streptavidin (Zymed Laboratories Inc.) at RT for 20 min using the labeled avidin-biotin method.
9. Wash with PBS and add AEC substrate solution.

3.3.9. Renal Tumor Proliferation Assay

1. Seed 3×10^4 renal tumor cells/well in 24-well culture plates for 24 h.
2. Withdraw supernatant and wash the cells twice with RPMI-1640 medium.
3. To each well add 1 mL of test-conditioned medium (triplicates). Test-conditioned medium contains various concentrations of IL-6 and/or mAb against IL-6.
4. Add 0.2 mCi [³H]dt to each well.
5. After 48 h remove supernatant and wash cells twice with RPMI-1640.
6. Add 0.5 mL of 0.5% SDS to each well and allow cells to disintegrate.
7. Transfer SDS into scintillation vials containing 10 mL scintillation cocktail (ScintiVerse II, Fisher Scientific, Fair Lawn, NJ), and count with a beta counter.

3.3.10. Clonogenic Assay

Methods used were as described before (**10**) with modifications.

1. Underlayer plated on 35 mm Petri dishes consisted of:
 - a. 0.5% agar with 25% FCS
 - b. 25% 1X RPMI-1640 medium
 - c. 25% 2X RPMI-1640 medium
2. Suspend cells in the upper layer consisting of:
 - a. 0.3% agar with 25% FCS
 - b. 25% 2X RPMI-1640 medium
 - c. Various concentrations of IL-6 and/or mAb
3. Plate tumor cells at a concentration of $2-3 \times 10^4$ cells/plate.
4. Incubate at 37°C in 5% CO₂.
5. Exam under inverted microscope every 2–3 d.
6. Final colony count is made at 10–14 d.

3.4. Interferon- α

Immunotherapy using systemically administered interferon- α (IFN- α) has demonstrated efficacy in the treatment of advanced RCC as a single agent and combination with IL-2 resulted in an improved clinical response rate (**11**). However, side effects associated with this therapy are significant, and to decrease the toxicity of this form of therapy we have evaluated the role of local production of cytokines at the tumor sites. The method involves the transfection of tumor with genes for human IL-2 and/or IFN- α . This alternative form of therapy has shown effective prevention and alteration of tumor growth in vitro and in vivo (**12,13**). The method for this purpose is shown as follows.

3.4.1. Gene Construction

1. Plasmids pIL-2-50A (Dr. T. Taniguchi, Japan Foundation for Cancer Research, Osaka, Japan), and Berg IFN- α (Shionogi Laboratory, Osaka, Japan).
2. Cleave plasmid pIL-2-50A using *Pst*I and Berg IFN- α A with *Eco*RI. This releases human IL-2 and IFN- α complementary DNA (cDNA).
3. Introduce *Not*I cutting site to both cDNAs using polymerase chain reaction.
4. Ligate cleaved cDNA to *Not*I cleaved and dephosphorylated pGEM3 Sra.neo expression vector (Shionogi Laboratory). This constructs IL-2 and IFN- α expression vectors under transcriptional control of simian virus 40 (SV40) promoter plus human T-cell leukemia virus enhancer.
5. Active transcription and translation of cytokine from the constructs can be confirmed by transfection into COS-7 cell line and using the DEAE dextran method.
6. Use plasmid vectors expressing the highest titer of cytokines were used to transfect R11 renal tumor cell line.
7. Transfect R11 cells using calcium phosphate precipitation.
8. Select cells for *Neo* gene expression by adding G418 (500 μ g/mL) (Geneticin; Gibco-BRL).
9. Select G418 resistant colonies and expand individually.
10. IL-2 secreted is measured by ELISA kit (Collaborative Research) using medium with 1×10^6 cells of transfectant clones.
11. IFN- α activity is measured by viral inhibition assay.

3.4.2. Coculture Experiments

1. Coculture $2-5 \times 10^5$ /mL parental tumor cells or 2×10^5 /mL peripheral blood lymphocytes (PBL) with $2-5 \times 10^5$ /mL transfected tumor cells.
2. Culture for 3 or 6 d using a cell culture device with a porous-bottom dish inserts (Transwell Costa, Pleasanton, CA). This device permits released cytokines to be freely transported between the upper and lower compartments.

3.4.3. Proliferation and Cytotoxicity Assays

1. Determine cell proliferation by tritiated thymidine ($[^3\text{H}]\text{dt}$) incorporation.
2. Seed 5×10^4 cells/ml in a 24-well plate in triplicate.
3. Incubate for 24, 48, and 72 h.

4. Pulse with 0.1 μ Ci of [3 H]dt for 24 h.
5. Harvest cells and measure cytotoxic activity using 4 hour or 18 hour chromium release assay.

3.4.4. Fluorescence-Activated Cell-Sorter (FACS) Analysis

1. Incubate 5×10^5 cells with appropriate mAbs for 30 min at 4°C.
2. Wash cells twice with PBS.
3. Incubate with fluorescein isothiocyanate-labeled goat anti-mouse antiserum for 20 min at 4°C.
5. Wash twice with PBS.
6. Analyze using a FACS scanner.

3.4.5. Northern Blot Analysis

The Northern blot analysis is prepared and conducted as previously mentioned.

3.4.6. Animal Studies and Immunohistochemistry

1. Tumors in mice are established by injecting 5×10^6 cells/0.3 mL subcutaneously in the right or left lower abdominal quadrant.
2. Use immune-deficient mice such as B mice (C3Hf/Sed/Kam mice rendered T-cell deficient by splenectomy, thymectomy, and supralethal irradiation. Mice are then reconstituted with anti-Thy 1.2-treated bone marrow cells).
3. For a mixed tumor transplantation assay, inject a mixture of 1×10^6 /0.7 mL transfected and parental R11 cells at a 1:1 ratio.
4. Measure tumors every 2–3 d using Vernier calipers.
5. For immunohistochemistry, tumors were dissected off the mice and fixed in 10% formalin.
6. Block in paraffin and section into 4 μ m slices.
7. Stain with hematoxylin-eosin and examine under the microscope.
8. For immunoperoxidase staining, embed tissue in OCT and snap freeze in liquid nitrogen.
9. Cryostat sections and stain with:
 - a. Mac-1 (TIB 128)
 - b. Lyt-2 (TIB 211)
 - c. L3T4 (TIB 207)
 - d. Preimmune serum used as control
10. Incubate sections with peroxidase-conjugated goat anti-rat IgGs.

Acknowledgment

We would like to convey our immense gratitude to Tracy Prinz for her patience and encouragement in preparing this manuscript.

References

1. Figlin, R. A., Pierce, W. C., Kaboo, R., Tso, C. L., Moldawer, N., Gitlitz, B., deKernion, J., and Belldegrun, A. (1997) Treatment of metastatic renal cell carci-

- noma with nephrectomy, interleukin-2 and cytokine-primed or CD8(+) selected tumor infiltrating lymphocytes from primary tumor. *J. Urol.* **158**, 740–745.
2. Steger, G. G., Pierce, W. C., Figlin, R., Czernin, J., Kaboo, R., deKernion, J. B., Okarma, T., and Belldegrün, A. (1994) Patterns of cytokine release of unselected and CD28+ selected renal cell carcinoma tumor-infiltrating lymphocytes (TIL). *Immunol. Immunopathol.* **72**, 237–247.
 3. Fidler, I. J. and Schroit, A. J. (1998) Recognition and destruction of neoplastic cells by activated macrophages: discrimination of altered self. *Biochem. Biophys. Acta* **948**, 151.
 4. Schwartzentruber, D. J., Hom, S. S., Dadmarz, R., White, D. E., Yanelli, J. R., Steinberg, S. M., Rosenberg, S. A., and Topalian, S. L. (1994) In vitro predictors of therapeutic response in melanoma patients receiving tumor-infiltrating lymphocytes and interleukin-2. *J. Clin. Oncol.* **12**, 1475–1483.
 5. Masucci, G., Ragnhammar, P., Wersall, P., and Mellstedt, H. (1990) Granulocyte-macrophage colony-stimulating factor augments the interleukin-2-induced cytotoxic activity of human lymphocytes in the absence and presence of mouse or chimeric monoclonal antibodies (mAb 17-1A). *Cancer Immunol. Immunother.* **31**, 231–235.
 6. Steger, G. G., Kaboo, R., deKernion, J. B., Figlin, R., and Belldegrün, A. (1995) The effects of granulocyte-macrophage colony-stimulating factor on tumor-infiltrating lymphocytes from renal cell carcinoma. *Br. J. Cancer* **72**, 101–107.
 7. Kohase, M., Henriksen-DeStefano, D., May, L. T., Vilcek, J., and Sehgal, P. B. (1986) Induction of B2-interferon by tumor necrosis factor: a homeostatic mechanism in the control of cell proliferation. *Cell* **45**, 659–666.
 8. Lee, T. Y., Koo, A. S., Peyret, C., Shimabukuro, T., deKernion, J. B., and Belldegrün, A. (1991) The effects of Interleukin-6 on tumor infiltrating lymphocytes derived from human renal cell cancer. *J. Urol.* **145**, 663–667.
 9. Koo, A. S., Armstrong, C., Bochner, B., Shimabukuro, S., Tso, C. L., deKernion, J. B., and Belldegrün, A. (1992) Interleukin-6 and renal cell cancer: production, regulation, and growth effects. *Cancer Immunol. Immunother.* **35**, 97–105.
 10. Hamburger, A. W. and Salmon, S. E. (1977) Primary bioassay of human tumor stem cells. *Science* **197**, 461–463.
 11. Figlin, R. A., Belldegrün, A., Moldawer, N., Zefferen, J., and deKernion, J. B. (1992) Concomitant administration of recombinant human interleukin-2 and recombinant interferon alpha-2A: an active outpatient regimen in metastatic renal cell carcinoma. *J. Clin. Oncol.* **10**, 414–421.
 12. Belldegrün, A., Cho-Lea, T., Sakata, T., Duckett, T., Branda, M. J., Barsky, S. H., Chai, J., Kaboo, R., Lavey, R. S., McBride, W. H., and deKernion, J. B. (1993) Human renal carcinoma line transfected with interleukin-2 nad/or interferon-alpha gene(s): implication for live cancer vaccines. *J. Natl. Cancer Inst.* **85**, 207–216.
 13. Hathorn, R. W., Cho-Lea, T., Kaboo, R., Pang, S., Figlin, R., Sawyers, C., deKernion, J. B., and Belldegrün, A. (1994) In vitro modulation of the invasive and metastatic potentials of human renal cell carcinoma by interleukin-2 and/or interferon-alpha gene transfer. *Cancer* **74**, 1904–1911.

Monoclonal Antibodies

Generation and Clinical Use

Egbert Oosterwijk

1. Introduction

Originally, the term "antibody" referred to an unknown entity in serum, which had the capacity to neutralize pathogenic bacteria. Ehrlich discovered that the so-called antibody had to be a discrete substance, and was the first to propose a theory on antibody formation (**1**). A few years later, he hypothesized that antibodies might be applied for selective treatment of cancer, provided that the antibody showed specificity for the tumor tissue (**2**). Later studies showed that antibodies could be produced against a wide variety of substances, including tumors.

The search for (tumor-related) antigens was given an enormous boost by the development of hybridoma technology in 1975 (**3**). The profound impact of this technology is reflected in the fact that the Nobel Prize was awarded to the discoverers of this technology.

In the study of renal cancer, investigations by various laboratories have provided numerous mAb probes with a high degree of specificity for kidney-related antigens (**4–11**). Expression of these antigens is in most cases specific for a particular segment of the nephron (**5,6,9,10**). Definition of the antigenic phenotype of the various cell types that comprise the normal adult nephron have provided a reference point for further studies in nephron development, the histogenesis of renal cancers, and studies examining normal and neoplastic renal epithelium cells in tissue culture (**12–14**). Clearly, molecular probes such as monoclonal antibodies (mAbs) can discriminate what is not apparent at the level of the microscope. There are multiple subtypes of renal cancer, which can be subclassified at the molecular level. As these subtypes are elucidated, these distinctions are shown to have clinical relevance.

In the early 20th century, Ehrlich suggested that antibodies could be used to selectively target cancer. The theory of selective targeting of cancer became widely known as the (popular) concept of using antibodies as “magic bullets.” The concept of selective tumor targeting with antibodies is based on the interaction between the antibody and an antigen, which is expressed in malignant cells but not in normal tissues. The term “tumor-specific antigen” should be avoided, because truly tumor-specific antigens have not been identified. Thus, a tumor-associated antigen can be defined as an antigen that is predominantly expressed by malignant cells of a certain tumor type. The ultimate goal of tumor targeting using antibodies is to develop an effective treatment for malignancies for which there is no effective therapy available yet. Targeting of labeled antibodies may also provide a useful tool for the detection of tumor lesions, which might alter treatment strategies.

For renal cell carcinoma (RCC) of the clear-cell type, clinical experience with the use of mAbs is most extensive with mAb G250. The initial decision to pursue clinical studies with this mAb was based on its unique tissue distribution: almost completely absent from normal tissues, whereas RCCs showed high, homogenous expression (4). This mAb is now known to recognize carbonic anhydrase IX, whose expression is absent in the normal kidney (15). However, mAb G250 is not tumor-specific in the absolute sense, as the mAb demonstrates some reactivity with normal gastric mucosal cells and with cells of the larger bile ducts (4). Clinical studies with radiolabeled mAb G250 in RCC patients have demonstrated the ability to selectively and specifically deliver mAb to RCC sites with a high absolute amount of mAb delivered to tumor sites. G250 can successfully target and image both primary and metastatic RCC, including both bone and soft-tissue metastasis (16–20). Quantitative analysis of tissue samples revealed peak ratios of tumor:serum of 178:1, tumor:normal kidney of 285:1, and tumor:liver of 92:1 at 1 wk after mAb administration, among the highest ever achieved with mAb (16). In addition, approx 25% of patients studied were imaged at sites not suspected on the basis of conventional imaging techniques. In many of these cases, these sites were pathologically confirmed, and the finding of these sites often influenced the treatment decisions.

In a phase I/II radioimmunotherapy study to determine the maximum tolerated dose (MTD_A) and therapeutic potential of ¹³¹I-G250 (19), 33 patients with measurable metastatic RCC were treated. Fifteen patients were studied with the maximum tolerated dose of activity (MTD_A) 90 mCi/m² ¹³¹I. There was targeting of radioactivity to all known tumor sites ≥ 2 cm, confirming the high fraction of G250 antigen-expressing tumors in patients with clear-cell morphology subset of RCC. Lesions ≥ 2 cm in size independent of location were visualized by scintigraphy by the first imaging scan, between 2 and 4 d after administration of ¹³¹I-G250. Seventeen of 33 evaluable patients had stable disease. There were no major responses.

Because the murine mAb G250 was highly immunogenic in patients, preventing multiple injections, chimeric G250 (cG250) was constructed, where the murine Fc region was replaced by a human Fc region. The excellent targeting and lack of immunogenicity of ^{131}I -cG250 in a clinical trial (17), led to the initiation of clinical trials to evaluate the utility of ^{131}I -cG250 in the radioimmunotherapy of RCC. In a phase I radioimmunotherapy study, the maximum tolerated dose (MTD_A) of ^{131}I -cG250 was determined (20), and phase I/II radioimmunotherapy trials are underway to evaluate the utility of high-dose administrations of ^{131}I -cG250 and multiple, outpatient administrations of ^{131}I -cG250 in patients with measurable metastatic RCC.

1.1. Generation of mAbs

Although antibodies can be extremely useful reagents, the most important question at the outset is: “What do we need the antibodies for?” The answer to this question will impose constraints on the experimental strategies used to obtain them. Several principles that are applicable in general to any antibody techniques should be taken into account:

1. Are we searching for antibodies of well-known, defined specificity, or antibodies of novel specificity?
2. What kind of immunogen is available?
3. What application are the antibodies to be used for?
4. How do we plan to establish antibody specificity?
5. Is it necessary to prepare polyclonal or mAbs?
6. How much antibody do we foresee we will need?
7. Is batch-to-batch variation an important issue?
8. What are the financial constraints?

It is a relatively straightforward approach to develop antibodies that recognize a known molecule or epitope, but it is often much more difficult and time-consuming to establish the specificity of antibodies raised against complex molecular mixtures. Furthermore, because the universe of antigens cannot be systematically tested, it is extremely important to bear in mind that antibodies—whether polyclonal or monoclonal—raised against a known molecule may cross-react with unrelated molecules. The latter may share with cognate antigen chemical characteristics that are easy to identify (i.e., primary amino-acid sequence), or may lack apparent structural relatedness. Therefore, when using antibodies, a word of caution is always necessary.

1.1.1. Antigen Source

1. Fresh tissue: The main advantage of using whole-tissue extracts is that one may aim at isolating mAbs, recognizing unknown molecules. The advantage over cell lines may lie in the observation that the phenotype of cell lines differs from the

progenitor tumor cells, and importantly, unidentified molecules may not be present on the cultured cells. The disadvantage is obviously contamination with nonrelevant tissue components—e.g., stromal cells, endothelial cells, and others.

2. Cultured cells. The same main advantage described for the use of whole-tissue extracts—i.e., the isolation of mAbs, recognizing unknown molecules—holds true for the use of cell lines as immunogen. Additionally, one works with a homogenous population of cells, without contaminating components. Yet important molecules may have been lost during the culturing procedure.
3. Recombinant proteins. Few investigators have reported the use of proteins produced from recombinant cDNAs in *E. coli* or baculovirus to make antibodies. Based on the scarcity of information available in the literature and the experience of our own laboratory, the isolation of recombinant proteins often presents solubility and/or purification problems, thus complicating their use. Despite these difficulties, more attention should be given to this strategy, since it is based on relatively less complex antigen preparations.
4. Other strategies. Several additional strategies have been used to obtain antibodies of novel specificity when using complex antigen preparations. Among them are the induction of tolerance in newborn mice (21) or the preincubation of antigen preparations with known antibodies in order to decrease the likelihood of raising antibodies with the same specificity (22). While these possibilities are intellectually stimulating and have been used with some success, there is limited information in the literature regarding their usefulness.

1.1.2. Polyclonal vs mAbs

Because the development of mAbs is relatively expensive and time-consuming, if the immunogen is available in reasonable amounts and high purity, it is reasonable to first produce polyclonal antibodies, analyze their specificity, and then assess the purpose of making mAbs. The major reason to prepare the latter is to have an indefinite source of reagents of identical specificity. When considering the preparation of polyclonal antibodies, several points should be taken into account:

1. Natural antibodies may contribute to substantial background; this is particularly true for antibodies that recognize carbohydrate epitopes, and is thus a relevant issue when dealing with mucins.
2. There may be considerable variation in the immune response obtained in animals from different species. In general, stronger immune responses are obtained across greater phylogenetic differences.
3. Detailed information on the homology of proteins across species may facilitate decision making. Greater homology is generally associated with lower immunogenicity.
4. It is possible to obtain very large amounts of antibodies from certain species, i.e., the horse. Some inexpensive and easy-to-handle laboratory animals, such as chickens, can provide substantial amounts of antibody, for example, in the egg yolk.

5. Even among animals that share a genetic background, significant interindividual variation can be observed in the immune response. Therefore, more than one animal should be immunized.
6. The immune response is a dynamic process, and subtle differences in the specificity of serum antibodies can be demonstrated when comparing different bleedings from the same animal.

1.1.3. Screening Strategies

The general principle that “you get what you look for” should not be forgotten. Antibodies—whether monoclonal or polyclonal—often work best when using certain, but not all, techniques. Therefore, when the application is known at the outset, it is most useful to devise screening strategies accordingly. For example, if we wish to use antibodies for studies on paraffin-embedded tissue sections, it is best to include immunohistochemical analysis on paraffin-embedded sections in the screening procedure. This is not always feasible when preparing hybridomas, because some methods are too tedious to be used for routine screening (i.e., immunoprecipitation). In such cases, it may be better to use a simple screening strategy that will allow the identification of a small number of antigen-reactive clones, and then apply a second round of screening with the specific technique desired.

1.1.4. Financial and Other Considerations

Making polyclonal antibodies is less time-consuming and cheaper than making hybridomas. The commercial cost of polyclonal antipeptide antibodies is in the range of \$3000 US. By contrast, the production of hybridomas will cost approx \$8000 US. Among the considerations to be taken into account is the experience of the group. For an inexperienced laboratory, setting up the hybridoma technology will require some effort, whereas it is easy to prepare polyclonal antibodies. Another consideration is time. Provided that the antigen preparation is reasonably immunogenic, it takes less time to prepare affinity-purified antibodies (3–4 mo) than to make hybridomas (6–12 mo until a purified antibody preparation is available).

2. Materials

Most materials needed to produce hybridomas are rather standard. The materials listed in **Subheading 2** are those used specifically for the filter-plaque technique which is less well known.

1. Agarose type VII (low melting temperature) (Sigma).
2. Nitrocellulose filters (0.45 μm , 6-cm diameter, Schleicher and Schuell).
3. Sintered glass funnel (Millipore).
4. UV light lamp (30-W Philips TUV).

3. Methods

3.1. Polyclonal Antisera

Several spp can be used to obtain polyclonal antibodies. Rabbits are most commonly used, but chickens provide certain advantages that should be considered, since it is relatively simple to house them. Up to 5 mg of total IgY can be isolated from the yolk of one egg. The procedure for making rabbit polyclonal sera is described in **steps 1–6**.

1. Prior to the first immunization, a preimmune serum sample is obtained from the auricular artery using a 20-gauge needle and a 20-cm² syringe. To dilate the artery, it is advisable to rub the ear with alcohol and warm it under a spotlight. If mice are used, the preimmune serum sample is obtained from the retro-auricular plexus by means of a Pasteur pipet.
2. Screen the preimmune rabbit sera for lack of reactivity using the assay that will be applied for testing the postimmune serum. This allows the selection of rabbits whose serum yields low background. Therefore, it is advisable to analyze preimmune serum from several rabbits.
3. Prepare the immunogen for inoculation by mixing 200 µg of the immunogen (in 500 µL) with 500 µL of Complete Freund's Adjuvant (CFA) (*see Note 1*) until a good emulsion is obtained (amount per rabbit). In general, 1 mL of mixture yields 0.8 mL of emulsion. For mice, 10–20 µg of antigen is used. It is best to mix both components using a 2-mL syringe with a needle until the mixture is hard. Alternatively, join two syringes (without needle) with a rubber tube and transfer the mixture from one syringe to the other until it is hard. Be careful, as the mix hardens the needle or the rubber can slip off the syringe and the immunizing material can be lost. The emulsion is ready when, upon applying a drop of it on water, it is not dispersed.
4. The first immunization is performed in the leg muscle with the mixture prepared as in **step 3**. It is better to split the immunogen between two injection sites. Subsequent inoculations are performed in the same way, except that the emulsion is prepared with Incomplete Freund's Adjuvant (IFA).
5. After the fourth immunization, bleed rabbits (or mice) as described in **step 1**. At this time, a screening is performed with the preimmune and post-fourth immunization serum samples to determine serum titer and specificity (*see Note 2*).
6. Immunization and bleeding proceed on a monthly basis following the same protocol. If the serum titer is good, it is advisable to bleed the animals regularly (every 2 wk) to quickly store a large amount of serum, because antibody specificity may change with time. Then, proceed to a final bleeding before sacrificing the animal.

3.2. Generation of mAbs

3.2.1. Liquid Culture Technique (*see Note 3*)

1. Immunization: Balb/c mice are given 3–5 ip immunizations with 20 µg of the corresponding immunogen in CFA/IFA as described for polyclonal antibodies (*see Note 4*). Four and three days before the cell fusion animals are boosted with the immunogen with IFA.

2. Feeder layer cells:

- a. To obtain peritoneal macrophages (PM), kill a normal nonimmunized mouse of the same strain as the immunized mice the day prior to the cell fusion. It is recommended to plate the cells 24 h before the cell fusion and check for contamination at the fusion time (*see Note 5*).
- b. Using a 25-gauge needle, inject 5 mL of cold serum-free RPMI-1640 intraperitoneally. Palpate the abdomen gently and withdraw the medium using a 21-gauge needle.
- c. Centrifuge at 600g for 5 min and wash the cells twice with RPMI-1640.
- d. Count the cells in a Neubauer chamber and check for viability by Trypan blue exclusion. Usually one mouse will yield 2.5×10^6 PM with >95 % viability.
- e. Plate PM in 96-well plates at $2-5 \times 10^3/100$ μ L/well in complete medium (RPMI-1640 supplemented with 10% fetal bovine serum (FBS), 1% glutamine, 1% nonessential amino acids, 1% penicillin/streptomycin). In general, PM from one mouse will suffice for fusion of one spleen.

3. Spleen cells:

- a. On the day of fusion, anesthetize the mouse with an ip injection of 0.5 mL avertin. Collect blood from the retro-orbital plexus by means of a Pasteur pipet. Serum is stored to test for specific polyclonal antibodies.
- b. Sacrifice the mouse, aseptically remove the spleen, and transfer to a 50-mm-diameter Petri dish filled with serum-free RPMI-1640 medium. Wash the spleen twice with medium under sterile conditions.
- c. Obtain a single-cell suspension of splenocytes by perforating the spleen tip with a 20-gauge needle and squeezing the splenocytes out with a forceps. Disperse cells gently with a Pasteur pipet or by passage through a fine-mesh metal screen.
- d. Transfer spleen cells into a 15-mL conical tube and fill with serum-free RPMI-1640.
- e. Centrifuge at 600g (1500–2000 rpm) for 5 min and discard supernatant.
- f. Lyse red blood cells by adding 10 mL of lysis buffer (0.150 M NH_4Cl 0.01 M KHCO_3 , 10^{-4} M ethylenediaminetetraacetic acid [EDTA], pH 7.0) and incubating for 5 min at 37°C.
- g. Centrifuge and wash the cells twice with cold serum-free medium. Resuspend splenocytes in 10 mL RPMI-1640, count, and assess viability with trypan blue. Approximately 100–200 million cells/spleen should be obtained.

4. Myeloma cells (*see Note 6*)

- a. Mouse myeloma cells are cultured in complete medium. It is best to use cells that are in an exponential growth phase. Four days before the fusion, the medium is changed and cells are seeded at $2-5 \times 10^5$ cells/mL. Viability and density are checked daily, and up to 50% of fresh medium is added daily to ensure that cells will grow exponentially.
- b. Harvest myeloma cells in a 50-mL conical tube and wash three times with serum-free cold RPMI-1640.
- c. Count the cells and assess viability by Trypan blue exclusion. It is important that viability is >95%.

5. Fusion

- a. Mix the splenocytes and myeloma cells in a 50-mL conical tube at a ratio of 5:1 to 2:1. Fill up the tube with cold RPMI-1640 and centrifuge at 300g (1000 rpm) for 5 min. Usually, ratios from 1:1 to 1:10 yield high-fusion efficiency.
- b. Discard the media and mix gently to soften the cell pellet.
- c. Add 0.5 mL (dropwise) of prewarmed (37°C) polyethylenglycol (PEG) 1500 over 1 min. Mix gently as the PEG solution is added to the cells.
- d. Let the cells rest for 1 min and add 10 mL of prewarmed RPMI-1640 dropwise, mixing gently over 10 min (1 mL/min).
- e. Centrifuge at 300g for 10 min.
- f. Resuspend the cells gently in complete RPMI-1640 medium (medium supplemented with 1 mM sodium pyruvate, 2 mM L-glutamine, 1% nonessential amino acids, 100 U/mL penicillin, 100 µg/mL streptomycin, and 10% FBS) supplemented with 2% hypoxanthine, aminopterin, and thymidine (HAT) in the appropriate volume to yield a suspension of 1×10^5 splenocytes/mL. Cells are extremely fragile at this phase, and violent pipetting must be avoided.
- g. Seed the cells in 96-well plates at 10^5 splenocytes/well. Incubate at 37°C in 5% CO₂ atmosphere (*see Note 7*).
- h. Check cell, by visualization with an inverted microscope, twice a wk for contamination and cell growth.
- i. Change 100 µL of medium weekly (optional if cells are kept in a wet incubator). After the second wk, the fusion medium may be replaced by complete medium supplemented with 2% HT (hypoxanthine, thymidine). Clones containing a few cells should be seen 1 wk after the fusion. Clones should be ready for screening (visible at the naked eye, approx 1-mm-diameter) at the end of the second wk.
- j. When clones are ready, remove 100 µL of supernatant for screening and replace with fresh medium (*see Note 8*).

6. Subcloning by limiting dilution (*see Note 9*):

- a. Clones producing antigen-reactive antibodies of the desired specificity are gently dispersed and cells are counted.
- b. Cells are cloned by limiting dilution: Seed in 96-well plates at densities of 1–1000 cells/well (approximately half-plate per dilution) in complete medium supplemented with 2% HT. If there are not enough cells, seed first in a well of a 24-well plate with 2 mL of medium/well.
- c. Several rounds of subcloning are performed until >95% of the clones seeded at 0.1–1 cells/well are reactive with the immunogen (*see Note 10*).
- d. Cloned hybridoma cells are first expanded in wells of 24-well plates, then frozen in liquid N₂ (in 90% FBS–10% dimethyl sulfoxide [DMSO]).

7. Scaling up antibody production. To obtain large quantities of specific mAb, two methods are generally used:

- a. Production of hybridoma culture supernatant: Seed the hybridoma cells in a 25-cm² tissue culture flask at a density of 10^5 cells/mL in complete medium (there are commercially available synthetic media that support hybridoma

growth in the absence of FBS). When cells reach the density of $1-2 \times 10^6$ or the medium becomes acidic, centrifuge cell suspension, collect the supernatant, and seed the cells in a 175-cm² tissue-culture flask with the appropriate amount of medium. Replace 80% of the medium regularly and substitute with fresh medium. A fraction of the cells will also have to be replaced, or the culture expanded, as indicated in **step 8b**.

- b. Several commercial systems are available for the production of mAb. E.g. hollow fiber based systems (so-called tecnomouse or minimouse systems) and membrane-based culture methods (e.g., Integra CELLine, Future Diagnostics). We have had positive experience with the latter system, which is easy to use (conventional culture techniques are used) and can be maintained for 3 mo without complex tissue-culture methodology. Additionally, cells do not need to be adapted. The culture fluid containing concentrated mAb is harvested twice a week

The spent medium is collected, stored at 4°C until used, or frozen at -40°C for long-term storage. If FBS-free medium is used, hybridoma culture medium can be concentrated in order to obtain high-titer antibody preparations.

8. Ascites fluid production (*see Note 11*):
 - a. Pristane (2,6,10,12, -tetramethylpentadecane) is injected intraperitoneally to nude mice or to mice of the same strain as those used for immunization (0.5 mL/mouse) 1 wk before inoculation with hybridoma cells.
 - b. Hybridoma cells are cultured as described in **step 7b**. Centrifuge the cells, and wash twice with PBS or medium without FBS. Count the cells and determine viability.
 - c. Inoculate 5×10^5 cells/per mouse.
 - d. Wait 1–2 wk for ascites formation.
 - e. To harvest ascites, wash mouse belly with 70% ethanol, insert an 18-gauge needle, and let ascites drop into a conical polypropylene tube.
 - f. To remove the cells, centrifuge ascites at 1000g for 10 min and discard the pellet (*see Note 12*).
 - g. Add 0.1% sodium azide (0.1% final concentration), make aliquots, and freeze at -80°C.
 - h. Continue to tap the animals at 1–3 d intervals.

3.2.2. Filter-Plaque Technique (*see Note 13*)

1. To prepare 20 agarose plates, 45 mL of a 3% agarose solution in 0.9% NaCl are sterilized and allowed to cool to approx 50°C. Forty milliliters are added to 160 mL complete HAT medium at 37°C (final concentration 0.6% low melting agarose).
2. When the yield of fused cells may be crucial, hybridoma-formulated media can be used. However, this is not really required: fusion efficiency is highly investigator-dependent, and is dependent on the quality of the fusion partners.
3. Add 10 mL fluid to each dish and allow the agarose to solidify at room temperature. Avoid bubbles on top of the agarose layer. Do not solidify the agarose at 4°C, as this will result in entrapment of air bubbles.

4. Fuse splenocytes and myeloma cells as described in **Subheading 3.2.5**.
5. The primary fusion products are gently resuspended in 30 mL complete HAT medium at 37°C, 4 mL 3% agarose solution at 40°C (*see Note 14*) is added and gently mixed, and the cell suspension is layered over the 20 dishes. Dishes are placed at 4°C for 20 min, and subsequently placed in a regular CO₂ incubator. The correct concentration of top agarose is crucial: concentrations that are too low result in semifluid top agarose, prohibiting subsequent screening.
6. Outgrowth of cells is examined at day 5 and every other day subsequently (*see Note 15*). Generally, colonies of 50–200 cells are present 9–10 d after seeding—a colony size sufficient for filter screening. In general 100–150 colonies are present per dish, accounting for 2000–3000 colonies per fusion.
7. Prepare nitrocellulose filters as follows: filters are cut from a larger nitrocellulose sheet, including a tab to facilitate filter handling (*see Fig. 1*). Alternatively, filters of 6-cm-diameter are available from Schleicher and Schuell. Filters are washed in 0.9% NaCl (*see Note 16*).
8. Coat filters with purified antigen or tissue-cell homogenates. Filters are placed on a sintered glass funnel, and 10 mL of the antigen solution is sucked through each filter (*see Note 17*).
9. Punch three small holes at the sides of filters coated with irrelevant antigen to shape a triangle to facilitate positioning (*see Fig. 1*).
10. Filters are air-dried and sterilized by UV light (20 min per side, twice) in a laminar flow hood (*see Note 18*). Wash several times in sterile water, and store filters overnight in sterile water. The next day, filters are soaked in complete medium supplemented with 2% HAT to block remaining protein-binding sites. Filters can be stored at –20°C or used immediately after preparation. Immediate use is preferable to reduce contamination problems.
11. To place the filters on top of the agarose layer, first completely remove excess fluid from the agarose plates with a Pasteur pipet. Unwanted excess fluid will result in flotation of the filters; tilt the plate to remove excess fluid (*see Note 19*).
12. Place two filters on every dish. One, coated with irrelevant protein, is placed directly, coated side up, on top of the agarose after briefly drying on a stack of sterile filter paper. The second filter is also briefly dried on sterile filter paper and placed on top of filter 1, coated side up (*see Fig. 1*) (*see Note 20*).
13. Gently place the filters on the brim of the dish and slide the filter onto the agarose. Punch through three small holes in the upper filter with an injection needle, corresponding to the larger holes in the lower filter. Using an inverted microscope, precisely label in the bottom of the plate the position of the three holes and the position of the filter tabs with a marker and incubate overnight in a regular CO₂ incubator at 37°C.
14. The next day the dishes are placed at 4°C for 1 h to facilitate further handling, and excess fluid is removed. Both filter tips are grabbed with a sterile forceps, the Petri dish is gently tilted again, and both filters are gently removed (*see Note 21*). Filters and dishes are numbered and placed in phosphate-buffered saline (PBS).
15. The filters are incubated for 1 h at room temperature with horseradish peroxidase-labeled rabbit-anti-mouse Ig (RAM-HRPO) at the appropriate dilution. After

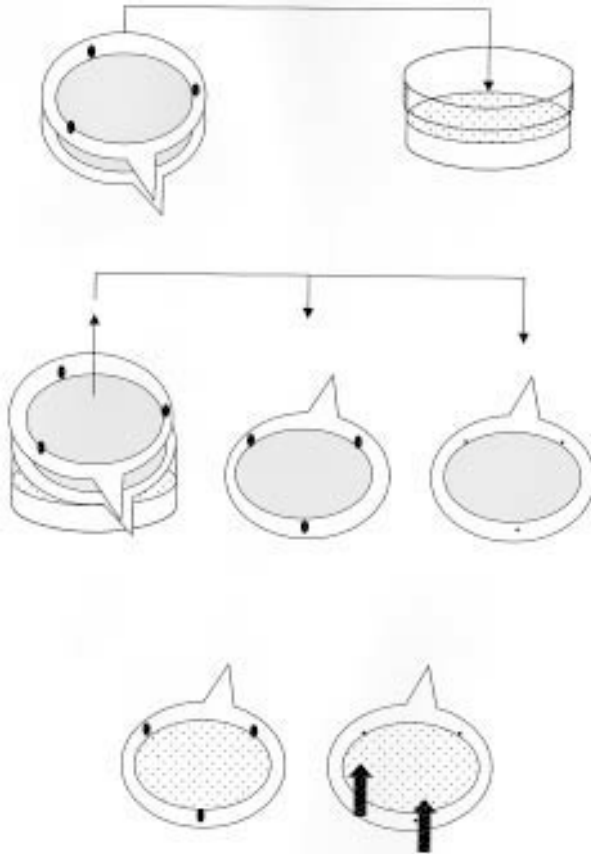


Fig. 1. Screening of fusion using the filter plaque technique. Placement of filters on top of the agarose layer and array of holes for filter positioning. Top left: Two aligned nitrocellulose filters, coated with relevant and irrelevant antigen(s). Note the prepunched holes in the top filter. After placement on the agarose, holes are punched in the lower filter with a sterile needle. Top right: Petri dish with (primary) fusion products in top agarose. Middle left: After overnight incubation filters are removed, numbered, and placed in PBS. Note holes in lower filter (middle right). After staining, comparison of the filters reveals specific spots on the filter coated with relevant antigen (bottom, arrows). In general, the reverse will also be observed: specific spots on the filter coated with irrelevant antigen, absent on the other filter. For the sake of clarity, this is not shown in the schematic drawing.

extensive washing with PBS or any other appropriate buffer, reactions are developed with 0.05% 3-3' diaminobenzidine and 0.03% H_2O_2 in 50 mM Tris-HCl pH 7.4.

16. A direct comparison of corresponding filters, using the holes as landmarks, allows the identification of spots specific for the protein of interest—i.e., those present in the antigen-coated filters and absent from the control filters. These spots are

punched out, and the filters accurately repositioned underneath the corresponding Petri dish, using the markings on the dish.

17. Pasteur pipets drawn in a flame to produce small bent tips and sterilized are used to retrieve, by gentle suction, the colonies that should be located in the position indicated by the punched-out hole. Retrieved colonies are grown in suspension in HAT medium in 96 wells. After 5–10 d, undiluted culture media can be tested from these monoclonal cultures.
18. If more than one colony is identified at the target position, retrieve each of them separately. When accurate repositioning is difficult, spots of colonies producing irrelevant antibody can be used as additional landmarks. Take up the colonies as neatly and cleanly as possible, without contaminating cells in the area.
19. Cultures of interest are subcloned two to three times by agarose seeding following the same basic strategy described in **steps 1, 3, and 5**: two dishes are prepared per clone and approx 1000 and 2500 cells/dish are plated.
20. After approx 10 d, 10–20 colonies are retrieved from the plates, grown in culture, and tested. Because the initial screening generally results in monoclonal populations, testing of more colonies is unnecessary. The methodology described above is adapted from the original reference by Sharon et al. (23).

3.3. Analysis of Antibody Specificity

Several points should be made regarding the analysis of antibody specificity:

1. Antibodies may bind to other molecules through their Fc region. The use of isotype-matched Ig of irrelevant specificity is always the best control. Omission of antibody is not an appropriate control.
2. Inhibition studies are useful in confirming the specificity of antibody binding, but cross-reactions cannot be evidenced using this type of assay.
3. Antibody “specificity” (in the sense of tissue-specificity) is highly concentration-dependent, and it is necessary to be cautious when drawing conclusions.
4. It is always best to use multiple antibodies to different epitopes of the same molecule in order to establish specificity.
5. When appropriate, alternative confirmatory techniques should be used (i.e., *in situ* hybridization can confirm results obtained using immunohistochemistry).

When defined molecular species are used for immunization, specificity analysis is relatively straightforward. In such cases, the major point to be made is that the antibodies raised may cross-react with related epitopes on other molecules.

The analysis of the specificity of antibodies is much more difficult when complex antigenic mixtures are used for immunization. In such cases, it may first be necessary to establish, for the sake of simplicity, whether the antibody recognizes a carbohydrate or a peptide epitope. Of course, complex epitopes that are dependent on both carbohydrate and peptide exist, and their precise identification is very complicated. If carbohydrate specificity is suspected, it will be useful to determine whether the epitope is present not only on glyco-

proteins, but also on glycolipids. In the latter case, it is preferable to pursue the specificity analysis on glycolipids, as these can be purified to homogeneity.

Obviously, when one is interested in defining new, tissue-specific molecules, extensive immunohistochemical fine-specificity analysis is required. Because mAb reactivity is also highly dependent on the tissue fixative (e.g., acetone, ethanol, methanol, paraformaldehyde), one should test for reactivity using several fixation liquids. This may reveal broader tissue reactivity than anticipated. In general, the mildest fixative (acetone) is used for screening purposes.

3.4. Advantages and Disadvantages of the Differential Filter-Screening Technique

1. Single-clone analysis: the filter-screening technique was specifically adapted for the isolation of antibodies used in diagnostic pathology. When using conventional hybridoma techniques (*see Subheading 3.2.1.*) several fused cells may grow out in a particular well. Therefore, immediate immunohistochemical screening cannot be performed: widely reactive antibodies produced by another hybridoma will mask the presence of cell-specific antibodies produced by one clone.
2. Workload: another limiting factor is the number of supernatants that can be tested using immunohistochemical assays. After a successful fusion, screening of 1500–2000 wells is needed, obviously well beyond a screenable number. Although initial screening by enzyme-linked immunosorbent assay (ELISA) may result in the isolation of useful hybridoma cultures, test conditions in ELISA differ considerably from immunohistochemical requirements. Coating conditions of protein on plates will impose conformational constraints. Therefore, it is not rare that antibodies that show appropriate reactivity by ELISA fail to react in immunohistochemical assays. Because this screening system is tuned for high-throughput screening of the initial fusion products, the number of clones of interest is quickly decreased to manageable numbers. Thus, many fusions can be performed in a relatively short period. This can be particularly advantageous in cases where mAb against poorly immunogenic molecules or molecules of low abundance are desired—which necessitates screening of many fusions.
3. Clone selection: by choosing the filter placed directly on the dish, one can actually loosely screen for hybridomas producing high avidity antibody/high-producer hybridomas. We generally prefer to place filters coated with relevant proteins on top of the filters coated with irrelevant antigen. Thus, clones producing low amounts of irrelevant antibody will be less likely to show up as colonies of interest.
4. In theory, coating with pure antigen should result in the identification of colonies producing only antigen-specific antibody. Nonetheless, we always find high numbers of spots on control filters as well as specific filters. We reason that this can be explained by the production of “sticky,” cross-reactive antibody by many fused cells. Therefore, we invariably use two filters for screening purposes. Obviously, two filters are necessary when crude tissue homogenates are used for

coating purposes to distinguish hybridoma colonies producing tissue-specific antibody from hybridomas producing cross-reactive antibody.

5. Subcloning: one of the main advantages of this technique is that monoclonal cultures are immediately available for screening purposes. Only 2–3 additional subcloning rounds are necessary. The latter are performed to stabilize the hybridoma for the antibody-producing phenotype, and are not really necessary to obtain a monoclonal culture. Instead of the regular limiting dilution method for subcloning purposes, we always use agarose seeding.
6. Agarose vs suspension cell growth: clonal stability. One should be aware that a small percentage of colonies will fail to grow in semisolid agarose. This may be a result of the absence of growth factors available in the vicinity of the clones when growing in agar. Alternatively, cells die—for example, because of instability—and the secreted antibody produced before death has been detected by this filter technique, regardless of the cells' status. Likewise, in conventional screening, wells may appear to contain cells excreting antibody with the desired specificity, which is lost upon further expansion. This is a possible result of similar events, i.e., when the cells secreting the antibody are not viable.
7. The differential filter-screening technique has also been successfully used to rescue extremely unstable hybridoma cultures. These are seeded at two or three different densities (1000–3000 cells per dish) and subsequently screened with anti-mouse Ig coated filters. Antibody-producing colonies can be detected by incubation with anti-mouse Ig conjugates. This alleviates cumbersome subcloning by limiting dilution, which may not be successful for extremely unstable hybridomas with a small percentage of cells still producing antibody. Additionally, filter screening can be performed within 2 wk—much more rapidly than with serial dilution subcloning.
8. Antigen source: we have used this method successfully in the isolation of tumor-specific mAbs, tissue-specific mAbs, carbohydrate-specific mAbs, and single cytokeratin-specific mAbs (4,5,24,25). Synthetic antigens, purified antigens—as well as whole-tissue homogenates—were used for screening purposes. For example in the isolation of carbohydrate-specific mAbs after immunization with a synthetic carbohydrate-carrier conjugate (24), a total of 102 colonies were retrieved. Additional ELISA screening showed carbohydrate specificity in 43 of 102 wells, 5 of 102 showed cross-reactivity with the protein carrier, and 54 of 102 did not show reactivity with any tested substance. The number of nonreactive colonies may seem high, but one must bear in mind that more than one colony is generally picked at each position identified. Obviously, the rate of success depends heavily on the requirements of the investigator and the immunogenicity of the antigen of interest. However, this also holds true for the conventional hybridoma technology.
9. It is noteworthy that in many cases, tissue- or tumor-specific mAbs were obtained that failed to react in Western blot analysis. This is most likely a reflection of recognized determinants that may be nonlinear. As mentioned earlier, this method may allow for a more native conformation of the antigens.

4. Notes

4.1. Specific Notes to the Protocols

1. The use of Freund's adjuvant has been recently contested because of the extensive inflammation it induces. Detoxified endotoxin represents a reasonable alternative as an adjuvant.
2. In general, after the fourth immunization, a good antibody titer should be obtained. Otherwise, consider other immunization strategies. However, when a crude mixture is used as immunogen, the titer of the antibody of interest will most likely be masked by contaminating antibodies.
3. As with all sterile techniques, great care should be taken to avoid contamination during the entire procedure.
4. Balb/c mice are normally used, but few studies have addressed the importance of mouse-strain use in hybridoma production. The optimal schedule and route of immunization have seldom been analyzed in a systematic way. Therefore, the final decision is left to the investigator. It is recommended to check the serum antibody titer prior to performing the fusion: in the absence of high antibody titers, the likelihood of achieving a high yield of specific hybrids is low.
5. Feeder-layer cells are used to produce soluble factors that increase hybrid growth. Alternative sources of feeder cells are mouse thymocytes, mouse spleen cells, and certain fibroblast cell lines. It is recommended to plate the cells 24 h before the cell fusion, and to check for contamination at the fusion time.
6. Several mouse myeloma cell lines are available. The choice may be determined by the fact that some lines (NS1) produce, but do not secrete, Ig light chains. However, since these can associate with Ig heavy chains produced by a hybridoma, and can be secreted, the preferred myeloma cells are the nonproducing lines P3X63-Ag8 or Sp2/O-Ag14. These lines are available from the American Type Culture Collection (Rockville, MD) or the European Collection of Cell Cultures (Salisbury, UK).

It is essential to make sure that the myeloma cells are free of Mycoplasma contamination, since this results in a dramatic drop in hybrid outgrowth. We recommend the regular testing of myeloma cells using polymerase chain reaction (PCR). If the hybridoma yield of fusions is low, or if cells appear to stop growing after a few cell divisions, one should first suspect that myeloma cells are not in good shape.

7. It is best to keep cells in a wet incubator, although this requires very careful control of sterility throughout the procedure. If a dry incubator is used, fill the outermost row of wells with PBS to avoid evaporation.
8. It is essential to optimize the screening method before the fusion is initiated because cells will grow very rapidly. It is also essential to perform the screening as rapidly as possible (maximum 2 d). In order to decrease the workload, it is also very important to devise a screening strategy that allows early identification of uninteresting clones (i.e., weak reactivity, wide reactivity, low avidity, false-positive).

9. It is very important to perform the subcloning rapidly, because nonproducing or low-producing cells tend to overgrow the cultures. Cloning efficiency generally increases when mouse PM are used as feeder layers.
10. It is recommended to confirm the persistence of antibody-producing clones after each step of expansion. Make sure to freeze cell stocks at each step of subcloning and expansion.
11. The animal Ethics and Experimentation Committees do not allow ascites production in certain countries.
12. It is useful to freeze stocks of cells adapted to grow as mouse ascites.
13. Myeloma cells to be used for fusion in the filter-plaque technique have previously been adapted to agarose growth using standard techniques. Although this is not absolutely required, this is advisable. This is also a way to become accustomed to the technique. Furthermore batch-to-batch variation of FCS does play a role in plating efficiency. It is advisable to test several lots of FCS, and to always test a new batch of FCS before ordering.
14. The temperature of the agarose to be added to the fused cells should not exceed 40°C. Do not add too-cold agarose to the cells—it will lump, resulting in uneven distribution of the toplayer and fluid toplayers and preventing any screening. The concentration of the top agarose should never be below 0.35%, otherwise it becomes too fragile and fluid.
15. Do not look at the plates before day 5, as it is detrimental to the cells.
16. Homemade filters can be prepared with a 6-cm-diameter stainless-steel punch with a sharpened edge. By leaving a 5-mm opening in the sharpened edge, a small triangle can be cut, resulting in filters shaped as shown in **Fig. 1**. Filter washing removes toxic reagents from the nitrocellulose, and is absolutely essential.
17. For purified molecules, 10–50 µg per filter is sufficient. Lower amounts can be used when the amount of material available for the assay is a limiting factor. For cell or tissue homogenates, 1 g of tissue is minced and homogenized in 20 mL PBS. Larger debris is removed by low-speed centrifugation at 1000g (3000 rpm) for 10 min. For coating purposes, a 10-fold dilution is prepared, and 10 mL of this solution are used per filter.
18. Filter sterilization should be carried out carefully. We find it convenient to place the filters in a laminar flow hood in rows at fair distances, enabling us to flip the sterilized side of the filters on the sterilized laminar flow bench as if reading a book. Try to avoid reaching over the filters during the sterilization process, to prevent contamination. Although repositioning of the filters appears cumbersome and difficult, this is not the case, provided care is taken to carefully mark the holes in the filters at the bottom of the Petri dish.
19. Remove as much fluid as possible from the Petri dishes. It facilitates screening, because the filters will adhere well to the agarose. If the top agarose appears too fluid, one can try to evaporate part of the excess fluid by overnight incubation in a dry CO₂ incubator.

If top agarose is removed during the screening, it may be helpful to place the dishes at 4°C again. This will solidify the agarose, making it less fragile. Also, it may be helpful to remove the filters one by one.

20. Placement of both filter tabs in exactly the same position will facilitate subsequent filter removal. Because contact between both filters is crucial, check for air bubbles between the filters. These show up as light spots.
21. Filter removal is a major concern. Obviously, the top agarose layer should not be disturbed, despite the intimate contact between the lower filter and the agarose. The position of the filter should never be changed: it will result in complete destruction of the integrity of the agarose. In rare cases, agarose will stick to the filter upon removal. Although we do not know why this happens, additional cooling of the remaining plates usually alleviates the problem.

References

1. Ehrlich, P. (1898) Über die constitution des diphtheriegiftes. *Dtsch. Med. Wochenschr.* **24**, 597–600.
2. Ehrlich, P. (1901) Die Schutzstoffe des blutes. *Dtsch. Med. Wochenschr.* **27**, 888–891.
3. Kohler, G. and Milstein, C. (1975) Continuous cultures of fused cells secreting antibody of predefined specificity. *Nature* **256**, 495–497.
4. Oosterwijk, E., Ruiter, D. J., Hoedemaeker, P. J., Pauwels, E. K., Jonas, U., Zwartendijk, J., and Warnaar, S. O. (1986) Monoclonal antibody G 250 recognizes a determinant present in renal-cell carcinoma and absent from normal kidney. *Int. J. Cancer* **38**, 489–494.
5. Oosterwijk, E., Ruiter, D. J., Wakka, J. C., Huiskens-van, D. M., Jonas, U., Fleuren, G. J., Zwartendijk, J., Hoedemaeker, P., and Warnaar, S. O. (1986) Immunohistochemical analysis of monoclonal antibodies to renal antigens. Application in the diagnosis of renal cell carcinoma. *Am. J. Pathol.* **123**, 301–309.
6. Bander, N. H., Finstad, C. L., Cordon, C. C., Ramsawak, R. D., Vaughan, E. D., Jr., Whitmore, W. F., Jr., Oettgen, H. F., Melamed, M. R., and Old, L. J. (1989) Analysis of a mouse monoclonal antibody that reacts with a specific region of the human proximal tubule and subsets renal cell carcinomas. *Cancer Res.* **49**, 6774–6780.
7. Finstad, C. L., Cordon, C. C., Bander, N. H., Whitmore, W. F., Jr., Melamed, M. R., and Old, L. J. (1985) Specificity analysis of mouse monoclonal antibodies defining cell surface antigens of human renal cancer. *Proc. Natl. Acad. Sci. USA* **82**, 2955–2959.
8. Luner, S. J., Ghose, T., Chatterjee, S., Cruz, H. N., and Belitsky, P. (1986) Monoclonal antibodies to kidney and tumor-associated surface antigens of human renal cell carcinoma. *Cancer Res.* **46**, 5816–5820.
9. Yoshida, S. O., Imam, A., Olson, C. A., and Taylor, C. R. (1986) Proximal renal tubular surface membrane antigens identified in primary and metastatic renal cell carcinomas. *Arch. Pathol. Lab. Med.* **110**, 825–832.

10. Vessella, R. L., Moon, T. D., Chiou, R. K., Nowak, J. A., Arfman, E. W., Palme, D. F., Peterson, G. A., and Lange, P. H. (1985) Monoclonal antibodies to human renal cell carcinoma: recognition of shared and restricted tissue antigens. *Cancer Res.* **45**, 6131–6139.
11. Moon, T. D., Vessella, R. L., Palme, D. F., Nowak, J. A., and Lange, P. H. (1985) A highly restricted antigen for renal cell carcinoma defined by a monoclonal antibody. *Hybridoma* **4**, 163–171.
12. Cordon, C. C., Bander, N. H., Fradet, Y., Finstad, C. L., Whitmore, W. F., Lloyd, K. O., Oettgen, H. F., Melamed, M. R., and Old, L. J. (1984) Immunoanatomic dissection of the human urinary tract by monoclonal antibodies. *J. Histochem. Cytochem.* **32**, 1035–1040.
13. Bander, N. H., Carroll, P. R., and Russo, P. (1997) Summary of immunohistologic dissection of the human kidney using monoclonal antibodies (Bander, N. H., Carlos Cordon-Cardo, C., Finstad, C. L., Whitmore, W. F., Jr., Darracott Vaughan, E., Jr., Oettgen, H. F., Melamed, M., and Old, L. J.) *Semin. Urol. Oncol.* **15**, 123–129.
14. Bander, N. H. (1984) Comparison of antigen expression of human renal cancers in vivo and in vitro. *Cancer* **53**, 1235–1239.
15. Grabmaier, K., Vissers, J. L., De weijert, M. C. A., Oosterwijk-Wakka, J. C., Van Bokhoven, A., Brakenhoff, R. H., Schendel, D. J., Mulders, P. A., Merks, G., Figdor, C. G., and Oosterwijk, E. (2000) Molecular cloning and immunogenicity of the renal cell carcinoma-associated antigen G250. *Int. J. Cancer* **85**, 865–870.
16. Oosterwijk, E., Bander, N. H., Divgi, C. R., Welt, S., Wakka, J. C., Finn, R. D., Carswell, E. A., Larson, S. M., Warnaar, S. O., Fleuren, G. J. and et al. (1993) Antibody localization in human renal cell carcinoma: a phase I study of monoclonal antibody G250. *J. Clin. Oncol.* **11**, 738–750.
17. Steffens, M. G., Boerman, O. C., Oosterwijk, W. J., Oosterhof, G. O., Witjes, J. A., Koenders, E. B., Oyen, W. J., Buijs, W. C., Debruyne, F. M. J., Corstens, F. H. M., and Oosterwijk, E. (1997) Targeting of renal cell carcinoma with iodine-131-labeled chimeric monoclonal antibody G250. *J. Clin. Oncol.* **15**, 1529–1537.
18. Steffens, M. G., Boerman, O. C., Oyen, W. J., Kniest, P. H., Witjes, J. A., Oosterhof, G. O. N., van Leenders, G. J., Debruyne, F. M. J., Corstens, F. H. M., and Oosterwijk, E. (1998) Intratumoral distribution of two consecutive injections of chimeric antibody G250 in primary renal cell carcinoma: implications for fractionated dose radioimmunotherapy. *Cancer Res.* **59**, 1615–1619.
19. Divgi, C. R., Bander, N. H., Scott, A. M., O'Donoghue, J. A., Sgouros, G., Welt, S., Finn, R. D., Morrissey, F., Capitelli, P., Williams, J. M., Deland, D., Nakhre, A., Oosterwijk, E., Gulec, S., Graham, M. C., Larson, S. M., and Old, L. J. (1998) Phase I/II radioimmunotherapy trial with iodine-131-labeled monoclonal antibody G250 in metastatic renal cell carcinoma. *Clin. Cancer Res.* **4**, 2729–2739.
20. Steffens, M. G., Boerman, O. C., de Mulder, P. M., Oyen, W. J., Buijs, W. C., Witjes, J. A., Van den Broek, E. J., Oosterwijk-Wakka, J. C., Debruyne, F. M. J., Corstens, F. H. M., and Oosterwijk, E. (1999) Phase I radioimmunotherapy of metastatic renal cell carcinoma with 131I-labeled chimeric monoclonal antibody G250. *Clin. Cancer Res.* **5**, 3268s–3274s.

21. Fradet, Y., LaRue, H., Parent, V. C., Bergeron, A., Dufour, C., Boucher, L., and Bernier, L. (1990) Monoclonal antibody against a tumor-associated sialoglycoprotein of superficial papillary bladder tumors and cervical condylomas. *Int. J. Cancer* **46**, 990–997.
22. Fradet, Y., Islam, N., Boucher, L., Parent, V. C., and Tardif, M. (1987) Polymorphic expression of a human superficial bladder tumor antigen defined by mouse monoclonal antibodies. *Proc. Natl. Acad. Sci. USA* **84**, 7227–7231.
23. Sharon, J., Morrison, S. L., and Kabat, E. A. (1979) Detection of specific hybridoma clones by replica immunoadsorption of their secreted antibodies. *Proc. Natl. Acad. Sci. USA* **76**, 1420–1424.
24. Oosterwijk, E., Kalisiak, A., Wakka, J. C., Scheinberg, D. A., and Old, L. J. (1991) Monoclonal antibodies against Gal alpha 1-4Gal beta 1-4Glc (Pk, CD77) produced with a synthetic glycoconjugate as immunogen: reactivity with carbohydrates, with fresh frozen human tissues and hematopoietic tumors. *Int. J. Cancer* **48**, 848–854.
25. Van Muijen, G., Ruiter, D. J., Franke, W. W., Achtstatter, T., Haasnoot, W. H., Poncet, M., and Warnaar, S. O. (1986) Cell type heterogeneity of cytokeratin expression in complex epithelia and carcinomas as demonstrated by monoclonal antibodies specific for cytokeratins nos. 4 and 13. *Exp. Cell Res.* **162**, 97–113.

Treatment Strategies in Metastatic Renal Cell Carcinoma

Cytokines, Vaccines, and Gene Therapy

Peter F. Mulders

1. Introduction

In recent years, the incidence of renal cell carcinoma (RCC) has increased dramatically (54% from 1975 to 1990), and in 1996, approx 30,000 new cases were diagnosed in the United States (1). In the same year, an estimated 12,000 RCC-related deaths occurred in the United States. The increased incidence of RCC in recent years may be linked to certain risk factors such as smoking, obesity, high-protein diets, and hypertension (2).

Nearly half of all RCC patients present with localized disease, one-quarter present with stage II disease, and nearly one-third of patients present with metastatic disease (3). In addition, as many as 40% of all patients treated for local tumors will ultimately relapse with metastatic disease. The prognosis of untreated patients with metastatic disease is unfavorable, with a 3-yr survival rate of less than 5% (4). Among patients who develop metastases within 1 yr of nephrectomy, the 2-yr survival rate is likewise very poor. In a few rare cases, however, in which patients develop metastases more than 2 yr postnephrectomy, long-term survival in excess of 5 yr has been observed (5). The prognosis for metastatic RCC remains highly unfavorable, mainly because RCC is usually resistant to radiotherapy and chemotherapy. One major challenge to the development of effective therapies for the treatment of metastatic RCC is to overcome this resistance. RCC typically exhibits a multidrug-resistant phenotype associated with expression of the multidrug-resistant-gene (MDR-1) and objective responses to chemotherapy occur in <10% of treated patients (6). How-

ever, RCC is known to be immunogenic, and immunotherapy with biological-response modifiers has had some success. A variety of approaches to immunotherapy are being investigated for the treatment of metastatic RCC. They include:

1. Immunomodulation with biological response modifiers.
2. Adoptive immunotherapy, which involves the transfer of cells with antitumor activity.
3. Therapeutic tumor-specific mAbs.
4. Vaccines designed to stimulate a specific antitumor response.
5. Gene therapy.

In human RCC, T cell-defined epitopes have not yet been identified. Therefore, the use of tumor lysate as a source of tumor antigen is an attractive approach because it circumvents the requirement of identifying tumor-specific antigens. The use of dendritic cells (DCs) loaded with tumor lysates has been explored in other tumors such as prostate carcinoma and sarcoma and a T-cell proliferation was observed *in vitro* (45,46). Moreover, mice vaccinated with DC pulsed with unfractionated tumor peptides showed a reduced growth of subcutaneously established, weakly immunogenic tumors (47). The use of unfractionated tumor proteins, compared to a single peptide-loaded DC vaccination strategy, may have advantages, although still hypothetical. Multiantigen-loaded DCs may be able to present undefined but important epitopes, whereas approaches that utilize peptide-pulsed DC require that the peptide is clearly defined. Therefore multiantigen-loaded DC are more likely to cause multiple clonal expansion of T cells, which may have an enhanced antitumor effect. This effect has been demonstrated in several human neoplasms, which have the capacity to elicit multiple specific immune responses in the autologous host (48). Second, peptides processed by the DC from the unfractionated tumor proteins will mainly be presented in a MHC class II manner, inducing a CD4+ T-cell proliferation (46). The induction of these T-helper 1 (Th1) cells has a proven stimulatory effect on the function of the DC to induce cytotoxic T-lymphocytes (CTL) (49,50). Th1 cells express CD40L on the surface, which ligates to the CD40 expressed on DC and subsequently triggers the DC to produce extremely high levels of bioactive IL-12, a cytokine known to have a proliferative effect on CTL and an enhancement of the antigen-presenting function of the DC (51). Also, other cytokines released by Th1 cells may provide an environment necessary for further maturation of DC. This may be similar to the effect accomplished by a recently described so-called monocyte-conditioned medium, which generates fully mature and stable DC (52,53). As compared with non-DC stimulation, a downregulation of natural killer (NK) cells with upregulation of CD3+CD4+ was observed in all four DC-stimulated tumor-infiltrating lymphocytes (TIL) cultures, which render a positive shift in the CD4+/CD8+ ratio. TIL

grown in low-dose IL-2 expressed reduced cytotoxicity against autologous tumor when compared to TIL costimulation with DC-TuLy. The addition of TuLy did not increase the cytotoxicity, suggesting a lack of activated antigen-presenting cells (APC) in the TIL culture. The demonstration of a lower cytotoxicity for both autologous and allogenic tumor targets in non-DC cultured TIL further implicates a loss of cytotoxic T-cell growth in IL2 alone, without DC stimulation. It appears that DC-TuLy-induced TIL do not represent single CTL clones, since the phenotypic analysis revealed a heterogeneous cell population in the cultures. Also, the cytokine profile of the restimulated TIL show patterns that correlate with tumor-specific lysis capacity of T cells (TNF α , IFN γ). Most likely, these cells represent multiple clones induced by multiantigens presented by DC using unfractionated crude TuLy. However, most of the autologous tumorlytic killing capacity of the DC-TuLy-stimulated TILs appeared to be cellular immune-mediated, as shown by the almost complete disappearance of this capacity with anti-CD3 blocking.

In summary, from the peripheral blood of patients with advanced RCC, we were able to obtain a significant number of DC with an *in vitro* granulocyte macrophage-colony stimulating factor (GM-CSF)/IL4-based culture technique suitable for clinical use. These cells have a profound morphological and phenotypic entity and a functional capacity characteristic for potent antigen-presenting cells. When loaded with unfractionated tumor proteins using liposomes, these cells were able to induce, from of TIL obtained from RCC tissue, a CTL with high autologous tumor-cell-killing capacity. Based on the results obtained from the present study, we proposed a DC-based vaccination strategy in patients with advanced RCC. Presently, such trials are ongoing in a phase 1 setting.

1.1. Gene Therapy

1.1.1. Genetically Engineered Tumor Cells

In an effort to stimulate a more potent antitumor immune response, researchers are experimenting with methods of increasing the immunogenicity of tumor cells in melanoma and RCC. One approach involves the introduction of MHC class I or cytokine genes into tumor cells to enhance tumor-antigen presentation and activation of tumor-specific CTLs (54). Genetically engineered tumor cells can be irradiated and reinfused into the patient, where they function as a vaccine.

1.1.2. GM-CSF Transfected Tumor Cells

Murine studies have demonstrated that GM-CSF is a potent stimulator of systemic antitumor immune responses (55). These findings have led to preclinical and clinical trials investigating the effectiveness of RCC cells genetically engineered to express GM-CSF in generating an anti-RCC immune

response. This type of tumor-cell vaccine has induced the complete eradication of established tumors in mice. Dr. Jonathan W. Simons described a clinical study in which several patients were injected with increasing numbers of GM-CSF-secreting tumor cells. An early infiltration of mononuclear cells (especially macrophages and DCs) at the vaccination site and an increased delayed-type hypersensitivity response were observed in patients injected with untransfected and GM-CSF-transfected tumor cells. However, two of three patients injected with GM-CSF-secreting tumor cells exhibited a fourfold increase in the magnitude of the delayed-type hypersensitivity response compared with controls, and there was no evidence of toxicity (56). Furthermore, one of these patients exhibited a partial response to the vaccine. These results suggest that adoptive transfer of GM-CSF-secreting tumor cells may stimulate an effective antitumor response. Unfortunately, this methodology is expensive and labor-intensive, which may limit its clinical application.

1.1.3. Intralesional Gene Therapy

The direct transfer of genes encoding MHC class I proteins or cytokines into tumor cells *in vivo* is a novel approach to enhancing the antitumor cellular immune response. One advantage of direct *in vivo* transfer of DNA into tumor cells compared with *ex vivo* transfer is the simplicity of the procedure, which does not require expensive and time-consuming manipulation of tumor cells in culture. One disadvantage may be the low efficiency of gene transfer. *In vivo* transfer of cytokine genes has been shown to reduce tumor growth in the murine renal adenocarcinoma model (RENCA) (57). The first Phase I clinical trial of *in vivo* intralesional gene transfer used cationic liposomes to deliver a plasmid harboring the IL-2 gene. No objective responses were observed; however, the procedure was demonstrated to be safe. The results of a dose-optimization trial are still pending.

Similar phase I trials are currently underway to examine direct gene transfer of the HLA-B7 gene and the β_2 microglobulin gene (58). The HLA-B7 gene was chosen for these studies because of evidence that it is involved in presentation of tumor-specific antigens in melanoma and RCC. Direct intralesional transfer of the HLA-B7 gene into melanoma tumors has produced clinical responses in some patients. However, to date, no clinical responses have been observed in RCC. The injection of the HLA-B7 gene into the tumors of 14 RCC patients by Dr. Nicholas Vogelzang and colleagues resulted in HLA-B7 RNA and protein expression in the majority of tumor samples. Although tumor infiltration by CD8⁺ T cells indicated induction of a cellular immune response, no clinical responses were observed (59). A recent phase II study involving 25 patients has likewise failed to demonstrate clinical efficacy. However, these studies have indicated, the overall safety and feasibility of intralesional HLA-B7 gene transfer.

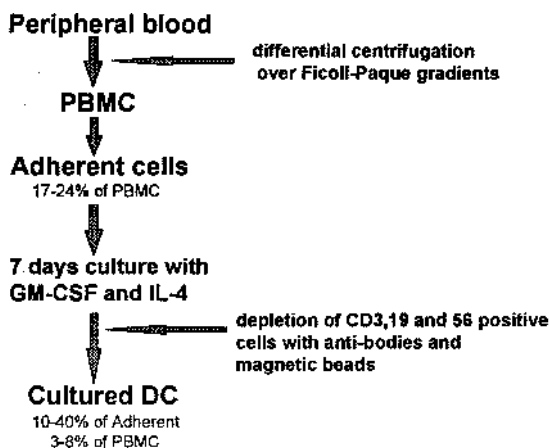


Fig. 1. Schematic presentation of materials.

2. Materials

(Schematically presented in **Fig. 1**)

1. Peripheral blood mononuclear cell (PBMC) must be isolated from peripheral blood of patients with RCC by a Ficoll-Hypaque gradient centrifugation (Pharmacia Biotech, Alameda, CA).
2. Cells are resuspended in culture medium RPMI-1640 (Bio-Whittaker, Walkersville, MD) or AIM-V (Gibco-BRL, Gaithersburg, MD) supplemented with different concentrations of heat-inactivated human-type (AB) or autologous serum (0%, 1%, 5%, or 10%), 0.01 M N-2-hydroxyethylpiperazine-N'-ethanesulfonic-acid buffer, and penicillin-streptomycin (50 IU/mL) (ICN Biomedical, Irvine, CA).
3. Cells are plated in 25-cm² cultured flasks at $2.5\text{--}5 \times 10^6$ cells/mL.
4. The cells are subsequently incubated at 37°C for 90–120 min, after which the nonadherent cells are removed with several gentle washes.
5. Adherent cells are incubated at 37°C in complete media supplemented with 800 U/mL of human recombinant GM-CSF (Genetics Institute, Boston, MA) and 1000 U/mL of human recombinant IL4 (R&D Systems, Minneapolis, MN).
6. After 7 d in culture, all free or loosely adherent cells are collected by vigorous rinsing. This results in a heterogeneous cell population containing DC, B cells, and T cells, and NK cells. DC are further purified by negative depletion.
7. The cell pellets are incubated for 30 min at 4°C with azide-free monoclonal anti-CD19, anti-CD3, and anti-CD56 antibodies (all from Immunotech, Westbrook, ME) at a concentration of 2 μ L of each per 1×10^6 cells.
8. Antibody-labeled cells are removed using magnetic beads coated with goat anti-mouse IgG (DynaL, Lake Success, NY). To test the purity of the DC, the cells are depleted with anti-CD14 (Immunotech, Westbrook, ME)

Finally, although GM-CSF is a crucial mediator of DC maturation and function, this method of DC maturation was also IL-4 dependent. In particular, the characteristic APC phenotype and function could only be demonstrated for DC grown in the presence of both GM-CSF and IL-4.

3. Methods

3.1. Immunomodulation with Biological Response Modifiers

3.1.1. Recombinant Interleukin-2 (rIL2)

1. Mechanism: proliferation of T-cells, monocytes, and NK cells.
2. Clinical status: FDA approved for clinical use in RCC patients.

In 1992, rIL-2 obtained approval from the United States Food and Drug Administration on the basis of demonstrated safety and efficacy in clinical studies involving 255 patients with RCC who were treated with high-dose rIL-2 regimens (7). The cumulative experience with high-dose rIL-2 therapy has demonstrated an objective response rate of approx a 15% (complete and partial responses)—mostly in patients with good clinical performance status—with a median survival of approx 40 mo for patients achieving a complete response and 24 mo for patients achieving a partial response. The objective response rate for RCC patients treated at the National Cancer Institute with high-dose iv bolus rIL-2 before 1992 was 20% (8). More than 75% of patients achieving a complete response remained disease-free for 3+ yr, and some complete responses have been durable for 5+ yr. The major challenge has been to develop new regimens and new strategies to further improve survival with manageable toxicity. The optimal schedule of rIL2 is still unknown. In a still ongoing three-armed randomized trial designed to establish the optimal dose of rIL-2, the three regimens are as follows (9):

1. High-dose i.v. bolus (720,000 IU/kg intravenously every 8 h).
2. Low-dose i.v. bolus (72,000 IU/kg intravenously every 8 h).
3. Subcutaneous (120,000 IU/d for 5 d each wk).

Toxicity—including hypotension, dyspnea, thrombocytopenia, malaise, and disorientation—was significantly greater with the high-dose regimen, and approx 50% of patients in this group required treatment for hypotension compared with less than 5% in the low-dose group. The response rate and toxicities observed in the sc group were similar to those observed in the low-dose iv group. The response percentages were 21% in the high-dose iv bolus group, and only 11% in the low-dose iv bolus group, and response durations were significantly longer in the high-dose group. Although the final results are still pending, it may be true that the differences will ultimately not be significant. Moreover, as with adequate monitoring of patients, it can be tolerated without risk of treatment-related mortality.

The role of nephrectomy in selected patients who responded to rIL-2 has also been addressed. In a study reported by Bennet et al., four of six patients whose renal tumors progressed after immunotherapy exhibited no evidence of residual disease after resection, and have remained disease-free for nearly 5 yr (*10*). The acceptance of rIL-2 as the standard therapy for metastatic RCC has led to the investigation of other biological-response modifiers for treating this disease.

3.1.2. *rINF α*

1. Mechanism: proliferation of T cells, upregulation of MHC molecules.
2. Clinical status: in Europe, approval for clinical use in RCC patients.

Since the first clinical trials in 1983 suggested that rINF- α was effective in the treatment of metastatic RCC, extensive studies have been conducted. The objective response rate from the treatment of more than 900 patients in 13 clinical trials with rINF- α was 18.4%, and duration of response ranged from 6–10 mo; however, complete responses are rare (*11,12*). Despite the large number of studies investigating the efficacy of rINF- α in metastatic RCC, the optimal dose and schedule have not been determined because of significant variability in reported response rates, which may stem from differences in regimens and patient populations. The published data, however, suggest that a dose of 10–20 mIU/d produces optimal response rates with single-agent rINF- α therapy. The impact of single agent rINF- α on overall survival has not yet been determined.

Certain variables appear to predict the likelihood of response to rINF- α therapy. Patients with a good performance status, prior nephrectomy, and nonbulky pulmonary and/or soft-tissue metastases who are asymptomatic or exhibit minimal symptoms have a higher likelihood for response. Indeed, response percentages of up to 30% and response durations of >27 mo have been observed in a select subset of patients (*13*). These patients had prior nephrectomy, good-to-excellent performance status, and no previous chemotherapy or radiotherapy. In contrast, patients with undersexed primary RCC, extensive prior treatment, and bulky metastases to viscera or bone were less likely to respond.

3.1.3. *Combination Therapy with rINF- α and rIL-2*

Preclinical murine tumor models have demonstrated synergistic antitumor effects with the combination of rINF- α and rIL-2, establishing a compelling rationale for their combined use (*14*). The mechanisms of synergy are unclear, but administration of rINF- α may augment the immunogenicity of tumor cells by enhancing expression of MHC antigens and presentation of tumor-associated antigens to T lymphocytes.

Clinical trials have established the safety and efficacy of combination therapy with rINF- α rIL-2 in metastatic RCC. The available data from 1200

patients treated with this combination collectively demonstrate an objective response rate of approx 20%, and approx 5% of patients achieved a complete response. Overall, responses have occurred at all disease sites—including bone, intact primary tumors, and visceral metastases—and have included patients with large tumor burdens such as bulky individual lesions. Some durable complete responses have been observed.

Several studies have also investigated the combination of rIL-2, rIFN- α , and 5-fluorouracil for metastatic RCC, with encouraging results (15,16). In a phase II outpatient study investigating the efficacy of sc IL-2 (20 mIU/m²) and rINF- α (6-9 mIU/m²) plus i.v. bolus 5-fluorouracil (750 mg/m²), an overall response rate of 39% was observed (11% complete responses and 28% partial responses) (17). Stratification of patients by risk factors revealed a significant survival advantage with this combination as compared to single-agent rIL-2 in low- and intermediate-risk patients. Others have reported similarly encouraging results, with an objective response rate of 47% (15). Confirmation of these efficacy data and additional information about toxicity associated with this regimen are needed.

3.1.4. *rIL12*

1. Mechanism: favors TH-1 type responses, macrophage, and NK cell activation; induces IFN- γ production.
2. Clinical status: Phase I.

Preclinical and phase I clinical trials are currently investigating the biological effects of rIL-12 and its antitumor activity in metastatic RCC. IL-12 is believed to induce expression of other cytokines and chemokines. Preclinical experiments have shown that administration of weekly pulses of rIL-2 in combination with rIL-12 additively enhanced the priming of macrophages for nitric-oxide production in culture and reversed tumor growth in mice far more effectively than either agent alone (18). Two phase I studies with systemic rIL-12 were performed, and in 50% of patients an induction of IFN- γ RNA was observed. In addition, two IFN-inducible chemokines were detected in rIL-12 treated patients—suggesting that rIL-12 induces IFN- γ expression, resulting in an enhanced antitumor immune response (19).

3.2. *Adoptive Immunotherapy*

A variety of adoptive immunotherapeutic approaches have been investigated in RCC, including:

1. Adoptive transfer of TILs.
2. Autologous activated memory T-cells (ALT).
3. Priming tumor-specific CTLs.

Lymphocytes with potential cytotoxic antitumor activity can be isolated from peripheral blood, tumor-draining lymph nodes, or tumor tissue. These cells are subsequently expanded *ex vivo* and reinfused into the patient—often in combination with biological response modifiers—with the hope of improving the rate and durability of response.

3.2.1. TILs

TILs can be isolated from the patient's tumor, expanded *ex vivo* in rIL-2, and reinfused, typically in conjunction with rIL-2 and/or rIFN- α therapy or chemotherapy. In an early study, 12% of RCC patients treated with rIL-2 plus TILs achieved a clinical response (20). The Departments of Urology and Medical Oncology at University of California Medical School at Los Angeles has shown a favorable experience with these regimens, according to Dr. Arie Belldegrun. Of the 55 patients treated with a combination of rIFN- α priming, TILs, and low-dose iv rIL-2, 35% achieved a clinical response (9% complete responses and 25% partial responses) with no significant toxicity (21). Among those patients who responded to therapy, 43% survived 2+ yr. Median survival among patients achieving a complete response was 42+ mo. High baseline levels of circulating NK cells were the only prognostic factor that correlated with response. These results demonstrate that immunotherapy in combination with radical nephrectomy and adoptive transfer of TILs can provide substantial therapeutic benefit. Combined therapy with rIL-2, rIFN- α , and TILs has become the standard at the University of California at Los Angeles.

3.2.2. ALT

ALT refers to adoptive immunotherapy with autologous activated-memory T lymphocytes that have been expanded and activated *ex vivo*. T lymphocytes are selected from peripheral blood leukocytes with anti-CD3 mAbs and then further enriched for activated-memory T lymphocytes that have presumably been exposed to tumor antigens. These memory T cells are then expanded and nonspecifically stimulated with cytokines to increase their cytolytic activity and multicytokine secretion. The resulting cell population presumably contains activated CTLs with potential antitumor activity. Early studies suggested that ALT, in combination with cimetidine (an agent postulated to inhibit suppressor T-cell activity), produced a survival benefit (22).

To assess the clinical benefit of ALT in metastatic RCC, 90 patients were randomized to receive cimetidine monthly for 6 mo, alone or in combination with ALT (23). Median survival in the ALT group was >2 times longer (17 mo) than in the group receiving cimetidine alone—a significant improvement. Ten of 45 patients (22%) survived 44+ mo, and toxicity associated with ALT was minimal. A phase III trial in which patients are randomized to rIFN- α plus cimetidine with or without ALT is currently underway.

3.2.3. Priming Tumor-Specific CTLs

Animal models have shown that adoptive immunotherapy can be effective against advanced malignancies when lymphocytes derived from tumor-draining lymph nodes are primed with *Corynebacterium parvum* ex vivo and subsequently reinfused. Clinical experiments involved patients with melanoma or RCC in which a portion of each patient's tumor mass was excised and used to prime tumor-specific CTLs. Tumor cells were irradiated and mixed with T lymphocytes from draining lymph nodes that had been stimulated in culture with bacillus Calmette-Guérin. By doing so, it was hoped that tumor-specific CTLs would proliferate in culture. As many as 10^{11} cells, primarily CTLs, could then be reinfused into the patient. These cells demonstrate autologous antitumor cytolytic activity in vitro, and have high GM-CSF and IFN- γ cytokine profiles, both of which are important for T-cell-mediated immune reactivity (24). In a recent clinical trial involving 12 patients with RCC, two complete responses and two partial responses were obtained with this treatment (25).

3.3. Vaccine Development—DC Immunotherapy

1. Mechanism: inducing a specific cellular immune response.
2. Clinical status: Phase I.

DCs are the most potent cells for antigen presentation, are critical for eliciting T-cell-mediated immune responses, and have initiated new directions in the treatment of cancer (26). The premise behind this approach is that DC can be isolated from patient's blood, armed with tumor antigens, and subsequently used to induce a specific antitumor response (27,28). Recently, several human phase I trials have been initiated using peptide/protein-loaded DC, and in different metastatic tumors promising results have been obtained, without significant side effects from the vaccinations (29–31). **Figure 2** depicts the flow of such a vaccination. It is known that a defective immune response exists in patients with advanced cancer (32,33). Although factors that contribute to tumor immunological escape are not well elucidated, inadequate presentation of tumor antigens by host APCs is one of potential mechanisms that renders tumor progression (34). In order to activate T-cell-mediated antitumor activity, APC must be capable of processing tumor-associated antigens, present them in the context of MHC class I or II molecules, and, provide costimulatory molecules (B7-1/B7-2) to interact with the T cell (35). **Fig. 2** schematically presents the interaction of DC and T cells. The recent finding that mature DC isolated from RCC tumor had a reduced capability of capturing soluble antigens indicates a close relationship between immunosuppression and defective DC *in situ* (36). This hypothesis is further supported by the study demonstrating that pretreatment of DC with transforming growth factor- β (TGF- β), a

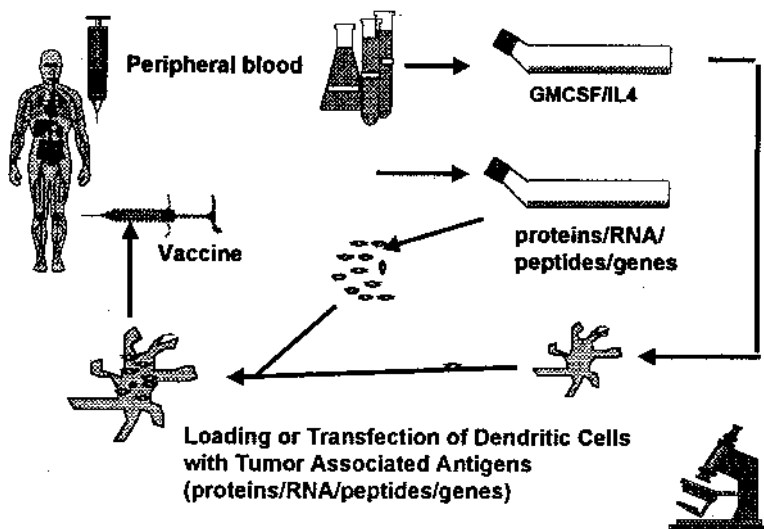


Fig. 2. Flow of vaccinations.

tumor-derived growth factor, could impair their antigen-presenting function (37). The lack of B7-1 and B7-2 expression by tumor-infiltrating DC was also reported (38). Likewise, vascular endothelial growth factor (VEGF) secreted by tumor cells was recently identified as an immunosuppressive factor that could block early stages of DC maturation from precursors (39). Therefore, the failure of RCC patients to elicit an antitumor response *in situ*, despite the presence of TIL and DC, suggests that the antigen presentation system *in situ* is functionally suppressed.

The DC play an important role in the immune system network, as the most potent APCs. This unique function provides a fundamental concept and rationale for clinical applications in the treatment of patients with advanced cancer. Efficacy of peptide-pulsed DC as APC for the induction of antigen-specific CTL *in vivo* has been demonstrated in a series of animal experiments using *in vitro* cultivated and cytokine-treated DC (42–44). There is evidence for a potent kidney-cancer vaccine that may be generated using autologous TuLy-loaded DC induced from adherent PBMCs using GM-CSF and IL-4. In order to develop a DC-based immunotherapy for the treatment of patients with RCC, the optimization of the DC culture technique suitable for clinical use is necessary. A DC culture technique with the use of serum-free medium (RPMI-1640 or AIMV) was not suitable because it obtained a heterogeneous cell population with a significant number of CD14⁺ macrophages with a low B7-2 expression, a phenotype which is correlated with a lack of antigen uptake capacity and

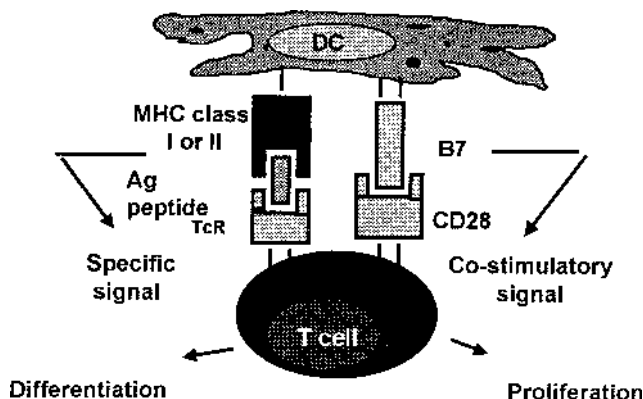


Fig. 3. Schematic interaction of DC and T cells.

presenting function. Moreover, only with the use of RPMI-1640 and 10% autologous serum DC can adequately be generated from CD14⁺ progenitor cells (macrophage/monocytes). A dose-dependent DC maturation by serum was only observed when DC were cultured in RPMI-1640 medium, but not in AIMV medium. This medium- and serum-dependent DC maturation is obligatory in the culture technique—in which, after the adherent step, the nonadherent cells are gently rinsed off and a significant number of lymphocytes are still present during the 7 d culture with IL4 and GM-CSF.

4. Notes

1. The frequency of response with this combination is equivalent to or greater than that reported with rIL-2 alone, and durable complete responses are reported with both regimens; however, no large randomized trial has directly compared the efficacy of rIL-2 alone vs rIL-2 plus rIFN- α .
2. The epidemiological correlation between the number of tumor-infiltrating DCs and survival (**40,41**) further indicates that activation of DC within the tumor site may be particularly important in the induction of a cellular immune response.
3. The combination of autologous serum and the presence of a small number of lymphocytes provides an adequate environment for monocytes to mature into potent APCs.
4. The successful treatment of metastatic RCC poses a significant therapeutic challenge. Because of the intrinsic multidrug resistance of renal cells, chemotherapy has proven ineffective. Immunotherapy with rIL-2 is the current standard for treating RCC, and a number of promising new immunotherapeutic strategies are now under investigation. Although none have demonstrated clear superiority over rIL-2 therapy, some combination regimens and adoptive immunotherapy strategies may improve response rates and prolong survival.

with less morbidity than single-agent rIL-2 therapy. Reducing the toxicity of therapy is important. Strategies to improve the antitumor activity of adoptively transferred leukocytes using cytokine priming, dendritic cells, or genetic manipulation are especially promising. Research aimed at defining the clinical parameters that can predict responses to immunotherapy is also beginning to bear fruit.

5. Perhaps the most potent weapon that we can yield against RCC is a tumor vaccine that will mobilize an effective in vivo, cellular, antitumor immune response. Currently, tumor-cell vaccines using genetically altered tumor cells are in the early stages of clinical testing, and researchers are experimenting with direct intralesional DNA transfer to deliver genes to tumor cells. Recent advances in the identification of tumor-associated antigens have improved the prospects for developing effective RCC-specific peptide vaccines. Continued preclinical and clinical research will undoubtedly lead to a better understanding of the factors critical to induction of an effective antitumor immune response, which may involve overcoming functional deficits in the host immune cells. This research, together with recent and continued advances in our understanding of the molecular genetics of RCC, will be critical to the development of a comprehensive strategy for treating this disease.

References

1. Parker, S. L., Tong, T., Bolden, S., and Wingo, P. A. (1996) *Cancer Statistics CA Cancer J.* **65**, 5–7.
2. Chow, W. H. and Gridley, G. (1994) Protein intake and risk of renal cell cancer. *J. Natl. Cancer Inst.* **96**, 1131–1139.
3. Golimbu, M., and Joshi, P. (1986) RCC: survival and prognostic factors. *Urology* **27**, 291–301.
4. deKernion, J. B., Ramming, K., and Smith, R. (1978) The natural history of metastatic renal cell carcinoma: a computer analysis. *J. Urol.* **120**, 148–152.
5. Franklin, J., Dorey, F., Gitlitz, B., and Belldegrun, A. (1996) Cytoreductive nephrectomy in 63 consecutive patients who received adoptive immunotherapy for advanced RCC. *J. Urol.* **155**, 500A.
6. Kakehi, Y., Kanamaru, H., Yoshida, O., Ohkubo, H., Nakanishi, S., Gottesman, M., and Pastan, I. (1988) Measurement of multi-drug resistance messenger RNA in urogenital cancers; elevated expression in renal cell carcinoma is associated with intrinsic drug resistance. *J. Urol.* **139**, 862–865.
7. Fyfe, G., Fisher, R. I., Rosenberg, S. A., Sznol, M., Parkinson, D. R., and Louie, A. C. (1995) Results of treatment of 255 patients with metastatic renal cell carcinoma who received high-dose recombinant interleukin-2 therapy. *J. Clin. Oncol.* **13**, 688–696.
8. Fyfe, G. A., Fisher, R. I., Rosenberg, S. A., Sznol, M., Parkinson, D. R., and Louie, A. C. (1996) Long-term response data for 255 patients with metastatic renal cell carcinoma treated with high-dose recombinant interleukin-2 therapy. *J. Clin. Oncol.* **14**, 2410–2411.

9. Yang, J. C., Topalian, S. L., Parkinson, D., Schwartzentruber, D. J., Weber, J. S., Ettinghausen, S. E., White, D. E., Steinberg, S. M., Cole, D. J., Kim, H. I., Levin, R., Guleria, A., MacFarlande, M. P., White, R. L., Einhorn, J. H., Seipp, C. A., and Rosenberg, S. A. (1994) Randomized comparison of high-dose and low-dose intravenous interleukin-2 for the therapy of metastatic renal cell carcinoma: an interim report. *J. Clin. Oncol.* **12**, 1572–1576.
10. Bennett, R. T., Lerner, S. E., Taub, H. C., Dutcher, J. P., and Fleischmann, J. (1995) Cytoreductive surgery for stage IV renal cell carcinoma. *J. Urol.* **154**, 32–34.
11. Wirth, M. P. (1993) Immunotherapy for metastatic renal cell carcinoma. *Urol. Clin. N. Am.* **20**, 283–295.
12. Motzer, R. J., Schwartz, L., Law, T. M., Murphy, B. A., Hoffman, A. D., Albino, A. P., Vlamis, V., and Nanus, D. M. (1995) Interferon α -2a and 13-*cis*-retinoic acid in renal cell carcinoma: antitumor activity in a Phase II trial and interactions *in vitro*. *J. Clin. Oncol.* **13**, 1950–1957.
13. Sarna, G., Figlin, R., and deKernion, J. B. (1987) Interferon in renal cell carcinoma. *Cancer (Phila.)* **59**, 610–612.
14. Chikkala, N. F., Lewis, I. Ulchaker, J. Stanley, J. Tubbs, R., and Finke, J. H. (1990) Interactive effects of α -interferon A/D and interleukin 2 on murine lymphokine-activated killer activity: analysis at the effector and precursor level. *Cancer Res.* **50**, 1176–1182.
15. Sella, A., Kilbourn, R. G., Gray, I., Finn, L., Zukiwski, A. A., Ellerhorst, J., Amato, R. J., and Logothetis, C. J. (1994) Phase I study of interleukin-2 combined with interferon- α and 5-fluorouracil in patients with metastatic renal cell cancer. *Cancer Biother.* **9**, 103–111.
16. Atzpodien, J., Kirchner, H., Hanninen, E. L., Deckert, M., Fenner, M., and Poliwoda, H. (1993) Interleukin-2 in combination with interferon- α and 5-fluorouracil for metastatic renal cell cancer. *Eur. J. Cancer* **29A(Suppl. 5)**, S6–S8.
17. Lopez Hanninen, E., Kirchner, H., and Atzpodien, J. (1996) Interleukin-2 based home therapy of metastatic renal cell carcinoma: risks and benefits in 215 consecutive single institution patients. *J. Urol.* **155**, 19–25.
18. Wigginton, J. M., Kuhns, D. B., Back, T. C., Brunda, M. J., Wiltrout, R. H., and Cox, G. W. (1996) Interleukin 12 primes macrophages for nitric oxide production *in vivo* and restores depressed nitric oxide production by macrophages from tumor-bearing mice: implications for the antitumor activity of interleukin 12 and/or interleukin 2. *Cancer Res.* **56**, 1131–1136.
19. Motzer, R. J., Rakhit, A., Schwartz, L. H., Olencki, T., Malone, T. M., Sandstrom, K., Nadeau, R., Parmar, H., and Bukowski, R. (1998) Phase I trial of subcutaneous recombinant human interleukin-12 in patients with advanced renal cell carcinoma. *Clin Cancer Res.* **4**, 1183–1191.
20. Bukowski, R. M., Sharfman, W., Murthy, S., Rayman, P., Tubbs, R., Alexander, J., Budd, G. T., Sergi, J. S., Bauer, L., Gibson, V., Stanley, J. Boyett, J., Pontes, E., and Finke, J. (1991) Clinical results and characterization of tumor-infiltrating lymphocytes with or without recombinant interleukin 2 in human metastatic renal cell carcinoma. *Cancer Res.* **51**, 4199–4205.

21. Figlin, R., Pierce, W. C., Kaboo, R., Tso, C. L., Moldawer, N., Dolan, N., Gitlitz, B., deKernion, J. B., and Belldegrun, A. (1997) Treatment of metastatic renal cell carcinoma with nephrectomy, interleukin-2 and cytokine-primed or CD8(+)-selected tumor-infiltrating lymphocytes from primary tumor. *Urol. Sept*; **158(3 Pt 1)**, 740–745.
22. Gitlitz, B. J., Belldegrun, A., and Figlin, R. A. (1996) Immunotherapy and gene therapy. *Semin. Urol. Oncol.* **14**, 237–243.
23. Graham, S., Babayan, R. K., Lamm, D. L., Sawczuk, I., Ross, S. D., Lavin, P. T., Osband, M. E., and Krane, R. J. (1993) The use of *ex vivo*-activated memory T cells autolymphocyte therapy) in the treatment of metastatic renal cell carcinoma: final results from a randomized, controlled, multisite study. *Semin. Urol.* **11**, 27–34.
24. Pierce, W. C., Belldegrun, A., and Figlin, R. A. (1995) Cellular therapy: scientific rationale and clinical results in the treatment of metastatic renal cell carcinoma. *Semin. Oncol.* **22**, 74–80.
25. Chang, A. E., Aruga, A., Cameron, M. J., Sondak, V. K., Normolle, D. P., Fox, B. A., and Shu, S. (1997) Adoptive immunotherapy with vaccine-primed lymph node cells secondarily activated with anti-CD3 and interleukin-2. *J. Clin. Oncol.* **15**, 796–807.
26. Steinman, R. M. (1991) The dendritic cell system and its role in immunogenicity. *Ann. Rev. Immunol.* **9**, 271–296.
27. Romani, N., Gruner, S., Brang, D., Kampgen, E., Lenz, A., Trockenbacher, B., Konwalinka, G., Fritsch, P. O., Steinman, R. M., and Schuler, G. (1994) Proliferating dendritic cell progenitors in human blood. *J. Exp. Med.* **180**, 83–93.
28. Celluzi, C. M., Mayordomo, J. I., Storkus, W. J., Lotze, M. T., and Falo, L. D. (1996) Peptide-pulsed dendritic cells induce antigen-specific, CTL mediated protective tumor immunity. *J. Exp. Med.* **183**, 283–287.
29. Hsu, F. J., Benike, C., Fagnoni, F., Liles, T. M., Czerwinski, D., Taidi, B., Engleman, E. G., and Levy, R. (1996) Vaccination of patients with B-cell lymphoma using autologous antigen-pulsed dendritic cells. *Nat. Med.* **2**, 52–58.
30. Mukherji, B., Chakraborty, N. G., Yamasaki, S., Okino, T., Yamase, H., Sporn, J. R., Kurtzman, S. K., Ergin, M. T., Ozols, J., Meehan, J., et al. (1995) Induction of antigen-specific cytolytic T cells in situ in human melanoma by immunization with synthetic peptide-pulsed autologous antigen presenting cells. *Proc. Natl. Acad. Sci. USA* **92**, 8078–8082.
31. Murphy, G., Tjoa, B., Ragde, H., Kenny, G., and Boynton, A. (1996) Phase I clinical trial: T-cell therapy for prostate cancer using autologous dendritic cells pulsed with HLA-A0201-specific peptides from prostate-specific membrane antigen. *Prostate* **29**, 371–380.
32. O'Sullivan, G. C., Corbett, A. R., Shanahan, F., and Collins, J. K. (1996) Regional immunosuppression in esophageal squamous cancer: evidence from functional studies with matched lymph nodes. *J. Immunol.* **157**, 4717–4720.
33. Young, M. R., Wright, M. A., Lozano, Y., Matthews, J. P., Benefield, J., and Prechel, M. M. (1996) Mechanisms of immune suppression in patients with head and neck cancer: influence on the immune infiltrate of the cancer. *Intl. J. Cancer* **67**, 333–338.

34. Gabrilovich, D. I., Corak, J., Ciernek, I. F., Kavanaugh, D., and Carbone, D. P. (1997) Decreased antigen presentation by dendritic cells in patients with breast cancer. *Clin. Cancer Res.* **3**, 483–490.
35. Melief, C. J. (1989) Dendritic cells as specialized antigen-presenting cells. *Res. Immunol.* **140**, 902–907.
36. Thurnher, M., Radmayr, C., Ramoner, R., Ebner, S., Bock, G., Klocker, H., Romani, N., and Bartsch, G. (1996) Human renal-cell carcinoma tissue contains dendritic cells. *Intl. J. Cancer* **68**, 1–7.
37. Bonham, C. A., Lu, L., Banas, R. A., Fontes, P., Rao, A. S., Starzl, T. E., Zeevi, A., and Thomson, A. W. (1996) TGF- β 1 pretreatment impaires the allostimulatory function of human bone marrow-derived antigen-presenting cells for both naive and primed T cells. *Transpl. Immunol.* **4**, 186–191.
38. Chaux, P., Moutet, M., Faivre, J., Martin, F., and Martin, M. (1996) Inflammatory cells infiltrating human colorectal carcinomas express HLA class II but not B7-1 and B7-2 costimulatory molecules of the T-cell activation. *Lab. Invest.* **74**, 975–983.
39. Gabrilovich, D. I., Chen, H. L., Girgis, K. R., Cunningham, H. T., Meny, G. M., Nadaf, S., Kavanaugh, D., and Carbone, D. P. (1996) Production of vascular endothelial growth factor by human tumors inhibits the functional maturation of dendritic cells. *Nat. Med.* **2**, 1096–103.
40. Zied, N. A. and Muller, H. K. (1993) S100 positive dendritic cells in human lung tumors associated with cell differentiation and enhanced survival. *Pathology* **25**, 338–343.
41. Becker, Y. (1992) Anticancer role of dendritic cells (DC) in human and experimental cancers—a review. *Anticancer Res.* **12**, 511–520.
42. Slingluff, C. L., Jr. (1996) Tumor antigens and tumor vaccines: peptides as immunogens. *Semin. Surg. Oncol.* **12**, 446–453.
43. Mayordomo, J. I., Zorina, T., Storkus, W. J., Zitvogel, L., Garcia-Prats, M. D., DeLeo, A. B., and Lotze, M. T. (1997) Bone marrow-derived dendritic cells serve as potent adjuvants for peptide-based antitumor vaccines. *Stem Cells* **15**, 94–103.
44. Porgador, A., Snyder, D., and Gilboa, E. (1996) Induction of antitumor immunity using bone marrow-generated dendritic cells. *J. Immunol.* **156**, 2918–2926.
45. Tjoa, B., Boynton, A., Kenny, G., Ragde, H., Misrock, S. L., and Murphy, G. (1996) Presentation of prostate tumor antigens by dendritic cells stimulates T-cell proliferation and cytotoxicity. *Prostate* **28**, 65–69.
46. Cohen, P. A., Cohen, P. J., Rosenberg, S. A., and Mule, J. J. (1994) CD4+ T-cells from mice immunized to syngeneic sarcomas recognize distinct, non-shared tumor antigens. *Cancer Res.* **54**, 1055–1058.
47. Zitvogel, L., Mayordomo, J. I., Tjandrawan, T., DeLeo, A. B., Clarke, M. R., Lotze, M. T., and Storkus, W. J. (1996) Therapy of murine tumors with tumor peptide-pulsed dendritic cells: dependence on T cells, B7 costimulation, and T helper cell 1-associated cytokines. *J. Exp. Med.* **183**, 87–97.
48. Sahin, U., Tureci, O., Schmitt, H., Cochlovius, B., Johannes, T., Schmits, R., Stenner, F., Luo, G., Schobert, I., and Pfreundschuh, M. (1995) Human neoplasms

- elicit multiple specific immune responses in the autologous host. *Proc. Natl. Acad. Sci. USA* **92**, 11810–11813.
49. Koch, F., Stanzl, U., Jennewein, P., Janke, K., Heufler, C., Kampgen, E., Romani, N., and Schuler, G. (1996) High level IL-12 production by murine dendritic cells: upregulation via MHC class II and CD40 molecules and downregulation by IL-4 and IL-10. *J. Exp. Med.* **184**, 741–746.
 50. Cella, M., Scheidegger, D., Palmer-Lehmann, K., Lane, P., Lanzavecchia, A., and Alber, G. (1996) Ligation of CD40 on dendritic cells triggers production of high levels of interleukin-12 and enhances T cell stimulatory capacity: T-T help via APC activation. *J. Exp. Med.* **184**, 747–752.
 51. Zeh, H. J., 3d., Hurd, S., Storkus, W. J., and Lotze, M. T. (1993) Interleukin-12 promotes the proliferation and cytolytic maturation of immune effectors: implications for the immunotherapy of cancer. *J. Immunoth.* **14**, 155–161.
 52. Romani, N., Reider, D., Heuer, M., Ebner, S., Kampgen, E., Eibl, B., Niederwieser, D., and Schuler, G. (1993) Generation of mature dendritic cells from human blood. An improved method with special regard to clinical applicability. *J. Immunol. Methods* **196**, 137–151.
 53. Bender, A., Sapp, M., Schuler, G., Steinman, R. M., and Bhardwaj, N. (1996) Improved methods for the generation of dendritic cells from nonproliferating progenitors in human blood. *J. Immunol. Methods* **196**, 121–135.
 54. Golumbek, P., Levitsky, H., Jaffee, L. and Pardoll, D. M. (1993) The antitumor immune response as a problem of self-nonsel self discrimination: implications for immunotherapy. *Immunol. Res.* **12**, 183–192.
 55. Dranoff, G., Jaffee, E., Lazenby, A., Golumbek, P., Levitsky, H., Brose, K., Jackson, V., Hamada, H., Pardoll, D., and Mulligan, R. C. (1993) Vaccination with irradiated tumor cells engineered to secrete murine granulocyte-macrophage colony-stimulating factor stimulates potent, specific, and long-lasting anti-tumor immunity. *Proc. Natl. Acad. Sci. USA* **90**, 3539–3543.
 56. Jaffee, E. M., Marshall, F., Weber, C., Pardoll, D. M., Levitsky, H., Nelson, W., Carducci, M., Mulligan, R., and Simons, J. (1996) Bioactivity of a human GM-CSF tumor vaccine for the treatment of metastatic renal cell carcinoma. *Proc. Am. Soc. Clin. Oncol.* **15**, 237.
 57. Sun, W. H., Burkholder, J. K., Sun, J., Culp, J., Turner, J., Lu, X. G., Pugh, T. D., Ershler, W. B., and Yang, N. S. (1995) *In vivo* cytokine gene transfer by gene gun reduces tumor growth in mice. *Proc. Natl. Acad. Sci. USA* **92**, 2889–2893.
 58. Nabel, G. J., Yang, Z. Y., Nabel, E. G., Bishop, K., Marquet, M., Felgner, P. L., Gordon, D., and Chang, A. E. (1995) Direct gene transfer for treatment of human cancer. *Ann. NY Acad. Sci.* **772**, 227–231.
 59. Vogelzang, N. J., Lestingi, T. M., Sudakoff, G., and Kradjian, S. A. (1994) Phase I study of immunotherapy of metastatic renal cell carcinoma by direct gene transfer into metastatic lesions. *Hum. Gene Ther.* **5**, 1357–1370.

Assessment of T-Cell Immune Dysfunction in Patients with Renal Cell Carcinoma

Robert G. Uzzo, Vladimir Kolenko, Andrew C. Novick,
and James H. Finke

1. Introduction

Functional T cells are the central component of an effective antitumor immune response. However, in patients with renal cell carcinoma (RCC), the growth of antigenic tumors proceeds in the absence of significant T-cell responses, posing a distinct obstacle to the development of effective immunotherapy strategies and cancer vaccines. The minimum required elements of a functional antitumor immune T-cell response have been identified, including T cells that can preferentially recognize tumor-associated antigens (1). However, despite increasing evidence that T-cells recognize discrete tumor antigen, transformed cells continue to evade immune destruction, and tumors thereby progress. There is now little doubt that the immune response to tumor antigens is altered in patients with cancer (2). This rarely manifests clinically as generalized immune suppression, which may reflect the antigen specificity of the immune dysfunction in the initial stages of the disease.

An orchestrated antitumor immune response depends on the ability of T lymphocytes to undergo normal activation and express cytokines necessary for clonal expansion and effector functions. In addition, this T-cell response must be appropriately maintained and must avoid premature downregulation mediated primarily through apoptotic pathways. Increasing evidence suggests these activities fail to occur or are inappropriately terminated in patients with malignancies including RCC. In tumor-bearing patients, T cells infiltrating the tumor bed exhibit a diminished capacity to proliferate (3), reduced cytotoxic activity (4), and reduced Th1 cytokine expression (5). Alterations in

select signal transduction pathways—including the transcription factor NF κ B—have been associated with this immune dysfunction in patients with RCC (6,7). Impaired NF κ B activity may contribute to reduced T-cell function, since this transcription factor controls the expression of a number of genes that encode for cytokines, their receptors, and other membrane-regulatory molecules central to T-cell activation, and protection of T cells from apoptotic stimuli (8,9,10,11).

The tumor itself may play a significant role in the development of immune dysfunction (7,12,13,14). Indirect evidence supporting the role of the tumor-T-cell interaction has been identified in the tumor bed, where defective T-cell signaling and function as well as T-cell death have all been detected. Similar defects have been demonstrated in circulating peripheral blood T cells, including decreases in the TCR- ζ chain (15), abnormal NF κ B-binding activity (7), and identification of preapoptotic markers on T-cells, such as the externalization of phosphatidyl serine (16). The magnitude of these defects may be related to tumor burden and clinical stage (17), and some defects may be reversed after complete tumor removal (7). Soluble tumor-derived products capable of altering T-cell function have been identified from our laboratory and others, and may account for these observations (18). Taken together, these data suggest that the tumor plays a central role in mediating T-cell defects. Here, we outline our techniques for isolating and identifying alterations in T-cell signaling elements and effector functions in patients with RCC.

2. Materials

2.1. Isolation of T-cells

2.1.1. Peripheral Blood T-cell Isolation by Negative Magnetic Selection

1. Equipment: pipettors, pipet aid, centrifuge, magnetic separator (MACS, Miltenyi Biotec, Sunnyvale, CA), magnetic column (Stem Cell Technologies, Vancouver, BC, Canada), pH meter.
2. Plasticware/Disposables: three-way stopcock, 21-gauge needle, 10-mL syringe, pipet tips, pipets (2-, 5-, and 10-mL), 50-mL conical polypropylene tubes (Becton Dickinson, Franklin Lakes, NJ), 15-mL polypropylene centrifuge tubes (Corning Inc., Corning, NY).
3. Medium: RPMI-1640, fetal calf serum (FCS), phosphate-buffered saline (PBS), bovine serum albumin (BSA), ethylenediaminetetraacetic acid (EDTA).
4. PBS/BSA/EDTA medium: 1% BSA with 5 mM EDTA in PBS (adjust to a pH of 7.2).
5. Reagents: Ficoll (LKD Biotech, Piscataway, NJ), T-cell antibody cocktail (α -CD14 (macrophages), α -CD16 (natural killer [NK] cells), α -CD19 (B cells), α -CD56 (NK cells), and glycophorin A (erythrocytes) and magnetic colloid (Stem Cell Technologies).

2.1.2. Tumor-Infiltrating T-Cells

1. Equipment: 37°C water bath, shaker, centrifuge, pipet aid, pH meter, 37°C incubator.
2. Plasticware/Disposables: scalpels, Petri dish, specimen container, mesh stainless-steel filter, nylon filters (150 μ M Nitex mesh, Tetko, Briarcliff Manor, NY), 50-mL conical centrifuge tubes, 60-mL syringe, nylon wool (PolyScience, Niles, IL), pipets.
3. Medium: Dulbecco's modified Eagle's medium (DMEM) (BioWhittaker, Walkersville, MD), RPMI-1640, FCS, PBS/BSA/EDTA (*see Subheading 2.1.1., item 3*).
4. Digestion solution (freshly made): 70 mg Collagenase II and 20 mg trypsin inhibitor in 20 mL warm DMEM.
5. Complete RPMI-1640: 10% FCS, 200 mM L-glutamine, gentamicin (50 mg/L), 100 mM sodium pyruvate, 10 mM nonessential amino acids. Adjust volume with RPMI-1640.

2.2. Characterization of Surface Antigens by Immunocytometry

1. Equipment: FACScan, microcentrifuge, pipet, pipet aids.
2. Plasticware/Disposables: eppendorf tubes, pipets, pipet tips, polystyrene round-bottom RIA tubes (Becton Dickinson).
3. Media: PBS, BSA.
4. Reagents: antibodies.
 - a. T-cell subsets and activation markers:
 1. CD3/CD4/CD8 (Becton Dickinson).
 2. CD25 (IL2R α) (Becton Dickinson).
 3. HLA-DR (Becton Dickinson).
 - b. Apoptotic proteins and receptors:
 1. CD95 (Becton Dickinson).
 2. CD95L (PharMingen, San Diego, CA).
 3. Annexin V (R & D Systems, Minneapolis, MN).
 4. Propidium iodide staining buffer (Phoenix Flow Systems, San Diego, CA).
 5. TNF R1 and 2 (R & D Systems).

2.3. Isolation of Cellular Extracts and Proteins

2.3.1. Whole-Cell Lysates

1. Equipment: microcentrifuge, pipettors, pipet aids, vortex, spectrophotometer.
2. Plasticware/Disposables: Eppendorf tubes, pipets, pipet tips, 50-mL conical centrifuge tubes.
3. Media: lysis buffer, 50 mM Tris-HCl, pH 7.6, 150 mM NaCl, 1% Triton X-100.
4. Reagents: ddH₂O, NaCl, phenylmethylsulfonyl flouride (PMSF), leupeptin, aprotinin, pefabloc, chymostatin.

2.3.2. Nuclear and Cytoplasmic Extracts

1. Equipment: microcentrifuge, pipettors, pipet aid, vortex, rock platform.
2. Plasticware/disposables: Eppendorf tubes, pipet tips, pipets, 50-mL conical centrifuge tubes.

3. Hypotonic buffer A: 10 mM HEPES (pH 7.9), 10 mM KCl, 0.1 mM EDTA, 0.1 mM EGTA.
4. Hypotonic buffer C: 20 mM HEPES (pH 7.9), 25% glycerol, 0.4 M NaCl, 1 mM EDTA (pH 8.0), 1 mM EGTA.
5. Protease inhibitors: 2 μ g/mL aprotinin, 2 μ g/mL leupeptin; 1 mM dithiothreitol (DTT); 100 μ g/mL pefabloc; 10 μ g/mL phenylmethylsulfonyl fluoride (PMSF); 0.1 μ g/mL chymostatin.
6. Nonidet P-40 detergent (Sigma).

2.4. Western Blotting for Signaling Proteins

1. Equipment: Electrophoresis apparatus, transfer apparatus, shaker, heating block, vortex, X-ray cassette, pipet aids, pipetors, heat sealer.
2. Plasticware/Disposables: PVDF or nitrocellulose membrane (MSI, Westborough, MA), clear-sheet protector, X-ray film, Eppendorf tubes, pipets, pipet tips, sealable clear plastic freezer bags, plastic containers for washes, scalpel, ruler.
3. Sample buffer (2X): 125 mM Tris (pH 6.8), 4% sodium dodecyl sulfate (SDS), 10% glycerol, 0.006% bromophenol blue, 2% β -mercaptoethanol.
4. Electrophoresis buffer (5X): 25 mM Tris-HCl, 192 mM glycine, 0.1% SDS. Bring up to 3 L with ddH₂O. Store at 4°C. Dil. 1:4 for use.
5. Transfer buffer (1X): 48 mM Tris, 39 mM glycine, 20% methanol, 0.037% SDS. Bring volume up to 1 L. Cool buffer before use.
6. Blocking buffer (1X): 5% nonfat dry milk in wash buffer.
7. Wash buffer (pH 7.4) (1X): 50 mM Tris-HCl, 150 mM NaCl, 0.1 % Tween-20.
8. Antibodies used:
 - a. Jak1 and Jak3 (Transduction Labs, Lexington, KY).
 - b. STAT 5 (Transduction Labs).
 - c. RelA and p50 (Santa Cruz Biotechnology, Santa Cruz, CA).
 - d. TCR α (Coulter Corp., Hialeah, FL).
 - e. p56^{lck} and p59^{fyn} (Upstate Biotechnology Inc., Lake Placid, NY).
 - f. Caspase 1,3,6,7,8 (Santa Cruz).
9. Molecular weight marker (Amersham Life Sciences).

2.5. Electrophoretic Mobility Gel Shift Assay (EMSA)

1. Equipment: Electrophoresis apparatus, pipet aid, pipettor, vacuum-gel dryer, X-ray film and cassette, liquid scintillation counter (Beckman, Fullerton, CA). A white light box and high-resolution CCD camera (Sierra Scientific).
2. Plasticware/disposables: Pipet tips, Eppendorf tubes, chromatography paper (Whatman International, Maidstone, UK), plastic wrap.
3. Running buffer: 0.25% TBE. Make 5X Tris-borate-EDTA (TBE) stock buffer solution with 54 g Tris, 27.5 g boric acid, 20 mL 0.5 M EDTA (pH 8.0). Dilute to a final concentration of 0.25% with ddH₂O.
4. Incubation buffer: 20 mM HEPES (pH 7.9), 80 mM NaCl, 0.1 mM EDTA, 1 mM DTT, 8% glycerol, 2 μ L poly (dI-dC) (Pharmacia, Piscataway, NJ).

5. Loading dye: 0.025 g bromophenol blue, 0.025 g xylene cyanol, 3 mL glycerol, 7 mL dEPC H₂O.
6. Reagents:
 - a. Gel: ddH₂O, polyacrylamide: *bis*-, 5X TBE, 10% ammonium persulfate, TEMED (Sigma).
 - b. Preparation of probes: Nick translation kit (Boehringer Mannheim, Germany), [α -³²P]-dCTP, NF κ B consensus sequence (Gibco-BRL, Gaithersburg, MD).
 - c. Sample preparation: poly (dIdC), DTT, loading dye.

2.6. RNA Isolation and PCR Protocol

2.6.1. RNA Isolation

1. Equipment: ultracentrifuge, SpeedVac, quartz cuvetts, spectrophotometer.
2. Plasticware/Disposables: 50-mL conical centrifuge tubes, 5-cc syringe, 21-gauge needle, SW50.1/SW55 polyallomer tubes.
3. Reagents: PBS, GITC/ β ME solution (25 mL of guanidine isothiocyanate plus 209 μ L of β -mercaptoethanol, cesium chloride, cold 70% ETOH, PCI extract (phenol:chloroform:isoamyl alcohol [Gibco-BRL])), 3 M sodium acetate (pH 5.0), dep H₂O.

2.6.2. PCR Protocol

1. Equipment: DNA thermal cycler, pipettor, pipet aid, X-ray film and cassette, water baths (42°C and 65°C), Southern blotting dish and apparatus, UV light box and crosslinker, heat sealer.
2. Plasticware/disposables: pipet, pipet tips, microwell dish, Tupperware, nitrocellulose paper, filter paper, absorbable towels, sealable plastic pouches, plastic wrap.
3. PCR primer and probe sets, AMV reverse transcriptase and buffer (Promega Corp., Madison, WI), RNase, *Taq* polymerase.
4. Reverse transcriptase (RT) mix: For each sample add 1 μ L 10X RT buffer, 1 μ L 10X dNTP's (2.5 mM), 1.25 μ L 3' primer (20 μ M), 0.5 μ L RNAsin enzyme, 0.5 μ L RT enzyme.
5. Polymerase chain reaction (PCR) mix: For each sample add 27.25 μ L depc H₂O, 5 μ L 10X PCR buffer, 5 μ L 10X dNTP's, 1.25 μ L 3' primer (20 μ M), 1.25 mL 5' primer (20 μ M), 0.25 μ L *Taq* polymerase.
6. Gel: 5X TBE, agarose gel, ethidium bromide, loading buffer.
7. Denaturing reagents: 60 mL 5 M NaCl, 20 mL 5 N NaOH, 120 mL ddH₂O.
8. Renaturing reagent: 60 mL 5 M NaCl, 80 mL 2.5 M Tris-HCl (pH8.0), 60 mL ddH₂O.
9. Gel transfer: 20X SSC.
10. Prehybridization solution: 30 mL formamide, 1.2 mL 50X Denhardt's solution, 3.0 mL 1 M phosphate buffer, 15 mL 20X standard saline citrate (SSC), 3 mL 20% SDS, 4.8 mL depc H₂O, 3.0 mL salmon sperm, which has been boiled for 10 min.
11. Hybridization solution: 5 mL 20X SSC, 0.3 mL NaH₂PO₄, 0.63 mL salmon sperm and 9.1 mL depc H₂O.
12. Probe cocktail: probe, polynucleotidekinase, DEPC H₂O, α -³²P adenosine triphosphate (ATP), 10X polykinase buffer.
13. Wash solution: 6X SSC, 20% SDS.

2.7. Generation of Tumor Supernatants from Explants

1. Equipment: Shaker, microcentrifuge, pipettors, pipet aids, CO₂ incubator.
2. Plasticware/disposables: Scalpels, Petri dish, tissue culture flasks, nylon filters, 50 mL conical centrifuge tubes, pipets, pipet tips.
3. Media: RPMI-1640, DMEM.

2.8. Determination of T-cell Apoptosis

2.8.1. TUNEL Assay

1. Equipment: FACScan, pipettors, pipet aids, microcentrifuge, Ventana Gen II *in situ* hybridization instrument Ventana Medical Systems (Tucson, AZ), Ventana 320 automated immunostainer, light microscope.
2. Plasticware/disposables: Eppendorf tubes, pipets, pipet tips.
3. Media: none.
4. Reagents: 1% Paraformaldehyde, 70% ethanol, PBS, APO-BRDU kit (Phoenix Flow) containing terminal deoxynucleotidyl transferase (TdT), dUTP, fluorescein-PRB-1 antibody, propidium iodide/RNase A solution, formalin and B5 fixed paraffin-embedded RCC, xylene, graded alcohol wash (70–100%), proteinase K (2 mg/mL diluted 1:100 in 10 mM Tris-HCl), nuclear fast red counterstain.

2.8.2. Assessment of Functional Caspase Activity by Fluorescent/Colorimetric Assays

1. Equipment: Fluorometer/spectrophotometer, pipettors, pipet aids.
2. Plasticware/disposables: 96-well plate, pipets, pipet tips, 50-mL conical centrifuge tubes, 37°C incubator.
3. Reaction buffer: 100 mM HEPES, pH 7.5, 20% vol/vol glycerol, 5 mM DTT, 0.5 mM EDTA.
4. Reagents: Fluorogenic/colorimetric caspase 1,3,6,8,9 specific substrates (Calbiochem, LaJolla, CA), glycerol, DTT, EDTA, ddH₂O.

2.8.3. Cytochrome c-Release Assays

1. Equipment: Pipettors, pipet aids, Kontes douncer and B pestle (Kontes Glass Co.).
2. Plasticware/disposables: Pipets, pipet tips.
3. Media: Cytochrome *c* buffer: 250 mM sucrose, 12.5 mM Tris, pH 4.0, DTT 1 mM, 0.125 mM EDTA, 5% glycerol, 1 μM PMSF, 1 μg/mL leupeptin, 1 μg/mL pepstatin, 1 μg/mL aprotinin.
4. Reagents: PBS.

2.8.4. Mitochondrial Permeability Transition (MPT) Assays

1. Equipment: Pipettors, pipet aids.
2. Plasticware/disposables: pipets, pipet tips.
3. Media: PBS.

4. Reagents: 3,3'-Dihexyloxacarbocyanine iodide (DiOC₆) (Molecular Probes, Eugene, OR), PBS, carbonyl cyanide m-chlorophenylhydrozone (mCICCP) (Sigma Chemical Co. St. Louis, MO).

3. Methods

3.1. Isolation of T-cells

3.1.1. Peripheral Blood T-Cell Isolation by Negative Magnetic Selection

3.1.1.1. ISOLATION OF MONONUCLEAR CELLS

1. Dilute blood 1:1 with RPMI-1640 at room temperature.
2. Add 12 mL of Ficoll to 50 mL centrifuge tubes.
3. Carefully layer 30 mL of diluted blood onto the Ficoll.
4. Centrifuge tubes at 1000 rpm for 30 min at room temperature.
5. Remove the upper yellow supernatant and discard leaving approx 5–6 mL of the top layer. Carefully collect the remaining yellow layer and the interface (buffy layer) containing the mononuclear cells.
6. Wash collected cells with RPMI-1640 at 1500 rpm for 5 min. Discard the supernatant and resuspend the cells in 30–50 mL of RPMI-1640. Count the cells, recentrifuge, and discard the supernatant. Resuspend the cells at 20×10^6 cells/mL in RPMI-1640.

3.1.1.2. TO REMOVE THE PLATELETS

1. Add FCS (twice the volume the cells are in) to a 15-mL centrifuge tube. Carefully layer the cells onto the FCS. Centrifuge at 1500 rpm for 5 min and discard the supernatant. Resuspend the cells at $2-8 \times 10^7$ cells/mL in PBS/BSA/ETDA.

3.1.1.3. IMMUNOMAGNETIC LABELING

1. Add 100 μ L of antibody cocktail for each mL of cells and mix well.
2. Incubate on ice for 30 min or for 15 min at room temperature.
3. Add 60 μ L of magnetic colloid for each mL of cells and mix well.
4. Incubate on ice for 30 min or for 15 min at room temperature.
5. Prepare the column during the incubation period.

3.1.1.4. COLUMN PREPARATION

1. Remove column from its sterile package. Avoid touching the luer fitting. Place column into the magnet.
2. Remove three-way stopcock from its sterile package and aseptically attach the luer lock to the column. Aseptically attach the 21-gauge needle to the luer fitting on the stopcock directly below column. Check all connections.
3. Set three-way stopcock to flow from the side port into the column. Fill a sterile syringe with PBS (no protein) and attach to the side of three-way stopcock. Slowly depress plunger of syringe to deliver PBS up the column until the level of PBS is above the stainless steel matrix of the column. Do not allow air bubbles to enter the mesh matrix.

4. To wash column, place a waste container below the exit needle. Add PBS/BSA/EDTA to top of column and turn the three-way stopcock so the flow is from column down through the needle (side exit closed). Continue adding media until you have collected three column vol of wash media. Do not let the column dry at any time. Turn the three-way stopcock to stop flow of media from the column. The column is now ready for separation procedure.

3.1.1.5. SEPARATION PROCEDURE

1. Load the sample on top of the column. Turn the stopcock to start the flow of media down through the needle into a collection tube. Allow the sample to run into the matrix of column. Add media to the top of the column until you have collected three column vol of media plus the vol of your start sample. Turn stopcock to stop flow of media.
2. Centrifuge the collected suspension at 1000 rpm for 10 min. Discard the supernatant and resuspend cells in the appropriate medium. This technique results in >95% CD3+ cell selection.

3.1.2. Tumor-Infiltrating T-Cell Isolation

3.1.2.1. NYLON COLUMN PREPARATION

1. Fill 60-mL syringe with 3.5 g of nylon and autoclave.

3.1.2.2. DIGESTION OF TUMOR

1. Trim tumor of fat and normal tissue and cut it into approx 2×2 -mm fragments with scalpels in a Petri dish under a sterile hood. Weigh tumor fragments and place into a specimen container. Wash with DMEM two or three times.
2. Add 2 mL of digestion solution per g of tumor. If tumor is less than 10 g, add 20 mL of digestion solution. Shake at 37°C for 2 h.

3.1.2.3. PREPARATION OF SINGLE-CELL SUSPENSION

1. Dilute digested tumor with DMEM and filter through mesh stainless-steel filter.
2. Centrifuge at 1000 rpm for 10 min and discard supernatant. Resuspend pellet in DMEM and filter through nylon filters. Centrifuge at 1000 rpm for 10 min. Discard the supernatant and resuspend pellet in DMEM.
3. Count the cells and dilute in RPMI-1640 to 2×10^6 cells/mL. Add 12 mL of Ficoll to 50 mL centrifuge tube and carefully layer 20 mL of diluted sample onto Ficoll. Next, centrifuge at 1000 rpm for 30 min at 18°C. Remove about two-thirds of the top layer and discard, leaving about 5–7 mL of the top layer. Carefully remove the remaining 5–7 mL of the top layer and the interface layer and place in 50-mL centrifuge tube. Centrifuge sample at 1500 rpm for 5 min and discard the supernatant. Resuspend pellet in RPMI-1640 and count the cells. Dilute the cells to 5×10^6 cells/mL in complete RPMI-1640.

3.1.2.4. SEPARATION OF MONONUCLEAR CELLS FROM TUMOR CELLS THROUGH NYLON COLUMN

1. Wet the nylon column completely with RPMI-1640 and evacuate the air. Fill the nylon column with complete RPMI-1640 and keep at 37°C for 2 h.
2. Add 10–15 mL of cell suspension into the nylon column and let it go into the column before adding more complete RPMI-1640. Keep at 37°C for 1 h and wash the column with 150–200 mL of warm complete RPMI-1640. Collect the eluate into 50-mL tubes. Centrifuge the samples at 1000 rpm for 10 min and discard the supernatant. Resuspend cells at $2\text{--}8 \times 10^7$ cells/mL in PBS/BSA/EDTA.
3. For isolation of T-TILs, follow procedures described in **Subheading 3.1.1.3.**

3.2. Characterization of Surface Antigens by Immunocytometry

1. All procedures should be performed under dimly lit conditions.
2. Resuspend cells at a density of approx 5×10^6 in 3% BSA/PBS. Add the first antibody solution or according to the protocol provided by the manufacturer. Incubate 30–45 min at 4°C.
3. Wash cells twice in 3% BSA/PBS for 5 min by centrifugation at 1500 rpm.
4. For labeled primary antibodies, analyze stained cells on the FACScan using appropriate emission and excitation wavelengths. Include the appropriately matched isotype control for each particular subclass of Ig and system employed.
5. For unlabeled primary antibodies, resuspend cells at a density of approximately 5×10^6 cells/mL in 3% BSA/PBS, then add the secondary antibody solution and incubate 30 min at 4°C. Wash cells twice in 3% BSA/PBS for 5 min at 1500 rpm. Analyze stained cells on the FACScan using appropriate emission and excitation wavelengths.

3.3. Isolation of Cellular Extracts and Proteins

3.3.1. Whole-cell Lysates

1. After isolation of T-cells as described in **Subheading 3.1.**, place $7\text{--}10 \times 10^6$ cells in media.
2. Wash cells three times with PBS (1500 rpm for 5 min each time).
3. Add inhibitors to the lysis buffer immediately prior to use for a final concentration of 10 $\mu\text{g/mL}$ PMSF, 2 $\mu\text{g/mL}$ leupeptin, 2 $\mu\text{g/mL}$ aprotinin, 100 $\mu\text{g/mL}$ chymostatin.
4. Resuspend cells in lysis buffer with inhibitors (100 μL per 1×10^7 cells). Vortex for 2 s, and incubate on ice for 15 min.
5. Centrifuge at 13000 rpm for 15 min and aliquot supernatant. This is the whole-cell lysate.
6. Measure protein concentration with a commercial kit (Bio-Rad, Richmond, CA).

3.3.2. Nuclear and Cytoplasmic Extracts

1. Wash cells three times with PBS (1500 rpm for 5 min each time). Resuspend cells in 100 μL of hypotonic buffer A per 10×10^6 cells. Add protease inhibitors

to buffer stock solution just before use (2 $\mu\text{g/mL}$ aprotinin, 2 $\mu\text{g/mL}$ leupeptin, 1 mM DTT, 100 $\mu\text{g/mL}$ pefabloc, 10 mg/ml phenylmethylsulfonyl fluoride (PMSF), 0.1 $\mu\text{g/mL}$ chymostatin). Vortex and incubate on ice for 20 min.

2. Add 10 μL of 10% nonidet P-40 detergent, vortex vigorously and centrifuge at 13000 rpm for 2 min. Aliquot the supernatant, which represents the cytoplasmic extract.
3. Rinse the pellet containing the nuclear extract with hypotonic buffer A, then resuspend it in buffer C (25 μL per 1×10^7 cells) with the protease inhibitors added to the stock solution at the same concentrations given above.
4. Incubate for 20 min at 4°C on a rock platform.
5. Centrifuge samples (13,200 rpm) at 4°C for 10 min and aliquot nuclear extracts.
6. Store at -70°C .

3.4. Western Blotting for Signaling Proteins (Jak-3, RelA, p56^{lck}, p59^{lyn} p50, STAT5)

3.4.1. Polyacrylamide Gel Electrophoresis

1. Mix equivalent amount of protein (10–50 μg) with equal volume of 2X sample buffer. Include one lane for the molecular weight marker. Vortex and boil for 3–5 min.
2. Load samples to each well of a polyacrylamide gel and electrophorese.

3.4.2. Western Blotting

1. Transfer proteins from gel to PVDF or nitrocellulose membrane using transfer apparatus (15 V, 3 mA/cm² for 30 min).
2. Remove the blot from transfer apparatus and place into blocking buffer. Incubate the blot for 1 h at room temperature or overnight at 4°C .
3. Dilute the primary antibody in the appropriate buffer as recommended on the product description sheet. Decant the blocking buffer from the blot and wash twice for 5 min with washing buffer. Place membrane in a clear plastic bag and add antibody solution. Carefully remove air and seal. Incubate with agitation for 1 h at room temperature or overnight at 4°C .
4. Decant the primary antibody solution, add wash buffer, and wash for 30 min with agitation, changing buffer every 5–10 min.
5. Dilute the enzyme-conjugated appropriate secondary antibody 1:2000–1:5000 in wash buffer containing 5% nonfat dry milk. Decant the wash buffer from the blot, add secondary antibody solution, and incubate with agitation for 30 min to 1 h at room temperature. Decant the secondary antibody solution, add wash buffer, and wash for 30 min with agitation, changing buffer every 5–10 min.
6. Decant wash buffer, and place the blot on clean tray containing chemiluminescent solution (0.25 mL/cm²). Incubate the blot for 1 min at room temperature.
7. Place blot in a clear sheet protector. Expose to X-ray film. Develop the film to an appropriate exposure.

3.5. Electrophoretic Mobility Gel Shift Assay (EMSA)

3.5.1. Generation of Sequence-Specific Double-Stranded Oligonucleotide Probes

1. The synthetic oligonucleotide containing a tandem repeat of the consensus sequence for the NF κ B DNA binding site corresponds to the κ B element from the IL-2R α gene. The sequence of the oligonucleotide is 5'CAACGGCAGGGGAATCTCCCTCTC-CTT3'. The underlined sequence represents the κ B motif.
2. Radiolabeled double-stranded oligonucleotide probes are prepared using a nick translation kit. A complementary DNA strand is synthesized using the 3' OH termini of the nick as a primer and incorporating [α - 32 P]dCTP as a label.
3. Perform binding reactions using 10 μ g of nuclear protein preincubated on ice for 10 min in a 20-mL total reaction volume of binding buffer.

3.5.2. Preparation of Gel and Samples

1. Prepare gel mixture using polyacrylamide:*bis* (9 mL), 5X TBE (2.3 mL), ammonium persulfate (0.45 mL), TEMED (22.5 μ L) and dd H $_2$ O to a total volume of 45 mL. Vortex and pour the gel.
2. Once crosslinked, remove the comb, rinse the wells and prerun the gel in the gel-shift tank using running buffer for 30 min.
3. Prepare samples with 6–10 μ g of protein, adding equivalent amounts for each sample on a given gel. Add appropriate amount of incubation buffer containing DTT and poly (dIdC) (*see Subheading 2.5., item 4.*). Incubate samples on ice for 10 min.
4. Add equal amount of probe to each sample using $1-4 \times 10^5$ counts/sample. The total volume of the reaction mixture should be 25 μ L. Incubate with probe at room temperature for 20 min to allow hybridization.
5. Unlabeled oligonucleotides may be added at 100-fold excess to the labeled probe to demonstrate specificity by competition.
6. Load samples into lanes after the addition of loading dye. Run gel at 150 V, cooling with circulating water in apparatus until dye is 1–2 cm from bottom of the gel (2–3 h).
7. Place gel on transfer paper and dry with vacuum gel dryer for 1 h.
8. Cover with Saran Wrap and expose to X-ray film in cassette at -80°C to desired exposure.
9. For quantitation of band density, place the developed X-omat AR film on the light box and capture its image using the CCD camera (Sierra Scientific). Analyze the density under each band using Image 1.57 software.

3.6. RNA Isolation and PCR Protocol

3.6.1. Isolation of Total RNA from T-cells or Tumor Samples

1. Wash cells (up to 10^8) twice with PBS.
2. Add 5.5 mL of (GITC)/ β ME solution per 100 mm dish and transfer to a sterile Falcon tube then vortex.

3. Layer the sample onto 2.0 mL of cesium chloride in a SW50.1/SW55 polyallomer tube. Top with mineral oil and balance buckets. Centrifuge at 30,000 rpm for 18–20 h.
4. Aspirate mineral oil and guanidine/cesium chloride from pellet and resuspend RNA pellet in 200 μ L DEP H₂O and transfer to labeled Eppendorf tube. Rinse each ultracentrifuge tube with an additional 200 μ L and transfer to same Eppendorf tube.
5. Add 45 μ L 3 M sodium acetate (pH 8) to each 400 μ L RNA solution. Mix well with pipet.
6. Add 1 mL absolute alcohol to each RNA sample and precipitate overnight at -20°C .
7. Spin Eppendorf tubes at maximum speed for 30 min and remove supernatants. Wash pellets three times with 70% EtOH.
8. Dry in rotovac 10 min, and resuspend each pellet in 30–100 μ L DEP H₂O.
9. Read optical density of 1:250 dilution in H₂O at 260 nm. (Concentration of RNA = OD 260 \times 50 \times dilution.)

3.6.2. RT-PCR Protocol and Southern Hybridization

1. Begin with an appropriate concentration of total stock RNA (1 $\mu\text{g}/\mu\text{L}$) resuspended in DEPC H₂O. In an autoclaved eppendorf, add 5 μ L of stock RNA to 7 μ L of DEPC H₂O. Incubate at 65°C for 5 min to denature the RNA into linear form.
2. Prepare the RT mix in bulk. Add the enzymes last. Next add 8.5 μ L of RT mix to each sample and incubate at 42°C for 1 h. If unable to continue at this point, the samples can be stored at -20°C until needed.
3. Prepare the desired number and kind of dilutions. For the total number of samples intended for PCR, add the dilutions as well as the positive and negative controls.
4. Transfer 10 μ L of RT product to each autoclaved PCR tube (0.8 mL Eppendorf). Make up the PCR mix in bulk adding the enzymes last. Add 40 μ L of PCR mix to each sample including a negative control. Top off each sample with approx 80 μ L of mineral oil and place in thermocycler for the appropriate number of cycles at the correct temperature.

3.6.3. Southern Hybridization

1. Prepare gel with 100 mL of 1X TBE and 1.5 g of agarose. Bring to a boil and pour gel into mold. Allow crosslinking of gel with appropriately sized comb in place.
2. Place gel into Southern blotting dish and fill with 1X TBE as running buffer.
3. Prepare samples for loading: Add 2 μ L of appropriate molecular weight marker into microwell dish for each sample. Add 18 μ L of sample to the corresponding wells and pipet up and down to mix thoroughly. Load the sample into the gel wells. Include one lane for the marker alone. Run the gel at 100 V for approx 1 h or until marker has migrated far enough along that resolution of bands will be adequate.
4. Remove the gel and examine it under UV light to evaluate band resolution. A polaroid can be obtained for recording the data.

5. Prepare denaturing and renaturing reagents and place gel in denaturing reagent for 15–30 min with gentle shaking. Next transfer to the renaturing reagent for an equal duration of time.
6. Gel transfer:
 - a. Make gel-transfer box using plastic container and 30–50 stacked sheets of 20X SSC-soaked 3MM filter paper. The stack of paper should fit in the container so that 1 inch of space between each side of stack and each side of box. Fill box to just below top to stack with 20X SSC.
 - b. Cut nitrocellulose and four pieces of blotting paper to size of gel to be transferred. Place two pieces of the gel-sized blotting paper on top of stack in transfer box. Turn gel upside down and place on top of these pieces. Wet nitrocellulose with 20X SSC and place on top of gel, removing bubbles with gloved finger. Place two additional pieces of blotting paper on top of the nitrocellulose.
 - c. Place 8-in. stack of flat paper towels above gel, and add weight to enhance wicking. Surround gel perimeter with parafilm to prevent wicking into towelings not covering the gel. Leave overnight at room temperature.
7. Hybridization
 - a. Remove towels from apparatus, and recover gel/nitrocellulose combination. Mark location of gel wells on the nitrocellulose paper. Crosslink the gel to the membrane using UV crosslinker.
 - b. Remove the gel from the membrane and discard. Place the membrane into a sealable pouch. Make prehybridization buffer and add 15 mL to the bag with the membrane. Remove all air and seal. Place in 42°C H₂O bath and agitate for 3 h. Prepare the 20- μ L probe cocktail/ with 1–2 μ L of probe, 2 μ L polynucleotidekinase, 2 μ L of 10X polynucleotidekinase buffer (final concentration = 1X), 2–4 μ L α -³²P ATP. Place the cocktail in 37°C bath for 30 min.
 - c. Make hybridization solution. Remove the membrane from the water bath and empty. Add 15 cc hybridization solution and 18 μ L of appropriately labeled probe. Remove all air bubbles and seal. Place in 42°C bath and agitate overnight.
 - d. The following day, remove the specimen from the bath and discard the hybridization solution. Make wash solution (6X SSC with 20% SDS) and place membrane in wash solution on agitator to remove excess, nonspecific ³²P binding. Wrap the membrane in plastic wrap and expose to X-ray film until the appropriate exposure is achieved.

3.7. Generation of Tumor Supernatants from Explants

1. Trim tumor of fat and normal tissue. Cut tumor into approx 3 × 3 mm fragments with scalpels in a Petri dish under a sterile hood. Shake tumor fragments overnight in RPMI-1640 at 4°C.
2. The next day, wash tumor fragments with RPMI-1640 2–3 times.
3. Place tumor explants into a tissue-culture flask and add 15 mL of DMEM per each gram of tumor. Incubate for 3–4 d at 37°C with 95% air and 5% CO₂.
4. Harvest supernatant fluid and filter through nylon filter. Centrifuge sample at 3000 rpm for 20 min. Aliquot and store at –70°C.

3.8. Determination of T-cell Apoptosis

3.8.1. TUNEL Assay

1. Fix cells in 1% formaldehyde for a minimum of 15 min.
2. Label cells with 50 μ L of DNA solution containing 10 μ L of terminal deoxynucleotidyl transferase (TdT) reaction buffer (0.75 μ L TdT enzyme, 8 μ L of Br-dUTP and dH₂O).
3. Rinse cells prior to resuspending in 0.1 mL of solution containing fluorescein-PRB-1 antibody.
4. Add propidium iodide/RNase A solution (0.5 mL) to each sample and incubate at room temperature for 30 min.
5. Perform flow cytometric analysis within 2 h of sample staining.
6. Percentages of apoptotic cells are obtained using quadrant analysis software (LYSIS II, Becton Dickinson, San Jose, CA).
7. *In situ* TUNEL assays:
 - a. Perform on formalin and B5-fixed RCC-embedded tumor tissue.
 - b. Deparaffinize and rehydrate in xylene for 5 min at room temperature.
 - c. Immerse and fix in graded alcohol washes (100–70% pure ethanol) then permeabilize using proteinase K (1 μ L of 2 mg/mL solution diluted 1:100 in 10 mM Tris).
 - d. TUNEL staining is performed as in **step 7a** and coupled to an automated chromogenic detection on the Ventana Gen II in situ hybridization instrument (Ventana Medical Systems) after nuclear fast red counterstaining.
 - e. Double-staining with anti-CD3 is performed using the Ventana 320 automated immunostainer.
 - f. Apoptosis in T-TIL was assessed using conventional light microscopy.

3.8.2. Assessment of Functional Caspase Activity

1. Incubate samples (20–30 μ g of cell lysates at 1 μ g/mL) with 180 μ L of reaction buffer containing 100 μ M of appropriate fluorogenic/colorimetric substrate in 96-well plate for 1–2 h at 37°C.
2. Perform negative controls with substrate alone and positive controls with substrate plus active caspase enzymes.
3. Monitor fluorescence/optical density on a microplate fluorimeter/colorimetric spectrophotometer using appropriate wavelengths.

3.8.3. Cytochrome c Release

1. Harvest cells and wash with PBS.
2. Add 20 mL of buffer and disrupt cells by douncing approx 80 times in a 0.3-mL Kontes douncer with the pestle.
3. Centrifuge at 13000 rpm for 15 min and collect the supernatant for Western blotting.

3.8.4. Mitochondrial Permeability Transition (MPT) Assay

1. Incubate cells with 100 nm 3,3'-dihexyloxacarbocyanine iodide (DiOC₆) in PBS for 15 min at room temperature.

2. Analyze cells with FACScan flow cytometer. Exclude dead cells by staining with propidium iodide and forward/sideward scatter gating.
3. Use cells incubated with mCICCP, which completely disrupts MPT, as a positive control.

4. Notes

1. Live gating of the forward and orthogonal scatter channels may be employed to exclude debris and to selectively acquire lymphocyte events.
2. When the RNA samples are finished, freeze to -20°C , remove the mineral oil, and transfer to new, clean tubes. Store at -20°C until needed.
3. For each mRNA amplified, the optimal cycle numbers and conditions must be determined.

References

1. Finke, J. H., Rayman, P., Edinger, M., Tubbs, R. R., Stanley, J., Klein, E., and Bukowski, R. (1992) Characterization of a human renal cell carcinoma specific cytotoxic CD8⁺ T cell line. *J. Immunother.* **11**(1), 1–11.
2. Finke, J., Ferrone, S., Frey, A., Mufson, A., and Ochoa, A. (1999) Where have all the T cells gone? Mechanisms of immune evasion by tumors. *Immunol. Today* **20**(4), 158–160.
3. Miescher, S., Stoeck, M., Qiao, L., Barras, C., Barrelet, L., and von Fliedner, V. (1988) Preferential clonogenic deficit of CD8-positive T-lymphocytes infiltrating human solid tumors. *Cancer Res.* **48**(24), 6992–6998.
4. Alexander, J. P., Kudoh, S., Melsop, K. A., Hamilton, T. A., Edinger, M. G., Tubbs, R. R., Sica, D., Tuason, L., Klein, E., Bukowski, R. M., and Finke, J. (1993) T-cells infiltrating renal cell carcinoma display a poor proliferative response even though they can produce interleukin 2 and express interleukin 2 receptors. *Cancer Res.* **53**(6), 1380–1387.
5. Wang, Q., Redovan, C., Tubbs, R., Olencki, T., Klein, E., Kudoh, S., Finke, J., and Bukowski, R. M. (1995) Selective cytokine gene expression in renal cell carcinoma tumor cells and tumor-infiltrating lymphocytes. *Int. J. Cancer* **61**(6), 780–785.
6. Mizoguchi, H., O'Shea, J. J., Longo, D. L., Loeffler, C. M., McVicar, D. W., and Ochoa, A. C. (1992) Alterations in signal transduction molecules in T lymphocytes from tumor-bearing mice. *Science* **258**(5089), 1795–1798.
7. Uzzo, R. G., Clark, P. E., Rayman, P., Bloom, T., Rybicki, L., Novick, A.C., Bukowski, R. M., and Finke, J. H. (1999) Alterations in NFkappaB activation in T lymphocytes of patients with renal cell carcinoma. *J. Natl. Cancer Inst.* **91**(8), 718–721.
8. Baeuerle, P. A. and Baltimore, D. (1996) NFkB: Ten years after. *Cell* **87**, 13–20.
9. Ullman, K. S., Northrop, J. P., Verweij, C. L., and Crabtree, G. R. (1990) Transmission of signals from the T lymphocyte antigen receptor to the genes responsible for cell proliferation and immune function: the missing link. *Annu. Rev. Immunol.* **8**, 421–452.

10. May, M. J. and Ghosh, S. (1998) Signal transduction through NF κ B. *Immunol. Today* **19**(2), 80–88.
11. Beg, A. A. and Baltimore, D. (1996) An essential role for NF-kappa B in preventing TNF -alpha induced cell death. *Science* **274**, 782–784.
12. Miescher, S., Whiteside, T. L., Carrel, S., and von Flidner, V. (1986) Functional properties of tumor-infiltrating and blood lymphocytes in patients with solid tumors: effects of tumor cells and their supernatants on proliferative responses of lymphocytes. *J. Immunol.* **136**(5), 1899–1907.
13. Yoshino, I., Yano, T., Murata, M., Ishida, T., Sugimachi, K., Kimura, G., and Nomoto, K. (1992) Tumor-reactive T-cells accumulate in lung cancer tissues but fail to respond due to tumor cell-derived factor. *Cancer Res.* **52**(4), 775–781.
14. O'Mahony, A. M., O'Sullivan, G. C., O'Connell, J., Cotter, T. G., and Collins, J. K. (1993) An immune suppressive factor derived from esophageal squamous carcinoma induced apoptosis in normal and transformed lymphoid lineage. *J. Immunol.* **151**, 4847–4856.
15. Finke, J. H., Zea, A. H., Stanley, J., Longo, D. L., Mizoguchi, H., Tubbs, R. R., Wiltrott, R. H., O'Shea, J. J., Kudoh, S., Klein, E., et al. (1993) Loss of T-cell receptor zeta chain and p56lck in T-cells infiltrating human renal cell carcinoma. *Cancer Res.* **53**(23), 5613–5616.
16. Uzzo, R. G., Rayman, P., Kolenko, V., Clark, P. E., Bloom, T., Ward, A. M., Molto, L., Tannenbaum, C., Worford, L. J., Bukowski, R., Tubbs, R., Hsi, E., Bander, N. H., Novick, A. C., and Finke, J. H. (1999) Mechanisms of apoptosis in T cells from patients with renal cell carcinoma. *Clin. Canc. Res.* **5**, 1219–1229.
17. Gastman, B. R., Johnson, D. E., Whiteside, T. L., and Rabinowich, H. (1999) Caspase-mediated degradation of T-cell receptor zeta-chain. *Cancer Res.* **59**(7), 1422–1427.
18. Uzzo, R. G., Rayman, P., Kolenko, V., Clark, P. E., Cathcart, M. E., Bloom, T., Novick, A. C., Bukowski, R. M., Hamilton, T., and Finke, J. H. Suppression of NF κ B activation in T cells by soluble products from renal cell carcinomas is mediated by tumor derived gangliosides. *J. Clin. Invest.* in press.

Transforming Growth Factor- β 1 as a Novel Marker of Response to Therapy for Renal Cell Carcinoma

Howard L. Adler

1. Introduction

Renal cell carcinoma is expected to account for 30,000 new cancer cases and 11,900 cancer deaths in the United States in 1999 (1). At the time of initial presentation, up to one-third of patients with renal cell carcinoma (RCC) have metastatic disease; furthermore, almost half of the patients resected for cure will relapse (2). Due to the poor results of cytotoxic chemotherapy in the management of metastatic RCC (3), physicians have explored the use of new therapies including immunotherapy and gene therapy. Some of these therapies are discussed in other chapters of this textbook. The use of these new therapies allows for the identification and utilization of new tumor markers that may allow investigators to identify patients at risk for advanced disease as well as establish new definitions of tumor response.

One example of a new marker of response to therapy for renal cell carcinoma is vascular endothelial growth factor (VEGF). VEGF is expressed by RCC (4) and has been demonstrated to play a role in angiogenesis (5,6). VEGF is elevated in the sera of patients with localized and metastatic renal cancer and has been shown to decrease after resection of localized disease (7). Serum VEGF levels have also been shown to decrease in patients who responded to treatment with subcutaneous interferon alpha-2b (INF- α -2b) (8). In addition, urine levels of VEGF were found to rise in patients with progressive RCC in a trial of Razoxane, which is a topoisomerase II inhibitor with antiangiogenic properties (9). Moreover, Baccala et al. (10) recently demonstrated the utility of serum VEGF levels in following the clinical course of a patient who was treated with an irradiated human granulocyte macrophage-colony stimulating

factor (GM-CSF) gene transduced tumor vaccine for metastatic RCC. In this patient, levels of serum VEGF were found to be elevated in the presence of diaphragmatic and pulmonary metastases and decreased when the patient had a partial response to treatment (10).

Circulating transforming growth factor-beta 1 (TGF- β 1) is also a potential new marker of tumor response to treatment. This chapter describes the utility of TGF- β 1 as a marker of response and the technique of obtaining plasma specimens suitable for TGF- β 1 measurement.

1.1. TGF- β 1 and Cancer

TGF- β 1 is a 25-kDa homodimer belonging to a large family of structurally related proteins (11,12). TGF- β 1 is expressed in several cells and organs (13) and has multiple functions (summarized in **Table 1**) including inhibition of epithelial cells (14), promotion of angiogenesis (15), and inhibition of immune cells (16,17). In fact, TGF- β 1 has both immunostimulatory and immunoinhibitory effects (summarized in **Table 2**) (18,19).

TGF- β 1 has been associated with several carcinomas. Systemic levels of TGF- β 1 have been found to be elevated in patients with breast, colorectal, hepatocellular, lung, and prostate cancers (20–26). Circulating TGF- β 1 levels have been shown to decrease in response to curative resection in patients with breast and colorectal malignancies (20,21). Furthermore, plasma TGF- β 1 levels have been shown to decrease in response to radiation therapy in patients with lung cancer. Patients who responded to therapy maintained a low level of plasma TGF- β 1, as opposed to those patients who had residual or recurrent disease (23).

TGF- β 1 has a strong relationship with RCC. Ramp et al. showed that TGF- β 1 was secreted into the supernatant by renal carcinoma cell lines (27). Knoefel et al. also demonstrated the production of TGF- β 1 and other cytokines by RCCs in primary culture (28). More importantly, TGF- β 1 has been shown to be significantly elevated both in the plasma (29,30) and sera (31) of patients with RCC. Wunderlich et al. (31) were able to show a decrease in serum levels of TGF- β 1 in 11 of 16 patients who underwent surgical resection for specimen-confined tumors. In contrast, all 5 patients who had distant metastases and/or lymph node involvement maintained elevated levels of TGF- β 1 the primary tumor was removed (31).

TGF- β has also been shown to be a potential marker for immunotherapy. Puolakkainen et al. (32) found that plasma levels of TGF- β increase during immunotherapy with IL-2 in patients who achieve clinical regression of cancer. They hypothesized that platelets were the source of the TGF- β in their patients as platelet counts decreased in those individuals receiving IL-2 (32). Adler et al. (33) demonstrated an increase in platelet-poor plasma TGF- β 1

Table 1
Roles of TGF-β1

Inhibition of growth of normal epithelial cells
Induction of stromal cell proliferation
Induction of angiogenesis
Inhibition of humoral- and cell-mediated immunity
Inhibition of natural killer cell activity

Table 2
Dual Role of TGF-β1

Immunostimulatory	Immunoinhibitory
Increase adhesion molecules	Inhibit activated inflammatory cells
Generate chemotactic gradient	Promote fibroblast recruitment and activation
Induce cytokine network	
Orchestrate leukocyte recruitment and activation	

levels in patients receiving suicide gene therapy for radiation resistant prostate cancer. Six of 18 patients receiving an intraprostatic injection of an adenoviral vector containing the herpes simplex virus thymidine kinase gene (ADV/HSV-tk) followed by 2 wk of intravenous ganciclovir were found to have elevation of TGF-β1 with simultaneous evidence of T-cell activation (CD4 or CD8 cells). Only one patient had thrombocytopenia, whereas the remainder did not. The authors hypothesized that this increase in TGF-β1 represented stimulation of the immune system and/or tumor necrosis with release of TGF-β1 into the circulation (33).

2. Materials

Only a few materials are necessary for the collection of plasma that is suitable for the measurement of TGF-β1:

1. 21-gauge butterfly.
2. 5.0-mL Syringe.
3. 4.0-mL ethylenediaminetetraacetic acid (EDTA) potassium 7.2-mg (EDTA-K₂) tubes.
4. Pipet.
5. 1.0-mL Eppendorf tubes.
6. Centrifuge.
7. -80°C freezer.

3. Methods

3.1. Rationale for Platelet-Poor Plasma

Although there are several reports of the use of TGF- β 1 as a marker of response to therapy for many cancers, there is no consensus as to the methodology used in obtaining patient samples. Investigators have used serum (25,31), plasma (20–24,29,30), and platelet poor plasma (26). There is a difference between the levels measured in each of these fluids, as the levels of TGF- β 1 are not comparable. Moreover, authors often do not indicate whether or a vacuum tube has been used for sample collection. Marie et al. showed that there is a small, but real, difference between platelet-rich and platelet-poor plasma levels of TGF- β 1 (34). Platelets may release from 5–25 ng of TGF- β 1/mL of blood collected (35,36). Furthermore, the use of a vacuum tube to collect samples and/or allowing blood to clot (for serum samples may allow for the release of TGF- β 1 from platelets. Adler et al. (26) showed that serum TGF- β 1 levels are greatly increased over platelet poor plasma levels; furthermore, they demonstrated that there was no correlation between the serum and platelet poor plasma levels. As there is only a slight discrepancy between platelet poor and platelet rich levels of TGF- β 1, either method may be acceptable for research studies. Serum levels of TGF- β 1 are probably the least useful of the three choices. Further research and discussion in this area are required so that a consensus can be reached as to the methods used in measuring systemic TGF- β 1 levels.

3.2. Technique for Collecting Platelet-Poor and Platelet-Rich Plasma

The method for collecting blood for use as platelet-poor plasma has been previously described (26). The techniques for obtaining both platelet-poor and platelet-rich plasma will be described. Both methods involve the use of no vacuum. Further research is needed to determine the significance of a vacuum tube on TGF- β 1 levels.

3.2.1. Platelet-Rich Plasma

1. Using a 21-gauge butterfly, blood is collected from a median antecubital vein.
2. 4.0 Milliliters (mL) of blood are collected into a 5.0-mL syringe by gentle aspiration of blood.
3. Remove the cap of a 4.0-mL EDTA potassium 7.2-mg (EDTA-K2) tube.
4. Gently place the blood into the EDTA tube.
5. Replace the cap of the EDTA tube.
6. Centrifuge at 1500 rpm for 10 min at room temperature.
7. Pipet off the platelet-rich plasma into 1.0-mL Eppendorf tubes.
8. Store at -80°C .

3.2.2 Platelet-Poor Plasma

1. Take the platelet-rich plasma that has been pipetted into the 1.0-mL Eppendorf tubes in **step 7**.
2. Centrifuge at 3000 rpm for 10 min at room temperature.
3. Pipet off the platelet-poor plasma into 1.0-mL Eppendorf tubes. A faint platelet clump will be visible at the bottom of the tube.
4. Store at -80°C .

3.3. Conclusions

Circulating TGF- β 1 and other cytokines are potentially useful as new markers for staging various malignancies as well as for demonstrating response to novel therapies. The collection and measurement of TGF- β 1 from plasma is easy, reliable, and reproducible. Levels of TGF- β 1 are stable in frozen specimens and are reproducible after multiple freeze–thaw cycles. Further research will elaborate on the utility of circulating TGF- β 1 and other cytokines in evaluating the response of tumors to novel therapies.

4. Notes

1. When pipetting off the platelet-rich plasma, do not pour off the plasma or red blood cells will also pour off.
2. When pipetting off the platelet-poor plasma, be careful to avoid disturbing the soft platelet pellet.
3. Although it is recommended to avoid multiple freeze–thaw cycles, TGF- β 1 is stable over several freeze–thaw cycles (26).
4. Once samples are ready to be assayed for TGF- β 1 levels, any of the commercially available enzyme-linked immunosorbent assay kits may be used.

References

1. Landis, S. H., Murray, T., Bolden, S., and Wingo, P.A. (1999) Cancer statistics, 1999. *CA Cancer J. Clin.* **49**, 8–31.
2. Figlin, R. A. (1999) Renal cell carcinoma: management of advanced disease. *J. Urol.* **161**, 381–387.
3. Yagoda, A., Abi-Rached, B., and Petrylak, D. (1995) Chemotherapy for advanced renal cell carcinoma, 1983–1993. *Semin. Oncol.* **22**, 42–60.
4. Nicol, D., Hii, S.-I., Walsh, M., Teh, B., Thompson, L., Kennett, C., and Gotley, D. (1997) Vascular endothelial growth factor expression is increased in renal cell carcinoma. *J. Urol.* **157**, 1482–1486.
5. Brown, L. F., Berse, B., Jackman, R. W., Tognazzi, K., Manseau, E. J., Dvorak, H. F., and Senger, D. R. (1993) Increased expression of vascular permeability growth factor (vascular endothelial growth factor) and its receptors in the kidney and bladder carcinomas. *Am. J. Pathol.* **143**, 1255–1262.
6. Takahashi, A., Sasaki, H., Kim, S. J., Tobisu, K., Kakizoe, T., Tsukamoto, T., Kumamoto, Y., Sugimura, T., and Terada, M. (1994) Markedly increased amounts of

- messenger RNAs for vascular endothelial growth factor and placenta growth factor in renal cell carcinoma associated with angiogenesis. *Cancer Res.* **54**, 4233–4237.
7. Dyrix, L. Y., Vermeulen, P. B., Pawinski, A., Prove, A., Benoy, I., De Pooter, C., Martin, M., and Van Oosterom, A. T. (1997) Elevated levels of the angiogenic cytokines basic fibroblast growth factor and vascular endothelial growth factor in sera of cancer patients. *Br. J. Cancer* **76**, 238–243.
 8. Vermeulen, P. B., Dirix, L. Y., Martin, M., Lemmens, J., and Van Oosterom, A. T. (1997) Serum basic fibroblast growth factor and vascular endothelial growth factor in metastatic renal cell carcinoma treated with interferon alfa-2b. *J. Natl. Cancer Inst.* **89**, 1316–1317.
 9. O'Byrne, K. J., Propper, D., Braybrooke, J., Crew, J., Mitchell, K., Woodhull, J., Dobbs, N., Ganesan, T. S., Talbot, D. C., and Harris, A. L. (1997) Razoxane: a phase II trial in renal cell cancer evaluating anti-angiogenic activity. *Proc. Annu. Meeting Am. Soc. Clin. Oncol.* **16**, A1160.
 10. Baccala, A. A., Zhong, H., Clift, S. M., Nelson, W. G., Marshall, F. F., Passe, T. J., Gambill, N. B., and Simons, J. W. (1998) Serum vascular endothelial growth factor is a candidate biomarker of metastatic tumor response to ex vivo gene therapy of renal cell cancer. *Urology* **51**, 327–332.
 11. Wahl, S. M., McCartney-Francis, N., and Mergenhagen, S. E. (1989) Inflammatory and immunomodulatory roles of TGF- β . *Immunol. Today* **10**, 258–261.
 12. Rifkin, D. B., Kojima, S., Abe, M., and Harpel, J. G. (1993) TGF- β : structure, function, and formation. *Thromb. Haemost.* **70**, 177–179.
 13. Assoian, R. K., Komoriyama, A., Meyers, C. A., Miller, D. M., and Sporn, M. B. (1983) Transforming growth factor- β in human platelets. *J. Biol. Chem.* **258**, 7155–7160.
 14. Shipley, E. D., Pittelkow, M. R., Wille, J. J. Jr., Scott, R. E., and Moses, H. L. (1986) Reversible inhibition of normal human prokeratinocyte by type β transforming growth factor-growth inhibitor in serum-free medium. *Cancer Res.* **46**, 2068–2071.
 15. Yang, E. Y. and Moses, H. L. (1990) Transforming growth factor- β 1-induced changes in cell migration, proliferation, and angiogenesis in the chicken chorioallantoic membrane. *J. Cell Biol.* **111**, 731–741.
 16. Rook, A. H., Kehrl, J. H., Wakefield, L. M., Roberts, A. B., Sporn, M. B., Burlington, D. B., Lane, H. C., and Fauci, A. S. (1986) Effects of transforming growth factor- β on the functions of natural killer cells: depressed cytolytic activity and blunting of interferon responsiveness. *J. Immunol.* **136**, 3916–3920.
 17. Tada, T., Ohzeki, S., Utsumi, K., Takiuchi, H., Muramatsu, M., Li, X.-F., Shimizu, J., Fujiwara, H., and Hamaoka, T. (1991) Transforming growth factor- β induced inhibition of T cell function. Susceptibility difference in T cells of various phenotypes and functions and its relevance to immunosuppression in the tumor-bearing state. *J. Immunol.* **146**, 1077–1082.
 18. Wahl, S. M. (1992) Transforming growth factor beta (TGF- β) in inflammation: a cause and a cure. *J. Clin. Immunol.* **12**, 61–74.
 19. Wahl, S. M. (1994) Transforming growth factor β : the good, the bad, and the ugly. *J. Exp. Med.* **180**, 1587–1590.

20. Kong, F.-M., Anscher, M. S., Murase, T., Abbott, B. D., Inglehart, D., and Jirtle, R. L. (1995) Elevated plasma transforming growth factor- β 1 levels in breast cancer patients decrease after surgical removal of the tumor. *Ann. Surg.* **222**, 155–162.
21. Tsushima, H., Kawata, S., Tamura, S., Ito, N., Shirai, Y., Kiso, S., Imai, Y., Shimomukai, H., Nomura, Y., Matsuda, Y., and Matsuzawa, Y. (1996) High levels of transforming growth factor β 1 in patients with colorectal cancer: association with disease progression. *Gastroenterology* **110**, 375–382.
22. Shirai, Y., Kawata, S., Ito, N., Tamura, S., Takaishi, K., Kiso, S., Tsushima, H., and Matsuzawa, Y. (1992) Elevated levels of plasma transforming growth factor- β in patients with hepatocellular carcinoma. *Jpn. J. Cancer Res.* **83**, 676–679.
23. Kong, F.-M., Washington, M. K., Jirtle, R. L., and Anscher, M. S. (1996) Plasma transforming growth factor-beta 1 reflects disease status in patients with lung cancer after radiotherapy: a possible tumor marker. *Lung Cancer* **16**, 47–59.
24. Ivanovic, V., Melman, A., Davis-Joseph, B., Valcic, M., and Geliebter, J. (1995) Elevated plasma levels of TGF- β 1 in patients with invasive prostate cancer. *Nat. Med.* **1**, 282–284.
25. Kaheki, Y., Oka, H., Mitsumori, K., Itoh, N., Ogawa, O., and Yoshida, O. (1996) Elevation of serum transforming growth factor- β 1 level in patients with metastatic prostate cancer. *Urol. Oncol.* **2**, 131–135.
26. Adler, H. L., McCurdy, M. A., Kattan, M. W., Timme, T. L., Scardino, P. T., and Thompson, T. C. (1998) Elevated levels of circulating interleukin-6 and transforming growth factor- β 1 in patients with metastatic prostatic carcinoma. *J. Urol.* **161**, 182–187.
27. Ramp, U., Jaquet, K., Reinecke, P., Scardt, C., Friebe, U., Nitsch, T., Marx, N., Gabbert, H. E., and Gerharz, C.-D. (1997) Functional intactness of stimulatory and inhibitory autocrine loops in human renal carcinoma cell lines of the clear cell type. *J. Urol.* **157**, 2345–2350.
28. Knoefel, B., Nuske, K., Steiner, T., Junker, K., Kosmehl, H., Rebstock, K., Reinhold, D., and Junker, U. (1997) Renal cell carcinomas produce IL-6, IL-10, IL-11, and TGF- β 1 in primary cultures and modulate T lymphocyte blast transformation. *J. Interferon Cytokine Res.* **17**, 95–102.
29. Junker, U., Knoefel, B., Nuske, K., Rebstock, K., Steiner, T., Wunderlich, H., Junker, K., and Reinhold, D. (1996) Transforming growth factor beta 1 is significantly elevated in plasma of patients suffering from renal cell carcinoma. *Cytokine* **8**, 794–798.
30. Wunderlich, H., Steiner, T., Kosmehl, H., Junker, U., Reinhold, D., Reichelt, O., Zermann, D. H., and Schubert, J. (1998). Increased transforming growth factor β 1 plasma level in patients with renal cell carcinoma: a tumor-specific marker? *Urol. Int.* **60**, 205–207.
31. Wunderlich, H., Steiner, T., Junker, U., Knoefel, B., Schlichter, A., and Schubert, J. (1997) Serum transforming growth factor- β 1 in patients with renal cell carcinoma. *J. Urol.* **157**, 1602–1603.
32. Puolakkainen, P., Twardzik, D., Ranchalis, J., Moroni, M., Mandeli, J., and Paciucci, P. A. (1995) Increase of plasma transforming growth factor beta (TGF β) during immunotherapy with IL-2. *Cancer Invest.* **13**, 583–589.

33. Adler, H. L., Lee, H.-M., McCurdy, M. A., Herman, J. R., Timme, T. L., Scardino, P. T., and Thompson, T. C. (1998) Adenovirus-mediated herpes simplex virus thymidine kinase gene therapy in men with radiorecurrent prostate cancer leads to stimulation of the immune system and increases in circulating cytokines. *Proc. 1st Annu. Meeting Am. Soc. Gene Therapy* **1**, A442.
34. Marie, C., Cavaillon, J.-M., and Losser, M.-R. (1996) Elevated levels of circulating transforming growth factor- β 1 in patients with the sepsis syndrome. *Ann. Int. Med.* **125**, 520–521.
35. Yang, E. Y. and Moses, H. L. (1990) Transforming growth factor β 1-induced changes in cell migration, proliferation, and angiogenesis in the chicken chorioallantoic membrane. *J. Cell Biol.* **111**, 731–741.
36. Miyazono, K., Hellman, U., Wernstedt, C., and Heldin, C.-H. (1988) Latent high molecular weight complex of transforming growth factor β 1: purification from human platelets and structural characterization. *J. Biol. Chem.* **263**, 6407–6415.

Static and Flow Cytometry

Ralph Madeb, Dov Pode, and Ofer Nativ

1. Introduction

It has been known for over 50 years that the amount of nuclear chromatin (DNA) in malignant neoplasms differs from that of homologous normal cells (*1*). More recently, it has been shown that nuclear DNA content correlates with the clinical outcome of various human neoplasms including urologic malignancies (*2–10*). An important problem in the care of patients with renal cell carcinoma (RCC) is the prediction of the neoplasms malignant potential, and in turn the patient's prognosis. Various parameters have been used to assess the malignant potential of renal cell carcinoma, including clinical and pathologic stage, histologic grade, tumor size, nuclear morphology, immunohistochemistry, age, elevated erythrocyte sedimentation rate, and hypercalcemia. To date, the most important predictors of prognosis in patients with RCC have been tumor pathologic stage, histologic grade and type (*11,12*). However, it has been shown that patients within a specified stage and grade may differ in their disease progression and survival (*13,14*). Furthermore, none of these variables alone or in combination has shown to provide total reliable prognostic information for the individual patient. These reasons led several groups to evaluate the prognostic value of nuclear DNA content in patients with renal cell carcinoma. Many researchers have found correlations between DNA ploidy pattern, histopathologic variables, and patient outcome (*4–6,9,10,13–16*). As a general rule, low-grade tumors have a normal DNA content that is, predominantly diploid. In contrast, high-grade tumors are usually characterized by an aneuploid DNA content with highly variable DNA values.

Currently, there are two techniques for the determination of DNA ploidy pattern in solid tumors—flow and static cytometry. Both methods are now used in RCC and allow analysis of fresh and archival samples embedded in paraffin blocks. Improvements in cell preparative and staining techniques have allowed cytometry to emerge as a powerful tool for the analysis of DNA content and proliferative activity. Static cytometry is based on the Feulgen staining reaction described in 1924 by Feulgen and Rossenbech in which nuclear DNA is stained reddish-purple (17). Microscopic analysis of the Feulgen-stained nuclei is carried out using a photomicroscope and the image of the investigated cells are projected either in a microscope or on a video screen. Suitable nuclei in the field are selected from the total sample by successively removing the unwanted cells, thus focusing on the population in question. It has been estimated that about 100 single cells is an adequate representation of the tumor cell population (18). The optical density of examined nuclei reflects the amount of DNA bound dye and is compared to that of normal cells. In turn, the determination of DNA ploidy is established. If the mean optical density is similar to that of the normal cell control group, then the tumor ploidy is classified as DNA diploid; otherwise the tumor DNA ploidy is considered aneuploid (*see Fig. 1*). A newer technique using fluorescence image analysis instead of optical density has been described (19). In view of the fact that static cytometry allows the direct visualization of the tumor sample, malignant cells are preferentially selected resulting in a population of cells with increased specificity. The main advantage of static cytometry is the ability to determine DNA ploidy from a small number of tumor cells, subsequently reducing the size of the tumor sample. Despite its advantages, DNA analysis by static cytometry has been criticized as being operator dependent, time consuming, and inefficient as each nucleus must be chosen and measured individually.

A distinctive feature of flow cytometry is the capability to rapidly analyze large populations of cells in suspension. In contrast to static cytometry, flow cytometry requires more tissue volume, which can be fresh or paraffin-embedded. The tissue must be disaggregated into single cells in suspension for flow cytometry to be performed. In 1983 Hedley and associates described a technique that analyzed the DNA content from nuclei extracted from formalin-fixed, paraffin-embedded archival tumor tissue (20) (*see Fig. 2*). His technique is widely used today and obviates the need for fresh tissue. The suspension of isolated nuclei is stained with fluorescent dyes according to the technique described by Vindeløv et al. (21) (*see Fig. 3*). The stained nuclear suspension is transferred to the flow cytometer for DNA analysis. As the cells pass through an intense beam of light they become excited and fluoresce. The cell's fluorescence-intensity is proportional to the amount of DNA in the nucleus and is stored in a computer. The entire examined cell population is later displayed as

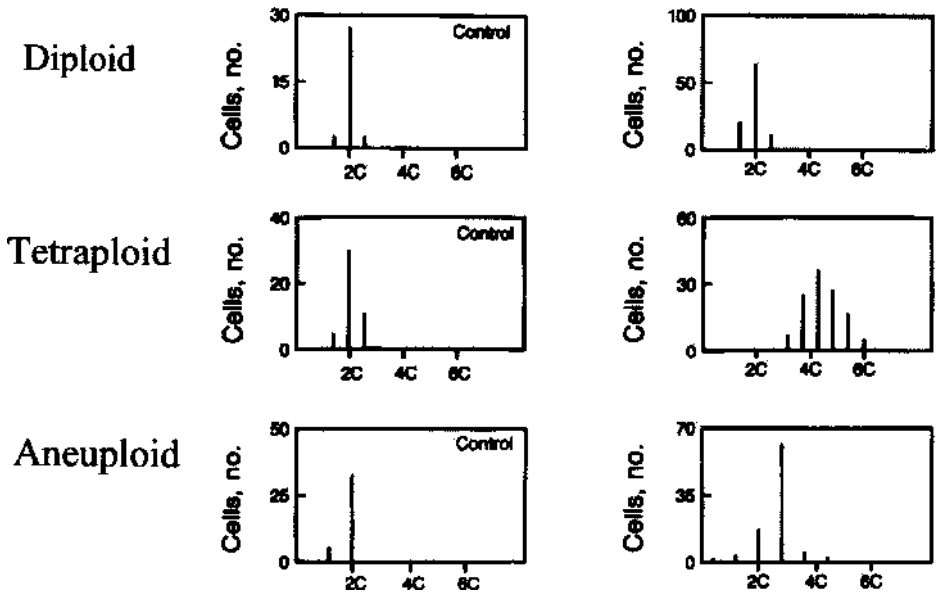


Fig. 1. Reconstructive DNA histograms of the integrated optical density obtained by static image cytometry from specimens of renal cell carcinoma and controls.

a histogram (*see Fig. 4*). Cell samples that have histograms that resemble those of benign normal tissues are classified as normal or DNA diploid. A population of tumor cells that contained a significant increase in the G2 (4C) peak of the cell cycle is characterized as being DNA tetraploid. The DNA ploidy pattern is considered aneuploid if there is a third separate peak that is different from the G0/G1 (2C) peaks (*see Fig. 5*). The ability to detect abnormal DNA ploidy by flow cytometry is limited when the proportion of tumor cells in the original specimen is less than 10–20%. Although flow analysis is rapid and commonly involves measurements of thousands of cells per sample, a major flaw with flow cytometric analysis is its inability to discriminate between normal host cells and tumor cells that have a DNA diploid content. In addition, the presence of a minority of aneuploid cells may also be masked when there is an abundance of non-malignant cells in the sample (22). Consequently, there will be errors in the interpretation of DNA histograms obtained using flow cytometry.

Because both static and flow cytometry have certain advantages and disadvantages, these methods may work in a complimentary fashion in order to increase the specificity of tumor detection along with improving the determination of prognosis. In this chapter we shall describe the methods used for the determination of DNA ploidy by static and flow cytometry.

Hedley Technique

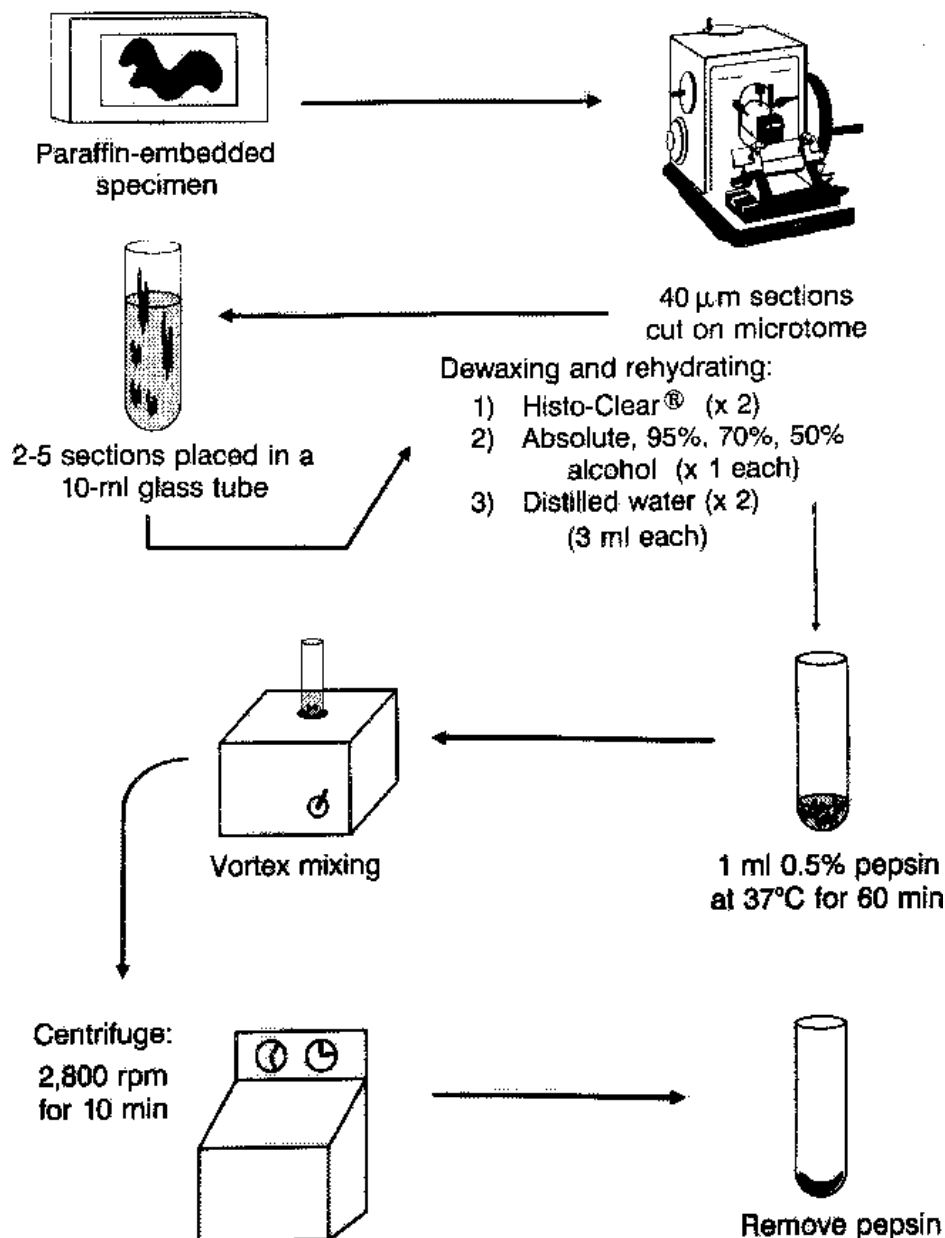


Fig. 2. Schematic diagram of the Hedley technique.

Vindeløv Staining Technique

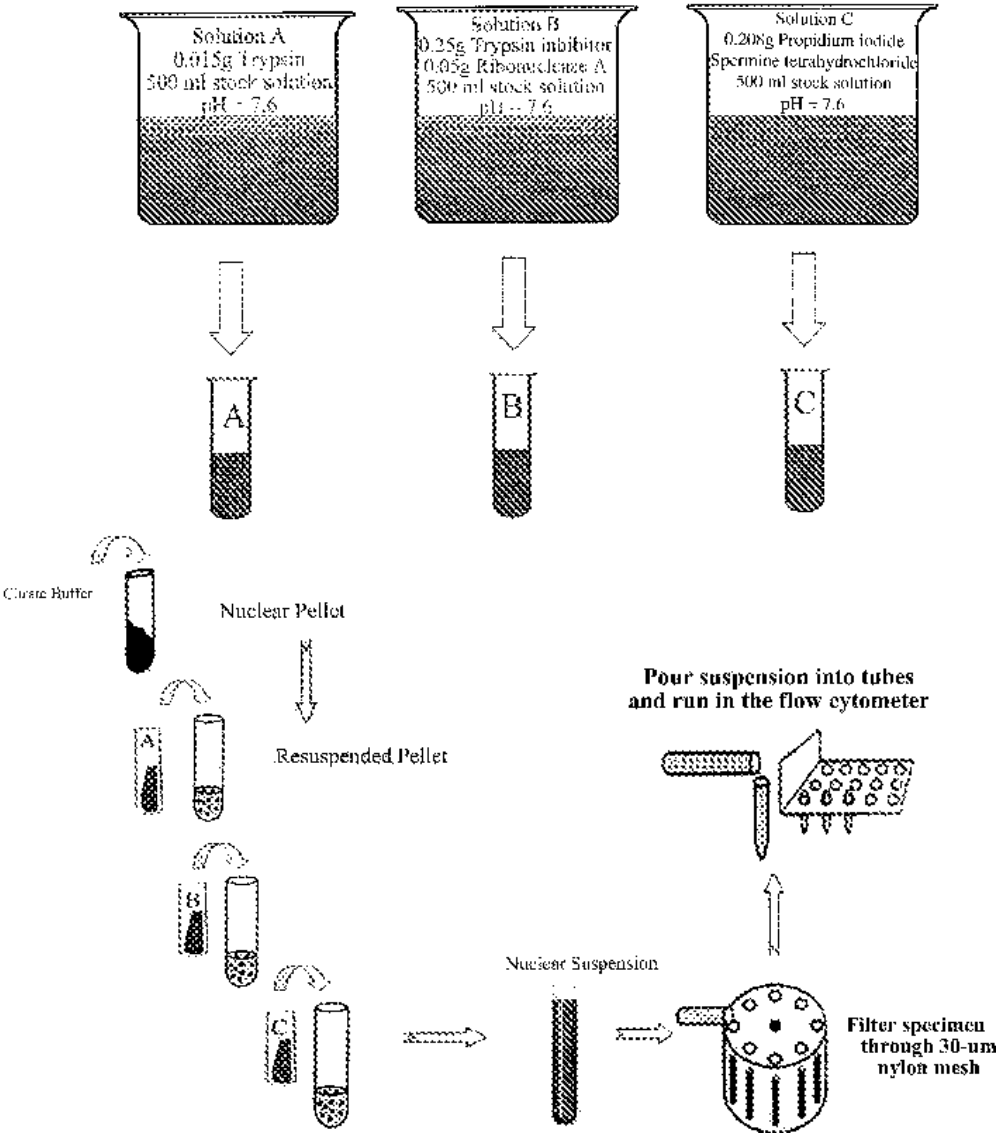


Fig. 3. Schematic diagram of the Vindeløv staining technique.

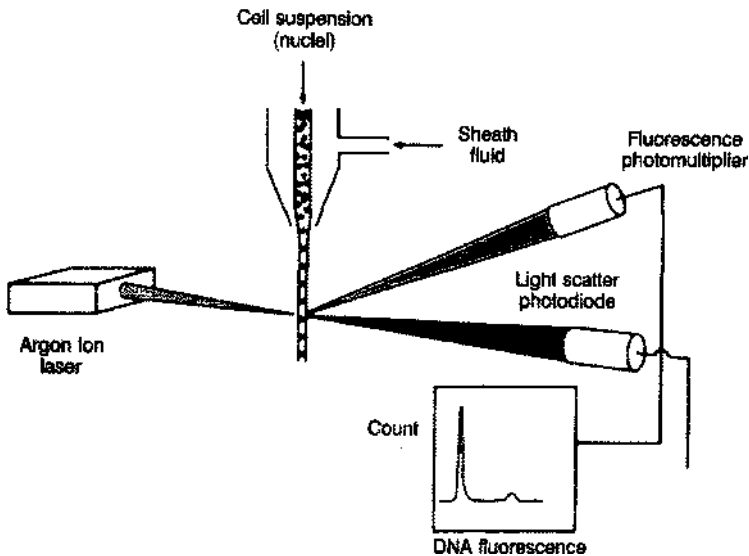


Fig. 4. Schematic illustration of the basic principles involved in flow cytometric DNA analysis using the fluorescence-activated cell sorter (FACS) for sorting nuclei from suspension. The nuclear suspension is transferred to the FACS where it passes through a narrow tube. The argon laser beam excites the fluorescent dyes at the same time as the photomultipliers monitor the emissions from each dye. The individual cell fluorescence-intensity is analyzed and stored in a computer which is displayed as a histogram of the entire examined population of cells.

2. Materials

2.1. Tissue Fixation, Embedding, and Sectioning for Static Cytometry

2.1.1. Tissue Fixation

1. Glass container.
2. 10% neutral buffered-formalin.
3. 100, 95, 70% Ethanol

2.1.2. Tissue Embedding

1. Paraplast Plus® (Oxford, St. Louis, MO).

2.1.3. Tissue Sectioning

1. Standard microtome.

2.2. Preparation of Slides and Coverslips

1. Water bath set at 40°C.
2. Elmer's glue.
3. Distilled water.

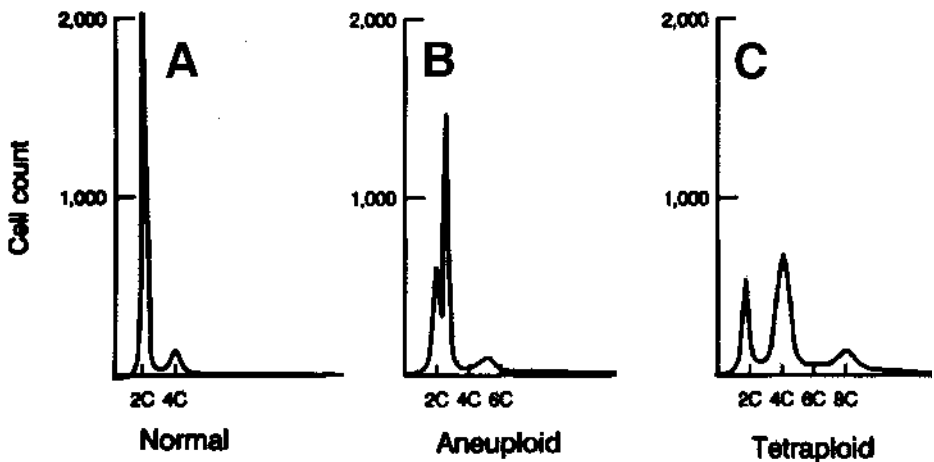


Fig. 5. Typical flow cytometric DNA histogram patterns found in patients with renal cell carcinoma. Samples with histograms similar to those seen in normal tissues are classified as DNA diploid (A). Samples that have a third separate peak, different from the G0/G1 (2C) peaks, are classified as aneuploid (B). If there is a significant increase in the G2 (4C) peak then the sample is classified as tetraploid (C).

2.3. Feulgen Staining Technique

1. Xylene.
2. 100, 95, 70, 50, and 30% ethanol.
3. Distilled water.
4. 5 N HCl.
5. Schiff reagent (Pararosaniline, distilled water, 1 N HCl, potassium metabisulfate).
6. Sulfurous acid (SO₂).

2.4. Image Analysis

1. Interactive image analyzer composed of a photomicroscope equipped with a 12 V halogen lamp.

2.5. Preparation of Single Cell Suspension

1. HistoClear.
2. 100, 95, and 70% Ethanol.
3. Distilled water.
4. Pepsin.
5. Sodium Chloride (NaCl).
6. 2 N HCl.
7. Water bath set at 37°C.
8. Vortex.
9. Centrifuge.

2.6. Vindeløv Staining Technique

2.6.1. Citrate Buffer

1. Sucrose.
2. Trisodium citrate · 2H₂O.
3. Distilled water.
4. DMSO (Dimethylsulfoxide).

2.6.2. Stock Solution

1. Trisodium citrate · 2H₂O.
2. Nonidet P40.
3. Spermine Tetrahydrochloride.
4. THAM (Tris(hydroxymethyl)methylamine).
5. Distilled water.

2.6.3. Solution A

1. Trypsin.
2. Stock solution.

2.6.4. Solution B

1. Trypsin inhibitor.
2. Ribonuclease A.
3. Stock solution.

2.6.5. Solution C

1. Propidium Iodide.
2. Spermine tetrahydrochloride.
3. Stock solution.
4. Tin foil.

2.6.6. Nylon Mesh Filter with a 30-μm Pore Diameter

2.7. Flow Cytometric DNA Analysis

1. Fluorescence-activated cell sorter (FACS) equipped with an argon ion laser.

3. Methods

3.1. Tissue Fixation, Embedding, and Sectioning for Static Cytometry

3.1.1. Tissue Fixation

1. The fresh surgical specimen is placed in a glass container and fixed in 10% neutral-buffered formalin.
2. The specimens are dehydrated with increasing concentrations of ethanol (EtOH), 70, 95, and 100%, for 30 min each at 40°C.
3. The specimens are then subjected to two changes of xylene for 15 min each at room temperature.

3.1.2 Paraffin-Embedding

1. The formalin fixed tissue is embedded in Paraplast Plus® (Oxford) at 60°C.

3.1.3. Tissue Sectioning

1. The paraffin-embedded tissue blocks are cut into 4–6 μm thick sections using standard microtome.

3.2. Preparation of Slides and Coverslips

1. Two to three tissue sections are placed in a water bath set at 40°C for 1 min.
2. The tissue sections are removed from the water bath with a slide that was previously immersed in a solution of 15 mL Elmer's glue dissolved in 85 mL of distilled water.
3. The tissue sections are then dried in an oven that was preset at 40°C for 12 h.

3.3. Staining

The formalin fixed paraffin embedded sections are stained according to the Feulgen method for DNA. This method was introduced by Feulgen and Rossenbeck (*see* **ref. 17**) in 1924 and is based upon the Schiff reaction for aldehydes. This staining technique is carried out in two steps:

1. Mild acid hydrolysis—which splits the purine bases from the carbohydrate moiety of the DNA molecule subsequently liberating the aldehyde group of the deoxyribose sugar molecule.
2. Aldehyde reaction: The second step where the liberated aldehyde group from the acid hydrolysis reacts with a decolorized or leuco Schiff reagent and is thereby converted into the colored form. This indicates that a covalent bond has been formed to the DNA.

After the reaction takes place the portions of the nuclei that contain DNA stain reddish-purple. Due to the fact that the Feulgen reaction is specific for DNA, removal of other cell components such as RNA, is not needed.

3.3.1. Feulgen Reaction

Table 1 summarizes the Feulgen staining schedule.

1. The tissue is deparaffinized by two changes of xylene for 10 and 5 min, respectively.
2. The sections are then put through a series of ethanol (EtOH) hydration of decreasing concentrations—100, 95, 70, 50, and 30% for 5 min each.
3. The sections are then washed with distilled water.
4. The sections are hydrolyzed with 5 *N* HCl for 1 h and then dipped in distilled water (*see* **Note 1**).
5. After the sections are hydrolyzed they are stained with the Schiff reagent, (*see* **Note 2**) adjusted to a pH of 1.5 with HCl just before use, for 1 h.

Table 1
Feulgen Stain Technique for Static DNA Measurement

Agent	Time
Xylene	10 min
Xylene	5 min
100% EtOH	5 min
95% EtOH	5 min
70% EtOH	5 min
50% EtOH	5 min
30% EtOH	5 min
Distilled water	5 min
5 N HCl (at room temperature)	1 h
Distilled water	1 dip
Schiff Stain (adjusted to pH 1.5 with HCl)	1 h
SO ₂ wash	10 min
SO ₂ wash	10 min
SO ₂ wash	10 min
Running tap water	5 min
Distilled water	5 min
30% EtOH	5 min
50% EtOH	5 min
70% EtOH	5 min
95% EtOH	5 min
100% EtOH	5 min
100% EtOH	5 min
Xylene	5 min
Xylene	25 min
Mounting	2 h

- When the sections are removed from the Schiff reagent they are placed into three successive sulfurous acid (SO₂) baths for 10 min each (*see Note 3*). The SO₂ solution should be prepared immediately before use.
- The SO₂ baths are followed by a wash in running tap water and distilled water for 5 min each. This is then followed by a dehydrating process with increasing concentrations of EtOH—30, 50, 70, 95, and 100% for 5 min each.
- Finally the sections are subjected to two changes of xylene for 5 and 25 min, respectively, and then mounted (*see Note 4*).

3.4. Image Analysis

1. Image analysis of the Feulgen-stained nuclei is carried out by using an interactive image analysis system composed of a photomicroscope equipped with a 12-V halogen filament lamp.
2. The microscopic fields are scanned with a video camera and projected to an external monitor.
3. The user selects 100–200 suitable tumor nuclei on the projected field, and all irrelevant cells are eliminated.
4. The integrated optical density (IOD) of all the remaining nuclei is measured by image measurement software.
5. The mean IOD value of the neoplastic nuclei is compared to that of 30–50 nuclei of surrounding normal cells, which serve as a control group.
6. Cell populations having a DNA index (mean IOD of the examined cells divided by that of the controls) equal to or less than the highest value obtained from the controls are classified as normal or diploid. The remaining cells are considered aneuploid.

3.5. Tissue Fixation, Embedding, and Sectioning for Flow Cytometry

3.5.1 Tissue Fixation

1. The fresh surgical specimen is placed in a glass container and fixed in 10% neutral buffered-formalin.
2. The specimens are dehydrated with increasing concentrations of ethanol (EtOH), 70, 95, and 100%, for 30 min each at 40°C.
3. The specimens are then subjected to two changes of xylene for 15 min each at room temperature.

3.5.2 Paraffin Embedding

1. The formalin fixed tissue is embedded in Paraplast Plus® (Oxford) at 60°C.

3.5.3. Tissue Sectioning

1. Three 40- μ m thick paraffin-embedded tissue sections are cut with the use of standard tissue microtome and are placed in a 10-mL glass culture tube. The specimens may be stored up till 3 d before running.

3.6. Preparation of Single-Cell Suspension

Nuclear suspension from paraffin-embedded sections is prepared by using the technique described by Hedley and colleagues (*see* **ref. 20** and **Fig. 2**).

1. The paraffin-embedded cut sections are dewaxed by two 4 mL washes of HistoClear for 10 min each.
2. The dewaxed remaining tissue is then rehydrated in a sequence of 3 mL of 100, 95, and 70% ethanol (EtOH) for 10 min each at room temperature.
3. The tissue is then washed twice in 3 mL of distilled water for 10 minutes each and resuspended in 1 ml of 0.5% pepsin in 0.9% sodium chloride (NaCl), adjusted to pH of 1.5 with 2 N HCl (*see* **Note 5**).

4. The tubes with the specimens are placed in a water bath set at 37°C for 60 min and subjected to intermittent vortex mixing.
5. The resulting nuclear suspension is centrifuged at 2800 rpm for 10 min to form a nuclear pellet, and the pepsin supernatant is discarded.

3.7. Staining

The isolated nuclei are stained with propidium iodide using the Vindeløv method described by Vindeløv and co-workers (*see* **ref. 21** and **Fig. 3**). The solutions that are needed for the staining technique have been labeled Solutions A–C, and their constituents are listed in **Subheading 4 (6–11)**.

1. The nuclear pellet is resuspended and gently mixed in 0.1 ml of citrate buffer (*see* **Notes 5, 11, and 13**).
2. 0.9 mL of solution A is added to the nuclear suspension and gently mixed for 10 min (*see* **Notes 8, 11, and 12**).
3. Then, add 0.75 mL of solution B and mixed gently for 10 min (*see* **Notes 9 and 11**).
4. Finally, add 0.75 mL of solution C to the suspension (*see* **Notes 10, 11, and 14**).
5. The solutions are mixed and the sample is filtered through a 30- μ m pore diameter nylon mesh filter to provide single nuclei and to eliminate nuclear clumps.
6. Samples are then processed on the flow cytometer (*see* **Note 15**).

3.8. Flow Cytometric Nuclear DNA Analysis

1. Nuclear DNA content is measured on a FACS (fluorescence-activated cell sorter) flow cytometer equipped with an argon ion laser.
2. Every group of specimens should be standardized with Fullbright Fluorospheres, to control day-to-day channel variations.
3. Histograms of 10–20,000 nuclei for each sample should be recorded at a maximal scanning rate of 1000 nuclei per second.
4. Cell-cycle evaluation of the DNA histograms and the coefficient of variation of the G0/G1 (2C) peak derived by flow cytometry are obtained by using a specifically designed computer program (e.g., Dean and Jett mathematical analysis).
5. Samples with histograms similar to those of benign normal tissues are classified as normal or DNA diploid.
6. A population of tumor cells that contain a significant increase in the G2 (4C) peak (more than three standard deviations above the observed mean of the G2 (4C) peak for non-tumor controls) are classified DNA tetraploid.
7. Samples that contain a third additional peak (different from the G0/G1 (2C) or G2 (4C) peaks) are classified as being aneuploid.

4. Notes

1. Hydrolysis is the most important step in the Feulgen reaction because at this point the nuclei are disrupted. In the reaction, purine bases are liberated from the nucleic acid molecule thereby unmasking the aldehyde group of the deoxyribose sugar moiety. The task of acid hydrolysis is to efficiently remove the purine bases

without destroying the DNA. Deitch and co-workers have demonstrated that acid hydrolysis for 1 h with 5 N HCl at room temperature is ideal for stain uptake (23).

2. The Schiff reagent can be prepared by dissolving 0.5 g of pararosaniline (basic fuchsin) in 100 mL of boiling distilled water. The solution is then cooled to 50°C, and then filtered. 10 mL of 1 N HCl and 2 g of potassium metabisulfate ($K_2S_2O_5$) is added to the filtrate. The solution is tightly closed in a chemically cleaned bottle and placed in the dark for 24 h. Note that during this time the pararosaniline is converted to a straw-colored compound. One teaspoon of activated charcoal is then added to the solution for decolorization. The solution is shaken and then filtered. The clear strain is stored in 46°C if needed. For optimal results the pH of the stain should be adjusted to 1.5 with HCl prior to usage.
3. The SO_2 wash is prepared immediately before use by dissolving 1 g of potassium metabisulfate ($K_2S_2O_5$) in 10 mL of 1 N HCl and 190 mL of distilled water.
4. We use mounting media with a refractive index ranging from 1.518 to 1.521.
5. If it is needed, it is possible to store the suspensions overnight *before* the trypsin is added.
6. The citrate buffer is composed of:
 - a. 17.1 g sucrose
 - b. 2.35 g trisodium citrate \cdot 2H₂O
 - c. 160 mL distilled water
 - d. 10 mL DMSO
 - e. Adjust pH to 7.6
7. The stock solution is composed of:
 - a. 2 g trisodium citrate \cdot 2H₂O
 - b. 2 mL Nonidet P40
 - c. 1.044 g spermine tetrahydrochloride
 - d. 0.121 g THAM
 - e. 2000 mL distilled water
 - f. Adjust pH to 7.6
8. Solution A is composed of:
 - a. 0.015 g trypsin
 - b. 500 mL stock solution
 - c. Adjust pH to 7.6
9. Solution B is composed of:
 - a. 0.25 g trypsin inhibitor
 - b. 0.05 g ribonuclease A
 - c. 500 mL stock solution
 - d. Adjust pH to 7.6
10. Solution C is composed of:
 - a. 0.208 g propidium iodide
 - b. 0.580 g spermine tetrahydrochloride
 - c. 500 mL stock solution
 - d. Adjust pH to 7.6
 - e. Wrap in foil to protect from light

11. Solutions A–C, and citrate buffer are good for 2 wk.
12. The pepsin is good for 1 wk.
13. If nuclear pellet is very small then it is recommended to use half the amounts of solutions A, B, and C.
14. Solution C, which contains propidium iodide, needs to be protected from light by use of tinfoil during the preparation, storage, and staining.
15. Samples should be processed on the flow cytometer within 30 min after the addition of solution C.

References

1. Caspersson, T. and Santesson L. (1942) Studies on protein metabolism of the cells of epithelial tumors. *Acta Radiol* (Suppl.)**46**, 1–105.
2. Auer, G. and Tribukait B. (1980) Comparative single cell and flow DNA analysis in aspiration biopsies from breast carcinomas. *Acta Pathol. Microbiol. Immunol. Scand. [A]* **88**, 355–358.
3. Nativ, O., Myers, R. P., Therneau, T. M., Farrow, G. M., and Lieber, M. M. (1996) Feulgen-stained histologic sections of prostate needle biopsy specimens: reliability of DNA static image analysis. *Forum* **6**, 313–318.
4. Raviv, G., Leibovich, I., Mor, Y., Nass, D., Medalia, O., Goldwasser, B., and Nativ, O. (1993) Localized renal cell carcinoma treated by radical nephrectomy: Influence of pathologic data and the importance of DNA ploidy pattern on disease outcome. *Cancer* **72**, 2207–2212.
5. Ellis, W.J., Bauer, K. D., Oyasu, R., and McVary, K. T. (1992) Flow cytometric analysis of small renal tumors. *J. Urol.* **148**, 1774–1777.
6. al-Abadi, H. and Nagel R. (1992) Transitional cell of the renal pelvis and ureter: Prognostic relevance of nuclear deoxyribonucleic acid ploidy studied by slide cytometry: 8-year survival time study. *J. Urol.* **48**, 31–37.
7. Stephenson, R. A. (1988) Flow cytometry in genitourinary malignancies using paraffin-embedded material. *Semin. Urol.* **6**, 46–52.
8. Brendler, C. B. (1988) Flow cytometric evaluation of urological malignancies. *J. Urol.* **139**, 342–343.
9. Ljungberg, B., Forsslund, G., Stenling, R., and Zetterberg, A. (1986) Prognostic significance of the DNA content in renal cell carcinoma. *J. Urol.* **135**, 422–426.
10. Baisch, H., Otto, U., and Klöppel, G. (1986) Malignancy index based on flow cytometry and histology for renal cell carcinomas and its correlation to prognosis. *Cytometry* **7**, 200–04.
11. Medeiros, L. J., Gelb, A. B., and Weiss, L. M. (1988) Renal cell carcinoma: prognostic significance of morphological parameters in 121 cases. *Cancer* **61**, 1639–1651.
12. Jonas, D., Thoma, B., Beckert, H., and Weber, W. (1985) The value of morphological prognostic criteria in the assessment of renal cell carcinoma. *Urol. Int.* **40**, 148–154.
13. Currin, S. M., Lee, S. E., and Walther, P. J. (1990) Flow cytometric assessment of deoxyribonucleic acid content in renal adenocarcinoma: does ploidy status enhance prognostic stratification over stage alone? *J. Urol.* **143**, 458–463.

14. Otto, U., Baisch, H., Huland, H., and Klöppel, G. (1984) Tumor cell deoxyribonucleic acid content in prognosis in renal cell carcinoma. *J. Urol.* **132**, 237–239.
15. Grignon, D. J., El-Nagger, A., Green, L. K., Ayala, A. G., Ro, J. Y., Swanson, D. A., Troncoso, P., McLemore, D., Giacco, G. G., Guinee, V. F. (1989) DNA flow cytometry as a predictor of outcome of Stage I renal cell carcinoma. *Cancer* **63**, 1161–1165.
16. Ljungberg, B., Stenling, R., and Roos, G. (1985) DNA content in renal cell carcinoma with reference to tumor heterogeneity. *Cancer* **56**, 503–508.
17. Feulgen, R. and Rossenbeck, H. (1924) mikroskopisch-chemischer nachweis einer nukleinsäure vom typus der thymonukleinsäure preparaten. *Hoppe-seyler's Z. Phys. Chem.* **135**, 203–248.
18. Tolles, W. E., Horvath, W. J., and Bostrom, R. C. (1961) A study of the quantitative characteristics of the exfoliative cells from the female genital tract. *Cancer* **14**, 347–454.
19. Hemstreet, G. P., West, S. S., and Weems, W. L., (1983) Quantitative fluorescence measurements of AO-stained normal and malignant bladder cells. *Int. J. Cancer* **31**, 577–585.
20. Hedley, D. W., Friedlander, M. L., Taylor, I. W., Rugg, C. A., and Musgrove, E. A. (1983) Method for analysis of cellular DNA content of paraffin-embedded pathological material using flow cytometry. *J. Histochem. Cytochem.* **31**, 1333–1335.
21. Vindeløv, L. L., Christensen, I. J., and Nissen, N. I. (1983) A detergent-trypsin method for the preparation of nuclei for flow cytometric DNA analysis. *Cytometry* **3**, 323–327.
22. Cope, C., Rowe D., Delbridge, L., Philips, J., and Friedlander, M. (1991) Comparison of image analysis and flow cytometric determination of cellular DNA content. *J. Clin. Pathol.* **44**, 147–151.
23. Deitch, A., Wagner, D., and Richart, R. (1968) Conditions influencing the intensity of the Feulgen reaction. *J. Histochem. Cytochem.* **16**, 371–379.